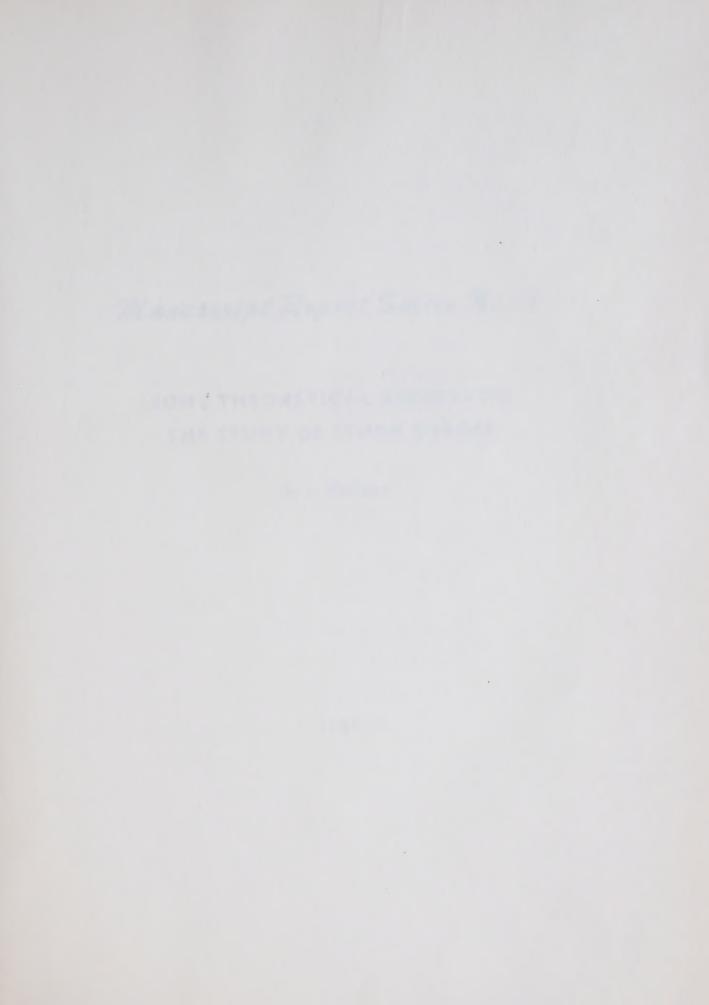


Digitized by the Internet Archive in 2023 with funding from University of Toronto

Canada. Marine Sciences Branch Manuscript report series. 11-17, 1969-71







CAI MT 47 - 72 RII

5936

Manuscript Report Series No. 11-17

THE STUDY OF STORM SURGES

G. L. Holland



SOME THEORETICAL ASPECTS DW

basilend & Reliend

QUEEN'S PRINTER
OTTAWA, 1969

ABSTRACT

Long waves generated by localised air pressure gradients and wind stresses acting on the surface are termed storm surges. This report investigates the equations of motion of these long waves and their solutions for particular cases.

The equations are simplified by using steps justified from physical considerations. In addition the advantages of using an averaged form of these equations is discussed.

Long waves propagated in a non-rotating system are not dispersive, but in general they are dispersive in a rotating system. The free oscillations of long waves are discussed for the cases of an unlimited sea and a circular basin in rotating systems. Special types of non-dispersive long waves are found and investigated. Modified forms of these waves are found when a simple frictional effect is included.

General solutions are found for the elevation and velocities of storm surges generated on an infinite rotating sea for which all bottom friction is neglected. Particular solutions are then derived for a given stationary generating force of constant amplitude suddenly applied and maintained over one half of the infinite sea. Extensions to the solutions are carried out to investigate non-instantaneous and non-infinite effects of such a force. The effect of a barrier at right angles to the motion is briefly considered. In addition a travelling generating force moving with the maximum

group velocity of the waves is shown to lead to an everincreasing surface elevation.

Lastly the equations of motion in cylindrical coordinates are used to investigate two simple axially symmetric cases. The generating forces used approximate well to cyclonic atmospheric conditions.

CONTENTS

		rage			
INTR	CODUCTION	1			
1.1	The physical problem	1			
1.2	The prediction of storm surges	2			
THE	DYNAMICS OF THE STORM SURGE	5			
2.1	The equations of motion	5			
2.2	The averaged equations	14			
2.3	The adequacy of the averaged equations	16			
EQU	ATIONS FOR THE ELEVATION & AND ITS FREE OSCILLATIONS	22			
3.1	The free oscillations on a rotating system	22			
3,2	The general two-dimensional equations	24			
3.3	Free oscillations on an unlimited rotating sea	26			
3.4	A modification to allow for bottom stress	31			
3.5	The general equation for \$\zeta\$ in cylindrical co-ordinates	34			
3.6	Free oscillations on a circular rotating sea	35			
THE GENERATION AND PROPAGATION OF SURGES ON AN INFINITE					
ROT.	ATING SEA	41			
4.1	The problem	41			
4.2	The general solution for \(\)	42			
4.3	The general solution for the velocities	45			
A PARTICULAR CASE					
5.1	The solutions	46			
5.2	Interpretation of the results for the Particular Case	49			

MODII	FICATIONS TO THE APPLIED FORCE	52	
6.1	A gradually applied force	52	
6.2	A finite generating width	56	
OTHE	R EFFECTS	61	
7.1	A barrier at right angles to the direction of propagation	61	
7.2	A travelling disturbance	63	
EXTE	NSIONS TO THE PROBLEM USING CYLINDRICAL CO-ORDINATES.	66	
8.1	A simple axially symmetric distribution	66	
8.2	A circular wind distribution	72	
DISCU	SSION	77	
9.1	Putting theory into practice	77	
BIBLI	OGRAPHY	82	
APPEI	NDIX	84	
ACKNOWLEDGMENTS			

NOTATION

Phase velocity of the surge. C Group velocity of the surge. C Acceleration due to gravity. g The depth of water. h Wave number, defined as $2\pi \times (\text{wavelength})^{-1}$. k K Coefficient of eddy viscosity, presumed constant. Pressure in the sea at depth z. p Pa Air pressure on the sea surface. (r, θ, z) A cylindrical co-ordinate system with r,0 in the mean sea surface and z vertically upwards. t Time. T Period of the surge. (u,v,w)Velocities relative to the (x,y,z) co-ordinate system. U,V Horizontal depth mean velocities in the x,y directions respectively. Velocities relative to (r, 0, z) co-ordinate (v_r, v_e, v_7) system. Horizontal depth mean velocities in the r,0 Vr, Ve directions respectively. A right-handed co-ordinate system with x,y in (x,y,z)the mean sea surface and z vertically upwards. Coriolis parameter equal to $2\Omega \sin \phi$. Υ Elevation of the sea surface above the mean ζ level.

Wavelength of the surge. λ Density of the water assumed uniform. ρ Frequency of the surge, defined as 2π x σ $(period)^{-1}$. (τ_r, τ_{Θ}) Horizontal components of the frictional stress in the r,θ directions respectively. $(\tau_{\rm X}, \tau_{_{
m V}})$ Horizontal components of the frictional stress in the x,y directions respectively. North latitude of the sea presumed constant. ф Ω Angular velocity of the Earth.

N.B. Other symbols used will be defined locally.

INTRODUCTION

1.1. The Physical Problem

The accurate prediction of variations in the level of the sea is of the utmost importance to all maritime nations. Engineers require this knowledge for the design of adequate sea-defences, harbour-masters for the economical use of their ports, captains for the safe navigation of coastal waters and the population of low-lying exposed coastal areas for ample warning should flooding prove imminent.

The changes in sea level can be initially separated into periodic (or tidal) and transient variations. The tidal variations, consisting mainly of the astronomical tides, can already be accurately forecast, so that the problem reduces to one of the prediction of the transient effects. Part of the transient variation in sea level is made up of the ordinary surface waves with periods of a few seconds. The remainder can be termed the "meteorological sea-level effect". There are rare occurences of strong seismic transients but these are neglected, along with the surface waves, in this treatment. The "meteorological sea-level effect" includes variations due to precipitation, evaporation, heating and cooling, but the effects due to these causes are small compared to the effect of the wind and pressure, at least over the reasonably short periods which are of interest.

The definition of a storm surge is that effect of wind and pressure on the sea surface associated with a single storm. Fortunately there does not seem to be a marked

interaction between the motions due to the different causes mentioned above, so that the motion of interest can be extracted from observations and studied separately. The amplitude of these surges is usually a few feet, but several times each century surges have been recorded whose amplitudes have reached a range of ten to fifteen feet or even more. These extreme, or major, surges created by severe storms occuring under the most unfavourable conditions have caused many catastrophies in the past, and a greater understanding of the generation and propagation of such surges is needed to avoid similar catastrophies in the future.

1.2. The Prediction of Storm Surges

In the past empirical forecasting methods, based on observational data, and prevailing meteorological conditions, have formed the basis for the prediction of storm surges, but in more recent years numerical methods using digital computers have been adopted successfully to this problem. In fact, the progress using this technique is being hampered by inaccuracy in weather forecasting, according to Welander (1961).

The exact mathematical treatment of the problem as it occurs in nature is impossible due to the complicated boundary conditions, generating forces and viscous effects. However the mathematical solutions to particular problems, where simplifying assumptions have been made, are important. Such solutions throw light on the properties of surges and these simplified models should be of use in more elaborate analyses

using computing techniques. The study of such theoretical aspects of the problem is the objective of the following report.

In the first section of the report the equations of motion are derived in a general manner. These equations are then simplified by neglecting certain terms using physical considerations. The difficulty of taking into full consideration the viscous forces within the liquid is overcome by averaging the equations throughout the depth. The equations which then result are approximate, in that they satisfy exact conditions only at the boundaries, yielding a mean solution for the rest of the fluid. Proudman (1954) justified the use of the averaged equations by a direct comparison with the solutions from the non-averaged equations for a particular case, Proudman and Doodson (1924). This paper is discussed briefly.

Bearing in mind the assumptions made in deriving the simplified equations of motion the equations are used to discuss the free oscillations of a rotating system. In these cases the generating forces and the viscous effects are taken to be zero. The free oscillations show how long waves propagate on a rotating system, and two special types of waves are found that can travel without change of shape. It is shown however that in general in a rotating system long waves are dispersive. The two special waves are called Kelvin waves and Poincaré waves, the former being described by Kelvin (1879) and the latter by Poincaré (1910). The basic forms of these waves were modified by Proudman (1954) to include a simple form of bottom stress,

and these modified waves, termed "damped" Kelvin and "damped" Poincaré waves are briefly discussed.

crease (1955) has considered solutions to the averaged equations of motion in which the forcing terms, that is the atmospheric pressure gradients and surface wind effects, have been taken into account. This paper is dealt with in detail. The system chosen is that of an infinite rotating sea of uniform depth, and the main purpose of his paper is to investigate the dispersive nature of long waves propagated on a rotating system. Extensions of his paper to include the effect of a moving generating force, and the effect on a barrier are considered more briefly.

The type of generating force assumed by Crease is of a very simple form, and extensions to his solutions by slight modifications to the assumed law of force are presented in the latter part of this report.

The equations of motion can be derived in cylindrical co-ordinates, but apart from a discussion by Lamb which is incorporated into the section dealing with free oscillations, the consideration of cylindrical co-ordinates seems to be largely neglected. Welander (1961) suggests that cartesian co-ordinates are preferable because of difficulties occuring at the origin when cylindrical co-ordinates are used. However by assuming axial symmetry the equations may be simplified and solutions are found when generating forces are included which approximate well to cyclonic atmospheric disturbances. These solutions are given in a form suitable for numerical analysis.

In the final discussion the place of exact mathematical theory in this complicated problem in relation to the other methods of prediction is evaluated.

Throughout the work treated in this report some overall assumptions have inevitably to be made in order to commence a mathematical analysis. The whole of the energy available from the atmospheric generating forces will be assumed to be used solely for the generation of that part of the wave spectrum under consideration, i.e. long waves. The actual partition of energy is still unknown and the above assumption is used generally. The interaction between the surge and the oscillations of the sea-surface due to astronomical and other effects is neglected, an assumption justified by most observations. Therefore the wave may be assumed to be propagated on a calm sea, and if necessary, the total variation of the sea-surface can be found by direct superposition of the different linear effects. The latitude of the seas in which the surges are supposed to take place is considered constant over the whole region of motion.

THE DYNAMICS OF THE STORM SURGE

2.1 The Equations of Motion

Equations of motion are required with respect to axes relative to an observer moving with the Earth on the Earth's surface. In the following diagram, figure 1, the Earth's centre is taken at C and the Direction $\overline{\text{CN}}$ is the North pointing axis of rotation of the Earth. It is assumed that the Earth is fixed in space.

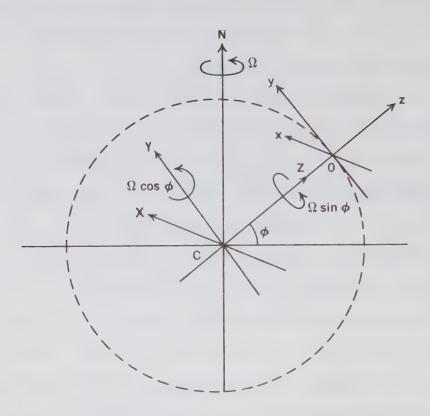


Figure 1. Axes of Rotation and Coriolis Components.

The accelerations of a particle relative to axes C(X'Y'Z') fixed in space are given by $\frac{D^2X'}{Dt^2}$, $\frac{D^2Y'}{Dt^2}$, $\frac{D^2Z'}{Dt^2}$ along the X', Y', Z' directions respectively, using $\frac{D}{Dt}$ in the usual Eulerian notation.

The axes C(XYZ) in the figure correspond to axes fixed in the Earth which is rotating about \overline{CN} with a constant angular velocity Ω . This rotation has components $\Omega \sin \phi$ about the axis \overline{CZ} and $\Omega \cos \phi$ about the axis \overline{CY} . The accelerations of a particle relative to, and in the direction of, these axes

C(XYZ) are
$$\left(\frac{D^2X}{Dt^2} - 2\Omega\sin\phi \cdot \frac{DY}{Dt} + 2\Omega\cos\phi \cdot \frac{DZ}{Dt}\right)$$
;

$$\left(\frac{D^2Y}{Dt^2} + 2\Omega\sin\phi \cdot \frac{DX}{Dt}\right)$$
 and $\left(\frac{D^2Z}{Dt^2} - 2\Omega\cos\phi \cdot \frac{DX}{Dt}\right)$ respectively, where the

squares of Ω have been neglected as being very small. Transferring the origin to a point in the Earth's surface alters the accelerations relative to the new axes only in the terms containing Ω^2 . Therefore the accelerations required relative to O(xyz) are $\frac{Du}{Dt} - 2\Omega \sin\phi \cdot v + 2\Omega \cos\phi \cdot w$; $\frac{Dv}{Dt} + 2\Omega \sin\phi \cdot u$ and

 $\frac{Dw}{Dt}$ - $2\Omega cos \varphi$.u , where (u,v,w) are the velocities at time t relative to these axes.

Hence if O(xyz) is a co-ordinate system fixed relative to the Earth at a latitude ϕ with x and y East and North respectively and z vertically upwards, (u,v,w) are the corresponding velocity components, p the pressure, ρ the density, g the acceleration due to gravity and (F_x,F_y,F_z) the corresponding general frictional terms, then the equations of motion are as follows:-

$$\frac{\partial \mathbf{u}}{\partial \mathbf{t}} + \mathbf{u} \frac{\partial \mathbf{u}}{\partial \mathbf{x}} + \mathbf{v} \frac{\partial \mathbf{u}}{\partial \mathbf{y}} + \mathbf{w} \frac{\partial \mathbf{u}}{\partial \mathbf{z}} - 2\Omega \sin \phi \cdot \mathbf{v} + 2\Omega \cos \phi \cdot \mathbf{w}$$

$$= -\frac{1}{\rho} \frac{\partial \mathbf{p}}{\partial \mathbf{x}} + \mathbf{F}_{\mathbf{x}}$$

$$\frac{\partial \mathbf{v}}{\partial \mathbf{t}} + \mathbf{u} \frac{\partial \mathbf{v}}{\partial \mathbf{x}} + \mathbf{v} \frac{\partial \mathbf{v}}{\partial \mathbf{y}} + \mathbf{w} \frac{\partial \mathbf{v}}{\partial \mathbf{z}} + 2\Omega \sin \phi \cdot \mathbf{u} = -\frac{1}{\rho} \frac{\partial \mathbf{p}}{\partial \mathbf{y}} + \mathbf{F}_{\mathbf{y}}$$

$$\frac{\partial \mathbf{w}}{\partial \mathbf{t}} + \mathbf{u} \frac{\partial \mathbf{w}}{\partial \mathbf{x}} + \mathbf{v} \frac{\partial \mathbf{w}}{\partial \mathbf{y}} + \mathbf{w} \frac{\partial \mathbf{w}}{\partial \mathbf{z}} - 2\Omega \cos \phi \cdot \mathbf{u} = -\frac{1}{\rho} \frac{\partial \mathbf{p}}{\partial \mathbf{z}} + \mathbf{F}_{\mathbf{z}} - \mathbf{g}$$

$$(2.1)$$

and since a liquid is being considered the continuity equation is

$$\frac{\partial \mathbf{u}}{\partial \mathbf{x}} + \frac{\partial \mathbf{v}}{\partial \mathbf{y}} + \frac{\partial \mathbf{w}}{\partial \mathbf{z}} = 0 \tag{2.2}$$

The approximations so far used in writing down equations (2.1) and (2.2) have assumed an incompressible sea of uniform density and neglected the effect of the curvature of the Earth's surface. The assumption concerning the density is consistent with physical considerations in seas well mixed by turbulence. The curvature of the Earth's surface can be considered negligible if the region under consideration is not too large in extent.

The above equations are in a general form and can be simplified by the use of an order of magnitude analysis developed by Charnock and Crease (1957) and used here in an adapted form.

The amplitude of the surge ζ_0 is assumed small compared with the depth h. The horizontal scale of the surge, denoted by its wavelength λ , is taken as large compared to h. These assumptions are based on observations and are generally true, however on rare occasions when large surges are propagated on shallow seas the ratio of the amplitude of the surge to the depth of water may not be negligible. An example of such an occasion was provided by the major surge in the North Sea in 1953, when the value of ζ_0/h reached an order of about 1/5 in the southern half of the sea. The corresponding value of h/λ for the same surge was about 10^{-4} .

The equations of motion can be reduced to a non-dimensional form by referring all velocities to \sqrt{gh} , lengths to h, times to $\sqrt{h/g}$, Ω to $\sqrt{g/h}$, pressure to pgh and the frictional forces to g. The non-dimensional equations are

$$\frac{\partial \mathbf{u'}}{\partial \mathbf{t'}} + \mathbf{u'} \frac{\partial \mathbf{u'}}{\partial \mathbf{x'}} + \mathbf{v'} \frac{\partial \mathbf{u'}}{\partial \mathbf{y'}} + \mathbf{w'} \frac{\partial \mathbf{u'}}{\partial \mathbf{z'}} - 2\Omega' \sin\phi \cdot \mathbf{v'} + 2\Omega' \cos\phi \cdot \mathbf{w'}$$

$$= -\frac{\partial p'}{\partial v'} + F_{X}' \qquad (2.3)$$

$$\frac{\partial \mathbf{v'}}{\partial \mathbf{t'}} + \mathbf{u'} \frac{\partial \mathbf{v'}}{\partial \mathbf{x'}} + \mathbf{v'} \frac{\partial \mathbf{v'}}{\partial \mathbf{y'}} + \mathbf{w'} \frac{\partial \mathbf{v'}}{\partial \mathbf{z'}} + 2\Omega' \sin\phi \cdot \mathbf{u'} = -\frac{\partial \mathbf{p'}}{\partial \mathbf{y'}} + \mathbf{F_{y'}}$$
(2.4)

$$\frac{\partial \mathbf{w'}}{\partial \mathbf{t'}} + \mathbf{u'} \frac{\partial \mathbf{w'}}{\partial \mathbf{x'}} + \mathbf{v'} \frac{\partial \mathbf{w'}}{\partial \mathbf{y'}} + \mathbf{w'} \frac{\partial \mathbf{w'}}{\partial \mathbf{z'}} - 2\Omega' \cos\phi \cdot \mathbf{u'} = -\frac{\partial \mathbf{p'}}{\partial \mathbf{z'}} + \mathbf{F}_{\mathbf{z'}} - 1 \quad (2.5)$$

and the continuity equation

$$\frac{\partial \mathbf{u'}}{\partial \mathbf{x'}} + \frac{\partial \mathbf{v'}}{\partial \mathbf{y'}} + \frac{\partial \mathbf{w'}}{\partial \mathbf{z'}} = 0 \tag{2.6}$$

where non-dimensional quantities are denoted by a prime.

The assumptions $\zeta_0 << h, \lambda >> h$ now become

$$\zeta_{0}^{\prime} << 1, \lambda^{\prime} >> 1$$
 (2.7)

The vertical velocity w varies from a value of zero at z=-h, that is the sea bottom, to $\frac{D\zeta}{Dt}$ at the sea surface. The fact that $w=\frac{D\zeta}{Dt}$ at $z=\zeta$ merely expresses the fact that the free surface must follow the fluid. The vertical velocity w therefore is of order ζ_0/T , where T is the period of the surge, and its dimensionless counterpart w' is of order ζ'_0/T' . No restrictions have been imposed on the horizontal directions, x' and y' are both taken to be of order λ' , whilst z' is of order unity. From the continuity equation considering orders of magnitude it follows that

$$\mathbf{u'} = O(\mathbf{w'}\lambda') = O(\underline{\zeta_0'\lambda'}); \quad \mathbf{v'} = O(\mathbf{w'}\lambda') = O(\underline{\zeta_0'\lambda'})$$
and
$$\mathbf{w'} = O(\underline{\zeta_0'})$$

$$\underline{T'}$$

Physically T is expected to have a value of several hours, so that, because of the smallness of $\boldsymbol{\Omega}$

$$T' >> \Omega'$$
 (2.9)

Using equations (2.7), (2.8), (2.9) the orders of magnitudes of the terms appearing in the equations of motion can be assessed. Taking equation (2.3) and writing the order of magnitude of individual terms beside each term.

Left hand side terms	Order of magnitude	Reduced order of Magnitude
∂u' ∂t'	$\frac{\zeta_0'\lambda'}{T'^2}$	[1]
u' <u>ðu'</u> ðx'	ζ <mark>ο</mark> λ'	[5]
v' <u>ðu'</u>	ζ <mark>'²λ'</mark> Τ' ²	[5,]
w' <u>ðu'</u> ðz'	ζ <mark>ο</mark> λ' Τ' ²	[5]
2Ω'sinφ.v'	Ω'ζ'λ' Τ'	[Ω'T'] (2.10)
2Ω'cosφ.w'	Ω'ζ' _O	$\left[\frac{\Omega'\mathbf{T'}}{\lambda'}\right]$
Right hand side terms		
<u>9p'</u>	<u>p'</u> λ'	[<u>T'²p'</u>] ζ'λ' ²
F _x '	F _x '	$\frac{\left[\frac{\mathbf{T'}^{2}\mathbf{p'}}{\varsigma_{0}^{'}\lambda^{'}}\right]}{\left[\frac{\mathbf{T_{1}}^{2}\mathbf{F_{x'}}}{\varsigma_{0}^{'}\lambda^{'}}\right]}$

 $\frac{\partial p'}{\partial x'}$ is assumed $O(p'/\lambda')$.

In any case $\frac{\partial p'}{\partial x'}$ is likely to be small and $\lambda'>>1$. The quantities in brackets denoting the orders of magnitude of the terms when referred to the first term as unity. It can be seen

from equation (2.10) that the non-linear terms can be neglected as being small and also the rotational term $2\Omega'\cos\phi.w'$ for the same reason. The remaining rotational term $2\Omega'\sin\phi.v'$ is retained since the value of $[\Omega'T']$ may approach unity. If it is further assumed that the forcing terms on the right hand side of the equation are of the same order as the acceleration term then this gives:

$$p' = O(\zeta_0'\lambda'^2), F' = O(\zeta_0'\lambda')$$

$$T'^2$$
(2.11)

A similar analysis of equation (2.4) leads to the omission of the non-linear terms from that equation

For the vertical equation (2.5) the orders of magnitude are as follows:

Left hand side terms	Order of Magnitude	Reduced order of Magnitude
<u>ðw'</u>	ζ <mark>ο</mark> Τ' ²	[1]
u' <u>ðw'</u>	50 T 1 2	[50]
Λ, 9 ^A ,	5°2 T'2	[50]
2Ω'cosφ.u'	Ω'ζ'λ' Τ'	[Τ'Ω'λ']
w ' <u>a w '</u>	ζ' ² Τ' ²	[50]

continued

Right hand side terms

$$\frac{\partial p'}{\partial z'} \qquad \frac{\zeta_0' \lambda'^2}{T'^2} \qquad [\lambda'^2]$$

$$F_z' \qquad \frac{\zeta_0' \lambda'}{T'^2} \qquad [\lambda']$$

$$1 \qquad 1 \qquad [\underline{T'}^2]$$

equation (2.11) being used for the orders of magnitude of the pressure and friction terms. From equation (2.12) it can be seen that the 1st. and 3rd. terms on the right hand side of the equation are an order of magnitude higher than any of the remaining terms, and therefore are the only terms retained.

With the above omissions, and replacing the frictional forces F_x , F_y with $\frac{1}{\rho} \frac{\partial^{\tau} x}{\partial z}$ and $\frac{1}{\rho} \frac{\partial^{\tau} y}{\partial z}$ respectively, $\left(\tau_x \text{ and } \tau_z\right)$

being the two horizontal components of the frictional stress, the equations of motion simplify to

$$\frac{\partial \mathbf{u}}{\partial t} - \gamma \mathbf{v} = -\frac{1}{\rho} \frac{\partial \mathbf{p}}{\partial \mathbf{x}} + \frac{1}{\rho} \frac{\partial^{\mathsf{T}} \mathbf{x}}{\partial \mathbf{z}}$$

$$\frac{\partial \mathbf{v}}{\partial t} + \gamma \mathbf{u} = -\frac{1}{\rho} \frac{\partial \mathbf{p}}{\partial \mathbf{y}} + \frac{1}{\rho} \frac{\partial^{\mathsf{T}} \mathbf{y}}{\partial \mathbf{z}}$$

$$0 = -\frac{1}{\rho} \frac{\partial \mathbf{p}}{\partial \mathbf{z}} - \mathbf{g}$$

$$(2.13)$$

 γ is used in the above equations as an abbreviation for $2\Omega sin\varphi$ and the quantities are again dimensional. The equation of continuity is unaltered being

$$\frac{\partial \mathbf{u}}{\partial \mathbf{x}} + \frac{\partial \mathbf{v}}{\partial \mathbf{y}} + \frac{\partial \mathbf{w}}{\partial \mathbf{z}} = 0$$

The vertical equation has reduced to the hydrostatic equation and can be integrated to give

$$p - Pa = \rho g(\zeta - z) \tag{2.14}$$

using the condition that the pressure is atmospheric p = Pa at the free surface where $z = \zeta$.

In the preceeding analysis no restrictions were taken in the horizontal scales, which were assumed to be the same. If however the y direction is restricted so that $0 < y < y_0$ (say), which could apply to a channel of width y_0 , then y' is $O(y_0')$ and from the continuity equation v' is $O(\zeta_0'\gamma_0')$. Using

this order of magnitude for v' in equation (2.3) the order of magnitude of the previously retained rotational term $2\Omega \sin\phi.v'$ is $O(\Omega'T'y'_0)$ when referred to the first term of the equation λ'

as unity. Hence for $y_0 << \lambda$ the rotational terms disappear from the equation, but for such channels ζ_0 is not necessarily small compared to the depth so the non-linear terms remain. Examination of equation (2.4) in the y direction shows that for such conditions $\frac{\partial p}{\partial y} = \text{Constant}$. To sum up it appears that in the

open sea the non-linear terms appearing in the equations may be neglected and the rotational terms retained, but in an estuary where the width y_0 may be small compared to the wavelength λ of the surge, and the amplitude ζ_0 need not be small compared to the depth h, the opposite may apply.

2.2 The averaged equations.

The motion of the surge is non-laminar and therefore the frictional forces taken in a general form in the previous section arise mainly from turbulence. In general therefore, additional equations expressing the turbulent motion of the sea are needed to relate the stresses given in equation (2.13) to the velocity field. Unfortunately very little is known about the relation of the stresses to the velocities in oceanic conditions, which mean further approximations have to be made. By analogy with laminar flow a virtual eddycoefficient of viscosity can be introduced, for example as defined by $\tau_{x} = K_{\rho} \frac{\partial u}{\partial z}$ but this relation means little unless K can be related to the mean flow. Apparently this can be done in certain cases, c.f. Schlichting Ch. 19 (1955). K can also be taken as constant so as to linearise the terms. However in general the best method of procedure, which at least partly avoids the difficulty, would seem to be the integration of the equations of motion throughout the depth of fluid. The stress, on integrating $\frac{\partial \tau}{\partial z}$ with respect to z throughout the depth h, enters the equations in the form

$$\int_{b}^{O} \frac{\partial \tau_{X}}{\partial z} \cdot dz = \tau_{X} \text{ (surface)} - \tau_{X} \text{ (bottom)}$$
 (2.15)

where $\tau_{\rm X}$ (surface) is the stress due to the drag of the wind on the surface of the sea, assumed to be a given force, and $\tau_{\rm X}$ (bottom) is the frictional stress on the bottom of the fluid, to be related in some manner to the mean flow. The usual and most simple assumption is that the bottom stress is directly proportional to the mean velocity, but as the action of the bottom stress may vary with the type of surge under consideration, c.f. Welander (1961) this assumption cannot be accepted unreservedly. The depth-mean velocities are defined as

$$U = \frac{1}{h} \int_{-h}^{\zeta} u.dz ; \qquad V = \frac{1}{h} \int_{-h}^{\zeta} v.dz \qquad (2.16)$$

From the hydrostatic equation (2.14) the pressure gradient $\frac{\partial p}{\partial x}$ is given by $\frac{\partial p}{\partial x} = \rho g \frac{\partial \zeta}{\partial x} + \frac{\partial Pa}{\partial x}$ so that on integrating with respect to z from z = -h to $z = \zeta$

$$\int_{-h}^{\zeta} \frac{\partial \mathbf{p} \cdot d\mathbf{z}}{\partial \mathbf{x}} = \rho g h \frac{\partial \zeta}{\partial \mathbf{x}} + h \frac{\partial Pa}{\partial \mathbf{x}}$$
 (2.17)

Consistent with previous assumptions ζ has been neglected against h in the above equation. The corresponding result for $\partial p/\partial y$ is found in a similar manner. The horizontal equations from (2.13) can now be integrated to

$$\frac{\partial U}{\partial t} - \gamma V = -g \frac{\partial \zeta}{\partial x} - \frac{1}{\rho h} \cdot \frac{\partial Pa}{\partial x} + \frac{1}{\rho h} \left(\tau_{xs} - \tau_{xb} \right)$$

$$\frac{\partial V}{\partial t} + \gamma U = -g \frac{\partial \zeta}{\partial y} - \frac{1}{\rho h} \cdot \frac{\partial Pa}{\partial y} + \frac{1}{\rho h} \left(\tau_{ys} - \tau_{yb} \right)$$
(2.18)

 $\tau_{\rm x}$ (surface) has been abbreviated to $\tau_{\rm xs}$, $\tau_{\rm x}$ (bottom) to $\tau_{\rm xb}$ etc.

The equation of continuity integrates to

$$\frac{\partial U}{\partial x} + \frac{\partial V}{\partial y} \simeq -\frac{1}{h} \frac{\partial \zeta}{\partial t}$$

$$\frac{D\zeta}{Dt} = \frac{\partial \zeta}{\partial t} + \frac{\partial \zeta}{\partial t} + \frac{\partial \zeta}{\partial y} \simeq \frac{\partial \zeta}{\partial t}; \int_{-h}^{0} \frac{\partial w}{\partial z} dz = \frac{D\zeta}{Dt}$$
(2.19)

In the averaged equations the theory requires only the boundary condition that the normal component of velocity (U,V) vanishes at the boundaries of the sea. For the equations to be solvable simplified boundaries are usually accepted that approximate to the physical coastlines.

Corrections are then applied to the solutions to allow for the local inshore effects.

The averaged equations are the most widely used in the theoretical treatment of storm surges, providing a basis for both mathematical treatment and numerical prediction methods. Proudman (1954) attempted to find the degree of approximation involved in using the averaged equations and a discussion of his paper is given in the following section.

2.3 The adequacy of the averaged equations

A paper by Proudman (1954) sets out primarily to show that approximate formulae for the time sequences in the response of the sea surface to atmospheric generating forces may be obtained without considering the vertical distribution of the current. These formulae, which are obtained from the averaged equations, are much simpler than those involving the variation of current with depth. In his paper Proudman obtains solutions from the averaged equations

and compares them directly with corresponding solutions from the non-averaged equations. The latter solutions are quoted from a previous paper Proudman and Doodson(1924). Both sets of equations are solved under the same boundary conditions.

In these papers the wave motion is assumed to take place in a non-rotating rectangular basin bounded by the planes x = 0, $x = \ell$, z = -h. The motion is assumed to lie entirely in the x,z plane. The mean free surface is taken as z = 0. The current, assumed sensibly parallel to the x axis, is denoted by u(x,z,t). K is the coefficient of eddy viscosity presumed constant, (c.f section 2.2 above), and the remaining terms are consistent in their notation with the previous The non-averaged equation of motion is:-

$$\frac{\partial \mathbf{u}}{\partial t} = -\frac{g}{\partial \mathbf{x}} - \frac{1}{\rho} \frac{\partial \mathbf{Pa}}{\partial \mathbf{x}} + \frac{\partial}{\partial \mathbf{z}} \begin{bmatrix} \mathbf{K} \cdot \partial \mathbf{u} \\ \partial \mathbf{z} \end{bmatrix}$$
and the continuity equation $\frac{\partial}{\partial \mathbf{x}} \int_{-\mathbf{h}}^{\zeta} \mathbf{u} \cdot d\mathbf{z} + \frac{\partial \zeta}{\partial t} = 0$

$$(2.20)$$

From these equations a single equation for the elevation ζ can be obtained in a manner described later in section 3.2. This equation is

$$\left[\frac{\partial^{2}}{\partial x^{2}} - \frac{1}{gh} \frac{\partial^{2}}{\partial t^{2}}\right] \zeta = -\frac{1}{\rho} \frac{\partial^{2} Pa}{\partial x^{2}} + \frac{K}{h} \left[\frac{\partial u}{\partial z}\right]_{z = \zeta} \left[\frac{K}{h} \frac{\partial u}{\partial z}\right]_{z = -h}$$
(2.21)

and is essentially a non-averaged equation as the function u = u(x,z,t) must be prescribed from the boundary conditions and equation (2.20). The boundary conditions are as follows (2.22)

u = 0 for x = 0, $x = \ell$ and z = -h

together with a prescription of the stress at the surface, [c.f. section 2.2] that is in equation (2.21) $\frac{K}{h} \left[\frac{\partial u}{\partial z} \right]_{z} = \zeta$

is given.

Proudman uses a one dimensional form of the averaged equations given by equation (2.18) and obtains an equation for $\boldsymbol{\zeta}$ which can be written

$$\left[\frac{\partial^{2}}{\partial x^{2}} - \frac{1}{gh} \frac{\partial^{2}}{\partial t^{2}}\right]^{\zeta} = -\frac{1}{\rho} \frac{\partial^{2} Pa}{\partial x^{2}} + \frac{1}{\rho h} \left[{}^{\tau}x\right]_{z = \zeta}$$

$$-\frac{1}{\rho h} \left[{}^{\tau}x\right]_{z = -h} \tag{2.23}$$

From the boundary condition above $\frac{K}{h} \left[\frac{\partial u}{\partial z} \right]_{\mathbf{Z}} = \zeta$ is equal

to $\frac{1}{\rho h} \begin{bmatrix} \tau_X \\ z = \zeta \end{bmatrix}$, so that equations (2.21) and (2.23) differ only by their bottom stress terms. Thus as far as the elevation is concerned the adequacy of taking the averaged form of the equations of motion depends entirely on what assumptions are made about the bottom stress law. In the non-averaged equations the term $\frac{K}{h} \begin{bmatrix} \partial u \\ \partial z \end{bmatrix}_{z=-h}$ is evaluated by

finding a solution for the velocity u = u(x,z,t) from the basic equations (2.18) and the boundary conditions. In the averaged equations some law has to be assumed relating the bottom stress to the mean flow. This statement comparing the two equations is quite general and applies equally well if K is not assumed constant in equation (2.20) and the

motion takes place under different boundary conditions.

Returning to the particular case, Proudman assumes a linear relationship between the bottom stress and the mean velocity $U\left(x,t\right)$ given by

$$\begin{bmatrix} \tau_{\mathbf{x}} \\ \overline{\rho \mathbf{h}} \end{bmatrix}_{\mathbf{z}} = -\mathbf{h} \tag{2.24}$$

where k is constant.

The generating functions are supposed created at t = 0 and thereafter maintained constant, with initial conditions $\zeta = 0$, u = 0 for $t \le 0$. The functions chosen by Proudman and Doodson were $K\left(\frac{\partial u}{\partial z}\right)_{z = \zeta} = ghW.sin\left(kx\right)$

and Pa = Constant + P $\frac{g\rho \cdot \cos(kx)}{k}$ (2.25)

where W and P are constants. The subsequent elevation from the non-averaged equation is given by

$$\zeta = -\frac{\cos(kx)}{k} \left\{ P + \frac{3W}{2} + \Sigma_s C_s \exp(\chi_s Kt/h^2) \right\}$$
 (2.26)

where χ_s is a root of the equation $\tan \chi^{\frac{1}{2}} = \chi^{\frac{1}{2}} + \alpha \chi^{\frac{5}{2}}$

with
$$\alpha = \frac{K^2}{gh^5k^2}$$

and
$$C_s = \frac{2P \cdot \alpha + 2W(\sec \chi_s^{\frac{1}{2}} - 1)/\chi_s^2}{\left[\frac{\tan \chi_s^{\frac{1}{2}}}{\chi_s}\right]^2 - 5 \alpha}$$
 (2.27)

Certain examples of this solution are evaluated in which $\alpha = 0.0615$ and in this case it is found that when the disturbance is produced by atmospheric pressure only

$$\zeta = \text{Hcos}(kx) \{1 - 1.062 \exp(-1.272\text{Kt/h}^2) \cos(3.435\text{Kt/h}^2) - 19.2^{\circ}\} + 0.003 \exp(-22\text{Kt/h}^2)\}$$
 (2.28)

where $H = - P/_{k}$, W = 0

and that when the disturbance is produced by wind stress only

$$\zeta = H\cos(kx) \{1 - 1.075 \exp(-1.272Kt/h^2) \cos(3.435Kt/h^2 - 22.8^0) - 0.009 \exp(-22Kt/h^2)\}$$
 (2.29)

on writing $H = -\frac{3W}{2}$, P = 0

In both equations, (2.28) and (2.29), H denotes a constant height and as $t \rightarrow \infty$, $\zeta \rightarrow H\cos(kx)$ in both cases. However though the elevation is the same in each of these two steady states the velocity distribution is totally different. For the case of no wind there are no currents, but for the case of wind stress and constant pressure there are currents flowing with the wind near the surface and opposing the wind direction near the bottom. The depth mean velocities for the currents in both cases being zero. The numerical values contained in (2.28) and (2.29) are so close together as to suggest (c.f. Proudman) "that as an approximation (2.28) may be used instead of (2.29) for the case when the disturbance is produced by the wind. And then this indicates that the formulae may still give a valid approximation when the currents do not folow the artificial laws assumed, but may have nonzero values at the bottom and a non-uniform coefficient of

eddy viscosity". However the forcing functions describing the pressure and the wind effects are so nearly the same when substituted into the equations as to suggest that this case may be a special one.

The averaged equation (2.23) when the bottom stress law given by (2.24) is used with the generating forces (2.25), yields a numerical solution that can be adjusted to the same form as the solutions (2.28) and (2.29), and this is given by

$$\zeta = H\cos\left(kx\right) \left\{1 - 1.058\exp\left(-1.326Kt/h^2\right) \cos\left(3.809Kt/h^2\right) - 19.2^{\circ}\right\}$$
where $-kg$ $H\sin\left(kx\right) = -\frac{1}{\rho} \frac{\partial P_a}{\partial x} + \frac{1}{\rho h} \left(\tau x\right)z = \zeta$ (2.30)

N.B. On substituting from equation (2.25)

$$-\frac{1}{\rho}, \frac{\partial Pa}{\partial x} + \frac{1}{\rho h}(\tau_x) = g(P + W)\sin(kx)$$

so that in the steady state for t $\rightarrow \infty$, $\zeta \rightarrow -(P + W)$ $\frac{\cos(kx)}{k}$ whereas previously (c.f. equation (2.26)

$$\zeta \rightarrow -(P + \frac{3}{2} \text{ W}) \frac{\cos(kx)}{k}$$
. Proudman (1953) indicates the

true value lies between these two.

Equation (2.30) approximates very nearly to that obtained by the non-averaged equations and Proudman concludes that the averaged solution (2.30) may be used as an approximation for the generation of a steady state in which $\zeta = \text{Hcos}(kx)$ whether this is caused by wind, pressure or both.

The numerical comparisons that have been made above apply only to the special case under consideration. It is

felt apart from the general statement made earlier in this section the adequacy of averaging the equations cannot be dealt with in general. Proudman's paper justifies the use of a certain bottom stress law in the averaged equations for a particular problem as an approximate method of solution. This linear law connecting the bottom stress and the mean velocity is widely used (c.f. Welander (1961), however Charnock and Crease (1957) refer to a series of papers by Nomitsu (1933, 1934, 1935) in which the author draws attention to the fact that the time response of the elevation to the generating forces will depend strongly on the type of bottom boundary condition assumed. Nevertheless the averaged equations offer many advantages and are adopted in complicated problems in order to obtain a solution. The solutions obtained using the averaged equations must approximate to the exact solutions but the degree of approximation will depend on the bottom boundary conditions assumed.

EQUATIONS FOR THE ELEVATION \$\footnote{\sigma}\$ AND ITS FREE OSCILLATIONS

3.1 The free oscillations on a rotating system.

A reasonable picture of the laws of propagation of storm surges in a rotating system can be obtained by the consideration of the laws governing their motion when forcing and frictional forces have been neglected. In particular such free motions would approximate well to cases where the

atmospheric conditions that excited the surge have disappeared, or alternatively where the surge created by external forces propagates into a region in which the conditions are uniform.

The equations of motion without forcing and frictional terms are relatively simple, and can be solved in particular cases. For a non-rotating system the surges would follow the laws of the classical long wave theory, that is all wavelengths travelling with the same velocity and without change of shape, assuming of course that first order theory is applied and $\gamma = 0$. However it will be shown in a following section that for a rotating system only special types of waves travel in this manner, and that in general the surges are dispersive.

Taylor (1920) used free oscillations to investigate the propagation of long waves in a uniform rectangular gulf. He discovered that when the dimensions of the gulf were chosen to approximate the shape to that of the North Sea, the mathematical model predicted a motion that agreed very well with observations taken from the prototype. Lamb (1932) gives the free oscillations for a rotating circular basin, and it will be shown that such a basin of roughly the same size as the North Sea gives the right order of magnitude for the periodic oscillations in the North Sea.

In the following sections the equations of motion for the elevation ζ are derived in both cartesian and cylindrical co-ordinates, and the free oscillations are discussed. Two cases are considered, the first an unlimited

rotating sea, and the second a circular rotating sea. The discussion of the free oscillations prepares the way to tackle the more difficult problems involving the generation and decay of the storm surge. The modification to the solutions for free oscillations, needed when frictional effects are not entirely neglected, is briefly discussed.

3.2 The general two-dimensional equations.

Because of the advantages mentioned previously the averaged form of the equations of motion is the most widely used in the theory of storm surges. From these equations a general two-dimensional equation for the elevation ζ can be derived. The pressure given by the hydrostatic equation is:-

$$p = Pa - \rho g (z - \zeta)$$
 (3.1)

and on averaging this equation throughout the depth h then

$$\frac{1}{\rho h} \int_{-h}^{\zeta} \frac{\partial p}{\partial x} \cdot dz = \frac{1}{\rho h} \int_{-h}^{\zeta} \left(\rho g \frac{\partial \zeta}{\partial x} + \frac{\partial Pa}{\partial x} \right) dz$$

or
$$\frac{1}{\rho h} \int_{-\delta}^{\zeta} \frac{\partial p}{\partial x} \cdot dz = g \frac{\partial \zeta}{\partial x} + \frac{1}{\rho} \frac{\partial Pa}{\partial x}$$
 (3.2)

where consistent with previous assumptions ζ has been neglected compared to h.

The equations of motion now take the form

$$\frac{\partial U}{\partial t} - \gamma V = -g \cdot \frac{\partial \zeta}{\partial x} + X$$

$$\frac{\partial V}{\partial t} + \gamma U = -g \cdot \frac{\partial \zeta}{\partial y} + Y$$
(3.3)

where
$$X = \begin{bmatrix} -\frac{1}{\rho}, & \frac{\partial Pa}{\partial x} + \frac{1}{\rho h} & (\tau_{xs} - \tau_{xb}) \end{bmatrix}$$
 and $Y = \begin{bmatrix} -\frac{1}{\rho}, & \frac{\partial Pa}{\partial y} + \frac{1}{\rho h} & (\tau_{ys} - \tau_{yb}) \end{bmatrix}$

The equation of continuity remains

$$\frac{\partial U}{\partial x} + \frac{\partial V}{\partial y} = -\frac{1}{h} \frac{\partial \zeta}{\partial t}$$
 (3.4)

By differentiating equations (3.3) with respect to time and then eliminating V from the first equation and U from the second by substitution,

$$\frac{\partial^{2} U}{\partial t^{2}} - \gamma \left[-g \frac{\partial \zeta}{\partial y} + Y - \gamma \cdot U \right] = -g \frac{\partial^{2} \zeta}{\partial x \partial t} + \frac{\partial X}{\partial t}$$
and
$$\frac{\partial^{2} V}{\partial t^{2}} + \gamma \left[-g \frac{\partial \zeta}{\partial x} + X + \gamma V \right] = -g \frac{\partial^{2} \zeta}{\partial y \partial t} + \frac{\partial Y}{\partial t}$$
(3.5)

Now equations (3.5) can be differentiated with respect to x and y respectively and the velocities eliminated by using the continuity equation (3.4) giving

$$\frac{\partial^{2}}{\partial t^{2}} \left[-\frac{1}{h} \frac{\partial \zeta}{\partial t} \right] - \gamma \left[\frac{\partial Y}{\partial x} - \frac{\partial X}{\partial y} \right] + \gamma^{2} \left[-\frac{1}{h} \frac{\partial \zeta}{\partial t} \right]$$

$$= -g \left[\frac{\partial^{2}}{\partial x^{2}} + \frac{\partial^{2}}{\partial y^{2}} \right] \frac{\partial \zeta}{\partial t} + \frac{\partial}{\partial t} \left[\frac{\partial X}{\partial x} + \frac{\partial Y}{\partial y} \right]$$
(3.6)

On collecting terms and dividing by g, this reduces to:-

$$\left[\frac{\partial^{2}}{\partial x^{2}} + \frac{\partial^{2}}{\partial y^{2}} - \frac{1}{gh} \left(\frac{\partial^{2}}{\partial t^{2}} + \gamma^{2}\right)\right] \frac{\partial \zeta}{\partial t} = \frac{\gamma}{g} \left[\frac{\partial Y}{\partial x} - \frac{\partial X}{\partial y}\right] + \frac{1}{g} \frac{\partial}{\partial t} \left[\frac{\partial X}{\partial x} + \frac{\partial Y}{\partial y}\right]$$
(3.7)

The full equation for ζ is found by substituting back for X and Y in the right hand side of (3.7).

$$\left[\frac{\partial^{2}}{\partial x^{2}} + \frac{\partial^{2}}{\partial y^{2}} - \frac{1}{gh} \left(\frac{\partial^{2}}{\partial t^{2}} + \gamma^{2}\right)\right] \frac{\partial \zeta}{\partial t} = \frac{\gamma}{\rho gh} \left[\frac{\partial}{\partial x} \left(\tau_{ys} - \tau_{yb}\right) - \frac{\partial}{\partial y} \left(\tau_{xs} - \tau_{xb}\right)\right] + \frac{1}{\rho g} \cdot \frac{\partial}{\partial t} \left[-\left(\frac{\partial^{2}}{\partial x^{2}} + \frac{\partial^{2}}{\partial y^{2}}\right)\right] + \frac{1}{h} \frac{\partial}{\partial x} \left(\tau_{ys} - \tau_{yb}\right) + \frac{1}{h} \frac{\partial}{\partial y} \left(\tau_{ys} - \tau_{yb}\right)\right] \tag{3.8}$$

If viscosity is neglected, so that the generating force consists of a pressure gradient only, the equation (3.8) can be integrated immediately and simplified to the following equation.

$$\left[\frac{\partial^{2}}{\partial x^{2}} + \frac{\partial^{2}}{\partial y^{2}} - \frac{1}{gh} \left(\frac{\partial^{2}}{\partial t^{2}} + \gamma^{2}\right)\right] \zeta = -\frac{1}{\rho g} \left(\frac{\partial^{2}}{\partial x^{2}} + \frac{\partial^{2}}{\partial y^{2}}\right) Pa$$
(3.9)

The integration constant being zero if at some time ζ and $\frac{\partial^2 \zeta}{\partial z^2}$ are zero and the pressure Pa is uniform.

3.3 Free oscillations on an unlimited rotating sea.

To study the natural propagation of surges, frictional effects are neglected and generating forces are taken to be zero giving uniform atmospheric conditions above the sea surface. The motion is supposed to take place on an unlimited sea so that complicated boundary conditions are avoided. The solutions will be approximately true for regions of finite seas that are far removed from any

boundaries. With these assumptions the simplified equations become, from (2.18) and (2.19)

$$\frac{\partial U}{\partial t} - \gamma V = -g \frac{\partial \zeta}{\partial x}$$

$$\frac{\partial V}{\partial t} + \gamma U = -g \frac{\partial \zeta}{\partial y}$$
(3.10)

The continuity equation

$$\frac{\partial U}{\partial x} + \frac{\partial V}{\partial y} + \frac{1}{h} \cdot \frac{\partial \zeta}{\partial t} = 0$$

From these equations, or directly from equation (3.9) the two dimensional equation for ζ is found to be

$$\left[\frac{\partial^2}{\partial x^2} + \frac{\partial^2}{\partial y^2} - \frac{1}{gh} \left(\frac{\partial^2}{\partial t^2} + \gamma^2\right)\right] \zeta = 0$$
 (3.11)

This equation reduces to the well known wave equation when $\gamma=0$. The wave equation describes the propagation of waves of different wavelengths all travelling with a velocity of \sqrt{gh} . However in the above equation (3.11) for $\gamma \neq 0$ this statement is in fact only true for special cases. In general the most that can be said is that the product of the group and phase velocities is gh, as is also for the non-rotational case $\gamma=0$. To demonstrate this a one-dimensional motion is assumed so that $\zeta=\zeta(x,t)$ and a wave of frequency σ is considered, where σ is defined as $2\pi \times (\text{Period})^{-1}$. Taking a time factor of $e^{i\sigma t}$ in ζ , such that $\zeta=e^{i\sigma t}$. f(x) and substituting this value for ζ in equation (3.11), then f(x) is given by

$$\frac{\partial^2 f}{\partial x^2} = -\left(\frac{\sigma^2 - \gamma^2}{gh}\right). f \tag{3.12}$$

From this equation it follows that the wave number k, defined as $2\pi \times (Wavelength)^{-1}$, is given by

$$k^2 = (\frac{\sigma^2 - \gamma^2}{gh}) \tag{3.13}$$

from which it can be seen that the phase velocity c is given by

$$c^2 = \frac{\sigma^2}{k^2} = gh + \frac{\gamma^2}{k^2}$$
 (3.14)

and the group velocity C is given by

$$C = \frac{d\sigma}{dk} = c + k \cdot \frac{dc}{dk} = \frac{ghk}{\left(\gamma^2 + ghk^2\right)^{\frac{1}{2}}}$$
(3.15)

Equations (3.14) and (3.15) prove the statement that the product Cc = gh. For positive values of k^2 the minimum possible wave velocity is \sqrt{gh} , and therefore the maximum possible group velocity must \sqrt{gh} . If $\gamma^2 > \sigma^2$ then k^2 is negative and the waves have no real wavelength and do not exist under the assumptions made.

A wave for which k=0 has both an infinite velocity and an infinite wavelength, so that the elevation can be taken as uniform over the whole sea at any given time. Hence ζ is a function of time only and the equations (3.10) give the velocities as

$$\frac{\partial^2 U}{\partial t^2} = -\gamma^2 U, \quad \frac{\partial^2 V}{\partial t^2} = -\gamma^2 V \tag{3.16}$$

Taking $U = C_0 \cdot \cos \gamma t \ V = C_0 \sin \gamma t$, these two velocities represent a current of constant speed C_0 whose

direction rotates in a direction opposing the rotation of the sea, see section 2.1, with a constant angular velocity γ , i.e.

$$\tan \Theta = \frac{V}{U} = \tan (-\gamma t)$$

$$\Theta = -\gamma t$$

$$\Theta = -\gamma$$

This type of current is called an inertia current and the period of rotation $2\pi/\gamma$ is called the inertia period, being half that of the period of rotation of the sea.

Apart from this instance it is evident that one-dimensional waves, that is waves with parallel horizontal crests, cannot propagate without change of shape in a rotating system. It can be shown however that the rotational forces can be balanced by allowing a slope of the wave crests in the transverse direction. The pressure gradient along the wave crests produced by such a slope can in certain cases balance the rotational forces. From a direct consideration of equation (3.11) it is seen that the rotational term can be balanced out if ζ is taken to be of the form

$$\zeta = A \exp \frac{1}{2} \cdot y \cdot f(x,t)$$
 A being a constant. (3.18)

The sign of the exponential index depending on the direction of motion of the wave. This wave has a complete solution of the form

$$\zeta = \exp \left(\frac{+}{\sqrt{gh}} \cdot y\right) \cdot F\left(x + \sqrt{gh} \cdot t\right)$$

$$U = -\sqrt{\frac{g}{h}} \exp \left(\frac{+}{\sqrt{gh}} \cdot y\right) \cdot F\left(x + \sqrt{gh} \cdot t\right); \quad V = 0$$
(3.19)

Such a wave is non-dispersive, all wavelengths propagating with a group and phase velocity of \sqrt{gh} . The transverse velocity is zero, and in this form a wave can travel along a coastline that is parallel to the direction of motion. However the exponential factor restricts the region over which the solution can be applied. This special wave is named a 'Kelvin Wave' after Lord Kelvin, who introduced geostrophic effects into the tidal dynamics of small seas, Thompson (1879).

Another form of wave that is non-dispersive when propagated on a rotating sea was noted by Poincaré (1910) and is called a 'Poincaré wave'. This wave is not subject to the restrictions imposed by the exponential term on the Kelvin wave since the variation of the elevation along the wave crests is assumed of the form

$$\zeta = e^{\frac{+}{iqy}} \cdot f(x,t)$$

It can be verified that this form of ζ satisfies equation (3.11) if $f(x,t) = Ae^{i(kx + \sigma t)}$, or taking the real part of f(x,t) then

$$\zeta = A \cos qy.\cos (kx + \sigma t)$$

and the corresponding velocities

$$U = -\frac{Ag}{\sigma^2 \gamma^2} \left[\gamma q. \sin(qy) + k\sigma. \cos(qy) \right] \cos(kx + \sigma t)$$
(3.20)

$$V = \frac{Ag}{\sigma^2 + \gamma^2} \left[\gamma k. \cos(qy) + \sigma q. \sin(qy) \right] \sin(kx + \sigma t)$$

Furthermore the quantities q, k, σ and γ are related by the equation

$$\frac{\sigma^2 - \gamma^2}{k^2 + q^2} = gh \tag{3.21}$$

From the equations (3.20) it can be seen that the velocity transverse to the motion, in this case in the y direction, is zero along lines given by

$$\tan(qy) = \frac{+ \gamma k}{\sigma q}$$
 (3.22)

Such waves may therefore propagate along coastlines coinciding with these directions.

3.4 A modification to allow for bottom stress.

If the equations of motions are modified to include the simple form of bottom stress mentioned in section 2.2, equation (2.24), then solutions can be obtained that represent "damped" Kelvin and Poincaré waves. This was done in 1954 by Proudman, and the equations, again assuming uniform and constant atmospheric conditions, are from equation (2.10)

$$\frac{\partial U}{\partial t} + 2k_{0}U - \gamma V = -g\frac{\partial \zeta}{\partial x}$$

$$\frac{\partial V}{\partial t} + 2k_{0}V + \gamma U = -g\frac{\partial \zeta}{\partial y}$$
(3.23)

and the continuity equation is unaltered being

$$\frac{\partial U}{\partial x} + \frac{\partial V}{\partial y} = -\frac{1}{h} \frac{\partial \zeta}{\partial t} \tag{3.24}$$

k is a coefficient of friction presumed constant.

Proudman quotes a general solution satisfying these equations of the form

$$\zeta = H \cdot \exp \left\{ l_1 x + m_1 y - \left(n_1 + 2k_0 \right) t \right\}$$

$$U = \frac{g}{n_1^2 + \gamma^2} H \cdot \left(n_1 l_1 - \gamma m_1 \right) \cdot \exp \left\{ l_1 x + m_1 y - \left(n_1 + 2k_0 \right) t \right\}$$

$$V = \frac{g}{n_1^2 + \gamma^2} H \left(n_1 m_1 + \gamma l_1 \right) \cdot \exp \left\{ l_1 x + m_1 y - \left(n_1 + 2k_0 \right) t \right\}$$
(3.25)

where H,l_1,m_1,n_1 are constants such that

$$1_1^2 + m_1^2 = \left(1 + \frac{2k_0}{n_1}\right) \frac{n_1^2 + \gamma^2}{gh}$$
 (3.26)

On taking $l_1 = i\psi$, $m_1 = -\frac{\gamma}{n_1} \cdot i\psi$ he finds the solutions

$$\zeta = \frac{1}{2} \operatorname{H.exp} \left\{ \overline{+} \frac{\sigma \gamma \psi y}{k_o^2 + \sigma^2} - k_o t \right\} \cdot \left[\cos \left(\psi x + \frac{k_o \gamma \psi y}{k_o^2 + \sigma^2} \overline{+} \sigma t \right) \right]$$

$$\overline{+} \frac{k_o \sin \left(\psi x + \frac{k_o \gamma \psi y}{k_o^2 + \sigma^2} \overline{+} \sigma t \right) \right]$$
(3.27)

$$U = \pm \frac{\psi g}{2\sigma} \cdot H \cdot \exp \left\{ \pm \frac{\sigma \gamma \psi y}{k_o^2 + \sigma^2} - k_o t \right\} \cdot \left[\cos \left(\psi x + \frac{k_o \gamma \psi y}{k^2 + \sigma^2} + \sigma t \right) \right]$$

$$V = 0$$

where $\sigma^2 = \psi^2 gh - k_0^2$, and states that equation (3.27) represents two Kelvin waves, travelling in opposite directions, damped by friction. Perhaps a clearer way of expressing this solution can be deduced from extending the results from the frictionless case. In fact we might expect a solution of

the form

$$\zeta = A \exp\left(\frac{1}{2} \frac{\gamma c}{gh}\right) \exp\left(i\psi(x + ct)\right) D(x,y,t)$$
 (3.28)

from equation (3.19). A is a constant, and D(x,y,t) an extra exponential term arising from the bottom stress assumption. On taking $l_1 = i\psi$ m = $-\frac{\gamma}{n_1}$. $i\psi$ the condition, equation (3.26)

reduces to

$$n_1^2 + 2k_0 n_1 + \psi^2 gh = 0$$

or $n_1 = -k_0 + i\psi c$ (3.29)
where $c^2 = gh - \frac{k_0^2}{\psi^2}$

This gives the elevation from equation (3.25) written in the form of (3.28) as

$$\zeta = A \exp\left(\frac{+ \gamma c \cdot y}{gh}\right) \exp\left(i\psi\left(x + ct\right)\right) \left\{\exp\left(-k_0 t\right) \exp\left(\frac{i\gamma k_0 \cdot y}{\psi gh}\right)\right\}$$
(3.30)

The elevation (3.30) represents a Kelvin wave travelling with velocity c decaying under the effect of the bottom stress at a rate given by $\exp(-k_0t)$, and also having an additional periodic variation in the transverse direction given by $\exp(\frac{i\gamma k_0 Y}{\psi gh})$. The real part of (3.30) gives the solution included in (3.27) where

$$\psi c = \sigma$$
 and $A = \frac{1}{2} \left(1 + \frac{ik_0}{\sigma}\right) H$

Taking the assumption $m_1 = \frac{+}{Y_1} i \frac{N\pi}{Y_1}$, where N takes integral

values, in equation (3.25) and following a similar but slightly more complicated analysis, values for l_1 and n_1 can be found that provide "damped" Poincaré waves. Proudman found that these waves had the special property that the transverse velocity was zero along the lines $y=\pm\frac{y_1}{2}$. He deduced that infinite series of these "damped" Poincaré waves can be added to the two "damped" Kelvin waves so as to satisfy the condition U=0 at x=0. The resulting solution will give the propagation of surges in a gulf of uniform width and depth, having boundaries at $y=\pm\frac{y_1}{2}$ and x=0, in the absence of atmospheric generating forces.

3.5 The general equation for ζ in cylindrical co-ordinates

The general equation for the elevation given in cartesian co-ordinates by equation (3.8) can readily be transformed into cylindrical polars by the transformation $x = r.\cos\theta$, $y = r.\sin\theta$, Z = z. The left hand side of this equation transforms straightforwardly into

$$\left[\frac{\partial^{2}}{\partial r^{2}} + \frac{1}{r} \frac{\partial}{\partial r} + \frac{1}{r^{2}} \frac{\partial^{2}}{\partial \theta^{2}} - \frac{1}{gh} \left(\frac{\partial^{2}}{\partial t^{2}} + \gamma^{2}\right)\right] \frac{\partial}{\partial t} \zeta(r, \theta, t) \quad (3.31)$$

The general transformation for the stress on the right hand side of the equation does not appear in any of the papers referred to, and since it is intended to use this transformation in a later section it is derived here. For convenience take stresses in the radial and cross-radial directions, and denote these in a similar notation to that used in referring to the cartesian stresses. i.e. $\tau_{rs} = 0$

radial stress in the surface, etc...

Therefore $\tau_x = \tau_r \cos \theta - \tau_\theta \sin \theta$; $\tau_y = \tau_r \sin \theta + \tau_\theta \cos \theta$. Using this notation and also substituting for x and y in terms of r and θ , the right hand side of equation becomes

$$\frac{\gamma}{\rho g h} \left[\frac{\partial}{\partial r} \left(\tau_{\theta s} - \tau_{\theta b} \right) + \frac{1}{r} \left(\tau_{\theta s} - \tau_{\theta b} \right) - \frac{1}{r} \frac{\partial}{\partial \theta} \left(\tau_{r s} - \tau_{r b} \right) \right] + \frac{1}{\rho g} \frac{\partial}{\partial t} \left[-\left(\frac{\partial^{2}}{\partial r^{2}} + \frac{1}{r} \frac{\partial}{\partial r} + \frac{1}{r^{2}} \frac{\partial}{\partial \theta^{2}} \right)^{Pa} + \frac{1}{h} \left(\frac{\partial}{\partial r} \left(\tau_{r s} - \tau_{r b} \right) + \frac{1}{r} \frac{\partial}{\partial \theta} \left(\tau_{\theta s} - \tau_{\theta b} \right) \right]$$

$$\frac{1}{r} \left(\tau_{r s} - \tau_{r b} \right) + \frac{1}{r} \frac{\partial}{\partial \theta} \left(\tau_{\theta s} - \tau_{\theta b} \right)$$

$$(3.32)$$

The general equation for the elevation given by (3.31) and (3.32) simplifies very much if axial symmetry is assumed, reducing to the equation.

$$\left[\frac{\partial^{2}}{\partial r^{2}} + \frac{1}{r} \frac{\partial}{\partial r} - \frac{1}{gh} \left(\frac{\partial^{2}}{\partial t^{2}} + \gamma^{2}\right)\right] \frac{\partial \zeta}{\partial t} = \frac{\gamma}{\rho gh} \left(\frac{\partial}{\partial r} + \frac{1}{r}\right) \left(\tau_{\theta s} - \tau_{\theta b}\right) \\
+ \frac{1}{\rho g} \frac{\partial}{\partial t} \left[-\left(\frac{\partial^{2}}{\partial r^{2}} + \frac{1}{r} \frac{\partial}{\partial r}\right)^{pa} + \frac{1}{h} \left(\frac{\partial}{\partial r} + \frac{1}{r}\right) \left(\tau_{rs} - \tau_{rb}\right)\right] \tag{3.33}$$

It can be seen that under certain conditions for the forcing functions, such as $\tau_{\theta s} = \tau_{\theta b} = 0$, the equation can be simplified still further, and these simplifications will be dealt with in a later section.

3.6 Free oscillations on a circular rotating sea

For the free oscillations on a circular rotating sea of uniform depth the equations of motion become, on neglecting the generating and frictional forces

$$\frac{\partial \mathbf{v}_{r}}{\partial t} - \frac{\gamma \mathbf{v}_{\theta}}{\partial r} + \mathbf{g} \frac{\partial \zeta}{\partial r} = 0$$

$$\frac{\partial \mathbf{v}_{\theta}}{\partial t} + \frac{\gamma \mathbf{v}_{r}}{r} + \mathbf{g} \cdot \frac{1}{r} \frac{\partial \zeta}{\partial \theta} = 0$$
(3.34)

 $v_{\text{r'}}$ v_{θ} being the radial and cross-radial components of the velocity respectively. The equation of continuity is

$$\frac{\partial \mathbf{v}_{\mathbf{r}}}{\partial \mathbf{r}} + \frac{\mathbf{v}_{\mathbf{r}}}{\mathbf{r}} + \frac{1}{\mathbf{r}} \frac{\partial \mathbf{v}_{\theta}}{\partial \theta} + \frac{1}{\mathbf{h}} \frac{\partial \zeta}{\partial \mathbf{t}} = 0 \tag{3.35}$$

and the corresponding equation for the elevation ζ is, from (3.31)

$$\left[\frac{\partial^2}{\partial r^2} + \frac{1}{r}\frac{\partial}{\partial r} + \frac{1}{r^2}\frac{\partial^2}{\partial \theta^2} - \frac{1}{gh}\left(\frac{\partial^2}{\partial t^2} + \gamma^2\right)\right]\zeta = 0$$
 (3.36)

Following Lamb (1932), ζ is assumed to be of the form

$$\zeta = f(r).\cos(m\theta + \sigma t)$$

and then f(r) is given by the Bessel equation

$$\frac{\partial^2 f}{\partial r^2} + \frac{1}{r} \frac{\partial f}{\partial r} + \left(K^2 - \frac{m^2}{r^2}\right) f = 0$$
 (3.37)

where $K^2 = (\sigma^2 - \gamma^2)/gh$

Taking the simple case of an open circular sea with vertical coasts and radius r_0 , a solution is required for f(r) that is finite at r=0. The general solution for f is, with m a real integer

$$f = A.J_m(Kr) + B.Y_m(Kr)$$

where A and B are constants and $J_{m}(Kr)$, $Y_{m}(Kr)$, are Bessel

functions of the first and second kind respectively. Retaining only the part of the solution remaining finite at r=0 gives

$$f = A.J_m(Kr)$$

 Y_{m} (Kr) becomes infinite at the origin so that B is taken to be zero. The required solution of (3.36) for ζ is therefore

$$\zeta = A.J_{m}(Kr).\cos(m\theta + \sigma t)$$
 (3.38)

In the general case the velocities are given by

$$v_{r} = V_{r}^{"}.\sin(m\theta + \sigma t); \quad v_{\theta} = V_{\theta}^{"}\cos(m\theta + \sigma t)$$

$$\text{where } V_{r}^{"} = \frac{-g}{\sigma^{2} - \gamma^{2}} \left\{ \sigma \frac{\partial f}{\partial r} + \frac{\gamma m}{r} \cdot f \right\}$$

$$\text{and } V_{\theta}^{"} = \frac{-g}{\sigma^{2} - \gamma^{2}} \left\{ \gamma \frac{\partial f}{\partial r} + \frac{\sigma m}{r} \cdot f \right\}$$

satisfying equations (3.34) and (3.35), and the solution (3.38) remaining finite over the region. The required boundary condition of $v_r = 0$ for $r = r_0$, i.e no radial velocity at $r = r_0$, gives,

$$\gamma m.J_m(Kr_0) + \sigma Kr_0 \frac{\partial}{\partial r} [J_m(Kr)]$$
 (3.40)

The values of the frequency σ of these oscillations may be obtained from a graphical construction in the following way. Again from Lamb write $K^2r_0^2 = x$, then from equation (3.37)

$$\frac{\sigma^2}{\gamma^2} = gh \frac{K^2}{\gamma^2} + 1$$

or
$$\frac{\sigma}{\gamma} = \frac{1}{\gamma} \left(1 + \frac{x}{\beta_0}\right)^{\frac{1}{2}}$$
 (3.41)

where
$$\beta_0 = \frac{\gamma^2 r_0^2}{gh}$$
 (3.41)

take
$$\phi(x) = m.J_m(\sqrt{x})$$
 where J_m denotes $\frac{\partial(J_m)}{\partial r}$

and then equation (3.40) can be re-written as

$$\phi(x) + (1 + \frac{x}{\beta_0})^{\frac{1}{2}} = 0 \tag{3.42}$$

The intersections of the curve - $\phi(x)$ with the parabole $y^2 = 1 + \frac{x}{\beta_0}$ will give by their ordinates the values of σ that are admissable for the solution (3.38). This solution represents a wave rotating relatively to, the water with an angular velocity $\frac{\sigma}{r}$, the rotation of the wave being in the same or opposite direction as that of the water according as σ is negative or positive. Obviously circular seas of uniform depth are exceptional if they exist at all, but the above solutions may be used as first approximations to certain cases of non-circular seas. For example the North Sea can be approximated to a circular basin of radius 200 kilometres and depth 50 metres. The period of rotation at latitude φ is $\Omega sin \varphi$, giving for the North Sea $2\Omega sin \varphi$ = γ \simeq 10^{-4} , and $\beta_0 \simeq 4/5$. The solutions of (3.42) for this particular case are shown in figure 2, for m = 1 which seems the most realistic value for the case of the North Sea. solutions of interest, from figure 2, give for the frequency of

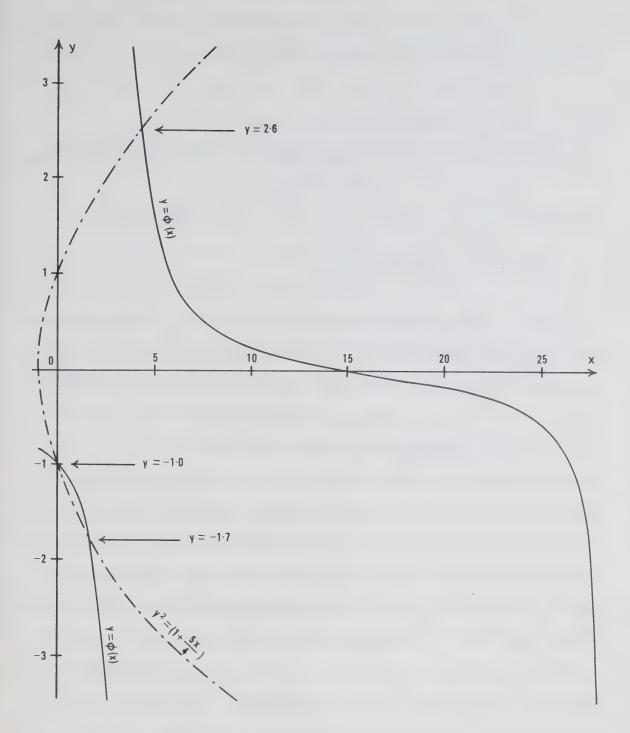


Figure 2

Solutions of the equation (3.42) giving the admissable parameters for the period of free oscillations of a particular rotating circular sea of constant depth.

$$\sigma_1 = 2.56\gamma, \ \sigma_2 = -\gamma, \ \sigma_3 = -1.7\gamma$$
 (3.43)

and the corresponding periods are as $T = 2\pi/\sigma$

$$T_1 \simeq 7 \text{ hrs.}$$
 $T_2 \simeq 17\frac{1}{2} \text{ hrs.}$ and $T_3 \simeq 12\frac{1}{2} \text{ hrs.}$ (3.44)

It is interesting to note that, for any integral value of m,

Lt.
$$\{\phi(x)\} = Lt.$$
 $x \to 0$

$$\frac{m.J_m(\sqrt{x})}{\sqrt{x}J_m'(\sqrt{x})} = 1$$

so that y = 1 is always a solution of (3.42). Therefore for any circular sea there is a natural oscillation rotating in the same direction as the water having a period $2\pi/\gamma$ which is half that of the rotation of the water.

Of the solutions above the periods T_2 and T_3 refer to oscillations rotating with the water, and the period T_1 refers to an oscillation rotating opposing the rotation of the water. In the North Sea the observed surge takes about 24 hours to travel around the North Sea (c.f. Charnock and Crease 1957 , Figure 2) and always travels with the rotation of the sea, that is in an anti-clockwise direction, travelling from the north of Scotland down the east coast of England and then up the west coast of the continent. Theoretically it appears to be possible for a surge to propagate in the opposite direction but such a surge has not been observed in the North Sea. The fact that the North Sea is a gulf and has not a continual boundary may be a possible explanation, however no papers referring to oscillations in enclosed seas

have been found to confirm such an opposite rotation. Taking into account the approximations made, the periods T_2 and T_3 would appear to be of the right order of magnitude.

THE GENERATION AND PROPAGATION OF SURGES ON AN INFINITE ROTATING SEA

4.1 The problem.

In a preceeding section the equations of motion were solved for surges propagated on an unlimited sea with generating and frictional forces neglected. The solutions obtained were reasonably simple, but with the introduction of even a simple generating function the solutions become much more difficult to obtain.

Crease (1955) discusses the problem of generating surges from rest on an infinite rotating sea. Friction is still neglected in the equations of motion except in so far as offering a method of surge generation by the action of the wind on the surface. In the integrated equations this means that the bottom stress disappears. Conditions are taken constant in the direction transverse to the direction of propagation of the surge. The main purpose of his paper is to show that the rotational effects lead to a dispersion of the waves, and to study this effect on the wave elevation and velocity. A generating force is assumed to act over a semi-infinite plane and is shown to produce a steady elevation at large times on a rotating sea. A similar force taken on

a non-rotating sea would lead to an ever-increasing surface elevation.

4.2 The general solution for ζ.

Taking the integrated form of the equation of motion given by equation (2.18), and using the approximations given in section 4.1, the equations reduce to

$$\frac{\partial U}{\partial t} - \gamma V = -g \frac{\partial \zeta}{\partial x} - \frac{1}{\rho} \frac{\partial P}{\partial x} + \frac{1}{\rho h} \tau_{xs}$$

$$\frac{\partial V}{\partial t} + \gamma U = 0$$
(4.1)

and the continuity equation from equation (2.19) is

$$\frac{\partial U}{\partial x} = -\frac{1.\partial \zeta}{h} \frac{\partial \zeta}{\partial t} \tag{4.2}$$

By eliminating the velocities from these equations, taking $E(x,t) = \frac{1}{\rho g} \left(\frac{\partial P}{\partial x} - \frac{\tau_{xs}}{h} \right), \text{ and proceeding as in section 3.2,}$ then the equation for ζ is,

$$\left[\frac{\partial^2}{\partial x^2} - \frac{1}{gh} \left(\frac{\partial^2}{\partial t^2} + \gamma^2\right)\right] \frac{\partial \zeta}{\partial t} = -\frac{\partial^2 E}{\partial x \partial t}$$
 (4.3)

Equation (4.3) can be integrated immediately, with respect to time, giving

$$\left[\frac{\partial^2}{\partial x^2} - \frac{1}{gh} \left(\frac{\partial^2}{\partial t^2} + \gamma^2\right)\right] \zeta = -\frac{\partial E}{\partial x}$$
 (4.4)

The integration constant being zero if at some time ζ , $\frac{\partial^2 \zeta}{\partial t^2}$ and $\frac{\partial E}{\partial x}$ are all zero.

To solve this equation Crease uses a Green function, but because operational calculus is employed in later sections of this report, the solution which follows will be derived by that method in order to be consistent.

The initial conditions are taken to be uniform, that is

$$\zeta = \frac{\partial \zeta}{\partial t} = 0$$
, E = constant for t<0 (4.5)

Taking the Laplace transform of equation (4.4) with respect to time, and taking

$$\overline{\zeta}(\mathbf{x},\mathbf{s}) = \int_0^\infty \zeta(\mathbf{x},t) \exp(t\mathbf{s}) \, dt, \, \overline{E}(\mathbf{x},\mathbf{s}) = \int_0^\infty E(\mathbf{x},t) \exp(t\mathbf{s}) \, dt$$

then the equation for $\overline{\zeta}$ is, using the conditions (4.5)

$$\left[\frac{\partial^2}{\partial x^2} - \frac{1}{gh} \left(s^2 + \gamma^2\right)\right] \overline{\zeta} = -\frac{\partial \overline{E}}{\partial x}$$

For convenience take $\psi^2=(s^2+\gamma^2)/gh$ and use the operator $D^2=\frac{\partial^2}{\partial x^2}$.

Then
$$\left[D^2 - \psi^2\right] \overline{\zeta} = -\frac{\partial \overline{E}}{\partial x}$$
 (4.7)

The particular integral becomes

$$\overline{\zeta} = \frac{1}{2\psi} \left(\frac{1}{D+\psi} - \frac{1}{D-\psi} \right) \frac{\partial \overline{E}}{\partial x}$$

that is

$$\overline{\zeta} = \frac{1}{2\psi} \left\{ \exp(-\psi x) \int_{a_0}^{x} \exp(\psi x_0) \frac{\partial \overline{E}}{\partial x_0} (x_0, s) . dx_0 \right\}$$

$$- \exp(\psi x) \int_{b_0}^{x} \exp(-\psi x_0) \frac{\partial \overline{E}}{\partial x_0} (x_0, s) . dx_0$$
(4.8)

ao, bo are constants to be evaluated in conjunction with the constants A and B given by the complementary function

$$\overline{\zeta} = A \exp(\psi x) + B \exp(-\psi x)$$
 (4.9)

Hence the complete solution for $\bar{\zeta}$ is

$$\bar{\zeta} = A \exp(\psi x) + B \exp(-\psi x) + \frac{1}{2\psi} \{ \exp(-\psi x) \int_{a_0}^{x} \exp(\psi x_0) \frac{\partial \bar{E}}{\partial x_0} \cdot dx_0 - \exp(\psi x) \int_{b_0}^{x} \exp(-\psi x_0) \frac{\partial \bar{E}}{\partial x_0} \cdot dx_0 \}$$

$$(4.10)$$

To ensure the convergence of the two integrals in (4.10) the constants can be chosen such that $a_0 = -\infty$, $b_0 = \infty$ are the integration limits. Also the boundary condition $\zeta = 0$ at t = 0 becomes $\overline{\zeta} = 0$ for $s = \infty$, i.e. $\overline{\zeta} = 0$ for $\psi = \infty$. Hence as finite values of $\overline{\zeta}$ are required for both negative and positive values for x when |x| becomes large, A = B = 0.

From tables of Laplace transforms it is found that the inverse Laplace transforms of f(s), where

$$f(s) = \exp(\frac{-Q\sqrt{s^2+R^2}}{\sqrt{s^2+R^2}}) \text{ is } J_O(R\sqrt{t^2-Q^2}.H(t-Q) = F(t)$$

where H(t-Q) is a step function. This is the form of the inverse transform required with respect to s for $\exp(-\psi(x-x_0))$ /2 ψ in equation (4.10), where $\psi = \sqrt{\frac{s^2 + \gamma^2}{gh}}$. Therefore using the convolution rule on this equation

$$\zeta = \sqrt{\frac{gh}{2}} \int_{-\infty}^{x} dx_{0} \int_{0}^{t} J_{0} [\gamma \{ (t-t_{0})^{2} - (x-x_{0})^{2} \}^{\frac{1}{2}}] \cdot H[(t-t_{0}) - (x-x_{0})] \frac{\partial E}{\partial x_{0}} \cdot dt_{0}$$

$$-\sqrt{\frac{gh}{2}}\int_{-\infty}^{x}dx_{0}\int_{0}^{t}J_{0}\left[\gamma\left\{\left(t-t_{0}\right)^{2}-\left(\frac{x_{0}-x}{gh}\right)^{2}\right\}^{\frac{1}{2}}\right]\cdot H\left[\left(t-t_{0}\right)-\left(\frac{x_{0}-x}{\sqrt{gh}}\right]\cdot\frac{\partial E}{\partial x_{0}}\cdot dt_{0}$$

where $\frac{\partial E}{\partial x_0}$ denotes $\frac{\partial E}{\partial x}$ evaluated at (x_0, t_0) . Finally the two integrals can be combined by a simple adjustment to the limits

of integration and the step functions giving the final equation

$$\zeta = \sqrt{\frac{gh}{2}} \cdot \int_{0}^{t} dt_{0} \int_{-\infty}^{\infty} \frac{\partial E}{\partial x_{0}} \cdot J_{0} \left[\gamma \left\{ (t - t_{0})^{2} - (\frac{x - x_{0}}{gh})^{2} \right\}^{\frac{1}{2}} \right].$$

$$H \left[(t - t_{0})^{2} - |\frac{x - x_{0}}{\sqrt{gh}}| \right] dx_{0}$$

$$(4.12)$$

4.3 The general solution for the velocities.

By eliminating V and ζ from equations (4.1) and (4.2) the differential equation for U is found to be

$$\left[\frac{\partial^2}{\partial x^2} - \frac{1}{gh} \left(\frac{\partial^2}{\partial t^2} + \gamma^2\right)\right] U = \frac{1}{h} \frac{\partial E}{\partial t}$$
 (4.13)

From a comparison with equation (4.4) for ζ it is seen that the only difference is that the term $\frac{1}{h} \cdot \frac{\partial E}{\partial t}$ now appears on the right hand side of the equation in place of $-\frac{\partial E}{\partial x}$. The solution for U can therefore be written down immediately from equation (4.12), giving

$$U = -\frac{1}{2} \sqrt{\frac{g}{h}} \cdot \int_{0}^{t} dt_{0} \int_{-\infty}^{\infty} \frac{\partial E}{\partial t_{0}} \cdot J_{0} \left[\gamma \left\{ (t - t_{0})^{2} - (\frac{x - x_{0}}{gh})^{2} \right\}^{\frac{1}{2}} \right] \cdot H \left[(t - t_{0}) - |\frac{x - x_{0}}{\sqrt{gh}}| \right] dx_{0}$$

$$(4.14)$$

Similarly the equation for the transverse velocity is found by eliminating the other two variables from the equations of motion, giving

$$\left[\frac{\partial^2}{\partial x^2} - \frac{1}{gh} \left(\frac{\partial^2}{\partial t^2} + \gamma^2\right)\right] V = -\frac{\gamma}{h}.E$$
 (4.15)

and again by direct comparison with the solution for ζ , the solution for V can be written down immediately as

$$V = \frac{\gamma}{2} \cdot \sqrt{\frac{g}{h}} \int_{0}^{t} dt_{0} \int_{-\infty}^{\infty} E \cdot J_{0} \left[\gamma \left\{ (t - t_{0})^{2} - (\underline{x - x_{0}})^{2} \right\}^{\frac{1}{2}} \right].$$

$$\cdot H \left[(t - t_{0}) - |\underline{x - x_{0}}| \right] dx_{0}$$

$$(4.16)$$

A PARTICULAR CASE

5.1 The Solutions.

To investigate these solutions Crease assumes a simple generating function given by

$$E(x,t) = -A.H(-x).H(t)$$
 (5.1)

which more clearly explained in terms of wind stress alone, represents a wind which starts to blow uniformly at time t=0 over the semi-infinite range $-\infty< x<0$ in the direction of x increasing. The derivatives of E needed for substitution, are given by:-

$$\frac{\partial E}{\partial x} = A.H(t).\delta(-x)$$
and
$$\frac{\partial E}{\partial t} = -A.H(-x).\delta(t)$$
 respectively

Substituting from equation (5.2), for $\frac{\partial E}{\partial x}$ into the solution for the elevation equation (4.12) and integrating with respect to x using the properties of the delta function

$$\zeta = \frac{A}{2} \sqrt{gh} \int_{0}^{t} H(t_{0}) .J_{0} \left[\gamma \left\{ (t-t_{0})^{2} - \frac{x^{2}}{gh} \right\}^{\frac{1}{2}} \right].$$

$$H \left[(t-t_{0}) - \frac{|x|}{\sqrt{gh}} \right] dt_{0}$$
(5.3)

This equation can be expressed in a non-dimensional form by putting $t-t_0=\tau$, and then using the parameters

$$\gamma \tau = \beta; \ \gamma t = b; \ \underline{\gamma x} = a$$
 (5.4)

The equation (5.3) for ζ then becomes the non-dimensional equation

$$\frac{2\gamma}{A\sqrt{gh}} \cdot \zeta = \int_{|a|}^{b} J_{o}\left[(\beta^{2} - a^{2})^{\frac{1}{2}} \right] d\beta$$
 (5.5)

This equation holds for all values of the parameter a, and shows that the distribution of ζ is symmetrical about a=o. The step functions have been incorporated into the limits of integration. Another way of expressing the upper limit would be to replace b by $\max |a|$, which is equivalent to the maximum distance a disturbance could travel in time t. The maximum group velocity is \sqrt{gh} (c.f. section 3.3).

Using these parameters the corresponding solutions for the velocities U, V, from the equations (4.13) and (4.16) are found to be given by

$$\frac{2\gamma}{Ag} \cdot U = \int_{a}^{\infty} J_{o} \left[\left(b^{2} - \alpha^{2} \right)^{\frac{1}{2}} \right] H \left(b - |\alpha| \right) d\alpha$$
 (5.6)

and
$$\frac{2\gamma}{Ag} \cdot V = -\int_0^b d\beta \int_a^\infty J_o\left[(\beta^2 - \alpha^2)^{\frac{1}{2}}\right] H(\beta - |\alpha|) d\alpha$$
 (5.7)

respectively.

The values of U and V depend to some extent on the parameter a. For example from equation (5.6) with a>o

$$\frac{2\gamma}{Aq}$$
 · U = H(b-a) $\int_{a}^{b} J_{o} \left[(b^{2} - \alpha^{2})^{\frac{1}{2}} \right] d\alpha$

the integral can be split into two separate integrals giving

$$\frac{2\gamma \cdot U}{Ag} = H(b-a) \left[\int_0^b J_o \left[(b^2 - \alpha^2)^{\frac{1}{2}} \right] d\alpha - \int_0^a J_o \left[(b^2 - \alpha^2)^{\frac{1}{2}} \right] d\alpha \right]$$

and hence

$$\frac{2\gamma}{Ag} U = H(b-a) \left[\sin b - \int_0^a J_0 \left[(b^2 - \alpha^2)^{\frac{1}{2}} \right] d\alpha \right]$$
 (5.8)

The full solutions for U and V in addition to equation (5.8), covering all the different cases for a are given below

For a>o,
$$\frac{2\gamma}{Ag}$$
. $V = -\left[1-\cos b - \int_0^a d\alpha \int_\alpha^b J_o\left[(\beta^2 - \alpha^2)^{\frac{1}{2}}\right] d\beta\right] H(b-a)$ (5.9)

For a<o,

i)
$$b>|a|$$
, $\frac{2\gamma}{Ag}$. $U=2\sin b-H(b-|a|)\int_{-b}^{a}J_{O}\left[(b^{2}-\alpha^{2})^{\frac{1}{2}}\right]d\alpha$ and $\frac{2\gamma}{Ag}$. $V=-\left[1-\cos b+\int_{O}^{|\alpha|}d\alpha\int_{\alpha}^{b}J_{O}\left[(\beta^{2}-\alpha^{2})^{\frac{1}{2}}\right]d\beta$ (5.10)

ii)
$$b < |a|$$
,
$$\frac{2\gamma \cdot U}{Ag} = 2\sin b$$

(5.11)

and $\frac{2\gamma}{Ag}$. $V = -2(1-\cos b)$

5.2 Interpretation of the results for the Particular Case.

The interpretation of the results depends on the relative magnitudes of the dimensionless parameters a and b as defined by equation (5.4). It follows from this definition that the time taken for a surge to travel a distance x with the maximum group velocity, is given in terms of these parameters by b = a. This is the minimum time that the surge can take to travel a distance x, so that it is possible to divide the effects of the surge into the two groups given by $b \le a$ and b > a respectively.

In this particular case at time t=0, a force is suddenly applied over one half of an infinite sea in a uniform direction parallel to the x axis over the area $-\infty < x < 0$. The immediate response to this force is the creation of some motion in the same direction as the force, and at this instant restricted to the region over which the force is applied. Simultaneously as a consequence to this motion a transverse velocity is set up balancing the resulting rotational forces. This can be seen by substituting for U and V from equation (5.11) into the equations of motion (4.1)

The generating force has a discontinuity at x=0 and as stated above the effect of this discontinuity cannot be propagated with a velocity greater than \sqrt{gh} . Before such time has elapsed for this effect to reach a particular

point, that is for b<|a|, there will be no motion at that point if it lies outside the generating area, a>0, and inertia - type motion, i.e. currents but no elevation [c.f Section 3.3], if it lies within the generating area a<0. This is shown by the equations (5.8), (5.9) and (5.11) and demonstrated by substituting these values for the velocities into the equations of motion (4.1), from which it is seen that the forces balance and $\frac{\partial \zeta}{\partial x} = 0$. Therefore there is no change in water level at a particular point until enough time has elapsed to enable the effect of the discontinuity, at x = 0, to reach that point. When this time is achieved b>|a|, and the water acquires a motion that by the continuity equation leads to an elevation of the surface, equations (5.8), (5.9) and (5.10).

The dispersive quality of surges propagating in a rotating system enable a steady state elevation to be reached as $t \to \infty$. In a non-rotating system the application of a similar applied force would lead to an infinite surface elevation, all wavelengths travelling with velocity \sqrt{gh} . In the rotating system however the pressure gradient resulting from this steady slope is balanced as $t \to \infty$, by the transverse velocity which also balances the applied force within the generating area.

The limiting values of \(\zeta\tau\text{U,V}\) when the time becomes very great are given by Crease to be:-

$$\frac{2\gamma}{A\sqrt{gh}} \cdot \zeta + \exp(-|a|)$$

$$\frac{2\gamma}{Ag} \cdot U + \sin b$$

$$\frac{2\gamma}{Ag} \cdot V + \cos b - \exp(-|a|) \qquad \text{for a>0}$$

$$+ \cos b + \exp(-|a|) - 2 \quad \text{for a<0}$$

Again by substituting these values into the equation of motion (4.1), it is seen that the applied forces are exactly balanced for a<0 by the term -2 in the transverse velocity, and the pressure gradient arising from the steady slope is balanced by the term $\exp(-|a|).a/|a|$. The sin b and cos b terms represent inertia type oscillations of the same period, $\frac{2\pi}{\gamma}$, and form as those discussed earlier in Section 3.2.

For the general period of the oscillations, it follows from equation (5.5) that the maxima and minima of ζ occur when

$$J_{o}\left[(b^{2}-a^{2})^{\frac{1}{2}}\right] = 0 {(5.13)}$$

Defining the local period of the surge at a point, given by the parameter a, as the time between two successive maxima n and n+1, $T_n(a)$, it can be shown that $T_n(a)$ is given by,

$$\frac{T_n(a)}{T_I} \approx 1 - \frac{a^2}{2j_{0,n} \cdot j_{0,n+1}} a << j_{0,n}$$

$$\frac{T_n(a)}{T_T} \simeq \frac{j_{0,n+1} + j_{0,n}}{2a}$$
 a>>j_{0,n} (5.14)

where $T_{\rm I}$ is the inertia period $2\pi/\gamma$, and $j_{\rm O,n}$ denotes the odd-order zero of $J_{\rm O}(x)$. Equation (5.14) shows that for points near to the generating area the local period is initially slightly less than the inertia period, but approaches it rapidly, whilst for large distances from the generating area the local period is much less than the inertia period and increases linearly for the first few oscillations.

Crease (1955) has plotted the values for ζ , U, V as functions of the parameters and the graphs appear in figures 1, 3 and 4, of his paper.

MODIFICATIONS TO THE APPLIED FORCE

6.1 A gradually applied force.

In the preceeding sections solutions have been found for the elevation and velocities resulting from the instantaneous application of a given force on an infinite rotating sea. In nature it would be expected that a generating force would build up from zero to its maximum value over a finite period of time. The effect of allowing for such finite growth period in the generating force can easily be found by taking the same system as in the previous section, and modifying the applied force given by equation (5.1) by the inclusion of a $tanh(\epsilon t)$ term, where ϵ is an

arbitrary constant. The results obtained can then be compared directly with those already obtained by Crease for an instantaneously applied force. The new generating function is given by

$$E_1 = A.H(-x).H(t).tanh(\varepsilon t)$$
 (6.1)

Proceeding in the same way as in section 5.1 the solution for the elevation using the new generating function is found to be

$$\frac{2\zeta}{A\sqrt{gh}} = \int_{0}^{t} \tanh(\varepsilon t_{0}) \cdot H(t_{0}) \cdot J_{0} \left[\gamma \right] (t-t_{0})^{2} - \frac{x^{2}}{gh} \right]^{\frac{1}{2}}.$$

$$H\left[(t-t_{0}) - \frac{|x|}{\sqrt{gh}} \right] dt_{0} \qquad (6.2)$$

putting

$$\frac{2.\zeta}{A\sqrt{gh}} = \int_{0}^{t} \tanh \epsilon (t-\tau) . J_{0} \left[\gamma \left\{ \tau^{2} - \frac{x^{2}}{gh} \right\}^{\frac{1}{2}} \right] . H \left[\tau - \frac{|x|}{\sqrt{gh}} \right] H(t-\tau) . d\tau$$

Using the non-dimensional parameters equation (5.4) and simplifying

$$\frac{2\gamma\zeta}{A\sqrt{gh}} = \int_{|a|}^{b} \tanh \varepsilon_{o}(b-\beta) .J_{o}\left[\left\{\beta^{2}-a^{2}\right\}^{\frac{1}{2}}\right] .d\beta$$
 (6.3)

where $\varepsilon_0 = \varepsilon/\gamma$

This equation (6.3) can be compared directly with the result given by equation (5.5) and it is seen that they differ only by the extra factor $\tanh\{\epsilon_0(b-\beta)\}$ in the integrand of the former. The length of the growth period for the generating

force is governed by the choice of the constant ϵ . Taking as a criterion that time during which the generating force achieves 90% of its maximum value, then for a growth period of 1 unit of time ε is required to be 1.5, [tanh $\theta \simeq .9$ when $\theta = 1.5$]. Similarly for double this growth period $\varepsilon =$ 0.75, and for half this period ϵ = 3 etc. Curves for the elevation ζ , at a = 0, have been computed and plotted, figure 3, for growth periods corresponding to 0.5 hours and 10 hours for latitudes such as that of the North Sea, $\gamma \simeq 10^{-4}$. These curves are compared with the corresponding curve for the elevation, at a = 0 computed from the solution using an instantaneous application of the force, given by equation (5.5). It can be seen from these curves, figure 3, that the maximum elevation attained decreases as the period of growth of the generating force increases. This would be expected both physically and from the form of the solutions. The instantaneous force therefore gives the maximum elevation of the sea surface, and if superimposed on known maximum tidal heights would give engineers the worst possible conditions that coastal defences would have to face. The required safety factors in the design of such defences could be adjusted accordingly. The fact that the quicker the generating forces develop the stronger the surge, has been borne out by observation, i.e. from Proudman and Doodson (1924). "Researches by one of the authors (Doodson) into the correlation between the unpredicted sea level at Liverpool and the neighbouring barometric distribution, led to a large

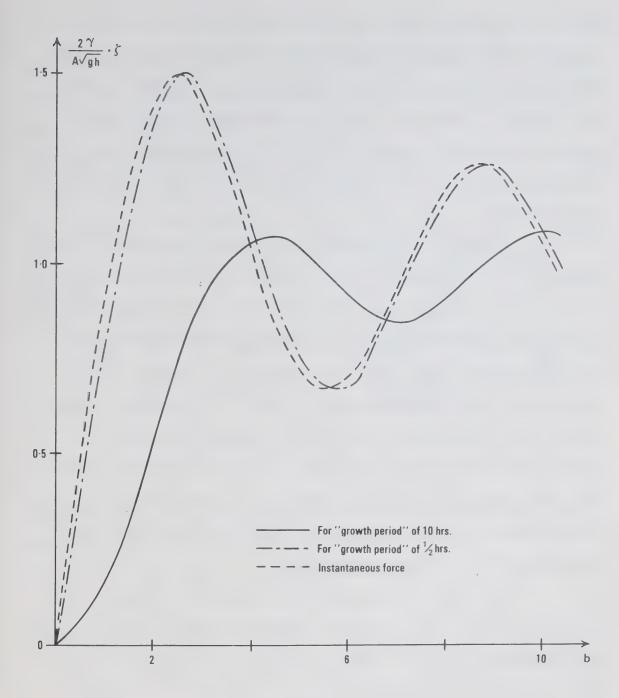


Figure 3

The elevation produced by generating forces on an infinite rotating sea with varying periods for the achievement of maximum force.

measure of success when the distribution did not change too rapidly. But a preliminary study of the effects of storms seemed to show that when the distribution changed suddenly, the effects on the sea level followed very rapidly and reached magnitudes greater than if the change had taken place slowly, oscillations of considerable amplitudes being often generated."

However an important point that should not be over-looked in this respect is that there is a difference in the time taken to reach a maximum elevation for different growth rates. This difference may be important when the surge is superimposed on the tidal oscillations to give the final elevation. For example a surge having a slow growth period could still produce greater effects merely because its maximum coincided with high tide. Crease (1955) has plotted the time taken to reach the maximum from the time of commencement of the surge, and a similar figure could be constructed for the modified force.

As would be expected the elevation reached by the sea surface for large times is identical with that of the instantaneous force as $\tanh \{\epsilon_O(b-\beta)\} + 1$ for $b + \infty$.

6.2 A finite generating width.

It would seem more realistic to impose a finite generating width on the applied force, and this modification can also be tried by simply including another step function in the generating function given by equation (5.1)

$$E_2 = -A.H(t).H(-x).H(L+x)$$
 (6.4)

Again the same system is used as that in section 5 and the generating force is now applied instantaneously at t=0 over the region - $L \le x \le 0$. Taking L > 0

and
$$\frac{\partial E_2}{\partial x} = A.H(t).H(L+x).\delta(-x)-H(-x).\delta(L+x)$$
 (6.5)

 $\frac{\partial E_2}{\partial x}$ is substituted into the general equation for ζ and using the properties of the delta function this equation becomes

$$\frac{2\zeta}{A\sqrt{gh}} = \int_{0}^{t} H(t_{o}) .J_{o} \left[\gamma \left\{ (t-t_{o})^{2} - \frac{x^{2}}{gh} \right\}^{\frac{1}{2}} \right] .H \left[(t-t_{o}) - \frac{|x|}{\sqrt{gh}} \right] dt_{o}$$

$$- \int_{0}^{t} H(t_{o}) .J_{o} \left[\gamma \left\{ (t-t_{o})^{2} - (\frac{x+L}{gh})^{2} \right\}^{\frac{1}{2}} \right] .$$

$$H \left[(t-t_{o}) - \frac{|x+L|}{\sqrt{gh}} \right] dt_{o} \tag{6.6}$$

As before put $t-t_0 = \tau$, use the parameters, equation (5.4) and also take an additional parameter

$$L_{o} = \gamma (x+L)/\sqrt{gh} = a + \gamma L/\sqrt{gh}$$

Then equation (6.6) simplifies to

$$\frac{2\gamma}{A\sqrt{gh}} \cdot \zeta = \int_{|a|}^{b} J_{o} \left[(\beta^{2} - a^{2})^{\frac{1}{2}} \right] d\beta - \int_{|L_{o}|}^{b} J_{o} \left[(\beta^{2} - L_{o}^{2})^{\frac{1}{2}} \right] d\beta \quad (6.7)$$

It can be seen that the first integral in equation (6.7) is identical with the solution for the elevation that is obtained using the generating force acting over the whole semi-infinite range, equation (5.5). The only difference

between the two solutions given by equations (5.5) and (6.7) is the inclusion of the extra integral

$$-\int_{\left|L_{O}\right|}^{b} J_{O}\left[\left(\beta^{2}-L_{O}^{2}\right)^{\frac{1}{2}}\right] d\beta$$

in the latter equation. This extra integral causes the solution (6.7) to be split into the two cases $|a|>|L_0|$ and $|a|<|L_0|$, whereas in the solution (5.5) this distinction does not exist. In fact the two cases $|a|>|L_0|$ and $|a|<|L_0|$ lead to equal and opposite solutions for the elevation. This can easily be shown by transferring the origin x=0 to x=-L/2 by the transformation $x=x_1-L/2$, or in non-dimensional terms by putting $a=a_1-\gamma L/2\sqrt{gh}$. The solution (6.7) becomes with this substitution

$$\frac{2\gamma}{A\sqrt{gh}} \cdot \zeta = \int_{\left|a_{1} - \frac{\gamma L}{2\sqrt{gh}}\right|}^{b} J_{o}\left[\left\{\beta^{2} - \left(a_{1} - \frac{\gamma L}{2\sqrt{gh}}\right)^{2}\right\}^{\frac{1}{2}}\right] d\beta - \int_{\left|a_{1}\right|}^{b} J_{o}\left[\left\{\beta^{2} - \left(a_{1} + \frac{\gamma L}{2\sqrt{gh}}\right)^{2}\right\}^{\frac{1}{2}}\right] d\beta \qquad (6.8)$$

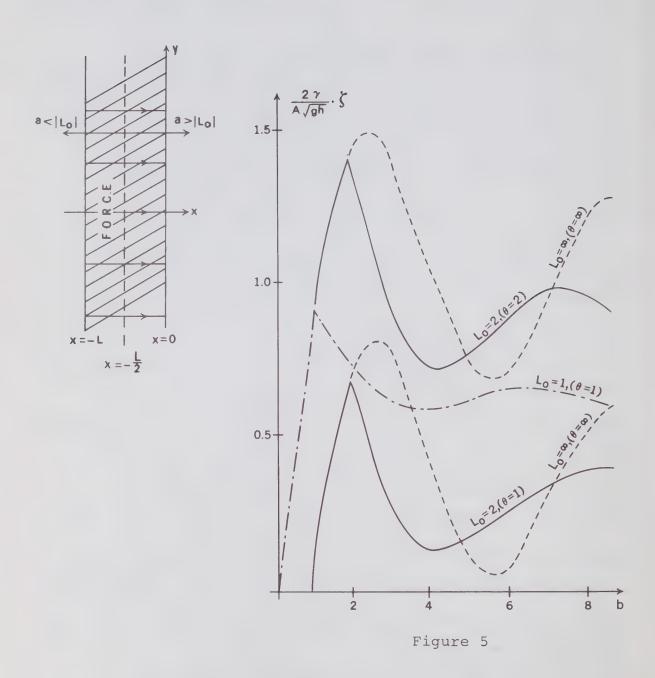
It can be seen that $(\zeta)_{a_1>0}=-(\zeta)_{a_1<0}$, and $a_1>0$ and $a_1<0$ correspond to the two cases $|a|>|L_0|$ and $|a|<|L_0|$ respectively, mentioned above. x=L is the line down the middle of the generating area, and it is of interest to note that on this line $a_1=0$, the elevation ζ is zero for all times.

To an observer at a particular point a where $|a|>|L_0|\text{, i.e. outside the generating area, there will be no disturbance until sufficient time has elapsed, after the}$

creation of the generating force at t = 0, for the effect of the force to be transmitted from the edge of the area x = 0to that point with the maximum group velocity \(\sqrt{gh} \). This period of time is given by b = |a|, exactly as in the previous section When this period has elapsed there is an initial elevation of the surface at that point. The actual elevation for the subsequent period, from b = |a| to $b = |L_0|$, being also exactly the same as that given in section 5.2. At the end of this period there is a decrease in the elevation due to the influence of the second integral in the solution (6.7) contributing for the first time, and the subsequent elevation ζ will depend on the width of the generating area, and the distance of the point of observation from the edge of the generating area. The elevation could be reinforced by the restriction of the generating area, if for instance, the first minimum of the second integral coincides with the second maximum of the first integral in equation (6.7). The condition for this can easily be found from equation (5.13). If the width of the generating strip L is represented by the parameter $\theta = \gamma L/\sqrt{gh}$, the condition is found to be $\theta = \{\sqrt{(a^2 + 54)}\}$ - a } For latitudes such as those for the North Sea, a = 1, θ = 1 correspond to lengths of the order of 200 kilometers, so that reinforcement is not physically possible owing to the large distances involved.

The case $|a|<|L_0|$ corresponds exactly to the previous case $|a|>|L_0|$ if the sign of ζ is reversed and the parameters L_0 and a are interchanged.

Figure 4
A generating force of finite width.



The elevation produced by generating forces of finite and infinite space dimensions on an infinite rotating sea.

As would be expected for large times, $b \rightarrow \infty$

$$\frac{2\gamma}{A\sqrt{gh}} \cdot \zeta \Rightarrow \exp(-|a|) - \exp(-|a+\theta|)$$

and the elevation ζ approaches zero as L+0. Also as L+ ∞ the limit for ζ approaches that of the case in Section 5.

Curves for particular values of a and θ are plotted in figure 5. Values of $\theta=1$ and $\theta=2$ are compared with the solution obtained when the generating area is the semi-infinite one, $\theta=\infty$, for a=0. Similarly the case $\theta=1$ is compared with $\theta=\infty$ for a=1.

OTHER EFFECTS

7.1 A barrier at right angles to the direction of propagation.

With the same infinite rotating system the equation for the velocity in the direction of propagation is equation (4.14).

$$U = -\frac{1}{2} \int_{0}^{\frac{\pi}{2}} \int_{0}^{t} dt_{0} \int_{-\infty}^{\infty} \frac{\partial E}{\partial t_{0}} (x_{0}, t_{0}) . J_{0} \left[\gamma \left\{ (t - t_{0})^{2} - (\frac{x - x_{0}}{gh})^{2} \right\}^{\frac{1}{2}} \right] . H \left[(t - t_{0}) - |\frac{x - x_{0}}{\sqrt{gh}}| \right] dx_{0}$$

The required condition for a barrier, taken at x=0 for convenience, is that U=0 at x=0. If E(x,t) is presumed to be a given force, then the velocity $U_{\rm I}$ produced by an image force $E_{\rm I}$ (x,t), where $E_{\rm I}$ (x,t) = - E(-x,t) is given by

$$U_{I} = \frac{1}{2} \sqrt{\frac{g}{h}} \cdot \int_{0}^{t} dt_{0} \int_{-\infty}^{\infty} \frac{\partial E}{\partial t_{0}} (-x_{0}, t_{0}) \cdot J_{0} \left[\gamma \left\{ (t - t_{0})^{2} - (\frac{x - x_{0}}{gh})^{2} \right\}^{\frac{1}{2}} \right] \cdot H \left[(t - t_{0}) - |\frac{x - x_{0}}{\sqrt{gh}}| \right] dx_{0}$$

and on substituting $x_0' = -x_0$ in this equation and then dropping the prime

$$U_{I} = \frac{1}{2} \sqrt{\frac{g}{h}} \cdot \int_{0}^{t} dt_{o} \int_{-\infty}^{\infty} \frac{\partial E}{\partial t_{o}} (x_{o}t_{o}) \cdot J_{o} \left[\gamma \left\{ (t-t_{o})^{2} - \left(\frac{x+x_{o}}{gh} \right)^{2} \right\}^{\frac{1}{2}} \right] \cdot H \left[(t-t_{o}) - \left| \frac{x+x_{o}}{\sqrt{gh}} \right| \right] dx_{o}$$

$$(7.1)$$

Therefore it can be seen that $(U)_{x=0} = -(U_I)_{x=0}$ and hence the effect of a barrier at x=0 could be interpreted as an image force acting in the opposite direction to the applied force at image points in the region beyond the barrier when the sea occupies either of the regions x>0 or x<0. This principle can be applied equally well if the barrier is at x=L by a simple adjustment of the origin.

It follows that ζ can be derived by the superposition of the incident and reflected waves. In fact for this particular system, taking the general equation for ζ given by equation (4.12), and adding the elevations ζ and $\zeta_{\rm I}$ due to the applied and image forces respectively, it is found that

$$\zeta + \zeta_{I} = \frac{\sqrt{gh}}{2} \cdot \int_{0}^{t} dt_{o} \int_{-\infty}^{\infty} \frac{\partial E}{\partial x_{o}} (x_{o}, t_{o}) \cdot J_{o} \left[\gamma \left\{ (t - t_{o})^{2} - (x_{o} - t_{o})^{2} \right\} \right] \cdot H \left[(t - t_{o}) - (x_{o} - t_{o}) \right] dx_{o} + \frac{\sqrt{gh}}{2} \int_{0}^{t} dt_{o}$$

$$\int_{-\infty}^{\infty} \frac{\partial E}{\partial x_{0}}(x_{0}, t_{0}) \cdot J_{0} \left[\gamma \left\{ (t - t_{0})^{2} - (\underline{x + x_{0}})^{2} \right\}^{\frac{1}{2}} \right] \cdot H \left[(t - t_{0}) - (\underline{x + x_{0}})^{2} \right] dx_{0}$$

$$\left[\frac{x + x_{0}}{\sqrt{ah}} \right] dx_{0}$$

$$(7.2)$$

Therefore at the barrier, x=0, the elevation is double that which would be present if the barrier was absent,

$$\zeta + \zeta_T = 2.\zeta$$

7.2 A travelling disturbance.

It has been indicated, c.f. Proudman (1929) that there would be a resonance effect if the disturbance creating the surge was not stationary but was moving with the surge with a velocity \sqrt{gh} . Crease demonstrates this resonance for the particular form of generating function E(x,t). The form of E(x,t) he uses is

$$E(x,t) = -A.H(t).H(V_0t - x)$$
 (7.3)

This is a force created at t=0 and maintained constant, acting over the region $-\infty < x < V_O t$. This means that the discontinuity in the force at the edge of the generating area is moving forward with a velocity V_O .

Substituting this value of E(x,t) in the general equation for the elevation ζ given by equation (4.12)

$$\frac{2\zeta}{A\sqrt{gh}} = \int_{0}^{t} H(t_{0}) \cdot J_{0} \left[\gamma \left\{ (t-t_{0})^{2} - (\underline{x-V_{0}t_{0}})^{2} \right\}^{\frac{1}{2}} \right] \cdot H\left[t-t_{0} \right) - \left[\underline{x-V_{0}t_{0}} \right] dt_{0}$$

$$(7.4)$$

By using the non-dimensional parameters given in equation (5.4), and taking in addition $V_0/\sqrt{gh} = \Phi$ then

$$\frac{2\gamma}{A\sqrt{gh}} \cdot \zeta = \int_{0}^{b} H(b-\beta) \cdot J_{0} \left[\left\{ \beta^{2} - (a-\Phi \cdot [b-\beta])^{2} \right\}^{\frac{1}{2}} \right] \cdot H\left[\beta - |a-\Phi(b-\beta)| \right] d\beta$$

that is

that is
$$\frac{2\gamma}{A\sqrt{gh}} \cdot \zeta = \int_{0}^{b} H(b-\beta) \cdot J_{0} \left[\left(\left\{ \beta \left(1+\Phi \right) + a - \Phi b \right\} \left\{ \beta \left(1-\Phi \right) - a + \Phi b \right\} \right)^{\frac{1}{2}} \right] \cdot H \left[\beta - \left| a - \Phi \cdot \left(b - \beta \right) \right| \right] \cdot d\beta \tag{7.5}$$

Crease omits the first step function in the integrand, but this function is relevant when discussing the case of the solution for a<o.

The particular velocity that is of interest is given by $V_0 = \sqrt{gh}$, or $\Phi = 1$, as mentioned above.

For $\Phi = 1$,

$$\frac{2\gamma}{A\sqrt{gh}} \cdot \zeta = \int_{0}^{b} H(b-\beta) \cdot J_{0} \left[\left(\left\{ b-a \right\} \left\{ 2\beta - (b-a) \right\} \right)^{\frac{1}{2}} \right] \cdot H \left[\beta - \left| \beta - (b-a) \right| \right] d\beta$$
(7.6)

Now the step functions impose the following limits on the integral

$$b>\beta> (b-a), b>|a|$$
 (7.7)

So that for a>o

$$\frac{2\gamma}{A\sqrt{gh}} \cdot \zeta = \int_{\frac{b-a}{2}}^{b} H(b-|a|) \cdot J_{C}\left[\left(\left\{b-a\right\}\left\{2\beta-(b-a)\right\}\right)^{\frac{1}{2}}\right] d\beta \qquad (7.8)$$

and for a < o putting a = -q', where q' is positive,

$$\frac{2\gamma}{A\sqrt{gh}} \cdot \zeta = \int_{\left(\frac{b+q'}{2}\right)}^{b} H(b-|a|) \cdot J_{o}\left[\left(\left\{b+q'\right\}\right\}\left\{2\beta - \left(b+q'\right)\right\}\right)^{\frac{1}{2}}\right] d\beta$$
(7.9)

Using the substitution (b-a) $[2\beta - (b-a)] = z_0^2$ these equations reduce to simple integrals, and can be combined in the solution

$$\frac{2\gamma}{A\sqrt{gh}} \cdot \zeta = H(\frac{b-|a|}{b-a}) \int_{0}^{(b^{2}-a^{2})^{\frac{1}{2}}} J_{0}(z_{0}) \cdot z_{0} \cdot dz_{0}$$

that is

$$\frac{2\gamma}{A\sqrt{gh}} \cdot \zeta = \left(\frac{b+a}{b-a}\right)^{\frac{1}{2}} \cdot J_1 \left[\left(b^2 - a^2\right)^{\frac{1}{2}} \right] \cdot H \left(b - |a|\right)$$
 (7.10)

From this solution, the elevation at the leading edge of the disturbance, $x = \sqrt{gh}$.t i.e. a=b, is given by

$$\frac{2\gamma}{A\sqrt{gh}} \cdot \zeta = \frac{1}{2} \text{ Limit}_{b \to a} \left[\frac{b+a}{b-a} \right]^{\frac{1}{2}} \cdot J_1 \quad (b^2 - a^2)^{\frac{1}{2}} = b$$
 (7.11)

Therefore ζ grows without limit at this leading edge and a discontinuity develops. The slope of the surface at the leading edge is found to be

b=a,
$$\frac{2\gamma}{A\sqrt{gh}} \frac{\partial \zeta}{\partial a} = \frac{1}{2} - \frac{a^2}{4}$$
 (7.12)

Thus immediately behind the discontinuity the surface gets progressively steeper.

For a point a<0 the elevation is zero for $b\leqslant q'$. The elevation at the origin is given simply by

$$\frac{2\gamma}{A\sqrt{gh}} \cdot \zeta = J_1(b) \quad \text{for a=0}$$
 (7.13)

The ratio of the elevations for points equidistant from the origin but on opposite sides at a time b>|a| is given by

$$\frac{\zeta_{+}}{\zeta_{-}} = \frac{b+a}{b-a} \tag{7.14}$$

EXTENSIONS TO THE PROBLEM USING CYCLINDRICAL CO-ORDINATES
8.1 A simple axially-symmetric pressure distribution.

The axially-symmetric form of the equation for the elevation ζ in cylindrical co-ordinates is given by equation (3.33), and if, to be consistent with assumptions in the preceding sections, the bottom friction is neglected this equation becomes

$$\left[\frac{\partial^{2}}{\partial r^{2}} + \frac{1}{r} \frac{\partial}{\partial r} - \frac{1}{gh} \left(\frac{\partial^{2}}{\partial t^{2}} + \gamma^{2}\right)\right] \frac{\partial \zeta}{\partial t} = \frac{\gamma}{\rho gh} \left(\frac{\partial \tau_{\theta S}}{\partial r} + \frac{\tau_{\theta S}}{r}\right) \\
+ \frac{1}{\rho gh} \frac{\partial}{\partial t} \left(\frac{\partial \tau_{rS}}{\partial r} + \frac{\tau_{rS}}{r}\right) - \frac{1}{\rho g} \frac{\partial}{\partial t} \left(\frac{\partial^{2}}{\partial r^{2}} + \frac{1}{r} \frac{\partial}{\partial r}\right)^{p} a \quad (8.1)$$

This equation can be integrated immediately with respect to time if $\tau_{\theta s}$ =0, that is no wind stress on the surface in a cross-radial direction. In fact more generally both wind stresses, $\tau_{\theta s}$ and τ_{rs} , disappear completely from the right hand side of equation (8.1) if they are taken to be of the form

$$\tau_{\theta S} = \frac{1}{r} \cdot f(t); \quad \tau_{rS} = \frac{1}{r} \cdot F(t)$$
 (8.2)

where f(t) and F(t) are general functions of time including the cases f(t)=0 and F(t)=0. There are difficulties in interpreting these functions near the origin into physical conditions unless it is assumed that $\tau_{\theta s} = \tau_{rs} = 0$. In the following case the assumption is that the wind effect on the sea surface is zero, or at least negligible compared to the effect created by the pressure distribution P_a . The simplified form of the equation (8.1) becomes

$$\left[\frac{\partial^2}{\partial r^2} + \frac{1}{r} \frac{\partial}{\partial r} - \frac{1}{gh} \left(\frac{\partial^2}{\partial t^2} + \gamma^2\right)\right] \zeta = -\frac{1}{\rho g} \left(\frac{\partial^2}{\partial r^2} + \frac{1}{r} \frac{\partial}{\partial r}\right) P_a \qquad (8.3)$$

the integration constant being zero if at some time ζ and $\frac{\partial \zeta}{\partial t}$ are zero, and P_a is constant.

Equation (8.3) can be solved by the use of a zero order Hankel transform.

let
$$\bar{\zeta}(q,t) = \int_{0}^{\infty} \zeta(r,t) . J_{O}(qr) . rdr$$
and $\bar{P}_{a}(q,t) = \int_{0}^{\infty} P_{a}(r,t) . J_{O}(qr) . rdr$

$$(8.4)$$

then the transformed equation becomes

$$-\left[q^{2} + \frac{1}{gh}\left(\frac{\partial^{2}}{\partial t^{2}} + \gamma^{2}\right)\right]\overline{\zeta} = \frac{q^{2}}{\rho g}\overline{P}_{a}$$
 (8.5)

By making the substitution $m^2 = (gh.q^2 + \gamma^2)$ and taking the operator $D = \frac{\partial}{\partial t}$,

$$(D^2 + m^2)\bar{\zeta} = -\underline{hq}^2. \bar{P}_a$$
 (8.6)

The complementary function $\bar{\zeta}_{C}$ is given by

$$\bar{\zeta}_{C} = A \exp(imt) + B \exp(-imt)$$
 (8.7)

where A and B are constants. The particular integral $\overline{\zeta}_{p}$ is given by

$$\bar{\zeta}_{p} = -\frac{hq^{2}}{\rho} \cdot \frac{1}{2im} \left[\frac{1}{D-im} - \frac{1}{D+im} \right] \bar{P}_{a}$$

that is
$$\bar{\zeta}_p = -\frac{hq^2}{2\rho \cdot im} \left[\exp(imt) \int_{a_0}^t \exp(-imt_0) \cdot P_a(q,t_0) \cdot dt_0 \right]$$

$$-\exp(-imt) \int_{b_0}^t \exp(imt_0) \cdot P_a(q,t_0) \cdot dt_0$$
(8.8)

where a_0 , b_0 are constants to be evaluated in conjunction with A and B. Therefore choosing $a_0=b_0=0$ for convenience and making the necessary adjustments to A and B

$$\bar{\zeta} = A \exp(imt) + B \exp(-imt) - \frac{hq^2}{\rho m} \left[\int_0^t \sin m(t-t_0) \cdot \bar{P}_a \cdot dt_0 \right]$$
(8.9)

Also for convenience take the pressure distribution to be created at t=0, that is

$$P_a = P_O + P(r) \cdot H(t)$$
 (8.10)

there being no initial oscillations, A=B=0 and

$$\overline{\zeta} = -\frac{h}{\overline{\rho}} \cdot H(t) \cdot \left(1 - \cos(mt)\right) \frac{q^2}{m^2} \cdot \overline{P}$$
 (8.11)

and taking the inverse Hankel transform

$$\zeta = -\frac{h}{\rho} H(t) \int_{0}^{\infty} \left\{ \left(1 - \cos(mt) \right) \frac{q^{2}}{m^{2}} \cdot qJ_{0}(rq) \int_{0}^{\infty} P(n) \cdot n \right\} dq$$

$$(8.12)$$

This equation is the general solution for the elevation

when the pressure distribution is of the form of equation (8.10), and to proceed further particular forms of P have to be taken. By consulting the tables of Hankel transforms the form of P can be chosen so that P̄ can be written down simply and yet still yield a physically interesting case. Such a case is the simple exponential variation given by

$$P = -C_1 \cdot \exp(-c_1 r)$$
 (8.13)

where C₁ and c₁ are positive constants, hence infinities in the pressure distribution are avoided. With this distribution

$$\zeta = \frac{h}{\rho} \cdot H(t) \cdot C_1 \int_0^\infty \left(1 - \cos(mt)\right) \frac{q^2}{m^2} \frac{c_1}{(c_1^2 + q^2)^{\frac{3}{2}}} \cdot q^{-1} \int_0^\infty (rq) dq$$
(8.14)

The equation for a similar non-rotating system can be deduced from this equation, for with $\gamma=0$ m² = gh.q²

and
$$(\zeta)_{\gamma=0} = \frac{H(t)}{\rho g}$$
. $C_1 \int_0^{\infty} \left(1 - \cos(\sqrt{gh} \ qt)\right) \cdot \frac{c_1}{(c_1^2 + q^2)^{\frac{3}{2}}}$.

 $q J_0(rq) . dq$ (8.15)

However returning to equation (8.14) and using the nondimensional parameters

$$b = \gamma t$$
, $a = \frac{\gamma r}{\sqrt{gh}}$, $q_0 = \frac{\sqrt{gh} \cdot q}{\gamma}$, $c_0 = \frac{\sqrt{gh} \cdot c_1}{\gamma}$ (8.16)

then

$$\zeta = \frac{1}{\rho g} \cdot H(b) \cdot C_1 \int_0^\infty \left(1 - \cos \left(b \sqrt{q_0^2 + 1} \right) \frac{q_0^2}{(q_0^2 + 1)} \frac{c_0}{(c_0^2 + q_0^2)^{\frac{3}{2}}} \right) dq_0$$
(8.17)

As c_1 , is arbitrary, take c_0 such that $c_0=1$, then

$$\zeta = \frac{H(b) \cdot C_1}{\rho g} \cdot C_1 \int_0^\infty \left(\frac{1 - \cos(b\sqrt{q_0^2 + 1})}{(q_0^2 + 1)^{\frac{5}{2}}} \right) \cdot q_0^3 \cdot J_0(aq_0) \cdot dq_0$$

Using the substitution $b^2(q_0^2+1) = \beta_1^2$

$$\frac{\rho g. \zeta = H(b).b \int_{b}^{\infty} \left(1 - \cos(\beta_1)\right) \left(\frac{1}{\beta_1^2} - \frac{b^2}{\beta_1^4}\right)^{J} o\left(\frac{a\sqrt{\beta_1^2 - 1}}{b}\right) d\beta_1$$
(8.18)

The integral can be evaluated numerically to give the elevation ζ for a given value of a in terms of the time parameter b. For the particular case a=0, see figure 5,

$$\frac{\rho g}{C_1} \cdot \zeta_0 = H(b) \cdot b \int_{b}^{\infty} \left(1 - \cos(\beta_1)\right) \left(\frac{1}{\beta_1^2} - \frac{b^2}{\beta_1^4}\right) d\beta_1$$
 (8.19)

which on integration by parts yields,

$$\frac{\rho g}{C_1} \cdot \zeta_0 = H(b) \cdot \left[\frac{2}{3} + \frac{\cos(b)}{3} - \frac{b}{6} \cdot \sin(b) - b(1 + \frac{b^2}{6}) \int_{b}^{\infty} \frac{\cos(\beta_1) \cdot d\beta_1}{\beta_1} \right]$$
(8.20)

and this reduces to

$$\frac{\rho g}{C_1} \cdot \zeta_0 = H(b) \cdot \left[\frac{2}{3} - \left(\frac{2}{3} + \frac{b^2}{6} \right) \cos(b) - \frac{b \sin(b) + b(1 + \frac{b^2}{6})}{6} \right]$$

$$\left(\frac{\pi}{2} - S_1(b) \right)$$
(8.21)

where $S_1(b) = \int_0^b \frac{\sin(\beta_1)}{\beta_1} d\beta_1$. This function can be evaluated for various values of b from existing tables, and hence $\frac{\rho g}{C_1}$. Can be plotted directly against b from equation (8.21). This is

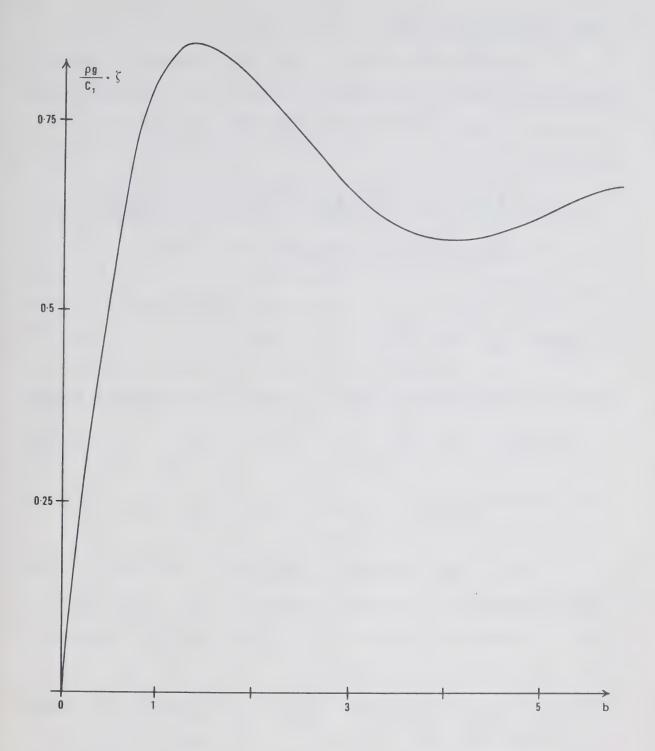


Figure 6

The elevation produced at the centre of a radial symmetric pressure distribution.

done in figure 6.

To find the value of ζ_0 for large times b+∞ equation (8.19) can again be integrated by parts, this time taking the functions in the reverse order to produce an asymptotic expansion for ζ_0 ,

i.e.
$$\frac{\rho g}{C_1} \cdot \zeta_0 = H(b) \cdot \left[\frac{2}{3} + \frac{2}{b^2} \cos(b) + \frac{14}{b^3} \sin(b) - \frac{96}{b^4} \cos(b) \right]$$

terms of $O(\frac{1}{b})^5$ and higher

Hence b→∞

$$\frac{\rho g}{C_1}$$
, $\zeta_0 \to \frac{2}{3} + \frac{2 \cos(b)}{b^2}$ (8.22)

whereas it can be found that on a similar non-rotating system

$$\left(\frac{\rho g \cdot \zeta_0}{C_1}\right)_{\gamma=0} \to 1 \quad \text{for } b \to \infty$$
 (8.23)

from equation (8.15).

8.2 A circular wind distribution.

Taking the atmospheric pressure to be uniform and the radial component of the wind stress to be zero, then the radially symmetric equation (8.1) for the elevation reduces to

$$\left[\frac{\partial^2}{\partial r^2} + \frac{1}{r}\frac{\partial}{\partial r} - \frac{1}{gh}\left(\frac{\partial^2}{\partial t^2} + \gamma^2\right)\right]\frac{\partial \zeta}{\partial t} = \frac{\gamma}{\rho gh}\left[\frac{\partial \tau_{\theta s}}{\partial r} + \frac{\tau_{\theta s}}{r}\right] \quad (8.24)$$

The right hand side of this equation vanishes for $\tau_{\theta s} = \frac{f(t)}{r}$, and becomes a function of time only for $\tau_{\theta s} = r.f(t)$. Combining these two forms of $\tau_{\theta s}$ to avoid infinities for

r=0 and $r\to\infty$ the generating force is taken to be of the form,

$$P_{a} = constant$$

$$\tau_{rs} = 0$$

$$\tau_{\theta s} = f(t) \left[\frac{T}{r} \cdot H(r-T) + \frac{r}{T} \cdot H(T-r) \right]$$

$$(8.25)$$

Hence the atmospheric disturbance consists of a circular wind blowing over the sea surface, whose magnitude varies with distance and time, and is zero for r=0 and r= ∞ . The variation of $\tau_{\theta s}$ with distance is shown in figure 7. This wind distribution approximates fairly well to that of a circular hurricane or similar disturbance, the wind velocity being zero in the 'eye' and at large distances from it. Substituting from equation (8.25) into equation (8.24)

$$\left[\frac{\partial^{2}}{\partial r^{2}} + \frac{1}{r} \frac{\partial}{\partial r} - \frac{1}{gh} \left(\frac{\partial^{2}}{\partial t^{2}} + \gamma^{2}\right)\right] \frac{\partial \zeta}{\partial t} = \frac{\gamma}{\rho gh} \cdot f(t) \cdot \left[-\frac{T}{r^{2}} \cdot H(r-T) + \frac{T}{r}\delta(r-T)\right]$$

$$+ \frac{1}{T} H(T-r) - \frac{r}{T} \cdot \delta(r-T) + \frac{T}{r^{2}} \cdot H(r-T) + \frac{1}{T} \cdot H(T-r)\right]$$
i.e.
$$\left[\frac{\partial^{2}}{\partial r^{2}} + \frac{1}{r} \frac{\partial}{\partial r} - \frac{1}{gh} \left(\frac{\partial^{2}}{\partial r^{2}} + \gamma^{2}\right)\right] \frac{\partial \zeta}{\partial t} = \frac{2\gamma}{\rho gh} \cdot f(t) \frac{1}{T} \cdot H(T-r)$$

The delta functions having zero value except at r=T, at which point they cancel each other.

For convenience and simplicity again choose the function of time to be a simple step function, that is, take $f(t) = A_0.H(t) \text{ where } A_0 \text{ is a constant.} \text{ The disturbance is}$ then suddenly created at t=0 and thereafter maintained constant. The initial conditions $t \le 0$ are assumed constant.

Taking the zero order Hankel transform of equation (8.26)

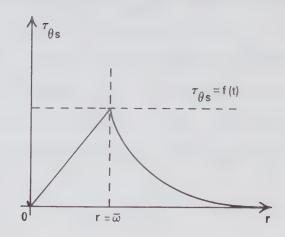


Figure 7

The wind distribution assumed to approximate to a circular atmospheric disturbance.

where
$$H_0$$
 $\frac{\partial \zeta}{\partial t}(r,t) = \frac{\partial \overline{\zeta}}{\partial t}(q,t) = \int_0^\infty \frac{\partial \zeta}{\partial t}(r,t) . J_0(qr).rdr$

and from tables of transforms

$$\begin{array}{c|c}
H_{O} & |H(T-r)| = \frac{T}{q} J_{1}(Tq) \\
\text{Transform}
\end{array}$$

then
$$\left[q^2 + \frac{1}{gh}\left(\frac{\partial^2}{\partial t^2} + \gamma^2\right)\right] \frac{\partial \overline{\zeta}}{\partial t} = -\frac{2\gamma}{\rho gh} \cdot A_0 \cdot H(t) \cdot J_1(\underline{\gamma}q)$$
 (8.27)

Multiply through by gh and take $m^2 = (gh.q^2 + \gamma^2)$; $D = \frac{\partial}{\partial t}$ then the complementary function

$$\frac{\partial \bar{\zeta}_{C}}{\partial t} = A \exp(imt) \rightarrow B \exp(-imt)$$
 (8.28)

where A and B are constants, and the particular integral reduces to

$$\frac{\partial \overline{\zeta}}{\partial t} = -\frac{2\gamma A_0}{\rho} \cdot \frac{J_1(\Upsilon q)}{q} \cdot \frac{1}{2im} \left[\frac{1}{D-im} - \frac{1}{D+im} \right] \cdot H(t)$$

i.e.
$$\frac{\partial \overline{\zeta}_{p}}{\partial t} = -\frac{2\gamma A_{o}}{\rho} \cdot \frac{J_{1}(Tq)}{q} \cdot \frac{1}{2im} \left[\exp(imt) \int_{a_{o}}^{t} H(t_{o}) \exp(-imt_{o}) \cdot dt_{o} \right]$$

$$-\exp(-imt) \int_{b_{o}}^{t} H(t_{o}) \cdot \exp(imt_{o}) dt_{o}$$
(8.29)

where a_0 and b_0 are constants to be evaluated in conjunction with A and B, so choose $a_0 = b_0 = 0$ and make the necessary adjustments to the constants A and B. The whole solution is then given by

$$\frac{\partial \overline{\zeta}}{\partial t} = A \exp(imt) + B \exp(-imt) - \frac{2\gamma A_0}{\rho} \cdot \frac{J_1(\Upsilon q)}{q} \cdot \frac{1}{m} \int_0^t \sin(m(t-t_0)) dt$$

$$H(t_0) \cdot dt_0$$

As there are no initial oscillations for t<0, A = B = 0

$$\frac{\partial \overline{\zeta}}{\partial t} = -\frac{2\gamma A_0}{\rho} \cdot J_1(Tq) \cdot H(t) \cdot (\frac{1-\cos(mt))}{m^2}$$
 (8.30)

Taking the inverse Hankel transform of equation (8.30)

$$\frac{\partial \zeta}{\partial t} = -\frac{2\gamma A_0}{\rho} \cdot H(t) \cdot \int_0^\infty J_{\frac{1}{q}} \frac{(Tq) \cdot (1-\cos(\sqrt{(ghq^2+\gamma^2)} \cdot t))}{(ghq^2+\gamma^2)} \cdot q \cdot J_0(rq) dq$$
(8.31)

This solution can be readily verified by substitution into equation (8.26).

By direct integration of equation (8.31) with respect to time

$$\zeta = -\frac{2\gamma A_{o} \cdot H(t) \cdot \int_{0}^{\infty} \left\{ \frac{\sqrt{(ghq^{2} + \gamma^{2}) \cdot t - \sin(\sqrt{(ghq^{2} + \gamma^{2}) \cdot t})}}{(ghq^{2} + \gamma^{2}) \frac{3}{2}} \right\}$$

$$J_{1}(Tq) \cdot J_{o}(rq) dq \qquad (8.32)$$

It is noticed that for $\gamma=0$; $\zeta=0$, that is on a non-rotating system the effect of a circular wind distribution would be to produce wind driven currents only, with no surface elevation. In contrast to the previous cases taken the above solution for the elevation leads to infinite values for ζ as $t\to\infty$. However such cyclonic disturbances in practice would not be in existence for infinite times and equation (8.32) could give the initial motion. For small values of t this equation simplifies to

$$\zeta = -\frac{2\gamma A_0}{2} \cdot H(t) \cdot \int_0^\infty \frac{t^3}{6} \cdot J_1(Tq) \cdot J_0(rq) \cdot dq$$
 (8.33)

DISCUSSION

9.1 Putting theory into practice.

The place of theoretical analysis in the practical problem of surge prediction is only partially obvious. The basic equations of motion, their simplification and in certain cases their integration will be required for most forecasting methods. Numerical methods using computers will probably be widely adopted for predictions in the near future, and the basic equations for these methods will be the general averaged equations in sub-section 2.2. However the usefulness of the exact mathematical treatment of idealised models is perhaps not so apparent.

In Section 2 the equations of motion are derived and simplified using an order of magnitude analysis. This method was developed by Charnock and Crease (1957) but has been adapted in Section 2.1, to the form of the boundary layer analysis given by Schlichting (1955) which is felt to be slightly more rigorous. The non-linear terms are neglected in this report but it has been indicated that these terms are important for the cases of estuaries and similar geographical features. The height of surges travelling up estuaries could effect major ports and cities and in recent years a number of papers have been published dealing with non-linear effects, see Charnock and Crease (1957).

The averaged equations provide an approximation to the equations of motion in that they satisfy conditions at the upper and lower boundaries and provide a mean solution for

the fluid between. In this respect the averaged equations resemble the Von Karman integral equation from boundary layer theory. Proudman (1954) justifies the use of the averaged form of the equations and a simple bottom stress relationship, for the case of a one-dimensional surge in a rectangular basin. In general however the adequacy of the averaged equations depends on the type of bottom stress law assumed (c.f. section 2.3) which in turn depends on other factors governing the motion (Welander (1961) ϕ 5.4).

The laws governing the propagation of the surges outside the influence of the generating forces are approximated to by the free motions described in Section 3. An example of such a surge would arise if a depression moved eastwards across the northern entrance to the North Sea. The associated surge would travel into and around the North Sea whilst the depression would disappear over the continent. Frictional effects would still be present however, but these are likely to be quite small except of course along the fringes of the sea. A simple allowance for such effects was discussed in sub-section 3.4.

The free propagation of surges also shows that on a rotating system the surges are in general dispersive, but two special types of non-dispersive waves were found. These two special waves, the Kelvin and Poincaré waves, together with the inertia currents provide a good indication of the laws of motion for surges in nature.

The general equations for the elevation are easily derived in both cartesian and cylindrical co-ordinates but are difficult to solve except when simple conditions are assumed. The particular model investigated in Sections 4-7, that is an infinite rotating sea of uniform depth with no bottom friction, would approximate well to mid-oceanic conditions. In deep water bottom stress can be safely neglected and a region far removed from boundaries would resemble an infinite sea. The usefulness of solutions in mid-ocean may be held in some doubt, nevertheless this particular model is a relatively simple one and can be useful in other ways. Solutions obtained on such simple models throw some light on the properties of surges occuring in more elaborate systems. In sub-section 6.1 it is shown that a gradually applied force will lead to a surge having an amplitude less than a surge generated by a more rapidly developing force. The travelling disturbance discussed in sub-section 7.2 indicates strong resonance when the disturbance moves at a velocity approaching \sqrt{gh} . Both of these properties are borne out by observation.

The particular forcing function chosen by Crease in Section 5, was shown to lead to a steady elevation for infinite times. On a non-rotating system a corresponding force would produce an ever-increasing elevation owing to the non-dispersive nature of its surges. The generation of the surge from rest was discussed in some detail in this section.

Other extensions considered were the effect of a barrier at right angles to the direction of propagation of the surge and a finite generating width.

The effect of a barrier is the same as that of an image force acting in the opposite direction to the applied force at image points with respect to the barrier, and for the particular applied force of Section 5 leads to an elevation at the barrier that is twice that which would have resulted if the barrier was removed. The restriction on the generating strip in general leads to a reduction of the surge amplitude, but it was shown in sub-section 6.2 that certain widths leading to a reinforcement of the surge are possible.

Finally the solutions were extended in Section 8 to cylindrical co-ordinates. This form of the equations appears to be neglected in theoretical works. With an axially symmetric form of the equations realistic forms of stationary atmospheric disturbances can be considered simply. However for travelling disturbances the equations would become more difficult to use. A simple form of pressure distribution was shown to lead to a well behaved solution for all values of r and t, whereas unfortunately a wind system leads to a solution that becomes infinite for $t \rightarrow \infty$. The second solution however remains finite for all values of r and so could be used as an indication of the solution for small times. A combination of these two generating functions gives an applied force that approximated very well to a cyclonic atmospheric

disturbance, and as the equations are linear the solutions can also be combined by addition.

In conclusion therefore it is considered that actual quantitative predictions must be left to computer techniques and to some extent empirical allowances for local geographical effects. Exact mathematical treatments are valuable in determining the laws of motion and properties of the surge and in this respect can direct the research into more realistic problems and provide a greater understanding of the dynamics of the motion. In some instances orders of magnitude of the various quantities of the motion can be determined. Tables for numerical values occuring in the solution for the infinite rotating sea are given in the Appendix.

BIBLIOGRAPHY

- Charnock, H., and Crease, J. 1957. North Sea Surges. Sci. Prog. 45.
- Crease, J. 1955. Propagation of long waves due to atmospheric disturbances on a rotating sea. Proc. Roy. Soc. A. 233.
- Lamb, H. 1935. "Hydrodynamics" (6th. ed.) Cambridge Univ.

 Press. Lond., N.Y.
- Nomitsu, T. 1933-35. Mem. Coll. Sci. Kyoto Ser. A. 16,17,18.
- Poincaré, H. 1910. Théorie des marées. Leçons de mécanique céleste 3. Paris.
- Proudman, J., and Doodson, A.T. 1924. Time relations in meteorological effects on the sea. Proc. Lond. Maths. Soc. (2) 24.
- Proudman, J. 1929. Mon. Not. R. Astr. Soc. Geophys. Suppl. 2.
- Proudman, J. 1953. "Dynamical Oceanography".
- Proudman, J. 1954. Note on the dynamical theory of storm surges. Arch. Met. Geophys. Biokl. (A). Defant-Heft.
- Proudman, J. 1954. Note on the dynamics of storm surges.

 Mon. Not. Roy. Astr. Soc. Geophys. Suppl. 7.
- Schlichting, H. 1955. "Boundary Layer Theory" Pergamon Press
 London.
- Taylor, G.I. 1920. Tidal oscillations in gulfs and rectangular basins. Proc. Lond. Maths. Soc. (2) 20.

- Thompson, Sir W. 1879. On gravitational oscillations of rotating water. Proc. Roy. Soc. Edin. 10.
- Welander, P. 1961. Numerical prediction of storm surges.

 Advances in Geophysics. 8.

APPENDIX

The numerical values of the parameters and physical quantities given by Crease (1955) are reproduced below for various oceanic conditions. The units of ζ ,U,V are equal to $A\sqrt{gh}/2\gamma$, $Ag/2\gamma$ and $Ag/2\gamma$ respectively. Column A' gives the values of these units for an air pressure gradient of lm.b./20 kms. equivalent to $A = \frac{1}{2}.10^{-6}$. Column B' gives the values of the same units when the generating force is derived from a wind stress $\tau = G.\rho_a.v_a^2$ where G is a numerical parameter, $G\simeq 0.002$, ρ_a and v_a the density and velocity of the air respectively. v_a is taken to be 20m./sec. By comparing columns A' and B' it is seen that the effect of wind stress is negligible in deep water but in shallow water it is somewhat greater than the pressure effect.

Location	Latitude	Average depth (m)	Approx.	Approx. units of b (hrs)	Approx. units of ζ (cms)		Approx. units of U, V (cm/sec.)	
		depth (m)	units of a (kins)	antes of D (mes)	A'	B'	A'	B'
N. Atlantic	50°	2500	1400	2.5	35.6	2.3	2.2	0.1
N. Atlantic Shelf	50°	150	350	2.5	8.7	9-3	2.2	2.4
North Sea	55 °	50	190	2.3	4.7	15.0	2·1	6.7

Numerical values of parameters and physical quantities.

ACKNOWLEDGMENTS

The author wishes to express his thanks to Dr. H.G.

Pinsent for his valuable suggestions and criticisms throughout
the period of this research undertaken at Chelsea College,
University of London for the degree of Master of Science. In
addition the author gratefully acknowledges the support of the
following members of the Marine Sciences Branch, Department of
Energy Mines and Resources, Ottawa who bore the brunt of the
tedious task of preparing this report for publication. Mr. F.G.
Barber for his never-failing assistance, Mr. M. Isabelle for
his excellent work in drafting and editing, Miss L. Britton and
Miss V. Freda for their cheerful cooperation with the typing.





MANUSCRIPT REPORT SERIES

No. 12

A Heat Budget of the Water in Barrow Strait for 1962

A. HUYER and F. G. BARBER



Marine Sciences Branch

Department of Energy, Mines and Resources

Ottawa, Canada

1970



Manuscript Report Series No. 12

EAST 73 11

A HEAT BUDGET OF THE WATER IN BARROW STRAIT FOR 1962

A. Huyer and F. G. Barber

The Queen's Printer for Canada Ottawa, 1970

CONTENTS

			Page
1.	Intro	oduction	1
2.	Disc	cussion of the budget	2
	2.1 2.2 2.3 2.4	Major limitations	3
3.	Ackı	nowledgements	10
4.	Refe	erences	11
5.	Appe	endix: Detail of the heat budget	17
	5.1 5.2	The heat budget equation	19 20
		5.2.1 Short-wave radiation	21 21 23 26
		5.2.2 Effective back radiation, Qb	26
	E 9	5.2.3. Net radiation balance, Qn	31 33
	ე. ა	Evaluation of the turbulent flux terms	33
		5.3.2 Sensible heat flux, Q _h	34
		5.3.3 Turbulent flux balance, Qt	36
	5.4	Total transport of heat across the air-sea boundary, QT	37
	5.5	Heat storage, Q_S	38
	5.6	Advected heat, $Q_V\dots$	41
	5 7	Glossary of symbols	42

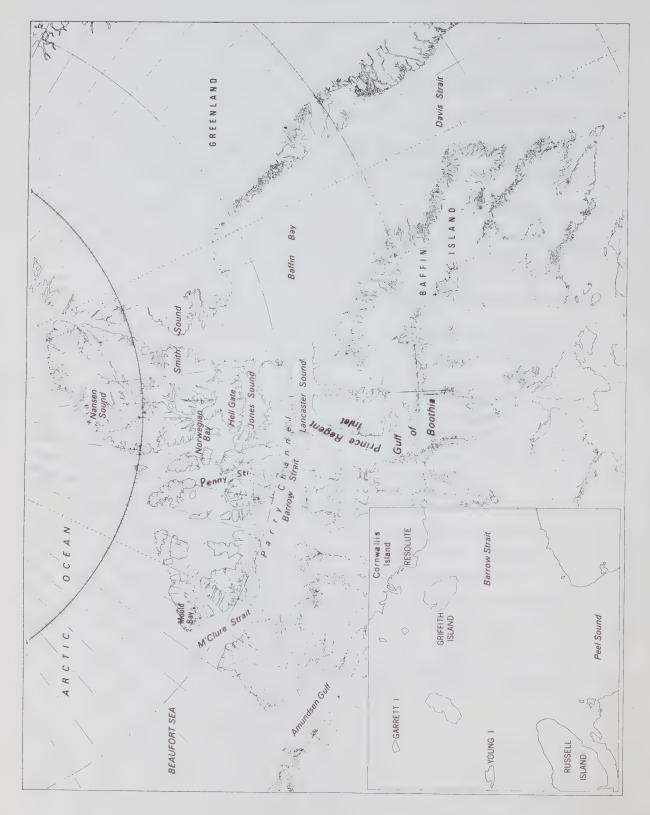


Fig. 1. Place names in the Canadian Arctic Archipelago.

1. INTRODUCTION

This assessment of the terms of the heat budget equation in Barrow Strait for 1962 was undertaken in connection with the study of oceanographic data observed in the Canadian Arctic during the navigation seasons of 1960, 1961 and 1962. Barrow Strait was selected as the area of study because radiation observations, as well as other meteorological data, are made at Resolute on nearby Cornwallis Island (Fig.1).

The oceanography and especially the water movements of the region are little known. It is considered (Collin, 1963; Collin and Dunbar, 1964) that a net water transport to the eastward occurs in Barrow Strait; however, the data are largely qualitative and, in the main, are restricted to the period of the navigation season (Collin and Dunbar, 1964). It is known (personal experience of one of the authors, F.G.B., in 1960 during a period of strong east wind) that a strong (2 knot) westward moving current can occur close inshore in Barrow Strait off Resolute, at least for short periods of 2 to 3 days. Bailey (1957, his figure 25 and table iv) inferred a small westward movement at the surface between Cornwallis and Griffith Islands with a general eastward movement throughout the remainder of Barrow Strait. Although icebergs have been observed as far west as Barrow Strait (Lindsay 1968, p 23) it is believed that the main surface drift is eastward.

Due to topography* this drift comprises water from the upper 150m in the Arctic Ocean. As this water is close to the freezing point it would be anticipated that the movement would contain little sensible heat. A consideration of the movement which likely occurs through Jones Sound and Smith Sound led to a similar conclusion, i.e. that water transport into Baffin Bay from the Arctic Ocean does not contribute significant sensible heat to Baffin Bay. This interesting hypothesis was another reason to locate the examination of the budget in Barrow Strait. Of course studies should also be made in the other areas (Jones and Smith Sounds) but they would be less meaningful because of the paucity of data there.

Thus, we are led to another reason for a heat budget study in an Arctic region which, and under the severe limitations which attend such studies generally, is further limited in the application through the lack of oceanographic data and hence understanding. It is clear that useful observa-

^{*} It is proposed to put off a detailed description of the bathymetric data and the likely influence of sill depth to another report. An examination of data obtained in CSS "Baffin" in 1962 in Barrow Strait (CHS field sheet 3182) indicates that the maximum sill depth probably does not exceed 130m (71 fathom) and that it likely exists in the section Russell to Young Islands, although there is a portion in the section Garrett Island to Bathurst Island not yet surveyed in which a deeper threshold may occur. Coupling with the Arctic Ocean may also occur to the north, via Wellington Channel, and to the south via Peel Sound, where from quite limited data the threshold depths appear to be 100m and 146m respectively.

tions will depend on the extent to which presently available material can be exploited. This may require considerable speculation initially and indeed the consideration of a number of assumptions quite impossible to assess even in the near future. No doubt a considerable modification will occur in a heat budget as presented here; it is partly for this reason that it is presented in some detail.

2. DISCUSSION OF THE BUDGET

The detail of the energy budget of the water of Barrow Strait, 1962 is presented in the Appendix. It is attempted there to estimate the monthly means of each of the terms in the heat budget equation. It is concluded that the total energy transfer at the surface in 1962 was a gain of 3.0 x 10 ly (3.0 kg-cal/cm²) to the water. Although the magnitude and even the sign of the balance remain in some doubt, some speculative conclusions can be drawn from the results.

2.1 Major limitations

The heat budget is not complete; it was not possible to obtain monthly estimates of the heat storage and hence the advected heat. The data needed to estimate heat storage include temperature-depth profiles of the water and the ice at regular intervals as well as the ice thickness data now available (Anon., 1962; 1963a). It is important to observe the water temperatures throughout the year; the temperature profile of the ice can be estimated without greatly increasing the error in the budget.

The balance obtained is limited by uncertainties in each term of the budget; these are discussed to some extent in the Appendix. Each of the surface heat fluxes depends on the ice cover so the error of the balance depends partly on the accuracy of ice concentration estimates. The error in estimating the concentration from aerial ice survey charts is probably about 10% and may sometimes be as high as 20%. It was assumed that during the winter the ice cover was complete. This may not be a good approximation; Dunbar (1954) in a representation of winter ice conditions shows eastern Barrow Strait to have some "semi-permanent open patches", and on May 21, 1964 (late winter) an area of open water was observed in this region (Anon, 1967a). It is not known how often such open areas occur. Since none were observed during the survey flights of April or May 1962 it was thought that assuming a complete ice cover from November to May was not unreasonable.

The heat balance is further limited by the lack of knowledge about ice transport. It is generally considered that the Arctic Ocean is a source of ice; Vowinckel and Orvig (1961) listed estimates of the annual ice export from the Arctic Ocean which range from ten to sixty percent of the ice formed and suggested that about twenty percent seems reasonable. There is little doubt that a portion of the ice which exists in Barrow Strait formed to the westward and northward. As well some of the ice which moves eastward out of Barrow Strait into Lancaster Sound formed in Barrow Strait. At the present time there do not appear to be any definitive data which would allow a quantitative assessment of this aspect. For the purpose of the budget it is as-

sumed that the surface ice condition throughout 1962 in Barrow Strait was due to ice formed within the strait. The aerial ice survey charts (Black, 1965; Anon., 1963b) suggest this is not unreasonable. Lindsay (1968, p40) estimated* the ice import in 1966 to be much greater than the export; he considered (p 39) that year to be "a normal, 'average', or typical ice year".

It was not possible to provide a realistic error estimate of the heat balance obtained in the Appendix. The magnitude of the error introduced by the assumptions concerning ice transport is completely unknown; it will only be possible to estimate it when the transports are known. There are also a number of terms in the heat budget for which no error estimate could be provided. No authoritative estimate of the error of the radiation observations is known to the authors; the precision appears to be high (section 5.2.1.1) but the accuracy is unknown. The albedo was derived from ice concentration estimates with about a 10% error, and a number of quite subjective criteria whose error can only be determined by more frequent measurements of the albedo. Neither the sensible heat flux nor the evaporation have been measured in this area, except for brief periods (Champ, 1965); again no realistic error estimate was possible. It is realized that the significance of any balance obtained is limited by this lack of error estimate.

2.2 Ice breakup

Ice formation and breakup are the results of the interaction of a variety of meteorological and oceanographic parameters. Currents and tidal streams often play a part in determining breakup patterns. The salinity of the water determines its freezing point. Air temperatures cause cooling or heating, i.e. growth or melt of the ice. The short-wave radiation from the sun causes heating and may be the heat source needed for melting. Wind stresses can cause cracks and leads, and ridging - contributing either to breakup or consolidation of the ice. These factors appear to contribute to breakup at different rates in various seasons, so that the condition at the surface may vary considerably from year to year.

Markham (1962) earlier had indicated that he considered the mean wind flow was significant in summer breakup patterns and that departures from normal temperatures were relatively unimportant. Some revision of this view seems to have occurred (Markham and Hill, 1963) in consideration of the distribution of sea ice in the summer of 1962. It is shown in the following that above normal air temperatures may be important.

* He estimated the area of ice imported and exported from Barrow Strait in 1966 as follows:

	Imports	Exports
	km ²	km ²
June July August Sept.	nil 6860 2500 1000	nil 1000 nil nil

The area of Barrow Strait was given as 25810 km². It is not known how reliable these estimates are.

In 1963, Lancaster Sound remained congested until mid-August and heavy ice obstructed passage from Lancaster Sound to Barrow Strait throughout the month. Usually these passages are open before the middle of August (Markham, 1963). In Baffin Bay, too, breakup was a month later than normal by mid-August (Hill, Cooper, and Markham, 1965). However, in the western Arctic, conditions were more open than usual. The clearing of Amundsen Gulf was the earliest reported since records began in 1953.

In 1964, Lancaster Sound had open water considerably earlier than normal. Baffin Bay remained more congested than normal. In the western Arctic, the extreme lateness of breakup in Amundsen Gulf was outstanding. Both the 1963 and 1964 ice distributions are attributed to the atmospheric pressure patterns (Anon., 1967 a, p 74):

In 1963, breakup was delayed in eastern Parry Channel by unfavourable winds and the lower than average frequency of lows in the area. In 1964 the reverse pattern had a similar effect on the western Arctic coast.

The dependence of the ice distribution on winds and thus on pressure patterns observed in 1963 and 1964 was noticeable partly because of the low air temperatures that prevailed. For both years the June, July and August temperatures were below normal. Because of these low air temperatures, thawing was only a minor factor in breakup, and the effects of winds and pressure systems were dominant. These effects have more influence on the distribution of ice than on the amount of it. Thus in a year when wind stresses are important we expect some open areas, and some very congested areas, as the wind stresses will cause the ice to move but not to melt. Such distributions were observed in both 1963 and 1964. In the former, the eastern Arctic was congested while the western channels were more open than usual. In 1964 the opposite was observed; Lancaster Sound was open while the western Arctic was congested.

In contrast to both the 1963 and 1964 seasons, the ice concentrations observed in 1962 were light throughout the Arctic Archipelago. Markham and Hill (1963) point out that "the extent of breakup in 1962 was greater than any summer of the past decade". When breakup is so widespread, it is not likely that wind speed or direction is the major factor in breakup, since this causes inhomogeneous ice conditions, as already mentioned. If breakup is widespread, the amount of ice must be considerably decreased, and it is likely that thawing is the more important factor in breakup.

The unusually high degree of breakup in 1962 was quite widespread* and it seems likely that more thawing than usual occurred. As the main

*Lindsay (1968, p.10) gave the percentage area of ice in the queen Elizabeth Islands at the end of the summer months for 1962, 1964 and 1966:

1962	June	July	August	September
	87	48	32	65
1964	90	85	72	79
1966	92	80	67	82

sources of heat available for melting are the absorption of short-wave radiation and sensible heat flux from the atmosphere, above normal thawing must be the result of either unusually high incident radiation or above normal air temperatures, or both. In 1962 both these conditions were observed. The effect of air temperatures on breakup is often discussed in terms of the thawing index (Markham, 1960; Thompson, 1963). This thawing index is the cumulative sum of melting degree-days where for each day the number of melting degree-days is defined as the excess in Fahrenheit degrees of the mean temperature over 32° F. For example when the mean temperature for one day is 40° F, the number of melting degree-days for that day is eight.

At Resolute, the mean thawing index is 495 melting degree-days for the season (H.A.Thompson, personal communication). The lowest index was observed in 1964 (200 melting degree-days) and the highest thawing index for the season was observed in 1958 (888 melting degree-days). 1962 has the second highest thawing index for the whole season (710 melting degree days). Once a region of open water has formed, thawing air temperatures contribute to a rise in temperature of the water rather than to continued ice-melt. Thus, it is more meaningful to consider the number of melting degree-days prior to breakup than the thawing index for the whole season. A large fraction of the melting degree-days in 1958 were accumulated after conditions of open water prevailed in Lancaster Sound, because of above normal August temperatures. In 1962 August temperatures were near normal. The number of thawing degree-days accumulated in June and July, that is before ice breakup, was highest in 1962. There then appears to be some correlation between a large extent of breakup and above normal air temperatures prior to breakup.

One way in which these temperatures can be brought about during a winter has been described by Thomas and Titus (1958) who concluded (p22):

A study of the normal temperature pattern during January in the Canadian Arctic indicates that the eastern coast adjoining Davis Strait and Baffin Bay often has much warmer temperatures than can be expected in the western Arctic. Besides the moderating effect of the water and ice, this coastal area is also subjected to maritime Arctic and maritime polar air thrusts from the south as low pressure systems move northward to the west of Greenland. The amount and extent of the warm air moving into the Arctic varies directly as the intensity and location of the cyclonic activity. On occasions when the surface low pressure system moves in a west-northwesterly direction across the top of Hudson Bay, the warm sector of the depression is extensive enough to move the warm air north not only over Baffin Bay but also over and to the west of Baffin Island. That is what occurred on January 19-24, 1958 and as a result the north-eastern Arctic experienced some abnormally high wintertime temperatures.

Such a circumstance may have occurred in the early summer* of 1962. According to Markham and Hill (1963, p3):

On the July mean pressure chart there was a low near Churchill, a smaller low over the Gulf of St. Lawrence and a flat ridge over Greenland and the Arctic Archipelago... The resulting extensive area of southeast winds gave above normal temperatures over the whole region...

Although air temperatures are important, the absorption of short-wave radiation is a much larger heat source than the sensible heat flux from the atmosphere, especially during the months immediately preceding breakup (See Figures 8 and 9). In July 1962 the amount of cloud was lower than normal (Table 1, Appendix) causing a higher than normal value for the incident short-wave radiation. The 1962 value was 557 gram calories per square centimeter per day, i.e. langleys per day (ly/day) for July; the normal is 456 ly/day. However, only the absorbed short-wave radiation can contribute to thawing. Thus it is necessary to examine the albedo as well. If the albedo is very high, say .90, then the difference in absorbed radiation becomes quite small - only about 10 ly/day. The difference is more important when a low albedo coincides with a high value of the incident radiation.

Before breakup begins, the albedo is dependent on the condition of the ice or snow surface. Havens (1964) found that the albedo increased during periods of snow fall and decreased during periods of melt. In 1962, measurable snow fell on only two days in June. This is less frequently than normal, and would tend to keep the albedo below normal. The early onset of melting (June 4; the mean for 1950-1965 is June 13) will also cause the albedo to be lower than usual since it drops sharply when the air temperature rises above 0°C (Langleben, 1966). After breakup begins, the albedo also depends on the concentration of ice left in the region. As the Arctic Ocean is a source of ice, and as, it is generally believed, a persistent water movement occurs through the waterways of the Archipelago from the Arctic Ocean to Baffin Bay it may be concluded that part of the ice in Barrow Strait originated in the Arctic Ocean. To what extent this occurs on the average or in an individual year is little known except perhaps for the 1962 season. Black (1965) provided a detailed description of ice movement which strongly suggests that less ice was advected into Barrow Strait than usual and that therefore the albedo was lower than usual. Combined with the high incident short-wave radiation this means that the absorbed radiation in 1962 was much higher than usual, and contributed much to the rate of thawing. Thus, the rate of thaw in 1962 was much higher than normal influencing the timing and extent of ice breakup that year.

Although the early breakup and its great extent in 1962 were largely due to the combination of high insolation and melting air temperatures, the correlation between breakup and radiation and air temperature will not be apparent every year. When the air temperatures remain below freezing, the influence of above normal radiation will be limited, because the albedo of

^{*}It is believed that the phenomenon occurred in March of 1962 but it is not considered significant in terms of the summer ice cover.

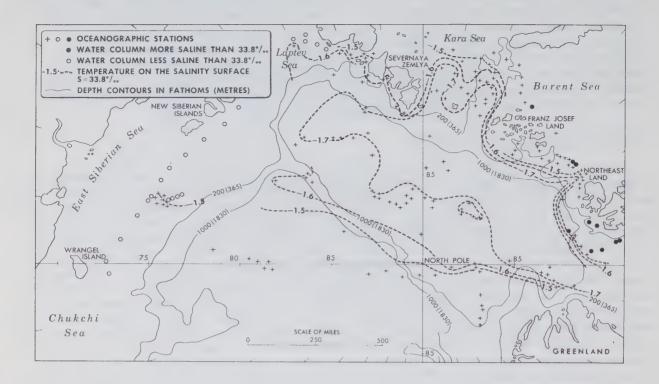
melting snow is much lower than that of a stable snow cover. When thawing is slower than normal, the effects of winds, currents and tides become more apparent, as was seen in 1963 and 1964. Thus, low thawing indices and low insolation in any given area do not necessarily cause congestion of ice, as breakup can occur by means other than melting. It is concluded, however, that much above normal air temperatures and higher than normal radiation, in combination will usually cause early breakup and relatively open water conditions. It is also concluded that in 1962 more seasonal heat than usual was absorbed by the surface water in Barrow Strait.

2.3 Oceanographic consequences

Generally in ice covered regions at high latitude a surface energy budget shows that a deficit in the radiative and flux terms occurs at the water surface. The deficit is usually small and generally balanced by an advection of warmer water (heat) into the region from lower latitude. For the Arctic Ocean, this deficit has been estimated by several authors; the most likely estimate seems to be 1.6 x 10³ ly/year (Untersteiner, 1964: Fletcher, 1965). It is met by the inflow of Atlantic water which remains in the Arctic Ocean six to eight years and during this time is somewhat modified due to the cooling at the surface (Coachman and Barnes, 1963). This longer term modification is superimposed on the seasonal cycle. Seasonal changes occur in the surface layer only; the modification due to the surface deficit extends to great depths. In the heat budget of Barrow Strait no annual deficit occurred. Consequently no net cooling of the water occurs and no advection of heat into the region is required. In the budget it was found that in 1962 a small surplus occurred at the surface. If this is usual, some heat must be advected out of the region but the amount will be small. It seems likely that there is usually no significant surplus or deficit in Barrow Strait, and that this is true over much of the water in the Canadian Arctic Archipelago. It follows that the observed vertical distribution of temperature and salinity at a position there is due to advection into the area and to mixing processes within the area. This implies that the observed distributions are nearly conservative even at relatively shallow depths.

Coachman and Barnes (1962) described the characteristics of the surface water in the Eurasian Basin of the Arctic Ocean and utilized the distribution of temperature and depth at 33.8% (Fig.2). They argued that water at 33.8% was part of the surface layer and that it moved out of the Arctic Ocean in the passage between Greenland and Spitsbergen. In their presentation the water at 33.8% close to Greenland is not warmer than -1.5°C. The temperature and depth of the 33.8% surface within the Archipelago were calculated from data obtained mainly in 1962 (Fig.3). West and north of the sills in Barrow Strait, Penny Strait (Fig.1) and Hell Gate the 33.8% surface is relatively shallow and warm. In M'Clure Strait the depth is about 150m; in Nansen Sound and Norwegian Bay it is about 100m. In most of the Archipelago the temperature is about -0.9°C; it is warmest in Norwegian Bay and Jones Sound (about -0.70c). Towards the Canadian Basin and Beaufort Sea temperatures were about -1.2°C while in Lancaster Sound and northern Baffin Bay they were colder at about -1.5°C. It is believed that the area of warmer water on the 33.8% surface within the Archipelago is due to the increased mixing which would occur in such a coastal area (as opposed to oceanic)*,

^{*} It is interesting to note that the warmest water on the 33.8% surface occurs in the vicinity of Hell Gate where mixing is probably more vigorous because of the topography of the strait and the strong current through it.



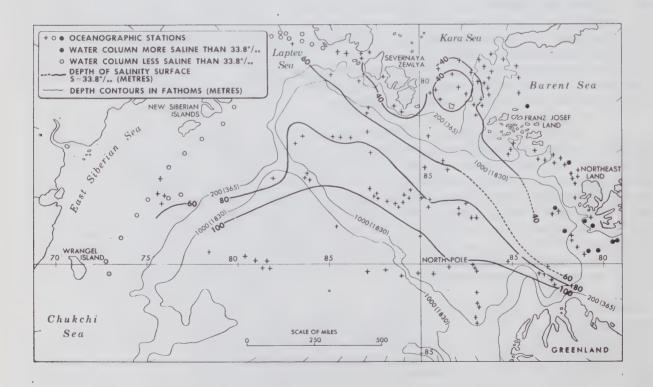
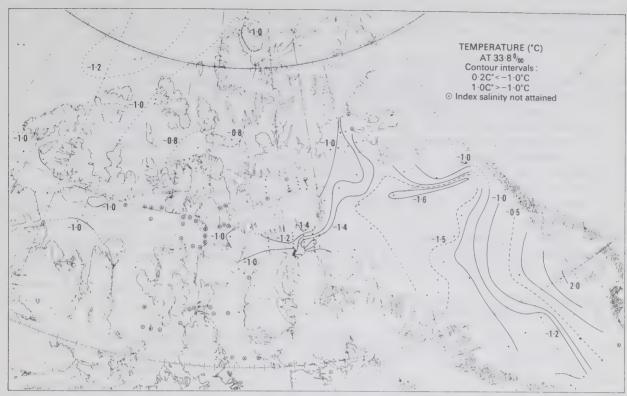


Fig. 2. Temperature and depth of the 33.8% surface from Coachman and Barnes (1962, their figures 7 and 8).



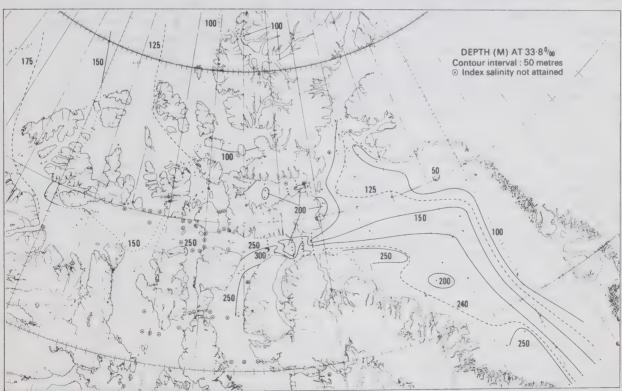


Fig. 3. Temperature and depth of the 33.8% surface in the Canadian Arctic based on 1962 data from CCGS "Labrador" (Anon., 1967b), CCGS "John A. MacDonald" (Anon., 1966c) and Ice Camps (Herlinveaux, 1963) and on data from Ice Pack, 1961 (Herlinveaux, 1961) and a few stations of the 1954 "Labrador" survey provided by the Canadian Oceanographic Data Centre.

the existence of relatively warm Atlantic water at depth below 33.8%, and a lack of net cooling at the surface as suggested by the heat budget.

In this it is assumed that in the region of the Archipelago westward of Barrow Strait and Jones Sound an advection of water occurs out of the Arctic Ocean. Eventually the water moves via Barrow Strait and Jones Sound into Baffin Bay. With knowledge of the threshold depths in these regions and the distributions within the surface layer of the Arctic Ocean one is led to the view, expressed here in the Introduction, that no significant sensible heat is transported with this advection. However, because of the coastal mixing which takes place, the temperature distribution is modified so that some warm water occurs at depths less than the sill depths and sensible heat may be transported with the advection. If the surplus of heat at the surface of Barrow Strait is usual, then it is also advected eastward. There is some evidence that this warm water is cooled in Lancaster Sound and Baffin Bay where some open water occurs during the cooling period of each year and a deficit in the radiative and flux terms occurs at the surface.

2.4 Suggestions for future work

One of the purposes of oceanographic heat budgets is to study the transport using the estimate of the advected heat. Although an annual estimate for the advected heat out of Barrow Strait, 1962, was obtained it was not possible to calculate the transport because the temperature data were too scarce. It is suggested that bathythermograph data be obtained in sections across the eastern and western ends, and across the entrances of Wellington Channel and Peel and McDougall Sounds for most of the shipping season. From such data it should be possible to estimate the change in temperature of water moving through the strait, and hence to estimate the transport. It is also suggested that temperature observations be made throughout the strait during an entire shipping season so that the heat storage and hence the advected heat can be estimated on a monthly basis, at least from July to October.

It was suggested in the previous section that coastal mixing is important in determining the structure of water moving through the Archipelago. It is suggested that a study be made of the vertical temperature and salinity distributions between the Arctic Ocean and Baffin Bay to see whether these properties are in fact conservative, as implied by the small annual surface energy balance. In such a study sill depths and known seasonal or sporadic variations in structure should be considered. The effects of winds and pressure patterns should also be examined. It is hoped that such studies will result in a model of the circulation through the Archipelago.

3. ACKNOWLEDGEMENTS

A considerable portion of the observations used originated with the Meteorological Branch of the Department of Transport; Mr. H.A.Thompson of the Meteorological Branch provided useful information and advice. The illustrations were prepared by Mr. Maurice Isabelle. Dr. G.L.Pickard read the manuscript and provided a critical review.

4. REFERENCES

- Anderson, E. R. 1952. Energy budget studies. Water loss investigations
 Lake Hefner Studies Tech. Rept., U.S. Geological Survey. Professional Paper 269, 71-117.
- Anonymous. undated, a. Monthly radiation summary.

 Meteorological Branch, Department of Transport, Canada.
 - undated, b. Arctic summary. Meteorological Branch, Department of Transport, Canada.
 - undated, c. Monthly record of meteorological observations in Canada. Meteorological Branch, Department of Transport, Canada.
 - undated, d. Monthly bulletin. Canadian upper air data. Meteorological Branch, Department of Transport, Canada.
 - 1962. Ice thickness data for selected Canadian stations, freeze-up 1961 break-up 1962. Meteorological Branch, Department of Transport, Canada. Cir. 3711. 24 pp.
 - 1963 a. Ice thickness data for Canadian selected stations, freeze-up 1962 break-up 1963. Meteorological Branch, Department of Transport, Canada. Cir -3918. 29 pp.
 - 1963 b. Aerial ice observing and reconnaissance, Queen Elizabeth Islands, 1962. Meteorological Branch, Department of Transport, Canada. Cir-3869. Ice -9. 57 pp.
 - 1963 c. Five Arctic surveys, Canadian Oceanographic Data Centre. 1963 Data Record Series. No. 4. 90 pp.
 - 1966 a. Normal cloud statistics. Meteorological Branch, Department of Transport, Canada. CDS #3 -66.
 - 1966 b. Mean radiation. Meteorological Branch, Department of Transport, Canada. Monthly Radiation Summary, December.
 - 1966 c. Arctic, Hudson Bay and Hudson Strait, August 5 October 4, 1962. Canadian Oceanographic Data Centre. 1966 Data Record Series, No. 4. 297 pp.
 - 1967 a. Ice summary and analysis, 1964, Canadian Arctic. Meteorological Branch, Department of Transport, Canada. 79 pp.
 - 1967 b. Baffin Bay 1962, September 25 to October 24, 1962. Canadian Oceanographic Data Centre. 1967 Data Record Series No.4 169 pp.
 - 1967 c. Mean daily net radiation. Meteorological Branch, Department of Transport, Canada. Monthly Radiation Summary, December.

- Badgley, F.I. 1961. Heat balance at the surface of the Arctic Ocean.

 Proceedings. Western Snow Conference. Spokane, Washington, 101-104.
- Bailey, W.B. 1957. Oceanographic features of the Canadian Archipelago. J. Fish. Res. Bd. Canada, 14 (5): 731-769.
- Barber, F.G. 1967. A contribution to the oceanography of Hudson Bay.

 Marine Sciences Branch. Department of Energy, Mines and Resources,

 Manuscript Report Series No. 4. 69pp.
- Black, W.A. 1965. Sea-ice survey, Queen Elizabeth Islands regions, summer 1962. Geographical Branch, Department of Mines and Technical Surveys, Geographical Paper No. 39. 44 pp.
- Budyko, M.I. 1956. The heat balance at the earth's surface. Teplovoi balons zemmoi poverkhnosti. Gidrometeorologicheskoe izdatelstvo, Leningrad. 255 pp. (Translated by Nina A. Stepanova, U.S. Weather Bureau, 1958).
- Champ, Donald Hillis. 1965. The energy budget at Resolute, N.W.T. A twenty-four study during the polar night. Unpublished thesis. University of Toronto. 155 pp.
- Coachman, L.K. and C.A.Barnes. 1962 Surface water in the Eurasian Basin of the Arctic Ocean. Arctic 15 (4): 251-277.
 - 1963. The movement of Atlantic water in the Arctic Ocean. Arctic 16 (1): 8-16.
- Collin, A.E. 1963. The waters of the Canadian Arctic Archipelago. Proceedings of the Arctic Basin Symposium, October 1962, Hershey, Pa. 128-136.
 - and M.J.Dunbar. 1964. Physical oceanography in Arctic Canada. Oceanogr. Mar. Biol. Ann. Rev. 2: 45-75.
- Dunbar, Moira. 1954. The pattern of ice distribution in Canadian Arctic seas. Transactions of the Royal Society of Canada. Vol 28: Series III: 9-18.
- Fletcher, J.O. 1965. The heat budget of the Arctic Ocean and its relation to climate. The Rand Corp. R-444-PR. 178 pp.
- Haltiner, George J., and Frank L. Martin. 1957. Dynamical and Physical Meteorology. McGraw-Hill, New York. 470 pp.
- Hanson, K.J. 1961. The albedo of sea-ice and ice islands in the Arctic Ocean basin. Arctic 14 (3): 188-196.
- Havens, J.M. 1964. Meteorology and heat balance of the accumulation and McGill Ice Cap, Canadian Arctic Archipelago summer 1961. Axel Heiberg Research Report, Meteorology No. 3. 87 pp.

- Herlinveaux, R.H. 1961. Data record of oceanographic observations made in Pacific Naval Laboratory underwater sound studies, 1961.

 Fisheries Research Board of Canada. Manuscript Report Series (Oceanographic and Limnological) No. 108. 85 pp.
 - 1963. Oceanographic observations in the Canadian Basin, Arctic Ocean, April-May, 1962. Fisheries Research Board of Canada. Manuscript Report Series (Oceanographic and Limnological) No. 144. 25 pp.
- Hill, R.H.W., A.B.Cooper and W.E.Markham. 1965. Ice conditions in the Canadian Arctic during the summer shipping season, 1963.

 Meteorological Branch, Department of Transport, Canada. Cir-4188, Tec-558. 10 pp.
- Laevastu, T. 1960. Factors affecting the temperature of the surface layer of the sea. Soc. Scient. Fennica, Comment. Physico-Mathem. 25(1). 136 pp.
- Langleben, M.P. 1966. On the factors affecting the rate of ablation of sea ice. Canadian Journal of Earth Sciences. 3(4): 431-439.
- Latimer, J.R. 1962. Laboratory and field studies of the properties of radiation instruments. Meteorological Branch, Department of Transport, Canada. Cir-3672, Tec. 414. 16 p.
- Leahey, D.M. 1966. Heat exchange and sea-ice growth in Arctic Canada.

 McGill Marine Sciences Centre, Manuscript Report No. 1. 48 pp.
- Lewis, E.L. 1967. Heat flow through winter ice. Physics of ice and snow. Proceedings of the International Conference on Low Temperature Science, 1966. Vol. 1. Edited by Hirobumi Oura. Hokkaido University. Sapporo, Japan. 611-631.
- Lindsay, D.G. 1968. Ice distribution in the Queen Elizabeth Islands. Paper presented at the Ice Seminar. Petroleum Society of the Canadian Institute of Mining and Metallurgy and the American Petroleum Institute, Rocky Mountain District, Calgary, May 6-7, 1968. 47 pp.
- Lonnqvist, O. 1954. Synthetic formulae for estimating effective radiation to a cloudless sky and their usefulness in comparing various estimation procedures. Ark. Geofys. 2(12): 247-94.
- Markham, W.E. 1960. Freezing and melting degree-day computations in spring and fall months. Meteorological Branch, Department of Transport, Canada. Cir-3350, Tec-325.
 - 1962. Summer breakup patterns in the Canadian Arctic, Meteorological Branch, Department of Transport, Canada. Cir-3586, Tec-386.
 - 1963. Preliminary study of ice conditions in Barrow Strait and Lancaster Sound during June, July and August 1963. Meteorological Branch, Department of Transport, Canada. Cir-3900, Tec-481.

- Markham, W.E. and R.H.W.Hill, 1963. Sea ice distribution in Canadian Arctic waters, summer 1962. Meteorological Branch, Department of Transport, Canada. Cir-3824. Tec-463. 12 pp.
- Mateer, C.L. 1955. Average insolation in Canada during cloudless days. Can. J. Technol., 33: 12-32.
- Milne, A.R. 1960. Shallow water under-ice acoustics in Barrow Strait, J. Acoust. Soc. Am., 32: 1007-1016.
- Mosby, Hakon. 1963. Water, salt and heat balance in the north polar sea, Proceedings of the Arctic Basin Symposium, October 1962.

 Arctic Institute of North America.
- Rae, R.W. 1951. Climate of the Canadian Arctic Archipelago. Met. Branch.

 Dept. of Transport, Canada. Toronto. 90 pp.
- Schule, John J., Jr., and Walter I. Wittman. 1958. Comparative ice conditions in North American Arctic, 1953 to 1955 inclusive. Transactions, American Geophysical Union 39 (3): 409-419.
- Swinbank, W.C. 1963. Long-wave radiation from clear skies. Quarterly Journal of the Royal Meteorological Society. 89 (381): 339-348.
- Tabata, S. 1964. A study of the main physical factors governing the oceanographic conditions at ocean station "P" in the Northeast Pacific Ocean. Unpublished thesis. University of Tokyo.
- Thomas, Morley K., and R.L.Titus. 1958. Abnormally mild temperatures in the Canadian Arctic during January 1958. U.S.Weather Bureau. Monthly Weather Review. 86(1): 19-22.
- Thompson, H.A., 1963. Air temperatures in northern Canada with emphasis on freezing and thawing indexes. Proceedings. International Conference on Permafrost, Lafayette, Indiana, 1963. N.A.S. N.R.C. Publication No. 1287: 272-280.
- Untersteiner, N. 1964. Calculations of temperature regime and heat budget of sea ice in the central Arctic. Journal of Geophysical Research 69 (22): 4755-4766.
- Vowinckel, E. 1966. The surface heat budgets of Ottawa and Resolute, N.W.T.

 McGill Arctic Meteorology Research Group. Publication in

 Meteorology, No. 85. 27 pp.
 - and S. Orvig, 1961. Water balance and heat flux of the Arctic Ocean, McGill Arctic Meteorology Research Group. Publication in Meteorology No. 44. 35 pp.
 - 1964. Energy balance of the Arctic II. Long wave radiation and total radiation balance at the surface in the Arctic. Arch. Met. Geoph. Biobl. B. Bd. 13, H.4. 451-479.
- Vowinckel, E., and B. Taylor, 1964. Evaporation and sensible heat flux over the Arctic Ocean. McGill Arctic Meteorology Research Group. Publication in Meteorology No. 66. 30 p.

- Walmsley, J.L. 1966. Ice cover and surface heat fluxes in Baffin Bay. McGill Marine Sciences Centre. Manuscript Report No. 2.
- Williams, G.P. 1959. Evaporation from snow covers in eastern Canada. National Research Council, Division of Building Research. Research Paper No. 73. 10 pp.
- Yamamoto, G. 1952. On a radiation chart. Scientific Reports, Tohoko University, Series 5 Geophys. 4(1).



APPENDIX

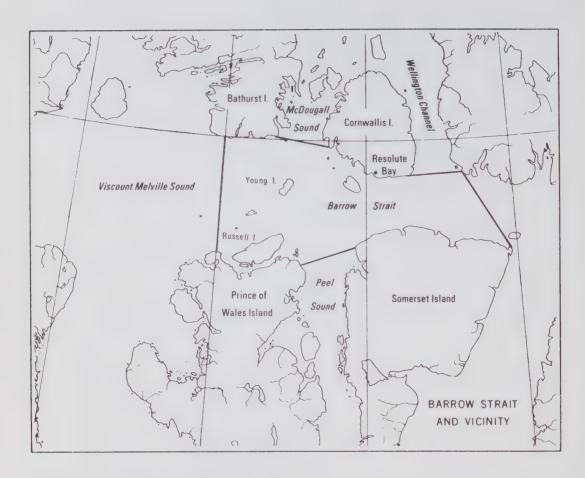


Fig. 4. The boundaries of Barrow Strait used in the heat budget, as defined by the Meteorological Branch in aerial ice survey reports (Anon., 1963b), and place names in the vicinity.

DETAIL OF THE HEAT BUDGET

5.1 The heat budget equation

A heat budget is an application of the principle of conservation of energy. In any arbitrary system the energy gained by the system from its surroundings is equal to the energy lost to its surroundings plus the energy stored in the system. In order to speak of heat fluxes between the system and its surroundings, it is necessary to choose boundaries for the system. In this study the system is the volume of sea water and ice in Barrow Strait. The lower boundary is the floor of the strait. Arbitrary lateral boundaries are shown in Fig. 4; the system is surrounded by Cornwallis Island, McDougall Sound, Bathurst Island, Viscount Melville Sound, Prince of Wales Island, Peel Sound, Somerset Island, Lancaster Sound and Wellington Channel. When there is no ice cover, the upper boundary is the air-sea interface; when the ice cover exists the upper boundary is chosen to be the air-ice interface, i.e. the sea-ice is part of the system.

The advected heat is the net heat exchange which accompanies the exchange of water or ice between Barrow Strait and the adjacent channels. If there is no net import of ice and if the mass of water flowing out is equal to that flowing in, then there is no net transport of the latent heat of fusion, and it need not be included in the advected heat. If there is a net import or export of ice but the total mass exchange is zero* then the advected heat must include the latent heat of the ice surplus or deficit. This advected latent heat is positive when there is a net export of ice from the region. In this heat budget it was assumed that there was no net import or export of ice in Barrow Strait.

Since the ice is included in the system, heat storage occurs in the ice as well as in the water. Heat storage in ice includes the heat utilized in melting or freezing at the top and bottom of the ice sheet and temperature changes of the ice. In long term heat budgets, the heat storage term is assumed to be zero; no net long term heating or cooling of the water is observed, and the ice thickness does not noticeably increase over the years. In short term budgets however, e.g. when monthly estimates of the terms are obtained, the heat storage in the ice must be included in the total heat storage.

Radiation incident on the air-sea boundary, $\mathbb Q$, is the chief gain of heat to the volume. The incident radiation is short-wave; part of it, $\mathbb Q_r$, is

^{*} It is conceivable that over short periods mass exchange may occur whereby the mass of the system is not conserved. If some of the water flowing into Barrow Strait freezes and becomes part of the ice cover and if the ice is landfast or moves more slowly than the water, there may be an increase in the mass of the system. The excess mass would be removed several months later when the ice melts and the outflow is greater than the inflow. For short term budgets, the latent heat of the water surplus or deficit should be included in the advected heat. It is not known whether such deficits or surpluses occur.

reflected at the surface, leaving an amount of \mathbb{Q}_a of absorbed short-wave radiation. The surface radiates in the long-wave region, as does the atmosphere; the balance between them is known as effective back radiation, \mathbb{Q}_b . These radiative terms add to give the net radiation, \mathbb{Q}_n :

$$Q_{n} = Q_{n} - Q_{n} \tag{1}$$

Turbulent heat fluxes, $\mathbb{Q}_{\mathbf{t}}$, occur as heat of evaporation, $\mathbb{Q}_{\mathbf{e}}$, and as sensible heat flux, $\mathbb{Q}_{\mathbf{h}}$:

$$Q_{t} = Q_{e} + Q_{h} \tag{2}$$

The total heat input through the air-sea boundary is:

$$Q_{\perp} = Q_{n} - Q_{\perp} \tag{3}$$

The advected heat, $\mathbb{Q}_{\mathbf{v}}$, is positive when it is a gain to the system. The heat conducted through the bottom of the strait is negligible. The change of heat storage of the system, $\mathbb{Q}_{\mathbf{s}}$, is the sum of the heat storage in the ice, $\mathbb{Q}_{\mathbf{i}}$, and in the water $\mathbb{Q}_{\mathbf{s}}$:

$$\mathcal{Q}_{s} = \mathcal{Q}_{1} + \mathcal{Q}_{\theta}$$
 (4)

Since heat is conserved,

$$Q_{\mathbf{v}} + Q_{\mathbf{v}} = Q_{\mathbf{s}} \tag{5}$$

This may also be written as

$$Q_{2} - Q_{1} - Q_{2} - Q_{1} - Q_{2} - Q_{1} + Q_{2} = 0.$$
 (6)

5.2 Evaluation of the radiative terms

There are two almost independent radiative terms, the absorbed short-wave radiation from the sun and sky, and the effective back radiation from the earth. The first is the difference between the incident short-wave radiation, Q, and the reflected radiation, Q, which depends on the albedo, A, of the surface:

$$Q_{r} = A Q \tag{7}$$

so that

$$Q_a = Q - Q_r = Q (1-A).$$
 (8)

The effective back radiation, $Q_{\rm b}$, is the difference between the long-wave radiation from the sea and that received from the atmosphere. The net radiation, $Q_{\rm n}$, is defined by (1).

5.2.1 The short-wave radiation

5.2.1.1 The incident short-wave radiation, Q

The Meteorological Branch of the Department of Transport publishes measurements of the incident short-wave radiation (also known as insolation) for Resolute (Anon., undated a). As little was known about the quality of the observations, data for the years 1962 to 1966 were examined in some detail.

Following a techinque described by Mateer (1955, p. 17) an insolation vs. time curve was obtained for days on which the cloud amount was reported as zero at each of the eight observation times. The cloud data (Anon., undated b) from January 1961 to June 1966 were examined. No cloudless days were observed in July, August, September or October, and only one was observed in June. For each cloudless day the observed insolation (Anon., undated a) was plotted (Fig.5). The scatter about the curve is very small - the deviation

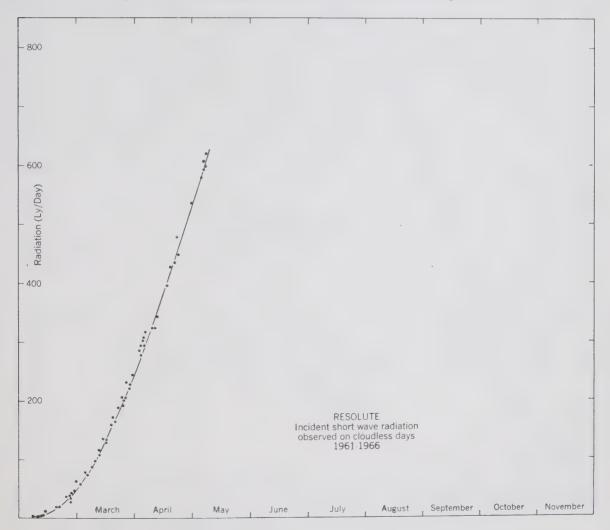


Fig. 5. Values of the short-wave radiation observed on cloudless days in 1962, 1963, 1964, 1965 and 1966.

of a point from the curve is usually less than 5%. Because of the lack of cloudless days in the later months of the year, certain of the other incident radiation data were also plotted. For 1962 the ratio of the diffuse shortwave to the total short-wave radiation was found. For each month a value was selected for which it was assumed that any larger ratio of diffuse to total radiation occurred on cloudy days. For the other years another criterion was used. Beginning in February, at first sunrise, days were chosen which had a higher insolation than any previous days. This selection process was applied to the data from February to June. In this period, increases of insolation from day to day are due to the increasing altitude of the sun; any decrease in the solar radiation can be attributed to cloud. For the rest of the year the data were examined in reverse order. The selected points were plotted in Fig.6. A symmetrical curve (Fig.7) drawn just below the highest points was obtained from the data of Fig. 6. Due to the increased cloudiness in the later half of the year, the curve is better defined from February to June than for the later months. It was found that the curve coincides well with the one obtained from data obtained on cloudless days (Fig.5). It may be inferred that Fig.7 shows the average insolation for cloudless days. The small scatter of short-wave

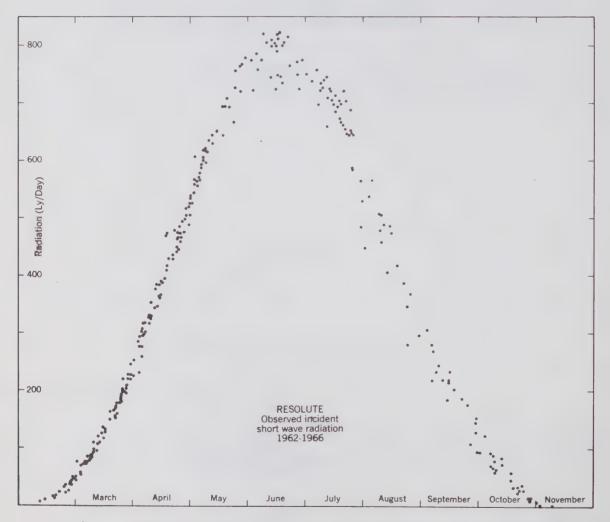


Fig. 6. Observations of the incident short-wave radiation at Resolute on days which were cloudless or had little cloud for the years 1961, 1962, 1963, 1964, 1965 and 1966.

radiation measurements on cloudless days implies that the precision of measurement is high. Direct measurements of $\mathbb Q$ are used in this energy budget. The monthly mean values of $\mathbb Q$ and of the cloud amount, $\mathbb C$, for 1962 (Anon., undated c) and the normals (Anon., 1966 a;b) are shown in Table 1. The low value of $\mathbb Q$ observed in June 1962 is accompanied by a higher than normal amount of cloud. In July 1962, $\mathbb C$ is much smaller than normal, resulting in a high value of $\mathbb Q$.

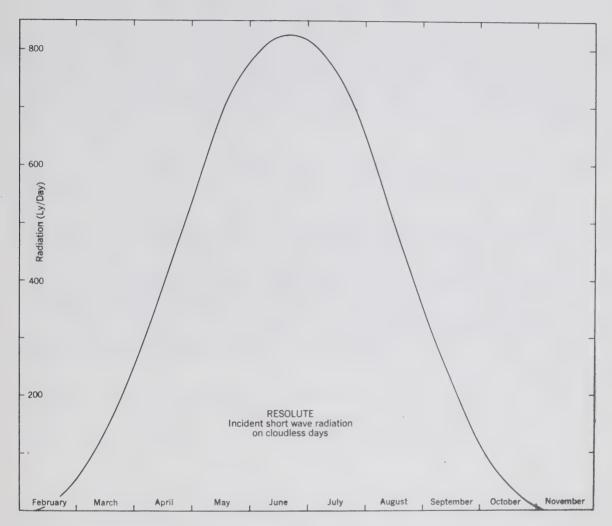


Fig. 7. The short-wave incident radiation on cloudless days, Q, obtained by finding the envelope of the points from February through June and assuming symmetry about the summer solstice.

5.2.1.2 The albedo, A

The albedo of any surface is defined as the ratio of radiation reflected from that surface to the radiation incident on it (7). Since the albedo of snow and ice is much different from the albedo of open water, the albedo of Barrow Strait depends on the concentration of ice, $I_{\rm c}$.

Table 1. Incident short-wave radiation, Q, in ly/day, and cloud amount, C, in fraction of sky covered, at Resolute. (i) Mean daily values of insolation during 1962. (ii) Mean daily solar insolation for 9 or 10 years, with standard deviation (iii). (iv) The cloud amounts observed in 1962. (v) The normal cloud amounts.

	J	F	М	A	M	J	J	A	S	O	N	D
(i)	()	17	120	369	570	533	557	294	118	28	4	0
(ii)	0	14	127	358	555	604	456	263	122	30	1	0
(iii)	0.0	2.2	8.1	12.1	26.4	37.7	47.6	39.6	10.3	3.8	0.5	0.0
(iv)	.24	.22	.52	.38	.77	.76	.50	.80	.88	.73	.36	.43
(v)	.39	.41	.40	.47	.69	.72	.75	.79	.82	.75	.46	.40

Table 2. Surface conditions and the albedo. (i) The estimated ice concentration, I, in fraction of surface covered. (ii) The number of observations from which I was estimated. (iii) The concentration of melt water puddles, P, as fraction of ice covered. (iv) The albedo for open water extrapolated from Budyko's table. (v) The albedo for open water from Anderson's equation (9). (vi) The albedo for observed ice concentration from Budyko. (vii) The albedo for observed values of P and I from Hanson's equation (10). (viii) The albedo at Resolute Airport from radiation measurements 1962. (ix) The albedo from mean radiation data for Resolute Airport. (x) The albedo accepted for Barrow Strait, 1962.

	J	F	М	А	M	J	J	A	S	()	N	D
(i)	1.0	1.0	1.0	1.0	1.0	0.7	0.4	0.1	0.1	0.9	1.0	1.0
(ii)	0	0	0	1	2	1	4	8	8	1	1	0
(iii)				0	0	.5	.7	.6	0	0	0	
(iv)					.10	.11	.10	.11	.15	.17		
(v)					.11	.09	.10	.12	.15	.30		
(vi)	.80	.80	.80	.80	.80	.20	1.3	.11	.15	.65	.80	.80
(vii)						.30	.15	.04	.03	.45		
(viii)		.65	.67	.66	.67	.32	.21	.20	.45	.71		
(ix)		.79	.74	.74	.72	.47	.24	.23	.45	.60		
(x)	.80	.80	.75	.75	.75	.30	.15	.11	.15	.55	.80	.80

The ice concentration and the amount of ice covered by melt-water puddles, P, was estimated for each month (Table 2) from aerial ice survey charts (Anon., 1963 b; Black, 1965) using the boundaries of the Barrow Strait region (Fig.4). The albedo of open water varies with the altitude of the sun for direct radiation, while it is almost constant for diffuse radiation, so that A for open water depends on cloud as well as the altitude of the sun. Anderson (1952) developed a formula for the albedo of Lake Hefner in terms of the mean altitude, \bar{h} , of the sun:

$$A = a \bar{h} b \tag{9}$$

where a and b are empirical constants depending on the cloud conditions. The albedo for open water in Barrow Strait was obtained (Table 2) from this formula using a = 0.78 and b = -0.68 for the mean summer cloud conditions at Resolute. It was also estimated (Table 2) by extrapolation from a table presented by Budyko (1956, p40) which shows A for each month for latitudes up to 70° N.

The albedo for snow and ice is also variable but does not seem to depend on cloud amount (Langleben, 1966). According to Budyko (1956, p37) the albedo for a stable snow cover north of 60° N is 0.80; for an unstable snow cover, the albedo is 0.45; the albedo of sea ice is 0.35. Williams (1961) estimated the following albedos: for new snow 0.8 to 0.9; for old snow 0.6 to 0.8; for melting snow 0.4 to 0.6 and for ice 0.4 to 0.5.

Using the estimated ice concentrations, I, Budyko's values of the albedo of snow and ice of open water were combined to give A for each month. For October it was assumed that the albedo of the ice was 0.7, as the ice would be covered with freshly fallen snow, so the albedo for the strait was A=0.65. Hanson (1961) developed a formula for calculating the albedo of puddled ice for diffuse incident radiation:

$$A = I_{c} (0.65 - 0.38P)$$
 (10)

This equation should only be used to calculate mean monthly values of the albedo when there is little direct radiation or when the ice concentration is high.

In winter, the albedo of the strait is about the same as the albedo at the airport since both the ice and the ground are covered by several inches of snow. The albedo at the airport may be calculated from the measured values of $\mathbb Q$ and $\mathbb Q_r$. The radiometer measuring $\mathbb Q_r$ receives most of it from a small area, several feet in radius. At Resolute, the snow may be several feet deep at one place while a nearby area is almost bare so the values of $\mathbb Q_r$, and therefore of the calculated A, may not be representative. A set of "mean" albedos was obtained (Table 2) from the mean incident and the mean reflected short-wave radiation data (Anon., 1966b). The low albedos calculated from the 1962 radiation data might seem to indicate less snow than usual, but this was not supported by the snow cover data. Even the June 1962 snow cover is not very unusual, though the measured albedo is very low. It was decided that the 1962 measured albedos could not be taken as representative of Barrow Strait.

The values accepted for the application of the heat budget of the strait for 1962 (Table 2) were derived from the foregoing. The albedos for

December to February were taken to be 0.80. For March to May the albedo of the ice would be higher than that of land since the latter was probably reduced by drifting. Drifting would have less effect on the albedo of Barrow Strait since the albedo of bare ice is much higher than that of bare land. For June, Hanson's value was adopted, because much of the radiation was diffuse and the ice was puddled. Since the water was not completely open in July, an albedo of 0.15 was chosen. For August and September, the open water values obtained from Budyko's table were adopted. Freeze-up began in October, and I was 0.9; the albedo was taken to be higher than Hanson's value, as his formula does not allow an adjustment for the fresh snow on the ice. In November the ice cover is complete and covered by fresh snow so A is once again 0.80.

5.2.1.3 Absorbed short-wave radiation, Q_a

Q was obtained for 1962 from the incident short-wave radiation (Table 1) and the albedo (Table 2) by (8). it is given here in ly/day:

J F M A M J J A S O N D
Q 0 3 30 92 142 373 473 262 100 13 1 0

5.2.2 Effective back radiation, Q

The effective back radiation is the balance between the long-wave radiation from the sea and that from the atmosphere. A variety of empirical formulae for estimating \mathbb{Q}_b is found in the literature, and it may be obtained from radiation measurements if both the net and the short-wave radiation fluxes are measured. Net radiation measurements at Resolute began in late 1963 so it was possible to calculate \mathbb{Q}_b from \mathbb{Q}_b , \mathbb{Q}_b and \mathbb{Q}_b for 1964, 1965, and 1966. \mathbb{Q}_b was also estimated (Table 3) for these years from a number of empirical formulae in an attempt to determine which if any was suitable for use at Resolute. All calculations were based on monthly means.

Was estimated from a linear formula developed by Laevastu (1960, p 43, equation 22) from Lonnqvist (1954) to find the effective back radiation under cloudless skies, \mathbb{Q}_{0} , and Moller's cloudiness factor to give \mathbb{Q}_{0} from \mathbb{Q}_{0} . Budyko (1956, p 42) presented a table for obtaining \mathbb{Q}_{0} and an equation (p 42, equation 31) to find \mathbb{Q}_{0} from \mathbb{Q}_{0} , and the amount of cloud; an alternative cloud correction given by Budyko (1956, p 43, equation 33) was also used. Anderson (1952, p 95) gave an empirical formula for Lake Hefner to find \mathbb{Q}_{0} in terms of cloud height, amount, the humidity and the surface temperature. Since mean cloud height data were not readily available for Resolute, his equation was used to find \mathbb{Q}_{0} and Moller's equation was applied to obtain \mathbb{Q}_{0} , as was Budyko's equation 33. Swinbank (1963) found that atmospheric long—wave radiation from clear skies may be calculated from the screen temperature alone; using his estimates of the atmospheric long—wave radiation and Stefan's law for the terrestrial radiation \mathbb{Q}_{0} was found. It was reduced to \mathbb{Q}_{0} by Budyko's cloud correction. Leahey (1966) calculated \mathbb{Q}_{0} from radiosonde data at Mould Bay and Yamamoto's (1952) radiation chart, and constructed a table to find \mathbb{Q}_{0} at Resolute. \mathbb{Q}_{0} was also obtained from measurements of \mathbb{Q}_{0} , \mathbb{Q}_{0} and \mathbb{Q}_{0} using the same equation as Vowinckel (1966):

Table 3. Effective back radiation, Q_b , at Resolute, 1964, 1965, and 1966 in ly/day from (i) Laevastu's and Moller's equations, (ii) Budyko's table and his equation (31), (iii) Budyko's table and his equation (33), (iv) Anderson's and Moller's equations, (v) Anderson's and Budyko's equations, (vi) Swinbank's and Budyko's equations, (vii) Leahey's table, and (viii) from the radiation measurements and (11).

						1964						
	J	F	M	A	M	J	J	A	S	0	N	D
(i)	192		197	154	117	66	61	63	69	150	132	174
(ii)					77	49	46	49	47	91	75	
(iii)					107	63	57	63	61	123	105	
(iv)	63		64	61	64	46	44	46	46	73	60	69
(v)	80		82	80	83	50	46	50	50	95	78	88
(vi)	140	146	142	129	115	62	56	61	65	142	120	145
(vii)	104	108	107	93	84	0			-1	115	82	112
viii)	72	72	77	87	56	79	106	77	67	82	56	72
						1965						
(i)		180	201	169	102	83	83	83	79	112	149	202
(ii)					78	61	67	67	58	72	87	
(iii)					108	84	94	94	79	101	119	
(iv)		66	75	73	64	64	61	60	50	58	70	73
(v)		84	93	93	83	79	76	75	59	74	91	91
(vi)	151	142	155	146	109	90	90	91	78	108	137	152
(vii)	116	108	123	118	79	51			30	72	115	118
viii)	53	65	72	101	93	137	161	142	76	53	72	72
						1966			,			
(i)			217	152	119	95	91	56	107	127	200	
(ii)					89	75	75	43	78	84		
(iii)					124	105	105	52	109	117		
(iv)			76	62	-71	65	67	42	70	66	55	
(v)			92	74	93	83	86	41	91	86	72	
(vi)	148	145	156	129	123	104	101	50	117	124	160	
(vii)	109	110	124	96	99	76			95	94	131	
\	72	74	85	53	71	129	162	69	111	72	89	

$$Q_{b} = Q - Q_{r} - Q_{n} \tag{11}$$

Since \mathbb{Q}_{r} is measured from a small area, and since the radiometer measuring \mathbb{Q}_{n} is not calibrated the same as those measuring \mathbb{Q} and \mathbb{Q}_{r} (Latimer, 1962; Champ, 1965) (11) will not give completely accurate results. It is believed that the error is less than 20%.

The values of \mathbb{Q}_b estimated from the empirical formulae show a minimum in summer and a maximum in winter, while \mathbb{Q}_b obtained from (11) shows the opposite trend, being largest in summer each year. Because the cloud conditions in the Arctic Archipelago are much different from those of more temperate climates (Rae, 1951), and also different from the central Arctic Ocean where ice cover persists, it seemed likely that the equations which give \mathbb{Q}_b and \mathbb{Q}_b were causing some of the difficulty. If this were true, we would expect better agreement between \mathbb{Q}_b from (11) and \mathbb{Q}_b from the empirical formulae on cloudless days.

The effective back radiation for cloudless days, \mathbb{Q}_{ob} , was calculated for each of the methods above except Budyko's table, which was not designed for the low temperatures observed on most cloudless days. Cloudless days were identified as before (see section 5.2.1.1) and \mathbb{Q}_{ob} was calculated for each date (Table 4) by Laevastu's, Swinbank's, and Anderson's equations, from Leahey's table, from the radiation measurements and from the radiosonde data (Anon., undated b; d) using Elsasser's radiation diagram (Haltiner and Martin, 1957, p 106-124). Laevastu's linear formula gives results that differ from the others by a factor of two or three. This supports a statement by Lonnqvist (1954, p 279) that a linear formula is probably not valid in situations with strong inversions such as usually exist during the Arctic winter; it was decided that the results from Laevastu's formula are not realistic for Resolute.

Swinbank's results are consistently higher than the others except Laevastu's. The differences between Swinbank's figures and those obtained from the radiation diagrams are smallest on days when there was a small atmospheric temperature inversion or none at all. When there is an inversion, the warm layer radiates more strongly than would a layer which is cooler than the surface so the atmospheric radiation is increased and $\Theta_{\rm b}$ is decreased. Since Swinbank used the surface temperature only, no account is taken of inversions and as a result, his values are too high. When there is no inversion as on April 19, 1965, his value agrees well with that obtained from the radiation diagram. Since inversions are common at Resolute in winter Swinbank's formula should not be used.

Anderson's values of \mathbb{Q}_{ob} are the lowest calculated. The only meteorological parameters used are surface observations so the effects of inversions are again neglected. Since his values are lower than those from the radiation diagram, we expect the difference to be largest on days when there is no inversion. This is observed. His values are the lowest estimates of \mathbb{Q}_{ob} when there is no inversion (April 19, 1965) and when the inversion is weak (March 28, May 6, May 7, 1966 and March 28, 30, 1964). Thus Anderson's results are not valid when there is no inversion, i.e. during most of the summer in the Barrow Strait area, and cannot be used in the heat budget calculations.

To obtain Q from Leahey's table the surface temperatures only are required. As the table is empirical the effect of inversions at Mould Bay is

Table 4. Effective back radiation on cloudless days, $Q_{\rm ob}$, in ly/day, at Resolute. (i) From Laevastu, (ii) from Swinbank, (iii) from Anderson, (iv) from Leahey's table, (v) from the radiation measurements and (11), (vi) from the radiosonde data and Elsasser's diagram.

(\(\) 110							
Date	8	(i) .	(ii) 170	(iii) 98	(iv) 138	(v) 115	(vi) 101
1964 Mar	28	297	168	96	134	129	165
	30	293	172	101	141	105	172
Apr	22	278	176	108	152	113	
Nov	15	269	175	107	150	120	116
	16	300	174	105	147	101	149
Dec	16	270	175	105	147	100	130
1965 Mar	10	29 6	169	97	13 6	74	135
1,00,110,1	19	298	165	92	130	82	147
	20	323	165	91	128	88	126
	24	293	171	100	140	77	108
Apr	3	297	171	100	141	105	128
-	4	276	179	114	158	118	149
	5	273	179	115	160	104	154
	19	26 7	181	119	166	149	172
Dec	19	315	168	95	133	98	114
1966 Feb	23	308	169	97	136	98	91
Mar	2	286	174	105	147	98	106
	6		158	84		88	91
	28	279	177	110	154	153	143
May	6	272	182	122	169	130	150
	7	275	180	117	163	143	151

implicit. As there seem to be fewer inversions in summer at Resolute than at Mould Bay the table is not necessarily valid for Resolute.

The last column (Table 4) gives \mathbb{Q}_{0} as calculated from the radiosonde data and Elsasser's radiation diagram. Although soundings were taken twice a day at 00 GMT and 12 GMT, only one was used in most of the calculations. For March 28, 1964, calculations were made using the data from both soundings; for one \mathbb{Q}_{0} was 196 ly/day and for the other it was 134 ly/day. This shows how variable the atmospheric radiation is and gives a measure of the reliability of using only one sounding. It is not known whether the value of \mathbb{Q}_{0} obtained from the radiosonde data and the radiation diagram is more or less accurate than \mathbb{Q}_{0} obtained from the radiation measurements.

The effective back radiation may be reduced by the long-wave radiation from cloud. If the cloud layer is thick enough it radiates as an almost perfect black body, so the long-wave radiation from the cloud and therefore \mathbb{Q}_b depends on cloud thickness and temperature as well as on the amount. It seems that the error in estimating the radiation from clouds, and thus the error in obtaining \mathbb{Q}_b from \mathbb{Q}_b will be larger than the error in calculating \mathbb{Q}_b from the radiation measurements (11).

As indicated earlier, net radiation measurements are not available for 1962, so (11) could not be used to estimate \mathbb{Q}_b . Although radiosonde data are available, they were not used to find \mathbb{Q}_b since there seems no good way to find \mathbb{Q}_b from \mathbb{Q}_b . It was decided to estimate \mathbb{Q}_b for 1962 by the use of a new empirical formula. Its form is not based on physical considerations — it is strictly empirical and applicable only to Resolute. The form is similar to that of the equation used by Anderson (1952) because the calculations from his equation were closest to the measured values. The second factor is the cloudiness correction used by Budyko (1956). The equation is:

$$Q_b = 1.141 \times 10^{-7} \theta_s^4 (a + be_a) (1 - 0.820^2)$$
 (12)

where Θ is the sea surface temperature in ${}^{\circ}$ K, e is the water vapour pressure in the atmosphere in millibars (mb) and C is the cloud amount in fraction of sky covered. For each month from January 1964 to November 1966 \mathbb{Q}_{b} , Θ , e and C were known. By the method of least squares, a and b were determined:

$$a = 0.191$$

 $b = 0.0369$

Using these values, Q 's were determined from the meteorological data observed at Resolute Airport:

	J	F	M	A	M	J	J	A	S	0	N	D
Q _b , 1964	61		63	64	84	79	81	96	75	86	67	71
Q _b , 1965		65	73	78	103	106	142	140	74	70	80	71
Q _b , 1966			70	65	102	126	167	74	126	79	80	

From comparison with the measured values of Table 3, the standard deviation was found to be 15, while the largest absolute error was 31 ly/day. In six cases out of 31 the difference between calculated and measured values was greater than 20 ly/day. This is better than any set of calculated values in Table 3.

To obtain Q for Barrow Strait in 1962, (12) was applied to the meteorological data adjusted to the strait. We assumed conditions over the strait to be the same as at the airport during the winter. In summer, the sea surface temperature will be lower than the screen level temperature measured at the airport. We assume the cloud amount will be the same over the strait as over the observing station. It is believed that the error in the back radiation arising from the assumption that the relative humidity over the strait is the same as at the airport, will be small. The effective back radiation in ly/day calculated for Barrow Strait in 1962 is then:

5.2.3 The net radiation balance Q_n

The estimates of the long-wave and short-wave radiative terms were combined to give the net radiation, Q_n , (1). Q_n for Barrow Strait in 1962 is shown in Fig. 8 and is given here in 1y/day:

Also shown are the three-year means* of $\mathbb Q$ at Resolute and the standard deviations (Anon., 1966b). The estimates of $\mathbb Q^n$ for 1962 seem to be of approximately the right magnitude. The value of $\mathbb Q$ for July 1962 reflects the higher than normal value of $\mathbb Q$ due to the low amount of cloud that month. The total net radiation for 1962, $\int \mathbb Q_n dt$ is 12.2 x 10 ly. Annual values at Resolute Airport were calculated for each year that $\mathbb Q_n$ was measured.**

^{*} The means were recalculated at the end of 1967 (Anon., 1967c) to give the four-year means and standard deviations:

	J	F	M	A	M	J	J	A	S	0	N	D
Q _n	-67	-6 6	-45	11	111	228	201	97	-6	-56	-70	-74
Std.Dev.	12:7	4.5	8.7	8.9	33.5	37.7	46.7	9.3	9.0	7.7	13.8	12.2

^{**}The 1967 data became available when work on the Appendix was almost completed. The total net radiation at Resolute in 1967 was 7.3 x 10^3 ly, which is within the range of the values for the three previous years.

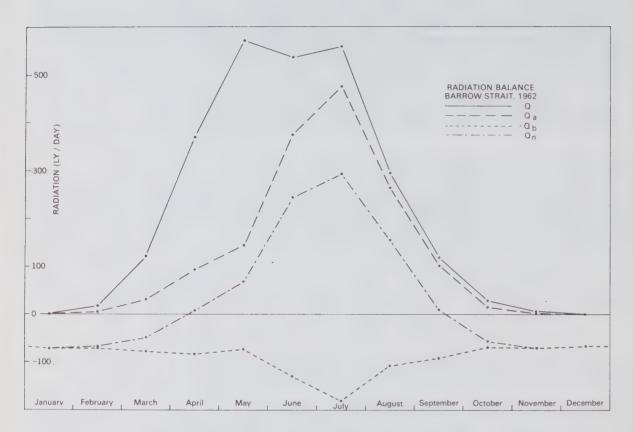


Fig. 8. The radiation balance showing the short-wave incident radiation, the absorbed short-wave radiation, the effective back radiation and the net radiation.

Year	$\int_{-Q_{\rm n}}^{-Q_{\rm n}}$ dt in ly
1964	9.8 x 10 ³
1965	9.2 x 10 ⁻³
1966	4.3×10^3

The radiation balance for each year is positive. Its magnitude appears to be quite variable, being twice as large in 1964 and 1965 as in 1966. The radiation balance obtained for Barrow Strait, 1962 is higher than any observed at the airport.

5.3 Evaluation of the turbulent flux terms

The sensible and latent heat fluxes are more uncertain than the radiative terms. Neither can be measured directly, so they must be calculated from other parameters. The best method to find the sensible heat flux (Badgley, 1961) is to measure near surface gradients of wind speed and temperature. To find the heat loss by evaporation the near-surface vertical gradient of water vapour should also be known. Although radiosonde data are available for Resolute, they are not sufficient to yield near-surface gradients so the turbulent fluxes must be estimated by empirical methods.

5.3.1 Heat of evaporation, Q

The rate of evaporation depends on the water vapour pressure in the air and the rate at which the air is mixed. Mixing depends on the turbulence of the air, which is a function of wind speed, and on the presence of convection. Laevastu (1960) revised Rohwer's formula to give daily estimates of the evaporation; he gave two formulae, one to be used when convection occurs and the other to be used when it does not, i.e. when the water is colder than the air. The amount of evaporation is often calculated from climatic data by the Sverdrup formula (Walmsley, 1966):

$$E = k \left(e_s - e_a \right) V \tag{13}$$

where E is the amount of water evaporated in mm/day; k is an empirical constant equal to 0.145; V is the wind speed in m/sec; e is the saturation water vapour pressure in mb at the sea surface temperature and e is the water vapour pressure in the atmosphere.

For most of August and part of September, 1962, daily weather observations were made on CSS "Baffin". The data were used to calculate the evaporation on a daily basis with both Laevastu's and Sverdrup's formulae. When the values for August were averaged, the difference between the two methods was small - from Laevastu's formulae E was 0.20 mm/day, and from Sverdrup's equation it was 0.19 mm/day. Although agreement between the two estimates for the first eight days of September (1.08 and 1.51 mm/day respectively) was less, it seemed that (13) gives reasonable estimates of the evaporation from the climatic data.

Monthly estimates of E were made from the mean meteorological data observed at Resolute. These data were adjusted to give estimates of the para-

meters over Barrow Strait both for open water and for a complete ice cover. It was assumed that the air temperature T_a , was the same as at the airport. The surface temperature, T_s , is written as T_s for an ice surface. T_s was obtained from T_s by applying corrections presented by Vowinckel and Orvig (1964) whenever $T_s < 0^{\circ}\text{C}$; when $T_s > 0^{\circ}\text{C}$ it was assumed that $T_s = 0.0^{\circ}\text{C}$. Since it did not seem possible to estimate the water surface temperature, T_s , from the observations from "Baffin" it was assumed that for June and September, $T_s = 0.0^{\circ}\text{C}$; for July and August, $T_s = 1.0^{\circ}\text{C}$; and for October $T_s = -1.0^{\circ}\text{C}$. The relative humidity T_s , over the strait was assumed to be the same as at the airport; since it was not measured during January and February an estimate was made. The vapour pressures over ice (s_s) and water (s_s) were found from the temperature and humidity data (T_s) . Wind speed measurements are published in the Monthly Record (Anon., undated, c). Then T_s was found for complete ice cover (T_s) and for completely open water (T_s) . T_s the heat of evaporation from ice, and T_s the heat of evaporation from water, were estimated from T_s and T_s and combined according to the ice concentration data to give T_s and T_s and combined according to the ice concentration data to give T_s and T_s and T_s and combined according to the ice concentration data to give T_s and T_s and T_s and T_s and combined according to the ice concentration data to give T_s and T_s and T_s and combined according to the ice concentration data to give T_s and T_s

The monthly values of Q were multiplied by the number of days in each month and summed to give $\int Q$ dt for 1962. Its value was found to be 5.1 x 10 ly. Since the heat of vaporization is about 600 cal/gm, the net evaporation from Barrow Strait in 1962 was about 8.5 cm. Barber (1967) estimated the evaporation from Hudson Bay to be about 20 cm/year. Estimates of the evaporation over the polar ocean range from 4 to 8 cm/year (Mosby, 1963; Vowinckel and Taylor, 1964) so the estimate of 8.5 cm/year for Barrow Strait seems reasonable.

5.3.2 Sensible heat flux, Q_h

The sensible heat flux at the surface may be either upward or downward, depending on the vertical temperature gradient. Although the radiosonde data may be used to estimate the gradient in the atmosphere they are not sufficiently detailed to calculate the sensible heat flux at the surface. When the temperature is known at two levels, one of which is the surface, when the temperature is known at two levels, one of which is the surface, when the temperature is known at two levels, one of which is the surface, when the temperature is many be estimated from empirical formulae. During summer, both sea and air temperatures are available. In winter, only the air temperature is measured.

During the winter the heat loss at the surface is met largely by growth and cooling of the ice cover. Lewis (1967) calculated the heat flow through winter ice in terms of the temperature difference across the ice sheet, its conductivity and its thickness. Neglecting the snow cover, the average heat flow through the ice in January 1962 was estimated to be 165 ly/day upward. The effective back radiation was about 70 ly/day. This would leave about 90 ly/day to be given off as upward sensible heat flux. If it is assumed that the snow cover maintained the ice surface at 100 higher than the air temperature the sensible heat flux at the surface would be estimated at 40 ly/day upward. However, it is apparent from the radiosonde data that an atmospheric temperature inversion existed so Q must have been downward. Therefore, Lewis' estimate of the heat flux cannot be used here, perhaps because not enough is known about the influence of a snow cover.

Empirical formulae may be used to estimate Q_h from the air temperature, the surface temperature and the wind speed. Estimates of the surface temperature were made previously (Table 5). Laevastu (1960) developed two equations for estimating daily values of Q_h , one to be used when convection

Table 5. Evaluation of the latent heat flux due to evaporation. (i) Mean air temperature in °C. (ii) Mean surface temperature in °C, (a) for open water; (b) for a complete ice cover. (iii) The relative humidity in percent. (iv) The difference between the water vapour pressure in the air and at the surface, (a) for open water; and (b) for a complete ice cover. (v) The wind speed, in m/sec. (vi) Evaporation in mm/day, (a) from open water; (b) from ice. (vii) The latent heat flux in ly/day (a) from open water; (b) from ice. (viii) The latent heat flux in ly/day for observed ice and puddling condition.

	J	F	M	А	М	J	J	A	S	0	N	D
(i)	-34.4	-34.6	-21.1	-23.1	-11.6	+1.5	+7.7	+3.0	-3.7	-14.7	-25.2	-28.7
(iia)						0.0	1.0	1.0	0.0	- 1.0		
(iib)	-36.4	-35.6	-22.1	-22.1	-10.6	0.0	0.0	0.0	-2.7	-14.7	-26.2	-29.7
(iii)	70*	70*	84	82	88	. 88	75	88	91	87	78	76
(iva)						.113-	-1.31-	102	1.87	3.97		
(ivb)	.025	.046	.063	.217	.481	.113-	-1.75-	565	.798	.221	.077	.062
(v)	4.51	5.81	6.88	5.81	5.23	5.63	4.42	5.50	7.29	5.86	5.63	6.79
(via)						.092	.841-	081	1.98	3.37		
(vib)	0.16	.039	.063	.182	.365	.092-	-1.12-	450	.843	.188	.063	.061
(viia)						6	-50	-5	118	202		
(viib)	1	3	4	12	24	. 6	-75	-30	56	13	4	4
(viii)	1	3	4	12	24	6	-60	-5	112	32	4	4

^{*}estimated

occurs (T > T), and the other when it does not (T < T). Vowinckel and Taylor (1964) used two empirical formulae developed by Shuleikin. The two sets of equations agree quite well for upward sensible heat flux but for the downward flux Laevastu's estimate is seven times greater than Shuleikin's. Estimates of Q were made for each month using both sets of equations (Table 6). Calculations were carried out separately for open water and for complete ice cover. These estimates were combined using the ice concentration data (Table 2). Both methods were also used with the daily temperature data observed from "Baffin" during August and the first week of September. For August, the mean value of Q was estimated to be 2 ly/day upward with Shuleikin's formulae and 19 ly/day with Laevastu's. In September Q was usually upward, so agreement between the estimates was better: 22 and 21 ly/day up respectively. These are the means for the first eight days of September; Q increased during the rest of the month since T drops more rapidly than T. The Bowen ratio (Anderson,

Table 6. Sensible heat flux, Barrow Strait, 1962. (i) T_i - T_a in C° . (ii) T_W - T_a in C° . Q_h for open water from Laevastu's (iii) and Shuleikin's formulae (iv). Q_h for a complete ice cover from Laevastu (v) and Shuleikin (vi). Q_h in 1y/day for the observed ice concentration from Laevastu (vii) and Shuleikin (viii).

	J	F	М	A	М	J	J	A	S	0	N D	
(i)	-2	-1	-1	1	1	-1.5	-7.7	-3.0	1	0	-1 -1	
(ii)						-1.5	-6.7	-2.0	3.7	13.7		
(iii)						-25	-88	-33	119	377		
(iv)						-4	-13	-5	112	414		
(v)	-27	-17	-21	28	26	-25	-102	-50	32	0	-17 -2	0
(vi)	-4	-2	-3	30	30	-4	-15	-7	30	0	-2 -3	
(vii)	-27	-17	-21	28	26	-25	-92	-35	110	38	-17 -2	0
(viii)	-4	-2	-3	30	30	-4	-14	-5	104	41	-2 -3	

1952) was used to estimate \mathbb{Q}_h for September from the evaporation. The result (140 ly/day) agrees quite well with the estimates obtained for open water from Shuleikin's and Laevastu's formulae using the monthly mean temperature data.

The estimates of \mathbb{Q}_1 adopted in this heat budget are those obtained from Shuleikin's formulae. It is thought that Laevastu's values are overestimates, since \mathbb{Q}_1 is usually small compared to the radiative terms (Langleben, 1966; Badgley, 1961). Both sets of \mathbb{Q}_1 were integrated for the year. From Laevastu's equations $\int \mathbb{Q}_1$ dt = -1.7 x 10³ly and from Shuleikin's the integral is +5.1 x 10³ly. Shuleikin's estimates seem preferable because the only large estimate of \mathbb{Q}_1 is in September when the open water is cooling rapidly. The ice and snow cover acts as an efficient insulator between the air and the water, so \mathbb{Q}_1 should be small in winter. During the summer the air-sea temperature diferences are small so the sensible heat flux would be small.

5.3.3 The turbulent flux balance, Qt

The sensible and latent heat fluxes \mathbb{Q}_e and \mathbb{Q}_h were summed (2) to give to total turbulent flux, \mathbb{Q}_+ , in ly/day:

The turbulent flux terms Q_p , Q_h and Q_t are shown in Fig. 9.

The total turbulent heat flux is 9.2×10^3 ly for 1962. This is less than the radiative flux (12.2×10^3) ly but of the same order of magnitude.

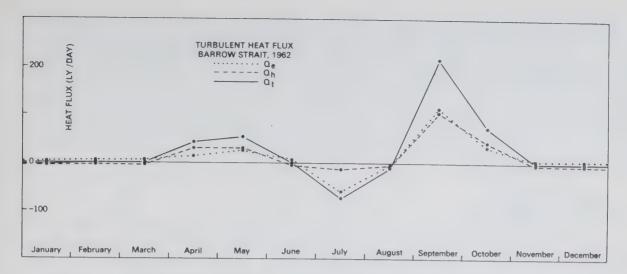


Fig. 9. The turbulent heat fluxes showing the sensible heat flux, the heat of evaporation and the total turbulent heat flux.

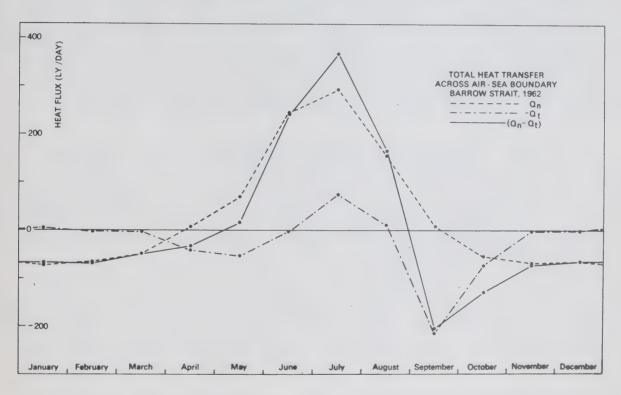


Fig. 10. The total heat transfer across the air-sea boundary, also showing the net radiative and net turbulent fluxes.

5.4 The total transport of heat across the air-sea boundary, Q

The net radiative flux, Q_n , (p. 31) and the net turbulent flux Q_t , (p. 36) combine (3) to give the total heat input through the air-sea boundary, Q_T , in ly/day.

J F M A M J J A S O N D

Q_T -68 -69 -50 -34 15 241 366 164 -208 -130 -72 -68

 $Q_{\rm T}$ and its components, $Q_{\rm t}$ and $Q_{\rm t}$ are shown in Fig. 10. Negative values of $Q_{\rm T}$ imply a flux from the water to the air; positive values are a gain to the water. In 1962 energy gains to the strait occurred across the air-sea boundary from May to August and were maximum in July. In each of the other months, heat was lost to the atmosphere, the greatest occurring in September. The total transport through the air-sea boundary, $\int Q_{\rm T}$ dt, was 3.0 x 10^{3} % ly downward and is a gain to the region. The integral of the absolute values of $Q_{\rm T}$ is 45.3 x 10^{3} ly for the year. The net gain is about 7% of this and may be less than the error which is difficult to estimate but is probably at least 10%, i.e. 4.5×10^{3} ly.

5.5 Heat storage, Qs

Although measurements of ice thickness were available for Resolute Bay (Anon, 1962; 1963 a) not enough was known about the ice to calculate mean monthly values of the heat storage in the ice Q. In the summer months there is no ice cover, and heat storage occurs only in water. According to Tabata (1964) the rate of change of heat storage may be calculated from its temperature depth profile. CCGS "John A. MacDonald" carried out a programme of ocean-ographic observations in the Arctic in 1962 which included a number of stations in Barrow Strait. At most of these stations the temperature was observed by a bathythermograph and by reversing thermometers at standard depths. Temperature observations were also obtained six times at a station off Assistance Bay ** by a land based party (Anon., 1963 c). The temperature data were used to obtain the temperature depth profiles. The initial condition at each station was assumed to be the same as that observed through the ice in late winter, 1959 (Milne, 1960).

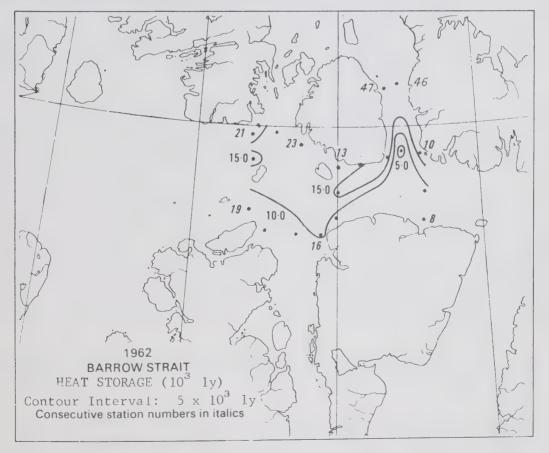
The heat storage to the bottom was calculated (Table 7) for each station occupied on August 7 or 8. It was generally lower in the southern portion of the strait (Fig. 11). The lowest is at station 11 where the water is also more saline between 10 and 75 meters than at the other stations in the vicinity. It is possible that upwelling occurs here, so that the warm surface water is advected away from this position. The heat storage shows large variations with location; it ranges from 5 x 10³ ly (at station 11) to 18 x 10³ ly (station 12). The low values may reflect a lingering of ice, or ice import, or advection of cool water; the higher values imply early removal of the ice cover or advection of warm water into the locality. It is thought that some of the heat in the northern portion of Barrow Strait was advected from McDougall Sound and Wellington Channel. Penny Strait usually has open water earlier than Barrow Strait (Lindsay, 1968, p 4) so heating begins early in this area. Since the flow through Penny Strait, Wellington Channel and McDougall Sound is pre-

^{*} This value would be 9.8 x 10^3 ly if Laevastu's estimates of the sensible heat flux had been used instead of Shuleikin's. This surplus seems too large at such a high latitude and supports rejection of the use of Laevastu's equations for \mathbb{Q}_h .

^{**} In the data record (Anon., 1963 c) this is referred to as Allen Bay. Examination of the position data and Canadian Hydrographic Service Chart 7056 shows it to be Assistance Bay.

Table 7. Heat storage to the bottom in Barrow Strait, 1962 calculated from observations on August 7 and August 8, 1962. (i) Consecutive station number, (ii) the depth in meters, (iii) the heat storage in units of 10³ ly.

(i)	(ii)	(iii)
8	137	5.7
9	300	. 8.1
10	121	16.7
11	157	5.0
12	135	18.1
13	117	12.9
14	179	15.2
15	194	8.4
16	205	10.3
17	212	6.3
18	267	8.6
19	134	8.6
20 ;	143	16.7
21	51	6.6
22	243	14.7
23	82	10.0



rig. 11. The heat storage on August 7-8, 1962 in Barrow Strait calculated from temperature data of the "John A.MacDonald" stations 8-2° and of the land based station in Assistance day.

dominantly southward, some of the warm water is advected into Barrow Strait.

It is possible to study the increase of heat storage with time at the station occupied on six occasions off Assistance Bay (Table 8). The depths show that observations were not made at exactly the same place. It is believed that the difference in heat storage due to the location are small compared to those due to the time between observations. The heat storage observed on June 28, 1962 in Assistance Bay is two thirds of the total surface energy exchange estimated for June. Assuming Q is zero and that each day Q is equal to its monthly mean, we concluded there was open water in this area on and after June 8. Black (1965, his figure 8) shows this area to have open water as early as June 21. The ice must have been transported out of the area, since there was not enough heat input to melt all of it (assuming that it was the same thickness as in Resolute Bay, i.e. 165 cm). Between June 28 and July 13 there was only a small increase in heat storage. It is possible that ice drifted in and melted but it is also possible that the low heat storage and the increase in the fresh water content observed* were due to advection of water.

Table 8 Change of heat storage with time, Barrow Strait, 1962. Heat storage calculations are based on observations made off Assistance Bay at 74° 36'N, 92° 13'W, by a land based party. (i) The consecutive station number, (ii) the date of occupation, (iii) the heat storage calculated from the serial temperature observations in units of 10° ly, (iv) the depth (m) at each station.

(i)	(ii)	(iii)	(iv)
1	June 28	4.8	55
2	July 6	5.0	52
3	July 13	6.0	52 62
5	July 25	10.6	60
6	August 7	14.3	55
7	August 14	15.7	41

Since the estimates of \mathbb{Q}_T are based on monthly means, it is probably better to consider the heat storage during a whole month. Between July 6 and August 7 the increase in heat storage is 9.3 x 10 ly; for the same period $\int \mathbb{Q}_T$ dt is about 10.3 x 10 ly. If the estimates of \mathbb{Q}_T are realistic for Assistance Bay, then from integrating (6) $\int \mathbb{Q}_V$ dt = -1 x 10 ly in this area in that month. This implies that warm water was advected out of this region or that ice moved into the area. It is possible that the time series stations are not representative of Barrow Strait and that \mathbb{Q}_V is much different in the main body of the strait.

The heat storage $Q_{\mathcal{Q}}$ could be estimated only for July and Part of June and August, and no estimates of $Q_{\mathcal{Q}}$ were made, so no monthly estimates of the heat storage $Q_{\mathcal{Q}}$ could be made.

^{*} Between June 28 and July 6 the fresh water content (Barber, 1967, p 32) using 33.8% as the base salinity increased from 1.6 m to 1.8 m; on July 13 it was 2.2 m.

5.6 Heat of advection, $Q_{\mathbf{v}}$

Since it was not possible to obtain monthly values for \mathbb{Q}_s , no monthly estimates of \mathbb{Q}_s can be found as the residue in the heat balance equation (5). Over the course of a year, there is no net heat storage in the surface mixed layer, since this is at the freezing point at both the beginning and the end of the year. It is possible for the depth of the mixed layer to vary from year to year, and some heat storage could result. It is believed that this contribution would be small and may be neglected. Variations from year to year in the thickness of the ice cover, and hence of \mathbb{Q}_1 must also be small since no large net long-term changes are observed.

The heat budget equation for the year is just the integral of equation (5):

$$\int Q_{T} dt + \int Q_{v} dt - \int Q_{s} dt = 0.$$

Since the third term is negligible

$$\int$$
 Q $_{\mathrm{V}}$ dt = $-\int$ Q $_{\mathrm{T}}$ dt

which is approximately -3.0×10^3 ly for 1962. Q was defined to be positive when it is a net gain to the region. Since it is negative, advection removes heat from the region, i.e. water flowing through Barrow Strait was heated in 1962. The net advected heat for the year is small; it is within the error estimate of the surface energy flux. For this reason it is dangerous to attach too much significance to either the numerical value or the sign of $\int Q_v dt$.

Because 1962 was an unusually open ice year (Anon., 1963 b; Lindsay, 1968) it seems likely that the value for the absorbed short-wave radiation was higher than normal. The low amount of ice would also enhance evaporation and sensible heat flux from the sea to the atmosphere. As the increased radiative and turbulent fluxes are in opposite directions it is believed that $\mathbb{Q}_{\mathbb{T}}$ dt is usually small and positive.

5.7 Glossary of symbols

Because of the large number of symbols used, they are listed here in alphabetical order for convenience and clarity. All heat fluxes are given in ly/day.

- A: the albedo of a surface, defined to be the ratio of the reflected to the incident radiation.
- a: an empirical constant.
- b: an empirical constant.
- C: the amount of cloud given as the fraction of sky covered.
- E: the amount of evaporation from the sea surface in mm/day.
- E,: the amount of evaporation from an ice surface in mm/day.
- E: the amount of evaporation from open water in mm/day.
- e: the water vapour pressure of the air at screen level in mb.
- e: the saturation vapour pressure over ice, in mb.
- es: the saturation vapour pressure at the temperature of the surface, either water or ice, in mb.
- ew: the saturation vapour pressure over open water in mb.
- h: mean altitude of the sun.
- I : the ice concentration as fraction of surface covered.
- k: an empirical constant.
- P: the concentration of puddles of melt water on the sea ice as the fraction of ice covered.
- Q: incident short-wave radiation from sun and sky.
- $\mathbf{Q}_{\mathbf{a}}$: the short-wave radiation absorbed at the sea surface.
- $Q_{\mathbf{b}}$: the effective back radiation from the sea surface.
- Q: the upward flux of latent heat through evaporation.
- \hat{Q}_{ei} : the flux of latent heat by sublimation from an ice surface.
- $Q_{\mathbf{ew}}$: the flux of latent heat by evaporation from open water.
- Q: the upward sensible heat flux, by turbulent conduction and convection.

Q: the amount of heat stored in the ice.

Q: the net radiation.

Q: the mean net radiation.

the short-wave radiation from sun and sky incident at the surface on cloudless days.

Q the effective back radiation on cloudless days.

 $Q_{\mathbf{r}}$: the short-wave radiation reflected at the surface.

 $Q_{\rm s}$: the heat stored in the ice and water.

 $\mathbf{Q}_{\mathbf{t}}$: the total turbulent heat flux from the sea to the atmosphere.

 \mathbb{Q}_{p} : the total transfer of heat across the air-sea boundary.

Q.: the storage of sensible heat in the water.

 Q_{v} : the heat brought in through advection.

 T_2 : temperature of the air at screen level, in ${}^{\circ}C$.

T_i: surface temperature of the ice in, °C.

 T_s : sea surface temperature, in $^{\circ}$ C.

 T_w : temperature of the water at the sea surface, in ${}^{\circ}C$.

 Θ_{c} : temperature of the sea surface, in ${}^{\circ}K$.

U: relative humidity of the air at screen level, in percent.

V: the wind speed, in m/sec.





MANUSCRIPT REPORT SERIES

No. 13

7hreeStatistical Programs to Process Limnological Data

H. E. SWEERS



Marine Sciences Branch

Department of Energy, Mines and Resources

Ottawa, Canada



CAT III. II =

Manuscript Report Series No. 13

THREE STATISTICAL PROGRAMS TO PROCESS LIMNOLOGICAL DATA

H. E. Sweers

The Queen's Printer for Canada
Ottawa, 1970

FOREWORD

The present report provides additional information on the computer programs used in the analysis of limnological data described by the author in Manuscript Report Number 10: Structure, Dynamics and Chemistry of Lake Ontario; Investigations Based on Monitor Cruises in 1966 and 1967. Computational techniques are described in more detail than was possible in the earlier report and program listings, clarified with comment statements, are reproduced. The report, however, is not intended to serve as a complete documentation of these programs; it only presents a general description of their scientific aspects and applicability.



ABSTRACT

Description of three programs, written in Fortran IV for a CDC 3100 computer, designed to calculate means, standard deviations, standard errors and other statistics of various limnological parameters. STATISTICS I gives weighted cruise-mean values, cruise-mean epilimnion and hypolimnion values, tabulations of the relation between temperature and other parameters, and near-bottom means. STATISTICS II is especially designed to study regional anomalies in the distribution of any parameter. STATISTICS III is a more specialized program analysing the variability in a set of data in terms of random and systematic components.



CONTENTS

		Page
Introduction		1
STATISTICS	I	3
STATISTICS	II	9
STATISTICS	III	14
Acknowledgen	nents	20
References		20
Appendix A:	Description of subroutines RETRIEVE AND TRNSLATE	23
Appendix B:	Listing of STATISTICS I	27
Appendix C:	Listing of STATISTICS II	39
Appendix D:	Description of STATISTICS III	45
Appendix E:	Listing of STATISTICS III	51



INTRODUCTION

In recent years a large volume of limnological data has been sampled on the Great Lakes by the Canada Centre for Inland Waters in cooperation with various other agencies. In an effort to facilitate analysis of these data the author developed a number of computer programs written in Fortran IV for use on the CDC 3100 computer of the Department of Energy, Mines and Resources. Three of these programs, called STATISTICS I, II and III, will be described in some detail in this report. They have been especially designed to cope with data from monitor-type of operations, in which a set of standard stations distributed evenly over the lake is revisited at regular intervals and sampled at a fixed number of standard depths. The data are grouped in various ways, and the means, standard deviations and standard errors of such parameters as temperature, specific conductance, pH, etc. are calculated for these groups. Extensive use has been made of the programs described herein to study data sampled in Lake Ontario during the 1966 and 1967 field seasons (Sweers, 1969). Some of these applications are briefly outlined under the appropriate heading in the program descriptions.

All data are coded in accordance with the STAR system, developed by the Canadian Oceanographic Data Centre (provisional description in Glennie et al., 1967), and are stored on magnetic tape. The stations are numbered consecutively on each cruise, but for purpose of the present programs they have also been assigned so called standard station numbers. For a series of

monitor cruises, in which the same locations are visited repeatedly, the planned station positions are numbered, and this standard number is assigned to any station taken at or near the planned position, regardless of its consecutive number. This information is, together with the weighting factors defined in the description of STATISTICS I and the consecutive station numbers, stored on a special tape, called the "editor" tape.

The first two programs contain two subroutines to read and interpret the data tape (designated as GLSP file in the program listing), which returns the data requested by means of special control cards preceding the program. All data from non-standard stations are rejected and information from the standard stations specified on the editor tape is stored in a matrix in sequence of the corresponding standard station numbers. These tape reading and interpretation subroutines, RETRIEVE and TRNSLATE, will probably be discussed in more detail in a future report on the STAR system; a basic description of their functions is given in Appendix A.

In the next chapters the purpose of each of the three programs will be defined, some possible applications discussed and the computational procedures outlined. Their listings, including many comment statements to facilitate understanding, are given in the appendices. In studying the listings it should be noted, however, that no special effort has been made to optimise the programs with respect to the use of computer time, and that they have been developed over a period of time and thus

may contain sections not essential to their functioning or adaptated to particular problems. The listings therefore are presented only to serve as an illustration.

The frequency distribution of values of any parameter sampled at a series of monitor stations is determined by random errors in the measurements, natural random fluctuations in the water and geographical or temporal effects. The distribution therefore does not necessarily correspond to a Gaussian random population, and a study of this must be made before standard deviations and standard errors of the mean, calculated in the programs, can be interpreted in terms of confidence limits.

STATISTICS I

Purpose

- 1. To calculate the weighted cruise-mean vertical distribution of a parameter P and its standard deviation and standard error of the mean at different depths.
- 2. To study the relation between the concentration of a parameter P and temperature T. A two dimensional plot of T versus P of the individual samples is made, and the mean, standard deviation and standard error of the mean of P for various temperature intervals are computed.
- 3. To indicate changes in the value of a parameter P near the bottom.

Applications

 To study seasonal variations in the lake-mean profile of a parameter.

- 2. To compare lake-mean profiles of various parameters.
- 3. To study the relation between P and temperature, or the differences in the mean values of P in different water masses defined by temperature limits.
- 4. To study variations of P with depth close to the bottom.
- 5. To study changes in the variability of P in different water masses, at different depths, or at different times.

Calculations

1. Each standard station is assigned a weighting factor W_i proportional to the area for which a measurement at that location can be considered to be representative; the sum of all weighting factors is proportional to the total area of the lake:

$$W = I = \sum_{j=1}^{J} W_{j}$$

where J is the total number of standard stations. This information is also stored on the "editor" tape, and is used to calculate weighted means.

2. For each standard depth * the mean, \overline{P} , weighted mean, M, standard deviation, S, and standard error of the mean, E, are calculated:

$$M_{k} = \frac{1}{\sum_{j=1}^{N} W_{j}} \sum_{j=1}^{N} W_{j} P_{jk}$$
 (1a)

$$\overline{P}_{k} = \frac{1}{J} \sum_{j=1}^{J} P_{jk}$$
 (1b)

$$S_{k} = \left[\frac{1}{J-1} \sum_{j=1}^{J} \left(P_{jk} - \overline{P}_{k}\right)^{2}\right]^{\frac{1}{2}}$$
 (1c)

$$E_{k} = \frac{S_{k}}{\sqrt{J}} \tag{1d}$$

where j is the station number, J the total number of stations, W_j the weight factor of station j, and $k=1,2,\ldots,K$ an index designating the depths Z_1,Z_2,\ldots,Z_K . No attempt is made to use the concept of weighted data in calculating other statistics but the mean. This may, depending on the station configuration, complicate interpretation of the results, but for a regular distribution of the stations the results are satisfactory. If desired, however, the standard deviation and standard error can also be computed for the weighted data:

^{*}In the sample listing the standard depths used are 1, 10, 20, 30, 50, 75, 100, 150, 200 metres, and values are accepted as measured at a standard depth if the sampling depth is within 1, 1, 2, 3, 5, 5, 10, 10, 10 metres respectively of the standard depths specified. These depths and intervals are defined in subroutine RETRIEVE.

$$S_{k}^{'} \simeq \left[\frac{\sum W_{j} (P_{jk} - \overline{P}_{k})^{2}}{J - 1} \sum_{j} W_{j}}\right]^{1/2}$$

$$(2a)$$

$$E_{k}^{'} \simeq \frac{S_{k}^{'}}{\sqrt{J}}$$
 (2b)

These approximate equations can be derived by assuming each observation to consist of a cluster of M_{i} identical observations, where M_{i} is proportional to the weighting factor W_{i} . The results of equations 2, however, can only be expected to improve upon those of the equations 1 if the variability in the data is caused by geographical factors. In this case, however, the standard deviation and standard error of the mean cannot be interpreted in terms of confidence limits. If the variability is largely determined by random variations in the water or by sampling and analysis errors, use of the equations 2 cannot be recommended, and in the limiting case of a purely Gaussian random distribution the equations 1 should be used if the calculated statistics are to be related to confidence limits.

3. For each cruise a two-way table is set up showing the distribution of P_{jk} over a number of temperature intervals. This can be interpreted as a scatter diagram of points (P_{jk}, T_{jk}) , where T_{jk} is the temperature at a station j and depth k, or as a bivariate frequency diagram of the parameter P versus a number of temperature classes. Using equations similar to

equation 1 above, the means, standard deviations and standard errors of the mean are calculated for data within each temperature interval and for the epilimnion (temperature > 11°C) and hypolimnion (temperature between 3.0 and 5.0°C) data respectively.

- 4. The equations 1 are also applied to monitor station data sampled less than 10 metres above the bottom. These observations are split into four groups: bottom depth less or more than 45 metres, and deepest and second deepest sample for any station, called BSHALLOW, BDEEP, BBSHALLOW and BBDEEP respectively in the output.
- 5. The percentage saturation of oxygen is calculated from the temperature T and the absolute oxygen concentration C:

SAT
$$O_2 = \frac{A \times C}{14.380 - 0.4105 \times T + 8.8 \times 10^{-3} \times T^2 - 9.5 \times 10^{-5} \times T^3}$$

where A = 100 at sea level and 98.8 at 80 metres above sea level, which corresponds to surface elevation of Lake Ontario (Dobson, 1968).

Input

- 1. Data in GLSP format on tape.
- 2. Editor tape to select desired stations from the GLSP tape, to renumber the stations using standard station numbers, and to assign weighting factors to the stations (see statement 101 of the main program for format of tape).

CRUISE NO. 12
PARAMETER SP CON (COMPAR

ER SP CON (COMPARED WITH TEMP)

Figure 1

ALL 275.8 239 5.0 250 279.6 72 2.3 281.0 150 280°2 6 100 280.1 17 2.1 279.0 20 20 2.4 2.4 279.4 27 2.7 2.5 .5 30 277.8 37 4.4 20 276.3 42 42 4.8 10 272.5 44 44 4.3 8.07S 2.3 MEAN NO OBS SU DATA SU MEAN

ALL	ALL	7	- 0	0	>	1	4	21	37	25	15	14	64	48	18	4	1		o c	275.8	530
≥ 11.00	≥ 11.00		0	c	S	0	*	18	36	24	15	5	4	2	-	0	0		o c	0 271.8	2-2
23.00	23.00	0	0	0	,	0	0	0	0	0	0	0	0	0	0	0	0	0	0		
21.00 ≥	23.00 ≥	0	0	0)	0	0	m	S	~		0	0	0	0	0	0		0	270.4	7
0.6	21.00 <	. 0	0	0	,	0	2	7	25	1	4		0	0	, ,	0	0	c	. 0	271.0	2.6
0	> 00.61	0	0	0		. 0	2	30	្រ	12	9		l emp	0	. 0	0	0	0	0	271.5	S.C.
5.0	> 00°2		0	0		0	0	0	-	, 2	2		1		0	0	0	0	0	273.2	6.2
	5.00 < 1	0	0	0		0	0	0	0	p=4	.0	2	→	-	0	0	0	. 0	0	277.0	2.5
•00 ≥ 1	3.00 < 1	0	_ 0	0		. 0	0	0	0	; ~	2	ent	1	0	0	. 0	0	. 0	0	275.4	ot
.00 > 1	.00 < 1.	0	0	0		~	. 0	0	0	0	0	r=1	0	2	1	0	0	0	0	276.6 5	7.4
7.00 ≥ 9	.00 < 11	0	0	0		0	0	0	0	0	0	2	: 4	9	2	0	0	0	0	279.6	6.1
۸۱	V		0	0		2	. 0	-	,r-4	. 3	0	: m	7	20	. 9	~4		. 0		279.6 28 1	3.7
AI .	> 00 ° c	0	0	0		0	[O	7	0	1	0	m	34	30	. 20	m	0	0		279.3 81	2.6
AI.	00 ×	0	0	0		0	. 0	0	0		0	0	0	0	0	0	0	0_	0	0	0
- İ	l l	260	262	564	264	266	268	270	272	274	276	278	280	282	284	286	288	290	290		SD DATA

BSHALLUW BBSHALLUW

BBULEP

BOTTOM SUMS

8DEEP 280.8 5.2 2.3

MEAN 2NO OBS SD DATA SD MEAN

6.6

3. Control cards to determine cruises, parameters and depths to be read (see description of the subroutine RETRIEVE, Appendix A).

Output See sample in Fig. 1.

STATISTICS II

Purpose

After rejecting the values of a parameter P outside prespecified limits the following statistics are calculated for each standard depth, using unweighted data:

- 1. The cruise-mean value and standard deviation of P.
- 2. The station-mean value and standard deviation of P using data from a series of monitor cruises.
- 3. The overall mean value and standard deviation of P using data from all stations and monitor cruises.
- 4. The relative deviation of individual observations from the cruise-mean value for the same depth, expressed in fractions of the overall standard deviation. This statistic allows a direct intercomparison of anomalies in the individual observations taken at any station or cruise.

Applications

1. The program is designed to give an indication of the persistency of local or regional deviations from the

^{*}A separate program has been developed to list rejected values for the purpose of quality control; this will not be described in the present report.

lake-mean value of a parameter at any particular depth by comparing the results from subsequent monitor cruises. It can also give an indication of local variations in the cruise-to-cruise variability of the data.

2. The program can alternately be used to find possible gross errors in unscreened data, if the check on whether a parameter falls within a predefined interval is omitted. A comparison of deviations at any one station for subsequent cruises can then show whether anomalous values occur in a regular pattern, suggesting a natural cause, or in an apparently random pattern, indicating possible gross errors.

Calculations

- 1. Values of P are rejected if they fall outside the range (P_1, P_2) , where P_1 and P_2 correspond to the range of calibration of the analytical technique used, or to some other, arbitrarily chosen, outer limits of credibility. The values P_1 and P_2 are read in from control cards.
- 2. For each standard depth the cruise-mean value and standard deviation, and the station-mean value and standard deviation, are calculated using the equations 1b and 1c. In the latter case the station index j must be replaced by the cruise index i, i = 1,.....I, where I is the total number of cruises.

See footnote on page 5.

3. The overall mean value \overline{P}_k of P_{ijk} at a depth Z_k is calculated by averaging its cruise-mean values; the overall standard deviation \overline{SD}_k by:

$$\overline{SD}_{k} = \left[\frac{\sum_{i \in I} SD_{ik}^{2}}{I}\right]^{1/2}$$
(3a)

where SD_{ik} is the standard deviation for cruise i and depth Z_k , and I the total number of cruises (Croxton and Cowden, 1962). This equation gives an approximation of the overall standard deviation, provided that a roughly equal number of stations is sampled at each cruise.

4. The respective deviations $\mathrm{RD}_{\mbox{ijk}}$ of individual observations are defined by:

$$RD_{ijk} = \frac{P_{ijk} - \overline{P}_{ik}}{\overline{SD}_{k}}$$
 (3b)

where P_{ijk} is an observation of the parameter P at cruise i, station j and depth Z_k , and where \overline{P}_{ik} is the unweighted mean of P_{ijk} for a particular cruise i and depth Z_k . In connection with this equation two points must be made:

(a) The cruise-mean value of a parameter may vary with time due to natural processes (for example seasonal changes), which do not necessarily affect the magnitude of natural geographical variations within the cruise. The variability of data sampled on different cruises thus may be

similar even if their cruise-mean values differ significantly. In equation 3a it is therefore assumed that data from various cruises can be considered as subsamples taken from equally many parent populations with the same true standard deviations but differing true means (true is used versus observed to indicate the hypothetical mean of the overall population which, of course, can only be approximated by measurements but never measured directly). Calculations of relative deviations by comparing individual observations with the overall mean (replacing \overline{P}_{ik} in equation 3a by \overline{P}_k) may systematically overestimate the deviations for some of the cruises, and more consistent results are obtained using \overline{P}_{ik} .

(b) The deviation of individual values is expressed in relative units by dividing ($P_{ijk} - \overline{P}_{ik}$) by the overall standard deviation \overline{SD}_k rather than by the cruise-mean standard deviation \overline{SD}_{ik} . This is done to keep values of RD_{ijk} directly comparable not only within a cruise but also between cruises.

Input

- 1. Data on GLSP format on tape.
- 2. Editor tape to select desired stations from the GLSP tape and to renumber the stations using standard station numbers. (See statement 100 of main program for format of tape).
- 3. Control cards to determine cruises, parameters and depths to be read. (See subroutine RETRIEVE, Appendix A).
- 4. Control cards to determine upper and lower limits of acceptability of a parameter to be read, and to indicate

DEPTH

stations to be processed (format: see statement 750 in main program). If the last four fields, ILIM (1) through ILIM (4) are left blank, all standard stations sampled on any cruise will be used. If only part of the stations is required, these variables can be filled out, but the stations must be grouped in one or two continuous blocks of numbers (for example, 1 through 4 and 10 through 21). No provision is made for a random choice of stations to be included.

- 5. Sequence of control cards:
 - (a) range control card
 - (b) station control card
 - (c) control cards specified in RETRIEVE

Output

See Fig. 2. The columns give deviations of individual observations from the cruise mean, relative to the summer-mean standard deviation (equations 3a and 3b).

STATISTICS III

Purpose

To analyse the relative importance of random and systematic variability in a set of measurements by means of Snedecor's F test, assuming a normally distributed population.

Applications

1. To study data sampled within a water mass by comparing the variability of the difference between samples taken close together in time and/or space with that of the

population of all samples. This gives an indication of the relative importance of variability due to random errors or random environmental fluctuations and to slow drifts in the measurements or naturally determined geographical or temporal effects.

- 2. To compare the variability of data sampled in different water masses, such as hypolimnion and epilimnion in a stratified lake, and to study the relation in time or space of the observed variabilities in these water masses.
- 3. Both techniques have been applied with success to estimate the magnitude of sampling errors occurring in specific conductance and chloride data collected on Lake Ontario in 1966 and 1967 (Sweers, 1969).

Calculations

1. For each standard depth, Z_k , the mean, \overline{P}_k , standard deviation, S_k , and standard error of the mean, E_k , are calculated as in equations 1b, 1c and 1d. These statistics are compared with the mean, $\overline{P}_{k1/k2}$ standard deviation, $S_{k1/k2}$, and standard error of the mean, $E_{k1/k2}$, calculated for the difference between paired observations. Let, for example, $Q_{j,k1/k2}$ be the difference between observations $P_{j,k1}$ and $P_{j,k2}$ sampled at station j at depths Z_{k1} and Z_{k2} respectively:

$$Q_{j,k_{1}/k_{2}} = P_{j,k_{1}} - P_{j,k_{2}}$$
 (4a)

The statistics $\overline{P}_{k1/k2}$, $S_{k1/k2}$ and $E_{k1/k2}$ are then calculated from the equations 1b through 1d by substituting $Q_{j,k1/k2}$ for P_{jk} .

2. For normally distributed, randomly sampled populations $P_{j,k1}$ and $P_{j,k2}$, $j=1,\ldots,J$, the statistics $P_{k1/k2}$ and $S_{k1/k2}$ are related to \overline{P}_{k1} (or \overline{P}_{k2}) and S_{k1} (or S_{k2}) respectively (Arley and Buch, 1950):

$$\overline{P}_{k,/k_2} = P_{k_1} - P_{k_2} \tag{4b}$$

$$S_{k_1/k_2} = \left[S_{k_1}^2 + S_{k_2}^2 \right]^{1/2} \tag{4c}$$

Assuming the two populations $P_{j,k1}$ and $P_{j,k2}$ to be subsamples from the same parent population $P_{j,kk}$, the mean and standard deviation of this population can be estimated:

$$\overline{P}_{kk} = \frac{1}{2}(\overline{P}_{k_1} + \overline{P}_{k_2}) \tag{4d}$$

$$S_{kk} = \left[\frac{1}{2} \left\{ S_{k_1}^2 + S_{k_2}^2 \right\} \right]^{1/2} \tag{4e}$$

3. These results can be used to test: (1) whether the means \overline{P}_{k1} and \overline{P}_{k2} and standard deviations S_{k1} and S_{k2} belong to populations that could have been sampled from the same parent population, and (2) whether the samples $P_{j,k1}$ and $P_{j,k2}$, $j=1,\ldots,J$, are independent. The difference of the means can be tested using Student's t-distribution by calculating:

$$t = \sqrt{J} \frac{\overline{P}_{k_1} - \overline{P}_{k_2}}{\left\{S_{k_1}^2 + S_{k_2}^2\right\}^{1/2}} = \sqrt{J} \frac{\overline{P}_{k_1} - \overline{P}_{k_2}}{S_{kk}}$$
(4f)

The difference between the standard deviations can be tested, using Snedecor's F-distribution, by calculating:

$$F_{k_1/k_2} = \frac{S_{k_1}^2}{S_{k_2}^2}$$
 (4g)

Tables for these distributions can be found in most testbooks on statistics (Arley and Buch, 1950; Mandel, 1964). The independence of the two populations finally also can be tested with the F-distribution by calculating:

$$F_{k_1/k_2} = 2 \frac{S_{kk}^2}{S_{k_1/k_2}^2}$$
 (4h)

If F, in this case, exceeds the 95% confidence limits, the assumption that the populations $P_{j,kl}$ and $P_{j,k2}$ are independent subsamples of the same parent population has to be rejected.

Discussion

The physical causes leading to rejection can be manyfold, and include dependence of both series of data on geographical or temporal variations naturally occurring in the sampling environment as well as drift type of errors in the

measurements. It will often not be possible to distinguish between these effects, but under certain conditions this technique can be helpful in establishing the reliability of the data. In an application described in detail in a recent report by the author (1969), the variabilities of data sampled at the 50, 75 and 100 metre levels in Lake Ontario are compared. It is shown that significant, non-random variations occur in some of the chloride and specific conductance data, which can be explained plausibly only by assuming drift errors in the chemical analyses.

The program does not actually calculate the F and t statistics, but provides all material needed for subsequent manual evaluations. It could, however, easily be expanded to include these calculations. In the output the following statistics are calculated for each of the levels, or for the difference between observations at the pair of levels specified in the page heading:

Number of observations (number of differences)
Mean

Reference mean, used as a median in the tabulation Standard deviation (S)

Standard error of the mean (E)

Tabulation of values (or differences) in intervals centered around the reference mean.

Input

1. Data in GLSP format on tape.

50M-100M	-1.1379 0 3.7940 .7045		29 -1.1379 3.7940 .7045	0 0 0 0 0 0 0 0 0 0 0 0 0 0 0 0 0 0 0 0
100 M	29 322.4621 324.0000 4.3607 .4098		29 322,4621 324,0000 4,3607	C C C C C V U
S0M-75M	.1500 .2.8857 .4563		.1500 .1500 .2.8857 .4563	N N N N N N N N N N N N N N N N N N N
75 M	40 322.1750 324.0000 3.9868		40 322.1750 324.0000 3.9868 6304	0 0 0 0 0 0 0 0 0 0 0 0 0 0 0 0 0 0 0 0
1M-50M	44. 7391 -4.0000 6.6999		45, -4.9111 -4.0000 6.6727	C C C C C T X X X C 4 X C - C C
1M-10M	46 -2.9348 -4.0400 4.0400		45 -3.0667 -4.0000 3.9855	0 0 0 0 0 0 0 4 8 % 0 0 0 0 0
S O S	46 322.3478 324.0000 6.4039		45 324.0000 324.0000 4.7282	100000000000000000000000000000000000000
10 M	46 320.5435 320.0000 5.7812	000	45 320.0000 4.1148	C C C C C C C C C C C C C C C C C C C
D• 1	46 317.6087 316.0000 6.8154 1.0049	ALUE 296,	45 320.0000 6.0730	, , , , , , , , , , , , , , , , , , , ,
SP.COND.	80 -3.1675 -4.0000 3.6209 .4048	J & .	-3.2405 -4.0000 3.5763	
PAHAMETEH 10 M	80 322-1500 324-0000 5-5365	1 ОЕРТН	79 324.0000 4.4887	C C C C C C C C C C C C C C C C C C C
22017 - 67 1 M	314.9875 320.0000 6.1268	STATION	319.2785 320.0000 5.5892 .6288	000004 m p 0 1 1 1 1 1 1 0 0 0 0 0 0 0 0 0 0 0 0
CRUISE 22017	MEAN REF MN ST DEV SD MN	DELETE S	NO OHS MEAN REF MN ST DEV SD MN	22 + 11GH 20 + 000 100 + 000 1

2. Control cards to determine cruises, parameters and depths to be read (see description in Appendix D).

Output

See sample in Fig. 3.

Note

The statistical technique is strictly speading valid only for normally distributed variables. For other distributions the F-technique may still yield useful results if they are single-peaked and reasonably symmetrical. For distributions deviating seriously from normality, however, reference should be made to non-parametric statistical techniques as, for example, described in Siegel (1956).

ACKNOWLEDGEMENTS

The author is greatly indebted to Mr. H.R. Steeves, not only for his assistance in developing the programs described herein but also for the formulation and preparation of the subroutines RETRIEVE, TRNSLATE and READC, which greatly facilitated handling of the data. Thanks is also due to Mr. R.T. Moore for writing and testing STATISTICS I and II and to Mr. D. Hill for developing the third program.

REFERENCES

Arley, N. and K.R. Buch. 1950. Introduction to the theory of probability and statistics. John Wiley, New York.

238 p.

- Croxton, F.E. and D.J. Cowden. 1962. Applied general statistics. Pitman, London. 843 p.
- Dobson, H. 1968. Principal ions and dissolved oxygen in Lake
 Ontario. Proc. 10th Conf. Great Lakes Res.,
 Milwaukee, Apr. 1967; Int. Ass. for Great Lakes Res.
- Glennie, C.J. and T.M. MacLeod. 1967. The STAR system for storage and retrieval of data. Canadian Oceanographic Data Centre. Internal report.
- Mandel, J. 1964. The statistical analysis of experimental data. Interscience Publ., N.Y.; 410 p.
- Siegel, S. 1956. Non-parametric statistics for the behavioral sciences. McGraw Hill, Toronto; 312 p.
- Sweers, H.E. 1969. Structure, dynamics and chemistry of Lake
 Ontario: Investigations based on monitor cruises in
 1966 and 1967. Dept. Energy, Mines and Resources,
 Canada; Marine Sciences Br. Rept. 10.



APPENDIX A

SUBROUTINES RETRIEVE AND TRNSLATE*

Control cards read in by RETRIEVE determine what data are to be read from the GLSP (Great Lakes Surveillance Program) tape. The subroutine has two entry points: RETRIEVE and CONTRET. An initial call to entry point RETRIEVE sets up the routine, reads in the first set of control cards, and returns the values of the parameters for the first consecutive station as specified by the control cards. Subsequent calls are to CONTRET, which returns values for the same parameters. New control cards are read in when what is asked for in the previous set has been satisfied.

The argument list for RETRIEVE (in sequence of listing) is:

ISTAT

0 normally

NODEPTH

NPARAM

IDM (10)

9 if an END parameter card is read no. of depths returned no. of parameter values standard depth code (1=0m, 2=10m, 3=20m, 4=30m, 5=50m, 6=75m, 7=100m, 8=150m, and 9=200m), which returns standard depths read in from control card 2; for example if required depths are 30, 50 and 100 metres, then

IDM(1) = 3, IDM(2) = 4 and IDM(3) = 6.

More information about these subroutines can be obtained by contacting the Systems and Programming group at the Marine Sciences Branch, 615 Booth Str., Ottawa, Ontario.

IPCODEO (10) parameter codes

IPVALUE (25, 10) coded parameter values for up to

25 depths and 10 different parameters

ISTDPTHO (10) standard depths requested, see control

card 2.

The control cards are read in groups of three; only the first one is checked for END in col. 1-4. The cards contain the following information:

- Card 1: The subroutine returns data sampled between cruises

 CM1 and CM2, between times TIME1 and TIME2, and

 between consecutive stations ISM1 and ISM2 within

 the cruises CM1 and CM2. Only data falling within

 all three ranges will be returned. Any one or more

 of the three ranges can be left blank, in that case

 the data only have to fall within the remaining

 specified ranges. If the card is left blank, all

 cruises are searched. (See statement 101 of

 RETRIEVE for card format).
- Card 2: Gives the standard depths to be searched; all other depths are ignored. If card is blank all depths are returned. (See statement 103 for card format).
- Card 3: Gives the list of parameter codes for which values are to be found. (See statement 102 for card format).

The tape is treated as a continuous loop and is rewound when E.O.F. is hit with no indication given to the main program.

To decode the data returned by RETRIEVE, call TRNSLATE, which has the following arguments (in sequence of listing):

IC parameter code

IVAL coded parameter value

VALUE decoded parameter value (floating)

LAB (2) standard label of that parameter, used to identify the printout (e.g. TEMP for temperature, etc.)

APPENDIX B

LISTING OF STATISTICS I

PROGRAM STAT I

C

C

000

C

C

 \subset

C

C

C

 \subset

000

C

C

C

C

C

C

C

C

C

C

C

C

C

C C C

C

C

C

C

C

 \subset

C

C

C

C

C

 \subset

THIS PROGRAM WAS WRITTEN FOR THE CDC-3100 IN THE EMR DEPT. OTTAWA. 12K WORDS OF CORE ARE REQUIRED PLUS 2 TAPE DRIVES.

THE TAPE DRIVE ASSIGNMENTS ARE

1.-LOGICAL UNIT 01. A STANDARD GLSP FILE.

2.-LOGICAL UNIT 20. A TAPE CONTAINING A SEQUENCEOF RECORDS ORDERED BY CRUISE NO. AND CONSEC NO. CONTAINING THE STD. STATION NO. AND A WEIGHT TO BE APPLIED TO DAT MEASUREMENTS AT THAT STD. STATION. WHERE THE STD. STATION FIELD IS BLANK THE DATA FROM THAT CONSEC IS IGNORED AND THE NEXT CONSEC IS READ IN.

THE OUTPUT FOR EACH CRUISE IS PREPARED IN THREE STAGES..

1.—ALL NON—STANDARD DEPTHS ARE DISCARDED EXCEPT THE TWO DEEPEST
THE FIRST SET OF OBSERVATIONS IN EACH DEPTH INTERVAL IS KEPT, THE SEC.
AND THIRD ETC. ARE DISCARDED. THE STATISTICS FOR EACH STANDRD DEPTH
INTERVAL ARE CALCULATED.

2.—CONTROL CARDS READ AT THE BEGINNING DEFINE INTERVAS FOR EACH
PARAMETER. READING PAIRS ARE CLASSIFIED ACCORDING TO WHICH PAIR OF
INTERVALS THE OCCUR IN. STATISTICS ARE CALCULATED FOR EACH INTERVAL.

3.—THE BOTTOM READINGS ARE CLASSIFIED ACCORDING TO WHETHER
THE SOUNDING ASSOCIATED WITH THAT STATION IS .GT. OR .LE. 45. M.
STATISTICS FOR THE BOTTOM READINGS AND THE BOTTOM BUT ONE READINGS
ARE CALCULATED

THE FOLLOWING IS A LIST OF THE VARIABLES USED IN THE ROUTINE AND A SHORT EXPLANATION OF THEIR USE.

BEG READ FROM CONROL CARD. BEGINNING OF RANGE FOR STAGE 2. STD. DEV. OF P2 IN EACH CLASS STD. DEV. OF MEAN OF P2 IN EACH CLASS BSD BSDM BSUM SUM OF P2 OBS. IN EACH CLASS SUM OF P2*P2 IN EACH CLASS **BSUMSQ** D INCREMENT VALUE FOR PARAMETER INTERVALS IN STAGE 2. STD. DEV. OF P2 OBS IN A DEPTH INTERVAL DSD STD DEV OF MEAN OF P2 OBS. IN A DEPTH INTERVAL D\$DM SUM OF P2 OBS. IN A DEPTH INTERVAL DSUM DSUMSQ SUM OF B2*P2 IN A DEPTH INTERVAL END END OF RANGE FOR STAGE 2. ICNTRY COUNTRY CODE ICRN CRUISE NO (CURRENT) ICSN CONSEC NO (CURRENT IDAY DATE, TIME OF MEASUREMENTS

```
IDEPTH
IDM
                      RETURNS CODED DEPTH CORRESPONDING TO LEVELS OF IPVALUE DUMMY ARRAY
C
C
        IHOUR
C
        TMTN
        IMONTH
C
                      INSTITUTE NO.
        INS
C
                      LOGICAL UNIT HOLDING GLSP FILE
        IO
C
        IOCTANT
                      OCTANT CODE
C
                      STORES PARAMETER CODES IN SAME ORDER AS ON CNTRL. CARD
        IPCODE
C
        IPCODOLD
                      STORES THE OLD PARAMETER CODE
C
        IPVALUE
                      RETURNS PARAM. VALUES FROM INP. ROUTINE. UP TO 25 DEP. 10 PAR
C
                      RANGES WITHIN WHICH A READING IS CONSIDERED TO BE AT A S.D.
        IRNG
C
        TSD
                      STANDARD DEPTHS USED
C
        ISNDG
                      SOUNDING
C
        IVAL
                      DUMMY ARRAY FOR RETURNING NDEC VALUE
\subset
                      USED BY INPUT ROUTINES ONLY
        IVALUE
C
        IYEAR
C
        LABEL
                      ARRAY HOLDING OUTPUT HEADINGS
C
        LATDEG
C
        LATMIN
                           LATITUDE OF CURRENT STATION
C
                      3
        LATSEC
        LONGDEG
C
                      1
C
                           LONGITUDE OF CURRENT STATION
        LONGMIN
                      2
C
        LONGSEC
C
        MAME
C
        MID
                      INDEX AT WHICH XMID OCCURS
C
        MODIFIER
                      CALCULATION. P1 SHOULD BE TEMP. P2 SHOULD BE D 02 P OR 02 W
C
        MODIFIER
                      READ FROM CONTR. CRD FOR P2. =1 INDIC
                                                                   PERFORM SATO2
                      ARRAY HOLDING NAMES OF PARAMETERS RETRIEVED
        NAME
C
C
        NBOTSUM
                      NO OF OBSERVATIONS IN AN INTERVAL OF
C
                      SUM OF WEIGHTS ASSOC. WITH OBSERVATIONS IN A P1 INTERVAL
        NBOTSUMW
                      ARRAY HOLDING NO. DECIMALS REQUIRED IN OUTPUT OF P1+P2 VALUE
C
        NDEC
C
        NDEPTH
                      NO. OF DEPTHS MEASURED
                      NO OF OBSERVATIONS OF P2 IN A STANDARD DEPTH INTERVAL
        NOBD
C
C
        NOBDW
                      SUM OF WEIGHTS IN A DEPTH INTERVAL
C
        NOBPI
                      NO OF OBSERVATIONS IN AN INTERVAL PAIR
        NOBPIW
                      SUM OF WGHTS. IN EACH PARAMETER INTERVAL PAIR.
\mathsf{C}
                      NO OF OBS. OF P2 IN EACH OF THE BOTTOM DEPTH CLASSES.
C
        NOBSB
C
        NOBSBW
                      SUM OF WEIGHTS IN EACH CLASS
\subset
        NOCBS
                      CONSECUTIVE BT SLIDE NO.
                      USED BY INPUT ROUTINES ONLY
C
        NOCDE
                            READ FROM CRUISE MASTER CARDS (NOT PROCESSED )
C
        NOPC
\subset
        NSOUND
\subset
        NSTO
C
        NTSC
                      DUMMY VARIABLE FOR SPACING IN COMMON DATA
C
        NUMMY
                       ARRAY CONT. PARAMETER INTERVAL BOUNDS FOR OUTPUT HEADINGS.
\mathsf{C}
        PINT
        PSD
                      STANDARD DEVIATION IN INTERVALS OF P1
C
                       STANDARD DEVIATION OF THE MEAN IN INTERVALS OF P1
C
        PSDM
                       SUMS OF SQUARES OF P2 VALUES IN P1 INTERVALS
C
        PSOMSQ
        PSUM
                      UNWEIGHTED SUMS OF P2 IN P1 INTERVALS
C
                       WEIGHTED SUM OF WEIGHTS IN EACH CLASS
C
        WBSUM
C
        WDSUM
                      WEIGHTED DSUM
                         WEIGHTED SUMS OF P2 IN P1 INTERVALS
C
        WPSUM
                      MIDDLE VALUE READ FROM FIRST CONTROL CARD USED ONLY FOR P1
C
        XMID
C
C
```

SUBROUTINES USED

C

```
RETREIVE WITH ENTRY POINTS SEARCH, CONTRET, REWIND
C
      TRNSLATE WITH ENTRY POINTS TAG, OUTPUT, NUMDEC
C
C
\subset
C
      COMMON INS, ICRN, ICSN, ICNTRY, IOCTANT, LATDEG, LATMIN, LATSEC,
     1 LONGDEG, LONGMIN, LONGSEC, IYEAR, IMONTH, IDAY, IHOUR, IMIN, ISNDG,
     2 NDEPTH, NOCBS, NCODE(9), IVALUE(9), IO, NSTO, MAME(4), NOPC,
     3 NSOUND, NTSC
      COMMON/DATA/ NUMMY(260), ISD(10), IRNG(10)
      DATA (ISD=1,10,20,30,50,75,100,150,200), (IRNG=1,1,2,3,5,5,10,10,
     1 10)
      DIMENSION BEG(2), END(2), D(2), NEND(2), MID(2), XMID(2), IPCODOLD(3), IP
     1CODE(10), PSUM(24), PSUMSQ(24), NOBSB(4), NOBD( 15), DSUM(15), DSUMSQ(
     215), BSUM(4), BSUMSQ(4), NOBPI(24,22), IPVALUE(25,10), DPTH(25), VALUE(4
     3), IPAR(2), NAME(4), NBOTSUM(24), PSD(24), PSDM(24), DSD(15), DSDM(15)
      DIMENSION BSD(4), BSDM(4), LABEL(2,5), NDEC(2), IVF(8), IVO(15), IVR(8),
      1 IVM(8), IVA(8), IVT(6), PINT(2, 25), IDPTH(25), IDM(10), IVAL(2)
      DIMENSION NOSPIW(24,22), NOSDW(15), NOBSBW(4), NBOTSUMW(24)
      1 .WDSUM(15), WPSUM(24), WBSUM(4)
(
      SET LOGICAL UNITS
      KR=60
      MT1=20
       IO=01
       LP=61
C
       READ FIRST CONTROL CARD GIVES RANGES OF P1
C
  997 READ(KR, 100) BEG(1), END(1), D(1), XMID(1)
\subset
C
       CHECK FOR END OF JOB
       GO TO (999,996) ECFCKF(KR)
  996 CONTINUE
       CALL REWND(IDM)
       REWIND MT1
\subset
\subset
      READ C.C. 2 GIVES RANGES OF P2 .
C
       READ(KR, 100) BEG(2), END(2), D(2), XMID(2), MODIFIER
  100 FORMAT(4F10.5,39XI1)
C
C
       CALCULATE NO OF INTERVALS FOR EACH PARAMETER
C
       AND INDEX OF MID POINT
C
       DO 10 K=1,2
       NEND(K) = (END(K) - BEG(K))/D(K) + .5
       MID(K) = (XMID(K) - BEG(K))/D(K) + 1.5
   10 CONTINUE
       CALL RETRIEVE(ISTAT, NODPTH, NPRM, IDM, IDPTH, IPCODE, IPVALUE, IDM)
C
\subset
       DETERMINE NO OF DECIMALS NEEDED IN OUTPUT (= NO DEC. IN INP. +1)
C
       DO 375 K=1,2
       CALL NUMDEC(IPCODE(K), IVAL, END(K), DUM)
       NDEC(K)=IVAL(1)
```

```
375 CONTINUE
IF(MODIFIER) 376,377
  376 NDEC(2)=1
C
      SET UP OUTPUT HEADINGS
C
\subset
  377 LABEL(1,1)=4HDEPT $LABEL(2,1)=4HH
      LABEL(1,2)=4HMEAN $LABEL(2,2)=4H
      LABEL(1,3)=4HNO O $LABEL(2,3)=4HBS
      LABEL(1,4)=4HSD D $LABEL(2,4)=4HATA
      LABEL(1,5)=4HSD M SLABEL(2,5)=4HEAN
C
      SET UP OUTPUT FORMATS
      ENCODE(32,103,IVF)NDEC(2)
  103 FORMAT(16H(1H 5X2A4,11(F9.I1,5H,1X)))
      NIM=NEND(1)
      N2M=NEND(2)
      N1P2=NEND(1)+2
       N2P2 = NEND(2) + 2
      M1P1=NEND(1)+1
       DC 380 J=1,2
       N2P1=NEND(J)+1
       DC 380 I=1.N2P1
  380 PINT(J, I) = BEG(J) + (I-1)*D(J)
       II=4H) , A2
       IDAT=2H )
       JDAT=4H 0
       NDCM1=NDEC(1)+1
       ENCODE(60,106,IV0)NDCM1,NEND(1),NDCM1,II,II,NDCM1,NDCM1
  106 FORMAT(15H(1H 2A4,2H CF6.II,1H,1I2,7H(A2,F6.II,A2,R2,4H,F6.II,
      17H, A2, F6, I1, 10H, 6H ALL)
       NDCM2=NDEC(2)-1
       NP3=NEND(1)+3
       ENCODE(32,108,IVR) NDCM2
  108 FORMAT(10H(1H A2, F6, I1, 13H, 2X15(I4, 4X)))
       IVM(1) = 4H(3X \$IVM(2) = 4H2A4 \$IVM(3) = 4H
                                                   SIVM(4)=4H 15
       NMD = NP3 + 1
    DO 1 I=5,8
1 IVM(I)=IVR(I)
       II = 4H))
       ENCODE(32,109, IVA) NMD, NDEC(2)
  109 FCRMAT(7H(3X2A4,12,4H(F6,11,5H,2X)) )
       ENCODE(24:112:IVT) NDEC(2)
  112 FORMAT(13H(1H 2A4,4(F6,I1,5H,4X)))
       INDIC=1
C
       INITIALIZE ARRAYS HOLDING MEANS ETC. TO O.
  155 IJ=-21
       JK=0
       DO 159 I=1,24
       IJ=IJ+22
       JK = JK + 22
       WPSUM(I) = 0.0
       PSUM(I)=0.
       PSUMSQ(I)=C.
       IF(I.GT.15) 156,157
  157 NOBD(I)=0
```

```
NOBDW(I)=0
WDSUM(I)=0.0
      DSUM(I)=0.
      DSUMSQ(I)=0.
       IF(I.GT.4) 156,158
  158 NOBSB(I)=0
      NOBSBW(I)=0
      WBSUM(I)=0.0
      BSUM(I)=0.
      BSUMSQ(I)=0.
  156 DO 159 J=IJ,JK
      NOBPIW(J) = 0
  159 NOBPI(J)=0
C
C
       STORE CURRENT CRN AND PARM. CODES
      ICRNOLD=ICRN
       IPCODOLD(1)=IPCODE(1)
       IPCODOLD(2) = IPCODE(2)
C
      ISTAT = 0 MEANS NORMAL RETURN

ISTAT = 9 MEANS END C.C. READ BY INP. SUBROUTINES. ERGO END OF JOBSTEP
Č
C
C
\subset
   49 IF(ISTAT.EQ.O) 51,172
   49 IF(ISTAT.EQ.0)71,172
       CHECK TO SEE IF STD. STATION
      IF NOT RETRIEVE NEXT STATION
\overline{}
   71 GO TO (51,160,70), INDIC
C
   51 READ(MT1,101)NOCN, NOSN, NSSN, IWGHT
  101 FORMAT(2X3(1XI3),1XI4)
      IF(IWGHT)61,62
   62 IWGHT=1
   61 CONTINUE
      GO TO (60,70), EOFCKF(MT1)
   60 REWIND MT1
      GO TO 51
       IF(NOCN-ICRN) 51,80,72
70
   80 IF(NOSN-ICSN) 51,90,72
   90 IF(NSSN.EQ.0)289,50
   72 INDIC=3
      GO TO 289
C
       IF END OF CRUISE .. CALCULATE AND PRINT STATISTICS
C
C
   50 IF(ICRNOLD.EQ.ICRN)160,172
C
  160 ID=1
       INDIC=1
       IF(IPCODE(1).EQ.IPCODE(2)) 1550,1560
 1550 DO 1555 I=1,25
       IF(IDPTH(I).EQ.4H
                            ) 1560,1555
1655 IPVALUE(I,2)=IPVALUE(I,1)
160 CONTINUE
      WGHT=FLOAT(IWGHT)
C
C
      REMOVE NON-STANDARD DEPTHS
C
      DO 250 I=1,25
```

```
IF(IDPTH(I).NE.4H )252,254
252 DO 210 J=1,9
IF((ISD(J)-IRNG(J))*10.LE.IDPTH(I))215,250
  215 IF((ISD(J)+IRNG(J))*10.GE.IDPTH(I))220,210
  210 CONTINUE
      GO TO 250
\subset
       TAKE ONLY THE FIRST FOUND IN EACH DEPTH INTERVAL
C
\subset
  220 IF(J.EQ.JOLD)250,230
  230 IDPTH(ID)=IDPTH(I)
       IPVALUE(ID,1) = IPVALUE(I,1)
       IPVALUE(ID,2)=IPVALUE(I,2)
C
       STORE CORRESPONDING STD. DEPTH INDEX
C
\subset
       IPVALUE(ID,3)=J
       JOLD=J
       ID = ID + 1
  250 CONTINUE
  254 IDN=ID-1
       JOLD=8388607
C
       STORE BOTTOM DEPTH S IF REQUIREMENTS MET
C
\mathsf{C}
       DO 264 K=1,2
       NN=I+K-3
       LL=1
       IF(IYEAR.LE. 66) 1250,1260
 1250 LL=10
 1260 CONTINUE
       IF((ISNDG*LL-IDPTH(NN)).LE.100)260,264
   260 IDPTH(ID) = IDPTH(NN)
       IPVALUE(ID,2) = IPVALUE(NN,2)
       ID=ID+1
   264 CONTINUE
 C
       COMMENCE STORING VALUES FOR STATISTICS
 \subset
 C
       DO 270 I=1,IDN
 C
       IF P2= BLANK GO TO NEXT DEPTH
 C
                                 ) 272,270
       IF(IPVALUE(I,2).NE.4H
               TRNSLTE(IPCODOLD(2), IPVALUE(1,2), VALUE(2), NAME(1))
   272 CALL
       KUMP=1
                                  1 266,265
       IF(IPVALUE(I,1).EQ.4H
   265 KUMP=0
               TRNSLTE(IPCODOLD(1), IPVALUE(I,1), VALUE(1), NAME(3))
        CALL
        IF(MODIFIER) 267,266
 C
       PERFORM SAT 02 CALCULATION
 C
   267 T=VALUE(1)
       VALUE(2)=98.8*VALUE(2)/(14.380+T*(.4105+T*(-8.8E-3+9.5E-5*T)))
   266 CONTINUE
        STORE IN APPROPRIATE DEPTH INTERVAL . INDICATED BY IPVALUE(3)
 C
 C
 C
```

```
KK=IPVALUE(I,3)
DSUM(KK)=DSUM(KK)+VALUE(2)
      WDSUM(KK) = WDSUM(KK) + VALUE(2) * WGHT
      NOBDW(KK) = NOBDW(KK) + IWGHT
      NOPD(KK)=NOBD(KK)+1
      DSUMSQ(KK) = DSUMSQ(KK) + VALUE(2) * VALUE(2)
      IF(KUMP) 270,273
  273 CONTINUE
C
      STORE VALUES FOR STAGE 2 OUTPUT
\subset
\subset
      DO 274 K=1,2
C
      SELECT APPROPRAITE PARAMETER INTERVAL
      IF(VALUE(K).GE.BEG(K))275,276
  275 IF(VALUE(K).LE.END(K))277,278
  276 IPAR(K)=1
      GO TO 279
  278 IPAR(K)=NEND(K)+2
      GO TO 279
  277 IPAR(K) = IFIX((VALUE(K) + 8EG(K))/D(K)) + 2
  279 IF(K.EQ.1)274,280
  280 II=IPAR(1)
\subset
C
      STORE IN COUNTERS FOR INTERVAL II
(
      WPSUM(II) = WPSUM(II) + VALUE(2) * WCHT
      PSUM(II) = PSUM(II) + VALUE(2)
       PSUMSQ(II) = PSUMSQ(II) + VALUE(2) # VALUE(2)
  274 CONTINUE
      JJ=IPAR(2)
      THOWI+(LL, II) WI980N=(LL, II) WI980N
      NOBPI(II,JJ)=NOPPI(II,JJ) +1
  270 CONTINUE
      JGO=ID-IDN
       ID=ID-1
       GO TO (289,281,282),JGO
C
C
       STORE BOTTOM VALUES IN PROPER COUNTERS
C
  281 NO=1
       GO TO 283
  282 NO=2
  283 IF(IDPTH(ID).GE.450) 284,285
  284 ND=0
       GO TO 286
  285 ND=2
  286 JG0=JG0-1
       IF(IPVALUE(ID,2).NE.4H
                                   1287,288
              TRNSLTE(IPCODOLD(2), IPVALUE(ID, 2), VAL, NAME(1))
  287 CALL
       IF(MODIFIER)9000,9001
C
\mathsf{C}
       PERFORM SAT 02 CALCULATION FOR BOTTOM VALUES IF MODIFIER=1
C
 9000 CALL TRNSLTE(IPCODOLD(1), IPVALUE(ID, 1), T, NAME(3))
       VAL=98.8*VAL/(14.380-T*(.4105+T*(-8.8E+3+9.5E+5*T)))
 9001 CONTINUE
       NNEW=NO/JGO+ND
```

```
WBSUM(NNEW)=WBSUM(NNEW)+VAL*WGHT
      BSUM (NNEW) = BSUM (NNEW) + VAL
      BSUMSQ(NNEW) = BSUMSQ(NNEW) + VAL * VAL
      NOBSB (NNEW) = NOBSB (NNEW) +1
      NOBSBW (NNEW) = NOBSEW (NNEW) + IWGHT
      ID = ID - 1
  288 IF(JGO.GT.1)286,289
C
      STATION FINISHED . RETRIEVE NEXT STATION
\subset
  289 CALL CONTRET(ISTAT, NODPTH, NPRM, IDM, IDPTH, IPCODE, IPVALUE, IDM)
      GO TO 49
(
C
      PERFORM SUM DOWN P1 INTERVALS
C
      NBOTSUM(24) HOLDS SUM OVER ALL NBOTSUM
      SIMILARLY FOR NBOTSUMW(24) . PSUM(24) . WPSUM(24) . ETC.
\subset
      NOBPI(24.1) HOLDS SUM ACROSS P2 INTERVALS
NOBPI(23.1) HOLDS SUM ACROSS P2 INTERVALS FOR P1 INTERVALS .GT. XMID(1)
\subset
  172 NBOTSUM(24)=0
      NBOTSUMW(24)=0
      DO 300 I=1,22
      NBOTSUM(I)=0
      NBOTSUMW(I)=0
      NOBPI(24,1)=0
      NOBPIW(24,1)=0
      PSUM(24) = PSUM(24) + PSUM(I)
      WPSUM(24) = WPSUM(24) + WPSUM(I)
      PSUMSQ(24)=PSUMSQ(24)+PSUMSQ(I)
      10 330 J=1,22
      MOBPI(24,1)=NORPI(J,1)+NOBPI(24,1)
      NOBPIW(24,I)=NOBPIW(J,I)+NOBPIW(24,I)
      NBOTSUM(I)=NBOTSUM(I)+NOBPI(I,J)
      NBOTSUMW(I)=NBC[SUMW(I)+NOBPIW(I,J)
       IF(J.EQ.MID(1))305,330
  305 NOBPI(23,I)=NOBPI(24,I)
      NOBPIW(23,I)=NOBPIW(24,I)
  330 CONTINUE
      NOBPI(23,1)=NOBPI(24,1)-NOBPI( 23,1)
      NOBPIW(23,1)=NOBPIW(24,1)-NOBPIA( 23,1)
      NBOTSUM(24)=NBOTSUM(24)+NBOTSUM(I)
      NBOTSUMW(24)=NBOTSUMW(24)+NBOTSUMW(I)
       IF(I.EQ.MID(1))310,32
  310 NBOTSUM(23)=NBOTSUM(24)
       NBOTSUMW(23)=NROTSUMW(24)
       PSUM (23) = PSUM (24)
      WPSUM(23) = WPSUM(24)
      PSUMSQ(23)=PSUMSQ(24)
  320 PSUM(I)=PSUM(I)/NROTSUM(I)
      WPSUM(I)=WPSUM(I)/NBGTSUMW(I)
       IF(NROTSUM(I).LE.1)325,335
  325 PSD(I)=PSDM(I)=0.
      GO TO 300
\subset
       CALCULATE SID. DEV. FROM UNWEIGHTED MEANS AND SUMS OF SQUARES
  235 PSD(I)=SQRTF((PSUMSQ(I)-NBOTSUM(I)*PSUM(I)*PSUM(I))/(NBOTSUM(I)-1)
     1)
       PSDM(I)=PSD(I)/SQRTF(FLOAT(NBOTSUM(I)))
```

```
300 CONTINUE
      NBOTSUM(23) = NBOTSUM(24) - NBOTSUM(23)
      NBOTSUMW(23) = NBOTSUMW(24) - NBOTSUMW(23)
      PSUM(23)=PSUM(24)-PSUM(23)
      WPSUM(23) = WPSUM(24) - WPSUM(23)
      PSUMSQ(23)=PSUMSQ(24)-PSUMSQ(23)
      DO 340 K=23,24
      PSUM(K)=PSUM(K)/NBOTSUM(K)
      WPSUM(K)=WPSUM(K)/NBOTSUMW(K)
      PSD(K) = SQRTF((PSUMSG(K) - NBOTSUM(K) *PSUM(K) *PSUM(K))/(NBOTSUM(K)-1)
     1))
      PSDM(K)=PSD(K)/SQRTF(FLOAT(NBOTSUM(K)))
  340 CONTINUE
C
      WRITE CRUISE HEADING
\subset
      WRITE(LP,120) ICRNOLD
  120 FORMAT (12H1CRUISE NO.
C
      CALCULATION FOR STAGE 1 DUTPUT
C
      DSUM(11), WDSUM(11), NOBD(11), ETC. HOLD TOTALS OVER ALL DEPTHS
      DSUM(10) , ETC. HOLDS TOTALS FOR ALL DEPTHS . GT. 50 M.
C
      DSUM(11)=0.
      WDSUM(11)=0.
      DSUMSQ(11)=0.
      NOBD(11)=0
      NOBDW(11)=0
      DO 350 I=1,9
      DSUM(11) = DSUM(11) + DSUM(I)
      WDSUM(11) = WDSUM(11) + WDSUM(I)
      DSUMSQ(11)=DSUMSQ(11)+DSUMSQ(I)
      NOBD(11) = NOBD(11) + NOBD(1)
      NOBDW(11) = NOBDW(11) + NOBDW(I)
      DSUM(I)=DSUM(I)/NOBD(I)
      WDSUM(I)=WDSUM(I)/NOBDW(I)
      DSD(I) = SQRT((DSUMSQ(I) - NOBD(I) *DSUM(I) *DSUM(I))/(NOBD(I) - 1))
      DSDM(I) = DSD(I) / SQRT(FLOAT(NOBD(I)))
      IF(I.EQ.4)351,350
  351 DSUM(10) = DSUM(11)
      WDSUM(10) = WDSUM(11)
      DSUMSQ(10)=DSUMSQ(11)
      NOBD(10) = NOBD(11)
      NOBDW(10)=NOBDW(11)
  350 CONTINUE
       WRITE(LP,121)(NAME(I), I=1,4)
  121 FORMAT(12H PARAMETER 2A4,18H
                                        (COMPARED WITH 2A4,1H)///)
      DSUM(10) = DSUM(11) - DSUM(10)
       WDSUM(10) = WDSUM(11) - WDSUM(10)
      DSUMSQ(10) = DSUMSQ(11) - DSUMSQ(10)
      NOBD(10) = NOBD(11) - NOBD(10)
      NOBDW(10) = NORDW(11) + NORDW(10)
C
\subset
      WRITE STAGE 1 HEADING
\mathbf{C}
      WRITE(LP,102)(LABEL(I,1),I=1,2),(ISD(I),I=1,9)
  102 FORMAT(1H 5X2A4,5X9(I3,7X),3H)507X3HALL)
\subset
       CALCULATION OF MEANS, S. D. PETC. FOR TOTALS OVER ALL DEPTHS AND
(
```

```
DEPTHS .GT. 50 M.
      DO 360 I=10,11
      DSUM(I)=DSUM(I)/NOBD(I)
      WDSUM(I) = WDSUM(I) / NOBDW(I)
      DSD(I) = SQRT((DSUMSQ(I) - NO3D(I) * DSUM(I) * DSUM(I)) / (NOBD(I) - 1))
  360 DSDM(I)=DSD(I)/SQRT(FLOAT(NOBD(I)))
      WRITE(LP, IVF)(LABEL(I,2), I=1,2), (WDSUM(I), I=1,11)
\subset
C
      STAGE 3 CALCULATIONS
\subset
\subset
      INDEX = 1
                     BOTTM READING FOR BOTTOM DEPTH .GE. 45 M.
C
       INDEX = 2
                     BOTTM BUT 1 READING FOR BOTTOM DEPTH .GE. 45 M.
                     BOTTM READING FOR BOTTOM DEPTH .LT. 45 M.
C
       INDEX = 3
C
       INDEX = 4
                     BOTTM BUT 1 READING FOR BOTTOM DEPTH .LT. 45 M.
(
      DO 370 I=1,4
      WBSUM(I) = WBSUM(I): / NOBSBW(I)
       BSUM(I)=BSUM(I)/NOBSB(I)
       BSD(I) = SQRT((BSUMSQ(I) - NOBSB(I) * BSUM(I) * BSUM(I)) / (NOBSB(I) - 1))
      BSDM(I)=BSD(I)/SQRT(FLOAT(NOBSB(I)))
  370 CONTINUE
      WRITE(LP,104)(LAREL(I,3),I=1,2),(NOSD(I),I=1,11)
  104 FORMAT(1H 5X2A4,5X11(I4,6X))
C
       WRITE MEANS ETC. FOR STAGE 1
C
       WRITE(LP, IVF)(LABEL(I,4), I=1,2), (DSD(I), I=1,11)
       WRITE(LP, IVF)(LABEL(I,5), I=1,2), (DSDM(I), I=1,11)
       WRITE(LP,105) NAME(3), NAME(4)
  105 FORMAT(1H-10X28HNO OF OBSERVATIONS IN EACH
                                                           2A4,9H INTERVAL
       WRITE(LP, IVO) NAME(3), NAME(4), PINT(1,1), ( IDAT, PINT(1,1), I=1, NIM)
      1, IDAT, END(1), IDAT, XMID(1)
       NAME(3) = NAME(4) = 4H - -
C
       WRITE HEADING FOR STAGE 2
WRITE(LP, IVO) (NAME(I), I=3,4), PINT(1,1), ((JDAT, PINT(1,1)), I=2,N1P1)
      1, IDAT, END(1), IDAT, XMID(1)
       WRITE(LP,107) NAME(1), NAME(2)
  107 FORMAT(1H 2A4,10HINTERVALS$ )
(
       WRITE TOTALS FOR EACH INTERVAL PAIR WITH HEADINGS AT SIDE OF PAGE
C
C
       DO 800 I=1.N2P1
       WRITE(LP, IVR) JDAT, PINT(2, I), (NOBPI(J, I), J=1, N1P2), NOBPI(23, I),
      1NOBPI(24,1)
       IF(I.EQ.N2P1)801,802
  802 WRITE(LP, IVR) IDAT, PINT(2, I)
  800 CONTINUE
  801 WRITE(LP, IVR) IDAT, END(2), (NOBPI(J, N2P2), J=1, N1P2), NOBPI(23, N2P2),
      1NOBPI(24, N2P2)
\subset
       WRITE MEANS ETC. FOR STAGE 2
C
C
       WRITE(LP, IVA)(LABEL(I,2), I=1,2), (WPSUM(I), I=1, N1P2), WPSUM(23),
      1WPSUM(24)
       WRITE(LP, IVM)(LABEL(1,3), I=1,2), (NBOTSUM(1), I=1, N1P2), NBOTSUM(23),
      1NBOTSUM(24)
```

```
WRITE(LP.IVA)(LAREL(I.4).)=1.92).(PSD(I).I=1.N1P2).PSD(23).PSD(24)
WRITE(LP.IVA)(LAREL(I.5).F=1.92).(PSDM(I).F=1.N1P2).PSDM(23).PSDM(2
      14)
C
       WRITE HEADINGS FOR STAGE 3 OUTPUT
C
       WRITE(LP,110)
  110 FORMAT(12H-BOTTOM SUMS/10X5HBDEEP4X6HBBDEEP3X8HBSHALLOW2X9HBBSHALL
      10W
       WRITE(LP . IVT) (LABEL(I . 2) . I = 1 . 2) . (WBSUM(I) . I = 1 . 4)
       WRITE(LP+113)(LABEL(I+3)+I=1+2)+(NOBSB(I)+I=1+4)
       WRITE(LP, IVT)(LABEL(I, 4), I=1,2), (BSD(I), I=1,4)
       WRITE(LP, IVT)(LABEL(I,5), I=1,2), (BSDM(I), I=1,4)
  113 FORMAT(1H 2A4,1X4( I4,6X))
C
       IF ISTAT = 0 RETURN FOR NEXT CRUISE
IF ISTAT = 9 ALL CRUISES SPECIFIED BY CURRENT SET OF CONTROL CARDS
\subset
\subset
C
       HAVE BEEN READ AND AN END CARD HAS BEEN READ. IN THIS CASE IF
       FURTHER PROCESSING IS REQUESTED TWO MORE CONT. CRDS. GIVING PARAMETER
\subset
       INTERVALS MUST BE READ. AN EOF ON THE CARD READER INDICATES JOB FND.
\subset
\subset
       IF(ISTAT.FQ.0)155,999
       INDIC=2
       IF(ISTAT.EG.0) 155,997
  999 END
```

APPENDIX C

LISTING OF STATISTICS II

```
PROGRAM STAT II
\subset
C*******
C*****THIS PROGRAM REQUIRES 2 MAG. TAPES AS INPUT
      1 GLSP DATA FILF
(
      2. STANDARD STATION TAPE
THE PROGRAM WAS WRITTEN FOR THE CDC-3100 EMR DEPARTEMENT IN OTTOWA
C*****IT REQUIRES THE USE OF SUBROUTINES RETREIVE, READC, TRNSLATE, CODE
       ENTRY POINTS OF RETRIEVE ARE SEARCH, CONTRET, REWND ENTRY POINTS OF TRNSLATE ARE TAG, OUTPUT, NUMBEC
(
C**********************************
                                                                              表长者公司名者有者表表长
C
       COMMON INS, ICRN, ICRN, ICNTRY, IOCTANT, LATDEG, LATMIN, LATSEC,
      1 LONGDEG, LONGMIN, LONGSEC, IYFAR, IMONTH, IDAY, IHOUR, IMIN, ISNDG,
      2 NDEPTH , NOCBS , NCODE (9) , IVALUE (9) , IO , NSTO , NAME (4) , NOPC ,
      3 NSOUND, NTSC , IFILL (50), VAL (11, 5, 62)
      DIMENSION IDN(10), IDPTH(15), IPCODE(10), IPVALUE(15,10),
      IISTOPTH(10) : ILIM(4)
      DIMENSION SUM(11,5), VARI(11,5), SD(11,5), AVSD(5), NAMEP
      1(2), SUMC(5), XNOSD(11), NO(11,5), SUMSQ(11,5), BIGSM(1), SQSM(1), SDC(1)
      2, TOTAL(1)
       GET PARAMETER RANGE CHECKS AND STD STN RANGES
C
       A VALUE OF A PARAMETER IS REJECTED UNLESS IT LIES BETWEEN SVAL AND BVAL
C
       ALL DATA FROM ANY STATION US REJECTED UNLESS IT IS A STD STN AND
C
       ITS STD STN NO. LIES BETWEEN ILIM1 AND ILIM2 OR ILIM3 AND ILIM4
C
       IBARE = 0
 1887 READ(60,750) SVAL, BVAL, ILIM
  750 FORMAT(2F10.5/414)
C
       IF THE CARD IS BLANK ACCEPT ALL STD STN
C
       IF(ILIM(1)+ILIM(2)) 1971,1971,1972
 1971 ILIM(1) = 0
       ILIM(2) = 500
 1972 CONTINUE
C
        NCRK IS NUMBER OF CRUISES TO BE READ
NSTK IS MAXIMUM NUMBER OF STATIONS
C
C
C
        NDPK IS MAXIMUM NUMBER OF DEPTHS
C
        LAST TWO ARE MAXIMUM DIMENSIONS,
C
        NCRK ALSO ACTS AS COUNTER AND MUST BE PRECISE
       NCRK=8
       NSTK=62
       NDPK=5
       LP=61
       KR = 20
       10=01
\mathsf{C}
C
       INITIALIZE INPUT ROUTINE READC
Ċ
       CALL REWND(N)
\subset
C
       START MAIN LOOP CONTROLLED BY I. I SS INCREMENTED BY 1 FOR EACH CRUISE
       I = 1
\subset
```

```
INITIALIZE INPUT ARRAY
C
      DO 14 J=1 , NDPK
      DO 14 IC=1,NCRK
      NO(IC \cdot J) = 0
      DO 14 K=1.NSTK
   14 VAL(IC, J, K) = 99999.
C
\subset
      GET FIRST STATION
C
      STORE CRUISE NO.
      CALL RETRIEVE(ISTAT, NODEPTH, NPARAM, IDN, IDPTH, IPCODE, IPVALUE,
     1ISTDPTH)
      ICRNST=ICRN
      IPCODEST=IPCODE(1)
\subset
C
      A NEW CRUISE'IS INDICATED BY ISTAT .NE. O OR THE CRN CHANGING
\subset
      IF NEW CRUISE CHANGED GO PROCESS DATA FOR OLD CRUISE
\subset
      ISTAT .NE. 0 INDICATES JOB DONE . IN THIS CASE THE CRN WILL NOT CHANGE
C
   18 IF(ISTAT.EQ.0)1.3
    1 IF(ICRNST.NE.ICRN)3,4
C
      READ STD STN TAPE TO SEE IF THIS IS A STN READ STD STN TAPE TO SEE IF THIS IS A STD STN
C
      IF AN EOF IS HIT OR IF TOO FAR UP THE TAPE REWIND AND START AT BOT
(
      THIS CONSEC IS NOT A STD STN IF NSSN=C
(
    4 READ(KR, 100) NOCN, NOSN, NSSN
  100 FORMAT(3X,3(13,1X))
      IF(FOFCKF(KR).FQ.1)5,6
    5 REWIND KR
      GO TO 4
    6 IF(NOCN.EQ.ICRN)7,9
    7 IF(NOSN.FQ.ICSN)8,10
    9 IF(NOCN.LT.ICRN)4,5
   10 IF(NOSN.LT.ICSN)4,5
    8 IF(NSSN.NE.0)11,12
C
      IF IT IS A STD STN SEE IF IT IS INSIDE WANTED RANGE
C
   11 DO 1969 III=1:3:2
       IF(ILIM(III).LE.NSSN.AND.ILIM(III+1).GE.NSSN) 1970,1969
 1969 CONTINUE
      GO TO 12
\subset
      REJECT INPUT VALUES IF BLANK
      DECODE THEM IF NONBLANK AND STORE IN INPUT ARRAY IF THEY ARE INSIDE
0
      SPECIFIED RANGES
      FOR A GIVEN CRUISE ,STD STN, AND DEPTH, THE ENTRY IN THE INPUT ARRAY WILL
C
      RETAIN A VALUE OF 99999. IF NO ACCEPTABLE VALUE EXISTS
C
 1970 DO 13 J=1.NDPK
                                 113,16
      IF(IPVALUE(J,1).EQ.4H
   16 CALL TRNSLTE(IPCODEST, IPVALUE(J,1), WAIT, DUMMY)
 IF(WAIT-SVAL) 13,1965,1964
1964 IF(WAIT-BVAL) 1965,1965,13
 1965 IF(VAL(I, J, NSSN), EQ. 99999.) 1966, 1967
 1967 VAL(1,J,NS:N) = (VAL(1,J,NSSN)+ WAIT)/2
```

```
GO TO 13
1966 VAL(I.J.NSSN)=WAIT
C
      NO(IJ) STORES THE NO OF ACCEPTABLE VALUES OCCURING AT EACH STD STN
C
      NO(I,J) = NO(I,J) + 1
   13 CONTINUE
\subset
C
      GET NEXT CONSEC AND GO BACK STD STN CHECK
(
   12 CALL CONTRET(ISTAT, NODEPTH, NPARAM, IDN, IDPTH, IPCODE, IPVALUE, ISTDPTH
     1)
      GO TO 18
C
\subset
      THIS SECTION DOES THE PROCESSING REQUIRED FOR EACH CRUISE
C
\mathbf{C}
      GET THE NAME OF THE INPUT PARAMATER
C
C
    3 CALL TAG (IPCODEST, IDUM, DUMMY, NAMEP)
C
      CALCULATE THE MEAN AND STD DEV FOR EACH DEPTH OVER ALL THE STD STN FOR
\subset
\overline{C}
      THE CRUISE
C
      DO 20 J=1,NDPK
      NEND=NO(I.J)
      SUM(I,J)=0.
      SUMSQ(1,J)=0.
      DO 21 K=1 NSTK
      IF(VAL(I,J,K),EQ,99999,)21,121
  121 SUM(I,J)=SUM(I,J)+VAL(I,J,K)
      SUMSQ(I,J)=SUMSQ(I,J)+VAL(I,J,K)**2
      KLAST=K
   21 CONTINUE
      SUM(I,J)=SUM(I,J)/NEND
      VARI(I,J) = ABSF(SUMSQ(I,J) - SUM(I,J) **2*NFND)/(NEND-1)
      SD(I,J)=SQRTF(VARI(I,J))
      IF(NEND-1) 32,23,20
(
C
      IF THERE IS CNLY ONE VALUE FOR A GIVEN STN NEGATE THE VALUE
C
   23 VAL(I,J,KLAST) = -VAL(I,J,KLAST)
      GO TO 24
   32 SUM(I,J)=0.
   24 SD(I,J)=0.
   20 CONTINUE
   26 ICRNST=ICRN
      I = I + 1
C
C
      UNLESS LAST CONTROL CARD HAS BEEN READ IN GO BACK TO CET ANOTHER CRUISE
C
      IF(ISTAT.FQ.9)25,4
C
C*****OUTPUT SECTION ONE PAGE FOR EACH STD DEPTH SPECIFIED ON CONTROL CARDS
C
\subset
      CALCULATE THE AVERAGE STD DEV OF READINGS OVER ALL CRUISES AT EACH DEPTH
\subset
   25 DO 30 J=1,NDPK
      SUMC(J)=0.
```

```
DO 31 I=1 •NCRK
SUMC(J) = SUMC(J) + VARI(I•J)
      AVSD(J)=SQRTF(SUMC(J)/NCRK)
   30 CONTINUE
      DO 50 J=1.NDPK
C
      WRITE PAGE HEADING
      WRITE(LP,105)(NAMEP(I),I=1,2),ISTDPTH(J)
  105 FORMAT(1H1,9X,10H PARAMETER,2A4,20X,7H DEPTH ,13/1
      WRITE(LP, 106)
  106 FORMAT(8H STATION,107X,6HSTATN./,7H NUMBER, 4X1H17X1H37X1H57X1H7
     17X1H96X2H116X2H1?6X2H156X2H176X2H196X2H21
     28X, THAVERAGE, 4X, 13HSTANDAPD DEV.)
      USING THE MEAP STD DEV OVER ALL CRUISES AND STATIONS FOR A GIVEN DEPTH
C
      CALCULATE THE NO. OF STD DEV EACH READING LIES FROM THE MEAN FOR THE
      CRUISE IN WHICH IT OCCURS
      DO 51 K=1.NSTK
      BIGSM=0.
      SQSM=0.
      DO 52 I=1.NCRK
      IF(VAL(I,J,K).EQ.99999.)53,54
   53 XNOSD(I)=0.
      GO TO 52
   54 IF(VAL(I,J,K).LT.O.) 55,56
   55 XNOSD(I)=.001
      VAL(I,J,K)=-VAL(I,J,K)
      GO TO 58
   56 XNOSD(I) = (VAL(I, J, K) - SUM(I, J))/AVSD(J)
   58 KN=KN+1
C
      CALCULATE THE MEAN AND STD DEV FOR EACH STATION
C
      PIGSM=BIGSM+VAL(I,J,K)
      SGSM=SQSM+VAL(I,J,K)**2
   52 CONTINUE
       IF(KN-1) 59,57,57
   57 BIGSM=BIGSM/KN
       IF(KN-1) 63,63,60
   60 KJ=KN+1
       SDC=SQRTF((SQSM-KN* BIGSM**2)/KJ)
       GOTO 65
   59 BIGSM=0.
   63 SDC=0.
   65 CONTINUE
       WRITE(LP, 200)K, (XNOSD(I), I=1, NCRK), BIGSM, SDC
  200 FORMAT(2XI2,2X11(1XF5.1,2X),4XF7.3,4XF7.3)
   51 CONTINUE
       TOTAL=0.
       IJ=0
\overline{C}
       CALCULATE OVERALL MEAN FOR PAGE
\overline{\phantom{a}}
C
       DO 70 I=1,NCRK
IF(SUM(I,J) .EO.(.) 70,72
   72 IJ=IJ+1
```

```
TOTAL=TOTAL+SUM(1,J)
   70 CONTINUE
      TOTAL=TOTAL/IJ
\mathsf{C}
Č
      WRITE MEAN FOR EACH CRUISE AND FOR PAGE
      WRITE(LP,500)(SUM(I,J),I=1,NCRK),TOTAL
  500 FORMAT(8H CRUISE / +6H AVG
                                       11(1X,F7.3),4X,F7.3)
     WRITE(LP,300)(SD(I,J),I=1,NCRK)
  300 FORMAT(4H STD/,4H D2V1X11(1XF7.3))
     WRITE(LP,199)AVSD(J)
 199 FORMAT(27H OVERALL STANDARD DEVIATION, 81X, F8.3)
C
     AVSD STANDS FOR AVRAGE STANDARD DEVIATION, XNOSD FOR THE NUMBER OF AVSD@S
C
\overline{C}
     A READING DIFFERS FROM THE MEAN WHICH IS LABELLED SUM
   50 CONTINUE
      IPCODEST=IPCODE
      ICRNST=ICRN
     DO 40 I=1.NCRK
     DC 40 J=1 , NDPK
  40 NO(I,J)=0
      I = 1
     IF(ISTAT.NE.0)999,4
  999 STOP
     END
```

APPENDIX D

DESCRIPTION OF STATISTICS III

STATISTICS III consists of thirteen separate steps which are executed in sequence as they appear, except where otherwise indicated. The beginning of each step is indicated by a comment card (C**...). Each step is described below.

In the first step, variables used in the program are declared and some are given initial values. The tape unit (logical unit 1) which contains the data is rewound to its initial position.

In the second step the control cards are read (subroutine READC*, not listed herewith). The first control card contains a two digit number, NP, which is the number of parameters to be analysed. This is followed by NP cards, each of which has information about one of the parameters. These cards are formatted as follows:

	position	format	information
Card 1	1-2	I2	number of parameters to be
			analysed
Card 2	1-8	2A4	parameter name (abbreviated)
	9-13	I5	parameter code (right
			justified)
	14-18	F 5	position of the decimal point
			in the data on tape
	19-23	F 5	inverse of increment desired
			in table output

^{*}See footnote on page 24.

24-28 I5 minimum allowable value of the parameter

29-33 I5 maximum allowable value Card 3 and following cards as card 2.

The next step reads the data for a full cruise. If there is no other cruise on the tape, the program is terminated. Otherwise, all values of the required parameters taken at standard depths (0-2 m, 9-11 m, 45-55m, 70-80 m, 90-110 m) are noted. If they are outside the minimum or maximum indicated on the control card, they are printed out and rejected for further calculations. The useful values are stored in an array IA(5, NST, NP): 5 is the number of standard depths, NST is the number of stations in the cruise, and NP is the number of parameters.

The parameters are then analysed one by one. Step four sets up M as the index of the parameter to be studied, and fills the array A(I,J) with the scaled values IA(I,J,M)/DC(M) of parameter M, where DC is the scale factor defined in columns 19-23 on the parameter control cards. Also the heading is printed on the output listing.

The fifth step accumulates a count (N), sum (S) and sum of squares (SS) for each statistical variable. There are twelve of these sums, determined as follows:

For all stations at which values are recorded at 1 and 10 m:

- 1. value at 1 m
- value at 10 m
- 3. difference of values at 1 m and 10 m

For stations at which values are recorded at 1 m, 10 m and 50 m:

- 4. value at 1 m
- 5. value at 10 m
- 6. value at 50 m
- 7. difference between values at 1 m and 10 m
- 8. difference between values at 1 m and 50 m

 For stations at which values are recorded at 1 m, 10 m, 50 m,

 75 m:
 - 9. value at 75 m
- 10. difference between values at 50 m and 75 m For stations at which values are recorded at 1 m, 10 m, 50 m, 100 m:
 - 11. value at 100 m
- 12. difference between values at 50 m and 100 m
 To accumulate the sums, the subroutine ADD is used.

Once all the sums are formed, step six calculates the mean standard deviation and standard deviation of the mean for each statistical variable. If no values are measured in a cruise, these are all assigned the value zero.

For step seven, a rounded value of the mean (RM) is calculated, which will be used as the reference value for the centre of the data table to be calculated in step 8. Then all of the statistical results are printed out.

In step eight, a range VLIM equal to three times the largest standard deviation of the twelve variables calculated above (for every time one or more values are rejected in step 11, the multiplication factor is increased by one), is

calculated, and the intervals for the data table are taken from RM-VLIM to RM+VLIM in steps of 1/RINC(M) (where RINC(M) is the inverse of the increment specified on the control card for parameter M). If too many steps (over 50) are required, the size of each step is doubled, and the program goes back to step seven to calculate a new reference mean.

Otherwise, the data values are sorted by step ten into an array NOBS, which contains the number of values of the variable in each of the intervals defined in step eight above. Any values falling above or below the tabulation-range are counted in the arrays NHI and NLO respectively.

If any values do exist outside the range specified on the control cards, step eleven prints them out, and deletes them from the array A. Control then returns to step five to recalculate everything without the deleted values. If no values are deleted, the table of counts is printed, and the processing for this parameter is completed. If another parameter remains, control returns to step four to begin the new analysis. Otherwise, it goes to step two to get data for a new cruise.

The program concludes when the last cruise on the tape has been processed.



APPENDIX E

LISTING OF STATISTICS III

```
PROGRAM STAT III
        DECLARE AND INITIALIZE VARIABLES
    DIMENSION VM(12), RM(12), SD(12), SDM(12), NHI(12), NLO(12)
    DIMENSION NAM(2:11): IC(11): DC(11): RINC(11): DIFF(50): NOBS(12:50)
    DIMENSION ICAL(11), JCAL(11), IA(5,125,7)
    COMMON NCTY, INSCR, NST, NTST, NAME (4), NOPC, NSND, NTSC, NOCT, LAT, LON,
   1 NDAT,NTIM,NDSND,NOD,NBT,ICOD(9),IVAL(9),IO
    COMMON/DATA/N(12),S(12),SS(12),A(5,125),ID(2,5),ITL(24),IND(5)
    DATA (ID = 0,20,90,110,450,550,700,800,900,1100)
    DAFA (IND = 1,2,6,9,11)
      TA (ITL=4H ,4H 1 M,4H ,4H10 M,4H 1M,4H-10M,4H ,4H 1 M
4H ,4H10 M,4H ,4H50 M,4H 1M,4H-10M,4H 1M,4H-50M,4H
4H75 M,4H 50M,4H-75M,4H 1,4H00 M,4H50M-,4H100M)
    DATA (ITL=4H
                                                                    94H 1 M9
     4H
    10 = 1
    REWIND IO
* *
    2 READ CONTROL CARDS
    READ (60,99) NP
 99 FORMAT (12)
    READ (60,91) (NAM(1,1),NAM(2,1),IC(I),DC(I),RINC(I),ICAL(I),
       JCAL(I), I=1,NP)
91 FORMAT (2A4,15,2F5,2I5)
   3 READ CRUISE DATA (IF NO NEW CRUISE, GO TO END)
 86 DO 87 I=1.NP
    DO 87 J=1,125
    DO 87 K=1.5
 87 IA(K,J,I) = 0
  7 CALL READC(K)
    IF (K.EQ.9) 85,6
  6 IF (K.EQ.O) 7,18
 18 NDATE= NDAT/10000
    NSCR = INSCR
    L = 0
  1 IF (K.EQ.9.OR.INSCR.NE.NSCR) 4,5
  5 M = NST
    CALL READC(K)
    IF (INSCR.EQ.21001.OR.INSCR.EQ.22085) 100,101
100 INSCR = NSCR
101 IF (K.EQ.2) 3,1
  3 DO 10 I=1.5
   . IF (IVAL(1).GE.ID(1,1).AND.IVAL(1).LE.ID(2,1)) 11,10
- 10 CONTINUE
    GO TO 5
 11 DO 12 J=2.9
DO 12 K=1.NP
    IF (ICOD(J).EQ.IC(K)) 13.12
 13 IA(I,NST,K) = IVAL(J)
    IF (IVAL(J).GT.JCAL(K).OR.IVAL(J).LT.ICAL(K)) 15,12
 15 IF (L.EQ.O) 16,17
 16 L = 1
    WRITE (61,98) NSCR, NDATE
 98 FORMAT (70H1THE FOLLOWING VALUES ARE OUTSIDE THE RANGE OF CALIBRAT
   110N FOR CRUISE ,15,3H - ,12,1H. // 36H STATION
                                                          DEPTH PARAMETER
      VALUE //)
 17 \text{ KK} = IVAL(1) / 10
    VLIM = IA(I,NST,K)/DC(K)
    WRITE (61,97) NST, KK, NAM(1,K), NAM(2,K), VLIM
 97 FORMAT (218,4X,2A4,F8.3)
    IA(I,NSI,<) = 0
 12 CONTINUE
```

```
GO TO 5
4 BACKSPACE 10
C **
         PREPARE FOR INDIVIDUAL PARAMETER
      DO 80 M=1 NP
      KK = 2
      DO 9 I=1,5
      DO 9 J=1,NST
    9 A(I,J) = IA(I,J,M)/DC(M)
      WRITE (61,90) NSCR, NDATE, (NAM(I, M), I=1,2), ITL
   90 FORMAT (8H1CRUISE , 15, 3H - , 12, 12H PARAMETER , 2A4/8X, 12(X, 2A4))
C ** 5 CALCULATE COUNT, SUM, SUM OF SQUARES
  14 DO 8 I=1,12
    8 S(I) = SS(I) = N(I) = 0
      KK = KK + 1
      DO 20 J=1,NST
      IF (A(1,J).LF.0.0.0R.A(2,J).LF.0.0) 21,23
   21 00 22 1=1,5
   22 A(I,J) = 0.0
      GO TO 20
   23 CALL ADD (1,A(1,J))
      CALL ADD (2,A(2,J))
      CALL ADD (3,A(1,J)-A(2,J))
      IF (A(3,J).LE.O.O) 24,25
   24 A(4*J) = 0.0
      A(5,J) = 0.0
      GO TO 20
   25 CALL ADD (4,A(1,J))
      CALL ADD
               (5,A(2,J))
      CALL ADD (6,A(3,J))
      CALL ADD (7,A(1,J)-A(2,J))
      CALL ADD (8,A(1,J)-A(3,J))
      IF (A(4,J).LF.O.C) 26,27
   27 CALL ADD (9, A(4, J))
      CALL ADD (10,A(3,J)-A(4,J))
   26 IF (A(5,J).LE.O.O) 20,28
   28 CALL ADD (11, A(5,J))
      CALL ADD (12, A(3, J) - A(5, J))
   20 CONTINUE
C **
         CALCULATE MEAN AND STANDARD DEVIATION
      6
      DO 30 I=1,12
         (N(I).EQ.O) 33,31
   33 VM(I) = SD(I) = SDM(I) = 0.0
      GO TO 30
   31 VM(I) = S(I)/N(I)
      SD(I) = SS(I)/N(I) - VM(I)*VM(I)
      SDM(I) = SD(I)/N(I)
      SD(I) = SQRTF(SD(I))
      SDM(I) = SQRTF(SDM(I))
   30 CONTINUE
C **
          CALCULATE REFERENCE MEAN AND PRINT STATISTICAL TABLE
   32 DO 50 I=1,12
      RM(I) = VM(I) *RINC(M)
      J = R^{M}(I) + SIGNF(0.5)RM(I))
   50 \text{ RM}(I) = J/\text{RINC}(M)
      WRITE (61,92) N, VM, RM, SD, SDM
   92 FORMAT (///8H NO OBS +1219/8H MEAN +12F9.4/8H REF MN +12F9.4/
     1 8H ST DEV ,12F9.4/8H SD MN ,12F9.4/)
     8 CALCULATE RANGE AND INCREMENTS FOR DATA TABLE
```

```
VLIM = 0.0
      DO 40 I=1.5
      K = IND(I)
      IF (VLIM.GE.SD(K)) 40,41
   41 \text{ VLIM} = \text{SD(K)}
   40 CONTINUE
      AFIW = KK * AFIW
      DIFF(1) = VLIM \times RINC(M)
      J = DIFF(1) + SIGNF(0.5,DIFF(1))
      DIFF(1) = J/RINC(M)
      R = 1./RINC(M)
      J = 1
   51 J = J + 1
      DIFF(J) = DIFF(J-1) - R
     IF (J.GE.50) 54,53
9 IF TABLE TOO LARGE, REDUCE INCREMENTS AND RETURN TO STEP 7
   54 \text{ RINC}(M) = \text{RINC}(M)/2
      GO TO 32
   53 IF (DIFF(J).LE.-VLIM) 52,51
           SORT DATA AND ASSEMBLE TABLE
C ** 10
   52 DO 56 K=1.12
      NHI(K) = 0
      NLO(K) = 0
      DO 56 L=1,J
   56 \text{ NOBS}(K,L) = 0
      DO 60 I=1 NST
       IF (A(1,1).LE.O.O) 60,61
   61 CALL SORT (J, NOBS, NHI, NLO, DIFF, R, 1, A(1, I) - RM(1))
      CALL SORT (J, NOBS, NHI, NLO, DIFF, R, 2, A(2, I) - RM(2))
       CALL SORT (J, NOBS, NHI, NLO, DIFF, R, 3, A(1, I) - A(2, I) - RM(3))
       IF (A(3,1).LE.0.0) 60,62
   62 CALL SORT (J, NOBS, NHI, NLO, DIFF, R, 4, A(1, I) - RM(4))
       CALL SORT (J, NOBS, NHI, NLO, DIFF, R, 5, A(2, I) - RM(5))
       CALL SORT (J, NOBS, NHI, NLO, DIFF, R, 6, A(3, I) - RM(6))
       CALL SORT (J, NOBS, NHI, NLO, DIFF, R, 7, A(1, I) -A(2, I) -RM(7))
       CALL SORT (J, NOBS, NHI, NLO, DIFF, R, 8, A(1, I) -A(3, I) -RM(8))
       IF (A(4,I).LE.O.O) 64,63
   63 CALL SORT (J. NOBS, NHI, NLO, DIFF, R, 9, A(4, I) - RM(9))
       CALL SORT (J, NOBS, NHI, NLO, DIFF, R, 10, A(3, I) -A(4, I) -RM(19))
   64 IF (A(5,1).LE.O.O) 60,65
   65 CALL SORT (J, NOBS, NHI, NLC, DIFF, R, 11, A(5, I) -RM(11))
       CALL SORT (J, NOBS, NHI, NLO, DIFF, R, 12, A(3, I) -A(5, I) -RM(12))
   60 CONTINUE
C ** 11 IF A VALUE IS OUTSIDE THE RANGE, DELETE IT AND GO TO STEP 5
       DO 70 I=1.5
       K = IND(I)
       IF (NHI(K) + NLO(K)) 71,70
   71 L = 1
   79 IF (A(I,L).LE.O.C) 78,72
   72 IF (A(I,L).GE.VM(K)+VLIM.OR.A(I,L).LE.VM(K)-VLIM) 73,78
   73 WRITE (61,96) L, ITL. (2*K-1) . ITL. (2*K), A(I,L)
   96 FORMAT (16H DELETE STATION ,13,6H DEPTH,2A4,8H, VALUE ,F8,3)
       IF (I.LE.2) 74,75
   74 A(1,L) = A(2,L) = A(3,L) = A(4,L) = A(5,L) = 0.0
      GO TO 78
   75 IF (I.EQ.3) 76,77
   76 A(3,L) = A(4,L) = A(5,L) = 0.0
       GO TO 78
```

```
77 A(I,L) = 0.0
78 L = L + 1
IF (L.LE.NST) 79,70
   70 CONTINUE
      IF (L.EQ.0) 82,14
C ** 12 PRINT DATA TABLE
   82 WRITE (61,93) NHI
      WRITE (61,94) (DIFF(L), (NOBS(K,L), K=1,12),L=1,J)
      WRITE (61,95) NLO
   93 FORMAT (8H HIGH, 1219)
   94 FORMAT (F8.3,1219)
95 FORMAT (8H LOW:1219)
C ** 13 IF ANOTHER PARAMETER REMAINS: GO TO STEP 4: ELSE GO TO STEP 2
   80 CONTINUE
      GO TO 86
   85 RETURN
      END
       SUBROUTINE ADD (I,X)
       COMMON/DATA/N(12),S(12),SS(12)
       N(I) = N(I) + 1
       S(I) = S(I) + X
       SS(I) = SS(I) + X*X
       RETURN
       END
       SUBROUTINE SORT (J, NOBS, NHI, NLO, DIFF, R, K, X)
       DIMENSION NOBS(12,50), NHI(12), NLO(12), DIFF(50)
       A = R/2
       DO 1 I=1,J
       IF (X.GE.DIFF(1)-A.AND.X.LE.DIFF(1)+A) 2,1
     2 \text{ NOBS}(K,I) = \text{NOBS}(K,I) + 1
       RETURN
     1 CONTINUE
       IF (X.GT.DIFF(1)) 3,4
     3 \text{ NHI(K)} = \text{NHI(K)} + 1
       RETURN
     4 \text{ NLO(K)} = \text{NLO(K)} + 1
       RETURN
       END
```





MANUSCRIPT REPORT SERIES No. 14

A Numerical Study of Large-Scale Motions in a Two-layer Rectangular Basin

Kenneth B. Yuen



Marine Sciences Branch

Department of Energy, Mines and Resources

Ottawa, Canada



ζ______.

Manuscript Report Series

No. 14

A NUMERICAL STUDY OF LARGE-SCALE MOTIONS IN A TWO-LAYER RECTANGULAR BASIN

Kenneth B. Yuen

1969

The material in this report was originally submitted to the University of Waterloo, Waterloo, Ont. in partial fulfilment of the requirements for the degree of Master of Applied Sciences.

The Queen's Printer for Canada Ottawa, 1969

CONTENTS

		Abstract	Page 1
1.		Introduction	1
			_
2.	0 1	Theory	2
	2.1	General Two-Layer Hydrodynamical Equations	2
	2.2	One-Layer Non-rotating Rectangular Basin	5
		(a) One-dimensional Case	5
	2.3	One-Layer Rotating Rectangular Basin	5 6
	2.0	(a) Kelvin Waves	7
		(b) Poincare Waves	8
		(c) Reflection of Kelvin Waves	9
		(d) Effect of Rotation upon Frequency	11
	2.4	Two-Layer Rectangular Basin	17
		(a) One-dimensional Non-rotating Case	17
		(b) Two-dimensional Rotating Case	19
	2.5	Circular Basin	21
		(a) One-layer Non-rotating, Free Modes	21
		(b) One-layer Rotating, Free Modes	23
		(c) Two-layer Rotating, Free Modes	24
		(d) Two-layer Rotating, Forced Modes	26
3.		Free Oscillations of Lake Huron	28
	3.1	Calculation of the Free Modes	28
	3.2	Computational Errors	38
	3.3	Power Spectra of Lake Huron Water Levels	40
4.		Dynamical Model of Two-Layer Rectangular Basin Subject to	
	4 4	Wind Stress	44
	4.1	Differential Equations	44 46
	4.2	Difference Equations	51
	4.4	Energy in the Basin	51
	4.5	Numerical Stability of the Calculations	53
	4.6	Numerical Results	54
	-,-	(a) Case A	54
		(b) Case B	73
		(c) Case C	89
		(d) Case D	96
		(e) Case E	101
		(f) Case F	101
	4.7	Computational Errors	111
5.		Conclusions	114
6.		Acknowledgments	115
7		References	115

LIST OF SYMBOLS

The following is a list of the main symbols used in this thesis. If a symbol is not listed below, or if the meaning differs from that given in this list, the meaning will be defined in context.

Symbol	Meaning
A _n a b	area of cross-section n.radius of circular basin.breadth of a channel.wave speed.
â, d' f g	- wave speed.- equilibrium depth of top and bottom layers.- Coriolis Parameter.- acceleration of gravity.
h, h' J _n (x)	- total depths of top and bottom layers Bessel function of real argument.
I _n (z)	- Bessel function of imaginary argument. - kinetic energy.
L (m,n)	length of a basin.the nodality of the transverse and longitudinal modes in a rectangular basin.
(m,n)	- also, the nodality of the radial and azimuthal modes in a circular basin.
P p, p' Q R	potential energy.pressure in the top and bottom layers.volume flow.Rossby's radius of deformation.
r s T	radial co-ordinate.also the nodality of the azimuthal modes.period of oscillation.inertial period.
T _n T _q	period of n-th lowest longitudinal free mode.period of transverse free mode.
u, u'	 x-component of velocity in top and bottom layers.
V, V'	- y-component of velocity in top and bottom layers.
U _i , V _i	 equivalent flow per unit cross-section in the equivalent one-layer model of a two-layer system.
U,U', V,V' W x,y,z	components of the flow per unit cross-section.width of a rectangular basin.co-ordinates of a rectangular co-ordinate
$\nabla \mathbf{X}$	system grid length.
ρ	<pre>- time step density of air.</pre>
ρ,ρ'ω	density of top and bottom layers.angular speed of the Earth.

- latitude. φ - azimuthal co-ordinate. - shear stresses in the top layer. τ', τ' - shear stresses in the bottom layer. - angular speed. κη,η' η η - wave number. - surface and interface displacements. - equilibrium displacement for steady wind. - one-layer equivalent displacement. - wavelength. ψ β; β - stream function. - roots of Stokes' equation. - arbitrary phase lags. α_s , ϵ



ABSTRACT

The work of this thesis involves the prediction of large scale motion in the Great Lakes, through the use of computer-oriented mathematical models. In the first part of this work, a one-layer one-dimensional model is constructed for Lake Huron. Spatial integration of the hydrodynamical equations by finite-difference techniques yields the frequencies of the lowest longitudinal free barotropic modes of Lake Huron. The power spectral analysis of water level records is carried out to verify these calculated frequencies.

In the main part of this thesis, a numerical model is constructed for a two-layer rectangular basin of constant depth. The dimensions of the basin are that of a typical Great Lake. The response of the basin under the influence of wind stress is studied. Six cases were investigated, in which the wind stress was impulsive, constant or periodic in time. The behavior of the basin is discussed in terms of forced and free motions that have been theoretically predicted by other researchers. The work carried out here is intended as a first step towards the solution of wind induced motions in a real two-layer Great Lake.

1. INTRODUCTION

Wind stress is one of the major influences affecting the dynamical behavior of the Great Lakes, and therefore also the dispersal of pollutants. The numerical prediction of wind-induced abnormal water levels (storm surges) in one layer basins has been investigated by Platzman (1958; 1963), Welander (1957), Miyazaki (1965), Jelesnianski (1965; 1966), Hansen (1966), and many others.

During the period of summer stratification, the density structure of the Great Lakes can often be reasonably approximated by a two-layer model. Such a stratification gives rise to internal waves and related phenomena which are not found in one-layer basins. The analytical solution of twolayer basins under the influence of wind stress has been investigated by Veronis and Stommel (1956), Welander (1966), Heaps and Ramsbottom (1966), Csanady (1968), and others. However, little has been done in the numerical solution of such problems in real basins. Whereas the analytic solution of an ideal basin will reveal the general behavior of the real basin, only a numerical model will predict this behavior to great accuracy. The work of this thesis is a numerical approach to the problem and is intended as a first step towards the solution of the wind stress problem in real lakes during summer stratification.

In Chapter 2, a discussion is given of some of the theoretical results that have been derived by past researchers, regarding the free and forced motions in both circular and rectangular basins. Both the one- and two-layer cases will be discussed so that the basic differences between these two situations may be noted. The theoretical results will show What

types of motions can be expected in the numerical model. For the free modes, theory only tells us what motions are possible. The numerical model will show which free modes specifically will be excited and to what degree, under a given set of conditions.

A one-dimensional one-layer model of Lake Huron is also constructed (Chapter 3). Whereas the two-layer model to be discussed in Chapter 4 is concerned with the time integration of the hydrodynamical equations, the Lake Huron model will deal with the spatial integration of these equations. These calculations lead to numerical values for the frequencies of the six lowest longitudinal free modes of oscillation. The results are compared to those of Rockwell (1966). Power spectral analysis is applied to several sets of surface water level data from Lake Huron tide gauge stations. Not only do these spectra help in the verification of the calculated Lake Huron free modes, but also give an indication as to which modes are the most dominant.

The ideal two-layer basin discussed in Chapter 4 is $105 \times 270 \text{ km}$. The differential equations are transformed into difference equations and integrated in time. A $36 \times 14 \text{ grid}$ system (grid length = 7.5 km.) is designed to represent the basin. The longitudinal axis of the basin is arbitrarily taken in the east-west direction, and the following six cases of wind stress are investigated:

(a) eastward wind, blowing for 4 hours,

(b) eastward wind, blowing for all time,

(c) northward wind, blowing for all time,

(d) eastward wind, sinusoidal with 7.5 hour period,(e) eastward wind, sinusoidal with inertial period,

and (f) eastward wind, sinusoidal with diurnal period.

In each of the above cases, the wind is uniform over the whole basin. Each case is discussed in terms of the various free

and forced motions given in the Theory.

2. THEORY

A brief discussion is given of some of the theoretical results regarding free and forced motions in both circular and rectangular basins. The developments given here will provide a sound basis on which to construct the two-layer numerical model in Chapter 4, and on which to base the discussion and interpretation of the results from that model.

2.1 General Two-layer Hydrodynamical Equations.

As has been noted by Mortimer (1952), Csanady (1967), and others, the temperature structure of the Great Lakes during the summer period of stable stratification can be approximated by two layers, each of constant temperature. A shallow warm layer lies near the surface (epilimnion), with a thicker layer of colder water lying near the bottom (hypolimnion). In fresh water, temperature is sufficient to reasonably determine the density. In fact, the measurement

of internal motions is often carried out by measuring the variation in temperature, which is a quasi-conservative quantity under stable stratification (see Hale, 1965, p. 4). In this case, the isosteric (equal density) surfaces are parallel to the isothermal surfaces. Thus, a two-layer model should lead to reasonable predictions of the large scale motions in the Great Lakes during the summer months.

Consider, then, a two-layer body of water. It is assumed that the wavelengths or length scales of the motions within the basin are large compared with the depths of the two layers, so that the vertical accelerations are negligible. Also, the pressure may be expressed by the hydrostatic approximation, as

$$p = g\rho(z+\eta) \tag{2.1}$$

and
$$p' = g\rho(d+\eta - \eta') + g\rho'(z - d + \eta')$$
 (2.2)

where z, η , and η ' are positive in the upward direction. It then follows that

$$\frac{1}{\rho} \frac{\partial p}{\partial x} = g \frac{\partial \eta}{\partial x} \tag{2.3}$$

$$\frac{1}{p} \frac{\partial p}{\partial y} = g \frac{\partial n}{\partial y} \tag{2.4}$$

$$\frac{1}{\rho'} \frac{\partial p'}{\partial x} = g \frac{\rho}{\rho'} \frac{\partial \eta}{\partial x} + g(1-\frac{\rho}{\rho'}) \frac{\partial \eta}{\partial x}$$
 (2.5)

and
$$\frac{1}{\rho'} \frac{\partial p'}{\partial y} = g \frac{\rho}{\rho'} \frac{\partial \eta}{\partial y} + g \left(1 - \frac{\rho}{\rho'}\right) \frac{\partial \eta'}{\partial y}$$
 (2.6)

It is further assumed that the non-linear accelerative terms such as $u\partial u/\partial x$ are also negligible. If the displacements are not large compared with the equilibrium depths, then the continuity equations may be written as (Proudman, 1953, p. 234)

$$\frac{\partial}{\partial t} (\eta - \eta') = \frac{-\partial}{\partial x} \frac{(hu)}{\partial y} - \frac{\partial}{\partial y} \frac{(2.7)}{\partial y}$$

and
$$\frac{\partial \eta'}{\partial t} = \frac{-\partial (h'u')}{\partial x} - \frac{\partial (h'v')}{\partial y}$$
 (2.8)

where h and h' are the total depths, given by

$$h = d + \eta - \eta' \tag{2.9}$$

and
$$h' = d' + n'$$
 (2.10)

If the Coriolis parameter, f, is taken to be constant, then the equations of motion become (including shear stress)

$$\frac{\partial \mathbf{u}}{\partial t} = \mathbf{f} \mathbf{v} - \mathbf{g} \frac{\partial \mathbf{\eta}}{\partial \mathbf{x}} + \frac{1}{\rho} \frac{\partial}{\partial \mathbf{z}} \mathbf{x}$$
 (2.11)

$$\frac{\partial \mathbf{v}}{\partial t} = -\mathbf{f}\mathbf{u} - \mathbf{g} \frac{\partial \mathbf{\eta}}{\partial \mathbf{y}} + \frac{1}{\rho} \frac{\partial \mathbf{\tau}}{\partial \mathbf{z}} \mathbf{y} \tag{2.12}$$

$$\frac{\partial \mathbf{u'}}{\partial t} = \mathbf{f}\mathbf{v'} - \mathbf{g} \frac{\rho}{\rho'} \frac{\partial \eta}{\partial \mathbf{x}} - \mathbf{g}(1 - \frac{\rho}{\rho'}) \frac{\partial \eta'}{\partial \mathbf{x}} + \frac{1}{\rho'} \frac{\partial}{\partial \mathbf{z}} \mathbf{\tau'} \mathbf{x}$$
 (2.13)

$$\frac{\partial \mathbf{v'}}{\partial t} = -\mathbf{f}\mathbf{u'} - \mathbf{g} \frac{\rho}{\rho} \frac{\partial \eta}{\partial \mathbf{y}} - \mathbf{g}(\mathbf{1} - \underline{\rho}) \frac{\partial \eta'}{\partial \mathbf{y}} + \frac{1}{\rho'} \frac{\partial}{\partial \mathbf{z}} \mathbf{\tau'} \mathbf{y}$$
 (2.14)

These equations are similar to those derived in Proudman (1953, p. 235), with the exception of the stress terms. The stress terms are similar in form to those found in Platzman (1963, p. 24) where the one-layer Ekman equations are given. At this stage, the velocity components are still functions of x, y, and z. To eliminate the z-dependence, it is convenient to integrate each of the hydrodynamical equations over the appropriate layer and divide by the depth of that layer, thus arriving at depth mean values. For example, in (2.11), u(x,y) is defined as

$$u(x,y) = \frac{1}{(d+\eta-\eta')} \int_{-d+\eta'}^{\eta} u(x,yz) dz$$
 (2.15)

The stress term in (2.11) is integrated as

$$\frac{1}{h} \int_{-d+n}^{\eta} \frac{1}{\rho} \frac{\partial \tau}{\partial z} x \, dz = \frac{1}{h\rho} \left(\tau_{x}^{s} - \tau_{x}^{i} \right)$$
 (2.16)

where τ_X^S and τ_X^I are the stresses at the surface and interface boundaries, thus eliminating the vertical dependence of the stress. The interface and bottom stresses will be assumed negligible, leaving only the surface stress. The remaining equations may be similarly integrated.

The Rossby Number, given by U/fS (2.17)

represents the ratio of the inertial forces to the Coriolis forces, where S is a length scale. Csanady (1967) has noted that within the Great Lakes the Rossby number is of the order of 10^{-2} , so that the non-linear accelerative terms may be neglected.

The motions may be "current-like", or if "wave-like", have wavelengths comparable to the length scale of the Great Lakes. Examples of both types of motion will be discussed. Non-rotating systems will also be discussed briefly, to permit comparison with rotating systems.

2.2 One-layer Non-rotating Rectangular Basin.

(a) One-dimensional Case.

For a one-layer channel of constant depth, with the stresses neglected, the hydrodynamical equations are given by (Proudman, 1953, p. 225)

$$\frac{\partial \eta}{\partial t} = -h \frac{\partial u}{\partial x} \tag{2.18}$$

and

$$\frac{\partial \mathbf{u}}{\partial t} = -\mathbf{g} \frac{\partial \mathbf{n}}{\partial \mathbf{x}} \tag{2.19}$$

For a channel with both ends closed, the boundary conditions are

$$u(0) = u(L) = 0$$
 (2.20)

A wave-like solution is given by

$$\eta = H \cos \frac{n\pi x}{L} \cos \frac{2\pi t}{T} \tag{2.21}$$

and

$$u = -\frac{H2L}{hT_n} \sin \frac{n\pi x}{L} \cos \frac{2\pi t}{T_n}$$
 (2.22)

where n is the nodality of the standing wave. The period \textbf{T}_{n} is given by

$$T_{n} = 2L/cn \tag{2.23}$$

This is a gravity wave, because the wave speed, c, is given by

$$c = \sqrt{gh} \tag{2.24}$$

(2.23) is commonly called Merian's formula. The criterion for the neglect of vertical acceleration is the smallness of

$$h \frac{\partial^2 n}{\partial t^2} / gn \tag{2.25}$$

For the above solution, this is the smallness of h/L, which has already been assumed small. For a narrow lake many methods have been devised for the integration of the hydrodynamical equations (2.18) and (2.19) (see Defant, 1961, p. 160-173).

(b) Two-dimensional Case.

If the assumptions of the previous section are extended to the two-dimensional case (still non-rotating), the equations are (Proudman, 1953, p. 242)

$$\frac{\partial \eta}{\partial t} = -\frac{\partial hu}{\partial x} - \frac{\partial hv}{\partial y}$$
 (2.26)

$$\frac{\partial \mathbf{u}}{\partial t} = -\mathbf{g} \frac{\partial \mathbf{n}}{\partial \mathbf{x}} \tag{2.27}$$

and
$$\frac{\partial \mathbf{v}}{\partial t} = -\mathbf{g} \frac{\partial \mathbf{n}}{\partial \mathbf{y}}$$
 (2.28)

For a broad lake of width, W, the boundary conditions are

$$u(0) = u(L) = 0$$
 (2.29)

and
$$v(0) = v(W) = 0$$
 (2.30)

A particular standing wave solution is given by (Proudman, 1953, p. 242)

$$u = A \sin \frac{m\pi x}{L} \cos \frac{\eta \pi y}{W} \sin \frac{2\pi t}{T}$$
 (2.31)

$$v = B \cos \frac{m\pi x}{L} \sin \frac{n\pi y}{W} \sin \frac{2\pi t}{T}$$
 (2.32)

and
$$\eta = H \cos \frac{m\pi x}{L} \cos \frac{\eta \pi y}{W} \cos \frac{2\pi t}{T}$$
 (2.33)

where the amplitudes, A and B, are given by

$$\frac{AL}{m} = \frac{BW}{n} = \frac{1}{2} gTH \qquad (2.34)$$

The period is given by

$$\begin{bmatrix}
\frac{1}{gh} & \frac{1}{(m^2_2 + n^2_2)} \\
\frac{1}{L} & W
\end{bmatrix}^{\frac{1}{2}}$$
(2.35)

2.3 One-layer Rotating Rectangular Basin.

With the inclusion of the Coriolis term to account for the Earth's rotation, the two-dimensional equations become

$$\frac{\partial \eta}{\partial t} = -\frac{\partial}{\partial x} \text{ (hu)} - \frac{\partial}{\partial y} \text{ (hv)}$$
 (2.36)

$$\frac{\partial \mathbf{u}}{\partial t} = \mathbf{f} \mathbf{v} - \mathbf{g} \frac{\partial \mathbf{n}}{\partial \mathbf{x}} \tag{2.37}$$

and
$$\frac{\partial \mathbf{v}}{\partial t} = -\mathbf{f}\mathbf{u} - \mathbf{g} \frac{\partial \mathbf{n}}{\partial \mathbf{y}}$$
 (2.38)

For a wavelike solution with time dependence of the form $\mathrm{e}^{\mathrm{i}\sigma t}$, the equations become

$$i\sigma\eta = -\frac{\partial}{\partial x} hu - \frac{\partial}{\partial y} hv$$
 (2.39)

$$i\sigma u = fv - g \frac{\partial \eta}{\partial x}$$
 (2.40)

and
$$i\sigma v = - fu - g \frac{\partial \eta}{\partial y}$$
 (2.41)

If h is constant, the elimination of u and v from these equations gives

$$\frac{\partial^2 \eta}{\partial x^2} + \frac{\partial^2 \eta}{\partial y^2} + \frac{\sigma^2 - f^2}{gh} \eta = 0$$
 (2.42)

or
$$(\nabla^2 + k^2)\eta = 0$$
 (2.43)

where
$$k^2 = \frac{\sigma^2 - f^2}{gh}$$
 (2.44)

and ∇^2 is the Laplacian. u and v also obey (2.43), which is called the Helmholtz equation.

(a) Kelvin Waves. (see Defant, 1961, p. 206-208)
Consider a solution to (2.43) where v is everywhere
zero. A particular solution for a wave progressing in the
x-direction is

$$u = g\eta/c \tag{2.45}$$

$$v = 0$$
 (2.46)

where $c = \sqrt{gh}$

In this solution, the amplitude of $\,^{\,n}$ varies exponentially in the transverse direction. If the amplitude at one shore is n_{0} , then at the other shore it is

$$\eta_{O} = (f/c)y$$
 (2.48)

The sign of the current is always the same sign as η . Thus, at the crest of the wave (high water), the current is in the forward direction, and the surface slopes down from right to left, looking in the direction of propagation. At the trough of the wave (low water), the opposite occurs. Such waves, characterized by large surface displacements to the right and small ones to the left of the direction of propagation, are called Kelvin (1879) waves.

The absence of transverse oscillations with Kelvin waves holds true only for channels of constant depth. Suppose now that the depth is not uniform and assume a solution of

the form

$$\eta = Z \cos (\sigma t - \kappa x) \tag{2.49}$$

$$u = U \cos (\sigma t - \kappa x) \tag{2.50}$$

$$v = V \sin (\sigma t - \kappa x)$$
 (2.51)

Then
$$\sigma U = fV - \kappa gZ$$
 (2.52)

$$\sigma V = -fU - g\partial Z/\partial y \tag{2.53}$$

and
$$\frac{d}{dy} = \frac{(h \partial Z)}{\partial y} + \left[\frac{\sigma^2 - f^2}{g} - \kappa^2 h + \frac{f \kappa}{\sigma} + \frac{\partial h}{\partial y} \right] = 0$$
 (2.54)

If the boundaries of the canal are at $y = \pm a$, then the boundary conditions are given by

$$h\left(\frac{\partial Z}{\partial y} + \frac{f\kappa}{\sigma} Z\right) = 0$$
 (2.55)

Thus,

$$hV = \frac{\kappa^2}{\sigma} e^{-\frac{f\kappa y}{\sigma}} \int_{-a}^{y} \frac{(\sigma^2 - gh)}{\kappa^2} Ze^{-\frac{f\kappa y}{\sigma}} dy$$
 (2.56)

and at y = a

$$\int_{-a}^{a} \left(\frac{\sigma^2}{\kappa^2} - gh\right) \quad Ze \qquad \frac{-f\kappa y}{\sigma} dy = 0$$
 (2.57)

Assuming that Z is always positive, then

$$\frac{\sigma^2}{\kappa^2} - gh_1 = 0 \tag{2.58}$$

where h_1 is an average depth over the cross-section. If the depth is a maximum near the centre of the channel and slopes up to both shore, there will be two values of h equal to h_1 , at y_1 and y_2 . In this case, high $\frac{-f \kappa y}{\sigma}$ goes from a zero at y=a to a maximum at $y=y_1$, then to a minimum at $y=y_2$, and back to zero at the shoreline. The transverse current has a zero somewhere between y_1 and y_2 , and goes in opposite directions near opposite shores.

(b) Poincaré Waves. (see Defant, 1961, p. 208-210)
Poincaré (1910) waves are also possible in a canal.
If the depth is again taken constant, then (2.54) becomes

$$\frac{d^2 Z}{dy^2} + \left(\frac{\sigma^2 - f^2}{gh} - \kappa^2\right) Z = 0$$
 (2.59)

The boundary conditions are v = 0 at $y = \pm a$. If

$$\frac{\sigma^2 - f^2}{gh} - \kappa^2 = \left(\frac{n\pi}{2a}\right)^2 \quad (n = odd)$$
 (2.60)

then a complete solution is given by

$$u = A \qquad \left[\frac{\sigma}{\kappa h} \quad \cos \frac{n\pi}{2a} y + \frac{\pi g}{2af} \sin \frac{n\pi y}{2a} \right] \cos(\sigma t - \kappa x) \tag{2.61}$$

$$\mathbf{v} = -\frac{\mathbf{Af}}{\kappa \mathbf{h}} \left(1 + \pi \mathbf{c}^2 \right) \quad \cos \, \frac{\mathbf{n} \pi \mathbf{y}}{2\mathbf{a}} \quad \sin \, \left(\sigma \mathbf{t} - \kappa \mathbf{x} \right) \tag{2.62}$$

and
$$\eta = A \left[\cos \frac{n\pi}{2a} y + \frac{\pi\sigma}{2af\kappa} \sin \frac{\pi n}{2a} y \right] \cos (\sigma t - \kappa x)$$
 (2.63)

If $\mathbf{T}_{\mathbf{q}}$ is the period of the n-th transverse free oscillation given by

$$T_{q} = 4a/nc \tag{2.64}$$

and T_i , the inertial period, by

$$T_{i} = 2\pi/f \tag{2.65}$$

then (2.60) becomes

$$1 - \left(\frac{T}{T_i}\right)^2 - \left(\frac{T}{T_G}\right)^2 = \frac{C^2 \kappa^2}{\sigma^2}$$
 (2.66)

Thus, Poincaré waves are only possible if the period, T, is less than both T_i and T_q .

(c) Reflection of Kelvin Waves. (see Defant, 1961 p. 210 - 217)

The superposition of two Kelvin waves going in opposite directions does not give rise to standing waves, but rather to a system of cells along the length of the canal. Within each cell, there is a node at the centre of the cell. The amplitude of η increases away from the centre of the cell, with the largest amplitudes being at the corners. The wave system in each cell rotates in the anti-clockwise direction. Such a cell is called an amphidromic region (see Defant, p. 211)

In a rectangular basin which is closed at one end, the value of u must be zero at this boundary. The superposition of two Kelvin waves results in zero values of u only at certain values of x. Taylor (1920) has solved this problem by adding to the two superimposed Kelvin waves a particular Poincaré solution for which u is exactly that necessary to make the total u at the end of the basin equal to zero. The boundary

conditions on v are automatically satisfied by the Kelvin and Poincaré solutions. Taylor (1920) also showed that perfect reflection of Kelvin waves is possible only if the following condition is satisfied.

$$(\sigma^2 - f^2) < gh\pi^2/b^2$$
 (2.67)

where b is the width of the canal. (2.67) may be re-expressed

$$\left(\frac{T_{q}}{T}\right)^{2} < 1 + \left[\left(\frac{T_{q}\sin x}{12q hours}\right)\right]^{2}$$
 (2.68)

Taylor's (1920) solution is mathematically very elegant. Defant (1925, p. 25) has derived a simpler solution. In this solution, the origin of the rectangular co-ordinate system is taken at the geometric centre of the basin, and the y-co-ordinate has been re-defined so that the side boundaries of the basin are at $y = \pm \pi/2$. The position of the closed end has been set to some unknown $x = x_1$, at which point the superposition of two Kelvin waves going in opposite directions gives

$$u_0 = S \left[\cosh \alpha y \sin \frac{\sigma x_1}{c} \cos \alpha t + \sinh \alpha y \cos \frac{x_1 \sin \sigma t}{c} \right]_{2.69}$$

and $v_0 = 0$ where $\alpha = f/c$

A second solution satisfying v = 0 at $y = \pm \pi/2$, and extending over a small area in the x-direction has the form

$$v_1 = \Sigma \quad C_n e^{-S_n x} \sin ny$$
even n
$$-S_n x \cos ny$$
(2.70)

even n
$$-S_n x$$

and $v_2 = \Sigma$ c_n e $\cos ny$ (2.71)

where
$$S_n^2 = n^2 - k^2$$
 (2.72)

To keep the exponential factor real,

$$n^2 > k^2$$
 (2.73)

and since the smallest value of n is unity,

$$k^2 < 1$$
 (2.74)

Corresponding to
$$v_1$$
 and v_2 are
$$u_1 = \sum_{n=1}^{\infty} A_n e cos ny$$
(2.75)

and
$$u_2 = \sum_{n=1}^{\infty} A_n' e^{-S_n x} \sin ny$$
 (2.76)

The elimination of η from (2.39) to (2.41) gives

$$\frac{\partial \mathbf{u}}{\partial \mathbf{y}^1} - \frac{\partial \mathbf{v}}{\partial \mathbf{x}^1} + \frac{\mathbf{f}}{\sigma} \quad \frac{\partial \mathbf{u}}{\partial \mathbf{x}^2} + \frac{\partial \mathbf{v}}{\partial \mathbf{y}^2} = \mathbf{0} \tag{2.77}$$

and
$$\frac{\partial \mathbf{u}}{\partial \mathbf{y}^2} - \frac{\partial \mathbf{v}}{\partial \mathbf{x}^2} - \frac{\mathbf{f}}{\sigma} \frac{\partial \mathbf{u}}{\partial \mathbf{x}^1} + \frac{\partial \mathbf{v}}{\partial \mathbf{y}^1} = 0$$
 (2.78)

The co-efficients of \sin ny and \cos ny must vanish, so that the substitution of (2.70), (2.71), (2.75), and (2.76) into (2.77) and (2.78) gives

$$\frac{A_n}{A_n} = \frac{n}{\psi_n}$$
 for even n (2.79)

$$\frac{A_n}{A_n} = \frac{\psi_n}{n}$$
 for odd n (2.80)

where

$$\psi_{n} = f\sigma/S_{n}C^{2} \tag{2.81}$$

Thus, for
$$-\frac{\pi}{2} < y < \frac{\pi}{2}$$

$$\sin \frac{\sigma x}{c^1}$$
 $\cosh \alpha y = \sum_{n=1}^{\infty} A_n \cos ny$ (2.82)

$$\sin \frac{\sigma x}{\sigma^{1}}$$
 $\sinh \alpha y = \sum_{n=1}^{\infty} A_{n} \sin ny$ (2.83)

The co-efficients A_n and A' can now be determined, as can be x_1 , the point at which the incoming Kelvin wave is perfectly reflected and the u component is zero.

Taylor (1920) computed numerical solutions for a bay with the dimensions of the North Sea. More recently, Godin (1965) derived a similar solution but for a narrow sea, and subsequently applied it to a study of the tides in Labrador Sea, Davis Strait, and Baffin Bay. For a vivid pictorial description of Poincaré and Kelvin waves (also Sverdrup waves, or waves with horizontal crests), the reader is referred to Mortimer (1963, p. 14-18).

(d) Effect of Rotation Upon Frequency. (see Rao,1966)
An important aspect of rotating systems is the effect
of rotation upon the frequencies of the non-rotating free
modes. In discussing the non-rotating free modes, the terminology (m,n) will be used, where m and n refer to the
nodality in the transverse and longitudinal directions,
respectively. When the sum of m and n is odd, the mode is odd
or anti-symmetric, and when the sum is even, the mode is even

					f/ν_1				
Mode	0	0.25	0.50	1.00	1.25	1.50	1.75	2.00	2.25
				Squ	are				
(1, 0)	1.0	0.907	0.831	0.723	0.686	0.657	0.635	0.617	0.602
(0, 1)	1.0	1.110	1.235	1.509	1.630	1.706	1.737	1.739	1.730
(1, 2)	2.236	$2 \cdot 173$	2.119	2.058	2.074	$2 \cdot 151$	2.290	2.468	2.666
(2, 1)	2.236	$2 \cdot 307$	2.384	2.540	2.610	2.666	2.705	2.733	2.742
(3, 0)	3.0	2.997	3.012	3.092	3.157	3.241	3.347	3.471	3.612
(0, 3)	3.0	***************************************	3.057	3.181	3.263	3.356	3.453	3.547	3.625
				Rectangl	e (2×1)				
(1, 0)	1.0	0.995	0.982	0.942		0.897	0.876	0.857	0.840
(0, 1)	2.0	2.015	2.058	2.201		$2 \cdot 336$	2.364	2.369	2.361
(2, 1)	2.828	2.811	2.777	2.726	remonents.	2.776	2.868	2.998	3.150
(3, 0)	3.0	3.025	3.083	3.235		3.402	3.483	3.554	3.615
(1, 2)	4.123	4.127	4.138	4.177		4.233	4.272	4.325	4.397
(4, 1)	4.472	4.472	4.472	4.489		4.556	4.609	4.670	4.735

Table 1. Frequencies σ/ν_1 of antisymmetric modes as a function of rotation speed f/ν_1

			f/	ν_1		
Mode	0	0.25	0.50	1.00	1.50	2.00
			Square			
(1, 1)	1.414	1.405	1.380	1.313	1.253	1.20
(2, 0)	2.0	2.010	2.038	2.131	$2 \cdot 216$	2.25
(0, 2)	2.0	2.022	2.084	$2 \cdot 293$	2.577	2.90
(2, 2)	2.828	2.821	2.805	2.795	2.881	3.09
(1, 3)	3.162	3.166	3.176	3.213	3.254	3.29
(3, 1)	3.162	3.182	3.235	$3 \cdot 404$	3.624	3.87
		Rect	sangle (2×1)			
(2, 0)	2.0	1.978	1.930	1.828	1.742	1.67
(1, 1)	2.236	2.266	2.338	2.528	2.732	2.89
(3, 1)	3.606	3.599	3.584	3.547	3.542	3.62
(0, 2)	4.0	4.006	4.022	4.084	4.170	4.25
(4, 0)	4.0	4.013	4.049	4.172	4.342	3.54
(2, 2)	4.472	4.478	4.497	4.570	4.693	4.86

Table 2. Frequencies σ/ν_1 of symmetric modes as a function of rotation speed f/ν_1

Table 2.1 The effect of rotation upon the frequencies of the lowest symmetric and antisymmetric surface modes in a square and rectangular (2x1) basin (Tables 1 and 2 from Rao, 1966).

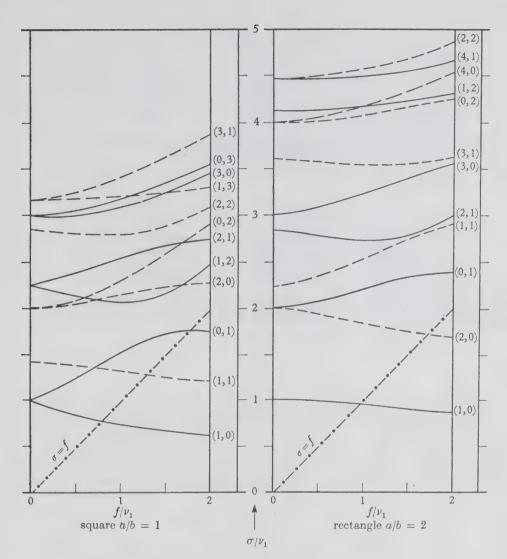


FIGURE 2. Frequency (σ/ν_1) vs. rotation speed (f/ν_1) for various modes in square and 2×1 rectangular basins.

Figure 2.1 The effect of rotation upon the frequencies of the lowest surface modes in a square and rectangular (2x1) basin (Figure 2 from Rao, 1966).

	f/ u_1					
a/b	0	0.5	1.0			
1	1.0	0.831	0.723			
2	1.0	0.982	0.942			
4	1.0	0.998	0.992			
6	1.0	. 0.999	0.997			

Table 3. Frequency σ/ν_1 of lowest longitudinal mode (1, 0) as a function of rotation speed f/ν_1 for various basin elongations a/b

	f/ u_1				
a/b	0	0.5	1.0		
1	1.0 (1.0)	1.235 (1.118)	1.509 (1.414)		
2	2.0 (2.0)	2.058 (2.062)	2.201 (2.236)		
4	4.0 (4.0)	4.030 (4.031)	4.117 (4.123)		
6	6.0 (6.0)	6.020 (6.021)	6.080 (6.083)		

Table 4. Frequency σ/ν_1 of lowest transverse mode (0, 1) as a function of rotation speed f/ν_1 for various basin elongations. Sverdrup-wave frequency $(\nu^2 + f^2)^{\frac{1}{2}}/\nu_1$ is given in parentheses

Table 2.2 The effect of rotation upon the (0,1) and (1,0) surfaces modes for various basin elongations (Tables 3 and 4 from Rao, 1966).

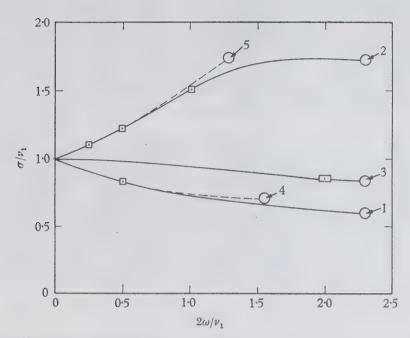


Figure 1. Frequency of oscillation (σ/ν_1) in square and rectangular basins of uniform depth, as a function of rotation speed $(2\omega/\nu_1)$. The solid curves are the results of the present calculation: curves 1 and 2 correspond to the slowest positive and negative modes in a square and curve 3 to the slowest positive mode in a 2×1 rectangle. Also shown are Corkan & Doodson's (1952) results for a square (\Box) and Taylor's (1922) result for a 2×1 rectangle (\Box). Curves 4 and 5 show the results of Van Dantzig & Lauwerier's (1960) perturbation analysis for the slowest positive and negative modes in a square, valid through the second order of $2\omega/\nu_1$.

Figure 2.2 The effect of rotation upon the frequencies of the (0,1) and (1,0) surface modes for a square and a rectangular (2x1) basin (Figure 1 from Rao, 1966).

or symmetric. A positive mode rotates in the same sense as the applied rotation, that is anti-clockwise in the Northern Hemisphere, and a negative mode rotates in the clockwise direction.

In his introductory chapter, Rao (1966) gives a brief survey of past studies on this topic. Such studies were carried out as early as 1903 by Rayleigh for a square sea, and 1909 for a rectangular basin. In these cases, only small rotation was considered. Taylor's (1920) analysis was the first complete study for a rectangular basin. This analysis was later simplified by Defant (1925), as was discussed in Section 2.3 (c).

Lamb (1942) showed that for a rectangular basin $(\sigma^2 - v_1^2) \ (\sigma^2 - v_2^2) = 256\pi \ \omega^2 \ \sigma^2$ (2.84)

where $_{0}$ is the angular speed with rotation, and v_{1} and v_{2} are the slowest longitudinal and transverse speeds in the non-rotating case. The angular speed is 2π times the frequency. (2.84) is also valid only for slow rotation. Lamb's (1924) results were confirmed by Goldsborough (1931). Later on, Corkan and Doodson (1952) treated the case of a square sea by a numerical approach. In connection with the North Sea, Van Dantzig and Lauwerier (1960) also examined rectangular basins. For a square sea subjected to small rotation, they obtained

$$\sigma/v_1 = 1 + 0.405 (2\omega/v_1) + 0.138 (2\omega/v_1^2) + \dots$$
 (2.85)

The minus sign refers to the slowest positive anti-symmetric mode and the plus sign to the slowest negative mode. For a rectangular basin with a length to width ratio of 2, they further obtained

$$\sigma/v_1 = 1 - 0.302 (2\omega/v_1)^2$$
 (2.86)

Clearly, most of the earlier studies had been approximated to cases of slow rotation. Rao (1966), however, investigated the effect of rotation over a larger range of rotation speeds; in the case of a square, this was carried out experimentally also.

In Table 2.1 (from Rao, 1966, Tables 1 and 2) is shown Rao's results for both the six lowest symmetric and antisymmetric modes, for a square and a 2 x 1 rectangular basin. The rotation and resulting angular speeds have been non-dimensionalized by the speed of the lowest non-rotating antisymmetrical mode. These results are also graphically displayed in Fig. 2.1 (from Rao, 1966, Fig. 2).

In Table 2.2 (from Rao, 1966, Tables 3 and 4) is shown Rao's results for the lowest longitudinal mode (0,1) and the lowest transverse mode (1,0), for various basin elongations. These same results are graphically given in Fig. 2.2 (from Rao, 1966, Fig. 1).

From Fig. 2.1, it is seen that certain frequencies in the zero-rotation spectrum are split up into doublets when rotation is applied; examples are the (0,1) and (1,0) doublet for a square basin, and the (2,0) and (0,1) doublet in a 2 x 1 rectangular basin. It is curious to note that the behavior of the (1,0) mode in a square is, within Rao's computational accuracy, the same as the (1,1) mode in the (r,θ) direction for a circular basin (see Lamb, 1932, p. 210). Such similarity is not found in any of the other modes, and Rao has concluded that this particular case is a coincidence.

An interesting feature found in Fig. 2.2 for the 2 x l rectangle is the non-monotonic behavior of some of the frequency curves; that is, for some modes, at certain values of rotation the frequency is the same as the non-rotating value. For example, in the (2,1) mode, this occurs at a value

for f/v of about 1.6.

Taylor (1920) has suggested that the frequencies of the symmetric modes may fall in between those of the antisymmetric modes. Rao's results show that this is not quite true, although it is true for the zero-rotation spectrum. Within the range of Rao's calculations, if m is constant and n is varied, or vice versa, then Taylor's suggestions are in this sense true. Rao feels that this may happen in general.

From Table 2.2, it is to be noted that the effect of rotation decreases as the basin elongation increases. In the limit, the oscillations are Kelvin waves (see Lamb, 1932, p. 208). In a very elongated basin, one would expect the purely transverse modes to approach the form of Sverdrup waves (waves with horizontal crests), providing the ends of the basin are sufficiently far away so as not to affect the main motion. Proudman (1953, p. 132) gives the frequency of a Sverdrup wave as

$$\sigma^2 = v^2 + f^2 \tag{2.87}$$

For the lowest transverse modes (Table 2.2) Rao has also included (in the brackets) the non-dimensionalized frequency calculated from (2.87). It is clear that as the basin elongation increases, the frequency of the transverse modes approaches that of the Sverdrup waves.

2.4 Two-layer Rectangular Basin.

(a) One-dimensional Non-rotating Case. (see Proudman, 1953, p. 338-341)

For a one-dimensional channel of constant depth, with no shear stresses present, the linearized hydrodynamical equations are (Proudman, 1953, p. 338)

$$\frac{\partial}{\partial t} (\eta - \eta') = -h \frac{\partial u}{\partial x}$$
 (2.88)

$$\frac{\partial \eta'}{\partial t} = -h' \frac{\partial u'}{\partial x} \tag{2.89}$$

$$\frac{\partial \mathbf{u}}{\partial t} = -\mathbf{g} \frac{\partial \mathbf{n}}{\partial \mathbf{x}} \tag{2.90}$$

and
$$\frac{\partial \mathbf{u'}}{\partial \mathbf{t}} = -\mathbf{g} \frac{\rho}{\rho}, \quad \frac{\partial \mathbf{n}}{\partial \mathbf{x}} - \mathbf{g} \left(1 - \frac{\rho}{\rho}, \frac{\partial \mathbf{n'}}{\partial \mathbf{x}}\right)$$
 (2.91)

The boundary conditions are given by

$$u = u' = 0$$
 at $x = 0$, L (2.92)

If
$$\beta = 4L^2/gh T^2$$
 (2.93)

then a solution for the lowest free mode of oscillation is

$$\eta = H \cos (\pi x/L) \cos (2\pi t/T) \qquad (2.94)$$

$$u = \frac{1}{\beta} \frac{2L}{hT} \text{ H sin } (\pi x/L) \text{ sin } (2\pi t/T)$$
 (2.95)

$$\eta' = (1 - \frac{1}{\beta}) \text{ H cos } (\pi x/L) \text{ cos } (2\pi t/T)$$
 (2.96)

and
$$u' = (1 - \frac{1}{\beta}) \frac{2L}{h'T} \sin (\pi x/L) \sin (2\pi t/T)$$
 (2.97)

Substitution of this solution into (2.91) gives an equation for β , known as Stokes' equation, given by

$$\frac{h}{h!} \beta^2 - (1 - \frac{h}{h!}) \beta + (1 - \frac{\rho}{\rho}) = 0$$
 (2.98)

The roots of this equation are

$$\beta = \frac{1}{2} \left(1 + \frac{h'}{h} \right) \pm \left[\frac{1}{4} \left(1 + \frac{h'}{h} \right)^2 - \left(1 - \frac{\rho}{\rho'} \right) \frac{h'}{h} \right]^{\frac{1}{2}}$$
 (2.99)

From the smallness of $(1-\rho/\rho')$ which is of the order of 0.001, the two approximate roots of (2.99) are

$$\beta = 1 + h'/h$$
 (2.100)

and
$$\beta_{i} = (1 - \frac{\rho}{\rho}) \frac{h!}{h+h!}$$
 (2.101)

For the first root, β_0 , (2.93) gives

$$T = 2L / \sqrt{g(h+h')}$$
 (2.102)

which is that given by (2.23) for the surface of barotropic mode. With the value $\beta=\beta_0$, (2.94) also agree with (2.21) and (2.22) for the surface mode. It appears then that excitation of the surface mode is possible even when stratification is present. This mode is characterized by maximum vertical displacement at the surface. The ratio of the displacements is given by

$$\frac{\eta'}{n} = \frac{h'}{h+h'} \tag{2.103}$$

The currents in both layers are equal in amplitude and direction.

Corresponding to $\ \beta_i$ is the internal or baroclinic mode, whose period is given by

$$T = 2L^{i} \left[\frac{\rho'}{\rho' - \rho} \frac{1}{g} \left(\frac{1}{h} + \frac{1}{h'} \right) \right]$$
 (2.104)

This mode can only exist with stratification; otherwise, the period is infinite and the amplitude is zero. It is characterized by maximum vertical displacements at the interface. The ratio of the displacements in the internal mode is

$$\frac{\eta}{\eta'} = \frac{(1 - \rho)}{\rho'} \frac{h'}{h+h'} \tag{2.105}$$

and the ratio of the velocities is

$$\frac{\mathbf{u}}{\mathbf{u}'} = \frac{\mathbf{h}'}{\mathbf{h}} \tag{2.105a}$$

(b) Two-dimensional Rotating Case. (see Veronis, 1956 and Csanady, 1967)

It has been seen that the two-dimensional equations in the one-layer basin are much more difficult to solve than the one-dimensional equations. Veronis (1956) has employed a special technique to simplify the solution of the two-layer equations. This technique has recently been used by Csanady (1967), and involves the transformation of the two-layer equations into an equivalent one-layer set.

Following Csanady (1967), the linearized hydrodynamical equations are

$$\frac{\partial U}{\partial t} = fV - gh \frac{\partial \eta}{\partial x} + F_x$$
 (2.106)

$$\frac{\partial V}{\partial t} = -fU - gh \frac{\partial \eta}{\partial y} + F_y$$
 (2.107)

$$\frac{\partial}{\partial t} (\eta - \eta') = -\frac{\partial U}{\partial x} - \frac{\partial V}{\partial y}$$
 (2.108)

$$\frac{\partial U'}{\partial t} = fV' - g \frac{\rho}{\rho}, \quad h' \frac{\partial \eta}{\partial x} - gh' \left(1 - \frac{\rho}{\rho}\right), \quad \frac{\partial \eta'}{\partial x} + F'_{x}$$
 (2.109)

$$\frac{\partial V'}{\partial t} = -fU' - g \frac{\rho}{\rho}, \quad h' \frac{\partial n}{\partial y} - gh' \left(1 - \frac{\rho}{\rho}, \frac{\partial \eta'}{\partial y} + F'\right)$$
 (2.110)

and
$$\frac{\partial \eta'}{\partial t} = -\frac{\partial U'}{\partial x} - \frac{\partial V'}{\partial y}$$
 (2.111)

where U, U', V, V' are the components of the flow per unit breadth, and F_x , F_x , F_y , and F_y are the components of the stress divided by the density of the appropriate layer.

With β_i as the two roots of the Stokes' equation, the following transformations are defined (Csanady, 1967, p. 4153-4154).

$$U_i = (1-\beta_i) U + U'$$
 (2.112)

$$V_{i} = (1-\beta_{i}) V + V'$$
 (2.113)

and
$$\eta_{i} = (1-\beta_{i}) (\eta-\eta') + \eta'$$
 (2.114)

where i = 1 or 2. The depths are transformed as

$$h_{i} = (1 - \rho_{i}) \frac{h'}{\beta_{i}}$$
 (2.115)

so that the equivalent depths are

$$h_1 = h + h'$$
 (2.116)

and
$$h_2 = (1-\frac{\rho}{\rho}) \frac{hh'}{(h+h')}$$
 (2.117)

The stresses are transformed as

$$F_{x,i} = (1-\beta_i) F_x + F_x^i$$
 (2.118)

and similarly for F_y and F_y' . For the free modes, these stress are set to zero. Under these transformations, the six original equations are transformed in to the following equivalent set of three equations.

$$\frac{\partial U}{\partial t}i = fV_{\underline{i}} - gh_{\underline{i}} \frac{\partial \eta}{\partial x}i$$
 (2.119)

$$\frac{\partial V}{\partial t}i = -fU_i - gh_i \frac{\partial \eta}{\partial y}i \qquad (2.120)$$

and
$$\frac{\partial \eta}{\partial t} i = \frac{-\partial U}{\partial x} i - \frac{\partial V}{\partial y} i$$
 (2.121)

This set is solved for i = 1 and i = 2, giving two sets of solutions. The two-layer solution is obtained by the following inverse transformations.

$$\eta' = (h'\eta_1 + h\eta_2)/(h+h')$$
 (2.122)

$$\eta = \eta_1 - (1-\rho) \eta_2 hh'/(h+h')^2$$
 (2.123)

$$U = (U_1 - U_2) h/(h+h')$$
 (2.124)

$$U' = (h' U_1 - hU_2) / (h+h')$$
 (2.125)

V and V' transform in the same manner as U, U'.

2.5 Circular Basin

(a) One-Layer Non-rotating, Free Modes.

(see Lamb, 1932, p.284-287)

Lamb (1932) has investigated the free modes in a onelayer, non-rotating circular basin of constant depth. The transformation to polar co-ordinates is given by

$$x = r \cos \theta$$
 $y = r \sin \theta$ (2.126)

where r is the radial co-ordinate and θ is the azimuthal co-ordinate. When the time dependence is of the form $cos(\sigma t + \epsilon)$, the wave equation for η becomes

$$\frac{\partial^2 \eta}{\partial r^2} + \frac{1}{r} \frac{\partial \eta}{\partial r} + \frac{1}{r^2} \frac{\partial^2 \eta}{\partial \theta^2} + k^2 \eta = 0$$
 (2.127)

where
$$k^2 = \frac{\sigma^2}{gh}$$
 (2.128)

The solution of this wave equation may be expanded in a Fourier series with terms of the form

$$f(r) \begin{cases} \cos s \\ \sin \theta \end{cases} = s\theta$$
 (2.129)

where s is a non-negative integer. This leads to

$$f''(r) + \frac{1}{r} f'(r) + (k^2 - \frac{s^2}{r^2}) f(r) = 0$$
 (2.130)

which is a Bessel's equation. A solution for the various modes for which η is finite is given by

$$\eta = A_s J_s (kr) \frac{\cos}{\sin} S\theta \cos(\sigma t + \epsilon)$$
 (2.131)

The values of $k\,\text{,}$ and thus of $\sigma\,\text{,}$ are determined by the boundary condition

$$\frac{\partial \eta}{\partial r} = 0 \qquad \text{at } r = a \qquad (2.132)$$

where a is the radius of the circular basin. Thus, k is determined by

$$J_{s}'(ka) = 0$$
 (2.133)

For the case s=0, η is symmetrical about the origin and has annular ridges and furrows. The lowest roots for s=0 are

$$\frac{ka}{\pi} = 1.2197, 2.2330, 3.2383, \dots$$
 (2.134)

 $\frac{\sigma a}{\pi}$ = 3.832, 7.016, 10.173,

The values of ka/ π tend to m + $\frac{1}{4}$, where m is an integer. For the m-th mode, there are m nodal circles, with the radii given by

$$J_{0}(kr) = 0$$
 (2.136)

or $\frac{kr}{\pi} = 0.7655, 1.7571, 2.7546, \dots$ (2.137)

When s>0, there are, in addition to the nodal circles, also s equidistant nodal diameters. In (2.131), the cosine and sine may be substituted by cos s(θ - α_s), where α_s is an arbitrary phase lag. The nodal diameters are given by

$$\theta - \alpha_S = \frac{2m + 1}{2s} \pi$$
 (2.138)

The frequencies of the normal modes given by $\sin s\theta$ and $\cos s\theta$ are equal, unless the boundary deviates from its exact circular shape. The symmetrical modes correspond to even s and the anti-symmetrical modes to odd s. For more detailed information, see Lamb (1932, p. 287-290).

or

(b) One-layer Rotating, Free Modes.

(see Lamb, 1932, p. 320-322)

Lamb (1932) also investigated the case of a circular basin rotating at speed ω . If the azimuthal dependence is of the form $e^{\mathbf{i}\mathbf{s}\theta}$, then the wave equation for η becomes

$$\frac{\partial^2 \eta}{\partial r} {}_2 + \frac{1}{r} \frac{\partial \eta}{\partial r} + \left(\kappa^2 - \frac{s^2}{r^2}\right) \eta = 0 \tag{2.139}$$

where

$$\kappa^2 = \frac{\sigma^2 - 4\omega^2}{\sigma h} \tag{2.140}$$

The boundary condition is

$$r \frac{\partial \eta}{\partial r} + \frac{2s\omega}{\sigma} \eta = 0 \tag{2.141}$$

Equation (2.139) is also a Bessel's equation, and a solution is

$$\eta = A_s J_s (\kappa r) e^{i (\sigma t + s\theta)}$$
 (2.142)

In this case, k 2 may be either positive or negative. For negative κ^2 , $J_{\rm S}(\kappa r)$ must be replaced by $I_{\rm S}(\kappa r)$, where κ is the positive square root of $(4\omega^2$ - $\sigma^2)/gh$ and $I_{\rm S}(z)$ is the Bessel's function of imaginary argument.

For positive κ^2 and s=0, then (in real form)

$$\eta = A J_0 (\kappa r) \cos (\sigma t + \varepsilon)$$
 (2.143)

where K is given by

$$J_{O} (\kappa a) = 0 \tag{2.144}$$

The free surface has the same form as in the zero-rotation case, but the frequencies are now different.

If
$$c^2 = gh$$
 and $\beta = 4\omega^2 a^2/c^2$ (2.145)

then
$$\sigma^2 a^2 /_{C^2} = \kappa^2 a^2 + \beta^2$$
 (2.146)

For the case s>o

$$\eta = A_S J_S (\kappa r) \cos (\sigma t + s\theta + \epsilon)$$
 (2.147)

The allowable values of κ and s are given by (2.141) which becomes

$$\kappa a J \frac{1}{s} (\kappa a) + \frac{2s\omega}{\sigma} J_s(\kappa a) = 0 \qquad (2.148)$$

Lamb (1932, p. 322) gives a technique by which the values of σ may be graphically estimated.

(c) Two-layer Rotating, Free Modes. (see Csanady, 1967).

Recently, Csanady (1967) has investigated the free modes in a two-layer circular basin of constant depth. In solving the two-layer problem, Csanady transformed the equations into an equivalment one-layer system, as discussed in Section 2.4(b). The wave equation for the equivalent displacement is given by

$$\frac{\partial^{2} \eta_{i}}{\partial t^{2}} - c_{i}^{2} \nabla^{2} \eta_{i} + f^{2} \eta_{i} = 0$$
 (2.149)

If the solution is assumed of the form

$$\eta_i = e^{i\sigma t} H(x,y)$$
 (2.150)

then the wave equation becomes

$$[\nabla^2 + (\sigma^2 - f^2)/c_i^2] \eta_i = 0$$
 (2.151)

which is again the Helmholtz equation. The boundary condition is given by

$$\frac{\partial^2 \eta}{\partial n \partial t} i \frac{f \partial \eta}{\partial s} i = 0$$
 (2.152)

at the shoreline; n and s are the normal and tangent to the shoreline. For a circular basin, polar co-ordinates are convenient. If η_i is periodic in the azimuthal co-ordinate, $^\varphi,$ then

$$H(x,y) = e^{in\phi} G(r)$$
 (2.153)

where n is an integer. (2.151) now becomes

$$\frac{\partial^2 G}{\partial r^2} + \frac{1}{r} \frac{\partial G}{\partial r} - \frac{f^2 - \sigma^2}{C_i^2} + \frac{n^2}{r^2} \quad G = 0$$
 (2.154)

Two solutions to this equation are Kelvin and Poincaré waves. Csanady (1967) distinguishes between the Kelvin and Poincaré modes accordingly as $|\sigma|$ is less than or greater than f. For the Kelvin modes, with $|\sigma| < f$, the solution is

$$G(r) = A I_{n} \left[\frac{(f^{2} - \sigma^{2})^{\frac{1}{2}} r}{r} \right]$$
 (2.155)

where
$$I_n(x) = J_n(ix)$$
, (2.156)

The boundary condition (2.152) gives

$$\sigma r \frac{dI}{dr} n + nf I_n = 0 (2.157)$$

which gives the permissible values of σ . If β (not to be confused with the roots of the Stokes' equation) is defined as

$$\beta = f^2 r_0^2/c_i^2$$
 (2.158)

then for each azimuthal mode (n = 0, 1, 2,....) there exists one Kelvin mode if

$$\beta > n(n+1) \tag{2.159}$$

From (2.157), if n = 0, then $\sigma = 0$. This zero-frequency mode is given by

$$G(r) = A I_o (fr/c_i)$$
 (2.160)

For the $n \gg 0$ Kelvin modes, (2.157) gives

$$\frac{(f^2 - \sigma^2)^{\frac{1}{2}}}{c_i} r I_{n-1} + n \left(\frac{f}{\sigma} - 1\right) I_n = 0 \qquad (2.161)$$

which shows that σ is negative. Thus the Kelvin modes are

$$\eta_{i} = e^{i(n\phi + \sigma t)} G(r)$$
 (2.162)

and rotate only in the anti-clockwise direction in the Northern Hemisphere.

For the Poincaré modes, that is $|\sigma|_{f}$, the solution to (2.154) is

$$G(r) = A J_n \left(\frac{\sqrt{\sigma^2 - f^2}}{c_i} r \right)$$
 (2.163)

The frequency equation (2,157) becomes

$$\sigma \frac{\text{rdJ}}{\text{dr}} + \inf_{n=0}^{n} = 0$$

$$r = r_0$$
(2.164)

The Poincaré solutions for the n_i surface are cellular, with undulations in both the azimuthal and radial directions. Whereas the Kelvin modes rotate only in the anti-clockwise direction, the Poincaré modes may rotate in either direction.

The case of $|\sigma|^{=f}$ corresponds to the inertial oscillations, in which the currents are circular but the displacements are zero.

(d) Two-layer Rotating, Forced Modes. (see Csanady, 1968)

In a subsequent paper, Csanady (1968) investigated the forced response due to wind stress in his (1967) circular basin. In his first case, a constant (in time) wind stress is considered, given by

$$F_{x} = F$$
 $F_{y} = 0$ (2.165)

If an equilibrium slope could be achieved, the mean surface would be described by

$$-c^2 \frac{\partial \overline{\eta}}{\partial x} + F = 0 \tag{2.166}$$

In polar co-ordinates, this is

$$\bar{\eta} = \frac{F}{c^2} r \cos \theta \tag{2.167}$$

Providing that the lake was at rest at time zero, then the integrated vorticity is given by

$$\zeta = \frac{\partial V}{\partial x} - \frac{\partial U}{\partial y} = f\eta \tag{2.168}$$

However, at equilibrium, U = V = 0, and thus η must also be zero. Therefore the equilibrium slope of (2.166) cannot be achieved. Instead the Earth's rotation would set up a quasisteady circulation.

Csanady gives a solution, which also conserves vorticity, as

$$\eta = \frac{Fr_0}{c^2} \quad \frac{I_1(r/R)}{I_1(r_0/R)} \cos \phi \tag{2.169}$$

where R = c/f is Rossby's "radius of deformation". The flows corresponding to (2.169) are

$$U = \frac{c^2}{f} \frac{\partial}{\partial y} (\eta - \overline{\eta})$$
 (2.170)

$$V = \frac{c^2}{f} \frac{\partial}{\partial x} (\eta - \overline{\eta})$$
 (2.171)

where $\overline{\eta}$ is given by (2.166). It becomes obvious that U and V can be derived from the stream function

$$\Psi = \frac{c^2}{f} \quad (\eta - \overline{\eta}) \tag{2.172}$$

The boundary conditions make it necessary that the boundary be a streamline. If Ψ at the shoreline is arbitrarily set to zero, then

$$\eta = \overline{\eta} = \frac{F}{c^2} r \cos \phi \quad \text{at } r = r_0 \tag{2.173}$$

so that the corrected stream function is

$$\Psi = \frac{\operatorname{Fr_0}}{f} \left[\frac{\operatorname{I_1}(r/R)}{\operatorname{I_1}(r_0/R)} - \frac{r}{R_0} \right] \cos \phi$$
 (2.174)

Under (2.174), vorticity is conserved and the surface streamlines now consist of two gyres, one each in the upwind and the downwind halves of the basin. The downwind gyre rotates anticlockwise, and the upwind gyre rotates clockwise.

Csanady (1968) also investigated the case of a periodic wind, given by

$$F_{V} = F \cos \sigma t \qquad F_{V} = 0 \qquad (2.175)$$

At low frequencies, the forced response is given by

$$\eta = \frac{Fr_0}{c^2} I_1(r/R^*) \begin{bmatrix} \frac{1 + f/\sigma}{r_0 I_1(r_0/R^*) + \frac{f}{\sigma} I_1(r_0/R^*)} & \cos(\phi + \sigma t) \\ \frac{1 - f/\sigma}{r_0 I_1(r_0/R^*) - \frac{f}{\sigma} I_1(r_0/R^*)} & \cos(\phi - \sigma t) \end{bmatrix}$$

$$R^* = R \left(1 - \frac{\sigma^2}{f^2}\right)^{-1/2}$$

This solution is a rotating seiche. If the multipliers of the cosine terms inside the brackets of (2.176) were equal, a standing wave in the direction of the wind would result. However, in general they are not equal and a rotating seiche is also produced. As $\sigma \rightarrow 0$, the rotating pattern vanishes, leaving only the $\cos \phi \cos \sigma t$ pattern, which is the same as the steady state solution for a constant wind.

Note that the denominator in the second term inside the brackets of (2.176) is identical to the frequency equation for the slowest Kelvin free mode. Thus as the forcing frequency approaches that of the Kelvin mode, resonance occurs. At higher values of σ , but still with $|\sigma| < f$ the standing wave pattern becomes $\sin \phi \sin \sigma t$, in which case, η is a maximum

goo to the right of the wind. For $|\sigma| > f$ the solution is given in terms of Bessel functions of real rather than imaginary argument. In this case, the denominator of the solution is identical to the frequency equation for the Poincaré modes. Thus, the system approaches resonance as the forcing frequency approaches any of the natural frequencies of the basin. This equally applies to the barotropic frequencies. At the same time, proximity to any of these natural frequencies may result in the excitation of the free modes themselves. Csanady (1968) cautions that the motions discussed above may be modified by friction, and possibly in a manner unlike damping in a non-rotating system.

3. FREE OSCILLATIONS OF LAKE HURON

3.1 Calculation of the Free Modes.

A one-dimensional model is now constructed from which the free surface modes of Lake Huron may be calculated. is expected that contributions from these free modes will often be present in surface water level data, so that the determination of these free modes will be of use in the processing of such data. This work will also demonstrate how the use of a simple model may give useful results, without involving the complex mathematics of a two-dimensional model.

The most serious objection to the use of a onedimensional model is the neglect of the Earth's rotation. ever, it will be seen that the period T of the non-rotating longitudinal surface seiche of Lake Huron is about 7 hours; the inertial period T; is about 17 hours, so that T/T; is

roughly 0.41. If Georgian Bay is neglected, the length to breadth ratio of Lake Huron is certainly at least 2, if not as large as 3. From Rao's (1966) calculations (see Fig. 2.2) the effect of rotation upon the lowest longitudinal mode is less than 1%, so that rotation may be safely neglected.

The one-dimensional hydrodynamical equations, subject to the assumptions of Section 2.1, and the neglect of the Earth's rotation, are (Proudman, 1953, p. 225)

 $\frac{\partial u}{\partial t} = -g \frac{\partial \eta}{\partial x}$

$$\frac{\partial \eta}{\partial t} = -\frac{h}{\partial x} \frac{\partial u}{\partial x} \tag{3.2}$$

where the depth has been taken constant. With the longitudinal axis of the lake in the x-direction, the boundary conditions are

$$u(0) = u(L) = 0$$
 (3.3)

For basins of variable depth, many methods of numerical solution have been developed (see Defant, 1961, p. 160-173). The method used below is a direct spatial integration of equations (3.1) and (3.2).

In recent years, this method has been used by Platzman and Rao (1964) in the study of the free modes of Lake Erie, and by Redfield (1961) in the study of tidal co-oscillations in Lake Maricaibo.

As suggested by Platzman and Rao (1964) and Redfield (1961), the free modes may be expressed in the form

$$Q(x,t) = Q(x) \sin \sigma t$$
 (3.4)

$$n(x,t) = Z(x) \cos \sigma t \tag{3.5}$$

so that (3.1) and (3.2) become

$$\frac{\partial Q}{\partial x} = b\sigma Z \tag{3.6}$$

$$\frac{\partial Z}{\partial x} = -\frac{\sigma}{gA} Q \tag{3.7}$$

where Q and Z are now only the x-dependent parts of the solution. To facilitate the integration of (3.6) and (3.7), the basin must be divided into a large number of cross-sections, so that the basin now consists of a large number of short channels, within each of which the breadth and depth are constant. In the following equations, Q_n shall refer to

 $Q[(n-1)^{\Delta}x]$ and similarly for Z. The factor (n-1) is introduced to ease computer programming. The central difference approximation, to lowest order, of the gradients can be written as

$$\frac{\partial Q}{\partial x}n = [Q_{n+1} - Q_{n-1}]/2\Delta x \tag{3.8}$$

$$\frac{\partial Z}{\partial x}_{n+1} = [Z_{n+2} - Z_n]/2\Delta x \tag{3.9}$$

so that (3.6) and (3.7) become

$$Q_{n+1} = Q_{n-1} + 2 \Delta x \sigma b_n Z_n$$
 (3.10)

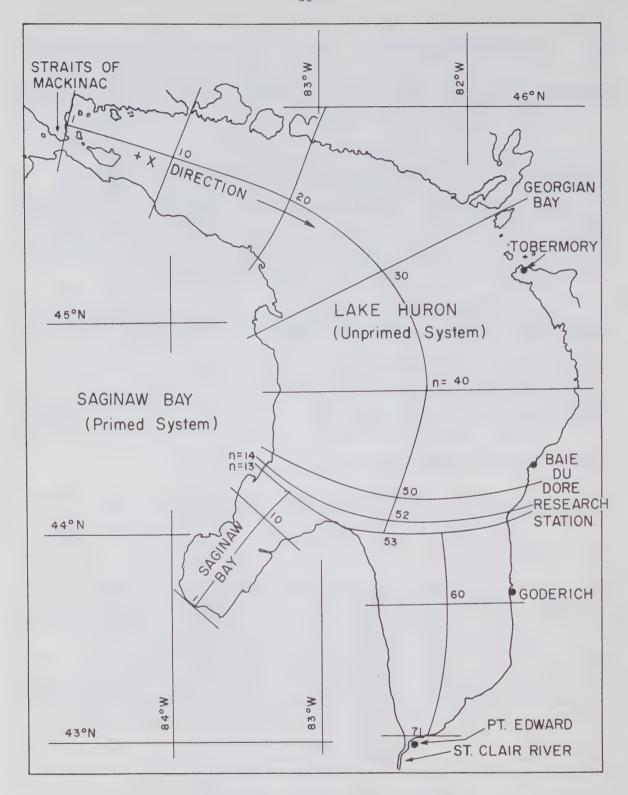


Figure 3.1 The one-dimensional grid system employed in the calculation of the free longitudinal surface modes of Lake Huron.

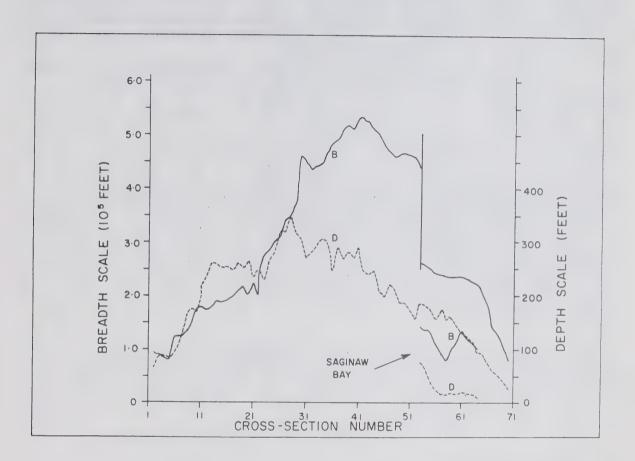


Figure 3.2 The longitudinal profiles for the mean depth (dashed line) and breadth (solid line) of Lake Huron.

$$Z_{n+2} = Z_n - 2\Delta x \quad \frac{\sigma}{g} \frac{Q_{n+1}}{A_{n+1}}$$
 (3.11)

For convenience, let n represent an even integer, and let n = 1 define the cross-section at one end of the lake. If Z_2 is known (Q_1 is zero), then the use of (3.10) gives Q_3 , (3.11) gives Z_4 , (3.10) gives Q_5 , and so forth along the entire length of the basin. In this manner, Z is calculated at even-numbered grid points and Q at odd-numbered ones. Such a grid system is similar to the R_1 -Richardson lattice (see Platzman, 1963, p. 34), and is logically called "step-over differencing", or more commonly, the "leap-frog method".

For the integration procedure, Lake Huron was divided into 71 cross-sections (from Canadian Hydrographic Service Chart No. 2200). The north end of the lake was set at n = 1and the south end at n = 71, with a grid spacing of 4.00 miles (see Fig. 3.1). In this schematization, Georgian Bay has been neglected. The breadth and depth are shown in Fig. 3.2. is assumed that the flows into Georgian Bay will not seriously alter the longitudinal free modes, although this may not be true for any transverse modes. At the two ends of the lake, the flows through the St. Clair River and Straits of Mackinac have also been neglected. At the time of these calculations, I was not aware of Rockwell's (1966) determination of the free modes of each of the Great Lakes. His results show that the neglect of the flows at either end of Lake Huron does not affect the free modes by more than a few percent. On the other hand, the presence of Saginaw Bay will be taken into consideration.

For the main part of Lake Huron, the +n-direction is taken as the +x-direction. For convenience, the +n-direction in Saginaw Bay will be taken as the -x-direction; that is, n increases from the head of the bay, so that in Saginaw Bay

$$x' = -(n-1)\Delta x$$
 (3.12)

The boundary conditions are

$$Q_1 = Q_{71} = Q_1' = 0$$
 (3.13)

The water surface must be continuous at all times, so that

$$Z_{14}' = Z_{52}$$
 (3.14)

At the junction at the mouth of Saginaw Bay, the continuity of flow is expressed as

$$Q_{J} = Q_{53} + Q'_{13} = Q_{51} + 2\Delta x b_{52} Z_{52} \sigma$$
 (3.15)

where $Q_{\mathbf{J}}$ is the total flow incident upon the cross-section at the junction.

Since (3.10) and (3.11) are linear equations, the amplitudes of the free oscillations may be arbitrarily set. Q_1 is zero, and Z_2 is set to unit height. (3.10) and (3.11) may now be used to obtain values of the variables up to and including Z_{52} and Q_J . However, Q_{13}^{\prime} is an unknown. Platzman and Rao (1964) continue the integration into Saginaw Bay in "continued-fraction form" (see Platzman and Rao, 1964, p. 364). I personally feel that such a procedure is tedious; it is not particularly practical if the secondary channel is long. At this point then, I deviate from their procedure.

For Saginaw Bay, the difference equations are

$$Q_{n+1}^{\dagger} = Q_{n-1}^{\dagger} - 2\Delta x \sigma b_{n}^{\dagger} Z_{n}^{\dagger}$$
 (3.16)

and

$$Z_{n+2} = Z_n + 2\Delta x \frac{\sigma}{g} \frac{Q'_{n+1}}{A'_{n+1}}$$
 (3.17)

 Q_1' is zero and Z_2' is arbitrarily set to unity. Repeated use of (3.16) and (3.17) yields values up to and including Q_{13}' and Z_{14}' , which shall be designated the intermediate solution. Since the system is linear, the intermediate solution may be multiplied by a constant; specifically, this constant is chosen to be

$$z_{52} / z_{14}$$
 (3.18)

This corrected solution satisfies the condition (3.14). With the correct value of Q_{13} now known, the value of Q_{53} is obtained from (3.15), and the integration can now be resumed for the remainder of Lake Huron, ending up finally with a value for Q71. Nothing has been said about the frequency, o, yet; the boundary condition of no flow at n =71 must also be satisfied. The establishment of the free modes consists of finding those values of o for which this boundary condition is satisfied. Initially, calculations are carried out for a set of coarsely spaced values of σ . The approximate behavior of Q71 is displaced in Fig. 3.3, from which the approximate zeroes may be estimated, either graphically or by numerical interpolation. Repeated trials with finer spaced values of o in the neighbourhood of these approximate roots will eventually yield the frequencies of the lowest free modes to the desired accuracy. In the actual calculations, three trials were sufficient to estimate the roots to within +2 in the 4th significant digit.

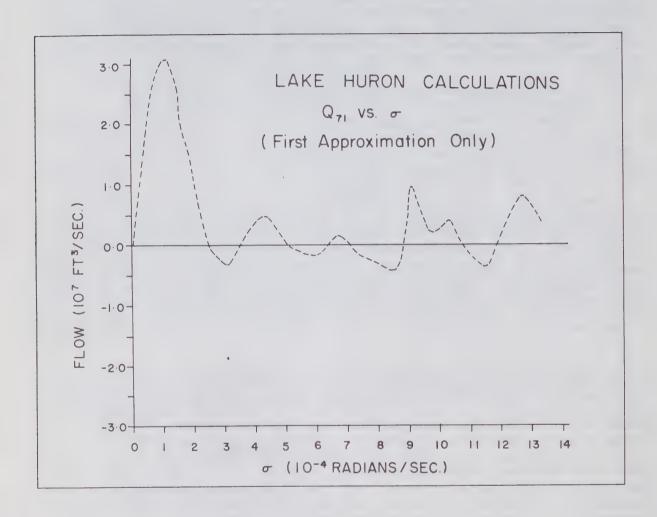


Figure 3.3 The value of \mathbf{Q}_{71} versus frequency calculated in the determination of the free modes of Lake Huron.

The frequencies for the six lowest modes are given in Table 3.1 below, along with Rockwell's (1966) values.

TABLE 3.1 Longitudinal Free Modes of Lake Huron.

m	<u>σ</u>	T	mT	Q*	<u>T</u> **
	-4 (10 /sec)	(hr)	(hr)	$(10^6 \text{ ft}^3/\text{se})$	R c) (hr)
1	2.500	6.98	6.98	-0.33	6.49(6.71)
2	3.522	4.96	9.92	+0.24	4.57(4.80)
3	4.964	3.52	10.52	-4.86	3.13(3.18)
4	6.378	2.74	10.94	-1.18	2.60(2.66)
5***	7.10	2.46	12.3		2.24(2.26)
6	8.855	1.97	11.82	+6.04	

- * flow at mouth of Saginaw.
- ** Rockwell's (1966) results
 - first value-Straits of Mackinac open.
 - bracketed value-Straits of Mackinac closed.
- *** 5-th mode was estimated only.

The flows and displacements for the free modes are shown in Fig. 3.4 and 3.5. Rockwell's (1966) results show that the flow through the Straits of Mackinac do not affect the results by more than a few percent. As the nodality increases, the neglected flow appears to be less important.

Comparison of Rockwell's (1966) and my results shows differences of up to 10%. These differences are principally caused by differences in the depth schematizations. For my model, the mean depth is 198.5 feet and the mean square root of the depth is 13.64 feet. From Merian's formula, given by

$$T = \frac{2L}{\sqrt{gh}} \tag{3.19}$$

these two values lead to periods of 10.28 and 10.62 hours, respectively, for the lowest mode. In comparison, Rockwell's model has an average depth of 65 meters, giving a Merian period of 9.77 hours, which is 7% less than my mean value of 10.45 hours.

From Table 3.1, it is seen that the period of the lowest mode is much less than the Merian period. For the higher modes, the value of mT is close to the Merian period. From these results, and those of Platzman and Rao (1966) and Rockwell (1966), it appears that the use of the Merian formula gives reasonable predictions for the free modes of a lake of variable depth, with the exception of the lowest mode.

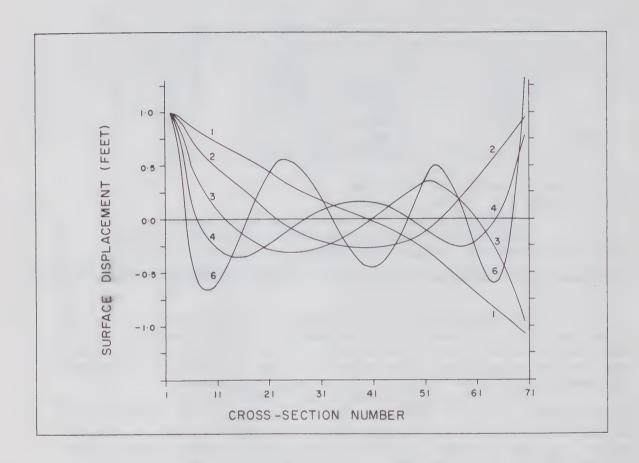


Figure 3.4 The configuration of the surface displacement for the lowest free surface modes of Lake Huron.

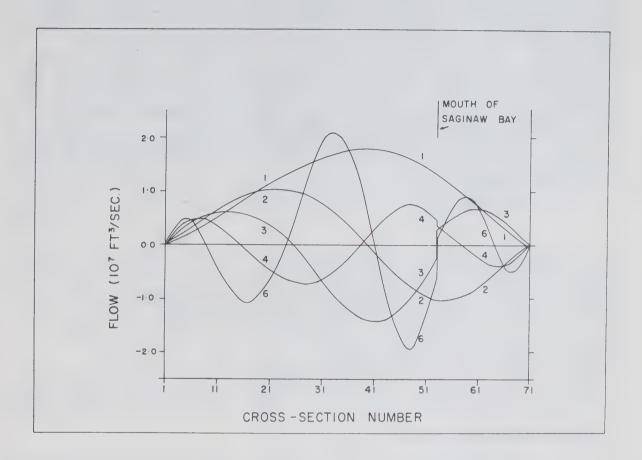


Figure 3.5 The configuration of the depth mean flow for the lowest free surface modes of Lake Huron.

Saginaw Bay is open at one end and closed at the other, thus acting as a one-quarter wave resonator; higher modes are 3/4, 5/4, 7/4, etc. A free mode or standing wave would consist of a flow field with a node at the head and an antinode at the mouth of the bay. The displacement, on the other hand, would have a node at the mouth and an anti-node at the head of the bay. In general, the oscillations in Saginaw Bay are forced to co-oscillate with those in the main part of Lake Huron. If the frequency of the Lake Huron motion tends to those of the free modes of Saginaw Bay, then the flow at the mouth of the bay will approach an extremum in that locality of the frequency spectrum, and the presence of Saginaw Bay will have a marked affect upon the Lake Huron modes.

The periods of the free modes of Saginaw Bay may be estimated by the following modification of Merian's formula for a quarter-wave resonator.

$$T = \frac{4L}{(2m-1)\sqrt{gh}}$$
 $m = 1, 2, 3, 4, \dots$ (3.20)

If the average depth is taken to be 23.4 feet, then the lowest free periods for Saginaw Bay are 10.30, 3.43, 2.06, and 1.45 hours. Rockwell (1966) obtained values of 10.0, 3.32, and 2.31 hours by numerical integration. It is seen that the third and sixth Lake Huron modes, with periods of 3.52 and 1.97 hours, respectively, are almost in tune with the second and third Saginaw Bay modes, with periods of 3.43 and 2.06 hours, respectively. The flows at the mouth of Saginaw Bay are included in Table 3.1. Indeed, the third and sixth Lake Huron modes show the largest flows going into (or out of) Saginaw Bay.

3.2 Computational Errors.

The central-difference approximations to the gradients given by (3.8) and (3.9) were derived from Taylor expansions whose errors, E, to lowest order are given by

$$E[Q_{X}, Z_{X}] = \frac{(\Delta X)^{2}}{3!} = \frac{\partial}{\partial X^{3}} [Q, Z]$$
 (3.21)

For the free modes, the solutions have the following general form (in complex form)

Q,Z
$$\sim \exp (i n \pi x/L)$$
 (3.22)

so that (3.21) becomes

$$E[Q_{X}, Z_{X}] = \frac{(\Delta X)^{2} (\pi)^{3} n^{3} [Q, Z]}{3! L^{3}}$$
 (3.23)

Thus,
$$\frac{E[\delta Q(x)]}{Q(x)} = \frac{E[\delta Z(x)]}{Z(x)} = \frac{(\Delta x)^3}{3} \frac{\pi^3}{L^3} \quad n^3$$
 (3.24)

Each of the equations (3.10) and (3.11) are integrated about 35 times each, so that the maximum possible accumulated error is

$$\frac{E[Q71]}{Q71} = \frac{E[Z70]}{Z70} = 9.6 \times 10^{-4} \text{ n}^3$$
 (3.25)

For the five lowest modes of Lake Huron, the relative error in \mathbf{Z}_{70} and \mathbf{Q}_{71} is 0.1, 0.8, 2.6, 6.1, and 12.0%.

This is not to be misconstrued as the error in the value for the frequency.

In Table 3.2 below, values of σ and Q_{71} for the second and third determination of σ for the fourth mode are given.

TABLE 3.2

Determination of the Frequency of the Fourth Free Mode for Lake Huron.

	σ (radians/sec)	Q_{71} (ft 3 /sec)
Second Determination	6.3×10^{-4} 6.4 6.5	-4.43×10^{5} +1.26 +6.67
Third Determination	6.370×10^{-4} 6.375 6.380 6.385 6.390	-4.40×10^{4} -1.56 $+1.27$ $+4.10$ $+6.93$

The maximum value of Q(x) is about 3 x 10^6 ft³/sec. From Table 3.2, interpolation would determine the value of σ to within 1.5 units in the second digit, so that the maximum possible error for the frequency of the fourth mode is at most 2%. Since the actual errors may occur in a sinusoidal fashion, the error in the frequency may be much less than this upper bound.

The error given above is only a measure of the computational error. There are many errors inherent in the model itself. The neglect of the Earth's rotation has already been mentioned. The schematization of the lake is also subject to error. Curvature of Lake Huron and the resulting centripetal acceleration has also been neglected. Despite these and many other errors, the results do look reasonable. The calculated frequencies will be further checked in the next section.

3.3 Power Spectra of Lake Huron Water Levels.

Power spectra of two sets of water level data will be presented here. The two data records are from the tide gauge stations at Point Edward and Goderich (see Fig. 3.1), which are maintained by the Tides and Water Levels Section of the Department of Energy, Mines and Resources. The duration of the records that are analyzed is for the 4 summer months June to September, 1966.

In providing a brief theoretical background for the calculation of these power spectra, I shall only deal with finite length discrete-time data (Blackman, 1965, p. 143-147). For a more comprehensive treatment, the reader is referred to Blackman and Tukey (1959), Munk, Snodgrass, and Tucker, (1959), and Muller (1966).

Consider a data record consisting of n + 1 consecutive values of X(t), sampled at regular intervals of Δt , given by

The Mean lagged products, C_r , computed at intervals of $\Delta \tau$, where $\Delta \tau = h \Delta t$ are given by

$$Cr = \frac{1}{n-hr+1} \sum_{q=0}^{n-hr} X_q X_{q+hr}$$
 (3.27)

with r up to some maximum m.

The choice of m will be discussed later, but certainly m \leq n/h If there is no drift in the data, and the mean is zero, then the raw spectral density estimates, $V_{\rm S}$, are given by (Blackman, 1966, p. 144)

$$V_{S} = \Delta t \left[C_{O} + C_{m} \cos s\pi + 2 \sum_{r=1}^{m-1} C_{r} \cos \frac{rs\pi}{m} \right]$$
 (3.28)

Smoothing of the ${\rm V}_{\rm S}$ gives the refined spectral estimates. The most common methods of smoothing are hamming, with weights

0.25, 0.50, and 0.25 (3.29)

and hanning, with weights

$$0.23$$
, 0.54 , and 0.23 , (3.30)

with the restrictions that $V_{-1} = V_1$ and $V_{m-1} = V_{m+1}$.

For example, the hanned value of V_{10} is

$$0.25 \text{ V}_9 \qquad 0.50 \text{ V}_{10} \qquad 0.25 \text{V}_{11}$$
 (3.31)

If only hanning or hamming is applied, the stability of the refined estimates is roughly that of a chi-square on k degrees of freedom (Blackman, 1966, p. 149), where

$$k = 2\left(\frac{n\Delta t}{m\Delta \tau} - \frac{1}{3}\right)$$

$$= 2\left(\frac{n}{mh} - \frac{1}{3}\right) \quad \text{for } f = \frac{s}{2m\Delta \tau}$$
(3.32)

This shows that the analysis of one long record is more stable than the analysis of several shorter records of the same total duration.

The 80% confidence limits may be expressed as (Blackman, 1966, p. 150)

7.8
$$\left[\frac{2}{3k-1} + \frac{1}{\sqrt{k-1}}\right]$$
 decibels, for k , 3 (3.33)

For the 90, 96, and 98% confidence limits, the leading factor of 7.8 must be changed to 10.0, 12.6, and 14.3, respectively. Thus the confidence limit gets smaller as k increases. General accepted procedure is to have the maximum lag no larger than 5 to 10% of the total record length, so that k is large.

For the data analyzed here, the mean is subtracted from each reading, giving a zero mean for the record. The drift is only several tenths of a foot. It is an annual variation, and will only affect the very low end of the spectrum. A method of correcting the drift is given in Blackman (1966, p. 152).

The data should be sampled at an interval Δt such that $1/\Delta t$ is at least twice the highest significant frequency. If not, "aliasing" or "overlapping of the side bands" will occur (see Blackman, 1966, p. 19), in which case power at higher frequencies is folded into the lower frequencies. The optimum frequency resolution is given by

$$\Delta f = 1/m\Delta \tau \tag{3.34}$$

It is not necessary to take $\Delta \tau = \Delta t$ but Δt should not be much smaller than $\Delta \tau$ so that an unnecessary number of measurement is avoided.

The record length of the data to be analyzed is 120 days, or 2880 hours. The sampling interval was 1 hour, and $^{\Delta t}$ is also set to this value. Thus periodicities as low as 2 hours can be measured without the danger of aliasing. The maximum lag, m $\Delta \tau$ was set to 120 hours, which is only 4.2% of the record length. This gives 47.3 degrees of freedom, and therefore fairly stable spectral estimates, since the 90% confidence limits are only 1.56 and -1.28 decibels. The maximum frequency resolution is 1 cycle per 240 hours. In the vicinity of the lowest Lake Huron mode, this gives a resolution in the period of about 0.22 hours; for the higher frequency range, the resolution in the period is even finer.

The data from Goderich and Point Edward were analyzed by the method described above, and subsequently hanned to give the refined estimates, which are plotted in Fig. 3.6 and 3.7. In view of their stability (47.3 degrees of freedom), I have not included the confidence limits in these two diagrams. Even when the spectral peaks are less than the confidence limits, which is not the case here, if the peaks are theoretically predictable, then if they occur consistently at the same frequencies, they are at least of physical significance, even if not of statistical significance.

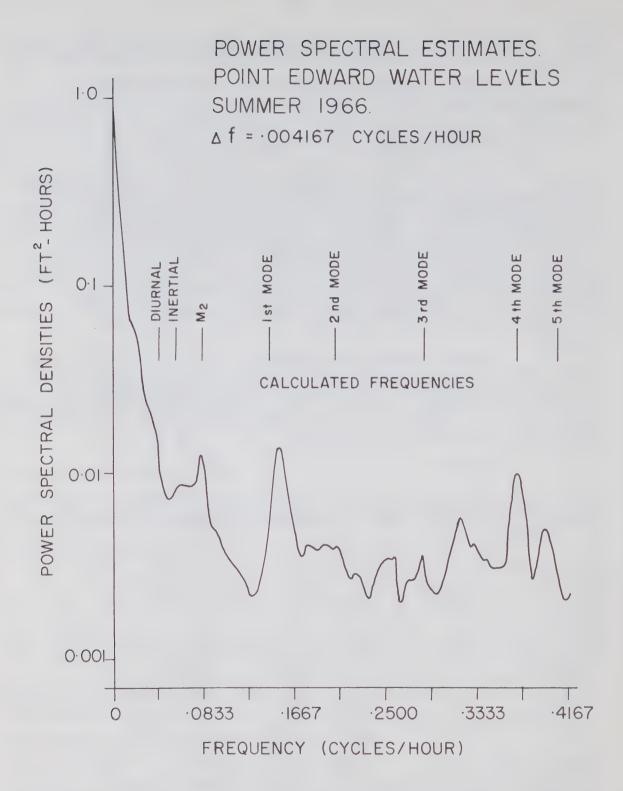


Figure 3.6 Power spectral estimates of Pt. Edward, Ontario water levels for summer, 1966; length of record, 4 months.

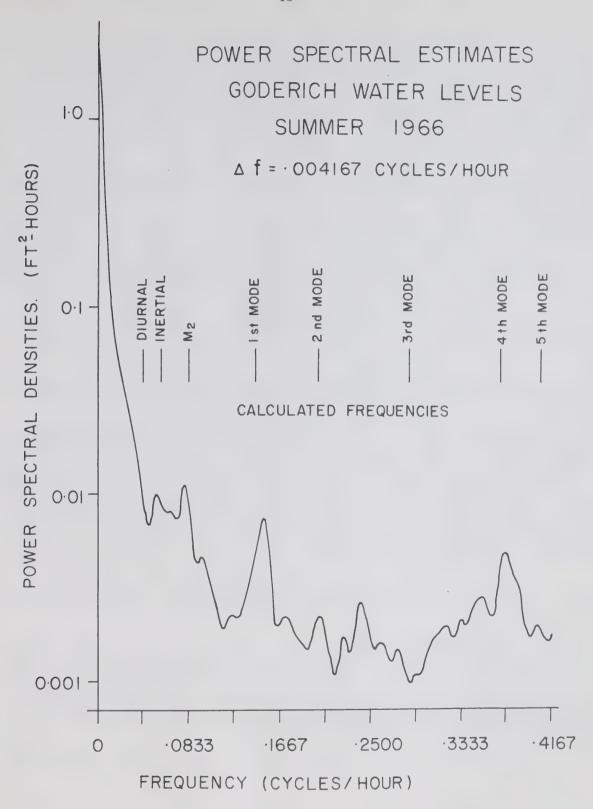


Figure 3.7 Power spectral estimates of Goderich, Ontario water levels for summer, 1966; length of record, 4 months.

Goderich lies at cross-section n = 55 of the Lake Huron model, whereas Pt. Edward lies at the south end of the lake, so that Pt. Edward is always at an anti-node for the surface displacement for the longitudinal free modes, while Goderich is near an anti-node only for some of the much higher free modes. It is therefore not surprising that the energy level of the Goderich spectral estimates is much lower than the level of the Pt. Edward spectra.

For the Pt. Edward spectra (Fig. 3.6), there is a faint peak at the inertial frequency. Power is also found at the frequency of the M₂, the major lunar constituent of the astronomical tide. Strong peaks are found near the frequencies of the first and fourth Lake Huron modes calculated in Section 3.1. For the first mode, the frequency is equivalent to a period of 6.67 hours, which lies between my calculated value of 6.98 hours and Rockwell's (1966) value of 6.49 hours. Lesser peaks are also found for the third and fifth Lake Huron modes.

The Goderich spectral estimates (Fig. 3.7) behave similarly to the Pt. Edward estimates, except that the energy level is much lower, and the inertial peak is stronger than that in the Pt. Edward spectra.

Many other peaks are also found in both spectra. Some of these must undoubtedly be related to the many possible transverse free oscillations in Lake Huron. Another source of energy is the many variations in the meteorological parameters, wind and atmospheric pressure, but there is neither time nor space to delve into these. In general, it appears that the one-dimensional model of Lake Huron, even though it is a very simple one, has nevertheless predicted the longitudinal free surface modes of Lake Huron quite well. The difference between the calculated periodicities and those found in the power spectra of the water level data was only about 5% for the lowest mode and less for the higher modes.

4. DYNAMICAL MODEL OF TWO-LAYER RECTANGULAR BASIN SUBJECT TO WIND STRESS

4.1 Differential Equations.

A numerical model of a two-layer rectangular basin subject to wind stress is developed for computer calculations. It consists basically of an integration of the hydrodynamical equations in time, and is therefore termed a dynamical model. The linearized hydrodynamical equations have been derived in Section 2.1, and are given by

$$\frac{\partial u}{\partial t} = fv - g \frac{\partial \eta}{\partial x} \qquad F_{x}$$
 (4.1)

$$\frac{\partial v}{\partial t} = -fu - g \frac{\partial n}{\partial y} + F_y \tag{4.2}$$

$$\frac{\partial u'}{\partial t} = fv' - g \frac{\rho}{\rho}, \frac{\partial \eta}{\partial x} - g \left(1 - \frac{\rho}{\rho}, \right) \frac{\partial \eta}{\partial x}'$$
 (4.3)

$$\frac{\partial \mathbf{v'}}{\partial t} = - \mathbf{f} \mathbf{u'} - \mathbf{g} \frac{\rho}{\rho}, \quad \frac{\partial \eta}{\partial y} - \mathbf{g} \left(1 - \frac{\rho}{\rho}, \right) \frac{\partial \eta}{\partial y}$$
 (4.4)

$$\frac{\partial \eta'}{\partial t} = -\frac{\partial}{\partial x} (h'u') - \frac{\partial}{\partial y} (h'v')$$
 (4.5)

$$\frac{\partial}{\partial t}$$
 $(\eta - \eta') = -\frac{\partial}{\partial x} (hu) - \frac{\partial}{\partial y} (hv)$ (4.6)

where the velocities are depth mean values. The assumptions inherent in these equations are as follows:

- the wavelengths of the motions are large compared with the depths of the two layers,
- (2) the vertical velocities are negligible,
- (3) the pressure may be expressed by the hydrostatic approximation, (2 and 3 follow from 1),
- (4) the velocities are small, so that the non-linear accelerative terms are negligible,
- (5) the bottom and interface stresses are negligible, and
- (6) The Coriolis parameter is constant over the whole of the basin.

The only serious objection to these assumptions is possibly the neglect of the bottom and interface stresses. During period of strong forcing, these stresses are relatively unimportant. The effect of friction is small over short periods of time, even though over longer periods, this neglect of friction is not valid. From general observations in the Great Lakes, Csanady (1967) has deduced that the effects of friction may only be neglected for possibly 5 or 6 inertial periods. In the calculations to be presented later, the duration of the calculations will generally be only 75 hours, which is 4 or 5 inertial periods, so that the neglect of friction will be valid. The terms $F_{\rm X}$ and $F_{\rm V}$ are components of the forcing term

F, given by $F = \tau/\rho h$

where T is the wind stress at the water surface. In each case treated in this thesis, the stress will always be taken to be uniform over the whole surface of the basin, but in time, they may be impulsive, constant, or periodic. Understanding of the model is enhanced if one can associate a certain wind speed with a given value of wind stress. Wilson (1960) has given an excellent review of wind stress laws used by past researchers. The most popular is the quadratic law, given by

$$\tau = C_{d} \rho_{a} W^{2} \tag{4.8}$$

where $C_{\rm d}$ is a wind stress co-efficient, $\rho_{\rm a}$ is the density of air and W is the wind speed. In the context of equations (4.1) to (4.4), $C_{\rm d}$ is dimensionless. Upon reviewing the work of 47

authorities, and adjusting their various stress laws to the quadratic formulation, Wilson (1960) found a mean value for $\rm C_d$ of 0.00147 for light winds, and 0.00237 for strong winds, with standard deviations of 0.00083 and 0.00056, respectively. For the work in this thesis, $\rm C_d\,\rho_a$ is arbitrarily set to a value of 2 x 10^{-6} gm/cm³.

4.2 Difference Equations.

In order that they may be numerical integrated, (4.1) to (4.6) are transformed into a set of difference equations. The following Taylor expansions are useful.

$$F(t+\Delta t) = F(t) + \frac{\Delta t \partial F(t)}{1 \partial t} + \frac{(\Delta t)^2}{2} \frac{\partial^2 F(t)}{\partial t^2} + \frac{(\Delta t)^3}{6} \frac{\partial^3 F(t)}{\partial t^3} + \cdots (4.9)$$

$$F(t-\Delta t) = F(t) - \Delta t \frac{\partial F(t)}{\partial t} + \frac{(\Delta t)^2 \partial^2 F(t)}{2 \partial t^2} F(t) - \frac{(\Delta t)^3}{6} \frac{\partial^3 F(t)}{\partial t^3} F(t) + \frac{(4.10)}{6}$$

The difference of these two series gives a central difference approximation to the time derivative, as

$$\frac{\partial F(t)}{\partial t} = \frac{F(t+\Delta t) - F(t-\Delta t)}{2\Delta t} + O\left[\frac{(\Delta t)^2}{6} \frac{\partial^3}{\partial t^3} F(t)\right]$$
(4.11)

The error term in (4.11) is of a higher order than that in a forward time difference, such as

$$\frac{\partial F(t)}{\partial t} = \frac{F(t+\Delta t) - F(t)}{\Delta t} + O\left[\frac{\Delta t}{2} - \frac{\partial^2 F}{\partial t^2}(t)\right] \tag{4.12}$$

The form of (4.11) is suitable for a grid system such as the R₁-Richardson lattice (see Platzman, 1963, p. 34), in which the continuity equations are evaluated at even time steps. Let t stand for an even multiple of the time step, Δt (4.1) may now be written as

$$\left(\frac{\partial \mathbf{u}}{\partial \mathbf{t}}\right)^{\mathbf{t}} = \mathbf{f} \mathbf{v}^{\mathbf{t}} - \mathbf{g} \left(\frac{\partial \mathbf{\eta}}{\partial \mathbf{x}}\right)^{\mathbf{t}} + \mathbf{F}_{\mathbf{x}}^{\mathbf{t}}$$
 (4.13)

If $u^{t-\Delta t}$ is known, then

$$u^{t+\Delta t} = 2\Delta t \left(\frac{\partial u}{\partial t}\right)^{t} + u^{t-\Delta t}$$
 (4.14)

Similarly for the other three equations of motion. The equation of continuity (4.5) may be approximated as

$$\left(\frac{\partial \eta'}{\partial t}\right)^{t+2\Delta t} = -\left(\frac{\partial}{\partial x} h'u'\right)^{t+\Delta t} - \left(\frac{\partial}{\partial y} h'v'\right)^{t+\Delta t}$$
(4.15)

If n' t is known, then

$$\eta, t+2\Delta t = 2\Delta t \left(\frac{\partial \eta'}{\partial t}\right)^{t+\Delta t} + \eta, t \qquad (4.16)$$

and similarly for the remaining equation of continuity. For the work here, all displacements are set to zero at time zero and all velocity components are set to zero at time Δt ; that is, the basin is initially at rest. Repeated integration of the hydrodynamical equations will give the displacements at time $2\Delta t$, the velocities at time $3\Delta t$, the displacements at time $4\Delta t$, and so on.

However, before the equations can be integrated in time, there still remains the problem of approximating the terms which are either functions of the space co-ordinates or are spatial derivatives. The notation to be used below is as follows.

$$F(M,N,T,)=F(y=[M-1]\Delta y,x=[N-1]\Delta x, t=T\Delta t)$$
 (4.17)

The -1 term is introduced into the spatial co-ordinates to ease translation into FORTRAN IV for computer calculation.

The approximations to the spatial derivatives may be expressed in the manner of (4.11), as

$$\frac{\partial}{\partial x}F(x) = \frac{F(x+\Delta x) - F(x-\Delta x)}{2\Delta x} + O\left[\left(\frac{\Delta x}{6}\right)^{\frac{2}{3}}\frac{\partial^{3}}{\partial x^{3}}F(x)\right]$$
(4.18)

$$\frac{\partial F(y)}{\partial y} = \frac{F(y + \Delta y) - F(y - \Delta y)}{2\Delta y} + O\left[\left(\frac{\Delta y}{6}\right)^2 \frac{\partial^3}{\partial y^3} F(y)\right]$$
(4.19)

The grid system is shown in Fig. 4.1; all similar grid points are 2 \triangle x apart, with \triangle y equal to \triangle x. The u-points are midway between the n-points (Z-points) in the x-direction, and the v-points are midway between the $\eta\text{-points}$ in the y-direction. This particular grid is used extensively by the Institut fur Meereskunde, Hamburg in tidal and storm surge prediction models (see for example, Hansen, 1956, and Brettschneider, 1965). Other grids are also possible, but require different finitedifference approximations. For example, Harris and Jelesnianski (1964) and Jelesnianski (1964) used a grid in which all variables were calculated at all grid points. However, the gradient approximations in that grid have errors proportional to $(2\Delta x)^2$, whereas in the grid in Fig. 4.1, the errors are proportional to $(\Delta x)^2$. In Jelesnianski's (1965) grid, forward differences are used in time, which have errors of a lower order than the errors in a central difference scheme. For the grid system used here,

M = even, N = even, T = even, for η -points M = even, N = odd, T = odd, for u-points,

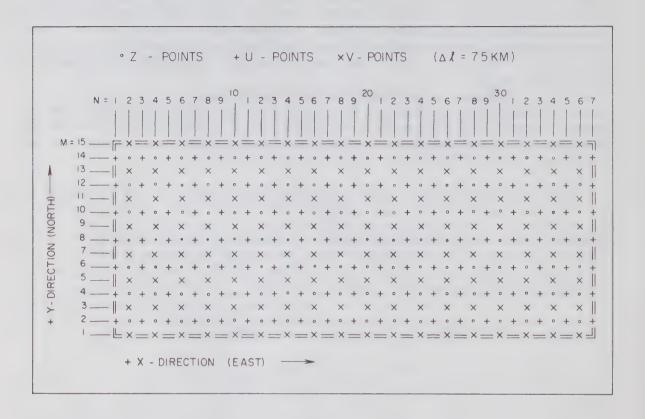


Figure 4.1 Grid system use to facilitate the calculations for the two-layer rectangular basin.

M = odd, N = even, T = odd, for v-points, so that the parity of the grid is even.

In the following equations let M,N, and T stand for even integers. Odd inters will be M ± 1 ,N ± 1 , and T ± 1 . The left hand side of (4.5) is approximated by

The first term on the right hand side of (4.5) is

where
$$h'(M,N\pm 1,T+1) = d(M,N\pm 1) + \eta'(M,N\pm 1,T+1)$$
 (4.22)

However, n' is not known at t=T+1, nor at $n=N^{\frac{1}{2}}$ 1, so the following approximation is used.

$$\eta'(M,N^{+}1,T+1) = \frac{1}{2} \left[\eta'(M,N,T) + \eta'(M,N^{+}2,T)\right]$$
 (4.23)

As long as $\eta << h'$, the error in (4.23) is not significant. The remaining term in (4.5) is similarly approximated.

Equation (4.6) is also approximated in the same manner as (4.5), with the added approximation that

$$h(M, N-1, T+1) = d(M, N-1) + \eta(M, N-1, T+1) - \eta'(M, N-1, T+1)$$
 (4.24)

The left hand side of (4.1) becomes

$$\begin{bmatrix} \frac{\partial u}{\partial t} \\ M, N+1, T \end{bmatrix} = \frac{u(M, N+1, T+1) - u(M, N+1, T-1)}{2\Delta t}$$
 (4.25)

The Coriolis term is approximated as

$$(fv)_{M,N+1,T} = \frac{f}{4} \begin{bmatrix} v(M+1,N,T-1) + v(M+1,N+2,T-1) \\ + v(M-1,N,T-1) + v(M-1,N+2,T-1) \end{bmatrix}$$
(4.26)

The gradient term is

Similar approximations are used for the remaining equations of motion.

In their final form, the six different equations are:

$$\eta'(M,N,T+2) = \eta'(M,N,T)$$

$$-\frac{\Delta t}{\Delta x} \begin{bmatrix} h'(M,N+1,T)u'(M,N+1,T) \\ -h'(M,N-1,T)u'(M,N-1,T) \\ +h'(M+1,N,T)v'(M+1,N,T) \\ -h'(M-1,N,T)v'(M-1,N,T) \end{bmatrix}$$
(4.28)

n(M,N,T+2) = n(M,N,T) + n'(M,N,T+2) - n'(M,N,T)

$$-\frac{\Delta t}{\Delta x} \begin{bmatrix} h(M,N+1,T)u(M,N+1,T) \\ -h(M,N-1,T)u(M,N-1,T) \\ +h(M+1,N,T)u(M+1,N,T) \\ -h(M-1,N,T)u(M-1,N,T) \end{bmatrix}$$
(4.29)

 $u(M,N+1,T+1) = u(M,N+1,T-1) = F_X(M,N+1,T) 2\Delta t$

$$+\Delta t f \left[v (M+1, N, T-1) + v (M+1, N+2, T-1) + v (M-1, N, T-1) + v (M-1), N+2, T-1) \right]$$

$$-g \Delta t \left[n (M, N+2, T) - n (M, N, T) \right]$$
(4.30)

$$v(M+1,N,T+1) = v(M+1,N,T-1) + F_y(M+1,N,T) 2\Delta t$$

$$- \frac{\Delta t f}{2} \left[u (M+2,N+1,T-1) + u (M+2,N-1,T-1) + u (M,N-1,T-1) \right]$$

$$-g\underline{\Delta t} \left[\eta \left(M+2,N,T \right) - \eta \left(M,N,T \right) \right]$$
 (4.31)

u'(M,N+1,T+1)=u'(M,N+1,T-1)

$$+ \frac{\Delta t f}{2} \left[\begin{array}{c} v'(M+1,N,T-1) + v'(M+1,N+2,T-1) \\ + v'(M-1,N,T-1) + v'(M-1,N+2,T-1) \end{array} \right]$$

$$-g\frac{\rho}{\rho}, \frac{\Delta t}{\Delta x} \left[\eta(M, N-2, T) - \eta(M, N, T) \right]$$

$$-g\left(1 - \frac{\rho}{\rho}\right) \frac{\Delta t}{\Delta x} \left[\eta'(M, N+2, T) - \eta'(M, N, T) \right]$$
(4.32)

v'(M+1,N,T+1) = v'(M+1,N,T-1)

$$-\frac{\Delta tf}{2} \left[\begin{array}{c} u'(M+2,N+1,T-1) + u'(M+2,N-1,T-1) \\ + u'(M,N+1,T-1) + u'(M,N-1,T-1) \end{array} \right]$$

$$-g\frac{\rho}{\rho}$$
, $\frac{\Delta t}{\Delta x}$ [n(M+2,N,T)-n(M,N,T)]

$$-g(1-\frac{\rho}{\rho}) \frac{\Delta t}{\Delta x} [n'(M+2,N,T)-n'(M,N,T)]$$
 (4.33)

4.3 Specifications of the Basin.

The rectangular model is characterized by the following:

L = 270 km.
$$(36 \Delta x)$$

W = 105 km. $(14 \Delta x)$
 $\Delta x = 7.5$ km.
h = 15. m.
h'= 60. m.
 $\rho'= 1.00000 \text{ gm/cm}_3^3$
 $\rho = 0.99826 \text{ gm/cm}$
 $(1-\frac{\rho}{\rho}) = 0.00174$
 $\phi = 45^{\circ}N. \text{ latitude}$
 $f = 0.0001029 \text{ radians/sec}$

The depths and density values are taken from Csanady (1967) and represent "typical" values in the Great Lakes. Csanady's (1967) and 1968) analytical solutions for a circular basin have already been discussed in Chapter 2; any similarities between his and my results which are due to the density or depth configuration may possibly be noted. The length to breadth ratio of the rectangular basin is 2.57, similar to that of Lake Ontario and Lake Superior. The actual size is similar to that of Lake Ontario.

The value of Δ x was arbitrarily set to 7.5 km. For the Poincaré modes, it is desirable to have an even smaller value, but this would increase the number of calculations greatly. On the other hand, a larger value of Δ x would further reduce the already limited spatial resolution.

The boundary conditions of no flow across solid bound-

Initially, all displacements are zero at time zero, and all velocity components are zero at time 1^{\triangle} t.

4.4 Energy in the Basin.

In studying the motions within the basin, it is informative to investigate the growth of energy in the basin. In particular, the partition of potential energy between the surface and the interface, and of kinetic energy between the two layers, is of some interest.

The total potential energy, P, can be expressed by the following surface integral over the whole of the basin.

$$P = \int_{A}^{\rho} g \eta^{2} dA + \int_{A}^{\rho} (\rho' - \rho) g \eta'^{2} dA \qquad (4.34)$$

The first integral refers to the surface and the second to the interface. In the approximations given earlier, the value of η (m,n) is a mean value, averaged over a square of side $2 \Delta x$, centred at the grid point (m,n). The integrals of (4.34) can thus be approximated by numerical quadrature, as

$$P = \frac{\rho}{2} \sum_{m=\text{even}} \sum_{n=\text{even}} \eta^{2}(m,n) (2\Delta x)^{2}$$

$$+ \left(\frac{\rho' - \rho}{2} \right) \qquad \sum \qquad \sum \qquad \eta'^{2}(m, n) \quad (2\Delta x)^{2} \tag{4.35}$$

m=even n=even

The kinetic energy, K, can be expressed as the volume

integral

$$K = \frac{\rho}{2} \int (u^2 + v^2) dV + \frac{\rho'}{2} \int (u'^2 + v'^2) dV \qquad (4.36)$$

However, the volume differentials, dV and dV', may be replaced by h dA and h' dA', respectively, so that (4.36) can be expressed by the following summations.

$$K = \frac{\rho}{2} \sum_{m=\text{even}} \sum_{n=\text{odd}} u^2(m,n) h (m,n) (2\Delta x)^2$$

+
$$\frac{\rho}{2}$$
 $\sum_{\text{m=odd}}$ $\sum_{\text{n=even}}$ v^2 (m,n) h (m,n) $(2\Delta x)^2$

+
$$\frac{\rho'}{2}$$
 $\sum_{m = \text{even } n = \text{odd}} \sum_{u'^2(m,n)h'(m,n)(2\Delta x)^2}$

$$+\frac{\rho}{2}'\sum_{m=\text{odd}}\sum_{n=\text{even}}v^{2}(m,n) h^{2}(m,n) (2\Delta x)^{2}$$
 (4.37)

The double summations above do not extend over the complete basin, however. For example, the first summation in (4.37) covers the complete width of the basin, from n = 2, to n = 36. At each end of the basin a strip of width Ax has been neglected. These two strips account for 1/17 th of the total area. Assuming that the velocities in the rest of the basin are of the same order of magnitude, then by linear interpolation, the mean velocities in these two end strips is only $\frac{1}{4}$ the magnitude of the other velocities. The error in the kinetic energy due to these two end strips is then $1/17 \times 1/16$, which is less than 1%. For the summations involving the v component, the area of the side strips is 1/7 of the total basin area, so that the error there is only $1/7 \times 1/16$, which is about 1%. Thus, the neglect of the side and end strips in the summations in (4.37) does not appear to be serious; certainly this will not be significant in a study of the large scale variations in time.

4.5 Numerical Stability of the Calculations.

In numerical calculations of the type performed here, stability criteria must be adhered to, else the results may be distorted by numerical instability, or even "blow up". For a detailed discussion of the topic, the reader is referred to Courant, Friedrichs, and Lewy (1928), Courant and Hilbert (1937), Kasahara (1965), and Fischer (1965). For a one-layer problem, the difference equations may be written in matrix form as

$$\begin{pmatrix} n^{t+2} \\ u^{t+1} \\ v^{t+1} \end{pmatrix} = (A) \quad x \quad \begin{pmatrix} n^{t} \\ u^{t-1} \\ v^{t-1} \end{pmatrix}$$

$$(4.38)$$

where A is a 3 x 3 matrix in this case. It may not always be possible to write out the system of equations explicitly in this form. When it can be so written, the condition of numerical stability is that the absolute value of the eigen values of the matrix A be less than unity (see Richtmeyer, 1957). For the system of difference equations in this study, the stability criterion for the non-viscous gravitational modes is (see Miyazaki, 1965)

$$\frac{\Delta x}{\Delta t} \ge \left((2gh_{max})^{\frac{1}{2}} \right)^{\frac{1}{2}}$$

During the calculations, spurious waves may develope between grid points spaced $2 \triangle x$ apart. (4.39) guarantees that the period of the gravitational oscillations under study in the model basin must be larger than the period of the spurious waves. (4.39) also refers to a one-layer basin, but since the internal periodicities are much longer than the surface periodicities, (4.39) also suffices for a two-layer basin.

The value of Δ x has already been set to 7.5 km, and since the maximum depth is 75m, the stability criterion becomes

$$\Delta$$
 t $<$ 196 seconds (4.40)

In the calculations that follow, \triangle t has been chosen to be

(4.41)

Δ t = 150 seconds

For a discussion of the stability of visco-gravitation al modes of oscillation, please refer to Platzman (1963, p.37). Harris (1964, p. 419) suggests certain smoothing operators to deal with the problem of spurious waves. He also states that a principal symptom of numerical instability is an unexplained growth or decay of the energy in the system. This is another reason for calculating the energy, as outlined in Section 4.4.

In the discussions that follow, the physical variables will be conveniently (to the author) referred to by their "names" in the computer programs that were written to carry out

the calculations. These are:

ZT = η , surface displacement, ZB = η' , interface displacement,

UT = u, x-component of velocity in top layer, VT = v, y-component of velocity in top layer,

UB = u', x-component of velocity in bottom layer. and VB = v', y-component of velocity in bottom layer.

4.6 Numerical Results.

(a) CASE A.

The length scale of passing cyclonic disturbances is often much larger than the size of any one of the Great Lakes. It is therefore not unreasonable to limit this study to wind stresses which are uniform over the whole of the basin, with only variations in the time dimension. Whereas the time scale of such disturbances may vary from a fraction of a day to many days, this initial calculation shall deal only with a wind impulse in the +x-direction of duration $100 \, \Delta \, t(4.17 \, hours)$. It is hoped that the free modes may be more clearly examined here than in cases where the time dependence of the wind is much more complex, and of longer duration.

The value of F_x was set to 10^{-3} cm/sec², corres-

ponding to a wind speed of 8.7 m/sec. The surface displacement, ZT, has been plotted against time for some sample grid points (Fig. 4.2), from which certain dominant periodicities are apparent. Although the time resolution is only 2\Delta tor 0.0833 hours, averaging over many periods will permit evaluation of the periodicities to within 0.01 hours. The longitudinal uninodal surface seiche is excited with a period of 5.56 hours, which is 0.03 hours longer than the Merian period. It appears that a longitudinally directed wind will excite the longitudinal surface modes. For points near the centre of the basin, the amplitude of the longitudinal seiche is small, and higher frequency oscillations are found. It is difficult to determine the period of these oscillations, but they may be transverse oscillations, the lowest period of which is 2.16 hours, calculated from the Merian formula.

In Fig. 4.3, I have attempted to demonstrate the rotational behavior of the surface, in a series of "time exposures". The contours have been plotted at half hour intervals, with a contour spacing of 0.5 cm. To simplify the discussions here, the x-direction will be arbitrarily taken to be the eastward direction. Initially, the basin is at complete rest, and as the eastward wind is applied, water piles up at the eastern end of the basin; the opposite occurs at the western end of the basin. Due to the Earth's rotation, the upward slope of the water surface is deflected to the south. Thus at time 48 (units of Δt are implied here), the surface slopes upwards to the southeast. At the ends of the basin, the initial surge due to the sudden imposition of the wind reaches a maximum of over 5 cm at time 72. After this time, the rotation of the surface is quite noticeable. From Fig. 4.3, it is seen that the orientation of the upward slope of the surface

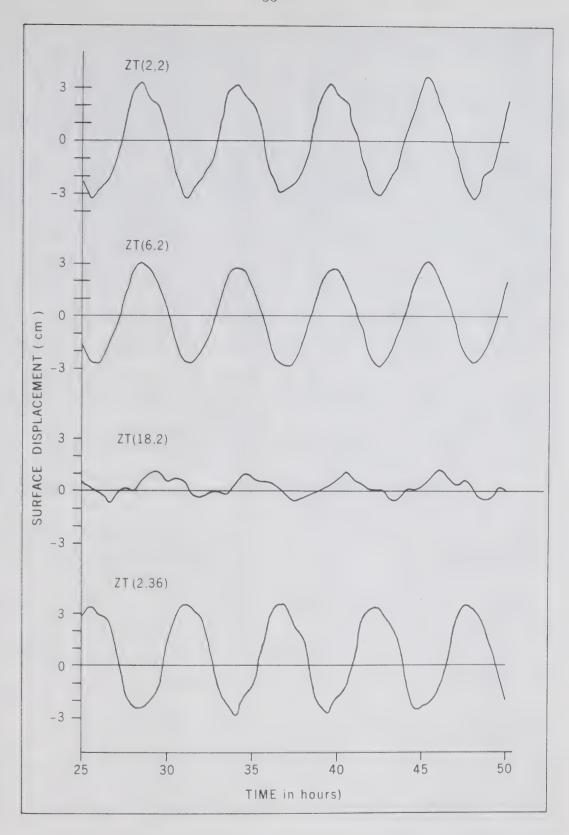


Figure 4.2 Case A. Surface displacements versus time.

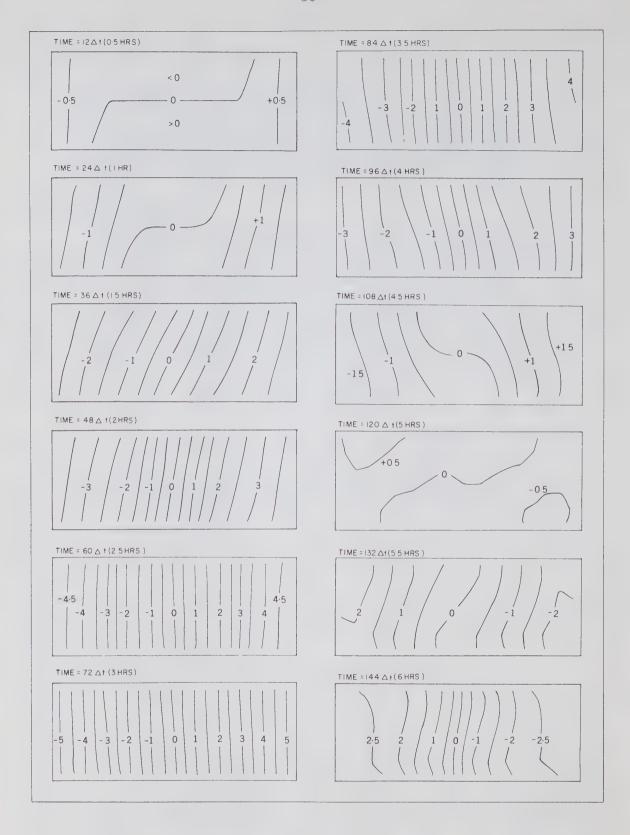


Figure 4.3 Case A. Configuration of surface displacement versus time, during initial stages.

"flips" from eastward to westward very quickly. For a circular basin the rotation is uniform, but the basin here is narrow so that the effects of rotation are small.

The wind ceases to blow at time 100, and at a much later time, the system is in a state of free oscillation. The surface contours are also plotted for a much later time (Fig. 4.4); the same behavior is found.

For the uninodal seiche, the surface is antisymmetrical; that is, at points diametrically opposite to each other with respect to the geometric centre of the basin, the surface displacement is equal and opposite. It is certainly obvious that rotation has little effect on the frequency, as predicted by Rao (1966), for the longitudinal surface seiche.

In Fig. 4.4, a quasi-static buildup of water is noticeable along the sides of the basin, roughly 0.5 cm along the south shore and -0.5 cm along the north shore. It will be seen later that at the interface, there is a quasi-static response of about -300 cm along the south shore and about 300 cm along the north shore. The ratio ZT/ZB is about -0.0017, which is in approximate agreement with the value of - $(1-\rho')$

(h'/[h+h']), which is -0.0014. Thus, the quasi-static response (abbreviated Q.S.R.) at the surface is a "reflection" of the Q.S.R. at the interface, and is of a baroclinic nature. Later, it will be shown that it is part of an internal Kelvin wave. Its period is in the order of 500 hours, and thus appears to be static over short periods of observation. It is also quasi-geostrophic, and can be regarded as a current-like rather than a wave-like motion (see Csanady, 1967).

The oscillations in ZB away from the shoreline are dominated by the near-inertial oscillations (Fig. 4.5), which have amplitudes of less than 100 cm. Near the shore, the Q.S.R. is dominant, and the near-inertial oscillations, which appear to be transverse oscillations, are not as noticeable.

To accurately map out the Kelvin waves, one would have to filter out the near-inertial oscillations, a tedious process which is not justified here. However, the Q.S.R. is dominant near the shore. Thus, a mapping of the interface displacement along the shoreline would show the large scale behavior of the Kelvin wave in a general qualitative way; the near-inertial oscillations would only perturb this picture slightly.

The time scale of the integrations were thus extended well past 75 hours, and indeed a reasonable picture of the Kelvin wave was obtained (Fig. 4.6). The path of these mappings follows a route along the near-boundary Z-points in an anticlockwise manner, starting at ZB (2,2). The wave is initially set up by the wind with a negative loop along the south shore and a positive loop along the north shore. The wave then slowly progresses around the shoreline of the basin in an anti-clockwise direction. At large times, spurious waves seem to develop, with wavelength 4Δ x. One probable source of instability causing these spurious waves is the corners of the basin. Error buildup is also large at large

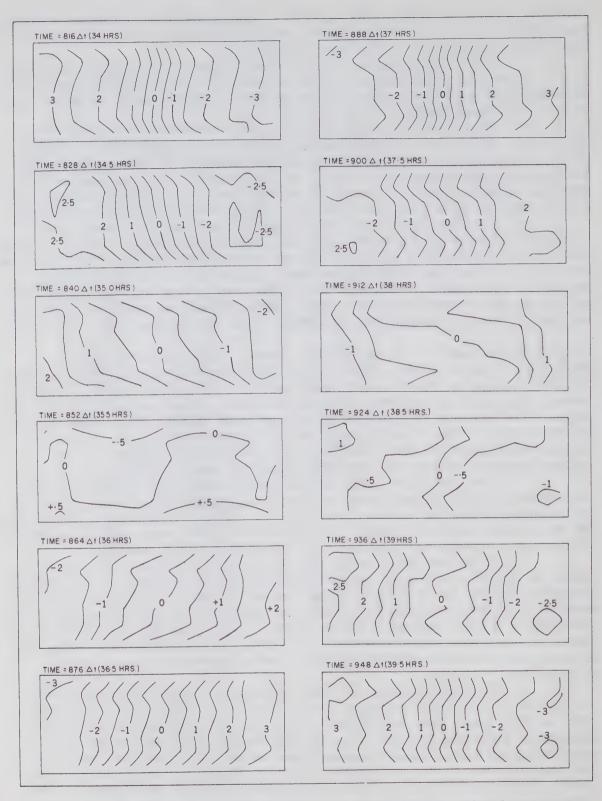


Figure 4.4 Case A. Configuration of surface displacement versus time, during later stages of free oscillations.

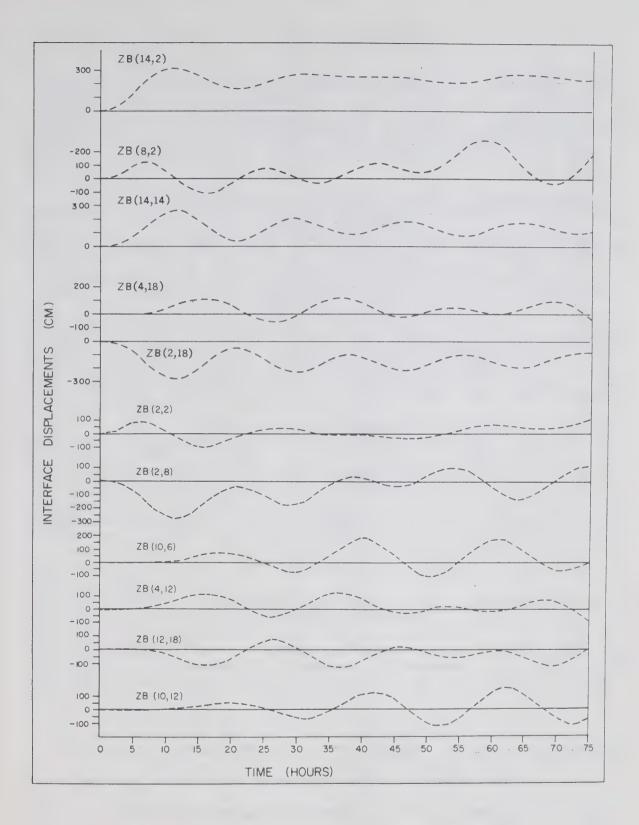


Figure 4.5 Case A. Interface displacement versus time.

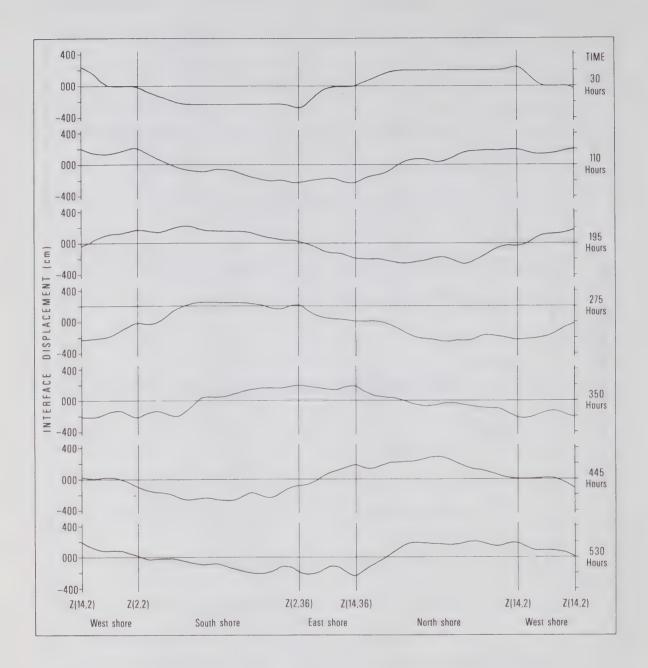


Figure 4.6 Case A. Display of the Kelvin wave progression; the interface displacements have been plotted along a path joining all the near boundary %B points, in the anticlockwise direction.

times. Nevertheless, the general behavior of the Kelvin wave is quite clear.

The period of the Kelvin wave is 470 ± 20 hours; the uncertainty is due to the presence of the near-inertial oscillations. For an extremely narrow basin, the period is proportional to the double length of the basin. In this case, the width is finite, and the period is proportional to the perimeter of the basin. The theoretical period is thus 461 hours, so that the observed period is in good agreement with theory.

It must be noted that this long calculation is not realistic since friction is not included. Indeed, Kelvin waves are rarely observed over any substantial portions of a complete cycle. The above is intended as an exercise to verify the predictions of the non-viscous theory, and to show the physical makeup of the apparently quasi-static motions.

In Fig. 4.7, the interface displacement has been plotted in time. Away from the ends of the basin, there is little variation of ZB in the longitudinal direction. ZB away from the boundary oscillates near the inertial period and shows a Sin nNy/W variation in the transverse direction. These observations indicate the existence of possibly a 3-noded Poincaré wave, or more specifically, a Sverdrup wave. The interface configuration is also antisymmetrical.

The u component in the top layer has been plotted in Fig. 4.8. Initially, the acceleration is in the + x-direction. At time 100 when the wind ceases to blow, the adverse surface gradients that have been built up immediately cause a deceleration. The dominant period is very near the inertial period, while at times the barotropic period is noticeable. At various grid points, there are cases of both growth and decay in the amplitude. For points along the sides of the basin, a net current is found, in the direction of the wind stress. This is the "coastal jet" discussed by Csanady (1968) and is part of the Q.S.R.

The UB component in the bottom layer oscillates in a similar manner to UT (Fig. 4.9). Generally, UT/UB is very close to -4.0, indicating that the currents are predominantly of a baroclinic nature. The wind stress occurs directly in the equation of motion for UT, but not in the equation for UB. Thus when the wind stops, there is a very sharp deceleration in UT but not in UB. For the barotropic mode UT/UB is 1.0, but for the baroclinic mode it is -4.0. This explains why the barotropic oscillations are more noticeable in UB than in UT.

The VT component in the top layer has been plotted in Fig. 4.10. As expected from Coriolis considerations, the initial acceleration is negative. VT is linked to the wind stress through UT, so that the deceleration in VT is also not sharp when the wind stops blowing. In the co-ordinate system used here, UT is initially positive, but VT is negative; this introduces a phase difference of 180 ° and VT is 90 ° in advance of UT. Also, since VT is caused by rotation, it consists mainly of near-inertial oscillations, with little evidence of a barotropic component.

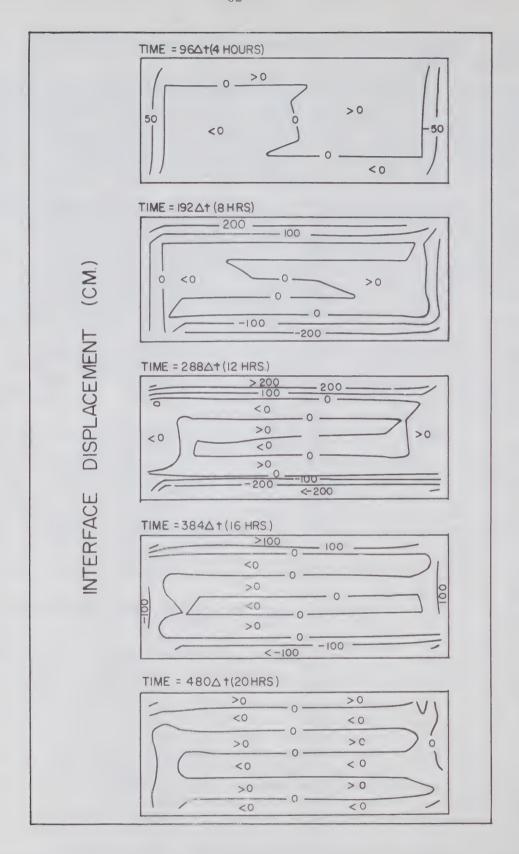


Figure 4.7 Case A. Configuration of the interface versus time, during initial stages.

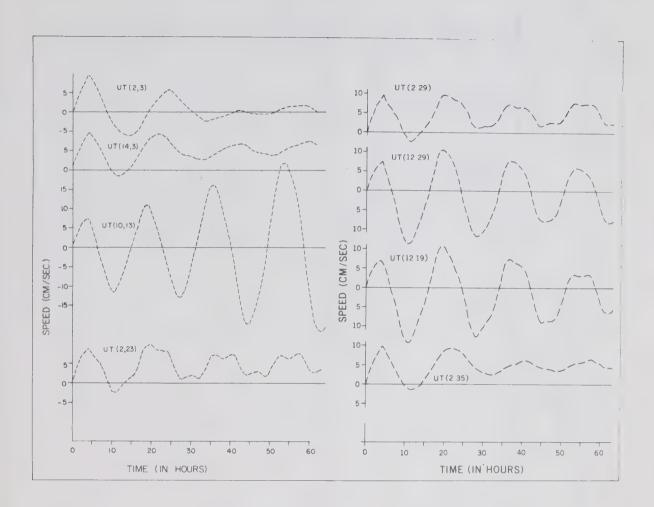


Figure 4.8 Case A. U component of velocity in the top layer versus time.

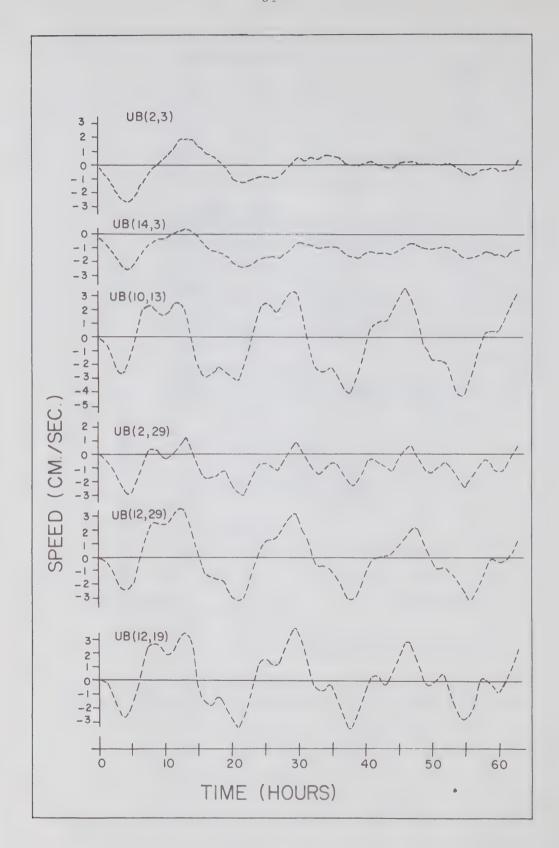


Figure 4.9 Case A. U component of velocity in bottom layer versus time.

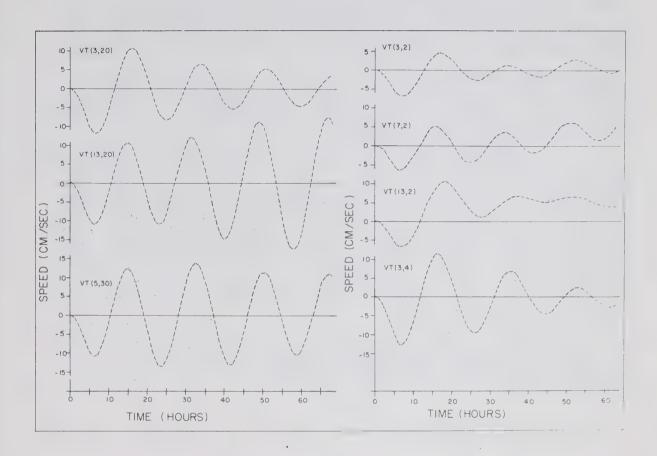


Figure 4.10 Case A. V component of velocity in top layer versus time.

The VB component also oscillates near the inertial frequency (Fig. 4.11). The ratio of VB/VT is also about -0.25. The duration for which the values have been plotted is small compared with the Kelvin period, so that there is only a small indication of a Q.S.R. in VB. After time 50 or 60 hours there is a Q.S.R., indicating that the coastal jet is turning the corners and progressing along the ends of the basin.

A few sample current ellipses have been plotted in Fig. 4.12. These are elliptical in the ratio UT/UB equal to $T/T_{\dot{1}}$, and since T is very near $T_{\dot{1}}$, these ellipses are nearly circular (excluding near shore points). Since the Earth's rotation causes a deflection to the right, these ellipses rotate in the clockwise direction. The ellipses in the bottom layer (Fig. 4.13) are similar, except that they are distorted by the barotropic oscillations.

A more complete picture is obtained by examining the current vectors over the whole of the basin. The currents are shown in Fig. 4.14 at 4 hour intervals. The arrows give the magnitude and direction of the current for the point at the base of the arrow. The clockwise rotation is also seen. In this case, the coastal jet is small compared with the currents in the interior of the basin. Unlike the displacements, the currents in this case are symmetrical over the basin. The currents in the bottom layer are displayed in Fig. 4.15, and are similar to the currents in the top layer, except for the roughly -0.25 reduction.

Most of the energy in the basin (see Fig. 4.16) is in kinetic form, and most of this is in the top layer because of the higher velocities there. Before investigating the periodicities in the energy components, consider a motion of the form

$$\zeta = A + B \sin \sigma t \tag{4.42}$$

The energy is proportional to

$$\zeta^2 = A^2 + B^2/2 + 2AB \text{ sinot } -\frac{B^2}{2} \cos 2\sigma t$$
 (4.43)

The predominant frequency in the energy will be either σ or 2σ depending on whether or not A is larger than B. One can consider A as an analogy to the Q.S.R. and B as an analogy to the oscillatory part of the basin response. At the surface, the surface seiche is dominant, so that the potential energy of the surface oscillates at twice the barotropic frequency. At the interface, the Q.S.R. is dominant so that the potential energy there oscillates at one times the inertial frequency. For the kinetic energies the oscillations are near one times the inertial frequency, with the barotropic oscillations superimposed upon these. Three times the barotropic period is 16.59 hours, which is only 0.39 hours away from the inertial period. There is thus a reinforcement of these two periodicities in combination almost every inertial period, with a

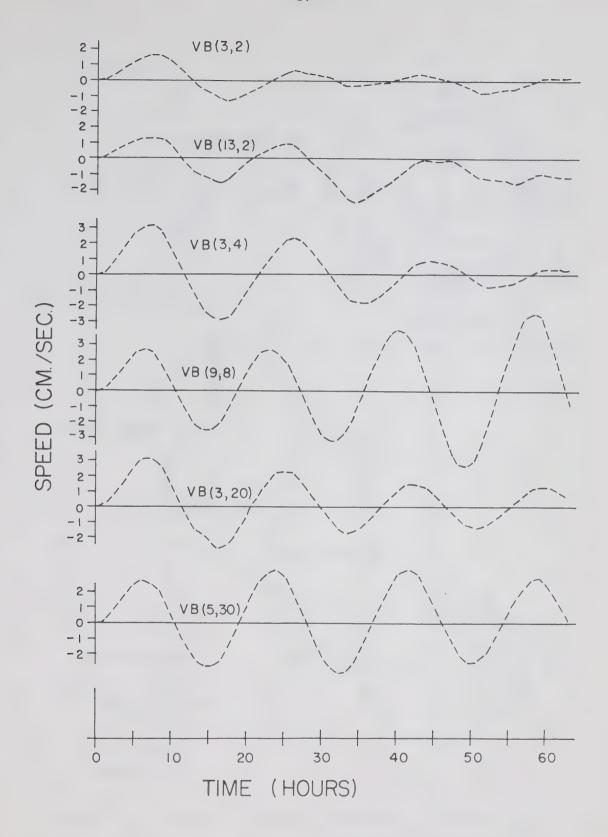


Figure 4.11 Case A. V component of velocity in bottom layer versus time.

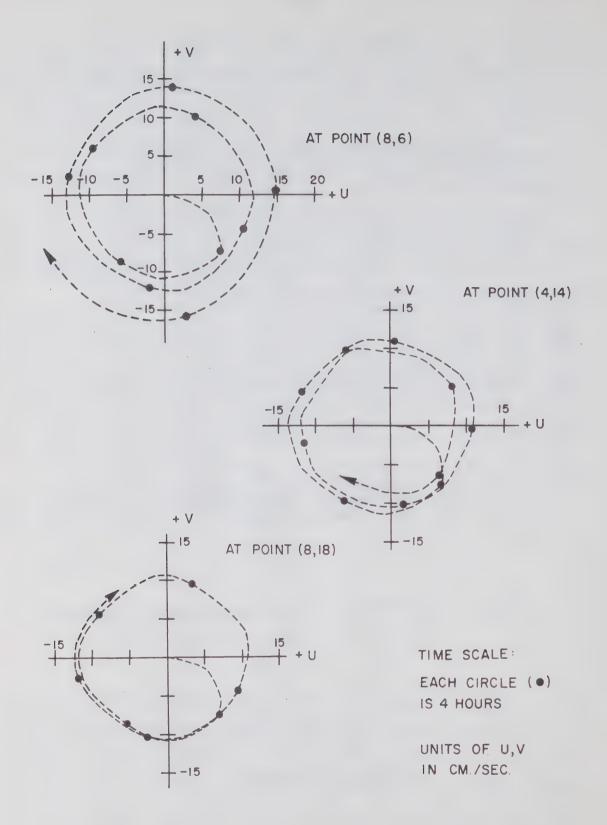


Figure 4.12 Case A. Current ellipses in top layer versus time.

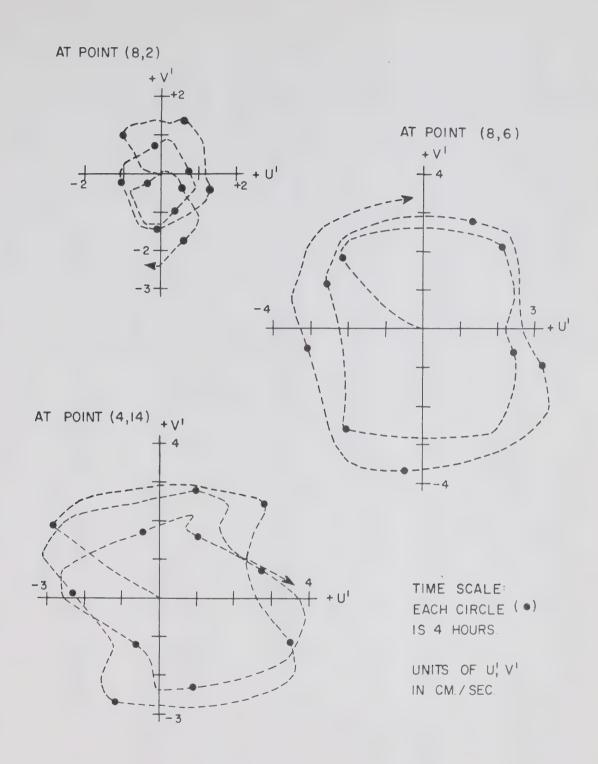


Figure 4.13 Case A. Current ellipses in bottom layer versus time.

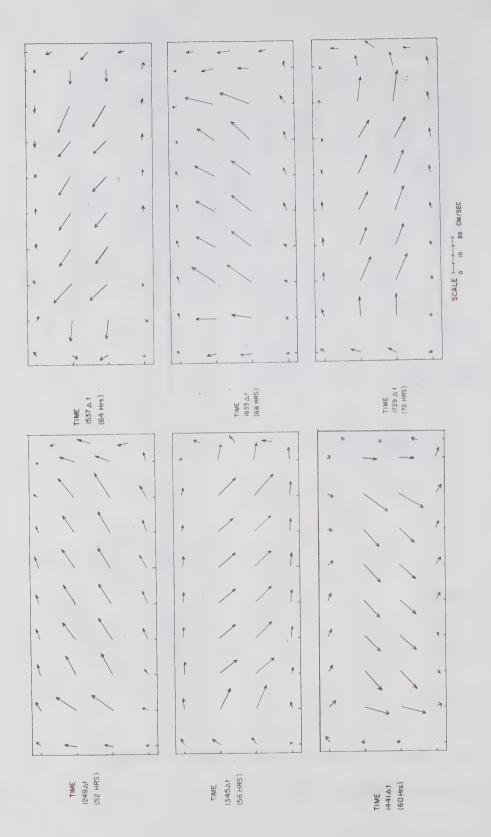


Figure 4.14 Case A. Velocity field in top layer

versus time.

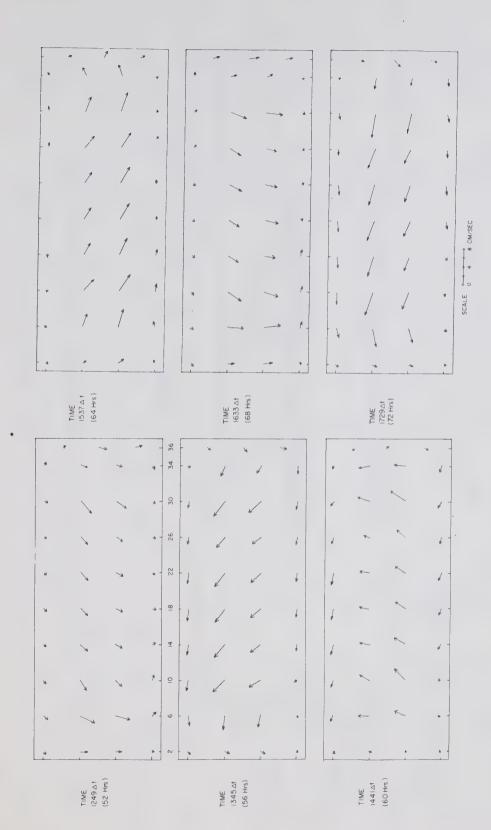
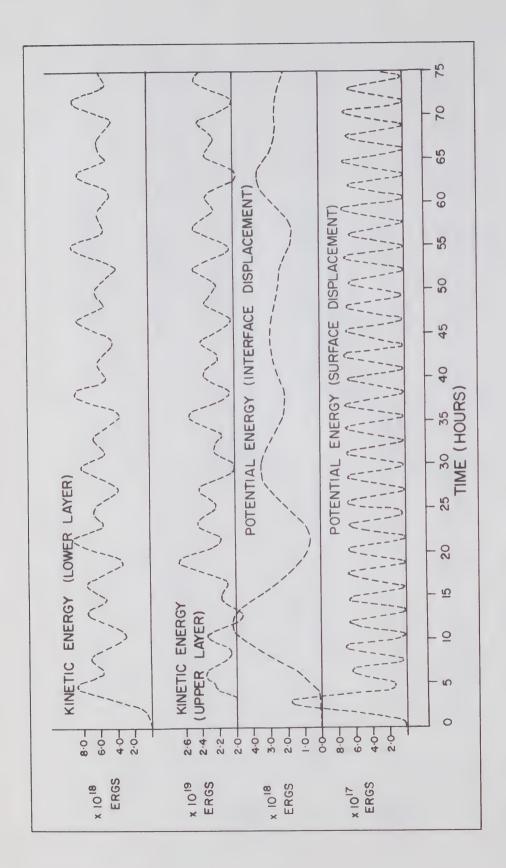


Figure 4.15 Case A. Velocity field in bottom layer versus time.



Components of the energy in the Case A. Figure 4.16

basin versus time.

slowly changing phase relationship. The total energy in the basin remains at a constant value of 3.1 x 10^{19} ergs after the wind stops blowing, which also shows that the calculations are fairly stable. Thus, the energy components give a fairly good indication of the dominant frequencies in the basin response. Attention should be restricted only to the large scale fluctuations, to avoid misinterpretation of the errors inherent in the summations (4.35) and (4.37).

(b) CASE B.

In this case, the wind is also in the eastward direction, but is now applied for the total duration of the calculation. In order to keep the interface displacements small and avoid intersection with the surface, the value of the wind stress is set to 8 x 10^{-5} cm/sec²; this corresponds to a wind speed of 2.7 m/sec.

Even though the wind is constant after its sudden imposition, some energy does enter into the surface mode. From the plots of ZT (Fig. 4.17), it is seen that the dominant period is again that of the lowest longitudinal surface mode, that is 5.56 hours. This is 0.03 hours longer than the Merian period. Rao (1966) has predicted such a lengthening of the surface period. For the model, the rotation is 0.326 times the non-rotating frequency, and the length to width ratio of the basin is 2.57. Interpolation from Table 2.2 (from Rao, 1966) predicts an elongation of 0.03 hours. The uncertainty in the period from the model is less than 0.01 hours, so that the 0.03 elongation of the longitudinal surface seiche found here is significant and at least roughly agrees with theory.

The surface again rotates in the anti-clockwise direction (see Fig. 4.18). A Q.S.R. contribution also exists at the surface but is obscured by the rotating seiche. The mean water levels have been plotted in Fig. 4.19, where the barotropic oscillations have been filtered out. As expected, the line of steepest descent in the mean surface lies upward slightly to the right of the wind direction. At time 1700, the maximum mean displacements at the surface are about 0.6 cm at the corners. The corresponding quasi-static interface displacement is about 300 cm, so that the Q.S.R. at the surface is of a baroclinic nature, corresponding to the Kelvin wave at the interface.

The interface displacements (Fig. 4.20) are again dominated by the Q.S.R. and the near-inertial oscillations. At the points near the shoreline, the growth of the Q.S.R. is very apparent. At early times, the positive loop of the Kelvin wave lies along the north shore. Thus at early times, ZB (2,2) is dominated by the near-inertial oscillations. By time 60 hours, the arrival of the Kelvin wave at that point is seen. At ZB (8,2), the wave has progressed to that point by time 35 hours. The Kelvin wave is plotted in Fig. 4.21, the instability at the corners is again found. It is possible that the neglect of the non-linear accelerative terms is not valid at these corner points.

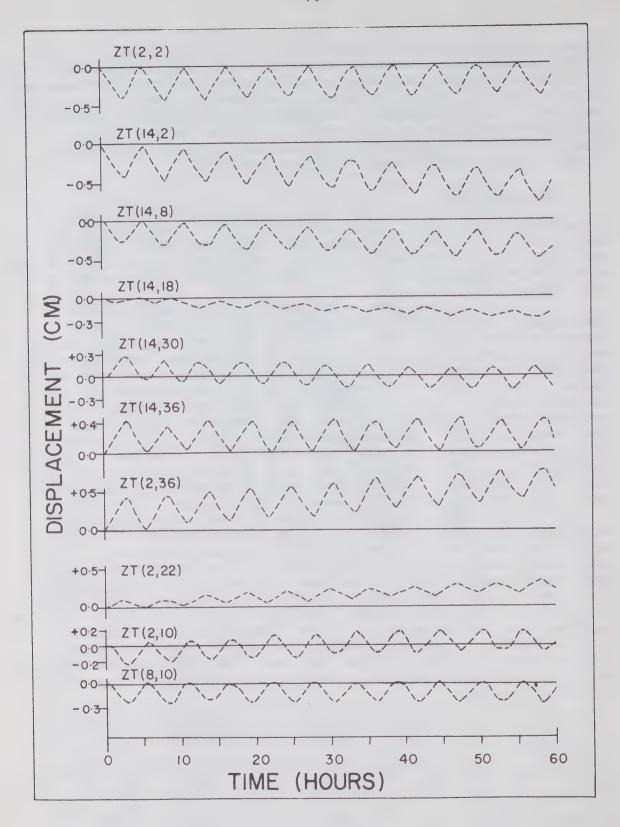


Figure 4.17 Case B. Surface displacement versus time.

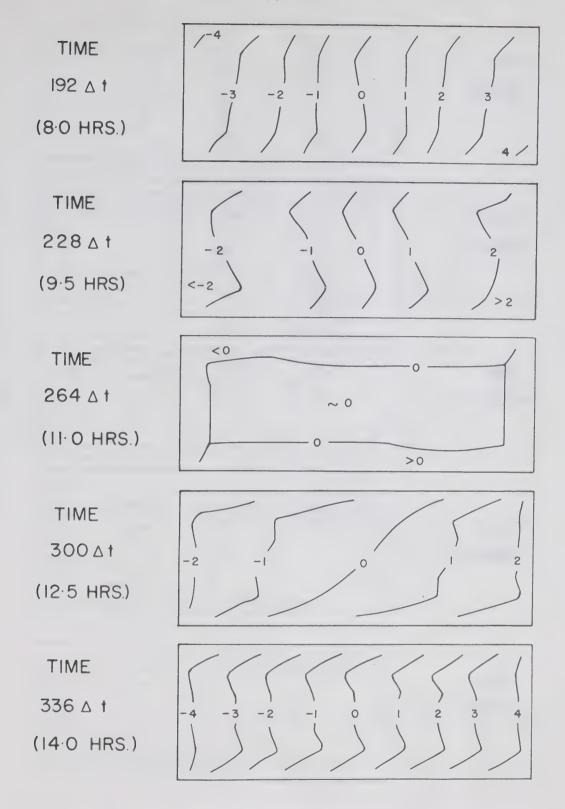


Figure 4.18 Case B. Configuration of the surface

versus time, showing rotating seiche

superimposed upon the quasi-static response.

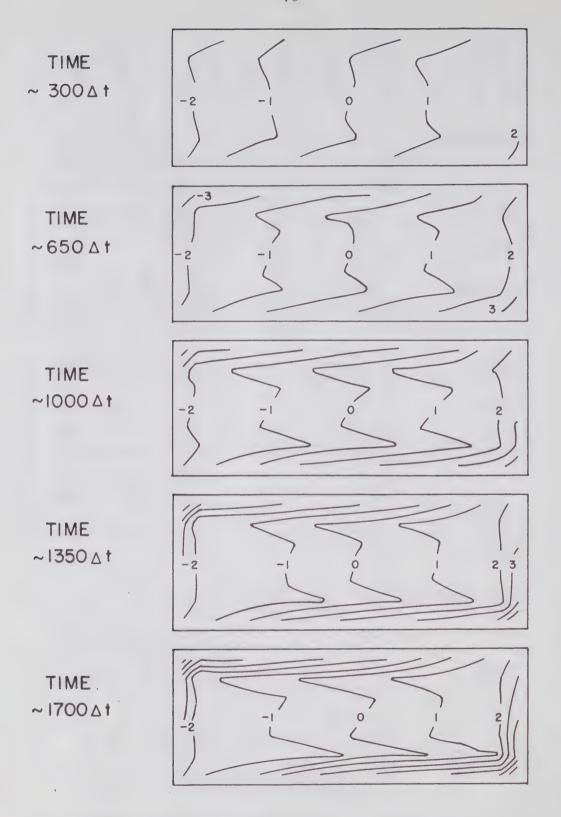


Figure 4.19 Case B. Configuration of the mean surface displacement versus time, showing the steady growth of the quasi-static response.

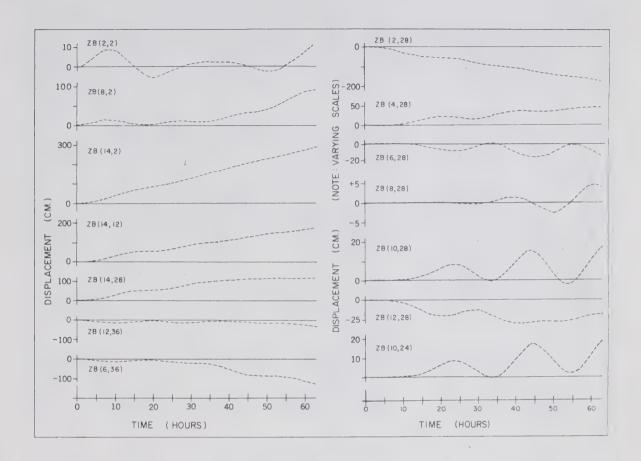


Figure 4.20 Case B. Interface displacement versus time.



Figure 4.21 Case B. Growth of Kelvin Wave during initial stages of development; the interface displacements have been plotted along a path joining all the near boundary % points, in the anticlockwise direction.

The transverse variation of the Poincaré motions is displayed in Fig. 4.22. On the left hand side of this figure, the exact cross-channel profile is shown, while on the right, the profile represents the near-inertial oscillations, obtained by filtering out the quasi-static response or Kelvin wave. There are only 7 ZB points in the transverse direction, which is really insufficient to give good resolution. On the other hand, decreasing the grid spacing by a factor of perhaps 3, for example, would increase the number of spatial calculations by a factor of 9. The number of time integrations would also be tripled. Thus, the increase in the total number of calculations is by a factor of 27. This astronomical increase in the number of calculations does not make it a practical move at this time.

The Q.S.R. and the near-inertial oscillations in UT are again seen in Fig. 4.23. Comparison with Fig. 4.20 shows that the quasi-static response in UT and ZB occur simultaneously at the same positions, indicating that they are both part of the same phenomenon. At 60 hours, the Q.S.R. at ZB (14, 2) is about 300 cm. For the baroclinic mode, theory predicts that UT should be 4.5 cm/sec. UT (14,3) is found to be about 5 cm/sec, which is in good agreement with theory. A further interesting point is brought out by examining UT over a transverse cross-section, say n = 19. Not only is there a coastal jet near the shore, but a return or counter coastal jet is found a little further away from the shore. A similar counter displacement is also found in ZB.

The VT component is plotted in Fig. 4.24. The slow progression of the Q.S.R. is seen along the ends of the basin. Here, too, there is evidence of a counter coastal jet. The coastal and counter coastal jet are more easily seen in Fig. 4.25, where the currents over the whole of the basin are displayed.

The UB component has been plotted in Fig. 4.26. The behavior of the Poincaré and Kelvin modes are similar to those in the top layer, except for the -0.25 reduction. The VB component has also been plotted (Fig. 4.27). In Fig. 4.28, the current vectors in the bottom layer have been plotted, and once again, the coastal and counter coastal jets are quite conspicuous.

With the exception of ZT, all the variables have been plotted for the point (6,12) (Fig. 4.29). The motions at this grid point are predominantly of the Poincaré type. Corresponding velocity components in each layer are 180° out of phase. VB and ZB are about 180° out of phase also, while VB is about 90° in advance of UB. The total behavior here is very complex, since it is comprised of free motions, forced motions, and computational errors or noise.

The energy (Fig. 4.30) grows steadily in time, because the wind is blowing for all time. For the kinetic energy of the bottom layer, there is only a small inertial oscillation because the motions there are dominated by the coastal jet feature. A small barotropic contribution is also seen. By far the largest components of the energy are the

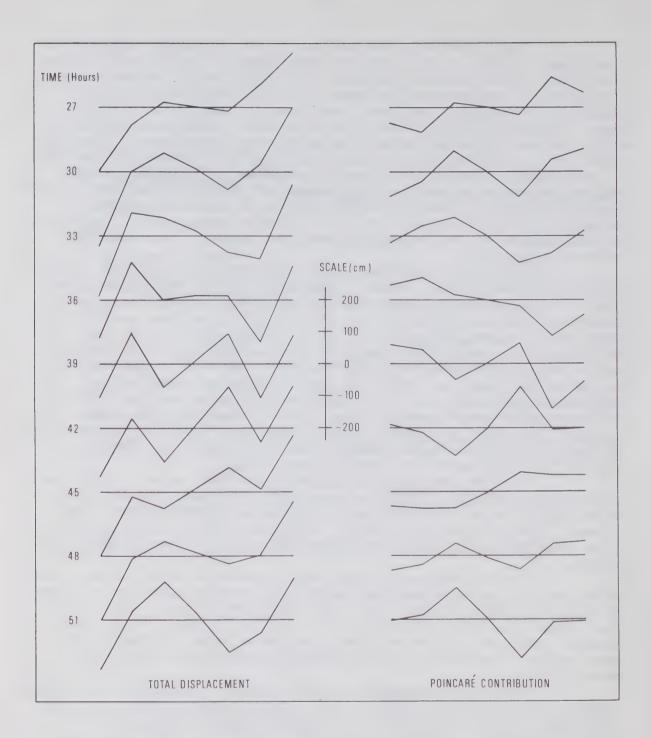


Figure 4.22 Case B. Cross channel profiles (n=22) of
the interface versus time; the profiles on
the left are the exact calculated values, while
on the right the quasi-static response has been
subtracted.

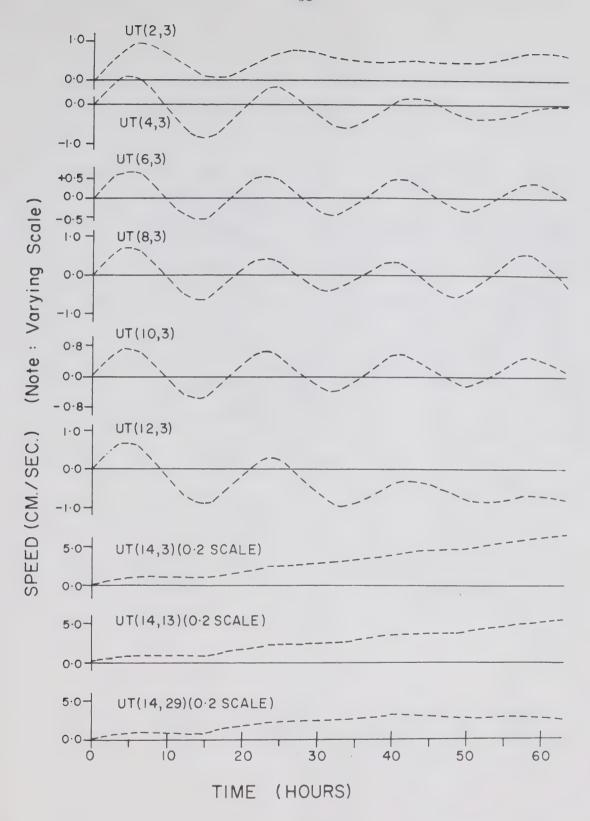


Figure 4.23 Case B. U component of velocity in top layer versus time.

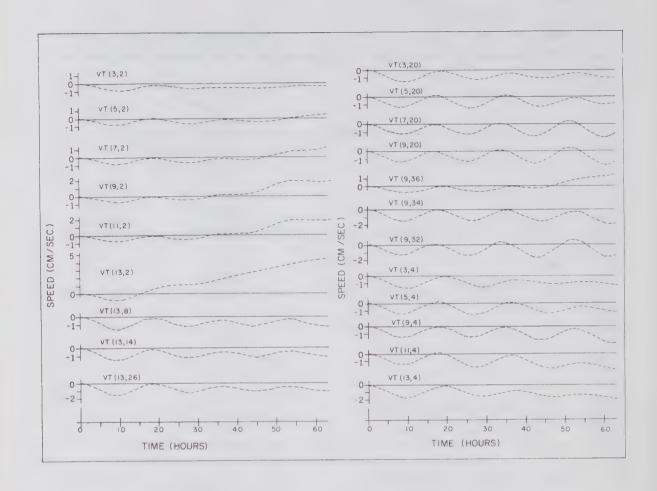
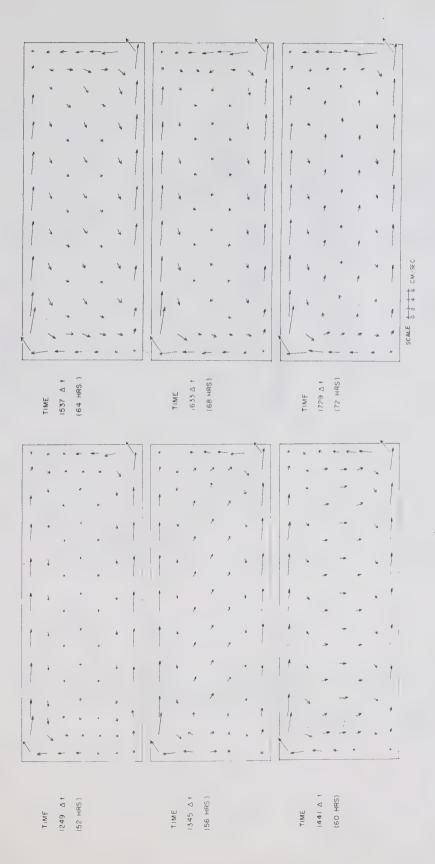


Figure 4.24 Case B. V component of velocity in top layer versus time.



B. Velocity field on top layer versus Figure 4.25 Case

time.

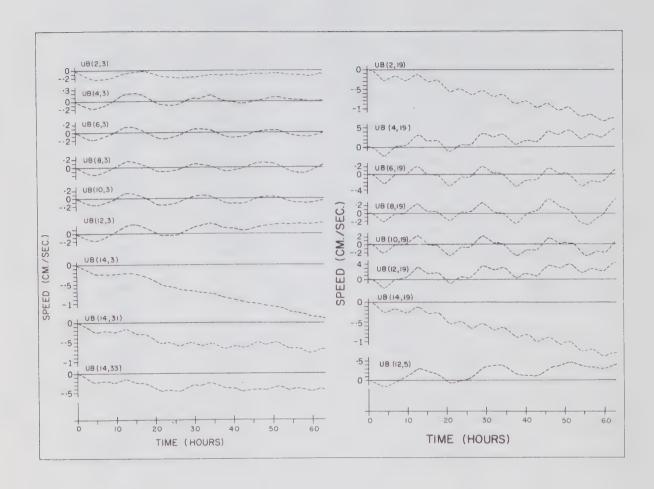


Figure 4.26 Case B. U component of velocity in bottom layer versus time.

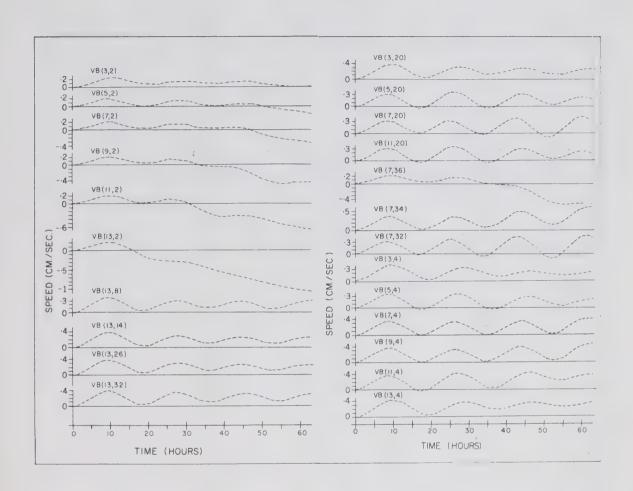


Figure 4.27 Case B. V component of velocity in bottom layer versus time.

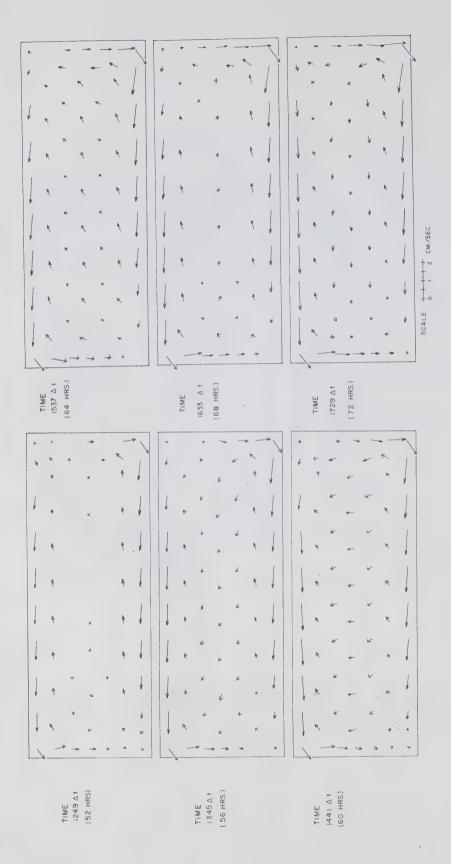


Figure 4.28 Case B. Velocity field in bottom layer

versus time.

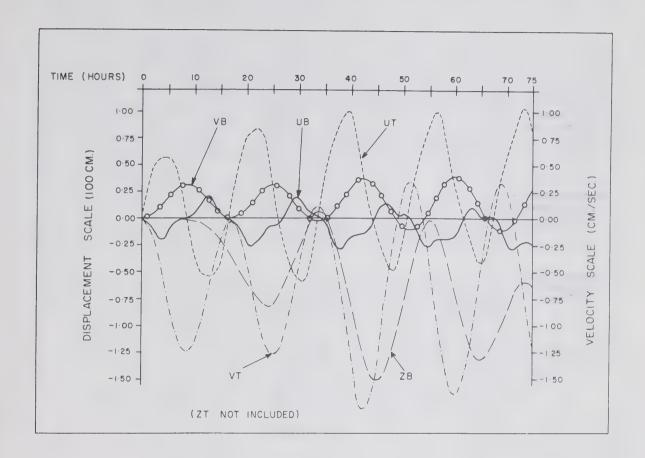


Figure 4.29 Case B. All variables versus time for the grid point (6,12), with the exception of the surface displacement.

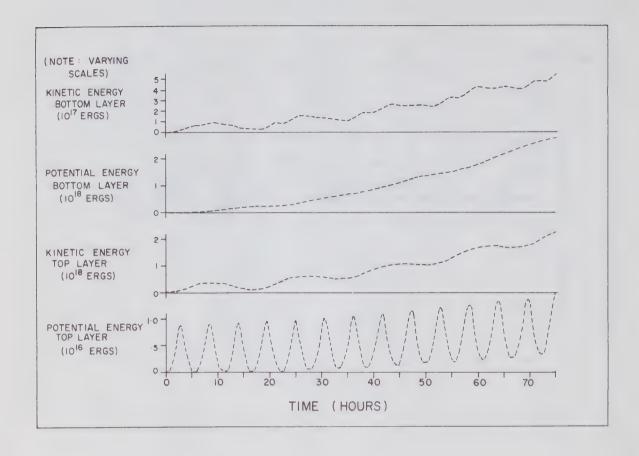


Figure 4.30 Case B. Components of the energy in the basin versus time.

potential energy of the interface and the kinetic energy of the top layer. The inertial contributions in both these components is small. Even at the surface, the Q.S.R. is much more important than the rotating seiche, so that the potential energy of the surface oscillates at one times rather than two times the barotropic frequency.

The magnitude of the wind stress remains at 8 x 10 ⁻⁵ cm/sec², but is now directed in the northward direction. In this case, the transverse uninodal surface seiche was excited, with a period of 2.16 hours. Since the wind is constantly blowing, there is a piling up of water produced in the vicinity of the northeast corner, with the opposite effect at the southwest corner. The mean surface is plotted in Fig. 4.31, obtained by filtering out the 2.16 hour oscillations. At time 1700, ZT at the northeast corner is about 0.45 cm, and ZB is about 280 cm. The ratio of ZT/ZB is -0.0016; at the southwest corner, this ratio has a value of -0.0017. These values compare favourably with the theoretical value of -0.0014 for the baroclinic mode.

The Kelvin wave is again displayed by a mapping along the shoreline (Fig. 4.32). The corners of the basin again appear to be sources of instability. The progression of the Kelvin wave around the basin is not too regular in this case. It "appears" to take until time 420 hours to travel half way around the basin, and yet it returns to its original position by time 500 hours. This apparently irregular progression is caused by the constant blowing of the wind. Initially, the wind produces a positive interface displacement along the western shore, and a negative one along the eastern shore, such as is found at time 35 hours. At a later time, the positive loop attempts to travel along the southern shore to the eastern shore but this is slowed down by the wind, which tends to cause fluid particles to leave the eastern shore and go towards the western shore. The progression of the negative loop to the western shore is also slowed down because the wind causes a piling up of water along the western shore. During the first half of the way around the basin, the Kelvin wave is thus "bucking the wind". During the second half of the way around the basin, it is "with the wind". One would expect that the period of the wave would be increased slightly, and indeed its period appears to be about 490 to 500 hours, as compared with the free period of 461 hours.

In attempting to show that the above explanation may be correct, I have plotted the Kelvin wave along the shoreline (Fig. 4.33), along with the along-shore component of the velocity. Clockwise currents are taken to be positive. The association of the Q.S.R. component in ZB and the coastal jet is certainly clear. In the vicinity of the crests or anti-nodes of the Kelvin wave, the currents and displacements are of the same sign, but along the south and north shores (in the vicinity of the nodes of the Kelvin wave), they are negatively correlated.

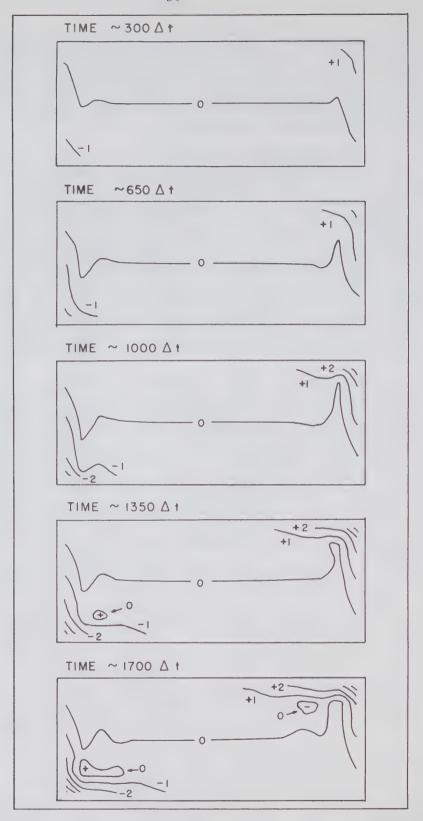


Figure 4.31 Case C. The mean surface versus time; that is, the barotropic oscillations have been removed.

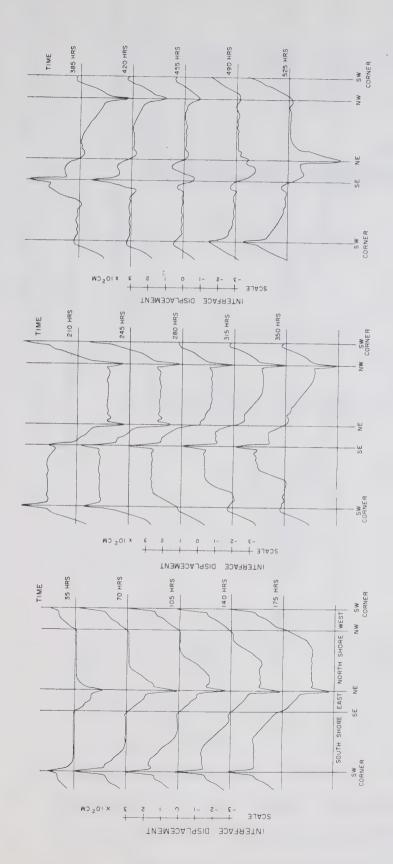


Figure 4.32 Case C. Display of the Kelvin wave progression; the interface displacements have been plotted along a path, joining all the near boundary #B points in the anticlockwise direction.

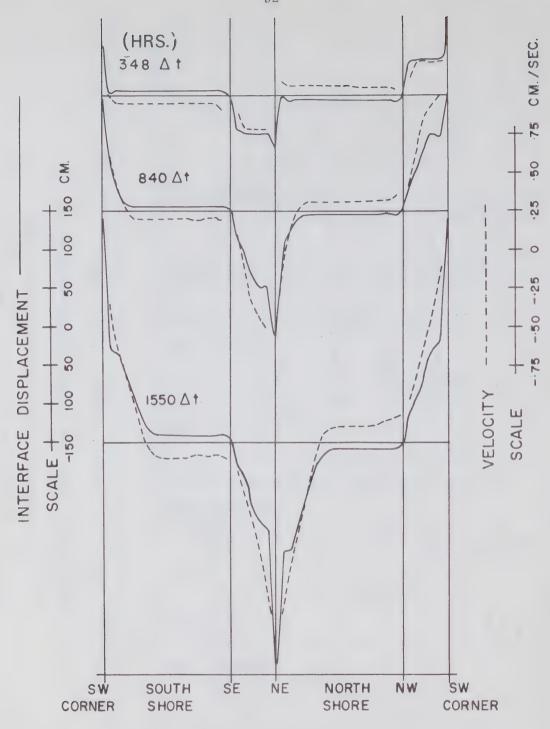


Figure 4.33 Case C. Relationship between the quasistatic response and the coastal jet, shown by
plotting the interface displacement (solid line)
and the component of the velocity parallel to the
shore; the current is taken positive in the
clockwise direction around the basin.

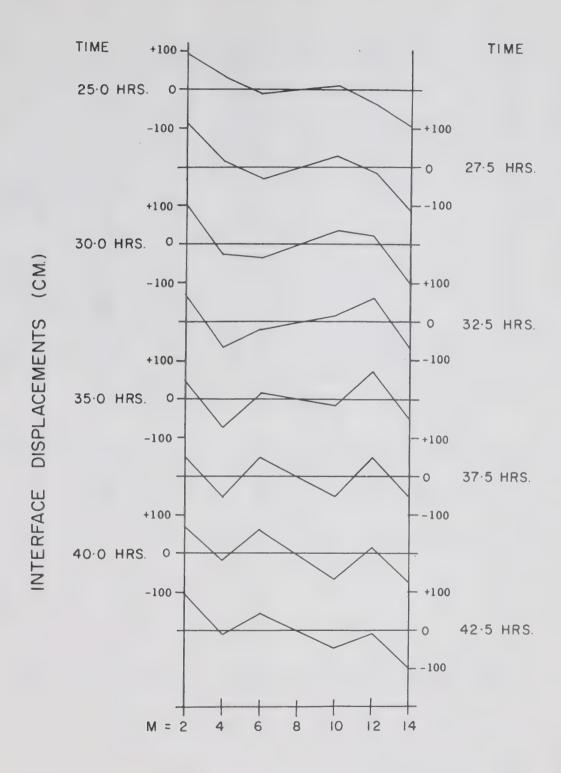


Figure 4.34 Case C. Cross channel profile (n=18) of the interface displacement versus time.

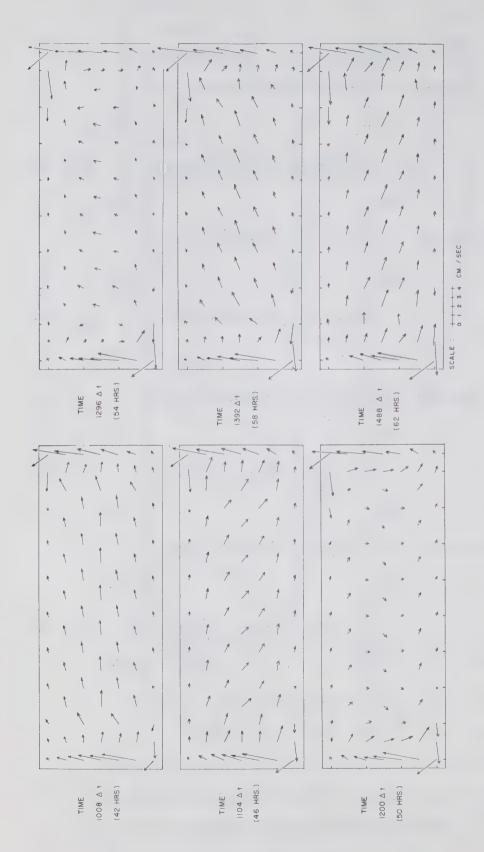


Figure 4.35 Case C. Velocity field in top layer versus

+ ime

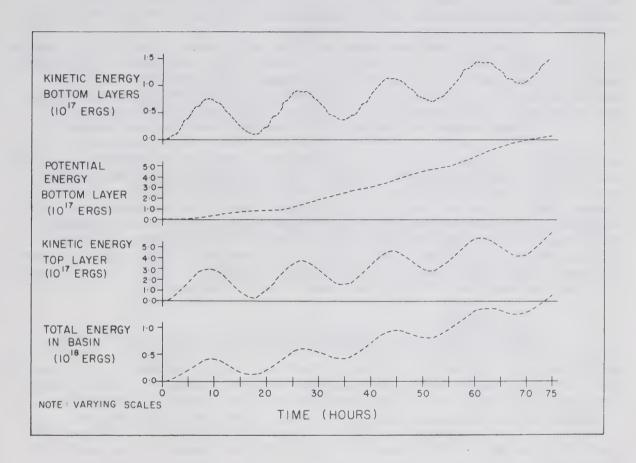


Figure 4.36 Case C. Components of the energy in the basin versus time.

It is apparent, then, that the Kelvin wave is "bucking the wind" in the first half of the cycle.

The Poincaré modes are again dominant away from the shoreline. The cross-channel variation for ZB over the cross-section n = 18 is displayed in Fig. 4.34, at 2.5 hour intervals. At times there appears to be 3 nodes, and at other times, 5 nodes. Possibly there are really only 3 nodes, with the Q.S.R. giving it the appearance of 5 nodes.

The current vectors in the top layer (Fig. 4.35) again exhibit the coastal and counter coastal jet features. At times when the currents are in the direction of the wind, the flow pattern is very orderly, but when the currents are going against the direction of the wind, the flow pattern is disorderely.

The potential energy of the surface is not shown, but in view of the large Q.S.R. at the surface, this component oscillates at one times the transverse surface frequency. Again all energy components (see Fig. 4.36) generally increase with time. For the interface, only a small inertial contribution is found for the potential energy, while the kinetic energies are dominated by strong inertial oscillations. The total energy supplied to the system is proportional to the scalar product of the wind stress and the surface currents. Since the surface currents oscillate near the inertial frequency, the total energy of the system also oscillates near this frequency.

(d) CASE D.

The three final cases (D, E, and F) in this study involve eastward blowing winds that are sinusoidal in time. The amplitude of the wind stress is set to 0.001 cm/sec². In Case D the period of the wind is taken to be 7.5 hours, a value which is slightly longer than the period of the lowest longitudinal surface mode, but yet much less than the inertial period.

The response in ZT is shown in Fig. 4.37. Since the forcing frequency is close to that of the lowest free surface mode, the response at both the forced and the free surface frequencies is relatively large. The forced and free oscillations appear to combine and produce wave packets, with nodes at 20, 43, and 65 hours. A light phase change is found at each of these nodes. The exact period of combination is 7.5 x 5.56 = 41.6 hours. However, 3 times the forced period is 22.5 hours, and 4 times the free period is 22.2 hours. This is apparently close enough to produce the almost periodic behavior that has been observed.

At the interface, the dominant frequencies are the forced and inertial frequencies. Little forced motion is found at ZB (14,8), but at ZB (8,2), every third inertial peak is slightly stronger than the rest (at roughly 51 hour intervals. The appropriate combination here seems to be 7 times the forced period (52.5 hours) and 3 times the inertial period (50.9 hours). The UT and UB components (Fig. 4.38) display the same type of behavior as ZB, but the forced oscillations are relatively much stronger than in ZB. The ratio UT/UB is approximately -4.0, showing substantial excitation in the baroclinic mode. ZT is of the order 10 cm, while ZB is of the order 50 cm,

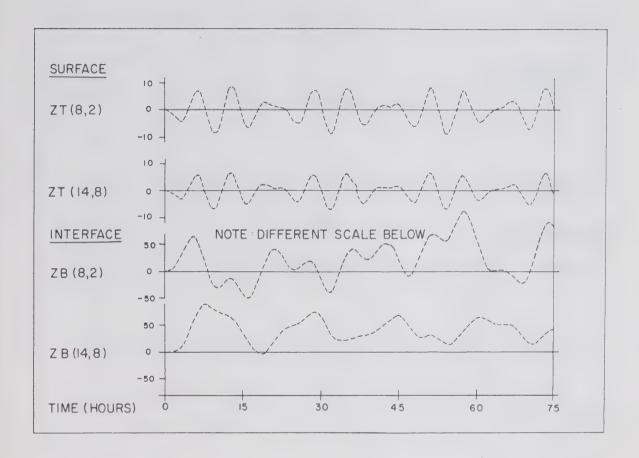


Figure 4.37 Case D. Surface and interface displacements versus time.

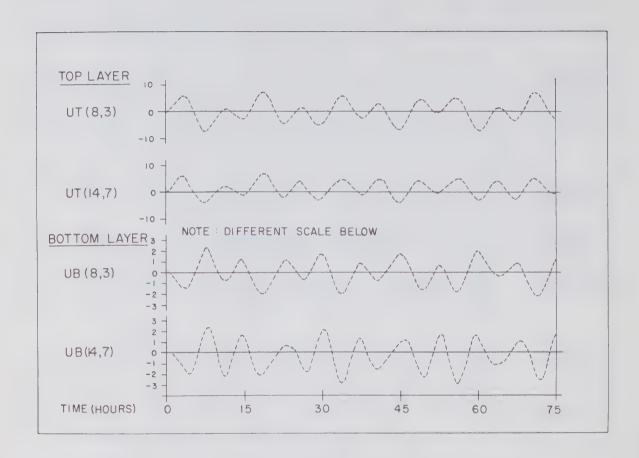


Figure 4.38 Case D. U component of velocity in both layers versus time.

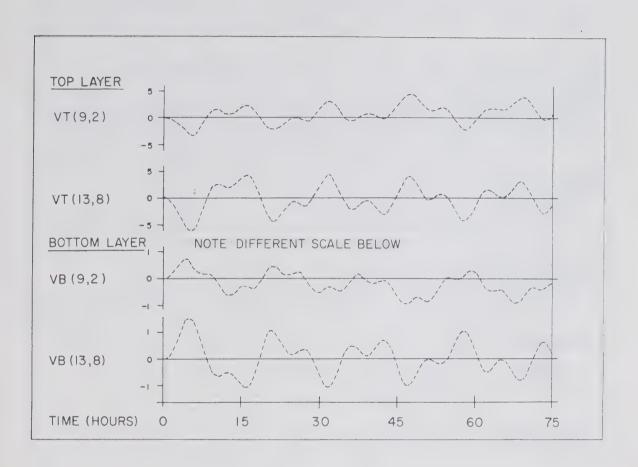


Figure 4.39 Case D. V component of velocity in both layers versus time.

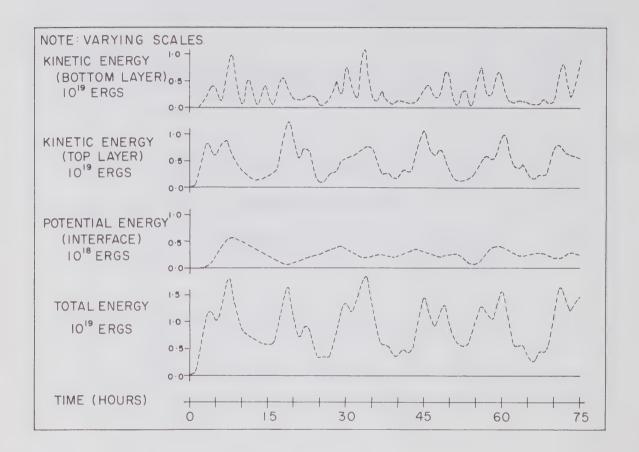


Figure 4.40 Case D. Components of the energy in the basin versus time.

indicating that the baroclinic mode is very easily excited.

The VT and VB components (Fig. 4.39) are dominated by near-inertial oscillations, which is logical because these components are produced by rotation. It is interesting to note that no substantial Q.S.R. is produced, because of the oscillatory nature of the wind stress. Finally, the energy components are displayed in Fig. 4.40.

(e) CASE E.

A more interesting case is a wind of inertial period. From Fig. 4.41, it is seen that excitation of the surface mode is much less than in Case D. Even the forced response in ZT is smaller than in Case D. The forcing frequency is extremely close to the frequency of the internal Poincaré modes, so that resonance is found in ZB. For example, at time 70 hours, ZB in this case is about 800 cm, while in Case D it is about 100 cm.

The behavior of the entire surface is also different. from previous cases. In past calculations, the geometric centre of the basin was a nodal point for ZT, and the nodal lines radiated from this point and rotated about it. Now, the

centre of the basin is not a nodal point (Fig. 4.42).

Instead, the nodal line is curved around the centre point; sometimes it is a closed curve, and at other times it intersects the shoreline. The surface on the inward side of the nodal line is negatively displaced, and on the shoreward or outward side the displacement is positive. The configuration rotates in the anti-clockwise direction.

The level of resonance in the velocities is also intense (Fig. 4.43 and 4.44). The magnitudes of the velocities

are from 8 to 12 times as large as those in Case D.

The growth of energy in the basin is also large (Fig. 4.45). At time 75 hours, the total energy is 2×10^{21} ergs, as compared with the value of 2×10^{-19} ergs in Case D. Since the Q.S.R. is almost non-existent in this case, all the energy components oscillate at twice the inertial frequency.

(f) CASE F.

This last case is concerned with a wind stress of diurnal variation (24 hour period). The forced response in ZT is very small (Fig. 4.46), although the oscillations of the lowest free surface mode (of period 5.56 hours) is still discernible. The values of ZB are dominated by the forced oscillations, as are the velocity components (Fig. 4.47 and 4.48). In general the response is baroclinic, but not to the large extent observed in Case E. The calculations have not been carried out long enough to reveal the common period of the diurnal and baroclinic oscillations. However, there is interference at about time 60 hours, indicating that the common period may be about 120 hours; indeed, 5 times the diurnal period (120 hours) does roughly coincides with 7 times the inertial period (119 hours).

The energy (Fig. 4.49) is mostly in kinetic form, and is dominated by the semi-diurnal variations. The potential energy is almost periodic every 36 hours. The combination of

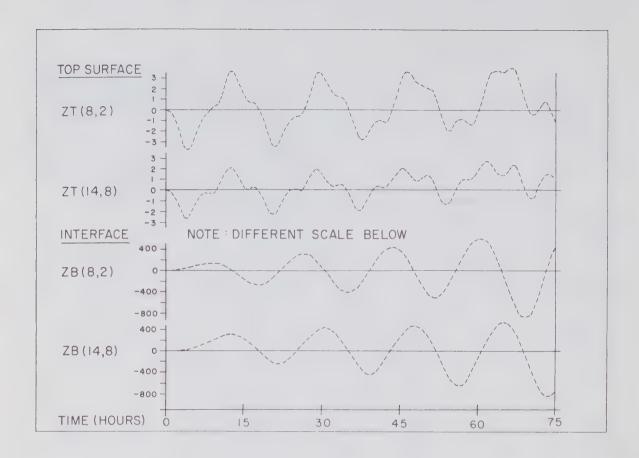


Figure 4.41 Case E. Surface and interface displacements versus time.

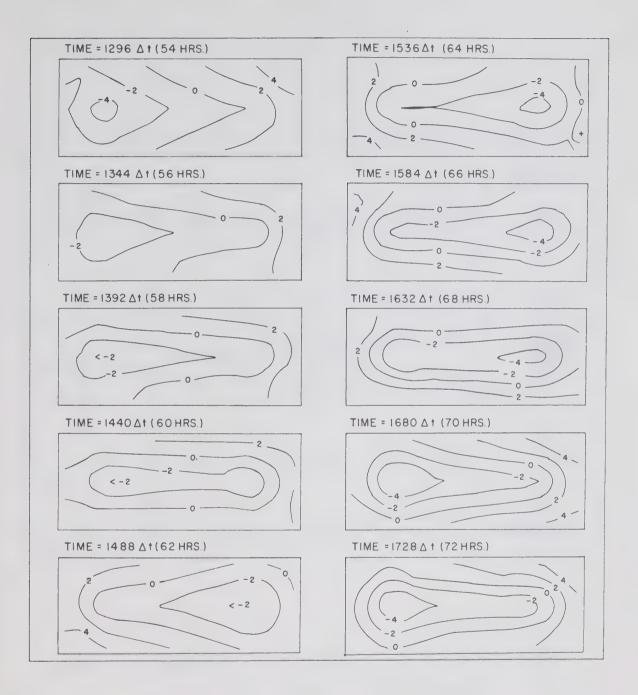


Figure 4.42 Case E. Configuration of the surface versus time.

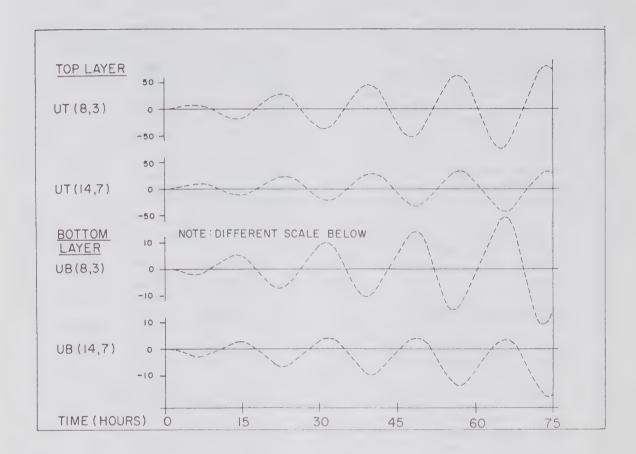


Figure 4.43 Case E. U component of velocity in both layers versus time.

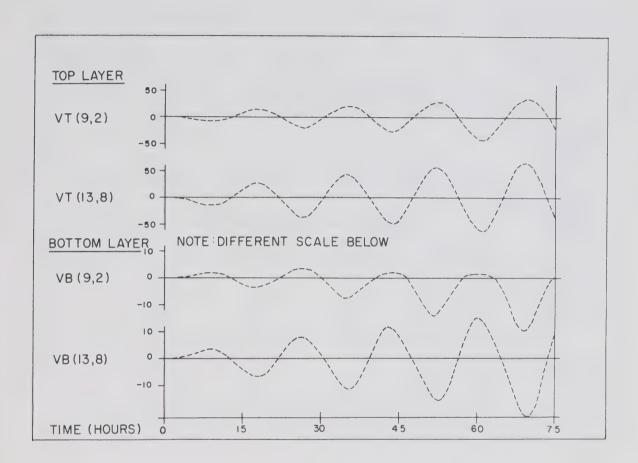


Figure 4.44 Case E. V component of velocity in both layers versus time.

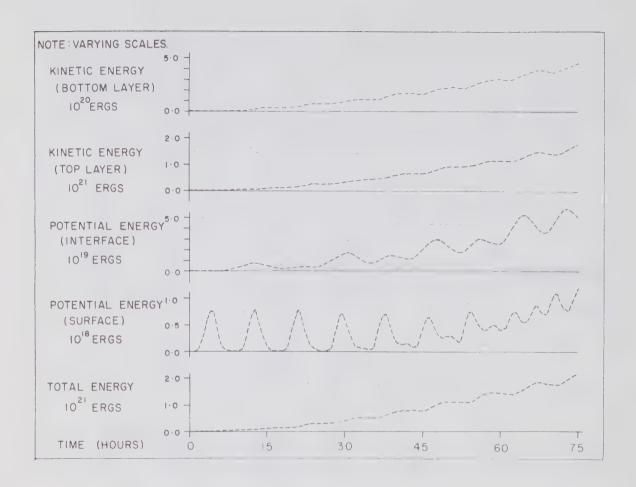


Figure 4.45 Case E. Components of the energy in the basin versus time.

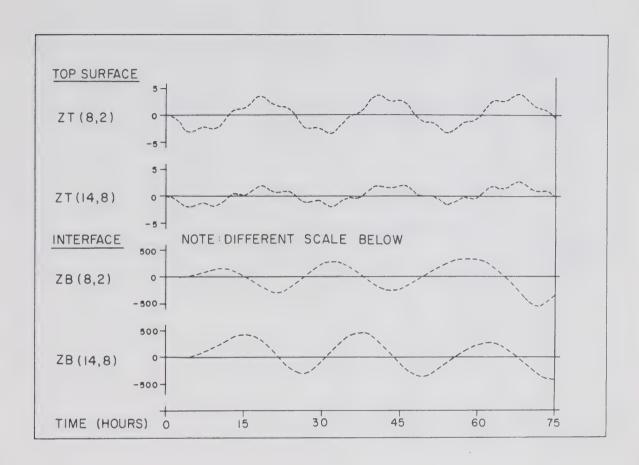


Figure 4.46 Case F. Surface and interface displacements versus time.

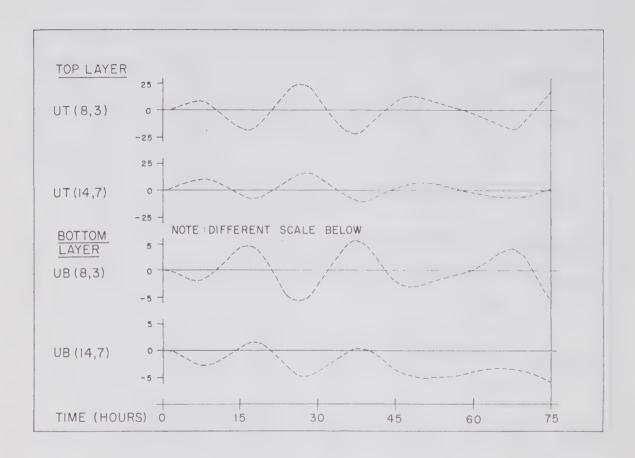


Figure 4.47 Case F. U component of velocity in both layers versus time.

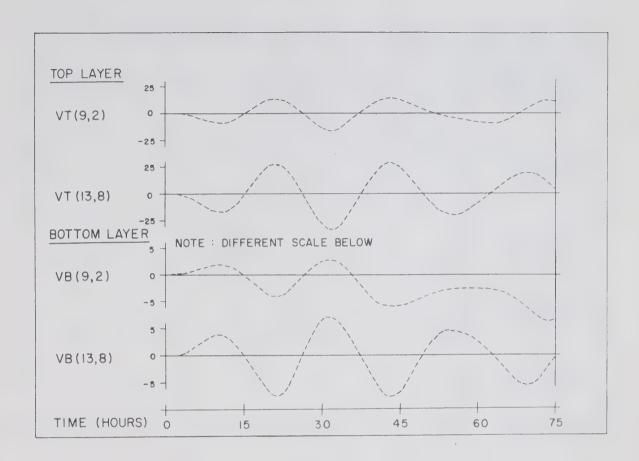


Figure 4.48 Case F. V component of velocity in both layers versus time.

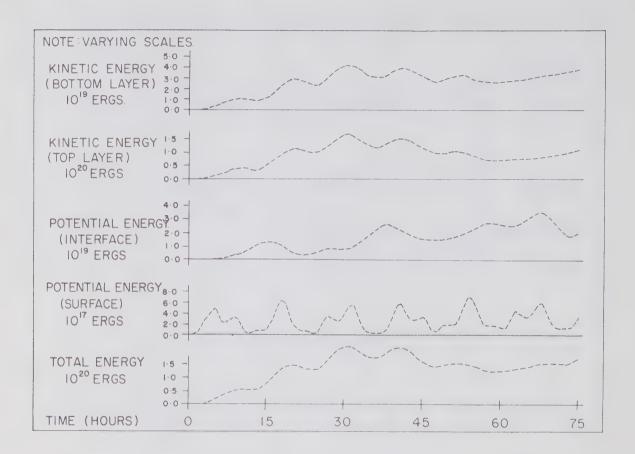


Figure 4.49 Case F. Components of the energy in the basin versus time.

the free and forced periods is 13 times the free period of the surface (72.3) and 3 times the diurnal period (72.0 hours). Due to the closer proximity of the forced frequency to the inertial frequency than to the surface frequency, the response of the basin is principally in the baroclinic mode. It is thus not surprising that the baroclinic response in this case is much higher than in Case D.

4.7 COMPUTATIONAL ERRORS.

Assuming that instability is of no concern in the above calculations, there still remains the problem of estimating the magnitude of the errors inherent in those calculations. The source of these errors arises from the approximations to the derivatives in the hydrodynamical equations. The form of those equations governs the manner in which the errors grow in time. The calculations to be presented here are only carried out to obtain an order of magnitude estimate of the upper limit of these errors.

The system of difference equations may be re-written as

$$\delta u(t) = f'v - A \frac{\partial \eta}{\partial x}$$
 (4.44)

$$\delta v(t) = -f'u - A \frac{\partial n}{\partial y}$$
 (4.45)

$$\delta u'(t) = f'v' - B \frac{\partial \eta}{\partial x} - C \frac{\partial \eta'}{\partial x}$$
 (4.46)

$$\delta v'(t) = -f'u' - B\frac{\partial \eta}{\partial y} - C\frac{\partial \eta}{\partial y}$$
 (4.47)

$$\delta \eta'(t) = -E^* \frac{\partial u'}{\partial x} - E^* \frac{\partial v'}{\partial y} \qquad (4.48)$$

$$\delta \Pi(t) = \delta \Pi'(t) - D\frac{\partial u}{\partial x} - D\frac{\partial v}{\partial y}$$
 (4.49)

where

$$f' = 2 \Delta tf$$

$$A = 2 \Delta tg$$

$$B = 2 \Delta tg \frac{\rho}{\rho'}$$

$$C = 2 \Delta tg (1 - \frac{\rho}{\rho'})$$

$$D = 2 \Delta th$$
and
$$E *= 2 \Delta th'$$

This set of equations may be used to represent the errors in the physical variables rather than the variables themselves. If at each time step the errors are assumed to accumulate in a positive manner, then the errors may be described by the following equations.

$$E'(u) = E_{+}(u) + E(u) + f'E(v) + AE(\eta_{v})$$
 (4.50)

$$E'(v) = E_{t}(v) + E(v) + f'E(u) + AE(n_{v})$$
 (4.51)

$$E'(u') = E_t(u') + E(u') + f'E(v') + BE(\eta_X) + CE(\eta'_X)$$
 (4.52)

$$E'(v') = E_{t}(v') + E(v') + f'E(u') + BE(\eta_{y}) + CE(\eta'_{y})$$
 (4.53)

$$E'(n') = E_t(n') + E(n') + E^*[E(u'_r) + E(v'_v)]$$
 (4.54)

$$E'(\eta) = E_{t}(\eta) + E(\eta) + \delta E(\eta') + D[E(u_{x}) + E(v_{y})]$$
 (4.55)

where

E' = error at new time step,

E = error at old time step, and

E_t = error at each time step due to approximation of the time derivative.

The above set of equations defines an iteration by which the errors may be calculated.

Assuming that the time dependence is of the form e , then the maximum value of \mathbf{E}_{t} at each time step is given by

$$E_{t}(F) = \frac{8}{3} (\Delta t)^{3} \frac{\Pi^{3}}{\Pi^{3}} F$$
 (4.56)

From Case A, T for η is 5.56 hours, and for the remaining variables it is roughly the inertial period.

For the spatial gradients, the errors are

$$E(\partial F/\partial x) = \left(\frac{\Delta x}{6}\right)^2 \frac{\pi^3}{L^3} \quad n^3 F \tag{4.57}$$

and
$$E(\partial F/\partial y) = \frac{(\Delta x)^2}{6} \frac{\pi^3}{N^3} m^3 F$$
 (4.58)

The following typical values are used.

Variable	Amp1:	itude	m	n
η	3 (cm	1	1
n '	75 (cm	3	1
ů	10 0	cm/sec	1	1
u'	10	cm/sec	1	. 1
V	3 (cm/sec	1	1
V	3 (cm/sec	1	1

The equations (4.50) to (4.55) were then iterated 900 times. The results are shown in Table 4.1 below.

Table 4.1 Error Bounds (maximum)

time	ZT	ZB	UT
step	(cm)	(cm)	(cm/sec)
200	1.32	0.72	0.04
400	2.64	1.44	0.28
600	3.96	2.16	1.38
800	5.27	2.88	6.47
1000	6.59	3.59	30.
1200	7.91	4.31	138.
1400	9.23	5.03	642.
1600	10.55	5.75	2973.
1800	11.87	6.47	13755.

Only the error in UT has been shown. The errors in UB, VT, and VB are the same size as the errors in UT. The errors in the displacements are additive, but the errors in the velocity components are exponential in time because of the Coriolis term. Unfortunately, the errors in the velocity components are much larger than the results themselves.

This calculation is not a realistic estimate of the errors in the model, obviously. To find a lower and more realistic limit, a probabilistic approach may be applied. Consider the additive error in the displacements. At each time step this error is ±X, so that the accumulated error is at most 900 X. However, the accumulation of these errors may be considered as a random walk process, the probability being 50% of being X or - X. Since the standard deviation is 30X, the probability of the total additive error being within ±90X after 900 time steps is 99.7% (see Lindgren and McElrath, 1959, p. 253). Thus, it is very probable that the total additive errors in the displacements is only a very small fraction of that listed in Table 4.1. Subsequently, I again carried out the iterations defined by (4.50) to (4.55), but assuming that the effective value of each term on the right hand side of those equations to be reduced by a factor of 1/3. These results are shown in Table 4.2.

Table 4.2 Error Bounds (1/3 maximum)

time	ZT	ZB	UT
step	(cm)	(cm)	(cm/sec)
200	0.28	0.24	0.006
400	0.56	0.48	0.019
600	0.84	0.72	0.044
800	1.12	0.96	0.088
1000	1.40	1.20	0.161
1200	1.68	1.44	0.285
1400	1.96	1.68	0.491
1600	2.24	1.92	0.846
1800	2.52	2.16	1.413

It is thus seen that reduction of the errors at each time step by the modest factor of 1/3 gives rise to reasonable upper bounds for the errors. If a reduction of say 10% were applied, the errors would be very small. No definite values will be given, but it is seen that the error bounds are extremely small even if only a 90% confidence or probability is desired. Recall also, from equations 4.18 and 4.19, that the errors are proportional to the third derivatives. Since the spatial and time dependence of the variables is generally harmonic, the errors will be quasi-periodic and thus will tend to cancel out to a large extent if integrated over a large time period. In any case, it seems clear that the errors in the calculations due to the gradient approximations are "probably" small.

5. CONCLUSIONS

A one-dimensional one-layer analysis was carried out for the free longitudinal surface modes of Lake Huron. Such ar analysis was possible because the effect of rotation upon the longitudinal free surface modes of a narrow basin is very small. The frequencies calculated for the free modes compared favourably with the results of Rockwell (1966). Further verification of the results was carried out by power spectrum analysis of several water level records from Lake Huron tide gauge stations. The results also indicated that Merian's formula is generally satisfactory for estimating the periods of the higher barotropic free modes of oscillation in a narrow basin, but is very poor for the lowest mode.

A numerical model was constructed for a two-dimensional two-layer rectangular basin of constant depth, under the influence of wind stress. In all cases investigated, the wind was kept uniform over the whole of the basin. In the first three cases, the winds were either impulsive or constant in time. From the results, many large scale phenomena were found, which have been predicted by various theories. For the surface mode, it was found that a longitudinally oriented wind excited the longitudinal free modes and that a transverse oriented wind excited the transverse modes. In each case, the Earth's rotation causes the surface modes to rotate in the anti-clockwise direction. It was verified that small rotation slightly lengthened the period of the lowest longitudinal mode, as predicted by Rao (1966).

The baroclinic modes were much more easily excited than the barotropic modes. Poincaré motions were observed in the transverse direction at the interface. One of the outstanding features of the basin response was the quasi-static response, as predicted by Csanady (1968). The currents were generally of a baroclinic nature, with only a small barotropic contribution. Away from the solid boundary, the currents were almost circular and oscillated near the inertial frequency. At the boundary, the existence of the coastal jet was observed, as predicted by Csanady (1968), corresponding to the quasi-static response of the interface displacement. At times, a counter coastal jet was also observed, at a further distance from the

boundary. Superposition of the elliptical currents and the coastal jet corresponds to the "crescent-shaped" currents observed by Verber (1966). The Kelvin waves that were studied are only valid for a non-viscous theory. In reality, friction and variations in the forcing functions do not permit Kelvin waves to exist for more than a small fraction of a complete cycle (their periods, in this case, are in the order of almost 500 hours). Over a short period of observation, these Kelvin waves appear to be static, or nearly so.

Three cases of sinusoidal winds were also studied, with periods of 7.5, 17.0, and 24.0 hours. In each case, growth of the quasi-static response. The forced response of the basin to a periodic wind increased rapidly as the frequency of the wind approached any of the natural frequencies of the basin. The response near the baroclinic frequencies is much greater than that near the barotropic frequencies. Indeed, a high level of resonance was found in the case of a wind of inertial period. Furthermore, the free modes themselves may also become excited. These results are in general qualitative agreement with the predictions of Mortimer (1953) and Csanady (1968).

6. ACKNOWLEDGEMENTS

This research project was carried out while the author was at the University of Waterloo, Waterloo, Ontario. The author is indebted to Dr. G.T. Csanady of the Department of Mechanical Engineering for guidance and encouragement throughout the course of this work. Mrs. Hamlin, of the University, and Mr. M. Isabelle, of the Marine Sciences Branch, Ottawa, are both commended for their good work on the numerous diagrams. Thanks are extended to the Tides and Water Levels Section of the Department of Energy, Mines and Resources for supplying the Lake Huron tide gauge data. Also the author, extends his warmest appreciation to the Faculty and students in the Department of Mechanical Engineering in helping to make his stay a most fruitful and enjoyable one.

The author's return to University to carry out this research was made possible by the granting of educational leave from the Marine Sciences Branch, Department of Energy, Mines, and Resources.

7. REFERENCES

Birchfield, G.E. 1967. Horizontal transport in a rotating basin of parabolic depth profile. Journal of Geophysical Research, 72, 6155-6164.

Blackman, R.B. 1965. Data smoothing and prediction.

Addison-Wesley Publishing Co. Inc.

Blackman, R.B. and J.W. Tukey. 1959. The measurement of power spectra from the point of view of communications engineering. Dover Publications.

- Brettschneider, G. 1965. Andwendung des Hydrodynamisch-Numerischen Verfahrens zur Ermittlung der M₂ - Mitschwingungezeit der Nordsee. Diplomarbeit, Universität Hamburg.
- Bryson, R.A. and R.A. Ragotzkie. 1960. On internal waves in lakes. Limnology and Oceanography, 5, 397-408.
- Cahn, A. Jr. 1945. An investigation of the free oscillations of a simple current system. Journal of Meteorology, 2, 113-119.
- Chrystal, G. 1908. An investigation of the seiches of Loch Earn by the Scottish Lake Survey. Part V: Mathematical appendix on the effect of pressure disturbances upon the seiches in a symmetric parabolic lake. Transactions, Royal Society of Edinburgh, 46, 499-516.
- Royal Society of Edinburgh, 46, 499-516.

 Corkan, R.H. and A.T. Doodson. 1952. Free tidal oscillations in a rotating square sea. Proceedings of the Royal Society of London, A215, 147.
- Courant, R.H., K. Friedrichs, u. H. Lewy. 1928. Uber die partiellen Differential Gleichungen der mathematischen Physik. Math. Ann. Bd., 100, S. 32-74.
- Courant, R.H. u. D. Hilbert. 1937. Methoden der mathematisschen Physik. Verlag von Julius Springer, Berlin.
- Csanady, G.T. 1964. Hydrodynamic studies on Lake Huron at Baie du Dore, Summer 1964. Great Lakes Institute, University of Toronto PR 19.
 - 1967. Large Scale Motion in the Great Lakes. Journal of Geophysical Research, 72, 4151-4162.
 - 1968. Wind driven summer circulation in the Great Lakes. Journal of Geophysical Research, 73, 2579-2589.
- Defant, A. 1925. Gezeiten probleme des Meeres in Landnähe. Probl. kosm. Physik, 6, 80.
- 1961. Physical Oceanography. Pergamon Press. Fischer, G. 1965. A survey of finite-difference approximations
- to the primitive equations. Monthly Weather Review, 93, 1-10.
- Fjeldstad, J.E. 1933. Interne Wellen. Geofysiske Publikasjoner 10, No. 6.
- Godin, G. 1965. Some remarks on tidal motion in a narrow rectangular sea of constant depth. Deep-Sea Research, 12, 461-468.
 - 1965. M₂ tide in Labrador Sea, Davis Strait, and Baffin Bay. Deep-Sea Research, 12, 469-477.
- Deep-Sea Research, 12, 469-477.

 Goldsborough, G.R. 1931. The tidal oscillations in rectangular basins. Proceedings of the Royal Society of London, A132, 689.
- Hale, A.M. 1965. Internal waves in Lake Huron. M.A. Sc. Thesis, University of Waterloo.
- Hansen, W. 1956. Theorie zur Errechnung des Wasserstandes und der Stromungen in Randmeeren nebst Anwendungen. Tellus, 8, 287-300.
 - 1966. The reproduction of the motion in the sea by means of the hydrodynamical-numerical method. Nr. V. Mitteilungen des Instituts fur Meereskunde der Universität Hamburg.

Harleman, D.R.F., R.M. Bunker, and J.B. Hall. 1964. Circulation and thermocline development in a rotating lake model. Publication No. 11, Great Lakes Research Division, University of Michigan.

Harris, D.L. 1957. The effect of moving pressure disturbances on the water level in a lake. Meteorological Monographs,

2, No. 10, 46-57.

1962. Equivalence between certain statistical prediction models and linearized dynamical methods. Monthly Weather Review, 90, 331-340.

Harris, D.L. and C.P. Jelesnianski. 1964. Problems involved in the numerical solution of tidal hydraulics equations.

Monthly Weather Review, 92, 409-422.

Haurwitz, B. 1948. The effect of ocean currents on internal waves. Journal of Marine Research, 7, 217-228.

Heaps, N.S. 1965. Storm surges on a continental shelf. Philosophical Transactions of the Royal Society of London, A257, 351-383.

Heaps, N.S. and A.E. Ramsbottom. 1966. Wind effect on the water in a narrow two layered lake. Philosophical Transactions of the Royal Society of London, A259, 391-430.

Jelesnianski, C.P. 1965. Numerical calculation of storm tides induced by a tropical storm impinging on a continental shelf. Monthly Weather Review, 93, 343-358. 1966. Numerical computations of storm surges without bottom stress. Monthly Weather Review, 94, 379-394.

Jensen, H.E. and S. Weywadt. 1966. Forecasting of storm surges in the North Sea. The Institute of Mathematical Statistics and Operations Research, The Technical University of Denmark

Copenhagen.

Kasahara, A. 1965. On certain finite-difference methods for fluid dynamics. Monthly Weather Review, 93, 27-31.

Lamb, H. 1932. Hydrodynamics. Sixth edition. Dover Publications.

Lindgren, B.W. and G.W. McElrath. 1959. Introduction to Probability and Statistics. The Macmillan Co.

Loucks, R. 1966. Notes on a set of programs for power spectrum analysis. BIO Computer Note 66-3-C, Bedford Institute of Oceanography, Dartmouth, N.S.

Miyazaki, M. 1965. Numerical computation of the storm surge of Hurricane Carla, 1961, in the Gulf of Mexico. Ocean-

ographical Magazine, 17, 109-140.

Mortimer, C.H. 1952. Water movements in lakes during summer stratification: Evidence from the distribution of temperature in Windermere. Philosophical Transactions of the Royal Society of London, B236, 355-404.

1953. The resonant response of stratified lakes to wind.

Schweiz. Z. Hydrol., 15, 94-151.

1961. Motion in the thermoclines. Verh. Internat.

Verein. Limnol., XIX, 79-83.

1963. Frontiers in physical limnology with particular reference to long waves in rotating basins. Publication No. 10, Great Lakes Research Division, University of Michigan.

- Muller, F.B. 1966. Note on the meteorological application of power spectrum analysis. Canadian Meteorological Memoirs, Meteorological Branch, Department of Transport, Toronto.
- Munk, W.H. 1941. Internal waves in the Gulf of California.

 Journal of Marine Research, 4, 81-91.
- Munk, W.H., F.E. Snodgrass, and M.J. Tucker. 1959. Spectra of low frequency ocean waves. Bulletin of the Scripps Institution of Oceanography of the University of California, 7, No. 4, 283-362.
- Neumann, G. and W.J. Pierson, Jr. 1966. Principles of Physical Oceanography. Prentiss-Hall, Inc.
- Phillips, O.M. 1966. The dynamics of the upper ocean. Cambridge Monographs on Mechanics and Applied Math. Cambridge at the University Press.
- Platzman, G.W. 1958. Lattice structure of the finite-difference primitive and vorticity equations. Monthly Weather Review, 6, 285-292.
 - 1958. Numerical computation of surge of 26 June, 1954 on Lake Michigan. Geophysica, 6, 407-438.
 - 1963. Dynamical prediction of wind tides on Lake Erie.
- Meteorological Monographs, 4, No. 26.

 Platzman, G.W. and D.B. Rao. 1964. Free oscillations of Lake Erie. Studies on Oceanography (Hidaka Volume), University of Washington Press, 359-382.
- Poincaré, H. 1910. Theorie des Marees. Lecon de mecanique celeste, 3, Paris.
- Proudman, J. 1929. The effects on the sea of changes in atmospheric pressure. Monthly Notices of the Royal Astronomical Society, Geophysical Supplement 2, 197-209.

 1953. Dynamical Oceanography. Metheun and Co. Ltd.
- Rao, D.B. 1966. Free gravitational oscillations in rotating rectangular basins. Journal of Fluid Mechanics, 25, 523-555.
- Rayleigh, Lord. 1903. On the vibrations of a rectangular sheet of rotating liquid. Philosophical Magazine, 5, 297.
- Redfield, A.C. 1950. The analysis of the tidal phenomena in narrow embayments. Papers in Physical Oceanography and Meteorology, 2(4).
 - 1961. Tidal system of Lake Maracaibo, Venezuela. Lim-nology and Oceanography, 6, 1-12.
- Reid, G.K. 1961. Ecology of inland waters and estuaries. Reinhold Publishing Corporation.
- Richtmeyer, R.D. 1957. Difference methods for initial value problems. Interscience Publishers.
- Rockwell, D.C. 1966. Theoretical free oscillations of the Great Lakes. Publication No. 15, Great Lakes Research Division, University of Michigan.
- Rossby, C.G. 1937. On the mutual adjustment of pressure and velocity distributions in certain simple current systems. Journal of Marine Research 1, 15-28.
- Sverdrup, H.U., M.W. Johnson, and R.H. Fleming. 1942. The Oceans. Prentiss-Hall, Inc.

- Taylor, G.I. 1921. Tidal oscillations in gulfs and rectangular basins. Proceedings of the London Mathematical Society, Series 2, XX, 148-181.
- Thomson, W. 1879. On the gravitational oscillations of rotating water. Proceedings of the Royal Society of Edinburgh, 10, 92 (paper 4, p. 141).
- Ufford, C.W. 1947. The theory of internal waves. Transacttions of the American Geophysical Union, 28, 96-101.
- Van Dantzig, D. and H.A. Lauwerier. 1960. The North Sea Problem: IV. Free oscillations of a rotating rectangular sea. Konink. Nederl. Akad. Wetensch., Proc. Ser. A, 63, 170-187.
- Verber, J.L. 1964. The detection of rotary currents and internal waves in Lake Michigan. Publication No. 11, Great Lakes Research Division, University of Michigan. 1966. Inertial currents in the Great Lakes. Publication No. 15, Great Lakes Research Division, University of Michigan.
- Veronis, G. 1956. Partition of energy between geostrophic and non-geostrophic oceanic motion. Deep-Sea Research, 3, 157-177.
- Veronis, G. and H. Stommel. 1956. The action of variable wind stress on a stratified ocean. Journal of Marine Research, 15, 43-75.
- Welander, P. 1957. Wind action on a shallow sea. Some generalizations of Ekman's theory. Tellus, 9, 45-52. 1961. Numerical prediction of storm surges. Advances in Geophysics, 8, 315-379.
 - 1966. A two layer frictional model of wind driven motion in a rectangular oceanic basin. Tellus, 8, 54-62.
- Wilson, B. 1960. Note on surface wind stress over water at low and high wind speeds. Journal of Geophysical Research, 65, 3377-3382.
- Yuen, K.B. 1967. Effect of tidal barriers upon the M₂ tide in the Bay of Fundy. Manuscript Report Series, No. 5, Marine Sciences Branch, Department of Energy, Mines and Resources, Ottawa.





MANUSCRIPT REPORT SERIES NO. 15

Oceans IV: A Processing, Archiving and Retrieval System for Oceanographic Station Data

H. E. SWEERS



Marine Sciences Branch
Department of Energy, Mines and Resources

1970





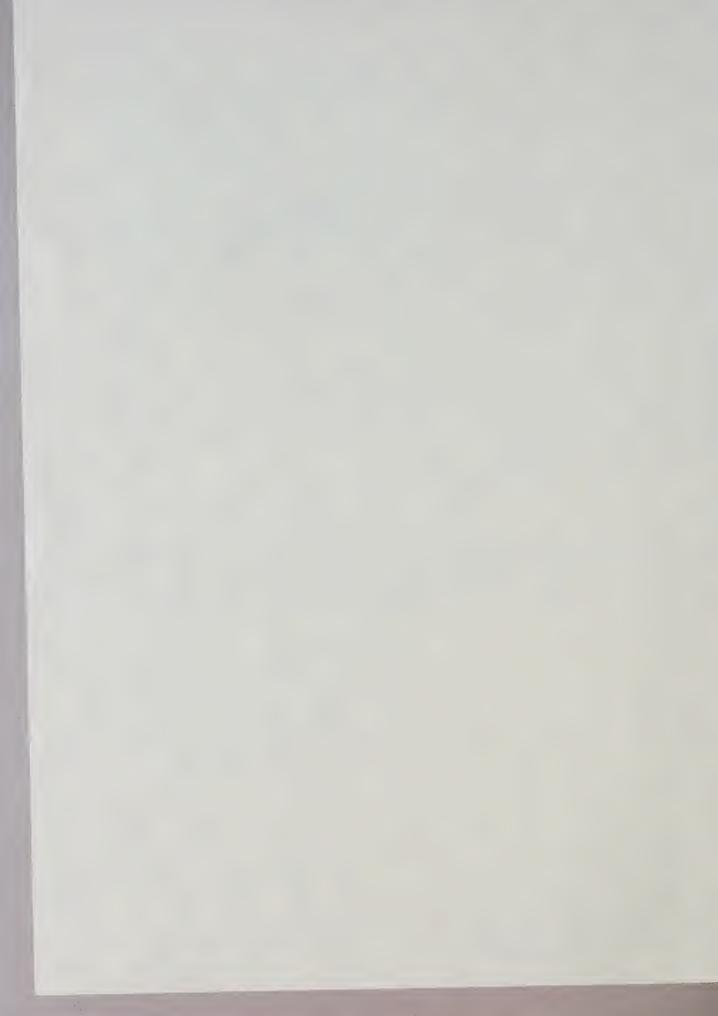


ERRATA

to

Manuscript Report Series No. 15
(January, 1971)

OCEANS IV: A Processing, Archiving and Retrieval System for Oceanographic Station Data, by H.E. Sweers, Marine Sciences Branch, Department of Energy, Mines and Resources, Ottawa.



/1 P. 14 - second line from Replace five degree square bottom number 1 by 0. 2 P. 15 - third line Replace five degree square number 4 by 1. 3 P. 17 - 3.2.5 2) last All stations with at least one observed level deeper sentence should read than the minimum level but shallower than the maximum level are extracted. P. 30 - footnote to the words *Pressure for oceanographic "oceanographic pressure"* calculations is normally last line second paraexpressed as oceanographic graph from the bottom. pressure, which equals true pressure minus atmospheric pressure. /5 P. 31 - insert in line 5 at 4°C and under atmospheric between words "water" pressure. and "now" 6 P. 31 - replace lines 6 The influence of this on through 9 by sigma-t is negligibly small, since the latter is defined as the difference between two specific gravity or two specific density values, respectively. 7 P. 32 - third line, add one ... specific gravity and specific density is word. It should read discussed... and is usually given in units 8 P. 32 - add between second of 10^5 cm 3 /gr. The difference equation and section 4.3.3.2 in the definitions of specific density on δ thus is a negligibly small, second order effect. ... Deep Sea Res... 9 P. 44 - Reference "Keyte, F.K. 1964" the second line should read

10 P. 63 - right hand side of the

"MPR data..."

page in column "Explan-

paragraph which starts

ation" after second

XBT data can be marked with

of XBT data in the file is

not recommended but can be

done if desired.

a Q in column 33. Inclusion



- 11 P. 77, 78, 79 Replace by new pages 77, 78, 79.
- 12 P. 131 footnote should read

This appendix will also be published in "Limnology and Oceanography" under the title "An Improved Code to Classify the Location of Marine and Terrestrial Data".

- 13 P. 132 in table F1 change lines 4 and 6 as shown
- X = 90-(Lat. + 1)Y = 360-(Long. + 1)



Manuscript Report Series No. 15

EAR BY MY

OCEANS IV: A PROCESSING, ARCHIVING

AND RETRIEVAL SYSTEM

FOR OCEANOGRAPHIC STATION DATA

H. E. SWEERS

ABSTRACT

OCEANS IV is a powerful system of programs used by the Canadian Oceanographic Data Centre to manage its oceanographic station data file. This file, at present, contains 30,000 stations consisting of, on the average, 10 observed levels each. The data are stored in geographical order on magnetic tape. The system can accept up to 35 different physical and chemical parameters in a partially open ended format. To date only 16 parameters have been assigned codes.

The four basic functions of the OCEANS IV system are:

- (1) Processing of reversing thermometer readings.
- (2) Preparing temperature, salinity and chemical data for archival in the oceanographic station data file.
- (3) Printing data reports on request.
- (4) Providing a flexible retrieval of data from the file.



CONTENTS

				Page
1.	INTE	RODUCI	FION · · · · · · · · · · · · · · · · · · ·	1
	1.1 1.2 1.3 1.4 1.5 1.6	Types Data Data Limit Envir	ose s of Data Output Files tations ronment and Languages mparison with OCEANS III	1 2 3 3 4 4 4
2.	INPU	IT AN	D DATA EDITING	6
	2.1 2.2 2.3	Erro	Forms and Formatsr Checks on Reversing Thermometer Datar Checks on Data Summary Entries	6 8 9
3.	DATA	RETI	RIEVAL AND OUTPUT	12
			Output Extraction	12 13
	3. 3. 3. 3.	2.1 2.2 2.3 2.4 2.5 2.6 2.7	Area Search	15 15 15 17 17 17
4.	4. CALCULATIONS		IONS	19
	4.		Correcting the Readings	19 19 20
			sure and Depth	23
		2.1	Calculations Justification	23 24
	4.3	Deriv	ved Parameters	29
	4. 4. 4. 4.	3.1 3.2 3.3 3.4 3.5 3.6 3.7 3.8	Gravity	29 30 31 34 37 38 38

		Page
	4.4 Interpolation Routines	38 39 40 41
5.	ACKNOWLEDGEMENTS	43
6.	REFERENCES	44
	APPENDICES	
A	System Summary and Flow Charts	47
В	Input Forms and Coding Instructions	53
	1. Cruise Master	55 57 60 67 71
С	Data Retrieval Forms	75
	 Data Extraction Form Data Output Form 	77 79
D	Data Output Print Outs	81
	1. Thermocheck Listing 2. OCEANS IV Edit Listing 3. Data Report 4. Cruise Master Catalogue (Data Acquisitions) 5. Data Counts 6. Station Master Catalogue 7. Data Inventory Type I 8. Data Inventory Type II 9. Data Inventory Type III 10. Distribution of Means and Standard Deviations	83 89 90 106 107 108 109 110 111 113
E	Data Output Card and Tape Formats	115
	1. OCEANS IV	117 122
F	The COTED Squares System for Sequencing Data in Geographical Order on Magnetic Tape.	129

LIST OF TABLES

Table

- 2.a Summary of the alternative combinations of forms that can be used to submit data to CODC.
- 2.b Coding, units and range tests for oceanographic parameters.
- 2.c Coding, units and range tests for meteorological parameters.
- 4.a Depth-density tables.
- 4.b Influence of ρ_m on the determination of depth from pressure.
- 4.c Sigma-t constants.
- 4.d Specific volume constants.
- 4.e Sound velocity constants.
- E.1 File units for parameters that have a choice of units that can be used for submission of the data.
- E.2 Conversion of Beaufort estimate to windspeed in m/sec.
- E.3 Conversion of $P_{\rm W}$ code (WMO3155) to period in seconds $(P_{\rm W}P_{\rm W})$.
- E.4 OCEANS III Station Master record (type 1).
- E.5 OCEANS III Observed Detail record (type 3).
- E.6 OCEANS III Interpolated record (type 6).
- F.1 Decision table to calculate the COTED square number of a station.

LIST OF FIGURES

Figure

- 3.a Graphical explanation of the method of setting up an areal search.
- 4.a Stations used to test effect of the depth-density table on depth-pressure conversions.
- A.1 Summary flow diagram for OCEANS IV.
- B.1.1 Cruise Master coding sheet.
 - 2 Cruise Master coding instructions.
- B.2.1 Deck Sheet
 - 2 Deck Sheet coding instructions.
 - 3 Deck Sheet coding instructions (continued).
- B.3.1 Data Summary.
 - 2 Data Summary coding instructions.
 - 3 Data Summary coding instructions (continued).
 - 4 Data Summary coding instructions (continued).
 - 5 Data Summary coding instructions (continued).
 - 6 Data Summary coding instructions (continued).
 - 7 Data Summary coding instructions (continued).
- B.4.1 Bridge Log.
 - 2 Bridge Log coding instructions.
 - 3 Bridge Log coding instructions (continued).
 - 4 Bridge Log coding instructions (continued).
- B.5.1 Thermometer Calibration Sheet.
 - 2 Thermometer Calibration Sheet coding instructions.
 - Thermometer Calibration Sheet coding instructions (continued).
- C.1.1 Data Extraction form.
 - 2 Data Extraction form (continued).
- C.2 Data Output form.
- D.1.1 Output of the Thermocheck program.
 - 2 Depth-density table used for the pressure-depth conversions.
 - 3 Sample listing of the thermometer calibration data.
 - 4 Sample output of the corrected temperatures and calculated pressures.
 - 5 Statistical analysis of the performance of paired thermometers (part 1), showing the distribution of observed differences over the interval -0.11°C to +0.11°C in steps of 0.01°C.

Figure

- D.1.6 Statistical analysis of the performance of paired thermometers (part 2), showing the mean temperature observed with each pair, the mean difference, the standard deviation of the differences, the standard error of the observed mean difference, and the number of observations in each of 7 depth intervals.
- D.2 Sample output of the Edit program.
- D.3.1 Sample Data Report page.
 - 2 Sample Data Report page showing interpolated data.
 - 3 Explanation of the Data Record headings.
 - 4 Explanation of the Data Record headings (continued).
 - 5 Explanation of the Data Record headings (continued).
 - 6 Explanation of the Data Record headings (continued).
 - 7 Explanation of the Data Record headings (continued).
 - 8 Explanation of the Data Record headings (continued).
 - 9 Explanation of the Data Record headings (continued).
 - 10 Explanation of the Data Record headings (continued).
 - 11 Explanation of the Data Record headings (continued).
 - 12 Explanation of the Data Record headings (continued).
 - 13 Explanation of the Data Record headings (continued).
 - 14 Explanation of the Data Record headings (continued).
 - 15 Explanation of the Data Record headings (continued).
 - 16 Explanation of the Data Record headings (continued).
- D.4 Cruise Master Catalogue.
- D.5 Sample Data Count.
- D.6 Station Master Catalogue.
- D.7 Data Inventory Type I, showing a summary by one-degree squares (COTED system) and by month of the available data.
- D.8 Data Inventory Type II, showing a summary by one-degree squares (COTED system) and by year-ranges of the available data.
- D.9.1 Data Inventory Type III, showing a summary of available data in a semi geographical lay-out by one-degree squares.
 - Data Inventory Type III, showing a summary of available data in a semi geographical lay-out by ten-degree squares.
- D.10 Distribution of Means and Standard Deviations, showing per one-degree square (COTED system) a count, mean and standard deviation of all data retrieved as specified on the Data Extraction form.

Figure

- E.1 Sample OCEANS IV input or output card.
- E.2 Sample OCEANS III input or output card.
- F.1 Key to the Marsden and COTED ten-degree square numbers.
- F.2 Key to the numbering of one-degree squares in the Marsden system.
- F.3 Key to the numbering of one-degree squares in the COTED system.

1. INTRODUCTION

1.1 PURPOSE

The Canadian Oceanographic Data Centre manages, among other files, a rapidly growing file of oceanographic stations. At present this file holds about 30,000 stations, but with the increasing global interest of Canadian oceanographers, it may well expand to ten times this size due to foreign data acquisitions. The usefulness of such a file is mainly determined by the availability of an efficient and flexible retrieval routine. The new OCEANS IV system meets these requirements, and has also been designed to extensively edit the input in an effort to make the system as "foolproof" as possible.

The OCEANS IV system fulfills the following four basic functions:

- (1) Processing of reversing thermometer readings.
- (2) Preparing temperature, salinity and chemical data for archival in the Oceanographic Station Data File.
- (3) Printing data reports on request.
- (4) Providing a flexible retrieval of data from the file.

Unlike its predecessor, OCEANS III, it can accept a fairly wide range of different physical and chemical parameters. At present it accepts 16 parameters, but it can be expanded to take up to 35 different variables.

This report will help the following categories of readers to understand the OCEANS IV system:

- (1) Anyone submitting data to CODC for processing and/or archiving.
- (2) Scientists or engineers using CODC's data bank.
- (3) Other data centres interested in an outline of the OCEANS IV system.

A separate manual "Specifications for the OCEANS IV System", has been written by Mr. A.S. Adams of DCF Systems Limited. It gives detailed specifications on the system and all individual components, and is useful mainly for programmers and clerical staff involved in the maintenance and usage of the system. A limited number of copies of Mr. Adams' report can be made available on special request to those wishing to make a more detailed study of the system.

A brief summary of the OCEANS IV system, including flowcharts and a description of the individual programs, is given in Appendix A. The main text of this report, however,

can be read without reference to the systems flowcharts. In the following sections a "black box" approach has been used to describe only the inputs to and outputs of the system with minimum reference to its actual structure.

1.2 TYPES OF DATA

The system can presently accept 16 different oceanographic parameters and a limited number of meteorological
observations. The range of meteorological parameters has been
limited to those which most directly influence surface
conditions in the ocean, such as wind, waves, temperature, etc.
Most oceanographic vessels submit regular marine weather
reports to the Department of Transport, and more complete
data (for the standard observation hours) are available from
their files.

The oceanographic parameters include depth, temperature, salinity, soundspeed, oxygen, PO4-P, total P, NO2-N, NO3-N, SiO3-Si and pH, all included in the former OCEANS III file, and a number of new parameters. Codes have presently also been assigned to fluoride, dissolved and particulate organic carbon, total and carbonate alkalinity, and ammonia. A further 19 parameters can be added in the future up to a total of 35, making OCEANS IV far more flexible than the old system.

One of the most important newly introduced parameters is pressure. Both pressure and depth are retained in the OCEANS IV file; either one of these can be used as the "independent" variable for data retrievals. If pressure has been observed, depth will be calculated, as outlined in Section 4.2, and stored as a "dependent variable", and vice versa if depth has been observed.

Temperature and salinity data sampled with STD probes can also be entered into the system, and can be marked to distinguish them from Nansen cast data. This is described in some detail in Appendix B3. It must be noted, however, that OCEANS IV is essentially designed to handle observations from a limited number of discrete levels for each station; analog or digital traces obtained with STD's therefore must be reduced to a maximum of 99 points per station. This is sufficient detail for climatological studies, but it may be inadequate for some other demands that could be put on the data bank. Separate programs still have to be developed to convert digitized STD data into OCEANS IV input format.

All data have to be corrected and calibrated before submission, with one exception only: Reversing thermometer data can be submitted as raw readings. They will be calibrated and corrected as outlined in Section 4.1 by the Thermocheck program.

1.3 DATA OUTPUT

The data output is very flexible. Major output options are listings of data being processed, data reports ready for publication, data inventories, horizontal distributions of means and standard deviations, or just plain copies of the data on paper, punch cards or magnetic tape. These options will be discussed in detail in Section 3.

The data input forms are described in some detail in Section 2, which also outlines the error checking procedures and summarizes the resulting error messages. Copies of the input forms and of the coding instructions are shown in Appendix B.

All data are thoroughly edited before inclusion in the file, and error messages will signal all violations of the edit conditions. The identifying information is subject to "presence" checks, most data are tested for being numerical and for remaining within acceptable ranges. These checks are discussed in some detail in the Sections 2.2 and 2.3.

1.4 DATA FILES

New data are entered into the system on cards, and are, after acceptance by the Edit program, accumulated on the OCEANS IV transaction tape. This file contains all Cruise Masters, Station Masters and Observed Details in sequence of entry, but no derived or interpolated data. All information that can be obtained mathematically from the observations, is re-calculated (upon demand) when the data are retrieved from the files.

Once every six to nine months the three oceanographic master files are updated. The Cruise Master file consists of cards and is only used for internal reference. The station data are separated into two master files on magnetic tape: The Station Master and Level Master files, containing the Station Master and Observed Detail records respectively. The reason for creating two master files for the station data is twofold: reduction of overall file size and of the cost of running inventory control type of requests. The number of stations that will be extracted under a set of retrieval conditions, for example, can be determined from the Station Master file in a fraction of the time needed to pass a tape containing both Station Masters and Observed Details.

The Station Master file contains, apart from the information given on the Station Master section of the input

forms, also a summary of the observations taken at the station. Major entries in this part are minimum and maximum observed depth, parameters observed and the percentage of the levels at which each of the parameters has been measured. The major reason for including this summary in the Station Master file is to decrease the cost of data extractions and the production of data inventories.

The Level Master file contains observed parameters, depth and pressure. No derived parameters, such as sigma-t, etc., are stored. These are all calculated upon demand when data are retrieved from the file.

The master files are in a geographical sequence. The traditional Marsden square system has been replaced by the more convenient COTED system described in detail in Appendix F. Marsden square numbers are only used in the output as shown in Appendix D3. Both the COTED and the Marsden ten-degree square keys are shown in the Fig. F1, and the one-degree square keys are shown in the Figs. F3 and F2 respectively.

1.5 LIMITATIONS

Within the range of input and output formats defined elsewhere, the system is also subject to some limitations set to reduce internal memory requirements and computing time. These are a maximum of 999 stations per cruise, 99 levels per station and 10 different parameters per station. The latter two limitations can be extended relatively easily if necessary.

1.6 ENVIRONMENT AND LANGUAGES

The system is written in COBOL F and FORTRAN IV G; the first of these is used for input-output, data manipulation and editing, while all calculations are written in FORTRAN. The use of special language features has been avoided as much as possible, and the system should be transferable to other computers with a minimum of modifications.

The computer presently used is the IBM System/360 Model 85, operating under MVT, at Systems Dimensions Limited in Ottawa. Internal memory requirements have been limited to 200 k bytes. The peripheral equipment needed consists of 5 tape drives (9 track, 1600 bpi), 1 card reader, 1 card punch and 1 line printer.

1.7 A COMPARISON WITH OCEANS III

The OCEANS IV system replaces the OCEANS III system in use until spring, 1970. The new system has a large number

of improvements over OCEANS III and is expanded with a fairly sophisticated data retrieval program. The major improvements are:

- (1) OCEANS IV has a partially open ended format, accepting up to 35 different parameters, of which 16 have been specified at present. OCEANS III had a closed format, accepting only 10 different pre-defined parameters.
- (2) Reversing thermometer data can be submitted for archiving and no longer have to be recopied onto Data Summary forms after calibration in the new system.
- (3) Depth and pressure are both accepted as independent variables and can both be used to retrieve data or as a reference level for dynamic height and other calculations. OCEANS III, as do systems used by most data centres, uses only depth for vertical reference.
- (4) Data retrieval is much more flexible in OCEANS IV.
- (5) More significant digits are allowed for several parameters to improve the accuracy of the system. Identifying information, such as location and depth, can also be specified with greater accuracy to improve the system's usefulness for storing nearshore and estuarine data.
- (6) The production of regular catalogues of data holdings has been greatly facilitated.

6 Section 2

2. INPUT AND DATA EDITING

2.1 DATA FORMS AND FORMATS

To provide some flexibility of input, a set of four forms has been designed:

The <u>Cruise Master</u> provides general information on a cruise and controls the conversion of "acceptable units" into OCEANS IV "file units".

The <u>Deck Sheet</u> is used to submit to CODC uncorrected temperature readings, obtained with reversing thermometers, for correction and subsequent archiving.

The <u>Data Summary</u> is used to submit, for archiving, and/or data report production, calibrated and corrected oceanographic station data such as temperature, salinity, oxygen, etc.

The <u>Bridge Log</u> can be used instead of the Station Master section of the Data Summary to submit station identifying information, such as time and location, and environmental data such as bottom depth and meteorological conditions.

Provisions have furthermore been made to accept data on the old OCEANS III forms and on tape in the NODC format.

The multitude of forms outlined above may, at first sight, appear to be somewhat confusing. They have been designed, however, to allow optimal flexibility. The combinations of input forms that can be used to cover various different situations is summarized in Table 2.a. The forms and their coding instructions are reproduced in Appendix B.

A separate form has also been designed to enter reversing thermometer calibration data for the Thermocheck program. This form, however, will be completed by CODC from the calibration certificates, and therefore will not be distributed to data submitting institutes. A sample of this Thermometer Calibration Sheet is also reproduced in Appendix B.

In the near future programs will be developed to accept STD data on magnetic tape. The Cruise Master and Bridge Log forms then could be used to record auxiliary information.

Section 2.1

Table 2.a

SUMMARY OF THE ALTERNATIVE COMBINATIONS OF FORMS
THAT CAN BE USED TO SUBMIT DATA TO CODC
(AT THE OPTION OF THE DATA ORIGINATOR)

		Possibl	e Form (Combinati	ons
Data	Purpose	Cruise Master	Deck Sheet	Data Summary	Bridge Log
Temperature readings	Correcting				
Temperature readings	Correcting and archiving				
Temperature readings plus other data	Correcting temp. and archiving all data				, Air
Temperature (corr.) and/or other data	Archiving				}

2.2 ERROR CHECKS ON REVERSING THERMOMETER DATA

Apart from a large number of edit checks performed on the input, the data is also subjected to a number of validity tests based on the results of the calculations described in Section 4.1. All terms used below are defined in Section 4.1.2. The following conditions are flagged in the output, but the data are accepted into the Thermocheck transaction file:

- (1) A difference between the two readings of a main thermometer exceeding 0.02°C or of an auxiliary thermometer exceeding 5.0°C is signalled by a verbal error message.
- (2) A difference between the calibrated mean temperatures of two protected thermometers, used at the same depth, exceeding 0.04°C is signalled by an asterisk following Mean Protected Temperature. If three protected thermometers have been used, all three are compared with each other.
- (3) If two unprotected thermometers are used, a difference between the calculated pressures exceeding (5.0 + $\Delta P/400$) is signalled by an asterisk following Observed Pressure.
- (4) A difference between observed and smoothed pressure at any level exceeding 5 dbar or 0.5%, whichever is larger, is indicated by an asterisk following Smoothed Pressure.
- (5) A smoothed pressure exceeding nominal pressure by more than 5 dbar or 0.5%, whichever is larger, is indicated by an asterisk following Wire Out.
- (6) Observed main and auxiliary temperature readings more than 1.5°C and 5°C respectively outside the calibration range are flagged by a verbal error message.

A number of other errors can be picked up by the edit routines of the program, such as the occurrence of non-numerical values in a numerical field, the absence or improper coding of the thermometer serial number, the absence of essential station identifying information, etc. These will cause rejection of individual levels or stations and the printing of a verbal error message.

2.3 ERROR CHECKS ON DATA SUMMARY ENTRIES

All data entered on Data Summary forms are subject to edit checks to determine the acceptability of each entry. These tests are described in the Systems Manual. Whenever applicable, the data are also subjected to the range checks summarized in Tables 2.b and 2.c, and to the following validity tests:

(1) Time-distance checks for consecutive stations:

where A is the vessel's cruising speed and B is given by:

$$B = \frac{1}{\Delta t} \left[(\Delta lat)^2 + (\Delta long \times cos \varphi)^2 \right]^{1/2}$$

where Δt is the time passed between two consecutive stations, ϕ their mean latitude (counting south latitudes as negative), and Δl and Δl ong the difference in their latitudes and longitudes respectively.

(2) Sigma-t check for consecutive levels. An error message is printed whenever:

where $Z_{i+1} > Z_i$ are two consecutive observed levels.

															_				
Remarks	Independent variable.	Note method codes on Cruise Master.	Can optionally be used as independent variable for retrievals. The M/C column following pressure provides room to indicate whether it is Measured or Calculated.	Note method codes on Cruise Master.	Note method codes on Cruise Master.	Note measured/calculated code on Observed Detail.	Note method codes on Cruise Master.												
Other Allowable Input Units (Decimals Allowed)	feet (1) fathoms (1)	feet (1) fathoms (1)	1	ı	1		mg-at/1 (3)	1	1	ı	1	1	1	ı	1	î	1	i	· ŧ
Range Check	a a	f	ş	-2.0 <t<30.0< td=""><td><40.0</td><td></td><td><15.0</td><td><4.0</td><td><20.0</td><td><4.0</td><td><45.0</td><td><300.0</td><td>6.5<ph<8.5< td=""><td>ı</td><td>ı</td><td>1</td><td>1</td><td>i</td><td>ı</td></ph<8.5<></td></t<30.0<>	<40.0		<15.0	<4.0	<20.0	<4.0	<45.0	<300.0	6.5 <ph<8.5< td=""><td>ı</td><td>ı</td><td>1</td><td>1</td><td>i</td><td>ı</td></ph<8.5<>	ı	ı	1	1	i	ı
Decimals Allowed	Н	Н	Н	3	m	П	2	2	2	2	Н	Н	С	2	2	0	0	0	2
Pre-printed Decimal Point	yes	yes	Yes	yes	yes	yes	no	no	no	no	no	no	ou	no	no	no	no	no	no
File Units	ш	E	ф	o.	g/kg	m/sec	m1/1	µg-at/1	µg-at/1	µg-at/1	μg-at/l	ug-at/1	pH units	mg/1	mg/1	mg/m3	µ-eq/1	µ-eq/1	µg/1
Doubtful data				*	*		*	*	*	-je	*	+	*	*	*	*	44	*	-je
Parameter	Depth of Sample	Sounding	Pressure (water)	Temperature	Salinity	Soundspeed	0xygen	PO4-P	Total P	NO2-N	NO3-N	SiO3-Si	hф	Fluoride	Diss. Org. C	Particulate C	Total Alkalinity	Carb. Alkalinity	NH3-N
eboo	1	1	1	1	1	1	4	2	9	7	00	6	A	m	O	Q	口	Ŀ	O

CODING, UNITS AND RANGE TESTS FOR OCEANOGRAPHIC PARAMETERS

Table 2.c

Parameter	File Unit	Pre-printed Decimal Point	Decimals Allowed	Other Allowable Input Units (Decimals allowed)	Remarks
Cloud Amount	WMO code 2700	N/A	1	1	
Wind Direction	WMO code 0877 ('68)	N/A	ı	ı	
Wind Speed	m/sec	ou	0	<pre>knots (0), feet/sec (0), Beaufort, stat. miles/ hour (0)</pre>	<pre>knots (0), feet/sec (0), Beaufort, stat. miles/ hour (0)</pre>
ww Code	WMO Code 4677	N/A	ı	1	
Pressure (Air)	mbar ¹⁾	Yes	Н	mm (1)	Corrections for barometer height and outside air temperature can optionally be made. Corrections are not made by the program.
Air Temperature	°C ¹)	Yes	H	°F (0)	For negative temperatures in °C add 50 to the absolute value; To enter °F, see instructions.
Wet Bulb	°C ¹⁾	Yes	П	°F (0)	See Air Temperature; Wet Bulb must be & Air Temp.
Wave Period	sec	ou	0	ı	
Wave Height	WMO code 1555	N/A	1	ı	
Swell Direction	WMO code 0885	N/A	I	ı	
Period	WMO code 3155 ('68)	N/A	1	sec (0)	
Height	WMO code 1555	N/A	1	1	

CODING, UNITS AND RANGE TESTS FOR METEOROLOGICAL PARAMETERS

12 Section 3

3. DATA RETRIEVAL AND OUTPUT

Data output from the OCEANS IV system is controlled I two programs: RETRIEVE and REPORT. The first of these can extract data from the master file according to any number of conditions as described in Section 3.2. The REPORT program takes the output of the RETRIEVE program, or the OCEANS IV transaction file, and produces printed data reports, a summary of the data or a copy of the data on punch cards or magnetic tape as described in the next section. Some data summaries, such as Station Master Catalogues, Data Inventories and Station Counts are produced directly by the RETRIEVE program; these are described in Section 3.2. The operation of both programs is determined by control cards that can be coded using the Data Extraction and Data Output Forms shown in Appendix C. Sample outputs are shown in Appendix D.

The system also produces a number of secondary output such as listings of processed Thermocheck data with a summary of reversing thermometer performance, and listings of edited data with error messages. A sample of all possible printed outputs is shown in Appendix D.

3.1 DATA OUTPUT

The REPORT program controls the output of data on punch cards, magnetic tape or in printed listings. Its major functions are:

- a) Production of Data Reports. Note that both depth and pressure are always given in the Data Reports.
- b) Computation of derived parameters and interpolated data as required for the output. The equations used are described in Chapter 4.
- c) Punching of cards or writing of magnetic tapes with data in OCEANS IV format. An auxiliary program is available to translate the OCEANS IV format into the previously used OCEANS III output format.
- d) Printing of tables with the means and standard deviations of data extracted from the master file by program RETRIEVE.

The choice of these functions, and some other details, is determined by control cards. A special form has been designed to code these control cards (Appendix C). Samples of all output listings and a description of all punch card and magnetic tape formats is given in Appendix D.

Section 3.2

The interpolation is relatively flexible and includes the following features:

- a) Interpolation can be requested for any of the chemical parameters specified on the Data Output Form. The code numbers to be used are defined on the Data Extraction Form. Temperature, pressure, salinity and soundspeed are always interpolated, if the interpolation control card is used, and need not be specified on the control card.
- b) A choice can be made between the two interpolation techniques, Reiniger and Ross' and Rattray's, both described in the next chapter.
- c) Interpolation can be requested to predefined standard depth levels (Table 7 in Fig. D.3.16) or to numerically identical standard pressure levels.
- d) If desired, the standard levels can be replaced by an arbitrary set of levels by using the "Levels to be Used for Interpolation" cards defined on the Data Output Form.

3.2 DATA EXTRACTION

Data can be extracted from the master files using program RETRIEVE. This is one of the most flexible and probably most useful programs of the OCEANS IV system. Its major functions are:

- a) To extract data from the master files according to a certain set of search conditions.
- b) To produce a count of the number of stations that would be extracted according to certain search conditions.
- c) To print a Station Master Catalogue.
- d) To print a Data Inventory (3 possible formats).

The choice of these functions is determined by control cards; in the first case RETRIEVE has to be followed by program REPORT to calculate derived and interpolated parameters and to format the data for output.

A special form has been developed to code the control cards (Appendix C). The search conditions specified are additive; e.g. any station (or level) not satisfying any of the search conditions is rejected. Any arbitrary subset of the search conditions discussed in the following subsections forms a legitimate set of control cards.

14 Section 3.2

On the "Request By" card the type of output desired is specified, along with requester name and address and a key used for sequencing the data. The output options ("search modes") are to:

- 1. Reproduce the stations successfully passing the search conditions onto an intermediate tape. Program REPORT then accepts this tape and produces punch cards, magnetic tape or a print out of the data as requested. The formats of these output options are described in Appendix D.
- 2. Count the number of stations and levels that meet a set of search conditions. The data are not actually retrieved in this case.
- 3. List a summary of all station masters accepted by the search (Appendix D). The entries are sequenced as specified on columns 65-67 on the "Request By" card. The summary shows for each station (i) the number of levels sampled, (ii) minimum and maximum sampling depth, (iii) number of samples within depth intervals delineated by the 0,75,225,500,1000, 2000,3000,5000, and 10000 metre levels, (iv) the parameters observed and (v) the percentage of levels at which each parameter is observed.
- 4. Print Data Inventory Type I. The data extracted from the file are counted, and for each one-degree square the totals counted for each of the up to 12 parts of the annual cycle specified in the "Time Interval or Season" search table. The data are counted over all years shown in the year-range field of the search table (Appendix D).
- 5. Print Data Inventory Type II. The output is similar to that of the type I inventory, except that the count within each one-degree square is broken down into up to 12 year ranges.
- 6. Print Data Inventory Type III. The data passing a search are counted by one-degree squares and printed in a semi-geographical format. The totals for one-degree squares within each Marsden square are printed in a two-dimensional grid as shown in Appendix D.

With the "Inventory Option" the one-degree square totals in the Data Inventories can be suppressed and only the totals by five and ten-degree squares will be printed. The five-degree squares are numbered in a counter-clockwise direction within each ten-degree square, and summarize the number of stations in the one-degree squares as shown:

five-deg. sq.

one-deg. squares

2

00-04, 10-14, 20-24, 30-34, 40-44 50-54, 60-64, 70-74, 80-84, 90-94 five-deg. sq.

one-deg. squares

3 # 1 55-59, 65-69, 75-79, 85-89, 95-99 05-09, 15-19, 25-29, 35-39, 45-49

The ten and one-degree squares are coded using the COTED squares system outlined in Appendix F.

The extracted data can be sorted in a sequence determined by the sort key specified under "Data Sequence". The geographical sequence is determined by the COTED squares system described in Appendix F. The data can be put into cruise sequence by using the identification "I" as first part of the sort key. The sequence then will be determined by country, institute code, CODC cruise number and consecutive station number.

All data extractions are based on the Station Master file unless otherwise noted. If a station is accepted, all levels will be brought forward to the intermediate output utilized by the REPORT program. In those cases where individual levels are searched, the levels not meeting the search conditions are marked by a "not acceptable" key, and these can optionally be rejected in the output of the REPORT program.

3.2.1 Area Search

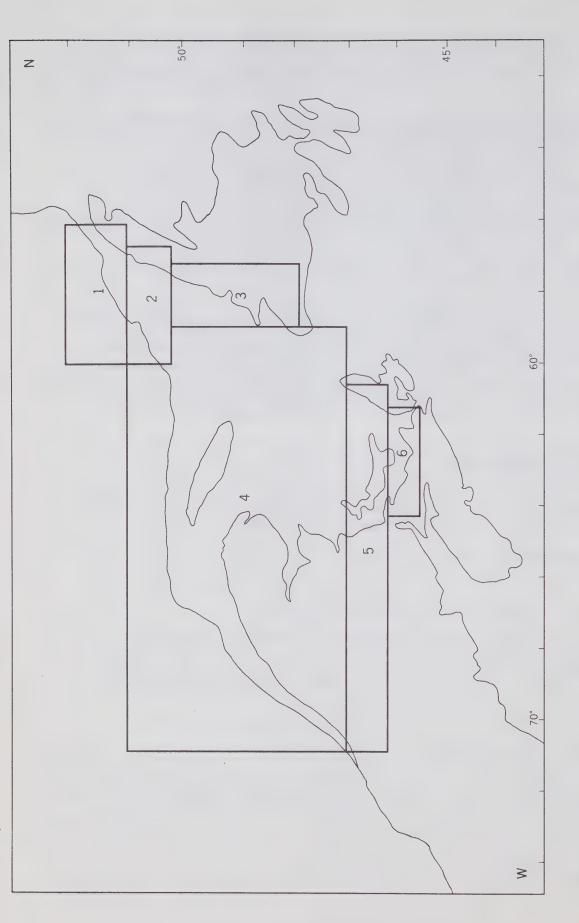
Up to ten different rectangular areas can be specified for an area search. All data in the Gulf of St. Lawrence, for example, can be retrieved using the six rectangles shown in Fig. 3.a. In this case no Bay of Fundy or Atlantic Ocean data will "contaminate" the retrieved data.

3.2.2 Time Interval or Season Search

Data can be extracted for a certain continuous period or for certain seasons over all years. Up to twelve entries can be made, mainly for the purpose of controlling the Inventory Options 1 and 2. For a straight data retrieval, however, multiple entries can also be made.

3.2.3 Cruise Search

Data for up to ten individual cruises can be extracted simultaneously. Larger numbers can be retrieved if the cruise numbers can be grouped as suggested on the Data Extraction Form.



areas such as the Bay of Fundy or the Atlantic Ocean. The numbers 1-6 indicate the six rectangles used in this case. Graphical explanation of the method of setting up an area excludes from the extracted data file all data from other search for all data in the Gulf of St. Lawrence, which Fig. 3.a

Section 3.2.4

3.2.4 Parameter Search

The simultaneous availability of up to 14 different parameters can be checked. Optionally, an upper and lower limit of acceptability can be assigned to each parameter. This search acts on both the Station Master and the Level Master files. If a parameter has been observed on a station, then all individual levels are checked for its presence. Any levels where the parameter in question has not been observed is marked by a "not acceptable" key, and can optionally be rejected by program REPORT when the data are punched on cards or written on magnetic tape.

3.2.5 Depth Search

Stations can be extracted from the file according to three different conditions:

- 1) The bottom depth must be observed and must be between the minimum and maximum values indicated.
- 2) Bottom depth is not always indicative of the depth to which a station extends. The sampling levels therefore can also be compared to a minimum and a maximum value. All stations with at least one observed level deeper than the minimum level and at least one level shallower than the maximum level are extracted.
- 3) Finally, the relation between sampling levels and bottom depth can be examined and all stations with at least one observed level within a specified distance off the bottom extracted.

This search is done on the Station Master file. A special routine can be used, however, to mark all levels, except the deepest, of the extracted stations as "not acceptable" thus deleting them from the output generated by the REPORT program.

3.2.6 Meteorological Data Search

The availability of any meteorological parameter on a Station Master can be checked, and only stations containing the desired information are extracted.

3.2.7 Data Distribution Search

For some derived parameters, such as geopotential anomaly, it is important that a sufficiently large number of adequately spaced levels have been observed. In this search the presence of at least one observed level within each of the defined intervals is checked for all levels between the surface and the

18 Section 3.2.4

deepest observed level of the station. The search condition can be made somewhat less stringent by allowing a certain number of "blank" intervals, that is intervals without any observed levels. This number can be defined under "a" (See Data Extraction form, Appendix C). If left blank, "a" is taken as zero. This is obviously a search into the Level Master File. Data outside the interval defined by the first and last levels specified are marked as "not acceptable" and can optionally be suppressed by program REPORT when the data are punched on cards or written on magnetic tape.

4. CALCULATIONS

4.1 REVERSING THERMOMETER CORRECTIONS

4.1.1 Correcting the Readings

The calibrated temperature T is calculated from the raw temperature readings R by applying two corrections. The index correction compensates for errors in the etched thermometer scale and the expansion correction compensates for the difference between reversal temperature and reading temperature (as indicated on the auxiliary thermometer). The mean temperature and pressure are then calculated for each level and, if more than one observation is taken at any level, the overall means are determined. The index and expansion corrections are calculated as follows:

4.1.1.1 Index Correction

The index correction I is added to (or subtracted from, if negative) the auxiliary and the main thermometer readings. This correction is defined for a number of points on the thermometer calibration cards. For intermediate points linear interpolation is used, for points outside the scale the nearest calibration point is used.

4.1.1.2 Expansion Correction for a Protected Thermometer

For a protected thermometer, the expansion correction C is calculated (Hansen, 1934) by:

$$C = \frac{(T_{p}' - t) (T_{p}' + V_{o})}{K - 1/2 (T_{p}' - t) - (T_{p}' + V_{o})}$$

where T_p' is a main thermometer reading adjusted by the index correction, t the corresponding auxiliary thermometer reading adjusted by its index correction, and V_O and K calibration constants. The latter of these is the reciprocal thermal coefficient of expansion of the main thermometer, and V_O is the volume below the 0°C mark at a 0°C temperature. The corrected protected temperature then is given by: $T_p = T_p' + C = R + I + C$.

4.1.1.3 Expansion Correction for an Unprotected Thermometer

For an unprotected thermometer, the expansion correction (Keyte, 1964) is given by:

$$C = \frac{(T'_{u} + V_{o}) (T_{p} - t_{u})}{K - 1/2(T_{p} - t_{u})}$$

where Tu is a reading of an unprotected thermometer adjusted by the index correction, tu the corresponding auxiliary thermometer reading similarly adjusted, and Tp the mean calibrated and corrected protected thermometer temperature. The corrected unprotected temperature then is given by: $T_{ij} = T_{ij}^{\dagger} + C = R + I + C$.

4.1.2 Calculating Observed and Smoothed Pressures

"Observed" pressure is calculated for all levels where unprotected thermometers have been used. A curve is fitted to the observations and a smoothed pressure value determined for each observed level. The procedure is outlined stepwise following a definition of all variables used. All depths are in metres and pressures in decibars.

4.1.2.1 Definitions

Lm Total Wire Out

= Distance in metres along the wire between the water surface and the deepest bottle. (Given on the Deck Sheet).

L; Wire Out

= Distance between the surface and bottle number i, measured along the wire.

L_{ni} Planned Wire Out = Planned distance along the wire for bottle number i; may or may not be equal to Wire out. Differences occur, for example, when wire out is adjusted to get the deepest bottle at a fixed distance from the bottom. (Given on the Deck Sheet).

Pn; Nominal Pressure = A function of wire out.

Poi Observed Pressure = A function of protected and unprotected thermometer readings.

P si Smoothed Pressure = Pressure obtained after smoothing observed pressures. Alternately this term is used to describe pressures obtained by other techniques, such as straight interpolation or from depth using the hydrostatic equation.

α Wire Angle = Angle between the vertical and the wire at the surface. (Given on the Deck Sheet)

4.1.2.2 Wire Out

Wire out L_i is calculated from total wire out and planned wire out. The difference between total wire out and planned wire out of the deepest bottle of a cast is ΔL . Wire out at any other depth then is given by:

$$L_i = L_{pi} + \Delta L = L_{pi} + (L_T - L_{pi} max)$$

4.1.2.3 Nominal Pressure

Nominal pressure P is calculated:

$$P_{\text{ni}} = \frac{9.80665}{10} (1.02736L_{i} + 2.465 \times 10^{-6}L_{i}^{2} - 1.847 \times 10^{-11}L_{i}^{3})$$

where L_i is wire out for planned wire out $L_{\rm pi}$. This equation has been derived by Fofonoff (pers. communication) for the North Pacific, but it can be used anywhere as a first approximation.

4.1.2.4 Observed Pressure

Observed pressure is calculated from the mean protected temperature \textbf{T}_{i} at $\textbf{Z}_{n\,i}$ and the unprotected temperature $\textbf{T}_{u\,i}$:

$$P_{oi} = \frac{T_{ui} - T_{i}}{Q} \times g_{o}$$

where the pressure coefficient Q is given in ${}^{\circ}\text{C/kg/cm}^2$ and g = 9.80665 is standard gravity. If two unprotected thermometers are used at any level, P_{Oi} is calculated for both observations and the mean is used for further computations.

4.1.2.5 Smoothed Pressure

22

Smoothed pressure is calculated from true depth as outlined in Section 4.2 if pressure has not been observed. Otherwise, it is calculated as described below.

If pressure has been observed at one level only, a second degree curve is fitted to the observation. The curve is constrained to meet the surface ($P_{n1} = P_{o1} = 0$) under the observed wire angle α :

$$P_{nk} - P_{ok} = a_2 P_{nk}^2 + (1 - \cos \alpha) \cdot P_{nk}$$

where k=1. The unknown constant a₂ is solved exactly and the smoothed pressure P_{sj} at all other levels is then calculated using the same equation, substituting P_{ok} by P_{sj} and P_{nk} by P_{nj} .

Below the level L_K of the deepest pressure observation pressure is determined by linear extrapolation from P_{SK} and $P_{S,T}$ at a level L_T = 0.8 L_K :

$$P_{sj} (L_{j} > L_{k}) = \frac{P_{sK} - P_{sJ}}{L_{K} - L_{J}} (L_{j} - L_{J}) + P_{sJ}$$

For levels $L_j > 1.15 \times L_K$, however, smoothed pressure is calculated by:

$$P_{sj}$$
 (L_j > 1.15 x L_k) = P_{sK} + (P_{nj} - P_{nk})

If pressure has been observed at K = 2 or 3 levels, a polynomial of order K is fitted by least squares to the difference between nominal and observed pressures. If K \geqslant 4, a fourth order polynomial is fitted. In all these cases the polinomial is restrained to reach the surface (P_{n1} = P_{o1} = 0) under the observed wire angle α :

$$P_{nk} - P_{ok} = a_4 P_{nk}^4 + a_3 P_{nk}^3 + a_2 P_{nk}^2 + (1 - \cos \alpha) P_{nk}$$

Section 4.2

where k = 1,...,K. The unknown constants a_2 , a_3 and a_4 are solved by least squares and the smoothed pressure P_{sj} at all observed levels is then calculated using the same equation, replacing P_{ok} by P_{sj} and P_{nk} by P_{nj} .

At levels below the deepest observed pressure, P_{sj} is again determined as outlined above for the case of K = 1.

4.1.2.6 True Depth When Pressure Not Observed

True depth is only calculated from wire out and wire angle if pressure has not been observed. In this case, true depth is given by:

$$Z_{ti} = L_{i} \cos \alpha$$

down to the deepest observed depth above 110 metres, \mathbf{Z}_{tj} , and below that by:

$$Z_{ti} = Z_{tj} + (L_i - L_j).$$

4.2 PRESSURE AND DEPTH

4.2.1 Calculations

Both the Thermocheck and the OCEANS IV Edit program convert depth to pressure and vice-versa. In the Thermocheck program pressure is calculated and smoothed before conversion to depth. If no reversing thermometers are used, depth is calculated from wire out and then converted to pressure. The OCEANS IV Edit program can accept either pressure or depth, and the missing level indicator is calculated (if both are given, no calculations are performed). The depth to pressure and pressure to depth conversions are outlined below and justified in the next subsection.

The hydrostatic equation relates depth, Z, to the pressure, P, and the density, ρ , of the water column:

$$z_{i} = 10 \int_{0}^{Pi} \frac{1}{\rho g} dp \qquad 4-2-1$$

24 Section 4.2.2

where $g = g_0 = 9.80665$ is standard gravity in the Thermocheck program and $g = g(\phi z)$ in the OCEANS Edit program (see Section 4.3.1). This equation can be integrated, using Simpson's rule to find the depth of a level of known pressure. For stations with few or no observations near the surface, however, the results may become erratic, and nearby stations with differing distributions along the vertical of the observations then may give incompatible results. A fairly sophisticated logic would be required to determine the validity of the results.

For these reasons a simplified version of the hydrostatic equation is used in OCEANS IV:

$$Z_{i} = 10 \frac{P_{i}}{\rho_{mi} g} \qquad 4-2-2$$

where ρ_{mi} is the mean density above the level Z_i (Table 4.a). In a first approximation Z_i^i is calculated for ρ_{mi} at a depth numerically equal to P_i . This is followed by a second approximation taking ρ_{mi} at the calculated depth Z_i^i . The depthdensity table can, for special projects, easily be substituted by another depth-density relationship.

Pressure can similarly be computed from depth by inverting equation 4-2-2:

$$P_{i} = \frac{\rho_{mi} g}{10}$$
 Z_{i} 4-2-3

using the same depth-density table.

4.2.2 Justification

Integration of the hydrostatic equation undoubtedly gives the best numerical conversion of pressure to depth, provided that density has been observed at an adequate number of levels. The difference between this and using a standard depth-density table, however, is small compared with the uncertainty in \mathbf{Z}_i caused by errors in the pressure measurement. The argument will be carried through for pressure determinations with a

Section 4.2.2 25

Table 4.a

DEPTH-DENSITY TABLES

The North Atlantic table for ρ_m is used as the standard depth-density relationship in OCEANS IV. The tables are taken from the "Handbook of Oceanographic Tables" (NAVOCEANO, 1966).

Depth (meters)	North Atlantic ρm	Northeast Pacific Pm	Arctic Pm	Mediterranean
0 100 200 300 400	1.0262 1.0264 1.0267 1.0270 1.0274	1.0248 1.0255 1.0261 1.0267	1.0279 1.0281 1.0283 1.0285 1.0288	1.0282 1.0286 1.0289 1.0293 1.0296
500 600 700 800 900	1.0278 1.0281 1.0285 1.0288 1.0291	1.0272 1.0276 1.0280 1.0283 1.0286	1.0290 1.0292 1.0295 1.0297 1.0299	1.0300 1.0302 1.0305 1.0307 1.0310
1,000 1,500 2,000 2,500 3,000	1.0294 1.0308 1.0321 1.0334 1.0346	1.0289 1.0304 1.0318 1.0331 1.0344	1.0302 1.0314 1.0326 1.0338 1.0351	1.0312 1.0324 1.0335 1.0346 1.0358
3,500 4,000 4,500 5,000	1.0358 1.0370 1.0383 1.0395	1.0356	1.0363 1.0375 1.0387 1.0400	0 C A C B B

26 Section 4.2.2

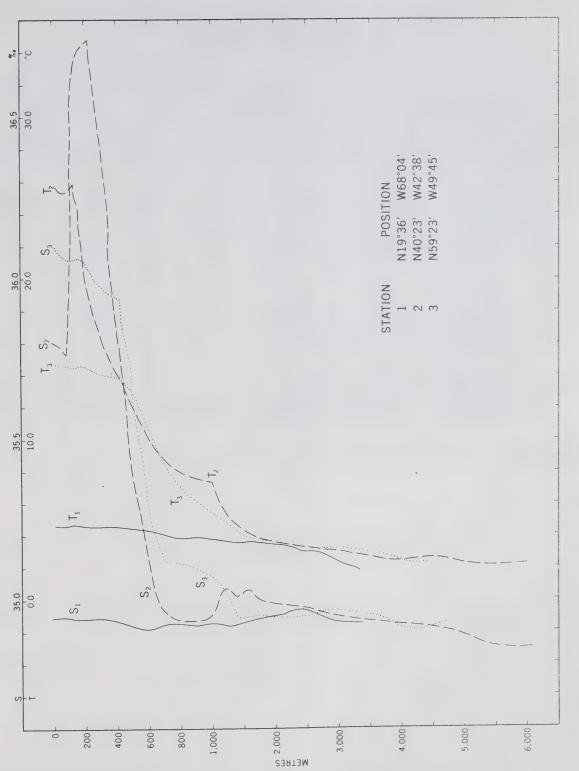
reversing thermometer. The results will be valid in general unless either depth or pressure determinations can be significantly improved.

In the past decades several studies have been published relating to the accuracy of depth determinations obtained with reversing thermometers. Wüst (1933) originally estimated a mean depth error of 5 metres for levels between 100 and 1000 m and of 0.4 to 0.6% for deeper levels. This estimate is based on an estimate of the errors in Q, ρ_{m} and $\Delta t = T_{u} - T_{p}$ for thermometers used on the German Meteor Expedition in 1925-1927. Whitney (1957), in a more detailed analysis of possible error sources involved in the usage of reversing thermometers, but excluding the effect of ρ_{m} , finds a somewhat lower probable error range of 0.2 - 0.5% for depths below 1000 m. These are estimates of the depth error, but can equally well be considered as estimates of the pressure error, since the effect of gravity changes have not been taken into account.

Whitney's and Wüst's lower estimates may well be on the low side in view of the results of a recent comparison of thermometer calibrations carried out by four different laboratories (Martin et al, 1968). They found a mean error in the Q-factor determinations of 0.36% and a standard deviation of the differences between laboratories of 0.41% (for Q measurements under pressures of 2000 and 3000 db). Martin et al also found significant systematic deviations between the determinations of the index correction (S.D. = .016°C), and small deviations for Vo, but these may not affect thermometers calibrated by the same laboratory. Errors in pressure are determined by the relative errors in the index correction and Vo between the thermometers used, but by the absolute error in Q. These results suggest a 95% confidence limit for the pressure measurements of at least 0.8% instead of the 0.2 to 0.6% indicated by Whitney and Wüst.

A second source of errors originates from the horizontal and vertical variability of the gravity field. In the Thermocheck program gravity is taken as constant. In actual fact it varies with latitude (± 0.26%), increases with depth (0.1% at a depth of 5000 m) and is subject to a local variability (usually remaining well within ±0.01% over the open ocean). The major variability factor thus is dependent on latitude, which may introduce errors in the pressure to depth conversion up to plus or minus 0.26%. This effect was pointed out by Sturges (1968), who argued that equation 4-2-2 should be replaced by:

$$Z_{i} = 10 \frac{P_{i}}{\rho_{mi} g(\phi)}$$
 4-2-4



Stations used to test effect of the depth-density table on depth-pressure conversions. 4.9 Fig.

Table 4.b

INFLUENCE OF $\rho_{\,\,\text{m}}$ ON THE DETERMINATION OF DEPTH FROM PRESSURE.

	Z			ΔZ		Max.
Stat. Number	Station Data	N. Atl.	Arct.	N.E. Pac.	Med.	deviation in %
1	972.0 2131.2 2996.5 3953.9 4907.3	-0.6 -0.7 -0.9 -1.2 -2.1	-1.3 -1.7 -2.3 -3.0 -4.0	-0.1 -0.1 -0.3 -0.9	-2.3 -3.4 -3.6 -	.24 .16 .12 .07
2	999.4 1965.4 2962.2 3960.4 4664.7	0.0 0.0 -0.1 -0.4 -1.2	-0.7 -1.0 -1.6 -2.3 -3.2	+0.5 +0.6 +0.4 +0.0	-1.7 -2.7 -3.6 -	.17 .14 .12 .06
3	1002.3 2083.3 3370.1	+0.6 +0.6 +0.5	-0.2 -0.3 -1.1	+1.1 +1.2 +1.2	-1.1 -2.1 -	.11 .10 .04

Section 4.3

where $g(\phi)$ is gravity as a function of latitude. In the OCEANS IV edit, the areal variability of gravity has been taken into account (see Section 4.3.1 on gravity). The Deck Sheet data do not include location, and the Thermocheck program therefore cannot include the latitude correction.

The errors due to incorrect calibrations and gravity variations can be compared with differences introduced by varying the depth-density table, which under normal conditions remain within 2.5 metres at a depth of 1000 m and less than 0.2% for deeper levels. These figures have been determined experimentally by taking three stations, one in the Labrador Sea (N59°23', W49°45') and two in the North Atlantic Ocean (N40°23', W42°38' and N19°36', W68°04'), see Fig. 4.a, and calculating the depth using the actual observations and four different depth-density tables. The depth-density tables used are given in Table 4.a and the results in Table 4.b. Errors are small even when the Mediterranean depth-density table is used. Excluding this area, where $\rho_{\rm m}$ is exceptionally high due to a high salinity, errors remain within 1.3 metres at 1000 m and within 0.08% at deeper levels.

The use of a standard depth-density table thus seems to be justified for all open ocean waters. The error introduced is less than 0.08%, which can be compared with an estimated error in the pressure measurement of 0.5 to 0.8%. If standard gravity is used, as in the Thermocheck, an additional error, increasing from 0 at latitudes of 45° to plus or minus 0.26% at the equator or the poles respectively, is introduced due to the difference between local and standard gravity.

4.3 DERIVED PARAMETERS

4.3.1 Gravity

Gravity is calculated as a function of latitude $\boldsymbol{\varphi}$ and depth $z\colon$

$$g(\phi) = 9.780356 \times \{1 + 5.2885 \times 10^{-3} \sin^2 \phi - 5.9 \times 10^{-6} \sin^2 (2\phi)\}$$

$$g(z\phi) = g(\phi) \times (1 + 2.28 \times 10^{-7} \times z)$$

The equations for $g(\phi)$ are, for example, given in the Smithsonian Tables (List, 1966) and in the Handbook of Physics and Chemistry (CRC, 1965); the equation for $g(z\phi)$ as a function of $g(\phi)$ in Proudman (1953, page 2).

30 Section 4.3.2

Gravity varies over a range of 0.052 m/sec^2 with latitude, increases by 0.011 m/sec^2 at a depth of 5000 m and is subject to a local variability usually remaining within a range of plus or minus 0.001 m/sec^2 over the open ocean.

The effect of gravity on the pressure-depth conversion is discussed in some detail in Section 4.2.2. For the purpose of the pressure-depth conversions in the OCEANS IV Edit and in the calculations of the potential energy anomaly, the above equations for gravity are used.

In the pressure-depth conversions and the observed pressure calculations in the Thermocheck, however, a constant value of gravity, $g_0 = 9.80665$, is used. It is based on early measurements of g_0 at a latitude of 45°. This value is presently also used to define the relation between a kilogramforce and the Newton (Anderton et al, 1967), although more recent measurements show that it is slightly too high. List (1966) indicates a value of 9.8062 for g_0 , at 45°. The difference between these two values of g_0 , however, is negligibly small for the present purpose.

4.3.2 Sigma-t

4.3.2.1 Definition

The specific gravity anomaly of seawater at atmospheric pressure, sigma-t, is defined by:

where $\rho_{s,t,\rho=0}$ is the specific gravity of seawater as a function of salinity S, temperature T, and oceanographic pressure P = 0.

Traditionally the terms specific gravity and density have been confused (see, for example, Cox, 1964). Strictly speaking, specific gravity is defined as the ratio of the mass of volume of water over the mass of an equal volume of pure water at a temperature of 4°C and under a pressure of one standard atmosphere; it is a dimensionless parameter. Density, on the other hand, is defined as the mass of a unit volume of water, and has a dimension of mass over volume. Up to 1964 the accepted unit of volume, the litre, was defined as the volume of l kilogram of pure water at 4°C and l atm., and the numerical values of specific gravity and density were equal. At the

Section 4.3.3

General Conference of Weights and Measures in October 1964 the unit of volume has been redefined to be the volume of 1 cubic decimetre. This introduces a slight, but noticeable, difference between specific gravity and density, as the density of pare water now is equal to 1.000.027 g/cm³ instead of unity (CRC, 1965).

The influence of this on sigma-t is negligibly small, since the latter is defined as the difference between two specific gravity or two specific density values, respectively.

4.3.2.2 Equations

Tables and formulae giving σ_t as a function of temperature and salinity have been developed emperically by Knudsen (1901). His original equations have been rewritten by analytical expansion to give the polynomials presented below, rounding off the coefficients to a maximum of 10 significant digits:

$$G_{t} = \frac{\sum a_{i}T^{i}}{T + a_{o}} + \sum_{i} \sum_{j} A_{ij} G_{o}^{i} T^{j}$$

$$G_{0} = \sum_{j} b_{j} (S - 35)^{j}$$

where a_i, A_{ij} and b_j are constants given in Table 4.c. This version of Knudsen's equations was derived by Fofonoff et al. in 1958, small corrections have since been made in the coefficients a₁, a₃ and a₄.

The modified Knudsen's equations given above have originally been developed to save on memory requirements in a small computer. With the computers presently in use this is no longer necessary, and it would be theoretically more correct to use Knudsen's original equations. This however, is not done in OCEANS IV, mainly because Fofonoff's equations have been much more widely accepted for computerized routine calculations than Knudsen's.

4.3.3 Specific Volume Anomaly

4.3.3.1 Definition

Specific volume, α , is defined as the volume occupied by a unit weight of water with a salinity S, temperature T and under an oceanographic pressure P, and it is expressed in units of cubic centimetres per gram. Specific volume thus is the inverse of the density d of a sample. The relation between α , d

and the specific gravity ρ , used to define σ_t , is given by:

$$\alpha_{stp} = \frac{1}{d_{stp}} = \frac{1}{\rho_{stp} \times 1.000.027}$$

The difference between specific gravity and density is discussed in the preceding section. The specific volume anomaly δ_{stp} is a measure of the difference between the specific volume of a sample and that of water with S = $35^{0}/00$, T = 0°C and under the same pressure P:

s,t,p =
$$\alpha$$
s,t,p - α 35,0,P

and is usually given in units of 10⁵ cm³/gr. The difference in the difficultions of specific density on 8 this is a negligible small, when we order leftered 4.3.3.2 Equations

The equations for α_{stp} have been developed emperically be Ekman (1908). They have been rewritten for ease of programming on a small computer by Fofonoff et al. (1958). The derivations, which are based on an analytical expansion of the original equations and a recombination of terms, have not been fully documented, but have been thoroughly checked (personal communication, Fofonoff). The equations are:

$$\alpha'_{tsp} = \frac{1}{1+10^{-3}\sigma_{t}} \left\{ 1 + \frac{a_{i}P}{1+a_{2}P} + \underbrace{\xi \xi \xi}_{ijk} A_{ijk} P^{i}\sigma_{o}^{j}T^{k} \right\}$$

$$\alpha'_{35,0,p} = \underbrace{\xi d_{i}P^{i}}_{a_{2}+a_{3}P}$$

and the specific volume anomaly is given by:

$$\delta(stp) = (\alpha_{stp} - \alpha_{st,o,p})$$

Table 4.c

SIGMA-T CONSTANTS

a_0	=	67.26	A 2 0	=	0
a ₁	=	+4.53168 42620	A 2 1	=	$+1.8030 \times 10^{-5}$
a ₂	=	-0.54593 91107	A 2 2	=	-8.164×10^{-7}
a ₃	=	-1.98248 39871 x 10^{-3}	A 2 3	=	$+1.667 \times 10^{-8}$
a ₄	=	$-1.43803\ 0609\ x\ 10^{-7}$			
A 1 0	=	1.00000 00000	b ₀	=	28.12634 861290
A	=	-4.7867×10^{-3}	b ₁	=	+0.80597 373759
		$+9.8185 \times 10^{-5}$	b ₂	=	+2.28129 3021 x 10 ⁻⁴
Α	=	-1.0843×10^{-6}	b,	=	$+6.76786$ 1356 x 10^{-6}

Table 4.d

SPECIFIC VOLUME CONSTANTS

a ₁ a ₂ a ₃	=	-4.886 x 10 ⁻⁶ 1.0 1.83 x 10 ⁻⁵	$A_{2\ 0\ 0}$ $A_{2\ 0\ 1}$ $A_{2\ 0\ 2}$		-6.68×10^{-14} -1.24064×10^{-12} $+2.14 \times 10^{-14}$
A ₁₀₀ A ₁₀₁ A ₁₀₂ A ₁₀₃	=	-2.2072×10^{-7} +3.6730 × 10 ⁻⁸ -6.63 × 10 ⁻¹⁰ +4.00 × 10 ⁻¹²	A ₂₁₀ A ₂₁₁ A ₂₁₂		-4.248×10^{-13} +1.206 × 10^{-14} -2.000 × 10^{-16}
A ₁₁₀	=	$+1.725 \times 10^{-8}$ -3.28×10^{-10} $+4.00 \times 10^{-12}$	A ₂₂₀ A ₂₂₁ A ₃₀₁	=	$+1.8 \times 10^{-15}$ -6.0×10^{-17} $+1.5 \times 10^{-17}$
A ₁₂₀ A ₁₂₁		-4.50×10^{-11} +1.00 × 10^{-12}			

The constants a_i , $A_{i\,j\,k}$ and d_i are given in Table 4.d and σ_o and σ_t have been defined in the preceding section.

Ekmen's original equations are not used in OCEANS IV for reasons similar to those leading to the rejection of Knudsen's original equations for sigma-t (see preceding section).

4.3.4 Sound Speed

4.3.4.1 Definition

Sound speed is the speed of propagation of sound waves through the water. It is independent of frequency, except in very shallow water or for very low frequencies when the wave length is of the same order of magnitude as the bottom depth.

4.3.4.2 Equation

Sound speed is a function of salinity, temperature and pressure, and is calculated using Wilson's (1960) equation:

$$V = \sum_{ijk} V_{ijk} Q^{i} (S - 35)^{j} T^{k}$$

where Q is the absolute pressure in kg/cm^2 , which can be calculated from P (CRC, 1965):

$$Q = 1.003,23 + 0.101,971,6 \cdot P$$

The constants V_{ijk} are given in Table 4.e. Wilson's equation has been calibrated for the full range of salinities, temperatures and pressures normally occurring in the open ocean.

4.3.5 Geopotential Anomaly

4.3.5.1 Definition

Two alternate methods of calculating geopotential anomaly (frequently also called dynamic height anomaly) are available, depending on whether output is required for predetermined depth levels or isobaric surfaces.

If output is required for fixed depth levels, the same calculations formerly used in OCEANS III will be provided:

Section 4.3.5

Table 4.e

SOUND VELOCITY CONSTANTS

V 000	=	+1449.14	V 110	=	+7.7016	X	10 5
V 0 0 1	emany emanys	+4.5721	V 111	==	+3.1580	X	10-8
V 0 0 2	emparis	-4.4532×10^{-2}	V ₁₁₂	==	+1.5790	X	10-9
V 0 0 3	-	-2.6045 x 10 ⁻⁴					
V 0 0 4	=	$+7.9851 \times 10^{-6}$	V 200		+1.0268	X	10-5
			V 2 0 1		-2.5294		
V 0 1 0	-	+1.39799	V 2 0 2	=	+1.8563	X	10-9
V 0 1 1	==	-1.1244×10^{-2}					
V 0 1 2	opens.	+7.7711 x 10 ⁻⁷	V ₂₁₀		-1.2943	X	10-7
V 0 2 0	==	+1.69202 x 10 ⁻³	V 3 0 0		+3.5216		
			V 3 0 1	=	-1.9646	X	10-10
V ₁₀₀	=	$+1.60272 \times 10^{-1}$					
V_{101}	=	-1.8607 x 10 ⁻⁴	V 400	=	-3.3603	X	10-12
V 1 0 2	=	$+7.4812 \times 10^{-6}$	400				
V 103	=	+4.5283 x 10 ⁻⁸					

$$\Delta D(z_n) = \int_{0}^{P(z_n)} \left[\alpha_{stp} - \alpha_{3s,o,p} \right] dp = \int_{0}^{P(z_n)} \delta(stp) dp$$

where $\Delta D(Z_n)$ is the geopotential anomaly in dynamic metres (10⁵ ergs/g), $P(Z_n)$ the pressure at a depth Z_n , and $\delta_{\text{stp}} = \frac{1}{\alpha_{\text{stp}}}$ is defined in Section 4.3.3.

If output is required for isobaric surfaces, the following equation will be used:

$$\Delta D(P_n) = \int_0^{P_n} \delta(stp) dp$$

where P_n is the pressure at the desired isobaric surface. This method is presently used by Bedford (personal communication, W. Forrester; see also Reiniger et al, 1968-A).

4.3.5.2 Calculations

Both equations are evaluated using the trapezoidal rule:

$$\Delta D(Z_n) = \frac{1}{2} \sum_{i=1}^{n} \left\{ \delta(\operatorname{stp}(z_i)) + \delta(\operatorname{stp}(z_{i-1})) \right\} \times \left\{ P(z_i) - P(z_{i-1}) \right\}$$
4.3.1

and

$$\Delta D(P_n) = \frac{1}{2} \sum_{i=1}^{n} \left\{ \delta(stp_i) + \delta(stp_{i-1}) \right\} \left\{ P_i - P_{i-1} \right\} 4.3.2$$

where $i = 1, \ldots, n-1$ are the observed levels Z_n and P_n respectively.

The accuracy then is improved by making successive approximations. Using Reiniger and Ross' interpolation method (Section 4.4.2), the density profile is defined, and the number of points used to evaluate (4.3.1) or (4.3.2) is successively doubted until the difference between successive approximations falls below 0.001 dynamic metres. Doubling the number of points is accomplished by taking values for levels midway between each pair (Z_i, Z_{i-1}) or (P_i, P_{i-1}) respectively.

Section 4.3.6 37

The basic assumption behind this approximation procedure is that the true profile of a parameter can be approximated better by a series of hyperbolic interpolations than by a series of straight lines connecting the observed points. No study has been made to determine whether this leads to a real improvement of the results.

4.3.5.3 Limitations

Geopotential anomaly is not calculated if the first observed depth Z_1 (or pressure P_1) exceeds 10. For $0 < Z_1 \leqslant 10$ or $0 < P_1 \leqslant 10$ the surface value of δ is taken to be equal to $\delta(Z_1)$ or $\delta(P_1)$ respectively.

4.3.6 Potential Energy Anomaly

4.3.6.1 Definition

The potential energy anomaly χ_n at a depth \mathbf{Z}_n relative to the surface is defined by:

$$\chi_n = \frac{1}{9} \int_{0}^{P(Z_n)} P \delta d\rho$$

where g is the gravity acceleration (Fofonoff, 1962). It is expressed in units of 10^8 ergs/cm². If output for fixed pressure levels is required, $P(Z_n)$ is replaced by P_n .

4.3.6.2 Calculations

The above equation is evaluated using the trapezoidal rule:

$$\chi_{n} = \frac{1}{2g} \sum_{i=2}^{n} (P_{n} \delta_{n} + P_{n-i} \delta_{n-i}) (P_{n} - P_{n-i})$$

The accuracy of the result can be improved by a similar procedure as outlined for geopotential anomaly, using successive approximations doubling the number of levels. For these intermediate levels δ is given by Reiniger and Ross' interpolation formula (Section 4.4.2).

Similar calculations can be made to standard pressure levels.

4.3.6.3 Limitations

The potential energy anomaly is not calculated if the first observation is taken at a pressure level P₁>10; for 0<P₁ \leqslant 10 the surface value of δ is taken equal to δ (P₁).

4.3.7 Potential Temperature

4.3.7.1 Definition

Potential temperature is the temperature that a water sample would attain if raised adiabatically to the sea surface.

4.3.7.2 Calculations

The equations to calculate the potential temperature θ have been developed by Fofonoff et al (1958). The equations below are taken from Ralya (1968).

$$\Delta \theta = \sum_{i} \sum_{j} \sum_{k} A_{ijk} P^{i} S^{j} T^{k}$$

where

$A_{100} = -1.60 \times 10^{-5}$	$A_{120} = +4.1 \times 10^{-9}$
$A_{101} = +1.014 \times 10^{-5}$	$A_{200} = +9.14 \times 10^{-9}$
$A_{102} = -1.27 \times 10^{-7}$	$A_{201} = -2.77 \times 10^{-10}$
$A_{103} = +2.7 \times 10^{-9}$	$A_{202} = +9.5 \times 10^{-13}$
$A_{110} = +1.322 \times 10^{-6}$	$A_{300} = -1.557 \times 10^{-13}$
$A_{111} = -2.62 \times 10^{-8}$	300

4.3.8 Sigma-θ

Sigma- θ is calculated as Sigma-t, replacing temperature T by the potential temperature θ .

4.4 INTERPOLATION ROUTINES

A choice of two interpolation methods is provided to interpolate observed or derived parameters to non-observed levels: the modified Rattray (1962) and the Reiniger and Ross (1968) methods. Both methods use two hyperbolic functions, fitted to partially overlapping groups of three points around the desired interpolation depth $Z_{\bf i}$. The value $A_{\bf i}$ of the observed variable A

Section 4.4.1

at the depth \mathbf{Z}_{i} is obtained by taking the arithmetric mean or a weighted mean of the two hyperbola respectively.

4.4.1 Modified Rattray Interpolation Method

Let the parameter A take the values A_{j-2} , A_{j-1} , A_{j} , A_{j+1} at the depths Z_{j-2} , Z_{j-1} , Z_{j} , Z_{j+1} , and let A_{i} be its interpolated value at a depth Z_{i} such that $Z_{j-2} < Z_{j-1} < Z_{i} < Z_{j} < Z_{j+1}$. Rattray (1962) then gives for A_{i} the following equation:

$$A_i = \frac{1}{2} \left(A_i' + A_i^2 \right)$$

where A_i^1 and A_j^2 are obtained by three-point interpolations using Z_{j-2} , Z_{j-1}^1 , Z_{j}^1 and Z_{j-1} , Z_{j}^2 , Z_{j+1}^2 respectively:

$$A_{i}' = Y_{j-2}' A_{j-2} + Y_{j-1}' A_{j-1} + Y_{j}' A_{j}$$

$$\chi'_{j-2} = \frac{(Z_i - Z_{j-1})(Z_i - Z_j)}{(Z_{j-2} - Z_{j-1})(Z_{j-2} - Z_j)}$$

$$Y'_{j-1} = \frac{(Z_i - Z_{j-2})(Z_i - Z_j)}{(Z_{j-1} - Z_{j-2})(Z_{j-1} - Z_j)}$$

$$\chi_{j}' = \frac{(Z_{i} - Z_{j-2})(Z_{i} - Z_{j-1})}{(Z_{j} - Z_{j-2})(Z_{j} - Z_{j-1})}$$

and A_1^2 is calculated similarly from the function χ^2 by replacing j with j+l in the above equations.

The interpolated values are assigned an error estimate P_i , which is based on the distance between the two hyperbola at the interpolation depth:

$$P_{i} = \frac{1}{3} |A_{i}^{1} - A_{i}^{2}|$$

The "goodness of interpolation" estimate P_i is coded as described in Fig. D.3.15.

4.4.2 Reiniger and Ross' Interpolation Method

Let the parameter V take the values V_1 , V_2 , V_3 , V_4 at the depths Z_1 , Z_2 , Z_3 , Z_4 , where Z_1 through Z_4 are the levels used for the interpolation in order of increasing depth. Let V_P be the interpolated value at a depth Z such that $Z_1 < Z_2 < Z < Z_3 < Z_4$. Reiniger and Ross (1968) then calculate a weighted mean for the two hyperbola, using the following equations:

$$V(P) = \frac{|V_R - V_{P_1}| |V_{P_2} + |V_R - V_{P_2}| |V_{P_1}|}{|V_R - V_{P_1}| + |V_R - V_{P_2}|}$$

where:

$$V_{R} = \frac{1}{2} \left\{ V_{23} + \frac{(V_{23} - V_{34})^{2} V_{12} + (V_{12} - V_{23})^{2} V_{34}}{(V_{23} - V_{34})^{2} + (V_{12} - V_{23})^{2}} \right\}$$

$$V_{P_{1}} = C_{23}^{'} V_{1} + C_{31}^{2} V_{2} + C_{12}^{3} V_{3}$$

$$V_{P_{2}} = C_{34}^{2} V_{2} + C_{42}^{3} V_{3} + C_{23}^{4} V_{4}$$

$$C_{jk}^{i} = \frac{(Z - Z_{j})(Z - Z_{k})}{(Z_{i} - Z_{j})(Z_{i} - Z_{k})}$$

$$V_{ij} = \frac{V_{i} (Z - Z_{j}) - V_{j} (Z - Z_{i})}{Z_{i} - Z_{j}}$$

An error estimate P of the interpolated value is calculated by:

$$P = \frac{1}{3} \left[\left| \left\{ V(P) - V_{P_1} \right\} \left\{ V(P) - V_{P_2} \right\} \right| \right]^{\frac{1}{2}}$$

and the "goodness of interpolation" estimate P is coded as described in Fig. D.3.15.

Section 4.4.3

4.4.3 Special Cases

In general the interpolation schemes require two observed values of a parameter A above, and two below the interpolation depth. When this is not the case, a linear interpolation is performed or the data are not interpolated at all. If linear interpolation is used, the interpolated value is followed by a W in the precision code column. The following special cases can be distinguished:

- 1. When less than four depths have been observed. In this case no interpolations are performed.
- 2. Near the surface. If less than two observations occur above Z_1 , a linear interpolation using the two upper observations is performed. No extrapolations are made over a distance exceeding 13 metres or 1.3 x (Z_2 Z_1), whichever is smaller.
- 3. Near the bottom. If less than two observations occur below Z_i , a linear interpolation using the lowest two observations is performed. No extrapolation is performed to depths exceeding the deepest observation by more than 10% of the depth difference between the deepest two observed levels.

Other special cases occur when:

- 1. The desired standard depth coincides with an observed depth.

 In this case the observed variables are transferred without change to the standard depth. If two or more observations have been taken at this depth, only the first one will be used.
- 2. Observed depths are spaced too far apart or too irregularly. This can occur if bottles are purposely spaced closely at some levels, or if two or more partially overlapping casts are taken, or if values of A are missing at two or more consecutive depths. Sample spacing therefore is checked as shown below and judged unacceptable if:

$$\frac{Z_{j-1} - Z_{j-2}}{Z_{j} - Z_{j-1}} < \frac{1}{5}$$
4.4.1

or

$$\frac{Z_{j+1} - Z_{j}}{Z_{j} - Z_{j-1}} < \frac{1}{5}$$

Section 4.4.3

In the first case, with too small an interval between the upper two points, interpolation is carried out using z_{j-3} , z_{j-1} , z_{j} , z_{j+1} instead of z_{j-2} , z_{j-1} , z_{j+1} . If the lowest interval is too small, that is if equation is not satisfied, A_{j+1} will be replaced by A_{j+2} . In either case the equations (4.4.1) and (4.4.2) are tested again before interpolation is completed, and the procedure is repeated until they are satisfied, or until surface or bottom is reached. When that happens, A_{j} will be determined by linear interpolation using z_{j-1} and z_{j} .

3. The interpolation error is too large. Linear interpolation will be used when the error estimator P_i exceeds 0.1 for temperature, 0.01 for salinity or 20 units for any chemical parameter.

43

5. ACKNOWLEDGEMENTS

Scientific specifications and general requirements for the system were defined by the author, but the actual systems design was done under contract by DCF Systems Limited. The contractors also were responsible for writing the programs and converting the old OCEANS III file into OCEANS IV format. The author is especially indebted to Mr. A.S. Adams of DCF Systems for his determined but undogmatic approach to the job at hand. Messrs. B. Wainwright and A. Treichel of the Computer Science Division, Department of Energy, Mines and Resources, have been very helpful in writing contract specifications and giving many helpful suggestions throughout the project.

The author is grateful for the support given by members of CODC's Advisory Board and by several of his colleagues working in the Bedford Institute and other oceanographic research centres. Dr. W.D. Forrester and Messrs. R.F. Reiniger and C.K. Ross, through their helpful comments, have contributed significantly to the specifications of the OCEANS IV system.

Last but not least, the author is indebted to his colleagues at the Canadian Oceanographic Data Centre for their continuous support. Mr. C.J. Glennie's help in forms design, Mr. R.C. Pattison's constructive comments on many of the details of the forms and Mrs. G. Mowbray's assistance in the preparation of the manuscript are greatly appreciated. Mr. Pattison, with the assistance of Miss M. Vetter, has also greatly assisted in the conversion of the old file, the preparation of test data, and the proofreading of test data outputs and print proofs. The work has been greatly facilitated by the continuous moral and background support given by the Head of CODC, Mr. C.M. Cross.

44 Section 6

6. REFERENCES

- ANDERTON, P. and P.H. BIGG, 1967. Changing to the Metric System; conversion factors, symbols and definitions. Nat. Phys. Lab. Her Majesty's Stationery Office, London. pp. 59.
- CHEMICAL RUBBER CO. 1965. Handbook of chemistry and physics. Ed. R.C. Weast.
- COX, R.A. 1964. Proposed re-definition of the litre, and the effect on oceanographic data. Nature, 202 (4937), p. 1098.
- EKMAN, V.W. 1908: Die Zusammendrückbarkeit des Meerwassers nebst einigen Werten für Wasser und Quecksilber. Publ. Circ. Cons. Explor. Mer, No. 43, 47 pp.
- FOFONOFF, N.P. and C. FROESE. 1958. Program for oceanographic computations and data processing on the electronic digital computer ALWAC III-E. PSW-1 programs for properties of seawater. Fish. Res. Bd. Canada, Manuscr. Rept. 27. 39 pp.
- FOFONOFF, N.P. and S. TABATA. 1958. Program for oceanographic computations and data processing on the electronic digital computer ALWAC III-E. PSW-1 programs for properties of seawater. Fish. Res. Bd. Canada, Manuscr. Rept. 25. 37 pp.
- FOFONOFF, N.P. 1962. Dynamics of ocean currents. The Sea, ed. M.N. Hill; Interscience Publ., New York, pp. 323-395.
- HANSEN, W. 1934. Bermerkungen zu den Korrektionsformeln für das Tiefsee-Umkippthermometer. Ann. der Hydrog. und Marit. Meteor., 62 (146).
- KEYTE, F.K. 1964. On the formulas for correcting reversing thermometers. Seep Sea Res. 12, pp. 163-172.
- KNUDSEN, M., 1901: Hydrographische Tabellen, Copenhagen, 63 pp.
- LIST, R.J. 1966. Smithsonian Meteorological Tables. Smithsonian Miscellaneous Collections, Washington, Vol. 114 527 pp.
- MARTIN, L, W.R. BRYAN, C. CURTIS and G. WHITNEY, JR. 1968. Standardizing calibration of deep sea thermometers. UST. pp. 33-39.
- PROUDMAN, J. 1953. Dynamical oceanography. John Wiley & Sons Inc. New York. pp. 403.

- RALYA, J. 1968. Handbook for computer users, Woods Hole Oceanographic Institution, pp. 100.
- RATTRAY, M. 1962. Interpolation errors and oceanographic sampling. Deep-Sea Res. 9, pp. 25-37.
- REINIGER, R.F. and C.K. ROSS. 1968. A method of interpolation with application to oceanographic data. Deep-Sea Res., 15, pp. 185-193.
- REINIGER, R.F., C.K. ROSS, P. TRITES and D.J. LAWRENCE, 1968-A. Physical oceanography data reduction programs for the CDC 3100, Atlantic Oceanographic Laboratory. B.I. Comp. Note 68-10-C pp. 275.
- STURGES, W. 1968. Thermometric depth and gravity variations.

 Deep-Sea Research 15, pp. 645-646.
- U.S. NAVAL OCEANOGRAPHIC OFFICE, 1966. Handbook of oceanographic tables SP-68, pp. 423.
- WHITNEY, G.G. JR. 1957. Factors affecting the accuracy of thermometric depth determinations. J. du Conseil. 22 (2), pp. 167-173.
- WILSON, W.D. 1960. Speed of sound in sea water as a function of temperature, pressure, and salinity, J. Acoustical Society America. Vol. 32 No. 6 pp. 5.
- WUST, G. 1933. Thermometric measurement of depth. Hydrogr. Rev., 10 (2) pp. 28-49.



APPENDIX A

SYSTEM SUMMARY AND FLOW CHARTS



APPENDIX A

System Summary

The flow of data through the OCEANS IV system is summarized in the flow diagram shown in Fig. A.1. The major programs are:

- Thermocheck (4010), which accepts reversing thermometer readings and computes corrected temperature and pressure values which are output onto the Thermocheck transaction tape. The processed data are listed with, when necessary, the appropriate error messages and a summary of thermometer performance.
- 2) Edit (4022), which accepts all data entered on Data Summary and other input forms and the output of the Thermocheck program. All data are thoroughly edited for validity, reasonableness, existence where necessary (for example, for identifying information), and consistency. Editing of the data continues as long as possible even if errors are found invalidating individual cruises, stations or levels. Such data, however, are not passed on into the OCEANS IV transaction file. All processed data are listed, together with error messages and, for data not entered onto the transaction file, rejection messages.
- 3) Update (4041), which updates the Station Master and Level Master files. The OCEANS IV Transaction file is first sorted into geographical sequence, using the COTED key described in Appendix F. The Update program also prints a one-line summary of each cruise transferred onto the master files (Cruise Master Summary) and extends the Station Master records to include a summary of available information for each station. This summary shows minimum and maximum observed depth, parameters observed, etc. (see Station Master Catalogue for details).
- 4) Report (4052), which prints a Data Report from the OCEANS IV transaction file or from the Extracted Data file produced by program Retrieve. It can also reproduce the data on cards or magnetic tape in OCEANS IV format. A separate program, Convert (4002), is available to convert the data to the previously used OCEANS III format. The Report program calculates, upon demand, derived and interpolated data. (See sections 3.1, 4.3 and 4.4)
- 5) Retrieve (4050), which can selectively extract data from the master files. If Data Reports or data on cards or magnetic

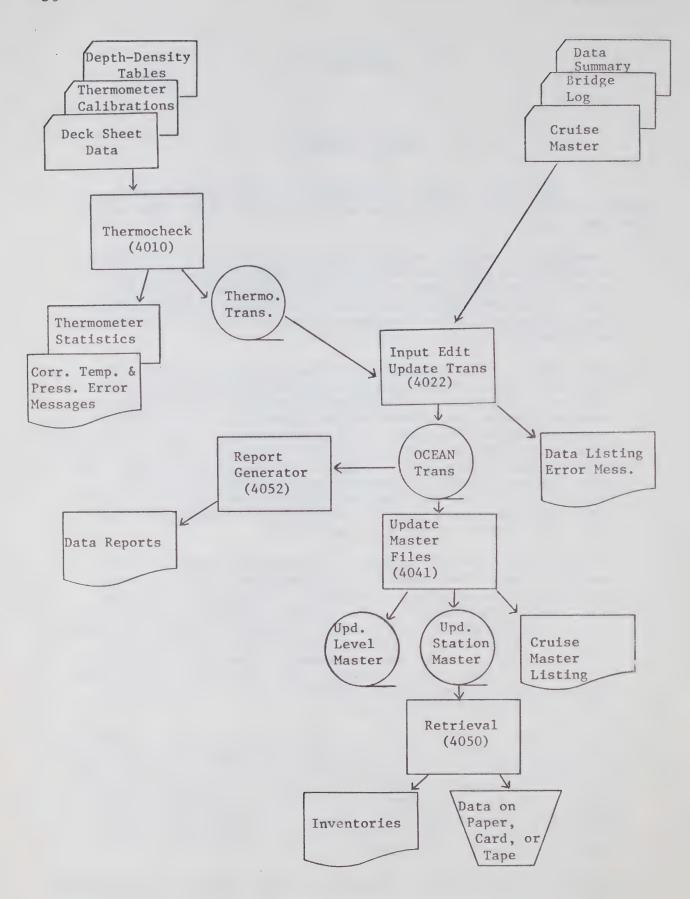


Fig. A.1 Summary Flow Diagram for OCEANS IV.

tape are required, this program can be followed by two further steps as described in Section 3.2.

A number of minor programs, such as a card-to-tape program preceding the Edit, or sort programs preceding several of the major programs, also form part of the system. For a discussion of these, however, reference must be made to the systems manual; their function is not essential for basic understanding of the OCEANS IV system.

The system utilizes strictly sequential processing. The Thermocheck and OCEANS IV transaction files are in cruise sequence and the master files in geographical sequence.

when the english this program can be followed by two further course to reserved in Schiell C.

A number of minor programs, such as a card-to-tape of tan preceding the Edit, or sort programs preceding several the major programs, also form part of the system. For a incussion of these, however, reference must be made to the systems manual; their function is not essertial for basic understanding of the OCHANS IV system.

The system utilizes strictly sequential processing. The Thermocheck and OCEANS IV transaction files are in cruise sequence and the master files in geographical sequence.

APPENDIX B

INPUT FORMS AND CODING INSTRUCTIONS

- 1. Cruise Master

- Deck Sheet
 Data Summary
 Bridge Log
 Thermometer Calibration Sheet



CODC CRUISE MASTER

					PARAMETERS OBSERVED	CHECK		Temperature	Vinited	Soundspeed	O A	+	+	+	7 NO2-N	8 NO3-N	9 SIO – Si	A pH	B Fluoride	C Diss. Org. C	D Part. C	E Total Alk.	F Carb. Alk.	G NH3			Vaccounty and Section 2017					
					OXYGEN	METHOD	1 Winkler 2 probe									000	CODCUSE				1 1	IAA	0				c Institution.					
						S L	1 1 µg-\$tom/1 2 10 µl/1*									00 5		d in				TFORM CODE	of oceanographi rship, light-vesse position platfor									
				. Indicate										SWELL PERIOD	1 Pw code ‡	2 Pw Pw, period in							OBSERVATION PLATFORM CODE	raphic duty; vessel in position. (Weather surface craft. ftc. n. n. n. rickes) towar, fixed ising small craft.								
					SALINITY	METH	1 titration 2 conductance	3 inductance 4 refrac. Index	5 in situ probe (a.g. STD) 6 hydrometer	Note: if two methods used, indicate both code numbers						CHA CHA	TEMPERATURE UNITS	1 °C*‡	2 °F					-		Table 2 OB	e of the state					
					SUB SURFACE TEMPERATURE	METHOD	1 reversing therm. 2 thermal probe (e.g. STD)	3 both, used alternately								-	CORRECTIONS		2 corr. for barometer	3 corr. for barometer	height and temperature					-	# 0					
-	0.43) E.D	(knots)		(kuosa)		SURFACE		go	ce temperetures												1000	AIR PRESSURE UNITS	1 mbar *‡	2 mm								The Commission of the Commission of the Commission of Comm
	PLATFORM COOD = 2 PLATFORM G See Table 2 PLATFORM G CRUISING G CRUISING G CRUISING G CRUISING G CRUISING G					4 tow frame																6	WIND SPEED UNITS	m/sec*‡	2 knots	Beaufort	statute miles per hour		1			INSTITUTE CODE
	VESSEL (PLATFORM) NAME				DEPTHOF	SAMPLE UNITS	1 metres* 2 feet	3 fathoms									ANEMOMETER HEIGHT IN M		010	9 1	۵				anation 1).	Table 1 INSTITU						
	VES				SOUNDING	UNITS	1 metres* 2 feet	3 fathoms								-									tation Data File.		Institute se Bellevus, P.O. iviers on antic Bedford Institute					
	CRUISE NUMBER	at'n consec	N O LL					0 4 1 2	PUBLICATION	000							ceanographic S 1968 DOT Coc		Group Group ion, Ste. Anne John's Mid. John's Mid. Alboris Mid. Bribment, Pas ablishment, Pas ic Laboratory, if Project													
CF INSTITUTE NU See Table 1 1st 1st 1st 1st 1st 1st 1st 1st 1st 1		80			SOUNDING CORRECTION	soundspeed of 1463 m/s soundspeed of 1500 m/s	Matthews Tables measured or calculated soundspeed	profile							140000000000000000000000000000000000000	DATA CODING	according to DOT code	card	see Note 5 on the back					File Units in CODC's Oceanographic Station Data File. Codes Specified by the 1968 DOT Code Card (See Explanation 1).		10 Marine Ecology Laboratory, Badford Institute 20 Pesific Coannagapho (Group 20 Bologies Station, St. Andrewa, N.B. 20 An Arctic Bologies Station, Sts. Andrewa, N.B. 20 Bologies Station, St. Andrewa, N.B. 20 Bologies Station, St. John's Wild. 20 Estation de Bloologies Marine, Graded Frieder 20 Marine Sciences Branch, Central Region 20 Marine Sciences Branch, Central Region 30 Defence Peasarch Establishment, Atlantic 30 Defence Research Establishment, Pacific 41 Atlantic Ocannogaphic Laboratory, Badford Institute 42 Great Lakes Institute 43 Great Lakes Institute						

Cruise Master coding sheet. The coding instructions are given in Fig. B.1.2. The Cruise Master is designed as a cardboard wallet in which all coding sheets made up during a cruise can be stored. Fig. B.1.1

CODC CRUISE MASTER CODING INSTRUCTIONS

GENERAL NOTES

1. A new Cruise Master must be made up for each cruise.

2. Acceptable units must be consistent throughout the entire cruise with the code entered on the Cruise Master. 3. If certain observations have not been made throughout an entire cruise, the appropriate columns may be left blank.

4. Up to 10 different coded parameters, plus any of the four uncoded parameters, can be entered for one cruise. Parameter codes are given on the reverse side; units on the Data Summary Coding Instructions. Additional codes can be supplied by CODC upon written request.

for Selected and Supplementary Ships" or as indicated in the columns 41-45 of the Cruise Master. If the DOT code card is 5. Metaorological data can be coded according to the Department of Transport's "International Meteorological Code used, the last two digits of its year of publication must be entered in the columns 37-38, and columns 41-45 can be left blank. The data fields on the CODC Data Summary and the CODC Bridge Log have been arranged to facilitate copying of the data from DOT's "Selected and Supplementary Ships N.B. According to the 1968 DOT code card, wind speed is given in m/sec, air and wet bulb temperatures in degrees Celsius, pressure in mbar corrected for barometer height and outside air temperature, and swell period in the Pw code.

SPECIFIC MOTES

See reverse side of this envelope.

OCEANS IV

CODC'S NEW SYSTEM FOR HANDLING OCEANOGRAPHIC STATION DATA

The OCEANS IV system will replace the OCEANS III system in April 1970. It is designed to increase the flexibility of CODC's data handling capabilities, and will fulfill such functions as:

Processing of reversing thermometer readings,

2) Preparing data for archival in the Oceanographic Station Data File,

3) Printing data reports on request,

Providing a flexible retrieval of data from the file.

The system is described fully in a separate report; below follows a summary of the input forms. Data submitted on different forms are merged by the system; no manual transcribing of data from form to form is necessary at any stage.

SUMMARY OF THE ALTERNATIVE COMBINATIONS OF FORMS THAT CAN BE USED TO SUBMIT DATA TO CODC (AT THE OPTION OF THE DATA ORIGINATOR)

Purpose				Ballie rom	rossillie rorm compinations	9
To provide general information on a cruise and to control conversion of "acceptable units" into OCEANS IV "file units"	Data	Purpose	Cruise	Deck	Data Summary	Bridge
(marked by a star on the Cruise Master form, see reverse). To submit to CODC uncorrected temperature readings, obtained with representation and subsemiant	Temperature readings	Correcting				
archiving. T. Annual of Child for makining and by data report productions	Temperature	Correcting and archiving			1	
To submit to Codo, or aromany and or set of the such as calibrated and corrected oceanographic station data such as temperature, salinity, oxygen, etc.	Temperature readings plus other data	Correcting temp, and archiving all data				
and be used instead to the Sustain mater section to the base Summary to submit station identifying information, such as time and location, and environmental data such as bottom depth and meteorological conditions.	Temperature (corr.) and/or other data	Archiving				

Deck Sheet

Data Summary

Bridge Log

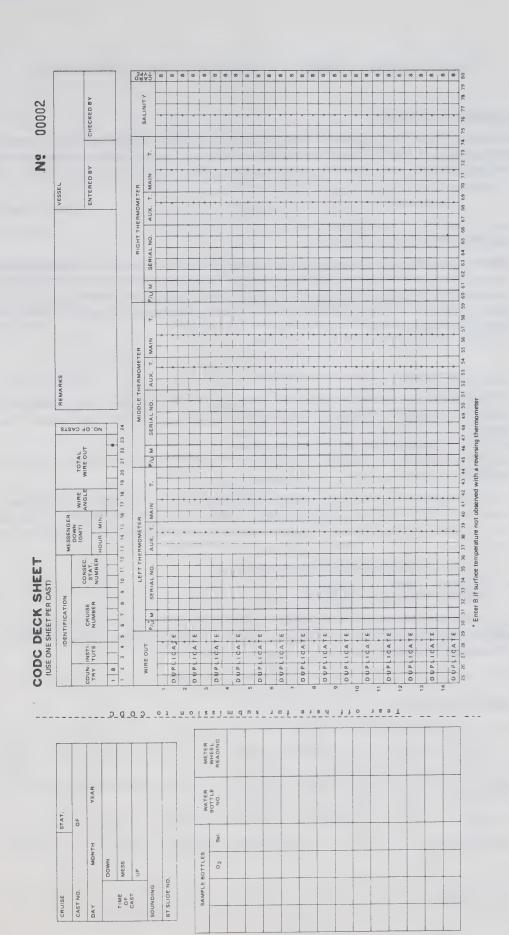
Cruise Master

Form

FORMS FOR THE OCEANS IV SYSTEM

the Of the back printed on L'S This instructions. coding wallet Master Master Cruise Cruise B.1.2

Fig.



B.2.3. and are given in Figs. B.2.2 "no carbon" copies. The coding instructions bound in pads of 50 with The form is Deck Sheet. B.2.1

Fig.

CODC DECK SHEET - CODING INSTRUCTIONS

USING THIS FORM

The CODC Deck Sheet is used to submit to CODC, for correction and/or archiving, temperature readings obtained with reversing thermometers. If salinity has been measured simultaneously, it may be entered on the same form or alternately, together with any other observations, on the CODC Data Summary.

COMPLEMENTARY FORMS

If the Deck Sheet is used to submit data to CODC only for correction of temperature readings, it must be accompanied by a CODC Cruise Master. If it is used to submit data for both correction and archiving, the CODC Bridge Log or the CODC Data Summary must be used to submit Station Master data such as sampling location, time, etc. In all cases thermometer calibration data should be made available to CODC.

GENERAL NOTES

- 1. The lines in the main part of the form are grouped in pairs, providing space for entering first and second readings of each thermometer on the two lines respectively. Second readings must be entered.
- 2. The left hand side of the form is provided for the user's convenience. It need not be returned to CODC.
- 3. Leading and trailing blanks are allowed in all fields except in the Cruise Number field, which must start with the last two digits of the year of observation of the first station. The last figure before a decimal point, however, must be entered; e.g. a temperature of 0.1 °C can not be coded as ".1".
- 4. Never enter data for different casts on the same sheet.
- 5. Shaded portions must be left blank.
- 6. Surface temperatures <u>not</u> observed with a reversing thermometer can, if desired, be entered in the Main Temperature field. In that case a "B" must be placed in the P/U column and columns 31 through 39 may be left blank.

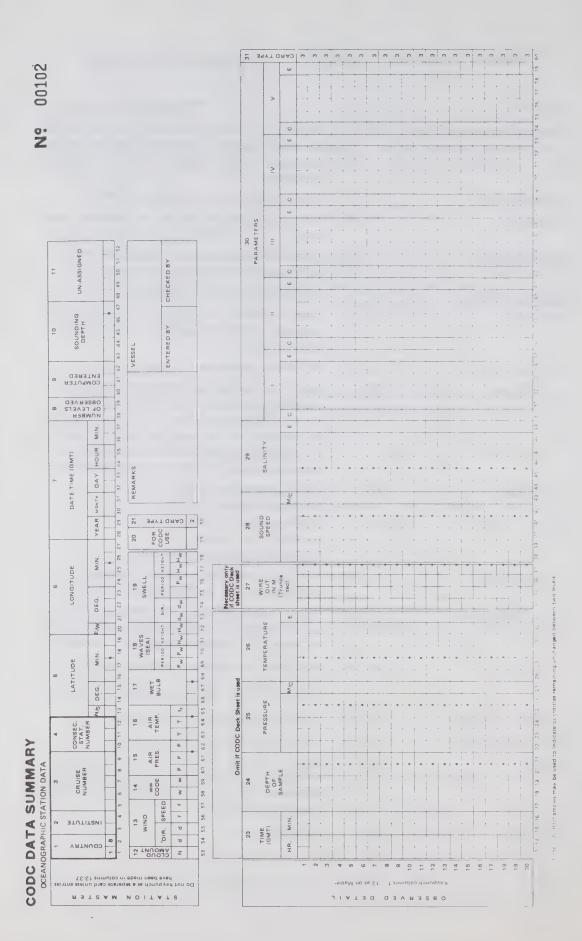
SPECIFIC NOTES

Field Name	Column	Explanation
Country	1 – 2	Same as on CODC Cruise Master; always 18 for Canadian Cruises.
Institute	3 – 4	Same as on CODC Cruise Master.
Cruise Number	5 – 9	Same as on CODC Cruise Master.

Fig. B.2.2 Deck Sheet coding instructions.

Field Name	Column	Explanation
Consecutive Station Number	10 – 12	Stations are numbered chronologically throughout the cruise; for the Thermocheck Program stations have to be in ascending order but not necessarily consecutive.
Messenger Down	13 – 16	Messenger time in hours and minutes GMT,
Wire Angle	17 – 18	Wire angle in degrees measured at Messenger Down time.
Total Wire Out	19 – 23	Distance in metres along the wire between the water surface and the deepest bottle on the cast.
Number of Casts	24	Number of casts taken on this station.
Wire Out	25 – 29	Distance between the surface and the bottle depth measured in metres along the wire. Note position of the decimal point.
Left Thermometer	30 – 44	See following breakdown by sub-fields.
P/U Code	30	Enter P or U to indicate whether the thermometer is protected or unprotected, or B when the temperature has been determined other than with a reversing thermometer. In this case columns 31-39 may be left blank, but the Main Temperature Field must be completed on both the first-and second-reading cards.
M Code	31	Enter manufacturer code: R = Richter & Wiese Y = Yoshino N = Negretti and Zambra (See also explanation of column 30).
Serial Number	32 – 36	Five digit thermometer number assigned by the manufacturer. (See also explanation of column 30).
Auxiliary Temp.	37 – 39	Enter Auxiliary Thermometer Reading in degrees Celsius. Minus signs, if applicable, should be entered in column 37. (See also explanation of column 30).
Main Temp.	40 – 44	Enter Main Thermometer Reading in degrees Celsius. Minus signs, if applicable, should be entered in column 40. (See also explanation of column 30).
Middle Thermometer	45 - 59	See instructions for Left Thermometer.
Right Thermometer	60 - 74	See instructions for Left Thermometer.
Salinity	75 – 79	Salinity may be entered if desired, in parts per thousand; note position of the decimal point. Alternately, salinities can be submitted on the CODC Data Summary sheets.
Card Type	80	Preprinted.

Fig. B.2.3 Deck Sheet coding instructions (continued).



through copies instructions are given in Figs. in pads of 50 with "no carbon" c pads . The coding form is bound Data Summary. B.3.7, The fo

CODC DATA SUMMARY CODING INSTRUCTIONS

USING THIS FORM

The CODC Data Summary is used to submit calibrated and corrected Oceanographic Station data to CODC. The form consists of two parts, the Station Master and the Observed Detail. The Station Master contains all information identifying the station in space and time as well as Sounding Depth and Meteorological Data. The Observed Detail contains all information observed at each sampling level.

COMPLEMENTARY FORMS

The Data Summary forms must be submitted together with a CODC Cruise Master for each cruise, and can, if desired, be combined with CODC Deck Sheets and/or CODC Bridge Logs.

The CODC Deck Sheet can be used to submit uncorrected Reversing Thermometer readings. After correction by our Thermocheck Program, the temperatures will be merged with other data contained on the CODC Data Summary. In this case field 27 on the Data Summary must be completed to match it with input from the Deck Sheet, whereas fields 23 through 26 can be left blank.

The CODC Bridge Log can be used instead of the Station Master section of the Data Summary to enter position, time, bottom depth and meteorological data. The first four fields on the Station Master, however, must still be completed to identify the station.

GENERAL NOTES

- 1. Leading and trailing blanks are allowed in all fields except the cruise number field.
- Any non-observed fields can be left blank; only the first seven fields on the Station Master must be completed.
- 3. The location of **decimal points**, whenever applicable, is indicated on the form.

- 4. A provision has been made to enter arbitrary station codes or any other alphanumeric information in the "Unassigned" field. (This information is reproduced in data listings, but cannot be used to search for a station in CODC's files.)
- 5. Any parameter for which a choice of units can be made, must, throughout the entire cruise, be entered in the units specified on the Cruise Master.
- 6. Meteorological data can, if desired, be taken from the appropriate columns in the Department of Transport's "Selected and Supplementary Ships' Meteorological Log", which is coded using DOT's "International Meteorological Code Card for Selected and Supplementary Ships". (See also Note 5 on the Cruise Master.) These codes have been set by the World Meteorological Organization. The codes accompanying the present instructions are based on DOT's coding instructions of January 1, 1968. If these are modified, data can be entered according to either the revised DOT Code Card or the 1968 Code Card, provided that the year of publication of toode card used is indicated. Optionally, data can also be entered in units specified on the Cruise Master.
- 7. If an entry in a certain column or field remains the same at a number of subsequent levels, it is sufficient to enter it in the highest and lowest of these levels only, connected by a **vertical arrow**.
- 8. Depth and Pressure need not both be entered; either one of the two can be left blank.
- 9. Up to ten different parameters can be entered for any one station. If more than five are given, enter parameters 6 through 10 on the next line of the form, repeating the level indication (Depth, Pressure or Wire Out, depending on which is used on the preceding line) on the second line. All other fields can be left blank on the second line.
- 10. The error columns following the Temperature and Salinity fields can be used to indicate data sampled with a MPR by entering a "P" (MPR = Multiple Probe Recorder such as STD, etc.).

	IFIC NOTES			No.	Field Name	Column	Explanation
	STA	ATION MA	ASTER		Wind Speed	56 – 57	Windspeed can be measured in metres per second, knots
ield No.	Field Name	Column	Explanation				feet per second or statut
1.	Country	1 – 2	Same as on CODC Cruise Master; always 18 for Canadian cruises.				miles per hour, or estimated on the Beaufort scale (Table 2). It must be entered a
2.	Institute	3 – 4	Same as on CODC Cruise Master.				ter. N.B. The DOT meteorolog
3.	Cruise Number	5 – 9	Same as on CODC Cruise Master.				ical Log code gives wind speed in knots.
4.	Consecutive	10 – 12	Stations must be numbered	14.	ww Code	58 – 59	Coded according to Table 3
	Station Number		consecutively throughout the cruise in a chronological order. A new consecutive number is required each time the station is reoccupied, even if no other locations are sampled in the intervening period. Other station code numbers can be entered in the "unassigned" field (num-	15.	Pressure		Enter the last three digits of the barometer reading, or of sea level pressure, in unit indicated on the Cruise Master. For example: 1026, mbar is coded as 264; 987. mbar as 873 and 768.3 mm a 683. Sea level pressure can be obtained from the baromete
5.	Latitude	13 – 19	ber 11) if the data originator so desires. Latitude of the station, Enter N or S in column 13 to				reading by applying corrections for barometer heigh and outside air temperatur using Table 4.
			indicate north or south lati- tude. Position is given in degrees and minutes with up	16.	Air	62 GE	N.B. The WMO code gives se level pressure in mbars. Enter air temperature in unit
			to two decimals.	10.	Temperature	03 - 05	stated on the Cruise Master
6.	Longitude	20 – 27	Longitude of the station. Enter E or W in column 20 to indicate east or west longi- tude. Position is given in degrees and minutes with up to two decimals.				Negative Celsius temperature are coded by adding 50 to the absolute value of the measurement (WMO) code). Negative Fahrenheit temperature are coded by placing a minu.
7.	Date Time	28 - 37	Sampling time of the first observed level is given in Greenwich Mean Time (GMT). The last two digits of the year (e.g. 70 for 1970)	4.7			sign in the last column (65 Omit decimals when codin in Fahrenheit. For example $14.2^{\circ}\text{C} \rightarrow 14.2$ $14.2^{\circ}\text{F} \rightarrow 14$. $-14.2^{\circ}\text{C} \rightarrow 64.2$ $-14.2^{\circ}\text{F} \rightarrow 14$.
			are followed by month (coded 01 through 12), day,	17.	Wet Bulb Wave Period	66 – 68	ture.
8.	Number of Depths Observed	38 – 39	hour and minute. Enter the number of levels at which observations are made.	18.	wave Feriod	69 – 70	sea waves in seconds. Whe the sea is calm, or the period indeterminate, enter // of
9.	Blank	40 – 42	These columns are reserved to insert a computer-calculated Marsden Square number.		Wave Height	71 – 72	leave blank. Estimate the average height of the larger well-former
10.	Sounding Depth	43 – 47	Sounding depth in units indicated on the CODC Cruise Master. Note location of the decimal point.				waves of the sea wave syste in multiples of 0.5 metre The height is then coded units of half-metres. For example, an observed wave
11.	Unassigned	48 – 52	These columns can be used to enter any alphanumeric in-				height of 5 metres is coded 10.
			formation the data originator wishes to be printed in provisional or published Data Reports produced by CODC.	19.	Swell Direction	73 – 74	True direction from which the waves are coming in terms of degrees. Enter 00 for call 01 for 10, 02 for 20, and
12.	Cloud Amount	53	Fraction of the sky covered by clouds of any type is coded on an octal scale where 0 stands for no clouds and 8		Swell Period	75 76	on by ten degree steps rig around to 36 for a wave fro due north. Code as Wave Period, see in
			for a completely clouded sky. (Table 1)		Owoll 1 GIOG	75 - 70	tructions for field 18, according to Table 5 as i
13.	3. Wind 54 – 55 Direction		True direction from which the wind is blowing, in tens of degrees. Enter 00 for calm, 01 for 10° 02 for 20° and so		0 1111		dicated on the Cruise Maste N.B. The WMO code giv swell as P _w .
			01 for 10°. 02 for 20° and so on by ten-degree steps right		Swell Height	11 - 78	Code as Wave Height.
				20.	For CODC Use	79	To be entered by CODC star

Fig. B.3.3 Data Summary coding instructions (continued).

Field		SERVED		No.	Field Name	Column	Explanation
No. 23.	Field Name Time GMT	13 – 16	Explanation Sampling time at each observed level in hours and minutes Greenwich Mean Time.				If the datum is based on triple measurement, P taken equal to the standard deviation:
24.	Depth of Sample	17 – 21	Enter sampling depth in units indicated on the Cruise Master. Can be left blank if Pressure is entered in field 25 or if Temperature and Depth				$P = \left\{\frac{1}{2}\sum_{i=1}^{3} \left(A_{i} - \overline{A}\right)^{2}\right\}^{1/2}$ where A_{i} are the measurements and \overline{A} the mean value of the observed parameter.
			are obtained from Reversing Thermometer observations submitted on the CODC Deck Sheet.				MPR data can be marked wit a "P" in this column. This necessary only if more that one measurement technique
25,	Pressure	22 – 26	Enter pressure in decibars. Can be left blank if Depth is entered in the preceding field				is indicated on the Cruis Master.
			or if Temperature and Pressure are obtained from Reversing Thermometer observations submitted on the CODC Deck Sheet.	27.	Wire Out	34 – 37	Has to be completed only in the temperatures are submitted on the CODC Deck Sheet. Wire out is entered in metres, no provision is made
		27	If both Pressure and Depth are completed, enter an M or a C to indicate whether Pressure is measured or cal- culated from depth. It can be				to enter fractions of metres Do not round decimals truncate them! 127.0 and 127.9 should both be be entered as 127.
	Temperatura		left blank if either Depth or Pressure is blank for the en- tire station.	28.	Soundspeed	38 – 42 43	Entered in metres per second Enter an M or a C to indicate whether soundspeed is meas ured or calculated at any
26.	Temperature	28 – 32	Temperature in degrees Celsius. Insignificant decimals can be left blank.	29.	Salinity	44 – 48	level. Enter in parts per thousand
		33	To be left blank unless the preceding datum is: 1) doubt-				The third decimal place car be left blank if not observed
			ul, or 2) the mean of a uplicate measurement, or 3) neasured with an MPR.			49	Enter doubtful mark or error code as explained under field 26, column 33, above.
			Doubtful data can be marked with an X by the originator or a Y by CODC. Error esti-	30.	Parameter I	50	Enter code number or letter in the first column; see Table 6.
			mates are coded A through I as follows: Let P be the dif- ference between the two			51 – 54	Enter measured quantity in units specified in Table 6.
			measurements, P then is coded in multiples of the last digit allowed for on the			55	Enter doubtful mark or error code as explained under field 26, column 33, above
			coding form as follows: P ≤ 1 Code A		Parameter II - V	Š6 − 79	Enter as specified for Parameter I.
		$\begin{array}{cccccccccccccccccccccccccccccccccccc$			Parameter VI — X	Second card	Enter on next line in field 30, as specified for Parameter I above. The level identifier (Depth, Pressure or Wire Out) used on the preceding line
			100 < P ≤ 200 Code H 200 < P Code I A temperature error P=0.003°C is coded as C, an error P=0.02°C as E, and a salinity error P=0.08 per mille				must be repeated; all other fields may be left blank. The maximum number of parameters that can be entered per station is 10.
			as G, etc.	31	Card Type	80	Preprinted.

Table 1 CLOUD AMOUNT (N - Code)

Fraction of the sky covered by clouds

Code	Cloud Cover	Code	Cloud Cover
0	Cloudless	6	6/8
1	1/8 or less but not zero	7	7/8 or more but not 8/8
2	2/8	8	8/8, sky totally covered
3	3/8	9	Sky obscured by dense fog, heavy
4	4/8	1	snow, etc., or amount cannot be
5	5/8		estimated.

Fig. B.3.4 Data Summary coding instructions (continued).

Table 2 WIND SPEED IN KNOTS (ff - Code)

The Beaufort force of the wind is estimated from the appearance of the see surface according to the table below. This table is only intended as a guide to show roughly what may be expected on the open sea, remote from land. Factors which must be taken into account are the 'lag' effect between the wind increasing and the sea getting up; and the influence of 'fetch', depth, swell, heavy rain and tide effect on the appearance of the sea. Estimation of the wind speed by this method becomes unreliable in shallow water or when close inshore, owing to the tidal effect and the shelter provided by the land.

Speed	Code ff (Speed in	Mean Speed	Beau-	Description	Appearance of Sea if the Fetch and Duration of the Blow Have Sean	Probabl seas in	
m/sec	Knots) (Knots) fort		Sufficient to Develop the See Fully	Aver.	Max.		
0.0 - 0.1	00	00	0	Calm	Sea like a mirror		_
0.2 - 1.8	01 - 03	02	1	Light Air	Ripples with the appearance of scales		
					are formed, but without foam crests	0.1	0.1
1.9 - 3.3	04 - 06	05	2	Light Breeze	Small wavelets; crests have a glassy		
					appearance and do not break , ,	0.1	0.3
3.4 - 5.3	07 – 10	09	3	Gentle Breeze	Large wavelets; crests begin to break;		
					foam of glassy appearance; perhaps		
					scattered white horses	0.6	0.9
5.4 - 8.4	11 16	14	4	Modt. Breeze	Small waves, becoming longer; fairly		
					frequent white horses	1.0	1.5
8.5 - 10.5	17 21	19	5	Fresh Breeze	Moderate waves; many white horses		
					are formed (chance of some spray), , ,	1.8	2.5
10.6 - 14.1	22 – 27	25	6	Strong Breeze	Large waves; white foam crests		
			_		everywhere (probably some spray)	2.8	3.9
14.2 – 17.2	28 – 33	31	7	Near Gale	See heaps up and white foam from		
					breeking waves begins to be blown in		
					streeks along the direction of the		
					wind	4.0	5.7
17.3 – 20.7	34 – 40	37	8	Gale	Moderately high waves; edges of crests		
					begin to break into the spindrift;		
					foam is blown in well-marked streaks		
					along the direction of the wind	5.4	7.5
20.8 – 24.4	41 47	44	9	Strong Gale	High waves; dense streaks of foam		
					along wind; crests begin to topple,		
					tumble and roll over; spray may effect		
	40 55		40	0	visibility	6.9	9.6
24.5 28.5	48 - 55	52	10	Storm	Very high waves with long overhanging		
					creets; foam in greet petches blown in		
					dense white streaks along wind; see surface takes a white appearance		
					tumbling becomes heavy and shock-		
					like; visibility affected	8.7	12.3
28.6 32.4	EC 62	60	11	Violent Storm	Exceptionally high waves (medium	0.7	12
26.0 - 32.4	30 - 03	00		A IOIGHT STORM	sized ships may be lost to view behind		
					waves); see covered with long white		
					patches of foam lying along wind;		
					everywhere edges of crests are blown		
					into froth; visibility affected	8.1	15.6
32.5 -	64 71	68	12	Hurricane	Air is filled with foam and spray; sea	0.1	10.0
72.0	J4 - /1	00	1.6	, , di i logire	completely white with driving spray;		
					visibility very seriously affected	13.5	

Table 3 PRESENT WEATHER (ww - Code)

Use the highest code figure applicable except that 17 has preference over 20 to 49 inclusive.

00-49	NO PRECIPITATION AT SHIP AT TIME	Code	Code
	OF OBSERVATION	10	0-12 MIST AND SHALLOW FOG
00-03 0	CHANGE OF SKY DURING PAST HOUR	10	Mist (visibility 1100 yds,
Code	Code		or more)
00	Cloud development not	11	Shallow fog in patches Fog not deeper
00	observable	12	Shallow fog-more or then 32 ft
01	Clouds dissolving or		less continuous
	becoming less developed	40	
02	State of sky on the whole	13-	-16 PHENOMENA WITHIN SIGHT
	unchanged		BUT NOT AT SHIP
03	Clouds generally forming or	13	Lightning visible, no
	developing		thunder heard
04	09 SMOKE, HAZE, SAND OR DUST	14	Precipitation in sight, not
04	Visibility reduced by smoke	45	reaching surface
04	(not ship's smoke)	15	Precip, beyond 3 naut.
05	Dry Haze	16	miles, reaching surface Precip, within 3 naut.
06	Widespread dust suspended	10	miles, reaching surface
	in air		
07	Blowing spray at ship	17-19 TI	HUNDER, SQUALLS, FUNNEL CLOUDS
08	Dust whirls in past hour	17	Thunder at time of obsn
	(not for marine use)		no precip, at ship
09	Dust or sandstorm in sight,	18	Squalls (no precip.) in past
	or at ship in past hour		hour or at time of obsn.

Fig. B.3.5 Data Summary coding instructions (continued).

Table 3 (C	Cont'd.) JNDER, SQUALLS,		Code 60-69	RAIN (NOT FALLING	Code (AS SHOWERS)
	INEL CLOUDS (Cont'd.)		Intermitte		Continuous
Code		Code	60	Slight rain	61
19	Funnel cloud(s) seen in		62	Moderate rain	63
	past hour or at time of		64	Heavy rain	65
	obsn.		Slight		Moderate or Heavy
òo oo	DISCOURAGE IN DACE HOLD	ID DUT	66	Freezing rain	67
20-29	PHENOMENA IN PAST HOU NOT AT TIME OF OBSN.	JK BUT	68	Rain or drizzle with s	now 69
20	Drizzle (not freezing) or snow grains		70 – 79 SO	LID PRECIPITATION I	NOT FALLING AS
21	Rain (not freezing)		Intermitter	nt	Continuous
22	Snow	Not falling	70	Slight snow in flakes	71
23	Rain and snow, or ice	as showers	72	Moderate snow in flat	
24	pellets Freezing drizzle or		74	Heavy snow in flakes	75
	freezing rain		76	Ice prisms (with or wi	ithout
25	Shower(s) of rain		77	fog) Snow grains (with or	
26	Shower(s) of snow, or of		• •	without fog)	
	rain and snow mixed		78	Isolated starlike snow	
27	Shower(s) of hail*, or of rain and hail* mixed			crystals (with or with	out
28	Fog (in past hour but not			fog)	
	at time of observation)		79	Ice pellets	
29	Thunderstorm, with or			80-84 RAIN SHOW	ERS
	without precipitation		80	Slight rain shower	
*I nelu	ides hail, ice pellets, or snow p	pellets	81	Moderate or heavy rai	n
			82	Shower Violent rain shower	
			83	Shower of rain and sn	ow
30-39	(Not likely to be used in ship	reports)		mixed, slight	
Slight or		Heavy	84	Shower of rain and sn	
Moderate				mixed, moderate or h	eavy
30	Duststorm or sandstorm,	33	8590 9	SOLID PRECIPITATION	IN SHOWERS
31	decreasing Duststorm or sandstorm, unchanging	34	Slight		Moderate or Heavy
32	Duststorm or sandstorm,	35	85	Shower of snow	86
	increasing		87	Shower of snow pellet	
36	Drifting snow, generally low			ice pellets*	
38	Blowing snow, generally high	39	89	Shower of hail, no the With or without rain and	
				HUNDERSTORM DUR	
40-49 FC	G AT THE TIME OF OBSER	VATION	ŀ	OUR BUT NOT AT TH	
40	Fog at a distance but not at			OF OBSERVATIO	
	ship during past hour			29 if there is no precip. a	it observation time
41	Fog in patches		91	Slight rain	
Sky	Visibility less than 1100 yard	s Sky	92	Moderate or heavy rain	Thunderstorm in
Visible	of time of observation	Invisible	93	Slight snow, or rain	past hour but not
42	Fog, has become thinner in	43		and snow mixed, or	now – precip.
	past hour		94	hail*	occurring at time of obsn.
44	Fog, no change in past hour	45	94	Moderate or heavy snow, or rain and	time of obsn.
46	Fog, has begun or thickened in past hour	47		snow mixed, or hail*	
48	Fog, depositing rime	49	*Inc	۔ ! ludes hail, ice pellets or	snow pellets
50-99 PE	RECIPITATION AT SHIP AT	TIME OF	95-	-99 THUNDERSTORM OF OBSERVATIO	N
55 56 11	OBSERVATION		95	Slight or modt, thunde	
	50-59 DRIZZLE			with rain and/or snow, hail*	, but no
I many It s		Continue	96	Slight or modt, thunde	erstorm
Intermittent		Continuous		with hail*	
50	Slight Drizzle	51 53	97	Heavy thunderstorm w	
52 54	Moderate Drizzle Heavy Drizzle	55	98	rain and/or snow, no h Thunderstorm with du	
		Moderate	96	or sandstorm	rac .
Slight		or Heavy	99	Heavy thunderstorm w	rith
56	Freezing drizzle	57		hail"	
56 58	Drizzle and rain mixed	59	*Incl	udes hail, ice pellets or s	now pellets

Fig. B.3.6 Data Summary coding instructions (continued).

Table 4 PRESSURE CORRECTION (MBARS)

The sea level correction must be added to the barometer reading.

			Outside A	ir Temperatui	re in °C.				
		-20°C	-10°C	0°C	10°C	20°C	30 °C		
	15	0.6	0.6	0.6	0.6	0.5	0.5		
	20	0.8	0.8	0.8	0.7	0.7	0.7		
	25	1.0	1.0	1.0	0.9	0.9	0.9		
	30	1.2	1.2	1.2	1.1	1.1	1.0		
	35	1.5	1.4	1.4	1.3	1.3	1.2		
3	40	1.7	1.6	1.5	1.5	1.4	1.4		
9	45	1.9	1.8	1.7	1.7	1.6	1.6		
9	50	2.1	2.0	1.9	1,9	1.8	1.7		
Height of Barometer above Sea Surface (Ft.)	55	2.3	2.2	2.1	2.0	2.0	1.9		
	60	2.5	2.4	2.3	2.2	2.2	2.1		
S	65	2.7	2.6	2.5	2.4	2.3	2.3		
o o	70	2.9	2.8	2.7	2.6	2.5	2.4		
76	75	3.1	3.0	2.9	2.8	2.7	2.6		
96	80	3.3	3.2	3.1	3.0	2.9	2.8		
0	85	3.5	3.4	3.3	3.2	3.1	3.0		
8	90	3.7	3.6	3.5	3.3	3.2	3.1		
9	95	4.0	3.8	3.7	3.5	3.4	3.3		
H	100	4.2	4.0	3.9	3.7	3.6	3.5		
Ŧ	105	4.4	4.2	4.1	3.9	3.8	3.7		
	110	4.6	4.4	4.2	4.1	4.0	3.8		
	115	4.8	4.6	4.4	4.3	4.1	4.0		
	120	5.0	4.8	4.6	4.5	4.3	4.2		
	125	5.2	5.0	4.8	4.7	4.5	4.3		

Table 5 SWELL (P_W - code)

Code	Period in sec.	Code	Period in sec.				
5	5 sec. or less	1	11 sec.				
6	6 sec.	2	12 sec.				
7	7 sec.	3	13 sec.				
8	8 sec.	4	14 sec. or more				
9	9 sec.	/	Period not determined.				
0	10 sec.						

Table 6 PARAMETER CODES

Code	Parameter	Units
4	Oxygen*	10 μl/ l or 1 μg-at/l
5	PO ₄ - P	0.01 µg-at/l
6	Total P	0.01 µg-at/l
7	NO ₂ - N	0.01 µg-at/l
8	NO3 - N	0.1 μg-at/l
9	SiO3 – Si	0.1 µg-at/l
Α	pH	0.001 pH units
В	Fluoride	0.01 mg/I
С	Dissolved organic carbon .	0.01 mg/l
D	Particulate carbon	mg/m ³
E	Total Alkalinity	1 μ-eq/1
F	Carbonate Alkalinity	1 μ-eq/1
G	NH3 - N	0.01 µg/l

For example: A Total Phosphate value of 17.12 μ_{0} -at/l is entered as $\boxed{117112}$, a Silicate (SiO $_3$ – Si) value of 12 μ_{0} -at/l is $\boxed{12}$, a pH value of 7.82 as $\boxed{7.82}$.

CANADIAN OCEANOGRAPHIC DATA CENTRE

OTTAWA APRIL 1970

Fig. B.3.7 Data Summary coding instructions (continued).

^{*}Oxygen units must correspond to those indicated on the Cruise Master.

			20 21		C nzE	HT.		2	2	5	2 2	2	2	2	2	~	2 2	7 0	2	2		2	7
				19	SWELL	DIR. PER.	3 p 3 p																
				801	WAVES (SEA)	PER. HT.	Pw Pw HwHw			-				- 1					1				
			ETEOROLOGY	17	WET			•	•		+	1		*	1	*		1		-			-
		A L	METEOR	16	AIR TEMP.		T T	•	•	-	•		•		•	*	•	1	-			*	
		N 01		15	AIR PRES.	-	<u>а</u>	•		•		•					•	•	+-				-0
		7 4 O		14	CODE	SPEED	3		-														
				13	WIND	DIR.	¢ Q Q			+													
			11 .	21	UNASSIGNED	10 13	Z								-,1		7						
REMARKS			10		SOUNDING										•	- +		-	+-				-
			00		BSEBAED	MBER O	DEP						-					+					_
ED BY				7 DATE-TIME (GMT)			HR. MIN.														1		
			7				DAY				- +	_		-			-	+-	1				
	CHECKED				DAT		YEAR MO.																
					ш		X X		•	*-	•						0 1		1				
PROJECT LEADER	ENTERED 8Y		9		LONGITUDE		DF G.									-		+					
PROJ	ENTE						E/w																
CRUISE NUMBER		7 8 9			UCE		ž.	•	•							-	•				-	-	
		۵. م	rc.		LATITUCE		N'S DEG.			_					+	~ / ^		+ ~	· · · · · · · · · · · · · · · · · · ·		1 -		
← YRTI	COUP	23	4		CONSEC. STAT. NUMBER						1	-						.,	;	+	1 .	1	

Bridge Log. The coding instructions are given in Figs. B.4.2 through B.4.4. The form is bound in pads of 50 with "no carbon" copies.

Fig.

CODC BRIDGE LOG - CODING INSTRUCTIONS

USING THIS FORM

The CODC Bridge Log is used to submit information identifying Oceanographic Stations in space and time and giving environmental data such as Bottom Depth and Meteorological Conditions.

COMPLEMENTARY FORMS

The Bridge Log is identical to the Station Master portion of the CODC Data Summary, and can be used optionally instead of the latter to submit the Station Master information. It can be used also in conjunction with CODC Deck Sheets. Bridge Log forms must be submitted together with a CODC Cruise Master for each cruise.

GENERAL NOTES

- 1. Leading and trailing blanks are allowed in all fields except the cruise number field. Note, however, that the last figure before a decimal point must be entered; e.g. 0.3 must not be entered as, ".3".
- 2. Any non-observed field can be left blank; only the first seven must be completed.
- 3. The location of decimal points, whenever applicable, is indicated on the form.
- 4. A provision has been made to enter arbitrary station codes or any other alphanumeric information in the "Unassigned" field. (This information is reproduced in data listings, but cannot be used to search for a station in CODC's files.)
- 5. Any parameter for which a choice of units can be made (see Cruise Master), must, throughout the entire cruise, be entered in the units specified on the Cruise Master.
- 6. Meteorological data can, if desired, be taken from the appropriate columns in the Department of Transport's "Selected and Supplementary Ships' Meteorological Log", which is coded using DOT's "International Meteorological Code Card for Selected and Supplementary Ships". (See also Note 5 on the Cruise Master.) These codes have been set by the World Meteorological Organization. The codes accompanying the present instructions are based on DOT's coding instructions of January 1, 1968. If these are modified, data can be entered according to either the revised DOT Code Card or the 1968 Code Card, provided that the year of publication of the code card used is indicated. Optionally, data can also be entered in units specified on the Cruise Master.
- 7. If an entry in a certain column or field remains the same at a number of subsequent levels, it is sufficient to enter it in the highest and lowest of these levels only, connected by a vertical arrow.

SPECIFIC NOTES

Field No.	Field Name	Column	Explanation
1.	Country	1 – 2	Same as on CODC Cruise Master; always 18 for Canadian cruises.
2.	Institute	3 – 4	Same as on CODC Cruise Master.
3.	Cruise Number	5 – 9	Same as on CODC Cruise Master.

Field No.	Field:Name	Column	Explanation
4.	Consecutive Station Number	10 – 12	Stations must be numbered consecutively throughout the cruise in a chronological order. A new consecutive number is required each time the station is reoccupied, even if no other locations are sampled in the intervening period. Other station code numbers can be entered in the "unassigned" field (number 11) if the data originator so desires.
5.	Latitude	13 – 19	Latitude of the station. Enter N or S in column 13 to indicate north or south latitude. Position is given in degrees and minutes with up to two decimals.
.6.	Longitude :	20 – 27	Longitude of the station. Enter E or W in column 20 to indicate east or west longitude. Position is given in degrees and minutes with up to two decimals.
7.	Date — Time	28 – 37	Sampling time of the first observed level is given in Greenwich Mean Time (GMT). The last two digits of the year (e.g. 70 for 1970) are followed by month (coded 01 through 12), day, hour and minute.
8.	Number of Depths Observed	38 – 39	Enter the number of levels at which observations are made.
9.	Blank	40 – 42	These columns are reserved to insert a computer-calculated Marsden Square number.
10.	Sounding Depth	43 – 47	Sounding depth in units indicated on the CODC Cruise Master. Note location of the decimal point.
11.	Unassigned	48 – 52	These columns can be used to enter any alphanumeric information the data originator wishes to be printed in provisional or published Data Reports produced by CODC.
12.	Cloud Amount	53	Fraction of the sky covered by clouds of any type is coded on an octal scale where 0 stands for no clouds and 8 for a completely clouded sky (Table 1).
13.	Wind Direction	54 55	True direction from which the wind is blowing, in tens of degrees. Enter 00 for calm, 01 for 10°, 02 for 20° and so on by ten degree steps right around to 36 for a north wind.
	Wind Speed	56 – 57	Windspeed can be measured in metres per second, knots, feet per second or statute miles per hour or estimated on the Beaufort scale (Table 2). It must be entered as indicated on the Cruise Master. N.B. The DOT Meteorological Log code gives windspeed in knots.

Fig. B.4.3 Bridge Log coding instructions (continued).

SPECIFIC NOTES (Cont'd)

Field No.	Field Name	Column	Explanation
14.	ww Code	58 - 59	Coded according to Table 3.
15.	Pressure	60 – 62	Enter the last three digits of the barometer reading, or of sea level pressure, in units indicated on the Cruise Master. For example 1026.4 mbar is coded as 264; 987.3 mbar as 873 and 768.3 mm as 683. Sea level pressure can be obtained from the barometer reading by applying corrections for barometer height and outside air temperature using Table 4. N.B. The WMO code gives sea level pressure in mbars.
16.	Air Temperature	63 – 65	Enter air temperature in units stated on the Cruise Master. Negative Celsius temperatures are coded by adding 50 to the absolute value of the measurement. Negative Fahrenheit temperatures are coded by placing a minus sign in the last column (65). Omit decimals when coding in Fahrenheit. For example: $14.2^{\circ}\text{C} \rightarrow 14.2$ $-14.2^{\circ}\text{C} \rightarrow 64.2$ $14.2^{\circ}\text{F} \rightarrow 14.$ $-14.2^{\circ}\text{F} \rightarrow 14.$
17.	Wet Bulb	66 - 68	Coding as for Air Temperature.
18.	Wave Period	69 - 70	Enter the estimated period of sea waves in seconds. When the sea is calm, or the period indeterminate, enter // or leave blank.
	Wave Height	71 – 72	Estimate the average height of the larger well-formed waves of the sea wave system in multiples of 0.5 metres. The height is then coded in units of half-metres. For example, an observed wave height of 5 metres is coded as 10.
19.	Swell Direction	73 – 74	True direction from which the waves are coming in tens of degrees. Enter 00 for calm, 01 for 10°, 02 for 20° and so on by ten degree steps right around to 36 for a wave from due north.
	Swell Period	75 – 76	Code as Wave Period, see instructions for field 18, or according to Table 5 as indicated on the Cruise Master. N.B. The WMO code gives swell as Pw.
	Swell Height	77 – 78	Code as Wave Height.
20.	For CODC use	79	To be entered by CODC staff.
21.	Card Type	80	Preprinted.

Fig. B.4.4 Bridge Log coding instructions (continued).

SEVENTH SIXTH FIFTH CORRECTIONS FOURTH CODC THERMOMETER CALIBRATION SHEET DATE OF CAL.

theet. The coding instructions are given in The form is bound in pads of 50. in pads Sheet. Thermometer Calibration Figs. B.5.2 and B.5.3, Fig.

CODC THERMOMETER CALIBRATION SHEET CODING INSTRUCTIONS

USING THIS FORM

The CODC Thermometer Calibration Sheet is used to code calibration constants for reversing thermometers. It is used in combination with the CODC Deck Sheet by the Thermocheck Program to calculate corrected and calibrated temperatures from reversing thermometer readings.

GENERAL NOTES

- 1. The rows on the form are grouped in pairs. The first of each, indicated by an M, contains Main Thermometer data, the second, indicated by an A, contains Auxiliary Thermometer data.
- 2. Shaded portions must be left blank.
- 3. Leading and trailing blanks are allowed in all fields.

SPECIFIC NOTES

Identification

Field Name

Column	Main Thermometer	Auxilian	Auxiliary Thermometer
-	Enter P or U to indicate whether the Will be copied from the Main Ther-thermometer is protected or un-mometer entry by the keypunch opprotected.	Will be copied mometer entry erator.	from the Main Therby by the keypunch op-
N	Enter manufacturer code: R = Richter and Wiese Y = Yoshino N = Negretti and Zambra	Will be copied mometer entry erator.	Will be copied from the Main Thermometer entry by the keypunch operator.
3-7	Five digit thermometer number as Will be copied from the Main Therassigned by the manufacturer. erator.	Will be copied mometer entry erator.	Will be copied from the Main Thermometer entry by the keypunch operator,

Field Name	Column	Main Thermometer	Auxiliary Thermometer
Date of Calibration	8 – 13	Year and month of last calibration.	Leave blank
°>	14 – 16	A calibration constant for individual thermometers, representing in degrees the volume of mercury below the 0° C mark when the thermometer is in a reversed position at 0° C. Enter in whole degrees Celsius.	Leave blank
O	17 – 20	Pressure coefficient of an unprotected thermometer, expressed in units of $0.0001^{\circ}\text{C/kg/cm}^2$.	Leave blank
Correction, lowest	21 – 23	Enter the lowest temperature at which a calibration is made in units of °C. Note the position of the decimal point. Enter a minus sign, if applicable, in column 21.	Same as for Main Thermometer.
	24 – 28	Enter the corresponding calibration correction in units of °C. Note the position of the decimal point. Enter a minus sign, if applicable, in column 24.	Same as for Main Thermometer.
Correction: second, third, etc.	29 – 76	Enter information for subsequent calibration points in ascending order. Not all fields need be used.	Same as for Main Thermometer.
\times	77 – 79	Reciprocal efficient of thermal expansion of the glass of which the thermometer is made, given in units of 10°C. Usually 610 x 10°C unless otherwise indicated on the thermometer certificate.	Leave blank
Card Type	80	Pre-printed	Pre-printed.

Thermometer Calibration Sheet coding instructions (continued).



APPENDIX C

DATA RETRIEVAL FORMS

- Data Extraction Form
 Data Output Form



DATA EXTRACTION FORM for OCEANS IV

GENERAL INSTRUCTIONS

- Use of all cards, except the Request card, is optional. Any number of cards within a subgroup, such as AREA, can be used up to the maximum number of cards shown.
 Any entry on a card can be left blank if a search for a particular option is not required.
 Any entry on a card can be left blank if a search for a particular option is not nequired.
 The output will only contain data meeting all search requirements specified. If an option is left blank, it will not be tested for.
 The Data Extraction Cards must be followed by the Data Output Cards specified on the Data Output Form, if data are to be retrieved. This is not necessary for Search Modes 2 6.

OUTPUT OPTIONS AND SEQUENCE SEARCH MODE 1: Retrieve 2: Station count 3: Station, Master Catalogue 4: Data Inventory 11 5: Data Inventory 11 6: Data Inventory 11 6: Data Inventory 11 6: Data Inventory 11	AD S T	16 17 18 19 20 21 22 23 24 25 26 27 28 29 30 3 INVENTORY OPTION blank: if Search Modes 1, 2 or 3 are used 1: optional with Search Modes 4, 5, 6, see Report	DATA SEQUENCE This is determined by a sort key consisting of the e and T in the sequence entered below, where: L = Location = Ten-degree square + One-degree square I = Identification = Country + Institute + Cruise + S T = Time = Year + Month + Day + Hour + Minure If left blank, data will be sorted in standard file sec	49 50 51 52 53 54 55 56 57 58 59 60 61 slements L, quence L-1-T
	ND SEQUENCE ND SEQUENCE Oralogue Sme Report Report for data west of the "From" but	6 17 18 19 20 21 22 23 24 25 26 27 28 INVENTORY OPTION blank: if Search Modes 1, 2 or 3 are used 1: optional with Search Mode see Report	7 32 33 3	53 54 55 56 57 58 59 60
	OD SEQUENCE Catalogue See Report for data west of the "From" but	INVENTORY OPTION blank: if Search Modes 1, 2 or 3 are used 1: optional with Search Mode see Report	33 33	53 54 55 56 57 58 59 60
	Oralogue See See	INVENTORY OPTION blank: if Search Modes 1, 2 or 3 are used 1: optional with Search Mode see Report		ements L, orion . rence L - I - T
SEARCH MODE 1: Retrieve 2: Station count 3: Station, Master 4: Data Inventory 5: Data Inventory 6: Data Inventory	Grandogue Sem Report Report From* but	INVENTORY OPTION blank: if Search Modes 1, 2 or 3 are used 1: optional with Search Mode see Report		ements L, re ation tre tence L - I - T
1: Retrieve 2: Station count 3: Station, Master 4: Data Inventory 5: Data Inventory 6: Data Inventory	See	blank: if Search Modes 1, 2 or 3 are used 1: optional with Search Mode see Report 64		ements L, objour
2: Station count 3: Station, Master 4: Data Inventory 5: Data Inventory 6: Data Inventory	See See	1, 2 or 3 are used 1: optional with Search Modesee Report See Report 64		otion
3: Station, Master 4: Data Inventory 6: Data Inventory 6: Data Inventory	Sme Sme Report Report Report From' but	1: optional with Search Modes see Report		ation
5: Data Inventory 6: Data inventory	63 for data west of the "From" but		T = Time = Year + Month + Day + Hour + Minute If left blank, data will be sorted in standard file set	
	for data west of the "From" but			
	for data west of the "From" but			
	for data west of the "From" but		92 99	
AREA (optional) The program searches		ance of the "To" Longitude	TIME INTERVAL OR SEASON (optional)	
The "From" latitude must be south of the "To" latitude.	must be south of the 'lo' tatifud	***************************************	YEAR RANGE IS DATE BANGE	
	LAT.	LONG.	CODE	HIGH required, regardless of the year
8000	FROM TO	FROM	5	MO. DAY Range" fields blank,
ž	DEG. MIN. NS DEG. MIN. EV	W DEG. MIN. E, DEG. MIN.	× :	
10 A R E A			T W T T	If only data for one year or one
A R E A			= Z	day are required, the "High"
12 A R E A			- I-	reids can be left blank
13 A R E A			× -	
R			W L	Successive month and year
W W			× -	ranges respectively can be
A E			₩ -	entered, each line determining
W W			25 T M E	one column in the print out.
+			× -	
A R E A			×	

Section See Data Extraction form. C.1.1 Fig.

COUNTRY INST.	CRUISES TO BE RETRIEVED (optional) If only one cruise or station is required, the "High" fields can be left blank	ed, the "High" field	s can be left blank		"	0 å 4 3	I parameters parameters code range vo blank for parameters with parameters with parameters.	re poramete fisted have been obser values as or meters code	ters are specified, stati tive been observed. A st reved at leoss at one le on Data Summary forms on A digits. If range ded in 4 digits. If range range or without parame	ied, statio ved. A state at one lever ary forms; ary forms;	ion is accion is accolute colutare reque	If one or more parameters are specified, stations will be returned only if all parameters listed have been observed. A station is accepted if each apparameter has been observed at least at one level. Code range volues as an Data Summary forms; leave columns 8 and 13 blank for parameters coded in 4 digits. If ranges are requested all levels with parameters out of range or without parameter will be flagged "no.".	
COMPANY NOTE: WE NO							000	PAR	AMETER				7-1
C C C C C C C C C C								7	חחח	-	ż	MAX.	
10 E N N N N N N N N N			RANGE	STATION			Δ A						
10 E N 1	COUNTRY INST.		HIGH	LOW H			α α α						
D E N N D E N N D E N N D D E N N D E D E N N D E D E N N D E D E D E N N D E	1 D E						02 0						
10 E M	ш I						K CK						
1 0 E N					Fluor	-	α α						
1 0 E N	_ D				Diss. Org.		A .						
D E N	П О				Part.	_	Y Q						
D E N 1 D E N 1 D E N 1 D E N	m í				Carb.	_	Z Y						
	ח ת				H.	_	∝						
2 5 1 1 2 3 4 5 5 7 1 1 1 1 1 1 1 1 1	U L					_	A						
Any one or more of the following politics come be searched for (meters)	1 2 3 4 5 6 7 88 9	11 12 13 14	1 18	77 77 77 77 70 70 70 70 70 70 70 70 70 7		700 1000 110	ATAG IA	011011011011	Ci+ac) VIN				
CODE Strike	SAMPLING LEVELS REQUIRED (option Any one or more of the following options	nai) s can be searched for	(meters)		EΨ	nter 1 in each b	ox below th	e parameter	s desired lea	ive blank f	or all othe	7.2	
CODE Retrieve only if depth Retrieve in depth Re	BOTTOM	АДЕРТН	8-	SAMPLING DEPTH	<u> </u>	1 C	CLOUD				WET		
DATA INVENTORY REPORT HEADINGS (optional)		Not more than:		servations available at levels Above:		ט ט	AMOUNT			\rightarrow	BULB	- 1	
2 3 4 5 6 7 8 9 10 11 12 13 14 15 16 17 18 19 20 21 22 23 24 25 26 27 1 2 3 4 5 6 0 7 8 9 10 11 12 13 14 15 16 17 18 19 20 21 22 23 24 25 26 27 1 2 3 4 5 6 0 7 8 9 10 11 12 13 14 15 16 17 18 19 20 21 22 23 24 25 26 27 28 29 30 31 32 33 34 35 36 37 38 39 40 41 42 43 44 45 46 47 48 49 50 51 52 53 54 55 56 57 58 99 60 60 62 63 64	P T H				08	E T Y		\dashv	-	- -	2	74 75 72	
Data Inventory REPORT HEADINGS (optional) Used only if Date Inventories are required; See Search Modes 4, 5, 6 on RQST card Level only if Date Inventories are required; See Search Modes 4, 5, 6 on RQST card Level only if Date Inventories are required; See Search Modes 4, 5, 6 on RQST card Level only if Date Inventories are required; See Search Modes 4, 5, 6 on RQST card Level only if Date Inventories are required; See Search Modes 4, 5, 6 on RQST card Level only if Date Inventories are required; See Search Modes 4, 5, 6 on RQST card Level only if Date Inventories are required; See Search Modes 4, 5, 6 on RQST card Level only if Date Inventories are required; See Search Modes 4, 5, 6 on RQST card Level only if Date Inventories are required; Search Modes 4, 5, 6 on RQST card Level only inventories are required; Search Modes 4, 5, 6 on RQST card Level only inventories are required; Search Modes 4, 5, 6 on RQST card Level only inventories are required; Search Modes 4, 5, 6 on RQST card Level only inventories are required; Search Modes 4, 5, 6 on RQST card Level only inventories are required; Search Modes 4, 5, 6 on RQST card Level only inventories are required; Search Modes 4, 5, 6 on RQST card Level only inventories are required; Search Modes 4, 5, 6 on RQST card Level only inventories are required; Search Modes 4, 6, 6, 6, 6, 6, 6, 6, 6, 6, 6, 6, 6, 6,	2 3 4 5 6 7 8	11 12	14 75	19 20 21	23 24 25 26	ω 4	9			=	12	14 15 16	
HE A D	DATA INVENTORY REPORT HEADING Used only if Data Inventories are requir	GS (optional) red; See Search Mode	5, 6 on RQST	card									
H E A D	CODE HEADING TO BE PR	SINTED IN POSITION	S 41 TO 100 OF 1		70	7.5	80		85	06		95	100
DATA DISTRIBUTION ALONG THE VERTICAL (optional) One data point has to be present in each interval specified an this card. This requirement can be relieved by entering under "a" the number of "empty" intervals allowed. CODE E V L	H E A D H E A D S S S S S S S S S S S S S S S S S S	13 14 15 16	18 19 20 21	23 24 25 26 27 28 29	32 33 34 35 36 37	40 41	44 45	47 48	50 57	54	57	59 60 61 62	64
This requirement can be relieved by entering under "a" the number of "empty" intervals allowed. CODE DATA DISTRIBUTION ALONG THE VI	ERTICAL (optional) ich interval specified	on this card.		Levels outside the reference in the output A blank or zero entry	unge of interva (see "Level B under "a" bot	Is specified Reject" entr	are marked y) mpty interv	with a "no"	flag and c	an options			
CODE de Code	This requirement can be relieved by en	ntering under "a" the	number of "empty ES BETWEEN DE	PTH INTERVALS	Lead zeros must be	entered; any nu	mber of field	is can be le	t blank; en	er trom let	100 11011		
л п э > >	∢z±												_
> =	m												
	L E <			-									7

Fig. C.1.2 Data Extraction form (continued).

DATA OUTPUT FORM for OCEANS IV

To be used: 1. To control data output or Data Report formats generated from the Transaction File
2. To control output of data retrieved from the Master File. In this case Data Extraction Cards must precede the Data Output Cards

L α					¥	REQUESTER	ADDRESS							
1 2 3 4 5	6 7 8	11 01 6	12 13 14 15	16 17 18 19	20 21 22 23	24 25 26	27 28 29 30	31 32 33 34	35 36 37 38 3	39 40 41 42 43	44 45 46 47	48 49 50 51 52	53 54 55 56	57 58 59 60 61
OUTPUT OPTIONS	ONS													
OUTPUT MEDIUM Enter 1 below output		DERIVED PA	~	GEOGRAPHICA Use only with N For means of st If INGE is not u	L DISTRIBUT laster File and andard levels a sed, means are	ROST option or derived par	GEOGRAPHICAL DISTRIBUTION OF MEANS Use only with Master File and ROST opino, I (see Date Retrieval Form) In means of strondard levels so derived parameters use INGE card (290) If INGE is not used, means are given for all data extracted but not flagged.	rieval Form) E card (290) Sut not flagged,			PILE TO BE USE	8	LEVEL REJECT Blank: reject levels marked "no" by the extract program	Page n
CARD TAPE	PRINT	red :		Blank: Not required to the state of the stat	uired jree sq.		Fill	n code of parar	Fill in code of parameter concerned		1: Transaction 2: Master	done o	Suppress the "ho" flag and accept all levels of each station extracted	of blank
77 67];												
	co	00			67				89		69		70	71 72
INTERPOLATION CONTROL (optional) This card need be present only if interpolation is required	ON CONTR	OL (optional) t only if inter	polation is re	quired										
CODE	CODES C Temps, se	of PARAMET	ERS TO BE I	CODES OF PARAMETERS TO BE INTERPOLATED Temps, sal. and sound speed are always interpolated if this card is used	ED ed if this care	Blank		INTERPOLATION METHOD 1: Rattray	QO		BASIS FO	FOR INTERPOLATION Depth Levels	TION	
C A L C	9 9	7 8	9 10	11 12	13 14	15 16		2				essure levels		
SPECIFICATION OF STANDARD LEVELS (optional) If this cord is not used, interpolations will be corried out to Sandard	N OF STAN	DARD LEVE	LS (optional)	S C C C C C C C C C C C C C C C C C C C		-							0	
CODE	LEVELS Fill ou	LEVELS TO BE USED FOR INTERPOLATION Fill out from left to right	FOR INTER	POLATION										
ı c∠														
-														
α ⊢ z														
2 3 4 5	5 6 7 8	9 10 11 12	13 14 15	16 17 18 19 2	20 21 22 23	24 25 26 2	27 28 29 30 3	37 32 33 34 3	35 36 37 38 39	9 40 41 42 43	44 45 46 47 48	3 49 50 51 52	53 54 55 56 57	58 59 60 6
CRUISE IDENTIFICATION (optional)	IFICATION	(optional)	1				GEOGRAPHIC	AI DISTRIBIL	GEOGRAPHICAL DISTRIBILITION OF MEANING CONTRACTOR		Table	le 1		able 2
Case only it a Data Report is printed from the Transaction File	ald Report	s printed from	The Iransac	- 1					10 m	3 CON 1 ROL	STANDARD LEVELS) LEVELS	Expl. see c	card 240 col. 11
CODE	COUNTRY	-NSH	CRUISE NUMBER	JMBER PAGE	E NUMBER OF		CODE	Indicate level for which means	el	Blank: If the observed parameter de- fined in co-	0 225	2,000 7,500 2,500 8,000		
O R U S										Jumn 68, card	300	3,000 8,500	_	· dello
C S									It If o	If a derived pa-	400		1 sigma-?	-
C R U S									rar	rameter is to be	200	4,000 9,500		
ے د									000	case a code	009	4,500	S sigma-	·9
2									0-0	0-5 has to be	700	5,000	3 geopot.	geopot, anomaly
2								***************************************	ra c	nn 68, card		5,500		
) :			,						2.00	200, See table	000,1	000,000	4 pot, en	pot, energy anomaly
2 2											1,200	2,000	5 SVA	
Σ (C											1,300	2000,	_	
C R C							(_	

See Section Data Output form, C.2 Fig.



DATA EXTRACTION FORM for OCEANS IV

GENERAL INSTRUCTIONS

Use of all cards, except the Request card, is optional. Any number of cards within a subgroup, such as AREA, can be used up to the maximum number of cards shown. Use of all cards, except the Request card, is optional. Any number of cards within a suk
 Any entry on a card can be left blank if a search for a particular option is not required.
 The output will only contain data meeting all search requirements specified. If an optior
 The Data Extraction Cards must be followed by the Data Output Cards specified on the I

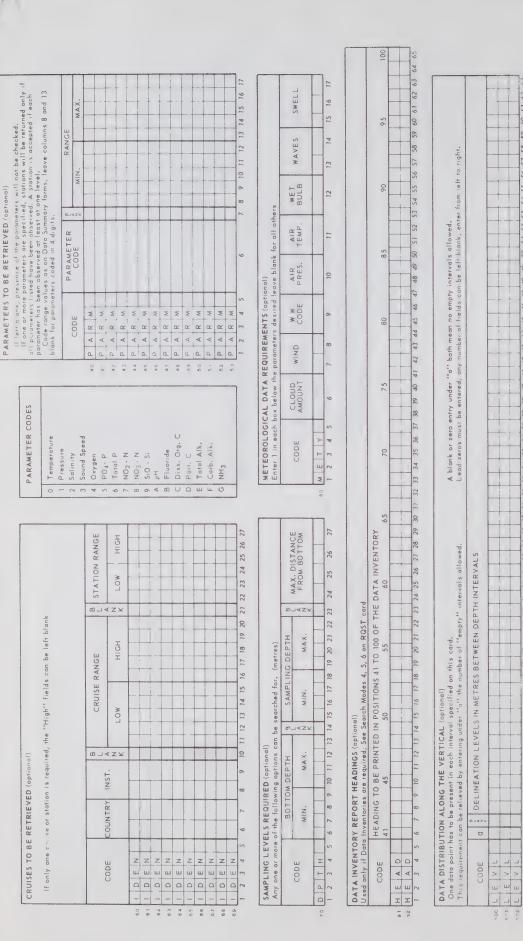
The output will only contain data meeting all search requirements specified. If an option is left blank, it will not be tested for.

The Data Extraction Cards must be followed by the Data Output Cards specified on the Data Output Form.

62 See reverse side If all data for a season are required, regardless of the year If only data for one year or one day are required, the "High" 67 of observation, leave "Year Range" fields blank, 9 freids can be isft blank 59 28 57 26 22 54 53 DAY If left blank, data will be sorted in standard file sequence L -1-T 52 18 19 20 21 HIGH This is determined by a sort key consisting of the elements L, 51 DATE RANGE MO. 8 | = Identification = Country + Institute + Cruise + Station L = Location = Ten-degree square + One-degree square 49 DAY 8 16 17 NO T 47 T = Time = Year + Month + Day + Hour + Minute 1 and T in the sequence entered below, where: MO. 46 99 11 12 13 14 15 45 QUAZX 4 65 \$ H16H TIME INTERVAL OR SEASON (optional) 42 YEAR RANGE 4 02 8 33 DATA SEQUENCE LOW 38 37 36 32
 W
 W
 W
 W
 W
 W
 W
 W
 W
 W
 W
 W
 W
 W
 W
 W
 W
 W
 W
 W
 W
 W
 W
 W
 W
 W
 W
 W
 W
 W
 W
 W
 W
 W
 W
 W
 W
 W
 W
 W
 W
 W
 W
 W
 W
 W
 W
 W
 W
 W
 W
 W
 W
 W
 W
 W
 W
 W
 W
 W
 W
 W
 W
 W
 W
 W
 W
 W
 W
 W
 W
 W
 W
 W
 W
 W
 W
 W
 W
 W
 W
 W
 W
 W
 W
 W
 W
 W
 W
 W
 W
 W
 W
 W
 W
 W
 W
 W
 W
 W
 W
 W
 W
 W
 W
 W
 W
 W
 W
 W
 W
 W
 W
 W
 W
 W
 W
 W
 W
 W
 W
 W
 W
 W
 W
 W
 W
 W
 W
 W
 W
 W
 W
 W
 W
 W</t - - -- - -34 CODE 33 32 2 optional with Search Modes 4, 5, 6, 8 2 2 2 2 8 30 8 82 27 × × searches for data west of the "From" but east of the "To" longitude. The "From" latitude must be south of the "To" latitude 26 24 25 26 1, 2 or 3 are used if Search Modes 20 25 ADDRESS TO DEG. 23 24 INVENTORY OPTION see Report 23 22 LONG. ×. 21 20 21 20 blank: FROM 02 19 DEG. 60 18 17 76 LU 3€ 36 2 E.Z. 11 12 13 14 15 14 DEG. 13 12 Prop. **DUTPUT OPTIONS AND SEQUENCE** 20 2 N. N. Swe Station, Master Catalogue 63 FROM DEG. 80 REQUEST BY (obligatory): = 9 Data Inventory Data Inventory Data Inventory Station count AREA (optional) SEARCH MODE Retrieve -CODE O 0 . 0 . 4 0 0 7 CONT.D

Section See Extraction form. Data Fig.

54 55



at levels below:" columns 15-22 on cards 100-102 "Retrieve if observations available card (70) the legend of ...above:" for columns 19-22. Also: 46 47 48 49 41 42 43 44 45 36 On the "Sampling Levels Required" 35 32 18 19 20 21 22 23 24 25 26 27 28 29 30 31 Extraction form (continued). road: modified to for columns 15-18 and 12 13 14 15 16 17 should be Note: Data C.1.2

Fig.

depths should be entered as four-digit numbers in metres

DATA OUTPUT FORM for OCEANS IV

To be used: 1, To control data output or Data Report formats generated from the Transaction File
2, To control output of data retrieved from the Master File. In this case Data Extraction Cards must precede the Data Output Cards

R P R T	TAPE CONTROL (optional) CODES OF PARAMETERS TO BE INTERPOLATED COPES OF PARAMETERS (optional) COPES TANDARD LEVELS (optional)	S	GEOGRAPHICAL DISTRIBUTION OF MEANS Use only with Master File and RQST options. Blank: Not required 1: One-degree sq. 2: Ten-degree sq. 57 67 67 67 68 11 Rattroy 2: Reiniger & Ross	5, 6 (see Date Retrieval Form) Il in code of parameter concerned BASIS FOR INTERPO D: Depth Levels P: Pressure level	52 53 54 55 56 57 58 59 FILE TO BE USED 1: Transaction 2: Master 69 LATION
TPUT OPTIONS TAPE CARD 63 64 TERPOLATION CONTROL (of This cord need be present only) ODE CODES OF PA	PRINT 65 67 pprional) y if interpolation is re ARAMETERS TO BE 8 9 70 RD LEVELS (optional)	DERIVED PARAMETER OPTION Blank: No derived par. 1 : Derived par. required 66 1 in TERPOLATED 11 12 13 14 15 11 12 13 14 15 11 12 13 14 15	GEOGRAPHICAL DISTRIBUTION OF MEANS Use only with Master File and RQST options. Blank: Not required 1: One-degree sq. 2: Ten-degree sq. 67 67 2: Reiniger & Ross 77	5, 6 (see Data Retrievo	FILE TO BE USED 1: Transaction 2: Master 69 LATION
UTPUT MEDIUM TARE CARD 63 64 TERPOLATION CONTROL (or This cord need be present onl) ODE CODES OF PA	PRINT 65 65 prional) y if interpolation is re ARAMETERS TO BE 8 9 10 RD LEVELS (optional)	DERIVED PARAMETER OPTION Blank: No derived par. 1 Derived par. required 66 1 INTERPOLATED 11 12 13 14 15 11 12 13 14 15 11 12 13 14 15	GEOGRAPHICAL DISTRIBUTION OF MEANS Use only with Master File and RQST options. Blank: Not required 1 : One-degree sq. 2 : Ten-degree sq. 57 INTERPOLATION METHOD 1: Rattrey 2: Reiniger & Ross	5, 6 (see Data Retrieve	FILE TO BE USED 1: Transaction 2: Master 69 LATION
CARD TAPE 64 CARD 64 TTERPOLATION CONTROL (o) This cord need be present only ODE CODES OF PA	PRINT 65 /y if interpolation is re ARAMETERS TO BE 8 9 10 RD LEVELS (optional)	required INTERPOLATED 11 12 13 14 15 11) sed out to Standard Levels (Table 1)	1 Ten-degree sq. 67 1 Rattroy 2: Reiniger & Ross	BASIS FOR INTERPODE D: Depth Levels P: Pressure level	
TERPOLATION CONTROL (or This cord need be present only	prional) y if interpolation is re ARAMETERS TO BE B B CONTROL EVELS (optional)	required INTERPOLATED 17 12 13 14 15 19 od out to Standard Levels (Table 1)	INTERPOLATION METHOD 2: Reiniger & Ross	BASIS FOR INTERPO D: Depth Levels P: Pressure level	
This cord need be present only CODES OF P.	y if interpolation is re ARAMETERS TO BE I	INTERPOLATED 11 12 13 14 15 1) sed out to Standard Levels (Table 1)	INTERPOLATION METHOD 1: Rattray 2: Reiniger & Ross	BASIS FOR INTERPO D: Depth Levels P: Pressure level	LATION
	ARAMETERS TO BE I	1) 12 13 14 15 11 19 19 19 19 19 19 19 19 19 19 19 19	INTERPOLATION METHOD 1: Reiniger & Ross 2: Reiniger & Ross	BASIS FOR INTERPO D: Depth Levels P: Pressure level	LATION S
The second secon	8 9 10	1) 12 13 14 15 [1] [1] [1] [1] [1] [1] [1] [1] [1] [1]			20
C A L - 1	RD LEVELS (optional)	(I) and to Standard Levels (Table I)			
SPECIFICATION OF STANDARD LEVELS (optional)	lations will be carried				
CODE LEVELS TO E	LEVELS TO BE USED FOR INTERPOLATION Fill out from left to right	ERPOLATION	and an artist and an artist and an artist and artist artist and artist and artist artist artist and artist artist artist and artist art		
α 					
F- 1					
2 3 4 5 6 7 8 9	10 11 12 13 14 15	5 16 17 18 19 20 21 22 23 24 25 26	27 28 29 30 31 32 33 34 35 36 37 38 39	40 41 42 43 44 45 46 47 48 49 50 51	52 53 54 55 56 57 38 39
CRUISE IDENTIFICATION (optional)	tional)			Table 1	EVELS
Use only it a Data Report is but	Delian our man pour			225	2,000 7,500
COUNTRY	INST. CRUIS	CRUISE NUMBER PAGE NUMBER	PAGE NUMBER OF PIROT PAGE		
-				400	3,500 9,000
2				200	4,000 9,500
2 0				009	4,500
2 0					5,000
2					5,500
N N				150 1,000	000,9
CRUS				1,200	2000
2					200,
2 C C C C C C C C C C C C C C C C C C C					

Note: On the "Requester Identification" card (200), a new column (70) should be added to indicate whether levels marked as not acceptable by program Retrieve should be rejected (blank) or accepted (mark "S") in the output produced by program Report. Also: on cards 220-222 depths should be entered as four digit numbers in whole metres. Data Output form. See Section 3. C.2



APPENDIX D

DATA OUTPUT PRINT OUTS

- 1. Thermocheck Listing
- 2. OCEANS IV Edit Listing
- 3. Data Report
- 4. Cruise Master Catalogue (Data Acquisitions)
- 5. Data Counts
- 6. Station Master Catalogue
- 7. Data Inventory Type I
- 8. Data Inventory Type II
- 9. Data Inventory Type III
 10. Distribution of Means and Standard Deviations



1 DENSITY-DEPTH TABLE USED FOR THERMOMETRIC DEPTH CALCULATIONS PAGE CORRECTED TEMPERATURES AND CALCULATED PRESSURES CALIBRATION DATA FOR THE THERMOMETERS USED 4 STATISTICS ON THERMOMETER PERFORMANCE CODC THERMOCHECK N OUTPUT CONSISTS OF

Output of the Thermocheck program. The output consists of the four elements listed above and shown in the Figs. D.1.2 through D.1.6. Fig. D.1.1

PAGE 2		
**************************************	TH DENSITY	1
DENSITY-DEPTH TABLE	ОЕРТН	2 0 0 0 0 0 0 0 0 0 0 0 0 0 0 0 0 0 0 0

See Depth-density table used for the pressure-depth conversions. Section 4.2. D.1.2

		P CORR			of James in Association					1		ı	1					
		TEMP			2													
	:	CORR		1	A control of the cont				060 00-	0.020		0.030	-0.030			:		
		TEMP			:	ļ			25.0	25.0		40.0	4000			1		
		CORR			Public consideration of constitute as a real				0.100	0.010	00000	0.010	0 0 0 30	00000	000000	0.020	0.000	0.070
	S	EMP			AND A LABORATE PROPERTY COST MINE OF THE			* * * * * * * * * * * * * * * * * * *	20.0	20.0	20.0	30.0	35.0 -	15.0	15.0	20.0 -	20.0	20.0
	ZOIL	CORR						0.010.0	0.0000	0.020	0.000	0.00000	0.000	0.000	0.020	0.000	0.000	0 2 0 2 0
	G.	 -			and Management of the Control of			4.0	15.0 -	15.0	15.0	25.0	30.00	10.0	10.0	15.0	15.0 -	15.0 -
TA	. C O R			1	a se am se management se management			0.00.0	0000000	0.020	0000000	0.020	0.050	000000	0.020	0.010	0.000	0~0~0
TION DATA	101	GW B			name			1.0	10.0 -	10.0	10.0	10.0	25.0 -	5.0 -	15.0	10.0	20.0	10.0 -
CALIBRATION	S ::		0.000	0.0000	0.000	0000	000000000000000000000000000000000000000	0000000	0.0000	0.010	0000	0.000	0.000	0.010	0.0000	0.020	0.030	0.000
THERMOMETER		150 40 00 00 00	15.0	15.0 -	40.0	0 ° 0 ° 0	40	00	10.0	5.0	10.0	30.0	20.0	15.0	10.0	15.0	5.0	10 a C
THERM	1	CORR 0.0000	0.010	-0.010	0.000	0000	0000	0000 • 0	0000 000	0.020	000000000000000000000000000000000000000	0000 000	-0.010	-0.010	0.020	00.050	0.000000	0 0 0 0 0
	1	TE 000	00	0.0	0000	-2.0	-2.0 0.0	-2.0	0000	000	00	000	0.0	1200	1200	0000	0.00	0.0
	۵ ۲	00 61	0000 6100	0000 0000	0000 6100	0000 6100	0000 6100	0000 6100	0000 0000	0000 6100	0000 0000	0920 6100	0928 6100	0000 6100	0000 6100	0000 6100	0000 0100	0000 6100
	0 ^	0 860	103 0	660	660	105 0	101	110	106	108) 260	100	260	084	067	660	112	112
	AL	D.	638	640	1641	657	629	1660	2753	2756	2765	2954	2963	2992	2995	960	3097	3104
	SERIAL	MAIN PR 1	MAIN PR 1	MAIN PR 1	AUX AUX	MAIN PR 1	MAIN PR 1	MAIN PR 1	MAIN PY 2	MAIN PY 2	MAIN PY 2	MAIN UY 2	MAIN UY 2	MAIN PY 2	MAIN PR 2	MAIN PY 3	MAIN PY 3	MAIN PY 3
		-	0	m	4	ın	ø	4	0	0	10	ged ged	12	(F)	4	5	16	1

Sample listing of the thermometer calibration data used with the Thermocheck program.

			SALIN E												•			:
			ERR															
			CALC	0 • 0	10.0	20.0	30°0	2000	75.1	10001	125,2	150.3	175.4	2000-4	250.6	300.8	401.1	₩ 98. • • • • • • • • • • • • • • • • • • •
σο 1.1			DRESS E													-2.2	1 • E	ιΩ •
PAGE			SMOOTH PRESS E	0 0	10.1	20.5	30.2	50.4	75.6	100.8	126.1	151.3	176.6	201.8	252.4	303.0	404.2	502.7
			AVG OBS	0 .0	0 • 0	0 0 0	0 • 0	0 • 0	0 • 0	0 • 0	0 • 0	0 • 0	0 • 0	0 • 0	0 • 0	300.8	40504	507.7
	SSURES		MEAN TEMP E	8.600	8 405	7.827	6.283	5.587	5.352	4.960	4.826	4 B33	4 • 685	4.360	4.003	3,789	3.711	3.677
	CULATED PRE		EMP DR	8.600G	8.403D 8.406D	7.8230	6.281D 6.286D	5.5870	5.350D 5.355D	4.958D	4.810D	4.836D 4.819D 4.8430	4.695D 4.696D 4.666D	4.350D 4.338D 4.392D	4.029D 3.985D 3.997D	3.787D 3.791D 7.899D	3.714D 3.708D 9.156D	3.682D 3.672D 10.531D
MOCHECK	CAL		DBS TE	TEMP	TEMP	TEMP	TEMP	TEMP	TEMP	TEMP	TEMP	TEMP	TEMP	TEMP	TEMP	TEMP	TEMP	TEMP TEMP PRES
DC THERMO	ATURES AND		RONG 2	00000	8.403	7.828	6.281	5.591	5.362	4.973	4.811	4 837 4 824 4 849	4.679 4.680 4.671	4 4 4 6 6 6 6 6 6 6 6 6 6 6 6 6 6 6 6 6	3.985 3.985 3.9885	3.787	3.718	3.686
COO	TEMPERAT		RONG 1	8.600	8 404 8	7.819	6.282	5.583	5.339	4.944	4 · 809	4 8 8 3 6 4 6 8 3 8 8 8 3 8 8 3 8 8 3 8 8 8 8 8 8 8	4.711	4 • 4 • 4 • 4 • 4 • 4 • 4 • 6 • 4 • 6 • 6	4 E O O O O O O O O O O O O O O O O O O	3.787	3.711	3.679 3.667 10.518
	CORRECTED	99002	SERIAL	BUCKET	PR 3438 PR 6239	PR 1641	PR 8881 PR 9273	PR 8876	PR 6246 PR 8878	PR 6241 PR 5383	PR 9276 PY 3104	PR 9278 PR 8746 PR 1635	PY 2756 PY 3720 PR 1638	PR 1640 PR 6245 PY 3095	PY 2765 PR 9264 PY 3097	PR 8883 PR 7749 UR 8517	PR 6451 PR 6455 UR 8518	PR 7756 PR 6461 UR 6161
:		CRUISE	PLANNED WIRE OUT	0.0	1000	20.0	30.0	50.0	75.0	100.0	125.0	150,0	175.0	20000	250.0	3000	40000	50000
		INSTITUTE 02	TOTAL WIRE DUT	400°0	40000	40000	0 • 0 0 4	40000	4000	40000	40000	400 0	4000	4000	4000	4000	400.0	4200.0
1		INST	WIRE		000	000	000	000	000	-	000	000	000	000	000	000	000	000
		COUNTRY 18	HAIMIN N	prd prd prd prd	1111	1111	1111	1111	1111	1111	1111	1111	1111	1111	1111			2222
		COU	SNS	001	001	001	001	001	001	001	001	001	001	001	001	001	001	100

Sample output of the corrected temperatures and calculated pressures for each level. Columns containing error indicators are headed by an "E". See Section 4.1 for a detailed explanation. Fig. D.1.4

		11		•		•	•	•	•	•	•	0 (0 4					9	•		0		•	D (0					
		11 ++ 0		•				•	•		•	9 () (•	•								•	0	•			
		+• 09 +• 10					•	•	•		•	•							0			0				a -											
		8 +•0				•	•				•															•	•								•	9	
		0 -+ 2												4																					0		
		.0 + • 9			•		•	•					•																								
		+.05 +.06 +.07 +.08			•		•	•	•		•						. ^							•													
	1			•	•	•		•	•		•	•											•	•								•			•		
	;	+004			•		•	•	•		•				,									•			^			. 10					•		0
	1	+.03		•	•	•	•	•	pref	•		• (4 **	- 61			. (\		•				-		9	911	,			, er)							0.020
CES		+•05			•	•	•	•	CV.		•	•	•		•	•			•	•			•			•					171						S I O
TEMPERATURE DIFFERENCES		+•01	2	•	*	•	•		8	•	•	•	•	• •	J		•	and American and	• •		មព	3	•		•	•	• 1	7 (•	. •	•	•	•	15 16 0 1
E DIF		01 0.00 +.01	-) grad	•	•	_	•	•	-	• (V	•			•	•	-	4 4	מיין פ		•	7	•	-	•	•	• n) 4		•			•	CA.	SSS
RATUR			~	14	****	m	N	-	•			V	•	•	•	•	•	1	0	10	1 6		2	•	-	•	•	•	1	•	•		-	CV	CAI	•	AN ONCE IS 35 IS 134 S NOT EXCEEDING
LEMPE		02		•	•	2	2		•	• 1	-	•	•	•	•	•	• •	100	3	• •			•	~			•	•	8 (e.	•	•	•	T 10
HO.		- 0 03		•	•	•	•	m	•	•		→	•	• !	•	•	•		9 =	• •	•	•	•	2	•	EV.	•	•	D	•		•		•	•		RS USED MORE THAN METER READINGS IS ALL DIFFERENCES N
3UT IO		04	•	•			•	•	0	•		•	•	•	• (4	•	1	•	•	•	•	•	•	-	~	•	•		b 4	•	•	•		•	•	USED M ER REA L DIFF
ISTRIBUTION		-• 0 £	•	•	•	•	•	•	•	•	•	•	•	• .		۰ ۳	-	• [· ·	• •	• •	• •		•	•	•	•	•	•	•. ·	•		•		•	•	•	MOL
٥		90 °-	•	•	•	•	•	•	•	•	•	•	•	• :	• •		7	• (• •		•	•	•	•	CV	•	•	•	P 1	• •				•	•	•	HERMOMET ED THERM VALUE O
FREQUENCY	002	07	•	•		•	•	•	•	•	•	•	•	•	•	• •	-		• •	•	•	•	•	•	•	•	•	•	•	• •		1 10			•		THER IRED TE VA
ű.	SE 99002	08	•	•		•	•	•	•	•	•	•	•	•	•	• •	-4	•, i	• •		•	•	•		•	4	•	•	•	9 6	•				•	•	IRS OF THE OF PAIRED ABSOLUTE V
	CRUISE	09	•	•	•		•	•	•	•	•	•	•	•	•	•	•	•	o (•	•		•	•	•	•	•	• •				•	•	•	MBER THE A
	02	10	,	• •	•	•	•	•	•	•:	•	•	•	0	•	•	•	•	0 1			•						•			•				•		NUMBER OF PAIR TOTAL NUMBER O
	INSTITUTE	-•11		• •	•			•	-	-	•	•	•	•	•	٠	•	•	• •				•		•		•		•	• •	•		•		•		MTN
	INSTI	RM 2	220	5685	1273	1878	1383	1104	3746	1635	635	3720	638	638	0740	3093	3095	1000	1000	7740	245	5461	7760	3888	3721	2753	8888	400	2000	1000	541A	8739	8877	1660	1657	1657	
	. 89	THER	0	1 0	a	ď	D.	λd	PR	ad	PR	λd	OL I	a c	1	J 1	a 0	7 0	1.0	1 0	2 0	0	0	PR	λd	Ad	0 1	10	7 0	10	1 0	0	d	0.00	DR	PR	
	COUNTRY	E E	34.30	1641	8881	6246	6241	9276	9278	9278	8746	2756	2756	3720	1040	1640	6245	2017	2000	2000	6000 6000	7756	8742	6464	7748	7595	2995	9205	7500	2000	0261	36.89	8876	1659	1659	1660	
	Cau	THERM	000	10	2	0	d	0	PR	PR	a a	ρ¥	7	d	2	2 1	2 2	7	20	1 0	K 0	DO	D	ď	a d	D'A	À 0	X (1,0	7 0	- 0	0.0	00	œ c	PR	PR	

Statistical analysis of the performance of paired thermometers (part 1), showing the distribution of observed differences over the interval -0.11° C to $+0.11^{\circ}$ C in steps of 0.01° C. The outer columns contain a count of all observations deviating by plus or minus 0.105° C or more Fig. D.1.5

respectively.

2.0_			!				-																						The second of the second of						
P'AGE 7			!				mane are named to over the				-							1																	
			NTERVAL DVER 2750		• •		•	•	•	• •		•	•	•	•	•	•	•	•	• •		•	•	•	0	•	•	• 1	ו (א	ا (د	۰ (۲	-	00	u c	u M
			DEPTH 1 1100 2750	•	• •	•	•	•	•	• •	1	•	•	•	•	•	•	•	• (• •		•	•	a i	m I	ו ליו	r) i	m	•,	•	•	•	0	•	• •
:			EACH 450 1100	•	• •	•	•	•	•	•	•	•	•	۰	•	•	•		•		i M	m	r 1	מי	۰		•		•	•	•		0	0	• •
LYSIS		RMANCE	225 450				•	•		• •	١.	•	0		•	• (ე •	4 4	\$ 14	n (r		•		•	•	D			•			•	•	•	
IL ANALYS		PERFOR	125 225			•		• •	0 1	יא כ	ıc	4	4	ហ	4	4	•	•	•	• •			•	•	•			•				•	•	•	• •
TISTICAL		ETER	08SE 40 125		• •	· 10	ısı	2	•	• •			•	•	•	•	•	•	•	• •	, 0		•	•	•	•		•	•		•	0 1	77)	۰	
STA		THERMOM	NO. 07	េ	ຄະດ			9		•				•	•		•	•	•	• (•	•	•	•				•	•		•	•	•		
HERMOCHECK		AIRED T	S FI	01	30	0	0	-11	ent h	n c	0	N)	CUI	0	(N)	m	N,	ed a	-0 C		000	00	0	03	02	02	0	0	01	a.	ores (0	(0 (000
THER		A d NO		0		0	0	0 (00		00	0	0	0	0		0 (00	00	0	0		0	0	0	0	0		0		0	o o		000
		STATISTICS	SD	000	0 0	010	0 0 1	e 0 2	000	9 0	0 0	0.4	.05	• 02	• 05	• 0 7	0 0 4 0 0 A	000	000			000	03	90°	· 03	e 03	000	000	000	0 0	• 02	000	000	000	0.00
	E 99002	STAT	DIFF	00	000	010	0 0 1	0 0 2	000			03	.04	020	e 04	90°	e 04	0 0	100			000	.02	• 05	• 03	• 03	000	000	00.	• 02	.01	.01	000	000	00000
:	CRUIS		EAN T																																• 518 • 521
:	TE 02	:	el O	6	σα	0 10	ů.	ID .	4	4 <	14	14	4	4	4	4	4	4	et i	ייו ח) (**) (P)	10	2	2	2	-	proj	944	prof	_		9,		
; ;	STITUT	:	Z N									4	- prod	-			e==0		pred o	. c	10	10	S	N	2	2	N	N	N	n	m) .	M	ו'נייו	ו נייו	35
!	ING		HERM	623	368	887	538	310	874	0 4	1700	163	163	624	309	309	926	309	300	4/1	545	776	888	372	275	888	645	889	936	538	641	873	887	166	1657
	100	i	1								1																								2 2
,	DUNTRY		M M	343	164	0 0	62.4	927	927	126	# W	275	372	164	164	624	276	276	926	00 4 00 4 0 00	775	874	646	774	759	299	926	956	927	299	956	368	887	165	1659
į	000		H	PR	0.0	r a	20	0	0.0	2 0	1 0	7	b	a	a.	d d	βA	a.	0. 0	0.0	2 0	d.	a.	O.	00	Ad	D.P.	DR	a	ÀG.	PR	D	0.1	2	a a,

Statistical analysis of the performance of paired thermometers (part 2), showing the mean temperature observed with each pair, the mean difference, the standard error of the observed ran deference, and the number of observations in each of 7 depth intervals.

D.1.6

Fig.

PAGE 73			SOUND CORR CRUISE MST MISSING		3 SIGMA-T LESS THAN PREVIOUS		3 SIGMA-T LESS THAN PREVIDUS	m		ריז	PD:	m		m	· · ·	2 SOUND CORR CRUISE MST MISSING		3 SIGMA-T LESS THAN PREVIOUS	m	3 SIGMA-T LESS THAN PREVIOUS	m	:	m	,	en en
OCFANDGPARHIC DXTA EDIT		122	306 12 62290 8 6407 562		14353C 30487	14356C 30567	14357C 30551	14397C 30739	14402C 31195	14408C 31546		14426C 33249	14415C 33510	14471C 34145	145¢0C 34409	330 09 00900 8 0410 516	14353C 30344	14347C 29849	14352C 30289	14355 <u>C</u> 39258	14395Ç 30415	14398C 30708	14407C 31462	14408C 32026	14422C 32801
000	1	2 1, 1 2	10 65 05 11 2	-168	-167	-164	m 9 = 1	-085	060-	0501	-114	-119	-159	-077	520-	00 65 05 11 2	-161	-160	-164	-160	-380	-086	060-	-112	100
And companies to the contract of the contract		1807 65001 LAND BASED 8 99	1807 650C1 0C1 N812290 W0771700	2000 00030	2000 00020	2000 00100	2000 00150	2000 00200	2500 00250	00000 0002	2000 00510	2000 00760	2000 01010	2000 61520	20000000	1807 65001 002 N812190 W0771500	2330 00030	2330 00050	2330 06100	2330 00150	2330 00210	2330 00260	2330 00310	2330 00520	2330 00770

Sample output of the Edit program. All data are accepted into the transaction file unless marked as "level rejected", "station rejected" or "cruise rejected". An error correction procedure is available to correct the anomalies signalled on the right hand side of the page. D.2

Fig.

		<	. Why V 100000000000000000000000000000000000	
		2	b) b) b c c c c c c c c c c c c c c c c	
	18 02 302	Ę	1 1 1 1 1 1 1 1 1 1 1 1 1 1 1 1 1 1 1	
	COUN INST RESTA UNAS	و د د د		
4FFF 002	WW F1	6	000\\\\\\\\\\\\\\\\\\\\\\\\\\\\\\\\\\\	
STATION NUMBER	190	0		
STAT	ND-DIR ND-SPD P-TEM T-BLA	T M	. 444MMUTACAAAAC . 000000000000000000000000000000000000	
58725	NO OO	∨ E ⊃		
RUISE NUMBER	AVE-P/F WEL-P/F WEL-D ARO 1011	C 3 S E R	OVO 0 0 0 0 0 0 0 0 0 0 0 0 0 0 0 0 0 0	W
CRU	₩ SS SS E		000000000000000000000000000000000000000	1
	1958 1958 2018	1 1	0 \ 0 \ 0 \ 0 \ 0 \ 0 \ 0 \ 0 \ 0 \ 0 \	15.
	YEAR MONTH DAY H/M	0		30
	50 T0.00 45 15.00	1	0 0 0 0 0 0 0 0 0 0 0 0 0 0 0 0 0 0 0	0
	LAT NS	1 1 1 1 1 1 1 1 1 1 1 1 1 1 1 1 1 1 1 1	T	240.0

Sample Data Report page. This listing is generated with program Report. It can snow up to 10 different chemical parameters per station. The entries are explained in Figs. D.3.3 througn D.3.8.

Fig.

			f ,	SVA	2389 2389 2304 2335 2319	2090		SWA 223362 223362 223362 223362 223366 2233669
		0 m	!	CHI	0-4000	2520	1	TI OH
		COUN INST RESTR UNAS		GEDA	0.534.00	310 310 40 40 40		232 232 232 339
	NUMBER 021	WW 03		SOUND	1483.0C 1483.0C 1483.9C	1444 0000 0000		\$00ND 1144883 144883 144883 144884 144884 144884 144884 144884 144884 14488 14
		310		SGPT	2555 2555 2555 2555 2555 2555 2555 255	0 10 10 10 10 10 10 10 10 10 10 10 10 10		\$ 6PT 2556 2556 2556 3556 3556 3556 3556 3556
	STATION	VO-DIR VD-SPD X-TEM I-BLB		SGMT	25553 25563 25563 25567 25567	2593 2593 2593 2593	C	S G M T 2 S G M T 2 S G M T 2 S G G M T 2 S G G G G G G G G G G G G G G G G G G
21	ER 68017	MIND- MIND- AIR- META-	RVED	SAL	######################################	0000	0 L A T E	SAL 3333 3333 3333 3333 3333 3333 3333 3
	CRUISE NUMBE	WAVE-P/H SWEL-P/H SWEL-D BARO 101	0 8 S E	POT. T	00000000000000000000000000000000000000	33.03	Œ	0 0 1 2 2 2 2 2 2 2 2 2 2 2 2 2 2 2 2 2
	CRU	1968 111 2000		TEMP	8 8 8 8 8 8 8 8 8 8 8 8 8 8 8 8 8 8 8	0004	gend	TEMP 88.700 88.700 88.700 89.8891 99.8891 99.8891 99.8891 99.8891
		OO WONTH		PRESS	0 0 0 0 0 0 0 0 0 0 0 0 0 0 0 0 0 0 0	37-10		PRESS 10.01 200.10 30.02 120.03 126.03 126.03 126.03
		N44 30.00 W 66 31.00 SQ 179.0		DEPTH	0000			0.00 100.00 220.00 30.00 50.00 755.00 1555.00
		LONG V DEPTH MARSD		GMT	20000 20000 20000	0000		5

Sample Data Report page showing interpolated data but no chemical parameters. The entries are explained in Figs. D.3.3 through D.3.8. Fig. D.3.2

_ Corrected For Bar. Height and Outside Air Temperature

GENERAL INFORMATION ON THE CRUISE

|--|

Explanation of the Data Record headings. Fig. D.3.3

DESCRIPTION OF THE DATA RECORDS

GENERAL REMARKS

This Data Report contains oceanographic station data for the cruise indicated on the title page. The data have been edited and processed by CODC's OCEANS IV program, and are archived in our Oceanographic Station Data File. Copies of the data can be provided in computer-compatible form on card or magnetic tape. A description of the OCEANS IV program and/or an outline of available output formats are available upon request. (OCEANS IV; A Processing, Archiving and Retrieval System for Oceanographic Station Data),

Most entries in the observed portion of the Data Records can be accompanied by an error code or doubtful marker. Errors are indicated only if the entry is based on duplicate or multiplicate measurements and are coded A through I in multiples of the last digit shown in the printout (see Table 6) The Data Records are broken into three "blocks": the station master, observed data, and interpolated data blocks. The station master contains the and salinity observations and derived parameters such as sigma-t, specific volume anomaly, etc. are given. It may be followed or replaced by a second group of identification. position, time and bottom depth of the station plus meteorological data and some general information. In the observed data block the temperature Observed data containing all observed parameters but no derived quantities. The third block contains interpolated values of all parameters at specified depth or pressure levels. It also can be replaced or followed by a second group of interpolated data containing all observed parameters but no derived quantities. This data block is included in the listing only if specifically requested by the data originator.

Interpolations can be carried out to standard oceanographic depth or pressure levels (see Table 7) or to depth or pressure levels specified by the data originator. Both observed and derived parameters are interpolated individually, using the nearest two observations (or calculated values) above and below the desired interpolation levels. Two hyperbola are fitted to these points and a weighted mean is determined as described by Reiniger and Ross (1968)* or by Raitray (1962).** Linear interpolation is used in all cases when fewer than two points above and two below the required level are available. On page 1 the interpolation technique used is specified (if applicable).

Record headings (continued) the Data Explanation of D.3.4 Fig.

^{*}Deep Sea Res., 15, p 185-193

^{**}Deep Sea Res., 9, p 25-37

EXPLANATION OF DATA RECORD HEADINGS

Insignificant trailing digits of any parameter can be left blank on the data entry forms, but will be shown as zeros in the listings of all data except temperature and salinity.

STATION MASTER HEADINGS	CRITISE NIMBER	2 STATION NIMBER		
		15. WND-DIR 19. 116. WND-SPD 20. 17. AIR-TEMP	WW CLD-A	
6. MARSD SQ 10. H/M	14. BARO	18. WET BLB		24. UNAS
(1) CRUISE NUMBER	The first two digits indiconsecutively by each inst	The first two digits indicate the year of the first station of the cruise; the next three digits are assigned consecutively by each institute commencing at 001 each year.	of the cruise; the never.	xt three digits are assigned
(2) CONSECUTIVE STATION NUMBER	Indicates the chronologic	Indicates the chronological order in which the stations are occupied.	occupied.	
(3) LATITUDE (4) LONGITUDE	Position of the platform decimals are printed as z N36 25.00.	Position of the platform at the sampling time in degrees and minutes with two decimals. Non-observed decimals are printed as zero's; e.g. observed latitudes of $N36^{\circ}25'$ and $N36^{\circ}25.00'$ will both be printed as $N36^{\circ}25.00$.	s and minutes with tw N36°25′ and N36°25.C	vo decimals. Non-observed 00' will both be printed as
(5) DEPTH	Bottom depth in metres w	Bottom depth in metres with one decimal; adjusted for soundspeed as indicated on page 1.	indspeed as indicated o	on page 1.
(6) MARSDEN SQUARE	A code to designate the te	A code to designate the ten-degree square in which the samples have been taken (Figure 1).	ples have been taken (Figure 1).
(7) YEAR (8) MONTH (9) DAY (10) HOUR and MINUTE	Time-date group defining Time).	Time-date group defining the moment at which the shallowest level is observed in GMT (Greenwich Mean Time).	west level is observed	in GMT (Greenwich Mean
(11) WAVE PERIOD and HEIGHT	Sea wave period in seconds (2 diy wave height of 3 m is coded as 06	Sea wave period in seconds (2 digits), followed by wave height (2 digits) in multiples of 0.5 metres; e.g. wave height of 3 m is coded as 06.	neight (2 digits) in mu	ultiples of 0.5 metres; e.g. a
(12) SWELL PERIOD and HEIGHT	See explanation of (11)			
(13) SWELL DIRECTION	Direction from which swe	Direction from which swell waves are coming. A calm is indicated by 000, waves from due north by 360.	licated by 000, waves f	from due north by 360.
(14) BAROMETER	Air pressure in mbar with one decimal have been applied as indicated on page 1	Air pressure in mbar with one decimal. Corrections for barometer height and/or outside air temperature nave been applied as indicated on page 1.	oarometer height and/	or outside air temperature
(15) WIND DIRECTION	Direction from which the 360.	Direction $from$ which the wind is blowing in degrees. A calm is indicated by 000, wind from due north by 360 .	alm is indicated by 000	0, wind from due north by

Fig. D.3.5 Explanation of the Data Record headings (continued).

(16) WIND SPEED	Wind speed is given in m/sec; original observations made on the Beaufort scale are converted to metres per second according to the scale given in Table 1.
(17) AIR TEMPERATURE (18) WET BULB	In degrees Celsius with one decimal.
(19) WW CODE	Present weather in WMO code 4677 (Table 2)
(20) CLOUD AMOUNT	Sky coverage in eighths according to WMO code 2700 (Table 3)
(21) COUNTRY	Country in which the institute responsible for collecting the data is situated (Table 4).
(22) INSTITUTE	A code identifying the institute responsible for collecting the data (Table 5).
(23) RESTRICTION	If desired, a restriction can be placed on the data by inserting a numerical code. Blank or zero stand for unrestricted and non proprietory data.
(24) UNASSIGNED	In this field any alphanumeric information, entered in the corresponding field on the Data Summary form used to submit the data to CODC, is reproduced. It can, for example, be used to indicate an arbitrary station coding.

ATTA.	JAIA;
ATTENT	AIEUI
AMERICAN	NIEKTOL
TOOUT	ED OK I
THE PARTY OF THE P	JESERV

2. DEPTH

1. GMT 6. SAL 11. CHI

10. GEOA	Time in GMT of in situ observation, e.g. time of reversal of a reversing thermometer. When a multiple cast is initiated prior to and continued after midnight, time may be indicated as 24, 25, 26, etc., hours plus up to
SGPT 9. SOUNDCHEMICAL PARAMETERS	tion, e.g. time of reversal of a revers d after midnight, time may be indi
8. SGPT 13 CHEM	Time in CMT of in situ observat initiated prior to and continued
7. SGMT 12. SVA	

59 minutes. Note that the station date is determined by the date of the shallowest observed level

Sample depth in metres with one decimal,

Pressure at the sampling level, in dbar with one decimal, with reference to a surface pressure of zero. It may be followed by an "M" or a "C" to indicate whether pressure is measured or calculated from a depth observation.

In degrees Celsius with three decimals, measured as indicated on page 1. It can be followed by one of the alphabetic doubtful data markers and error codes shown in Table 6, or by a "P" to indicate temperatures measured with an in situ probe.

the Data Record headings (continued). Explanation of Fig. D.3.6

(4) TEMPERATURE

(3) PRESSURE (2) DEPTH

(1) GMT

Potential temperature is the temperature that a water sample would attain if raised adiabatically to the sea surface. It is defined by:

(5) POTENTIAL TEMPERATURE

$$I_1 = T_1 + \int_{0}^{P_1} \frac{\partial T}{\partial p} \eta dp$$

where T_i is the in situ temperature, $\left(\frac{\partial T}{\partial p}\right)_{\eta}$ the derivate of temperature with respect to pressure under constant entropy, and P_i the pressure at the observed level. Θ_i is given in degrees Celsius with three

In parts per thousand (g/kg) with three decimals, measured as indicated on page 1. It may be followed by the alphabetic error codes shown in Table 6, or by a "P" to indicate salinities measured with an in situ

(6) SALINITY

The specific gravity anomaly, sigma-t, of seawater at atmospheric pressure is defined by:

$$\sigma_{\rm t} = 1000 \times (\rho_{\rm s,t,p=0} - 1.0)$$

where $\rho_{s,t,p=0}$ is the specific gravity of seawater as a function of salinity S, temperature T, and sea surface pressure. Sigma-t is given with two decimals; e.g. an entry of 2485 corresponds to $\sigma_{\rm t} = 24.85$ or $\rho =$

See definition of sigma-t, but substitute the potential temperature Θ for the in situ temperature T.

(8) SIGMA POTENTIAL TEMPERATURE

(9) SOUNDSPEED

Soundspeed is reported in m/sec with one decimal. It may be followed by an "M" or a "C" to indicate whether it is measured directly or calculated as a function of temperature, salinity and pressure using Wilson's equations.

Geopotential anomaly is defined as:

(10) GEOPOTENTIAL ANOMALY

$$\Delta D = \int_0^P \delta \, dp$$

where δ is specific volume anomaly. The integration over pressure is carried out either down to the pressure anomaly is expressed in dynamic metres (105 ergs/gram) with three decimals: a value of 0215 corresponds at the required depth level, or down to the required pressure level, as specified on page 1. The geopotential to $\triangle D = 0.215$ dynamic metres.

(11) POTENTIAL ENERGY ANOMALY (CHI)

Potential energy anomaly is defined by

$$\chi_{\eta} = \frac{1}{g} \int_{0}^{R(z_{\eta})} p \delta dp$$

It is expressed in units of 108 erg/cm2 and recorded with two decimals, e.g. a value of 11644 corresponds where g is local gravity as a function of latitude and depth, p is pressure and δ the specific volume anomaly. to $\chi = 116.44 \times 10^8 \text{ erg/cm}^2$.

(12) SPECIFIC VOLUME ANOMALY

The specific volume anomaly is defined by: $\delta_{\rm stp} = \alpha_{\rm stp} - \alpha_{\rm 35,0,\,p}$

where α_{stp} and α_{35} , 0, p are the specific volume at the in situ salinity, temperature and pressure, or a standard salinity of 35.0%, standard temperature of 0°C, and in situ pressure respectively, δ is expressed in 10^5 ml/gr with one decimal place; e.g. a reading of 1234 corresponds to $\delta = 123.4 \times 10^{-5}$ ml/gr.

Dissolved oxygen in ml/l with two decimals.

(13) OXY

(15) T-P (16) NO₂ (17) NO₃

 $(14) PO_4$

Phosphate-phosphorus in μ g-atoms per litre with two decimals.

Total phosphorus in μ g-atom per litre with two decimals.

Nitrate-nitrogen in µg-atom per litre with two decimals.

Nitrate-nitrogen in µg-atom per litre with one decimal.

Silicate-silicon in µg-atom per litre with one decimal.

The pH value with three decimals.

Fluoride in mg/l with two decimals.

Dissolved organic carbon in mg/l with two decimals.

Particulate organic carbon in mg/m³ with zero decimals.

Total alkalinity in micro-equivalents per litre with zero decimals.

(23) T ALK (24) C ALK

(22) P.C.

(21) D.C.

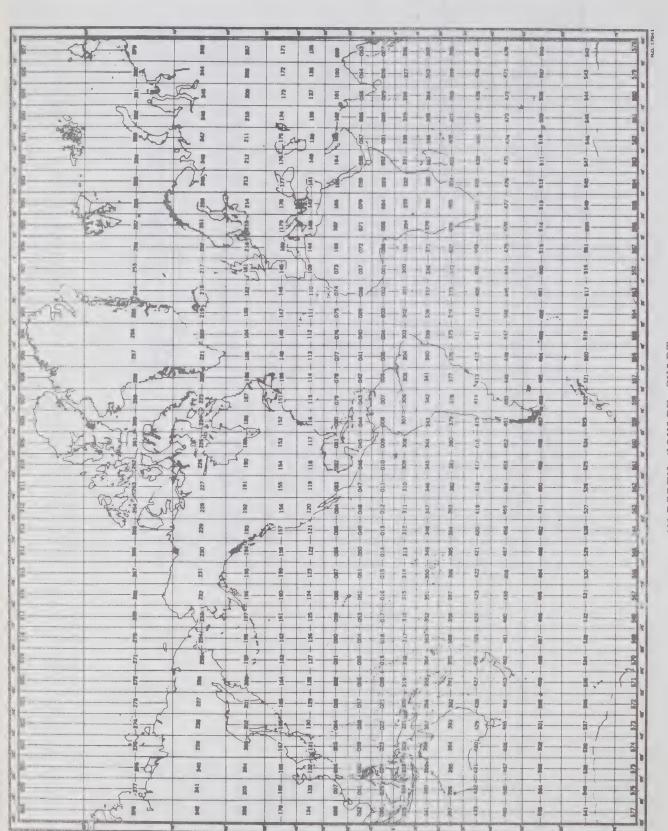
(19) pH (20) F

(18)

(25) NH₃

Carbonate Alkalinity in micro-equivalents per litre with zero decimals.

Annuonia in micrograms NH₃ per litre with two decimals.



MARSDEN SQUARE CHART

CODE TABLES

TABLE 1

CONVERSION OF BEAUFORT ESTIMATE TO WINDSPEED IN M/SEC

	Windspeed in m/sec	15	.19	22	26	30	34	
WINDSPEED IN M/SEC	Beaufort	7	∞	6	10	11	12	
WINDSPE	Windspeed in m/sec	00	01	02	04	07	60	12
	Beaufort	0		2	m	4	5	9

TABLE 2

PRESENT WEATHER (ww - Code)

Use the highest code figure applicable except that 17 has preference over 20 to 49 inclusive.

Code	04-09 SMOKE, HAZE, SAND OR DUST	04 Visibility reduced by smoke	(not ship's smoke)	O5 Dry Haze	06 Widespread dust suspended	in air	07 Blowing spray at ship	08 Dust whirls in past hour	(not for marine use)	09 Dust or sandstorm in sight,	or at ship in past hour	4	
	00—49 NO PRECIPITATION AT SHIP AT TIME	OF OBSERVATION	00-03 CHANGE OF SKY DURING PAST HOUR		Sold Control of the C	00 Cloud development not	observable	01 . Clouds dissolving or	becoming ess developed	02 State of sky on the whole	unchanged	03 Clouds generally forming or	developing

Explanation of the Data Record headings (continued) Fig. D.3.10

Table 2 (cont'd.)

e		26 Shower(s) of snow, or of rain and snow mixed	77 Showed Stoff or of	28 Fog (in past hour but not	29 I hunderstorm, with or without precinitation	Tricon Programming	*Includes hail, ice pellets, or snow pellets	30-39 (Not likely to be used in whin remorts)		Slight or Heavy	Moderate	30 Duststorm or sandstorm, 33	decreasing	31 Duststorm or sandstorm, 34	32 Duststorm or sandstorm, 35	increasing	36 Drifting snow, generally low 37	38 Blowing snow, generally high 39		40-49 FOG AT THE TIME OF OBSERVATION	40 Fog at a distance but not at	ship during past hour	41 Fog in patches	Visi	Visible of time of observation Invisible	42 Fog, has become thinner in 43	 Fog, no change in past hour	46 Fog, has begun or thickened 47	
Code	10-12 MIST AND SHALLOW FOG	10 Mist (visibility 1100 yds.		12 Shallow tog-more or than 33 ft. less continuous	13-16 PHENOMENA WITHIN SIGHT	BUT NOT AT SHIP	13 Lightning visible, no	thunder heard	14 Precipitation in sight, not	reaching surface	15 Precip. beyond 3 naut.	miles, reaching surface	16 Precip. within 3-naut.	miles, reaching surface	17-19 THUNDER, SQUALLS,	FUNNEL CLOUDS	17 Thunder at time of obsn. –	no precip. at ship	18 Squalls (no precip.) in past	hour or at time of obsn.	19 Funnel cloud(s) seen in	past hour or at time of	obsn.	20-29 PHENOMENA IN PAST HOUR BUT	NOT AT TIME OF OBSN.	20 Drizzle (not freezing) or	Rain (not freezing)	22 Snow Not falling	

Fig. D.3.11 Explanation of the Data Record headings (continued).

or Heavy 86 88

06

Shower of snow
Shower of snow pellets or
ice pellets*
Shower of hail, no thunder

85

88

*With or without rain and/or snow

Table 2 (cont'd.)"

70-79 SOLID PRECIPITATION NOT FALLING AS SHOWERS	Code	Intermittent	70 Slight snow in flakes 71 Moderate snow in flakes 73	out		78 Isolated starlike snow crystals (with or without fog)	79 Ice pellets	80–84 RAIN SHOWERS	80 Slight rain shower		82 Violent rain shower	83 Shower of rain and snow mixed, slight		85-90 SOLID PRECIPITATION IN SHOWERS	Slight Moderate
50–99 PRECIPITATION AT SHIP AT TIME OF	COSEN ALICA	SU-SY DRILLE	Code Intermittent Continuous	 50 Slight Drizzle 52 Moderate Drizzle 53 54 Heavy Drizzle 55 	Slight Moderate or Heavy	56 Freezing drizzle 57 58 Drizzle and rain mixed 59		60–69 RAIN (NOT FALLING AS SHOWERS)	Intermittent	60 Slight rain 61 63 .	64 Heavy rain 65	Slight Moderate or Heavy	66 Freezing rain 67 68 Rain or drizzle with snow 69		

Fig. D.3.12 Explanation of the Data Record headings (continued).

Table 2 (Cont'd.)

Modelate of fleavy liftle of obst.

snow pellets

TABLE 3

*Includes hail, ice pellets or snow pellets

CLOUD AMOUNT (N - Code)

Fraction of the sky covered by clouds

Code Cloud Cover	8/9 9	7 7/8 or more but not $8/8$	8 8/8, sky totally covered	9 Sky obscured by dense fog, heavy	snow, etc., or amount cannot be	400000000
Cloud Cover	Cloudless	1/8 or less but not zero	2/8	3/8	4/8	0/3
Code	0	_	7	3	4	V

Fig. D.3.13 Explanation of the Data Record headings (continued).

TABLE 4

COUNTRY CODES (abbreviated table)

Complete table see OCEANS IV Systems' Description.

46 Iceland	49 Japan	58 Norway	64 Netherlands	74 United Kingdom	90 Union of Soviet Socialist Republics
Germany	Australia	Canada	Denmark	United States	France

06 09 7 18 0 26 1 31 1 18 33 1 1 18

TABLE 5

INSTITUTE CODE

01 Marin 02 Pacifi 03 Biolo 04 Arctic 05 Biolo 06 Static 07 Marin 08 Defer 09 Defer 10 Atlan 11 Polar 11 Creat	01 Marine Ecology Laboratory, Bedford Institute 14 Institute of Oceanography,	02 Pacific Oceanographic Group Dalhousie University	03 Biological Station, St. Andrews, N.B. 15 Marine Sciences Branch, Pacific Region	04 Arctic Biological Station, 16 Department of Transport	Ste. Anne de Bellevue, P.Q.	05 Biological Station, St. John's Nfld. 18 Canadian Forces Maritime Command,	06 Station de Biologie Marine, Grande Rivière East Coast	07 Marine Sciences Branch, Central Region 19 Canadian Forces Maritime Command,	08 Defence Research Establishment, Atlantic West Coast	09 Defence Research Establishment, Pacific 20 Ontario Water Resources Commission	10 Atlantic Oceanographic Laboratory, 21 Dept. of National Health and Welfare		11 Polar Congnental Shelf Eroject Mines and Resources	Lakes Institute 23 Arctic Institute of North America	13 Institute of Oceanography, University of
00 00 00 00 00 00 00 00 00 00 00 00 00	Marine Ecology I	Pacific Oceanogra	Biological Station	Arctic Biological	Ste. Anne de Bell	Biological Station	Station de Biolog	Marine Sciences	Defence Research	Defence Research	Atlantic Oceanog	Bedford Institute	Polar Continental	12 Great Lakes Institute	Institute of Ocea
	01	02	03	04		05	90	07	08	60	10		11	12	13

British Columbia

TABLE 6

DOUBTFUL DATA MARKERS AND ERROR CODES

Explanation Code

Considered doubtful by the data originator.

×

Considered doubtful by CODC

Error estimates coded as shown below. The codes are used only as a measure of the spread between duplicate or multiplicate measurements at A-I

the same location and time.

Let P be the difference between two measurements. P is then coded in multiples of the last digit allowed for on the coding

form as follows:

 $2 < P \leqslant 5 \text{ Code C}$ $5 < P \leqslant 10 \text{ Code D}$ 10 < P ≤ 20 Code E 1 Code A 20 < P ≤ 50 Code F 50 < P ≤ 100 Code G 100 < P ≤ 200 Code H 2 Code B $\begin{array}{c} P \leqslant \\ 1 < P \leqslant \end{array}$

A temperature error P=0.003°C is coded as C, an error P=0.02°C as E, and a salinity error P=0.08 per mille as G, etc. If the datum is based on a triple measurement, P is taken equal to the standard deviation

where A_i are the measurements and \overline{A} the mean value of the observed parameter.

Note: A code "W" may follow interpolated data, indicating that linear instead of hyperbolic interpolation has been used. Explanation of the Data Record headings (continued). Fig. D.3.15

TABLE 7

STANDARD LEVELS

5500	0009	6500	7000	7500	8000	8500	0006	9500	
1200	1500	2000	2500	3000	3500	4000	4500	2000	
0200	0225	0250	0300	0400	0020	0090	0000	0800	1000
0000	0010	0000	0030	0020	0075	0100	0125	0150	0175

Note: The standard levels can refer to standard depths or to standard pressure levels as indicated on page 1.

Explanation of the Data Record headings (continued). Fig. D.3.16

0

0

0

0

	01		, ,	9 0	· c	, ,						0 0) 'C	0		0	· c	0	0		0	0	-0
	Q 0	0													i								
	z	0													i i								-
	Σ	c		, ,	0	0																	
	4	0	0	0	0	0	10	0	0	0	0	, ,	0	0	C	0	0	0					
	×	0											0	0	0	0	0	0	0		, 0	0	-
	~	0	0			0			0						1								(
	I	0	.0			0			0						1				0				0
	G	0	0	0	0	0	0	0	0		0				1				0				- 0
	<u>t</u> L	0	0	0	0	0	0	0	0	0	0	0	0	0	0	0	0	0	0	0			C
	Ш	0	0	0	0	0	0	0	0		0					0	0	0	0	0	0	0	c
	٥	0	. 0	0	0	0	0	0	0		0	0	0	0	0	0	0	0	0	0	0	0	C
	gr	0	0	0	0	0	0	0	0		0	0	0	0	.0	0	0	0	0	0	0	0	0
	≪	0	0	0	0	0	0	0	0	0	0	0	0	0	:0	0	0	0	0	0	0	0	C
	6	0	0	0	0	0	0	0	0	0	0	0	0	0	0	0	0	0	0	0	0	0	C
	© ~	0 0	0	0	0	0	0	0	0	0	0	0	0	0	0	0	0	0	0	0	0	0	0
	9	0	0	0	0	0	0	0	0	0	0	0	0	0	0	0	0	0	0	0	0	0	0
	ហ	0	0	0	0	0	0	0	c	. 0	0	0	0	0	. 0	0	0	0	0	0	0	0	0
	4	0	0	0	0	0	0	0	0	0	0	0	0	0	0	0	0	0	0	0	0	0	0
E D	SND	0	6	6	0	0	6	6	6	6	6	6	0	6	6	0	6	6	6	6	6	6	0
5 0	SAL	6	0	6	6	0	6	σ	c	6	6	6	0	0	Ċ.	6	0	0	6	0.	6	6	6
لــا	Σ																						
⊥ ∀	SSIF	6	O	0	6	6	O	C	0	φ.	0	6	C	6	6	6	6	C	O	6	6	6	0
O A	CLA	0	0	0	0	0	0	0	0	0	0	0	0	0	0	0	0	Ó	0	0	0,	0	0
~	UNDER 3000	0	0	0	0	C	0	0	C	C	0	0	0	0	0	0	0	0	0	0	0	0	C
ll.		0	0	0	0	0	0	0	0	0	0	0	0	0	0	0	0		0	0	0	0	0
Λ Ω:	STNS																						
∑	STNS	12	111	30	87	16	9.	24	64	43	111	4 1	4.3	42	30	1.3	102	1 2	66	26	66	2	m
S	UDE	#067	690M	W076	#069	W062	W065	¥064	W063	W065	690₩	W067	W065	M066	64	W065	690M	W057	W063	W058	W065	W066	69
⊃	-							*							W 0 4				0 %	3	0		€90M
ů U	LONGI	W056	#054	₩068	W064	#057	650%	W061	W059	W060	W064	₩055	09CM	w051	44CM	₩063	W064	W065	W054	W054	690≱	W054	W056
	LATITUDE FROM TO	245	N45	N39	N 4 5	N45	0 47	N4.0	N45	N4 0	N45	252	C 4N	0 4 N	N 4 N	Q. 4 N	N 4 5	N 4 N	N4 5	N4 5	0.47	0 4 N	141
	TIT	447	147	N33	N42	× 42	N46	746	N 42	N45	Z ¢ Z	246	N46	N45	N 4 N	V 47	Z 4 Z	4 4 N	NAZ	N42	N46 N		N39 N41
		ž	ž	Z	7.	2	7	Z	Z.	Ž	Z	7	Ž	S	Ż	マ	Z	Z	*Z	Z A	Z	N47	M
	PLAT		gard		-	1	1	***		gent.	gant			gard	-	gord	e4	-	1	part .	end	-	gred
		rus	N O	PRINCE	DRINCE	PRINCE	PRINCE	SO	90	SO.	CF	70	S	II.	Z	LIJ LIJ	W.	00	Ü	E CE	CE	S	Œ
	ī	L01	<u>∐</u>	K	212	Z Z	× ×	2	PRINCE	2	PAINCE	NOSGAH	2	DRINCE	Æ	PRINCE	BONING	10	151	DRINCE	PRINCE	2	I
	VESSFL	MALLOTUS	T CAMERON	C. LL	in o	a. Lui	<u>а</u>	HARENGUS	<u>a</u>	HARENGUS		Ī	HARENGUS	E E	T CAMERON	ū	ā	MALLOTUS	KAPUSKASING	0		HARENGUS	JUDITH
	>			112	III	Ш	ш	1	LLI	I	Lit		I	E.	ja-	147 183	12.7 0.1	Σ	U d I	ELJ	LJ 	Ī	7
			∢						-		100			d.	A	U.S	W.		X	<u>Li</u>	n:		
		21	20	04	90	80	60	10	PT)	14	91	80	50		100	5	9:	1	=	2	4	2	9
	I SE	66021	67002	67004	67006	67009	61000	57010	67013	57014	67016	67318	67020	57021	67023	67025	67026	67027	68001	68032	69004	68005	63006
	CRUISE IN NO	03 6	03 6	03 6	03 6	03 6	03 6	03 5	03 6		03 6												
		3	8 0	9 0	8	9	0			3 03		3 03	0.3	0 3	03	0 3	0.3	0.3	03	0 3	0 3	03	03
	Z		1	-	0.0	~	~	18	<u>c</u>	1.8	<u>a</u>	1.3	-	13	<u>~</u>	23	20	1.9	r	18	<u>~</u>	13	0

and longitudes shown indicate the cornerpoints of a "rectangular" Cruise Master Catalogue. A list of the cruises merged into the master files. The grid surrounding all stations observed on a cruise. The number of stations down to depths exceeding 1000 or 3000 metres is given as well as the total parameter has been observed at least once is summarised, using a code from 9 for non-observed to observed at 90% or more of all stations. The parameters are temperature (TEM), salinity (SAL), sound speed (SND) and the chemical parameters 4 through G listed in the table in Fig. C.1.2. in Fig. C.1.2. A data restriction can be entered in the "CLASS" field. In the remaining columns the number of stations at which any parameters H through Z have not yet been assigned number of stations. The latitudes

D.4

Fig

PAGE

RUN CONTHUL TOTAL SUMMARY

STATIONS GRANCHED 35.95 O

NUMBER OF SUCCESSFUL STATIONS 4, 2017 NUMBER OF SUCCESSFUL EPOFIES 4, 2017 NOT SUCCESSFUL SUCCESSFU

THE (WHITTEN) RECORD COUNTS INDICATE THE SIZE OF THE FILL IF YOU HAD REQUESTED CREATION -AN EXPROPARE OF PLANTE NOTE SEASON AN EXPACTED DATA FILE WAS NOT CHEATED

Sample Data Count, showing the number of data that satisfy a given set of data extraction conditions as specified on the Data Extraction form shown in Figs. C.1.1 and C.1.2. Fig. D.5.

		,				
-	Z (1		•		
:	٥				•	
LLI	SB					
PAG	D A O				!	
	0			ν.		
	7 80			1 40		
i	α φ,	i		1	1	
:	E TE					
:	Z d	rrr!	0000	9	;	00000
1	PAR.	000			00000000000	
	-				000000000	
	0	000	0000000	,00000000	000000000	000000
	M 000			İ	i I	
	500					
	000			g=d		ged
	m m					
	2001	-		N	erd	N
U E	1001	mmm	m m m	· e=t [¹])	en\$	maam
0 0 7	501	4 W IU	W44N	440m0	en (M)	ភេសស្
TAL	226	10 m m	4444	4 W M 4 4 +	. U U M M U 4 U	พทพพ
CA	70	444	ריו ריו ריו ריו	mm4m40	1 m m m m m m m m	ריז ליז ביה ליז ביה
α	75	m d m o	-444Nmm	mmmm	, co o o o o o o o o	-994-9
AST	LES	2308 2139 1969	222 244 244 244 25 25 25 25 25 25 25 25 25 25 25 25 25	10 10 10 00 00 10 10 00 0	04 m M 4 m U W Q m 00 0 0 0 0 0 0 0 0 0 0 0 0 0 0 0 0 0	40000
Σ	SAMPI					50
2 0 H	OCEAN	4645 4750 4628	00 67 00 00 00 00 00 67 00 00 00 00	4582 44758 44330 44330 14200 18286	22 4 4 4 4 4 4 4 4 4 4 4 4 4 4 4 4 4 4	600 600
T .A T	C.OF PTHS	20 00 00	- 85 64 M M	1900000mmm	- RODNO - RODN	
ഗ	NO DP	₩ E O	W 2000 4 10	0486084-1	2442 0000 0000 0000 0000 0000 0000 0000	04031-
	₩				1001100100	
	tij	111	MANANANA	Nmmmoo-N	1 - 2 - 2 - 2 - 2 - 2 - 2 - 2 - 2 - 2 -	M = 1 - 1 - 1 - 1 - 1 - 1 - 1 - 1 - 1 - 1
	DAT				0.000 0.000	
	NOILS				00000000000000000000000000000000000000	
	ICA				40 E O O O O O O O O O O O O O O O O O O	
	IT O					
	DENT	900		9000000000	11880 1180 11800 1	
	N S	500			전 로 로 로 로 로 로 로 로 로 로 로 로 로 로 로 로 로 로 로	
	α .τ	306-0	000000000000000000000000000000000000000		13066-10 13066-10 13066-10 13066-10 13066-10	

more of all lefels. The parameters are temperature (0), pressure (1), salinity (2), soundspeed (3) and the chemical parameters listed in the table shown Note that only the last three digits of the cruise given set of data extraction conditions as specified on the Data Extraction form. The area is given in the COTED square code (Appendix F), followed by maximum sampling depth are shown under "SAMPLES LO" and "HI" respectively; a blank under "LO" indicates a minimum sampling depth of zero metres. The number of observed levels is broken down over the intervals shown (0-75, observed is summarized by a scale of 0 through 9. The zero is suppressed and stands for not-observed at any level, the 9 for observed at 90% or satisfy 76-225, etc.). The number of levels at which each of the parameters is number are shown; the first two digits are, for Canadian data, equal to the year of observation of the first station of a cruise. Minimum and Station Master Catalogue, showing a summary of the stations that the Marsden square number. (2), soundspeed (3) D.6.

e 1																																														
	TEN-DEG SQUARE	0	0 0 0 0	0001	1306	1306	1306	0 (0	1300	1306	1306	1306		1300	1306	1306	100	0 0	1300	1306	1306	1306	0 0	1306	1306	1306	1306	1306	0000	1 300	1306	1306	1306	1306	1306	1306	1000	2 4	1300		1306	1306	1306	1306		1306
	FIVE-DEG SQUARE	•		0	0	0		> !	*7	0	0	C) (0	0	m) (), (0	0	C) [ກ	0	0	C	, (> <	0	m	0	0	0	0	C	> =			+	0	en4	N	rr's		
	DFC	(0	0	0	1	<	> <	0	ovel	C		> 0	0	g=-(C	0 (> (7 0	0	C	0	ų ¢	0	0	0	7	0 (VI (N	0	0	0	0		17		0 1	0		113	0	0	0		77
	> ON	<) c	0	0	0	0) (0	S	4	0	Ų (N	0	C	77	۱ (۱	S	0	00	. (٥.	4	N	N	0)	ŋ (10	0	<i></i>	11	φ	130	4	ı,	- 1	0		324	and	0	9		331
	GE)	6	3 :	0	0	0	(> 1	0	0	-	· C	> <	N	0	C	-	-0 1	6	0	17		-0 (0	0	0	24	0	iC -	4	0	0	4	2	100) be	3 (5	N		233	C)	0	0	1	235
	SEP OC	(0	0	0	0	-	4	0	0	C	0	، د	—	0	C	00	0	0	0	~) -	-4 (0	0	graf	***	3		61		-	pol	1	139	l la	0 9	0	2		244	N	0			247
	(YE A AUG		0	N	0	O	0	ų.	prof	g=4	-	c	V I	0	0	0	10		25		4	000	27	4	ಯ	16	24	10	21	4	m	O	6	18	157	11	7	0	ď		451	ď	0	10		465
>- C′	MONTH		0	-	0	O) (>	0	0	◁	<	0 (N	C)	C) =		្រ	4	20	16	/J - P	4	10	50	0	1.4	4 1	2		3	, prof prof	10	150	1 00	-1	0	et e		576		0	in.		585
0	D N N		0	0	0	С) (>	0		C) (0 1	O.J	0	C	0 0	0	0	0	4	3	0 1	0	Φ	S	- T	0 0	10	67	0	10	9	94	00	0 0	2 0	0	0		239	0	0	0		239
N N	MAY		0	0	ard	C	0 0	5	0	0	15) <	0	0	0	-	7 0	n :	12	4	O		d I	N	10	36	0) •	red i	0		10	17	0	134	4	1	0	0		401	0	0	ťΩ		404
Z	STAT		0	0	0	0		-0	0	0	C) ()	m	ហ	C	2 =	-0	10	الما	0	2 4	0	N	0	56	1 15	* 4	4 1	1	~	~	15	god	00	1 10	- 0	0	0		301	0	0	m		304
× +	MAR		đ	មា	4	-	4 (>	0	0	ı,) (V	Oh	***	() (0	0	16	0	- P	2	0	17	23	i u	10	10	ord ord	0	77	Ø	C)	76	2.0		-	0		333	~	0	0		336
V 0	FEB		0	0	0	C) (0	0	m	C) -		N	0	0	0 0	0	23	7		2 4	4	N	0	11	, d	10	J. 1	3	1	16	00	T.	155	0 (1	000	>	0		421	0	0	rr3		454
0	Z		0	0	0	C) (0	0	944	<	3 (0	0	0	0	0 (0	9	0	· C	0 (V	C/S	0	0) Q) (10	quité	4	m	C)	∀	0 0	0 <	0	0		110	0	0	m)		113
0 0	ONS																															~							0.1		€		^			
	TOTAL		7 7	70	10	0	j d	4	===(12	0	1		20			,	-	172	V	127) (7	20	0	-	٠.	- (ю.	O.	prof	N	93	-	1338) 4	3		pred COI		3748	14	0	36		3796
	ONE-DEG		00	01	000	1 10) (4	500	10	-	4 (7 7	gane)	14	. 12	7 0	20	21	20	10	7 (47	25	30	340	0.7	710	33	eř	35	40	4 3	69	A 3	\ \ \	rc	200	52							
	FIVE-DEG		0) C	> <	2	m	0	0	0	2	0) (*	n (0	0) (>	m		C) () (0	0	P ¹)	0	Ç			> <	· o		groß		0	and	2	r^)		
	TEN-DEG SQUARE		1306	1306	1306	2000	211	1300	1306	1306	700	000	1300	1306	1306	3000	0000	1300	1306	1306	700	0000	1300	1306	1306	1306	2000	2000	1306	1306	1306	1306	1306	1306	2000	0 4 5	0001	1300	1306							1306

Data Inventory Type I, showing a summary by one-degree squares (COTED system) and by month of the available data. The inventory can show all available data or all data satisfying a given set of data extraction conditions. Fig. D.7.

PAG			
	TEN-DEG SOUARE		00
	FIVE-DEG SOUARE	©UU0UUU0000000000000000000000000000000	
	1969	11	* 1
	1967	00000000000000000000000000000000000000	h
	NGE)	00000000000000000000000000000000000000	1
	1965	00000000000000000000000000000000000000	1
	(YE		1
≻	MONTH 963 1	00000000000000000000000000000000000000	
0 1	84 962 1	m	Ĺ
> N	10NS 961	00000000000000000000000000000000000000	-0
Z ₩	STAT 960 1		ż
∀	TOTAL 1955 1	00004w0000w000k44w000004000 6000	Ì
O A	950	1 000 00 00 00 00 00 00 00 00 00 00 00 0	300
0 0 0	1900 1	000001711717401000000000000000000000000)
	TOTAL	4	0
I c	ONE-DEG SQUARE	00000111111000000000000000000000000000	
	FIVE-DEG SQUARE	00000000000000000000000000000000000000	
	TEN-DEG SQUARE	11111111111111111111111111111111111111	0

Data Inventory Type II, showing a summary by one-degree squares (COTED system) and by year or year-ranges of the available data. The inventory can show all available data or all data satisfying a given of data extraction conditions. The year (ranges) are specified with the TIME cards coded on the Data Extraction form. D.8

Fig.

eri TOTAL 16068 OL I INVENTORY ម រ TEN-DEGREE SQUARE 1306 1.98 331 2140 DATA GEOGRAPHICAL 4 1 TEN-DEGREE SQUARE 1305 (C) 0 1 J. -9 1 3 3-

summary of available data in a semi (COTED system, Appendix F) squares Data Inventory Type III, showing a geographical lay-out by one-degree D.9.1. Fig.

i		000	0	0	m	0	0 .	0	0	0	0	0	0	0	_0	0	0	0	0	0
		010		0		0	0	9	0	0	0	0	0	0	0	0	0	0	0	0
		020	.0	0	21	13	ert :	7	0	0	.0	0	0	0	0	0	0	0	0	0
		030	0	0	43	59	50	23	0	0	0	0	O	0	0	0	0	0	0	0
		040	0	0	11	124	585	87	0	0	0	0	0	0	0	0	0	0	0	0
		050	0	15	544	1186	4188	50	0	0	0	0	0	0	0	0	0	0	0	0
ARE		0.000	15	86	331	260	15941	113	£ 3	12	0	0	0	0	0	0	0	0	0	0
SQUARE		070	126	189	368	4 20	55	67	21	0	0	0	0	0	0	0	0	0	0	0
10-DEGREE		080	81	215	422	. 91	0	9	7	0	0	0	0	0	0	0	0	0	0	0
BY 10-		100	O	334	52	5.5	0	0	0	0	0	0	. 0	0	0	0	0	0	. 0	0
		100		99	35	0	0	0	0	0	0	0	0	0	0	0	0	0	0	0
INVENTORY		110		68	193	0	0	9	pret	0	0	0	0	0	0	0	0	0	0	0
HICAL		120	0	65	150	1546	6544	10	0	0	0	0	0	0	O	0	0	0	0	0
GFOGRAPHICAL		130	0	17	18	1658	484	9	0	0	0	0	0	0	0	0	0	0	0	0
CCDC GF		150	0	-	0	247	363	no	·0	0	0	0	0	0	0	0	0	0	0	0
Ü	151	150	0	13	0	173	64	0	1	0	0	0	0	0	0	0	0	0	0	0
	LATITUDE WEST	160	0	0	0	15	On pred	***	0	0	0	0	0	0	0	0	0	0	0	0
	LATI	170	-	0	0	90	7	0	0	0	0	0	0	0	0	0	0	0	0	0
		LONG	06-08N	N70-80	N60-70	N50-60	N40-50	N30-43	N20-30	N10-20	N00-10	800-10	\$10-20	\$20-30	830-40	840-50	850-60	800-70	S70-80	06-085

α Data Inventory Type III, showing a summary of available data in semi geographical lay-out by ten-degree squares. Fig. D.9.2.

cr		m	190	4	283	0	35	0	469	00	0	00	C	e 0	0	00	0	000	C	00
1S 278		(A)	1271	- O	4152		-		5	13374	338	15200		14453	2.4	3	0	000	0	co
L 0951	ALL S	IC.	2200	20.2	C)	102	a.	75	100	13500	3743	11677	401	o.c	0	14971	4	000	С	CQ
< Y	3	300	2026	10277	396	2000	407	44	00 m	00	0	13210	453	16639	3400	17820	16	000	0	60
Z	. 4	12330	173	77	325	210	3.5	12826	Į 🖛	12742	10	13243	384	15200	185	15506	46		, C	00
D.		20	909	8 12051	4660	200	3263	1	2901	35011	4 (1)	12530	121		35	15167	170	16619) V	
0 20%)	7300)		199	,0	586	0.	00	00100	1 TO 1	-	203	10	164	good	193	15450	4	2456
011	_	00	00	00	00	C	D Q	0.0	00	- 8	2297	-	510	154	4	4000	172	14800	5	20169
Daco.	- m	00	0	ć	1747	:	00		00	A SALES	00	1 OHO.		1	110	0,0		15570	0 7	18520
S T R	0	0 (00	,	2120	:	2729	1	00	-		0:		00		00		000	, .	0 14500
000			•	:	X)	:	_		o o	1	r.		1		1		Į			
METEW 94	49		00	0	00	0	00	0	00	0	00	00	00	0.0	00	7 15614	162	20202		000
ADDALA	300	3	00	0	00	0	00	Ç	50	0	00	0	D 0	.0	1.911	14	115	0,00	9 (, 000
0 6 P	ALL S.		00	0	00	0	00	С	00	0	00	10	0004	1	363	00	0	000		000
101	00 10 10 10 10 10 10 10 10 10 10 10 10 1		00	0	00	0	00	0	00	C	00	0	00	0	00	0,9	00	00	0 (
2 0	<	, 0	00	0	00	0	СĢ	0	00	a	00	ol	00	0	00	00	0	00	0 9	0'00
0 0	tı	0	00	0	00	0	00	0	00	0	00	0	00	0	00	0.0	90	00	0 (000
	305	0	00	0	00	0	00	0	00	0	00	0	00	Q	00	0,0	00	00	0	000
	SOUARE 1		2500	0	00	· a	00	0	00	۲.	985U 50	quel	15363 2803	0	00	0,0	þ	90	0	000
	1	0C ===	18600 1	4	15800		00	0	00	0	00	9	8983	0	00	11	18300	00	0	000
	TEN-DEGREE	or m	16666 1	4			14933	m	10933	0	00	0	00	17	3401		00	00	0	000
			6		80		7		9		2		4		ers	21	N			0

Distribution of Means and Standard Deviations, showing per one-degree square (COTED system) a count, mean and standard deviation of all data retrieved as specified on the Data Extraction form. 10

о О

Fig.



APPENDIX E

DATA OUTPUT CARD AND TAPE FORMATS

- 1. OCEANS IV 2. OCEANS III



APPENDIX E

Appendix E.1 Format of OCEANS IV Cards or Tape

Five types of records occur in the OCEANS IV output:

Cruise Master (format type 1). This record will appear only in outputs from the transaction file. Cruise Master information is not included in the master files, and therefore cannot be retrieved from them.

Station Master (format type 2).

Observed Detail (format type 3).

Observed Detail Continuation (also format type 3).

Derived Parameters (format type 4). A sample output card for record types 2,3 and 4 is shown in Fig. El.

The format types 1,2 and 3 are identical to the input formats of OCEANS IV described in Appendices Bl and B3. Values in a number of fields, however, may differ, since all data are converted to the OCEANS IV file units. The parameters concerned, and their file units, are shown in Table El. All other parameters are given in the units specified on the data submission forms.

Minor differences also occur in the following fields of the Observed Detail record:

- a) Temperature, soundspeed and salinity fields are filled with 99999 if not observed.
- b) If more than five chemical parameters have been observed at a level, continuation records are used. These can be recognized by blanks in the temperature, salinity and soundspeed fields. Otherwise the format is identical to that of the Observed Detail record.
- c) If card type 3 is used for interpolated data, the letters "INTR" appear in columns 34-37.

In the Station Master one difference occurs: for nonobserved soundings (columns 43-47), blanks are replaced by zero's.

The <u>Derived Parameters</u> record (type 4) contains the same information as the printed data records described in Appendix D3. The columns used for each record are shown in

Fig. El. Note that the sign for potential temperature is given as an overpunch over its last digit, whereas the sign for temperature in record type 3 is given in the first column of its field. The latter is, strictly speaking, not an overpunch, since temperature never goes below -9.00°C.

The data can be in cruise, time or geographical <u>sequence</u>. In the latter case the COTED squares system is used to sequence the data (see Appendix F).

Data on magnetic tape are in card image, record length 80, blocking factor 1, BCD, not labelled, seven track, 556 b.p.i. unless otherwise indicated. Any alternative option standard to IBM system 360 is available on request.

Overpunches are not used on card types 1,2, and 3. Card type 4 may contain an overpunch in column 27 to indicate a negative value for potential temperature.

Table El

FILE UNITS FOR PARAMETERS THAT HAVE A CHOICE OF UNITS THAT CAN BE USED FOR SUBMISSION OF THE DATA

Parameter	Unit	Display	Remarks
sounding depth	. m	XXXX.X	
depth of sample	m	XXXX.X	
oxygen	m1/1	XX.XX	
wind speed	m/sec	XX	Wind force estimates are converted to m/sec as shown in table E2.
air pressure	mbar	XX.X	The first one or two digits are dropped, e.g. 1026.4 mbar is shown as 264 and 987.3 mbar as 873. If the high order digit shown is <5, pressure is assumed to be over 1000 mbar, if it is > 5, pressure is assumed to be between 950 and 1000 mbar. Pressures are not corrected for barometer height or outside air temperature unless this has been done by the data originator.
air and wet bulb temperature	°C	XX.X	Negative temperatures are coded by adding 50°C to the absolute value of the measurement.
swell period	sec	XX	P_{W} codes have been converted as shown in Table E3.

Table E2

CONVERSION OF BEAUFORT ESTIMATE TO WINDSPEED IN M/SEC

Beaufort	Windspeed in m/sec
0	0.0
1 2	01
3	02 04
4	07
5	09
6	12
7 8	15 19
9	22
10	26
11	30
12	34

Table E3

CONVERSION OF P_{W} CODE (WMO3155) TO PERIOD IN SECONDS ($P_{W}P_{W}$)

$\frac{P_W}{}$	$\frac{P_{W}P_{W}}{P_{W}}$
5	5
6	6
7	7
8	8
9	9
0	10
1	11
1 2 3	12
3	13
4	14
/	blank

THE PERSON NAMED IN	SAM .	and the second second	Man affect of Philadelphia	-	DET		on Service of Alberta Bellerina			GBVIB	
digitalization in terrorior report of	Personal value value	3	2	£	3477	4		00	♦ 3dl.	deligners - reconstitued	000
		E 25	Carl Carl		LLI	44		(2)		CO	on ;
F		3 6	2 2			4		9		CC CC	07 5
11-1		2 2	~		Þ	44		20		00	on a
SWFL		2 5	2.4			4		60		60	07 1
Sal		C 75	N		U	42		5		00	07 7
15		E 53	~		Ш	4		0		co	တ
	-	2 0	cu			4		9		00	တ
FR	-	=======================================	273		H	4		CLD		00	on :
WAYA PD P	(0 8	~		A	4		03		00	00 8
POA ON		C ?	2			44		0		00	90
7		C 36.	F3	SG	0	4		0		00	00 5
EOROLOGICAL	5	= 10	Cons	Til.	Lui	4		0		90	on (
0		3	~	Ĩ.		4		9		00	g (
0 0		CD 12	64	E W	Ħ	4		9		00	00 5
A A	TE,	3 C	CA	ET		4		0		00	
+			2	RAMET	0	4		0		00	හ දි භ
I a	200	61:62	2	PAR	Ш	4		2		00	on 3
d	0.	= 8 = 8	12	Ω.	1-	4		2		00	60 8
		(2) (2)	67			4		(2)		00	000
*		(J) (C)	CV		Ħ	4		00		00	07 (
		CD (5	2			4		CO		00	0
N.C.		5 %	CV		U	4		(2)		00	00 9
Z ~		(2) (S)	~		ш	4		ယ		00	on (
> 0		a .5	0		-	44		CO		00	on ;
THUMAA	surreitte de Mandelle de la	C 73	200			V		0		00	07
laurillhusters elables 1 mar		a 3	1 ~		н	42		0		00	00 3
	A SO CONTRACTOR	C> 55	N			4		0		00	00 3
ž Š	5	2 3	~		U	<		0		00	00 3
- 2	20	co \$	0		ш	4		0		00	on :
	4	C 3	, ~	>-		47		CD		00	60 3
		CD -	~	Z		43		0	SVA	00	00 :
ž į	E '	ت. نې د	1 ~	SALI		A		(0)	S	00	6
S	T .	C &	7	S		alife.		CO		00	on :
SOUNDING		CD 2	CV	_		44		ധ		ෙ	CD :
access stores are an arrangement	alle, i fallery y dylljenskame	3	C	ED	3/0	42		0	RG)	co	6
46	IMUNC	co 7	2	SPE		and .		9	POT ENERGY ANOMALY	00	o :
	SHVW	a \$	2			4		9	A A	co co	GD :
made all 1 at 1.00	AMERICA 1889 PT 1875-777		2	SOUND		dist.		3		00	- 07
	0.11	3 00 8	2 2	20		44		CE	GEOPOT.	00	on (
		C 'S	2	-	L	And-		9	O. O.	00	a) (
		S (5)	2		OUT INTR.	4		9	ANGE	00	on 8
		S 3	1 0		i.i.l	dillo.		(5)	0	00	00 ;
<u>™</u>	Ľ	2	CV.		WIR OR	4		60		00	00 3
	>	5)	~		121	44		co.	SIGMA	00	00 8
-	es c	<u>යා යු</u> සා බ	2			4		CD	(V)	00	တႈ
DATE	9	C 3	23	TEMP.		47		cas.	H	00	a :
	2	ED 5	1 01	E		W.S		CLD	¥ V	00	07.8
		四	500			4		(2)	SIGMA	00	g 8
		98	-			164		0		00	<u>ලා</u> ද
		cm 13	~	1.1	20	455.		(0)	₹.	600	00 00
36	2	4. K	1 67	PRESSURE		4		00	TEM	00	00 8
= 1			2	SS		47		9		CO	
ONGIT		S C	2	8		47		3	Po	00	G 20
20	n		64	CL.		47		0		00	60
- 0	-	2 2 2	64			4		CD	10		
Lul'		3 2	00		· û	25		CO	PRESS	00	07 8
- CLI		0 2	1 ~		OF SAMPLE	45		යා	O.	00	on 9
Ave .			6~1		SAN	47		co		CO	on 9
30:		6	27			WT.		cot		00	07:
+		c > 4	5~1		2	4		(0)	HL	00	5
A	0	a vi	1 ~	. w ≥	25	46.04		CO	E D I	00	5
The state of the s		9.0	1 000	=	II.	64		CE	0	00	07 3
Z	manuscript of Dead or Association for	co 12	CV		I	4		0		00	_ m
	Old	c 2	2			44		9		00	on :
			N			44		(0)		00	00 0
Annual Control	CONTE	<u> </u>	6-1			44		CCO		00	on s
5			CV			42.		CED!		00	900
FICATION	10.01	~ m	CV			4		(0)		00	on :
G 9.	CHOL	- ·	6-1			403°		00		00	00 0
			200			and I		50		00	00 0
2	\$500 per 1 and 10		(7)			- self.		CO		60	5
-1	ICMI	□ **	61			42		(2)		oc.	cm d
	-		2			42		co		00	cn c
			60			1		(0)		00	on -
1	7140					*3 :					

Fig. E.1. Sample OCEANS IV input or output card.

122 Appendix E.2

Appendix E.2 Format of OCEANS III Cards or Tape

Only a brief summary of the OCEANS III record formats will be given here, since it is not an essential output of the OCEANS IV system. Further details can be obtained by writing to the Canadian Oceanographic Data Centre.

The old OCEANS III system has four basic record types:

Cruise Master (type 0)

Station Master (type 1)

Observed Detail (type 3)

Standard (type 6).

A sample lay-out of the latter three records is shown in Fig. E2. The Cruise Master record will, unless specifically requested, not be included in the data punched on cards or written on magnetic tape.

No continuation records are used in OCEANS III. Interpolated data are written in a separate "standard" format (type 6). A summary of units used and overpunches is given in Tables E4, E5 and E6.

Data on magnetic tape are in card image, record length 80, blocking factor 1, BCD, not labelled, seven track and 556 b.p.i. unless otherwise indicated. Any alternative option standard to IBM system 360 is available on request.

Sample OCEANS III input or output card.

_		яэтг	ΔM		a	9880	QAAQNATS				
CD	TYPE 1 %	O 8	- Trans	2	E 39YT	4	22	Q	TYPE 6	တ	
		0 %		2	62	4	r.	۵	~	00	တ္ခ
E	23 CONSEC UTIVE NUMBER	0 %	quince	2	co	4	ru.	0	~	00	တာ 🖔
CONSECUTIVE	0 2	7.0	- proces	7	က	4	. rc	ယ	_	00	တ္
NSECU	SE F.	0 %	-	2	സ	4	5	9	-	00	တာ 🕾
00	CRUISE PEF, NUMBER	57 5	_	2	က	4	LC.	9	_	00	50 %
		0.0		2	0 10/11ND3	4	<u>.</u>	ယ		00	ලා දි ලා දි
0	ED	0 0	_	2 2	0 1081N03	4		-	ED	00	တာ ည
CRUISE PEF NUMBER	GNED	0 5		2	ŵ ŗ	4	TC)	1	25	00	တ္က
C.R.	UNASSI	0 2	-	2	- 4	4			SSI	00	on (5
34	Z	0 %	-	2		4	r.C		UNASS	00	တ ႏ
	>	0 %	-	2	17	4	23		٦	00	တ 🥳
DEG®	1, N M 3	0 6	****	2	0	4	2			00	00 %
0 2 NO 50.04	PC HRS AFTER	C 8		2	7	4	r.c.		SPECIFIC 70, 1ME ANOMALY 1105 B1	00	တ ဗ
0 0	D 'S1A	0 8	-	2	16	4	10	1-1	NOW.	00	o 59
-	B C S TAIN	0 3	-	2	2	4	5	- 4		∞	o ½
Z w		C 28	-	7	z	4	r.			00	တ ္ဖ
MAPSSEN	** CCDE (%2√59)	0 %		2	1.50N	4	_ rc	Z	POTENTIAL ENERSY ANOMALY (3X)	000	_ o
MAM		0 9	A-ma-	2		4	_ rc	-	OTENTIA ENERSY ANDMAL	00	o n 2
	2.00	0 00	= -	2	A P	4	5	0	PO	00	o 8
	WET BULB	0 88		2 2	14 101A.	4 4	- 23	-		00	
		57.5	=	7,7		4	2		S T T	00	9 6
PTH	10 C N	58815		2	10 0-	4	r.		DVY/ MIC DETTH ANOMALY (AD)	00	o . €
E G	- 4 B O	55 0	queen	2	P.C.		- E	0	A D O	00	- 60 %
0	- 5 th → 5 ch	54	=	2		4	2	10		00	6.5
		(C) (Z)		7	SOUND VELCOSTY IM/Sec)	4			SOUND VELOCATY (M/Sec)	00	- 6
	MET MET	25	-	7	SOUND SOUND FEEDOT	4	r.c	-	SOUND ELOCAT	00	တာ အ
	FORCE	0 5	-	2	1+	4	2		>	∞	_ on [
	N N N N N N N N N N N N N N N N N N N	0 8	· ·	2	-	4	5		-	00	တ ငွ
/10	3 8	0 4	-	2	11 GMA-T (O 1)	4	_ 5		SIGMA-T (O1)	00	- 05 th
-		0 8		7	SIGN	4	r.		Sig	00	90 0
		0 4		2		4		1		00	9 4
. × × ×	N S a	5 46	_	2	7 4	4	5	9	2 ~	00	9 9
HRS.	WAW Dwew	0 0		2 2	10 Y GE	4 4	r.	9	00 3	00	
I	<u> </u>	0.0	<u> </u>	2	XOE	414	- 5 -	919	X E	c5	- 65
-1 +		0 24	-	2		4	2	9	LW.	00	9
>	WAVES Da Pa	0 1	-	7	> 100	4	2	9	> 0	00	D 7
CA	3 0	0 4	-	2	0 2 00	4	2	9	0 7 (00)	00	တ ဗိ
		O 8	_	2	4 0	4	5	9	4 0	00	- 65 39
[]	TER (m)	0 %		2	(f)	4	LC .	9	0	00	တြ 🕾
WOAT Y	WATE	0 5	-	7	w w	4	rt.o	9	a w	00	3.0
≥	1			2		A.	T.	ڡ	-	00	98
-!	157	- W	quere	2	() ()	7	- rs	9	0 0	000	<u> </u>
	200	0 %	·	3	J.	4	5	က	× 0	00	တ ႏ
47	SAN	co 13	-	2		1	. 12	യ		00	
17	2 N 2	O 3	quer's	2		4		و	10	00	
11	. 2	3 0	- P	7	7	4	27	9	35, 15	00	5 5
- 2	10 10 10 10 10 10 10 10 10 10 10 10 10 1	8 0		2 2	2 72.7	4 4	5 5	9 9	COPTA CAMPI WETERS	တ	ာ 8 ဘ %
	19 8	0 0 0 28 28 28	-	2 2	5 z	4	מא	9	(*	00	න දි න
	p. gr	0.0	Marcal	2 2	5	4		9	1 2	00	9, 5
13		50.0	-	57	w 2	7 7	- Z	ت	E SAS	00	- 50 %
13 1	HOUPS THE	27 12	-	2	L SW	4	2	ယ	F SE	CO	25 50
- 1 1 3	1 [0 %	,	2	ري سيار سيا	D	Ľ,	9	-	00	es 2
1 ()	24.	0 8	quest	2	က	44	2	9	~	00	5 2
	41 - J	3 0	-	2	co	4	S	9	_	00	ಕಾ ಜ
2E68/	DATE TONT	0 5	quem	2	က	4	5	9	7	00	2 2
(,)	27.50	2 5	-	2	S	4	rcs	မ	7	00	5 8
	} 	0 5	=	2	<u>c</u>	4	r.	60		00	တ ္
917	2 W	C 20	-	2	S	2	73	9	_	00	on ∞
100	MARSDEN SC. ARE	0	- Quantum	2	S	4	5	9	-	00	00 1
10	3 0	0 0 21	<u> </u>	2	<u> </u>	- 	.5	9		00	9 9 9
JE G	·	0 1		1/2	- 8	<u> </u>	- 5	6	- = -	00	9. 4
MINUTES	CONGITUDE (W=+)	13 14	Quida.	2 2	co co	4 4	מא	9 9	-	00	00 00
115	0 =	0 0 12 13		2 2	62	4	rC.	9	_	00	on 22
10 7	LOH DEG*	0 =	-	2	62	4	ru.	9	-	00	on =
DEGREES	36	0 5	Anna	2 2	m	7	r.	2	-	00	တာ မ
DE	102	0 %		2	m	7	2	9	_	00	നേത
		0 0		2	~ ~ ~	4	<u>_</u>	6		00	∞
	AT:TUDE (N·+)	0 -	qc/mar	2	co.	4	LO	9	_	00	on ~
	LATITUDE (N-+) FGr MIN'	0	-	2	c2	4	ro.	9	_	00	တာ ဖ
TST NO	1	0 7	Stanton	2	m	47	r.C	က	_	00	6 0 %
INST	0				approximate the survivors made of		5	9	_	00	6
.r ICA		0 *	decide.	0	സ	42	10.7	-	1 -	00	0, 4
.r ICA	TODE	0 0	A	2 2	co co	4	ro.	9		00	6 0 0
COUNTRY INST		C) **	denne denne								

CANADIAN OCEANOGRAPHIC DATA CENTRE

Table E4

OCEANS III STATION MASTER RECORD (TYPE 1)

Field			
No.	Column	Contents	Remarks
1	1-4	Country and Institute	See Tables 4 and 5 of Appendix D3.
2	5-9 5-6	Latitude degrees	An overpunch (11 zone) in column 5 indicates south latitudes.
	7-8 9	minutes 1/10 minute	J Indicates South Ideledaes.
3	10-15 10-12	Longitude degrees	An overpunch (ll-zone) in column 10 indicates east longitudes.
	13 - 14 15	minutes 1/10 minute	To indicates east longitudes.
4	16-18	Marsden Square	
5	19-27	Date-time	Last two digits of the year, followed by month, day, hour and 1/10 hour in GMT.
6	28-31	Sounding depth	In metres.
7	32-33	Max. sample depth	Blank
8	34-35	No. of depths	
9	36-39	Water	Blank
10	40-43 40-41	Waves I direction	Same as wind direction except that the value is increased by 50 for wave heights in excess of 4.5m (code 9). Indeterminate or non-observed is coded 49 (or 99 for waves in excess of 4.5m).
	42	period	One digit P_W code, see Table E1.

Table E4 (cont'd)

24

80

Card Code

Table	E4 (CONT. d)	
Field No.	Column '	Contents	Remarks
	43	height	Wave height is coded in multiples of 0.5m, e.g. a wave height of 3m is coded 6. If the wave height code exceeds 9, 50 is added to wave direction and the high order digit of the wave height code is dropped.
11	44-47 44-45	Waves II direction	Coded as columns 40-41, but
	46 47	period height	giving true swell direction. Same as column 42. Same as column 43.
12	48-49	Wind Direction	Direction from which the wind is coming in tens of degrees. A calm is coded as 00.
13	50-51	Wind Speed	Units of m/sec.
14	52-54	Barometer	In mbars; if air pressure < 1000 mbar, an overpunch (11-zone) is inserted in column 52.
15	55-57	Air Temp.	In °C; negative temperatures are indicated by an overpunch (11-zone) in column 55.
16	58-60	Wet Bulb	In °C; negative values are indicated by an overpunch (11-zone) in column 58.
17	61-62	WW Code	See Table 2 in Appendix D3.
18	63-64 63 64	Cloud cloud type cloud amount	Blank. See Table 3, Appendix D3.
19	65	Visibility	Blank.
20	66-67	Hours after HW	Blank.
21	68-73	Unassigned	May contain miscellaneous alphanumeric information inserted by the data originator.
22	74-76	Cruise Ref. No.	
23	77-79	Consec Station No.	

Card code is 1.

126 Appendix E.2

Table E5

OCEANS III OBSERVED DETAIL RECORD (TYPE 3)

Field			
No.	Columns	Contents	Remarks
1	1-24	Station Data	Same as on Station Master record columns 1-24.
2	25-27	Time	In hours and tenths of hours.
3	28-31	Depth	In metres
	32	Error of Depth	Blank.
4	33-37 33-36	Temperature value	In 0.01°C, negative temperatures are indicated by an 11-zone in
	37	error code	column 33. See Table 6, Appendix D3. If numerical, it is a third decimal of temperature. Measurements with an STD are indicated by a P.
5	38-42 38-41 42	Salinity value error code	In ppm. See Table 6, Appendix D3. May also contain a P for measurements obtained with an STD or similar instrument.
6	43-46 43-45	Oxygen value	In 0.01 ml/1; the high order digit for oxygen values between 10.00 and 19.99 ml/1 is dropped and oxygen values > 10 ml/1 are implied by an 11-zone in column 43.
_	46	error code	See Table 6, Appendix D3.
7	47-50	Sigma-T	In 10^{-5} gr/gr.
8	51-54	Sound Velocity	In 0.1 m/sec; the high order "1" is dropped.
9	55-57	PO4-P	In hundredths of µg-at/l
10	58-60	Total-P	In hundredths of µg-at/l

Table E5 (cont'd)

Field No.	Columns	Contents	Remarks
11	61-63	NO2-N	In hundredths of µg-at/l
12	64-66	NO3-N	In tenths of µg-at/l
13	67-69	SI03-S1	In tenths of µg-at/l
14	70-72	рН	In hundredths
15	73 ;		Blank
16	74-79	Station Data	Same as on Station Master Record.
17	80	Code	Code 3.

Table E6

OCEANS III INTERPOLATED RECORD (TYPE 6)

This record is constructed in the same way as the Observed Detail record previously described, up to and including field number 8 (Sound Velocity). The remainder of the card is set up as follows, using OCEANS IV interpolated data:

Field No.	Columns	Contents	Remarks
1-8	1-54		Same as on Observed Detail Card.
9	55-58	Dynamic Height Anomaly	In dynamic metres with three decimals.
10	59-63	Potential Energy Anomaly	In units of 10^6 ergs/cm^2
11	64-67	_	In units of 10^{-6} ml/gr.
12	68-73	_	Blanks
	74-79		Same as on Station Master Record.
	80		Code 6.

APPENDIX F

THE COTED SQUARES SYSTEM FOR SEQUENCING DATA IN GEOGRAPHICAL ORDER ON MAGNETIC TAPE.



APPENDIX F

The COTED Squares System for Sequencing
Data in Geographical Order
on Magnetic Tape*

In a recent review of the oceanographic station data file of the Canadian Oceanographic Data Centre, we considered several methods of sequencing the data, in some geographical order, on magnetic tape. The traditional Marsden square system, being too cumbersome due to its irregularity, was rejected. A new system was designed, numbering the ten-degree squares consecutively in a two-dimensional grid. This system, called the Consecutive Ten-Degree, or COTED, squares system, greatly simplifies the logic of the data retrieval programs used to extract data on a geographical basis from our files, thereby reducing both complexity and running times for these programs.

Both the Marsden and COTED square systems divide the globe into 648 ten-degree squares and subdivides each of these into 100 one-degree squares, and a five or six digit key uniquely defines each one-degree square. In the Marsden system the ten-degree squares are numbered increasing from 1 to 288 and from 901 to 936 north, and from 300 to 587 south of the equator (Fig. F.1); the one-degree squares from 0 to 99 increasing away from an origin at the equator and the Greenwich meridian (Fig. F.2). In the COTED system, four instead of three digits are used to number the ten-degree squares. first two increase from 00 to 17 northwards from the south pole, the second two increase from 00 to 35 westward from the Greenwich meridian (Fig. F.1, bold numbers). The one-degree squares are numbered from 00 to 99 with the lowest number always in the southeast corner (Fig. F.3). The major advantage of this is that the relative geographical position of two onedegree squares is immediately obvious from their COTED numbers.

It may be noted here that the apparently simpler solution of numbering the ten-degree squares from -9 to +8 in a north-south direction, and from -18 to +17 in an east-west direction, leads to problems in sorting the data sequentially on the computer. The COTED square key numbers cause the data to be sorted in a continuous "strip" spiralling from pole to pole. A combination of positive and negative key numbers, on the other hand, may lead to a different sequence of the sorted data, unless the available software has special features.

^{*}This appendix will also be published, under a different title, as a letter to the editor in "Limnology and Oceanography".

The COTED square key NN WW D D for any station of known latitude (Lat.) and longitude (Long.) can easily be calculated, as outlined in Table F.1. For the Marsden square key MMMB B a similar table can be constructed. The number of program steps is approximately 10 in both cases.

Table F.1

Decision table to calculate the COTED square number of a station. All variables are integers; NN and WW are obtained by truncation.

is latitude north is longitude west	Y Y	Y	N Y	N N
X = Lat. + 90 X = 90 - Lat. Y = Long. Y = 360 - Long. NN = X/10 D _N = X - NN x 10 WW = Y/10 D _W = Y - WW x 10 COTED square = NNWWD _N D _W	X X X X X	X X X X X	X X X X X X	X X X X X X

A major advantage of the COTED system is the simplicity of the numerical relation between the keys of one and tendegree squares situated along an E-W or N-S line. As a result, the presence of a station within an arbitrary rectangular area can be established by only two range tests. This can best be explained by an example: Given a "rectangular" area between the latitudes 2°S and ll°N and longitudes 28°W and 35°W, and a station in the one-degree square $\text{NlNlWlD}_{\text{N}}\text{lD}_{\text{W}}\text{l}$, determine whether it falls within the defined area. This can be solved in two steps:

- (1) Calculate the COTED square numbers of the four one-degree squares in the corners: 080288, 080384, 100208, 100304.
- (2) Test whether N^1N^1D_N^1 and W^1W^1D_W^1 fall within the two ranges $088{\leqslant}N^1N^1D_N^1{<}100 \text{ and} \\ 028{\leqslant}W^1W^1D_W^1{<}034.$

To answer the same question for a unit area $M^1M^1B_1^1B_2^1$ in the Marsden square system, a much more elaborate system of tests is required.

Appendix F

A second advantage is that only one discontinuity line occurs, the Greenwich Meridian, instead of five at 0°W, 180°W, 80°S 0°N and 80°N. This also simplifies the writing of retrieval routines and saves computing time. Furthermore, the COTED system extends down to the south pole, and thus can also be used to store data obtained over the Antarctic land mass.

In our new Oceanographic Station Data File, OCEANS IV, the data are therefore sequenced in ascending order of the COTED key. This leaves the grouping of the data in basic units of one-degree squares unmodified, but the sequence of the one-degree squares is different from that determined by the Marsden square keys (except in the northwestern quadrant of the globe, south of 80°N).

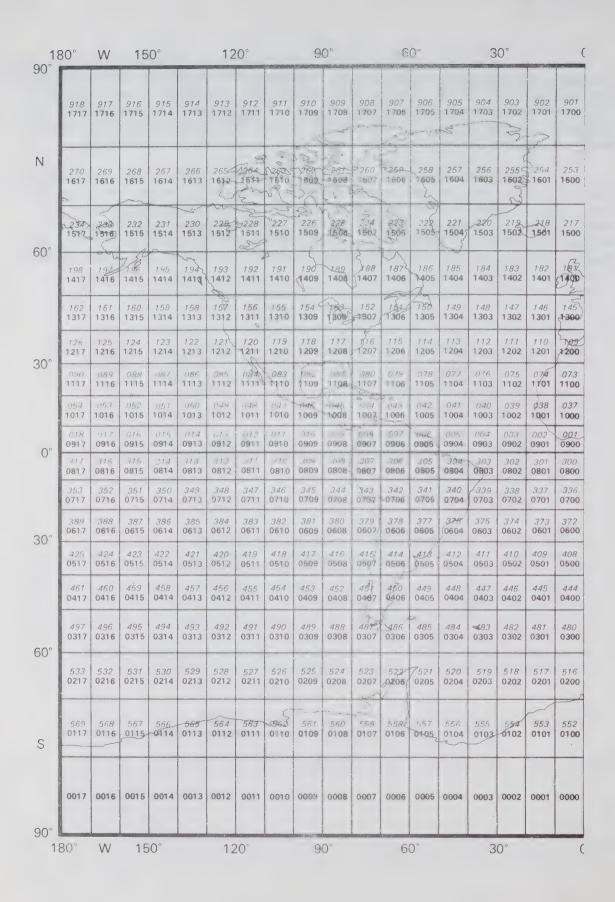


Fig. F.l Key to the Marsden and COTED ten-degree square numbers. The COTED square numbers are in bold print.

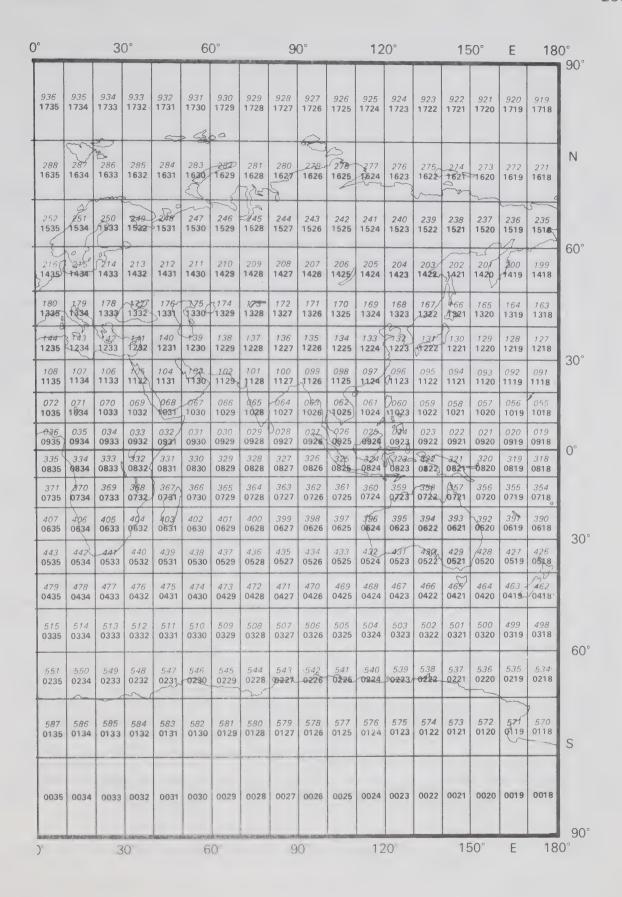


Fig. F.1 (cont'd) Key to the Marsden and COTED ten-degree square numbers.

11)°	WEST LONGITUDE)°			EA	0° EAST LONGITUDE							
10°	99	98	97	96	95	94	93	92	91	90	90	91	92	93	94	95	96	97	98	99	10°	
	89	88	87	86	85	84	83	82	81	80	80	81	82	83	84	85	86	87	88	89		
	79	78	77	76	75	74	73	72	71	70	70	71	72	73	74	75	76	77	78	79		
DE	69	68	67	66	65	64	63	62	61	60	60	61	62	63	64	65	66	67	68	69	NO	
LATITUD	59	58	57	56	55	54	53	52	51	50	50	51	52	53	54 —03	55	56	57	58	59	RTHL	
NORTH L	49	48	47	46	0 (44	43	42	41	40	40	41	42	43	44	45	46	47	48	49	NORTH LATITUDE	
NO	39	38	37	36	35	34	33	32	31	30	30	31	32	33	34	35	36	37	38	39	DE	
	29	28	27	26	25	24	23	22	21	20	20	21	22	23	24	25	26	27	28	29		
	19	18	17	16	15	14	13	12	11	10	10	11	12	13	14	15	16	17	18	19		
0°	09	08	07	06	05	04	03	02	01	00	00	01	02	03	04	05	06	07	08	09	0.	
0-	09	08	07	06	05	04	03	02	01	00	00	01	02	03	04	05	06	07	08	09		
	19	18	17	16	15	14	13	12	11	10	10	11	12	13	14	15	16	17	18	19		
	29	28	27	26	25	24	23	22	21	20	20	21	22	23	24	25	26	27	28	29		
DE	39	38	37	36	35	34	33	32	31	30	30	31	32	33	34	35	36	37	38	39	SO	
ATITU	49	48	47	46	45	44	43	42	41	40	40	41	42	43	44	45	46	47	48	49	UTH L	
SOUTH LATITUDE	59	58	57	56	3 0	54	53	52	51	50	50	51	52	53	54	55	56	57	58	59	SOUTH LATITUDE	
SOI	69	68	67	66	65	64	63	62	61	60	60	61	62	63	64	65	66	67	68	69	DE	
	79	78	77	76	75	74	73	72	71	70	70	71	72	73	74	75	76	77	78	79		
	89	88	87	86	85	84	83	82	81	80	80	81	82	83	84	85	86	87	88	89		
10°	99	98	97	96	95	94	93	92	91	90	90	91	92	93	94	95	96	97	98	99	10°	
1	0°			WE	ST LO	NGITU	DE			()°			EA	ST LO	NGITU	DE			1	0.	

Fig. F.2 Key to the numbering of one-degree squares in the Marsden system.

99	98	97	96	95	94	93	92	91	90	
89	88	87	86	85	84	83	82	81	80	
79	78	77	76	75	74	73	72	71	70	
69	68	67	66	65	64	63	62	61	60	
59	58	57	56	55	54	53	52	51	50	
49	48	47	46	45	44	43	42	41	40	
39	38	37	36	35	34	33	32	31	30	
29	28	27	26	25	24	23	22	21	20	
19	18	17	16	15	14	13	12	11	10	
09	08	07	06	05	04	03	02	` 01	00	
14/										

W----

Fig. F.3 Key to the numbering of one-degree squares in the COTED system.





MANUSCRIPT REPORT SERIES

No. 16

Computer Routines for Surface Generation and Display

J. Taylor, P. Richards and R. Halstead



Marine Sciences Branch

Department of Energy, Mines and Resources, Ottawa



Manuscript Report Series No. 16

CALL HE WA

12810

COMPUTER ROUTINES FOR SURFACE GENERATION AND DISPLAY

J. Taylor, P. Richards and R. Halstead

CONTENTS

		Page
1.0	Introduction	1
2.0	Section A 3-D Pictures	3 4 4 5 8 9 10 11 13
3.0	Section B Contouring Routines	21 22 22 22 23 26 26 27 28 29 30
4.0	Section C Surface Fit by Stepwise Regression 4.1 General description	35 36 36 38 38

Figures

			Page
Fig.	A-1	Hibberts Data K=0 NSM=0	11
Fig.	A-2	Hibberts Data K=0 NSM=2	12
Fig.	A-3	Hibberts Data K=10 NSM=0	13
Fig.	A-4	Hibberts Data K=10 NSM=0 Blanking included	14
Fig.	A-5	<pre>Z = X * * 2 - Y * * 2 One quad blanked</pre>	15
Fig.	B-6	Hibberts Data K=0 NSM=0	31
Fig.	В-7	Hibberts Data K=10 NSM=0	32
Fig.	B-8	Z = X * * 2 - Y * * 2	33
Fig.	B-9	Wind driven circulation in Lake Ontario Equilib. level	34
Fig.	C-10	<pre>3rd degree polynomial fit F-value in=0 F-value out=0</pre>	46
_	C-11	5th degree polynomial fit F-value in=0 F-value out=0	47

1.0 INTRODUCTION

Three sets of computer routines are described in this manuscript.

- A) A FORTRAN IV program package for fitting a single valued surface z(x,y) through arbitrarily placed data points and displaying a perspective (3-D) view of the surface on a plotter.
- B) A set of FORTRAN IV subroutines (with an optional driver program) for fitting a single valued surface z(x,y) through arbitrarily placed data points and displaying contours of the surface on a plotter.
- C) FORTRAN IV subroutines for fitting a surface by means of arbitrarily chosen functions of x and y using the stepwise regression technique. For display purposes these routines may be linked to the 3-D and contouring packages.

The surface fitting and contouring routines were initially developed at the request of Dr. T.S. Murty of the Division of Oceanographic Research.

We wish to thank Miss Tish Millington for preparing this report for publication.

The surface interpolation technique used in sections A) and B) is an extension of a method described in notes left by Mr. I. Crain who worked for the Computer Science Center, Energy, Mines and Resources Department in the summer of 1968.

We would like to thank Mr. P. Hibbert, also of the Computer Science Center, for his comments and suggestions concerning surface interpolation.



2.0 SECTION A

PROGRAM G10638 3-D PICTURES NOVEMBER, 1969

2.1 GENERAL DESCRIPTION

This program plots a perspective picture of a single valued surface Z(X,Y) defined over a rectangular grid in X and Y.

The data may be given as a set of points XP(K), YP(K), ZP(K), K=1...N arbitrarily placed over the region of the grid (and to be interpolated onto the grid), or as already gridded data.

The surface may be smoothed, the data points may be marked and labeled, contours may be drawn on the surface, and portions of the grid may be blanked out as desired.

The routines are written in simplified FORTRAN IV language and have been run on the CDC3100, IBM360 and SRUll08 computers. The changes needed to go from one computer to another are rather slight. The complete set of routines just fit into the CDC3100 which has 16,000 24 bit memory locations. The CALCOMP plotting routines PLOT, SYMBOL and NUMBER, and one magnetic tape to receive the plotter commands, are required.

2.2 ROUTINES REQUIRED

1)		rogram G10638 reads data and calls the outines needed to generate the picture
2)	ZGRIDP	Performs two dimensional interpolation onto grid Z
3)	SMOOTHS	smooths the surface Z
4)	XLINES	Routines to draw the surface Z and the
5)	YLINES	pase on which it rests
6)	BLINES	dase on which it lests
7)	CON3DD	raws contours on the surface Z
8)		Marks and labels data points on surface Z
9)		Determines if a point on the surface is visible
10)	i	Determines if a given point (X,Y) is inside or outside the so called planking polygon
11)		lots the projection of a line
12)	PROJ	Calculates the projection of any point (X,Y,Z)
13)	ZLEVEL	uxiliary routine to CON3D
14)	PLOTNY	Plots an ordinary, heavy or dotted ine. (dotted lines are used for contours)
15)	PLOT, SYMBOL, NUMBER	The CALCOMP plotting routines

Routines SUBDIV and FOURPT are not part of the package but may easily be inserted by the user and have been found very useful for subdividing the grid to make a smoother flowing surface.

2.3 DATA

In a computer run any number of pictures can be made. Each picture requires 7 types of data (types 0 to 6). Data types 1 to 6 control various sections of the program (grid construction, contouring, etc.). Type 0 merely controls the reading of types 1 to 6.

Data Type 0

One card containing KD1, KD2...KD6. FMT(6I1). If KDI is greater than or equal to 1, data type I will be read in. If KDI=0 data type I should be omitted and data from the previous picture will be used.

For example, if KDl=0 for picture 2 then the title card for this picture should be omitted and the title will be the same as that of picture 1 of the run.

KDl=KD2...KD6=0 denotes the end of the job.

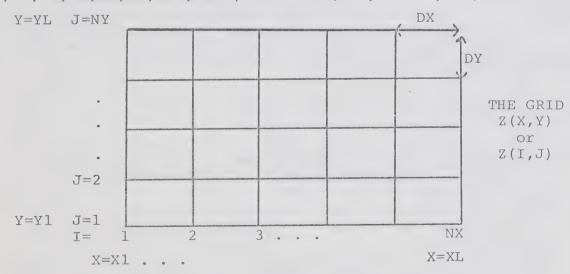
Data Type 1

One card containing any title of 80 characters or less for the picture. The title is .2 inches high and .5 inches below the bottom of the picture. (This can easily be changed by modifying the call to SYMBOL near the end of the MAINLINE).

Data Type 2

One card containing information on construction of the grid surface Z, as follows...

NX,NY,X1,Y1,XL,YL,CAY,NRNG,NSM FMT(2I5,5F10.0,2I5)



---NX,NY are the numbers of grid points along the X and Y directions. See illustration above.

---Xl,YL,XL,YL are the coordinates of the lower left and upper right corners of the grid. (Distance here is measured in what may be called data units; any unit convenient to the user. All other length-type inputs are in the same units, except XlPL,YlPL,XLPL,YLPL which are in inches.) --- CAY determines the type of interpolation used to fill in the grid Z from an arbitrarily placed set of data points.

If CAY=0.0, Laplacian interpolation is used. The resulting surface tends to have rather sharp peaks or dips at the data points (somewhat like a trampoline with poles pushed up into it). There is no chance of spurious peaks appearing in regions devoid of data.

As CAY is increased, Spline interpolation predominates over the Laplacian, and the surface passes more smoothly through the data points. Here the surface is somewhat like a lattice of flexible beams constrained to pass through the data points. The possibility of spurious peaks and steep extrapolations in areas lacking data increases with CAY. By adjusting CAY properly, a trade-off between smoothness and avoidance of spurious peaks can be obtained. CAY=5.0 or 10.0 often gives a good surface.

A relaxation procedure is used to perform the interpolation onto the grid. Each data point is shifted to the nearest grid intersection before the procedure is begun. An average ZP value is used if two or more data points are nearest the same grid intersection. (A version of the interpolation routine ZGRID which leaves the data in place is available. However, it is not used here in order that compatibility with the data marking routine might be maintained.)

If CAY=-1.0 the interpolation is bypassed (as well as the smoothing, blanking and data marking routines). In this case the user is expected to supply coding to read or generate the grid surface Z(I,J).

---NRNG...Any grid points more than NRNG grid spaces from the nearest data point are set to undefined. NRNG has somewhat the same effect as the blanking polygon (data type 6). NRNG = 5 or 10 is usually good for blanking ill-determined regions of the grid and improving the convergence of the grid interpolation.
---NSM is the number of Laplacian smoothings to be applied to the grid Z after the interpolation is done. This is useful for removing sharp peaks, or noise, from the surface, while leaving large scale trends undisturbed.

Data Type 3

There are two possibilities here...

1) If CAY is greater than or equal to 0.0, the data points XP(K),YP(K),ZP(K),K=1...N are read one point per card according to format statement 304 of the MAINLINE. End of the set is indicated by XP(N+1)=10**35.

The points XP, YP, ZP are the set from which the surface is interpolated. Any point not falling over the surface of the grid is ignored.

2) If CAY=-1.0 the user is expected to have inserted coding between statements 309 and 399 in the MAINLINE to generate the surface grid Z(I,J). Areas of the grid to be left blank should be set to 10**35. Control passes to statement 309 only if KD3 is greater than 0. If the user code calls for data to be read, this data must be placed in the type 3 spot.

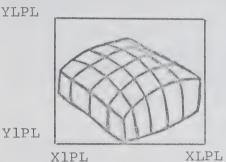
For example, the user might read from cards the entire grid

Z(I,J), I=1...NX, J=1...NY.

Data Type 4

Two cards are needed here giving information on the position of the picture and the labeling of data points Card 1... XIPL, YIPL, XLPL, YLPL, LABPT FMT(4F10.0,I5) Card 2... ZBASE, ZMAG, R, THETA, PHI FMT(5F10.0)

---XlPL, YlPL, XLPL, YLPL are the lower left and upper right corners of the rectangular space on the plotter in which the picture is to be drawn, in inches. Usually the picture cannot touch all four sides of the allotted rectangle and is justified to the lower left as illustrated below.



Y1PL X1PL XLP

---LABPT ≥ 0. Mark and label data points using LABPT figures after the decimal.

=-1. Omit decimal point.

=-2. Omit labels. (Mark data points only).

=-3. Omit data points altogether.

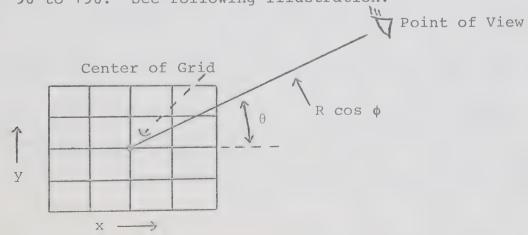
Note...All data points are marked at their closest grid points.
---ZBASE. All pictures are drawn on a boxlike base. ZBASE is the height (Z value) of this base. Blanked portions of the grid are drawn in at level ZBASE. It is usually a good idea to set ZBASE less (greater) than the lowest (highest) point of the surface to get a nice looking picture.

--- ZMAG. The Z values of the surface are magnified by a factor ZMAG about ZBASE. ZMAG may be positive or negative.

---R is the distance of the point of view from the center of the object consisting of the surface and its base. The center is taken to be (AV(X1,XL), AV(Y1,YL), ZBASE).

---THETA is the longitude of the point of view in degrees. THETA is zero along the positive X axis and increases counter clock wise.

---PHI is the latitude of the point of view in degrees. It varies from -90 to +90. See following illustration.



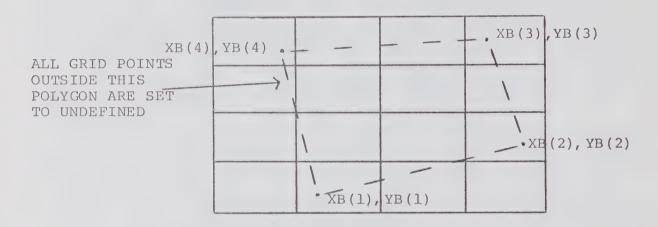
Data Type 5

The set of contour levels ZLEV(K), K=1...NLEV, one per card, FMT (F10.0). The set is ended by a card containing ZLEV(NLEV+1) = 10**35. If no contours are desired use this ending card only. There is no provision for the labeling of contours.

Data Type 6

A set of cards defining in sequence the vertices XB(K), YB(K), K=1...NB, of the blanking polygon; one point per card FMT (2F10.0). The set is ended by a card in which XB(NB+1)=10**35. If no blanking is desired use this last card only.

All grid points exterior to the polygon are set to undefined (10**35), as shown in the diagram. Blanking is useful for cutting out areas of the grid containing no data, where spurious extrapolations and peaks can occur.



2.4 PRINTER OUTPUT

All input data is printed out as it is read in. Any data points not falling over the area of the grid are noted on the printer. Entry to each of the major routines is noted.

A record is kept of each iteration in the relaxation procedure used to interpolate from the data points onto the grid Z. The relaxation factor W, an estimate of the largest root of the iteration matrix, and the maximum change in Z over all grid points relative to the range of Z are printed at each iteration. The process is continued until the estimated error in Z is less than 1 percent of the Z range or until 100 iterations are done.

2.5 PLOTTER OUTPUT

Five sample pictures are included to illustrate the features of the program. The data needed to produce these pictures are listed preceding the pictures. The coding used to generate the grid for Picture 5 is listed as well.

Picture 1 (FIG. A-1)

Here Laplacian interpolation (CAY=0.) is used and the surface is seen to peak sharply at many of the data points. The data points here are both marked and labeled. Note that each data point has been moved to the nearest grid intersection. (Of course the arrays XP,YP,ZP are left untouched.)

Picture 2 (FIG. A-2)

Same as Picture 1 only the surface has been smoothed, reducing the sharp peaks, the data points have been left off here.

Picture 3 (FIG. A-3)

Here Spline interpolation predominates (CAY=10.) and the surface is much smoother, and more satisfactory.

Picture 4 (FIG. A-4)

Same as Picture 3 except that contours have been included and a corner of the grid containing no data has been blanked out. Data points are marked only.

Picture 5 (FIG. A-5)

Here CAY=-1. and user code has been inserted between statements 309 and 399 in the MAINLINE to generate a simple function Z(X,Y) over the grid. One quadrant has been blanked out by filling all points in it with Z(I,J)=10**35.

Note

Each new picture starts a new block on the plotter tape and is shifted 3 inches from the right edge of the previous picture.

2.6 CAUTIONS

- 1) In routine ZLEVEL, entry ZCORN, note that the arguments must be included when using the 360 or 1108 and must be omitted with the 3100. (See Cols 73...80 of the card).
- 2) In reading the title of the picture (data type 1 in the MAINLINE) 4 characters are stored per word on the 3100 or 360 and 6 per word on the 1108. This means a change of four cards when changing from the 3100 or 360 to the 1108. (See Cols 73...80 of the cards in question).
- 3) In the call to PLOTS near the start of the MAINLINE, two arguments are needed when using the standard CALCOMP plotting routines. Three are needed when using the MODULAR MOORE PDP-8 routines. The third argument is the logical unit number of the plotter tape. We have used unit 13.

- The dimensions of the array Z must be at least (NX,NY).
 The dimensions of the first subscript of Z must be identical in the MAINLINE, ZGRID, SMOOTH, XLINES, YLINES, BLINES, CON3D, DATA3D, VISIBL (and SUBDIV if used). Z must be in common storage in the MAINLINE and VISIBL.
 The array INTZ should be dimensioned the same as Z in the MAINLINE and VISIBL, and should be equivalenced to Z. (In the 3100 version, INTZ requires three subscripts, the first being a 2, and the other two being the same as in Z. The coding involving INTZ in the 3100 version also reflects this difference). INTZ overlays Z and allows the visibility code of each grid point to be stored in the low order bit of Z.
- 5) The arrays XP,YP,ZP must be dimensioned large enough in the MAINLINE to hold all the data points plus one.
- 6) The array ZLEV must be dimensioned large enough in the MAINLINE to hold all contour levels plus one.
- 7) The arrays XB, YB must be dimensioned large enough in the MAINLINE to hold all vertices of the blanking polygon plus one.
- 8) The array IMNEW in routine ZGRID should be dimensioned at least as large as NY. It is now set at 110 which should be big enough in most cases.
- 9) The format 304 in the MAINLINE must correspond to the format in which the data points have been punched.
- 10) The hidden line procedure presently used in this program does not cover the case where one end of a line is visible from above the surface, the other end from below and part of the interior is hidden. This can cause no trouble if the surface is viewed from above (PHI is greater than or equal to 0) and all points of surface Z are greater than ZBASE. However in other cases, if care is not taken in selecting the view, some hidden lines might show through.

2.7 MODIFICATIONS

An effort was made to write the MAINLINE in a fairly straight forward way, in order that modifications could be made without too much trouble.

Aside from the setting up of routine PROJ (to fit the picture into the allotted plotter space), all the MAINLINE does is read in the data and call, one after the other, the routines needed to generate the picture. Listed below are several modifications which can be made fairly easily.

1) If all data is ready gridded and no contours are required, quite a bit of computer memory can be released by removing

the routines ZGRID, SMOOTH, CON3D, DATA3D and ZLEVEL, and the appropriate calls in the MAINLINE.

2) Coding for the labeling of axes could be inserted (say after statement 1320 of the MAINLINE).

To draw a label parallel to the projection of a given axis, two calls to PROJ and one to ATAN2 would be needed to get the position and angle of the label. Then a call to SYMBOL or NUMBER could be used to plot the label. (See the comment cards in PROJ for the use of this routine).

- 3) Extra lines can be added to the picture as desired by calls to PLOTP, which draws projected lines. (See comment cards in routine PLOTP).
- 4) Stereo pictures can be produced by making two pictures of the same surface with longitude THETA differing by 2 or 3 degrees.

The two pictures can be done in red and blue ink superimposed, then viewed through colored glasses, or can be plotted separately and brought together by straining the eyes.

To produce a stereo pair remove the C from Col.1 of the card marked STEREO in the MAINLINE.

5) Sometimes the data is given in gridded form, but on a very coarse grid. In this case the surface can be rather sparse and spiky looking. To get a smoother and fuller looking surface the routine SUBDIV can be used to subdivide the grid any number of times in both directions using third degree polynomial interpolation. (The auxiliary routine FOURPT is also required).

2.8 DATA SUMMARY SHEET

Data Formats

- 0) KD1, KD2, KD3, KD4, KD5, KD6 FMT (611)
- 1) IT(1 ... 20) FMT(20A4)
- 2) NX,NY,X1,Y1,XL,YL,CAY,NRNG,NSM FMT(215,5F10.0,215)
- 3) XP,YP,ZP One set/card Last XP=10**35 FMT NO. 304, or if CAY=-1.0 insert coding between 309 and 399 to generate Z(1...NX,1...NY).
- 4) X1PL, Y1PL, XLPL, YLPL, LABPT FMT (4F10.0, I5)
- 4B) ZBASE, ZMAG, R, THETA, PHI FMT (5F10.0)
 - 5) ZLEV One per card Last ZLEV=10**35 FMT(F10.0)
 - 6) XB, YB One set/card Last XB=10**35 FMT(2F10.0)

Data Description

KD1...KD6 = 0 Use previous set of data (All zeros = EOJ).

> 0 Read in new data.

data units.

CAY = 0. Laplace interpolation used to get grid Z.

> 0. As CAY is increased Spline interpolation predominates.

= -1. When interpolation not needed.

NRNG All grid points more than NRNG grid spaces from the closest data point are set to undefined (10**35).

NSM = Number of Laplacian smoothings to apply to Z. XP,YP,ZP = The set of N data points (in data units).

Z = Array of height values (Undefined Z=10**35).

XlpL, YlpL, XLPL, YLPL

= Lower left and upper right corners of space on plotter for the picture to fit into (inches).

ZBASE = Base level of the figure being plotted.

ZMAG = Magnification of Z to be used.

R, THETA, PHI = Point of vision relative to center of picture.

R = Radius in data units.

THETA = Longitude (Degrees) (Zero along X axis).

PHI = Latitude (Degrees).

LABPT ≥ 0. Number of digits after decimal on data point labels.

= -1 Omit decimal in data point labels.

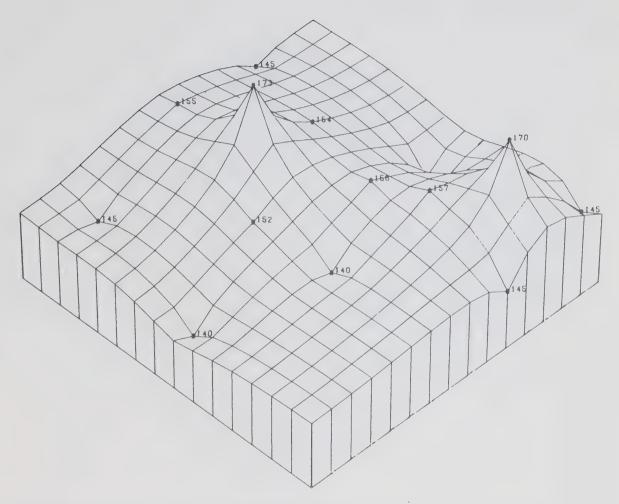
= -2 Omit labels on data points.= -3 Omit data points altogether.

ZLEV = Array of contour levels to be drawn. There are NLEV levels.

2.9 DATA USED TO PRODUCE PICTURES 1 TO 5 (FIGURES A-1 TO A-5)

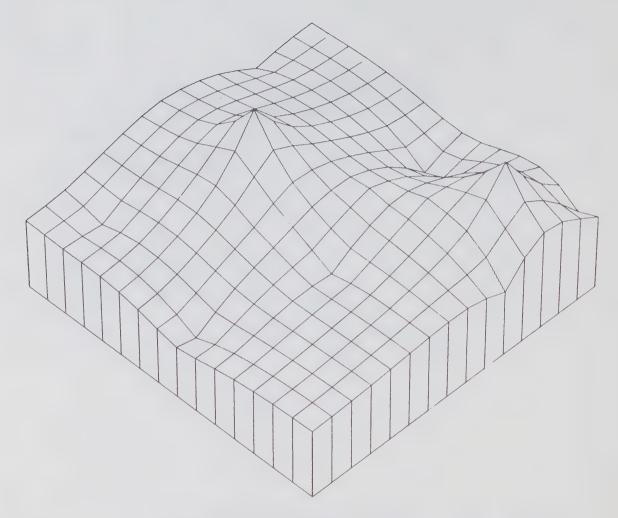
```
123400
HIBBERTS DATA K=0 NSM=0
 16 16 110. 120.
                       185. 195. 0.0
                                                       20 0
                140.
 148.
       125.
 122.
         131.
                  145.
 143.
         145.
                  152.
 158.
         149.
                  146.
 115.
         155.
                  155.
 135.
         157.
                  173.
 155.
         165.
                  156.
 185.
         168.
                  145.
 165.
         170.
                  157.
                  154.
 135.
         172.
 112.
         181.
                  145.
 175.
         182.
                  170.
 153.
         183.
                  143.
 149.
         186.
                  140.
      193.
 182.
                  145.
 1.0000E+35
                          7.5
 0.0
                  7.5
         0.0 7.5
1.6 1000.
 130.
                          -45.
                                   45.
 120400
 HIBBERTS DATA K=0 NSM=2
 16 16 110. 120.
                          185.
                                    195.
                                             0.
                                                       20
                                                              2
        0.0
 0.0
                  7.5
                          7.5
 130.
         1.0
                  1000.
                           -45.
                                    45.
 120400
 HIBBERTS DATA K=10 NSM=0
 16 16 110. 120.
                         185.
7.5
-45.
                                195.
-1
                           185.
                                             10.
                                                    20
                                                            0
 0.0
130.
1.0
                  7.5
                                    -1
                  1000.
 100450
 HIBBERTS DATA K=10 NSM=0 BLANKING INCLUDED
 0.0 0.0 7.5 7.5 -2
130. 1.0 1000. -45. 45.
 140.
 145.
 150.
 155.
 160.
 165.
 170.
1.0000E+35
105. 115.
158. 115.
 158.
        143.
 167.
         145.
 167.
         162.
 190.
         162.
 190. 200.
105. 200.
 1.0000E+35
```

```
123456
Z=X**2-Y**2 OHE QUAD BLANKED
  21 21 0. 0.
                             20.
                                      20.
                                                  -1.
0.
        0.
                    5.
                              5.
-100.
         . 1
                    75.
                             -35.
                                        55.
-50.
0.0
50 .
1.0000E+35
1.0000E+35
000000
      CODING INSERTED IN MAINLINE TO GENERATE
2.10
      GRID OF PICTURE 5 (FIGURE A-5)
309
      CONTINUE
C
C
      USER CODE FOR GRID Z GENERATION GOES HERE (ACTIVE IF CAY=-1.0
C
      AND KD3 GT 0 )
C
C
      Z=X**2-Y**2
      DO 350 I=1,21
      DO 350 J=1,21
      Z(I,J)=1.E35
      IF(I-11)340,340,330
330
      IF(J-11)350,340,340
340
      Z(I,J) = (I-11)*(I-11)-(J-11)*(J-11)
350
      CONTINUE
C
399
      CONTINUE
```



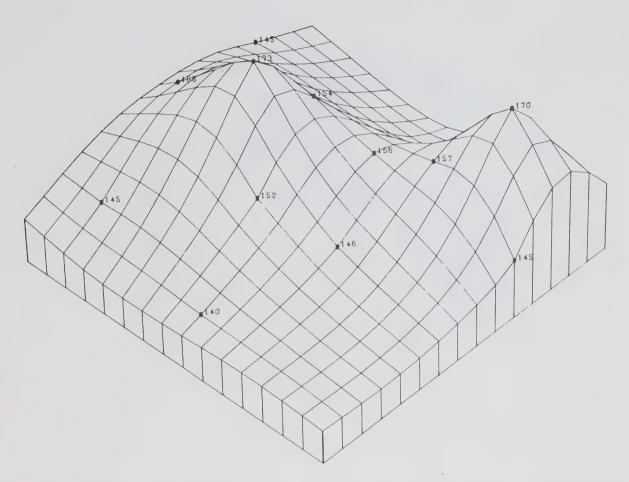
HIBBERTS DATA K=0 NSM=0

Figure A-1



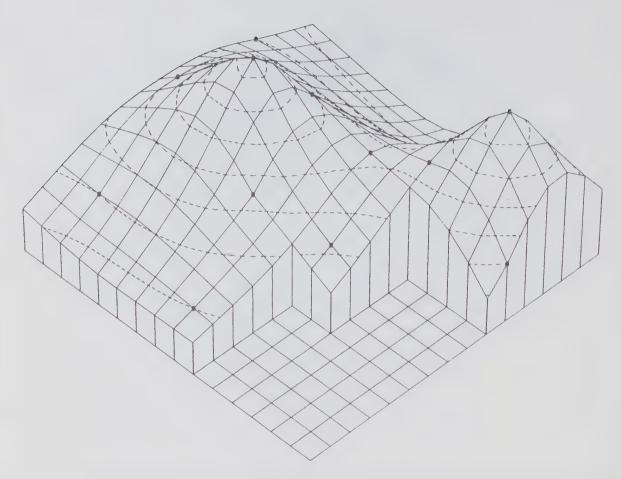
HIBBERTS DATA K=U NSM=2

Figure A-2



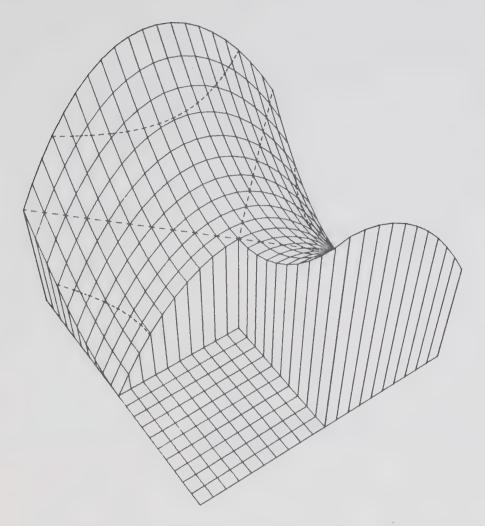
HIBBERTS DATA K=10 NSM=0

Figure A-3



HIBBERTS DATA K=10 NSM=0 BLANKING INC

Figure A-4



Z=X**2-Y**2 ONE QUAD BLANKED

Figure A-5



3.0 SECTION B

PROGRAM G10649 CONTOURING ROUTINES APRIL 1970

3.1 GENERAL DESCRIPTION

This is a set of subroutines for surface interpolation and contour plotting.

Arbitrarily placed data points XP(K),YP(K),ZP(K),K=1...N may be interpolated onto a rectangular grid Z(I,J) using two dimensional Laplace or Spline interpolation or a combination of the two. The surface may then be smoothed. Portions of the grid surface may be blanked out (set to undefined) as desired.

Contours of the surface Z(I,J) may be plotted. The grid may be subdivided to produce smooth flowing contour lines. The contours may be labeled. Three line types are available for contours. Data points may be marked and labeled.

The routines are written in a simplified FORTRAN IV language and have been run on the CDC3100, SRU1108 and IBM360 computers. The changes needed to go from one computer to another are minor. The complete set of routines takes about 12000 words of storage if the array dimensions are kept at a minimum. The CALCOMP plotting routines PLOT, SYMBOL and NUMBER and one magnetic tape to receive the plotter commands are required.

3.2 THE DRIVER PROGRAM

A driver program has been written which reads data supplied by the user and calls the various routines needed to produce a contour plot. We will describe the routines in terms of the driver program, as the data variables for the driver correspond quite closely to the arguments of the various routines. (However, it might be mentioned here that the routines are often more convenient to use by means of individual calls from user written programs. The calls to particular routines will be described briefly in a later section.)

3.3 ROUTINES REQUIRED WHEN USING DRIVER

1)	MAINLINE	. (Program	G10649)) This	is the	driver.	It
		reads the	data a	and cal	.1s the	routines	needed
		to genera	te the	contou	r plot	•	

- 2) ZGRID......Performs two dimensional interpolation from data points XP,YP,ZP onto grid Z(I,J).
- 3) SMOOTH.....Smooths the surface Z.
- 4) INSIDE......Determines if a given point is inside or outside the so called blanking polygon.
- 5) GETLEV......Given a contour interval, it produces an array of levels.
- 6) CONSEG......Calls DOUBLE and CONTUR to subdivide the grid and contour the surface Z in segments.
- 7) DOUBLE......Subdivides the grid by a factor of 2 using cubic polynomials.
- 8) CONTUR......Calculates contours as strings of (X,Y) points and plots them.
- 9) DATAPT......Marks and labels the data points.
- 10) ARC......Will create a series of smooth flowing arcs from a series of straight line segments.

- 11) PLOTNY......Plots an ordinary, heavy or dotted line segment.
- 12) PLOT, SYMBOL and NUMBER...The CALCOMP plotting routines.

3.4 DATA NEEDED BY DRIVER

In a computer run any number of contour plots can be made. Each plot requires 7 types of data (types 0 to 6). Data types 1 to 6 control various sections of the program (interpolation, blanking, contouring, etc.). Type 0 merely controls the reading of types 1 to 6.

DATA TYPE 0

One card containing KD1, KD2... KD6 FMT(6I1). If KDI is greater than or equal to 1, data type I will be read in. If KDI=0 data type I should be omitted and data from the previous plot will be used.

For example, if KDl=0 for plot 2, then the title card for this plot should be omitted and the title will be the same as that of plot 1 of the run.

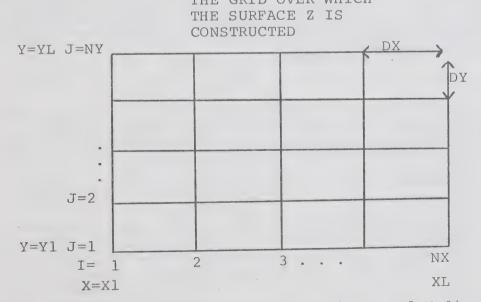
KD1=KD2=...KD6=0 denotes the end of the job.

DATA TYPE 1

One card containing any title of 80 characters or less for the plot. The title is 0.28 inches high and 0.5 inches below the bottom of the plot. (This can easily be changed by modifying the call to SYMBOL near the end of the driver).

DATA TYPE 2

One card containing information on construction of the grid Z, as follows...NX,NY,X1,Y1,XL,YL,CAY,NRNG,NSM FMT(2I5,5F10.0, 2I5).



--NX,NY...Number of grid points along the X and Y directions.
--X1,Y1,XL,YL...Co-ordinates of the lower left and upper right corners of the grid. (Distance here is measured in what may be called data units, any unit convenient to the user.)
See illustration above.

--CAY...Determines the type of interpolation used to fill in the grid Z(I,J) from an arbitrarily placed set of data points.

If CAY=0.0, Laplacian interpolation is used. The resulting surface tends to have rather sharp peaks and dips at the data points (somewhat like a trampoline with poles pushed up into it). There is no chance of spurious peaks appearing in regions devoid of data.

As CAY is increased, Spline interpolation predominates over the Laplacian, and the surface passes more smoothly through the data points. Here the surface is somewhat like a lattice of flexible beams constrained to pass through the data points. The possibility of spurious peaks and steep extrapolations in areas lacking data increases with CAY. By adjusting CAY properly, a trade-off between smoothness and avoidance of bad peaks can be obtained.

An over-relaxation process is used to perform the interpolation. The data points are initially moved to the nearest grid points, and then shifted back to their proper positions as the shape of the surface becomes evident. A value of CAY=5. often gives a good surface. To get a good rate of convergence of the relaxation process, it is wise to make the grid not much finer than is needed to resolve most of the data points into separate grid squares.

If CAY=-1.0 the interpolation is bypassed (as well as the smoothing, blanking and data posting routines). In this case the user is expected to supply coding to read or generate the

grid surface Z(I,J).

--NRNG...Any grid points more than NRNG grid spaces from the nearest data point are set to undefined. NRNG has somewhat the same effect as the blanking polygon (data type 6). NRNG=5 or 10 is usually good for blanking ill-determined regions of the grid and improving the convergence of the grid interpolation.

--NSM...The number of Laplacian smoothings to be applied to the grid Z after the interpolation is done. This is useful for removing sharp peaks, or noise, from the surface while leaving

large scale trends undisturbed.

DATA TYPE 3

There are two possibilities here...

1) If CAY is greater than or equal to 0.0, the data points XP(K),YP(K),ZP(K),K=1...N are read one point per card according to format statement 304 of the driver. End of the set is indicated by XP(N+1)=10**35.

The points XP,YP,ZP are the set from which the surface is interpolated. Any point not falling over the grid is

ignored. XP, YP and ZP are in data units.

2) If CAY=-1.0 the user is expected to have inserted coding between statements 309 and 399 of the driver to generate the surface grid Z(I,J). Areas of the grid to be left blank should be set to 10**35. Control passes to statement 309 only if KD3 is greater than 0. If the user code calls for data to be read, this data must be placed in the type 3 spot.

(For example, the user might read from cards the entire grid Z(I,J), I=1...NX, J=1...NY).

DATA TYPE 4

One card is needed here giving information on the position of the plot on the plotter, the labeling and subdivision of the grid as follows...

X1PL,Y1PL,XLPL,YLPL,HGTPT,HGTC,LABPT,NDIV,NARC FMT(6F10.0,315)
--X1PL,Y1PL,XLPL,YLPL = Lower left and upper right corners of
plot in inches.

--HGTPT = Height of labels on data points in inches.

-- HGTC = Height of labels on contours in inches.

--LABPT \geq 0 - Number digits after decimal on data point labels.

= -1 - Omit decimal in data point labels.

= -2 - Omit labels on data points.
= -3 - Omit data points altogether.

--NDIV = 1,2 or 4. The grid is subdivided NDIV times in both directions using cubic polynomials to produce finer looking contour lines. NDIV=1 has no effect.

--NARC = 1,2,3...10. This replaces each straight line segment of a contour by an arc of a smooth flowing curve. NARC is the number of subsegments in each arc. Care must be taken here as over-lapping of contours is a possibility. NARC=1 has no effect.

DATA TYPE 5

This gives the contour levels to be used. There are two possibilities here...

1) A set of cards containing ZLEV(K), LABC(K), LWGT(K), K=1...NLEV one group per card. FMT(F10.4,2I5). Column 25 must be blank. The set is ended by a card containing ZLEV(NLEV+1) = 10**35. If no contours are desired use this last card only.

--ZLEV(K) = Level of the Kth contour.

--LABC(K) \geq 0 - Number digits after decimal on contour label.

= -1 - Omit decimal on contour label.

= -3 - Omit label on contour.

--LWGT(K) ≤ 1 - Draw contour with ordinary line.

= 2 - Use heavy line.
= 3 - Use dotted line.

One card only containing DLEV, LABC, LWGT and the identifier INDC=1 in column 25. FMT(F10.4,315)

--DLEV = the contour spacing.

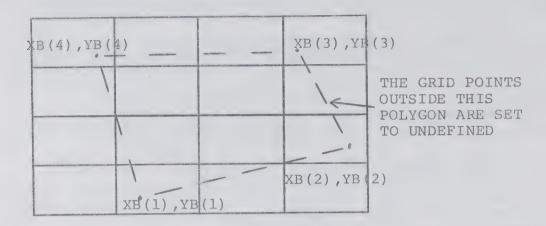
-- LABC and LWGT are as above.

DATA TYPE 6

A set of cards defining in sequence the vertices XB(K), YB(K), K=1...NB of the blanking polygon, one point per card, FMT(2F10.0). The set is ended by a card containing XB(NB+1)= 10**35. If no blanking is desired use this last card only. XB and YB are in data points.

units

All grid points exterior to the polygon are set to undefined (10**35), as shown in the diagram. Blanking is useful for cutting out areas of the grid containing no data, where spurious peaks and extrapolations may occur.



3.5 PRINTER OUTPUT USING THE DRIVER

All input data is printed out as it is read in. Entry to each of the major routines is noted.

A record is kept of each iteration in the relaxation process used to generate the grid Z(I,J). The relaxation factor W, an estimate of the largest root of the iteration matrix, and the maximum change in Z over all grid points relative to the range of Z, are printed at each iteration. The relaxation is continued until the estimated maximum error in Z is less than 1 percent of the range of Z, or until 100 iterations are done.

3.6 INDIVIDUAL USE OF THE ROUTINES

As mentioned earlier it is sometimes convenient to use the routines through individual calls from a user program. Some calls which may be useful are described below. Most arguments have been defined previously. Any new arguments are defined as they appear.

1) Interpolation of data onto a rectangular grid

The only routine needed here is ZGRID and the call is... CALL ZGRID(Z,NX,NY,X1,Y1,DX,DY,XP,YP,ZP,N,CAY,NRNG) where DX=(XL-X1)/(NX-1)

DY = (YL - Y1) / (NY - 1)

On input the undefined areas of Z(I,J) should be set to 10**35. All other points of Z should be 0.0. On output the 0.0 values will be replaced by Z values interpolated from data points XP,YP,ZP.

2) Smoothing of gridded data

The routine needed is SMOOTH and the call is... CALL SMOOTH(Z,NX,NY,NSM) The larger NSM the greater the smoothing. Any points of Z(I,J) set to 10**35 on input will be left untouched. All other Z points will be smoothed on output from the routine.

3) Blanking of portions of the grid

Routine INSIDE is needed here. For each point of the grid the following call should be made...
CALL INSIDE(XI,YJ,XB,YB,NB,IND)

where XI=X1+(I-1)*DX

YJ=Y1+(J-1)*DY

IND should be 999 on input to the first call only. On output IND=1 if (XI,YJ) is inside the blanking polygon and 0 if outside. For best efficiency do a series of YJ for each fixed value XI.

4) Contouring

Routines CONSEG, DOUBLE, CONTUR, ARC and PLOTNY are needed. (As well as PLOT, SYMBOL and NUMBER). The call is... CALL CONSEG(Z, NX, NY, X1PL, Y1PL, XLPL, YLPL, ZLEV, LABC, LWGT, NLEV, HGTC, NDIV, NARC).

The opening call to PLOTS and the closing call to PLOT must be made by the user. Also the user must draw the border around the plot if desired. No contours will be drawn in regions of the grid where Z(I,J)=10**35.

5) Getting an array of levels, given the contour interval

The routine needed is GETLEV and the call is... CALL GETLEV(Z,NX,NY,DLEV,ZLEV,NLEV)
The output here is the array ZLEV(K), K=1...NLEV of contour levels. Before calling CONSEG the user must set up the arrays LABC(K) and LWGT(K) K=1...NLEV. GETLEV ignores any Z values which are set to 10**35.

6) Posting the data points

Routine DATAPT is required (as well as PLOT, SYMBOL and NUMBER). The call is...
CALL DATAPT(NX,NY,X1,Y1,DX,DY,X1PL,Y1PL,DXPL,DYPL,XP,YP,ZP,N,LABPT,HGTPT)

where DXPL=(XLPL-X1PL)/(NX-1)

DYPL=(YLPL-Y1PL)/(NY-1)

The opening call to PLOTS and the closing call to PLOT must be made by the user. Also the user must draw the boundary around the plot if desired.

3.7 CAUTIONS

2)

1) In reading the title of the plot (data type 1) 4 characters are stored per word on the 3100 or 360 and 6 per word on the 1108. This means a change of four cards in the driver when changing from the 3100 and 360 to the 1108. (See cols 73...80 of the cards in question.)

In the call to PLOTS near the start of the driver, two arguments are needed when using the standard CALCOMP plotting routines. Three are needed when using the MODULAR MOORE PDP-8 routines. The third argument is the logical unit

number of the plotter tape. We have used 13.

The dimensions of the array Z in the driver must be at least NX,NY. The dimensions of the first subscript of Z must be identical in the driver,ZGRID,SMOOTH,GETLEV and CONSEG.

4) Arrays XP, YP, ZP must be dimensioned large enough in the driver to hold all the data points plus one. Arrays ZPIJ and KNXT in ZGRID must also be this large.

5) Arrays ZLEV, LABC, LWGT must be dimensioned large enough

in the driver to hold all contour levels plus one.

6) The arrays XB, YB must be dimensioned large enough in the driver to hold all vertices of the blanking polygon plus one.

7) Format 304 in the driver must correspond to the format in which the data points have been punched.

3.8 SOME POSSIBLE MODIFICATIONS

- 1) The arrays KNXT, ZPIJ and IMNEW of ZGRID, the array ZZ of CONSEG, and arrays X and Y of CONTUR are internal and may be put into some common/work/region to be re-used if storage is short.
- 2) The fractional distance to travel along a contour before labeling it and the distance between labels on a contour are given in SLABIF and DSLAB defined near the start of routine CONTUR. They are presently set at 0.4 and 100 inches respectively, but may be changed as desired. (Since a plot is done in segments which are labeled independently there is usually no need to put more than one label on each contour segment.)

As mentioned above, a plot is done in segments. The size of a segment in grid square units is LSEG by LSEG where

. . .

LSEG=(IZZ-1)/NDIV-2

IZZ=Dimension of array ZZ(I,J) in CONSEG. (Presently 57).

IZZ may be changed as desired but the dimensions of ZZ in routine CONSEG and the corresponding array Z in routine CONTUR should be changed accordingly. Also array IND10 of routine CONTUR should have dimensions of IZZ by IZZ/10 rounded up.

4) It is sometimes desirable to use heavy lettering for contour labels. This may be done by inserting two more calls to NUMBER after the call at Statement 860 in routine CONTUR. In the second call XLAB should be replaced by XLAB-.02 and in the third call XLAB should be replaced by

XLAB-.01 and YLAB by YLAB-.02.

from the grid points to their proper positions during the iteration process, we found that very steep slopes could be generated within a grid square if two data points were close in XP and YP but differed by quite a bit in ZP. To control this we set a limit DERZM upon the slope of the surface within a grid square. We have set DERZM = 4*(ZMAX-ZMIN)/MIN(XL-X1,YL-Y1). DERZM may be changed to suit the user. DERZM=0.0 causes all data points to be permanently shifted to their nearest grid points.

3.9 SAMPLE PLOTS TO ILLUSTRATE THE ROUTINES

Pictures 1 to 4 are small plots illustrating some of the features of the routines. The first 3 were done using the driver. The data needed to generate these plots is listed just before the pictures. Picture 4 was done with a user written MAINLINE.

PICTURE 1 (FIG. B-6)

This is a contour plot of a surface through 15 data points. We have used CAY=0.0 here.

PICTURE 2 (FIG. B-7)

This is similar to Picture 1. Here CAY=10. and a corner containing no data has been blanked out. The surface is seen to be smoother and more satisfactory than that for CAY=0.

PICTURE 3 (FIG. B-8)

This is a simple surface (with one quadrant blanked) generated by setting CAY=-1.0 and inserting the proper coding between statements 309 and 399 of the driver. The coding required is shown following the data listing.

PICTURE 4 (FIG. B-9)

The data here consisted of a 60 by 24 array Z(I,J) of levels in Lake Ontario. Points outside the lake were set to 10**35. A call to GETLEV was used to get the contour levels. CONSEG was then called to plot the contours. Then the points Z(I,J) interior to the lake were set to 100., points on the lake boundary were set to 0.0, and the Z=1.0 contour was plotted in a heavy line by another call to CONSEG. This produced the boundary of the lake.

Note:

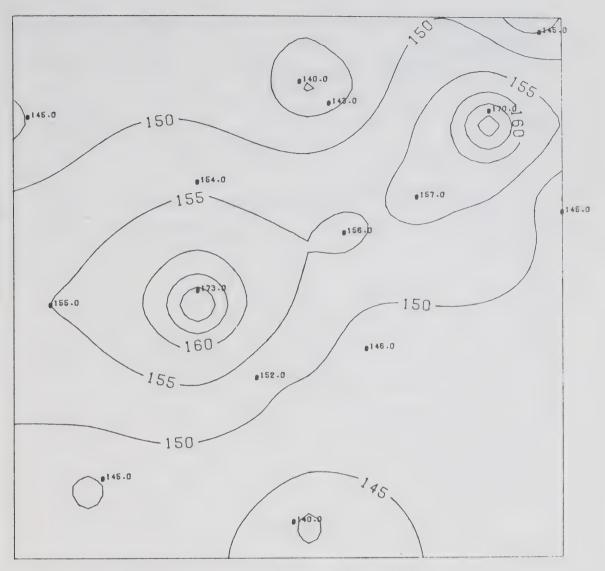
When the driver program is used, each new plot starts a new block on the plotter tape and is shifted 3 inches from the right edge of the previous picture.

3.10 DATA USED TO GENERATE PICTURES 1, 2, AND 3 (FIGURES B-6, B-7, AND B-8)

	AND B-	0)					
123456							
HIBBERTS	S DATA KEU	NSM=0					
16	10 110.	120.	185.	195.	0.0	10	()
148.	125.	140.					
122.	131.	145.					
143.	145.	152.					
158.	149.	146.					
115.	155.	155.					
135.	157.	173.					
155.	165.	156.					
185.	166.	145.					
105.	170.	157.					
135.	172.	154.					
112.	181.	145.					
175.	182.	170.					
153.	183.	143.					
149.	180.	140.					
	193.	145.					
182.		140.					
1.00001-		77 C	") (.	0.7	.14	1	- 4
U. U		7.5	7.5	.07	• 7.4	1	4
	-1	U 1					
1.000UE	+35						
120056							
	S DATA KET		4.0.6	1.05	10 0	1.0	0
	10 110.	120.	185.	195.	10.0	10	0
140.	-1	2					
145.	-1						
150.	-1						
155.	-1	5					
160.	-1						
165.	-1						
170.	-1	2					
1.0000F	+35						
105.	115.						
158.	115.						
158.	143.						
167.	143.						
167.	162.						
190.	162.						
190.	200.						
105.	200.						
1.0000E							
123450							
	Y**2						
/=X**2=		0.	5.	5.	-1.		
Z=X**2-		0.0		3.		1	ج
21		17.	5.		. 14		
0.	U.	5. 3. 1	5•		.14	-1	6
21	U. -1	5. 3 1	5.		.14		6

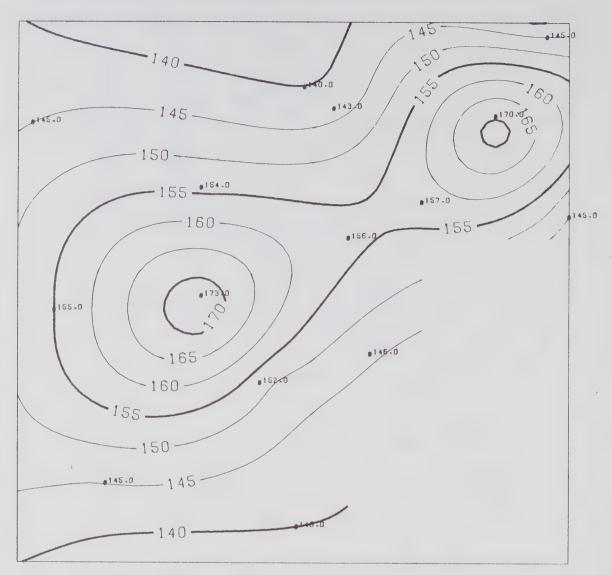
3.11 CODING INSERTED IN DRIVER TO GENERATE GRID OF PICTURE 3 (FIGURE B-8)

```
309
      CONTINUE
(
C
      USER CODE FOR GRID Z GENERATION GOES HERE (ACTIVE IF CAY=-1. AND
      KD3=3 )
C
      Z=X**2-Y**2
      DO 350 I=1,21
      DO 350 J=1,21
      Z(I,J)=1.E35
      IF(I-11)340,340,330
330
      IF(J-11)350,340,340
340
      Z(I * J) = (I-11) * (I-11) - (J-11) * (J-11)
350
      CONTINUE
399
     CONTINUE
```



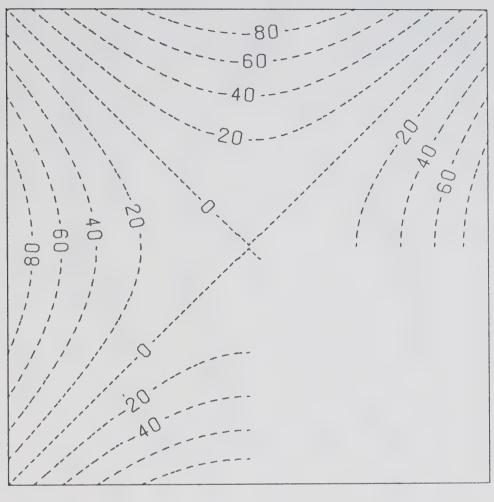
HIBBERTS DATA K=0 NSM=0

Figure B-6



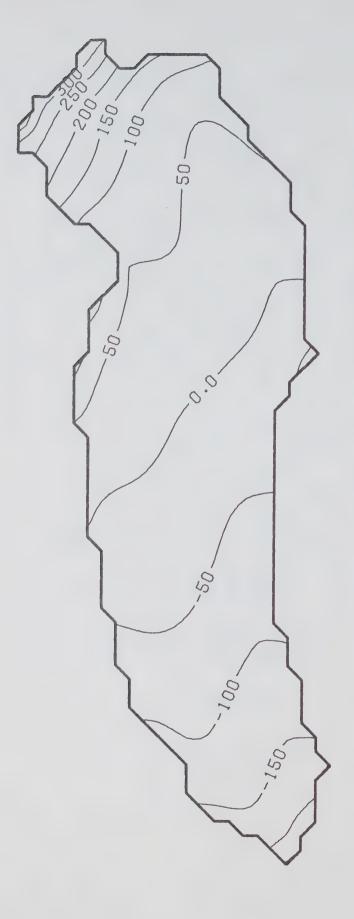
HIBBERTS DATA K=10 NSM=0

Figure B-7



Z=X**2-Y**2

Figure B-8



EQUILIB. LEVEL TOTL CURRENT . LAPLACIAN DEPTH SHOOTHING TSY=BETA+ALF2*X/L TSX=1-ALF1#Y/L WIND DRIVEN CIRCULATION IN LAKE ONTARIO ALF2 .250 RLF1 .750 BETA 1.000 .002500 .000100 5080. Ω 5080. X EXPONENT 10** 0

Figure B-9

4.0 SECTION C

PROGRAM TO FIT A SURFACE BY STEPWISE MULTIPLE REGRESSION ANALYSIS (LEAST SQUARES METHOD) MAY, 1970

4.1 GENERAL DESCRIPTION

Given a set of data points (XPi, YPi, ZPi), i=1,...NP, the program will calculate the least squares coefficients (Ao,SB1,...SBm) of the linear combination of suitable functions, Z(x,y)=AO+SBlfl(x,y)+...+SBmfm(x,y) which give a best fit to the ZPi data values. The functions fi(x,y)i=1,...,m are defined by the user.

The Regression Analysis is performed by a subroutine RESTEM which is resident in the statistical library on the UNIVAC 1108 computer.

It should be noted that only those functions fi(x,y) which contribute significantly to the fit are used. Those which do not are discarded by the Analysis.

The program is set up such that the user provides two short FORTRAN routines.

4.2 1 FORTRAN MAINLINE:

Purpose: to dimension arrays; to read data and limits; to call the subroutines which perform the analysis.

There are two calls to subroutines.

(i) Call SURFCE(XP,YP,ZP,VAR,SB,AO,M,NP,LIMIT,EFIN, EFOUT,IW,X,A,NPl).

This call is manditory. It performs the Regression Analysis and returns the least squares coefficients.

Name	Description	Туре
XP YP ZP	3,1 dimensional arrays of NP input data points	floating point array input
VAR	<pre>l dimensional array of functions fi(x,y) evaluated at (x,y). VAR has M elements.</pre>	floating point array output
SB	l dimensional array of M least squares coefficients. Those which the analysis decides do not contribute significantly to the fit are set to zero.	floating point array output
AO	constant least squares coefficient	floating point variable output
М	number of user defined functions $fi(x,y)$.	integer variable input
ИЪ	number of data points	integer variable input

Name	Description	Type
LIMIT	number of times regression is called. (Should be one more than number of functions fi(x,y)).	integer variable input
EFIN	F-value at which a function, fi(x,y), is entered into the regression.	floating point variable input
EFOUT	F-value at which a function, fi(x,y), is removed from the regression.	floating point variable input
IW	If IW=1, NP weights are applied to the NP data points. The weights are read in by subroutine SURFCE. There are 9 values per card under 9F8.0. Weight cards are placed immediately after the data cards containing the (XP,YP,ZP) data points. If IW=0 no weights need be provided.	integer variable input
х	2 dimensional array. User need not know the purpose of this array. He must dimension it. It is dimensioned as a NP by M+1 array.	floating point array
A	2 dimensional array. User need not know the purpose of this array. He must dimension it. It is dimensioned as a M+l by M+l array.	floating input array
NPl	Number of functions fi(x,y) plus l i.e. M+1.	integer variable input

Subroutine SURFCE initially prints out the correlation coefficients. At each stage of the analysis SURFCE also prints: function entering or leaving analysis; F-level of that function; standard error of Z; value of AO constant coefficient; list of values of least squares coefficients used at that point in the analysis.

At the end of the analysis a list of the input ZP values compared to a list of predicted Z(XP,YP) values using the least squares coefficients is printed.

(ii) Call VARS(X,Y,VAR)

This call is optional. Having called SURFCE to perform the analysis using the input data (XP,YP,ZP) and having obtained

the least squares coefficients (A0,SB1,SB2....SBm), the user may now wish to calculate the value Z for other (x,y) values. This can be done using the least squares coefficients and the functions fi(x,y).

Name Description Type

Y X and Y values for evaluation of floating point fi(x,y). VAR array of functions fi(x,y) floating point evaluated at (x,y). VAR has M array output elements.

The user could evaluate Z by Z = A0+SB(1)*VAR(1)+...+SB(m)*VAR(M)

4.3 2 SUBROUTINE VARS (X,Y,VAR)

Purpose: to define the user provided functions fi(x,y).

Each function fi(x,y) is evaluated at the given point (X,Y) and becomes one element of the array VAR. VAR can be dimensioned 2 as it is dimensioned in the calling routine.

4.4 THE FOLLOWING PAGES CONTAIN AN EXAMPLE OF THE USE OF THIS PROGRAM

FORTRAN MAINLINE:

NP = 96

M = 9

EFIN=EFOUT=2

IW = 0

LIMIT = 10

DIMENSION XP(96), YP(96), ZP(96), VAR(20), SB(21), X(96,10), A(10,10) LR=1

READ(LR, 3) M, NP, EFIN, EFOUT, IW, LIMIT

3 FORMAT(213,2F2.0,11,13)

READ(LR, 1) (XP(J), YP(J), ZP(J), J=1, NP)

1 FORMAT(3F9.0)

NPl=M+1

CALL SURFCE (XP, YP, ZP, VAR, SB, AO, M, NP, LIMIT, EFIN, EFOUT, IW, X, A, NP1) STOP

END

SUBROUTINE VARS:

In this example a 3rd degree polynomial is used to fit to.

SUBROUTINE VARS (X,Y,VAR)

DIMENSION VAR(2)

VAR(1) = X

VAR(2) = Y

VAR(3) = X*Y

VAR(4) = X*X

VAR(5) = Y * Y

VAR(6) = X*Y*Y

VAR(7) = X*X*Y

VAR(8) = X**3

VAR(9) = Y * * 3

RETURN

END

INPUT DATA

XP	YP	ZP	XP	YР	ZP
20.300	.000	1014.000	20.500	2.000	1014.000
20.800	3.000	1014.000	21.700	5.000	1014.000
22.200	6.000	1014.000	22.600	8.000	1014.000
22.400	9.000	1014.000	21.200	11.000	1014.000
20.300	12.000	1014.000	18.700	14.000	1014.000
18.200	15.000	1014.000	17.800	17.000	1014.000
17.900	18.000	1014.000	18.400	20.000	1014.000
18.500	21.000	1014.000	18.600	23.000	1014.000
18.900	24.000	1014.000	19.700	26.000	1014.000
19.800	27.000	1014.000	.000	1.900	1016.000
1.000	1.300	1016.000	3.000	.700	1016.000
4.000	.500	1016.000	6.000	.200	1016.000
7.000	.300	1016.000	8.200	2.000	1016.000
8.400	3.000	1016.000	8.300	5.000	1016.000
8.100	6.000	1016.000	8.000	8.000	1016.000
8.100	9.000	1016.000	8.500	11.000	1016.000
8.900	12.000	1016.000	9.600	14.000	1016.000
9.900	15.000	1016.000	10.000	17.000	1016.000
9.700	18.000	1016.000	8.600	20.000	1016.000
8.200	21.000	1016.000	7.700	23.000	1016.000
7.900	24.000	1016.000	9.700	25.000	1016.000
11.000	24.200	1016.000	13.000	22.800	1016.000
14.000	22.800	1016.000	15.600	24.000	1016.000
15.700	25.000	1016.000	15.600	27.000	1016.000
15.600	28.000	1016.000	1.000	7.000	1018.000
1.600	8.000	1018.000	1.600	10.000	1018.000
1.600	11.000	1018.000	1.800	13.000	1018.000
1.850	14.000	1018.000	2.000	16.000	1018.000
2.300	17.000	1018.000	2.400	19.000	1018.000
2.500	20.000	1018.000	2.500	22.000	1018.000
2.500	23.000	1018.000	2.700	25.000	1018.000
3.600	26.000	1018.000	6.000	28.000	1018.000

XP	ΥP	ZP
20.350 21.300 22.500 22.000 19.300	1.000 4.000 7.000 10.000 13.000	1014.000 1014.000 1014.000 1014.000
17.800 18.100 18.500 19.300 20.000	16.000 19.000 22.000 25.000 28.000	1014.000 1014.000 1014.000 1014.000
2.000 5.000 7.700 8.400 8.000	1.000 .250 1.000 4.000 7.000	1016.000 1016.000 1016.000 1016.000
8.200 9.300 10.100 9.300 7.800	10.000 13.000 16.000 19.000 22.000	1016.000 1016.000 1016.000 1016.000
8.700 12.000 15.000 15.700	25.000 23.200 23.100 26.000 7.300	1016.000 1016.000 1016.000 1016.000 1018.000
1.700 1.700 1.900 2.400 2.500	9.000 12.000 15.000 18.000 21.000	1018.000 1018.000 1018.000 1018.000 1018.000
2.550 4.600	24.000 27.000	1018.000 1018.000

Output:

List of the least square coefficients AO, SB(1),...,SB(M). Notice that not all the terms of the 3rd degree polynomial are used.

AO = 1015.24760

	Var	iable	Coefficient	Of Error of Coefficient
SB(1)	= X	(1)	09991	.01437
	X	(2)	.35049	.04532
	X	(3)	01337	.00251
	X	(5)	01978	.00360
	X	(6)	.00033	.00009
SB(M)	= X	(9)	.00039	.00009

Output: List of ZP input data values compared to a list of Z(XP,YP) predicted values, calculated using the least squares coefficients AO, SB(1),..., SB(M) and the 3rd degree polynomial.

	Actual	Predicted	Deviation
1 2 3 4 5 6 7 8 9 10 11 12 13 14 15 16 17 18 19 20 21 22 23 24 25 26 27 28 29 30 31 33 34 35 36 37 37 37 37 37 37 37 37 37 37 37 37 37	Actual 1014.0000 1016.0000 1016.0000 1016.0000 1016.0000 1016.0000 1016.0000	Predicted 1014.1300 1014.1907 1014.2137 1014.1910 1014.1129 1014.0238 1013.8962 1013.7836 1013.6563 1013.6575 1013.7455 1013.8650 1014.0183 1014.0959 1014.1615 1014.2154 1014.1883 1014.1499 1014.1022 1014.0475 1014.0596 1014.1175 1014.1763 1014.2157 1014.2629 1014.3445 1014.3445 1014.3445 1014.5305 1014.7326 1016.7554 1016.4645 1016.2633 1016.0666 1015.7284 1015.6120 1015.5343	Deviation130019072137191011300238 .1038 .2164 .3053 .3436 .3425 .2545 .13500183095916152154188309591615215418831499102204750596117517632157262934455305732775544645530573277554464526330666 .0975 .2716 .3880 .4657
38 39	1016.0000 1016.0000	1015.6195 1015.7554	.3805

	Actual	Predicted	Deviation
92 93 94 95 96	1018.0000 1018.0000 1018.0000 1018.0000	1018.0212 1018.0830 1017.9968 1017.9189 1017.7893	0212 0830 .0032 .0811 .2107

The following two pages contain two pictures comparing the results of this program using the data as shown in the example. In FIG. C-10 the least squares coefficients were obtained using the 3rd degree polynomial used in the example. This polynomial with the coefficients, was interpreted over a grid. The resulting Z values were contoured. The lines of black dots are the (XP,YP) positions of the input ZP value.

FIG. C-ll was produced with a 5th degree polynomial instead of a 3rd.

Note that the 3rd gives a better fit.

3RD DEGREE POLYNOMIAL FIT. F-VALUE IN=0 F-VALUE OUT=0

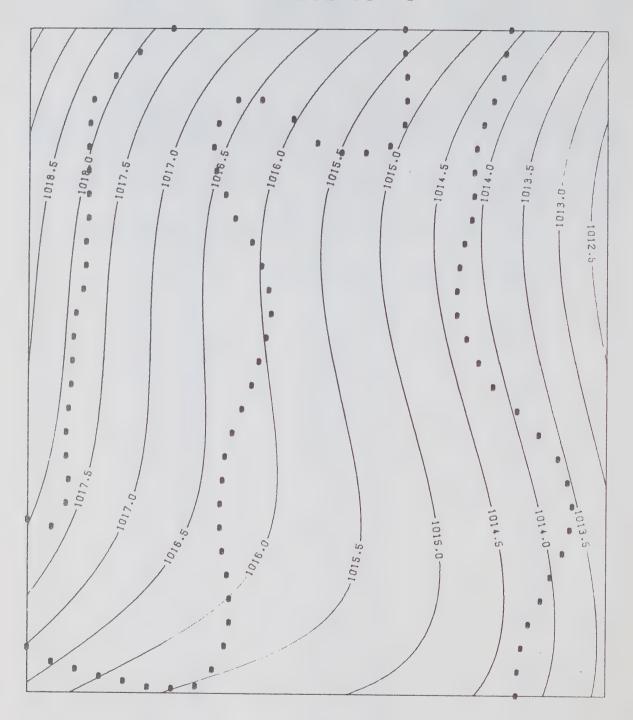


Figure C-10

5TH DEGREE POLYNOMIAL FIT. F-VALUE IN=0 F-VALUE OUT=0

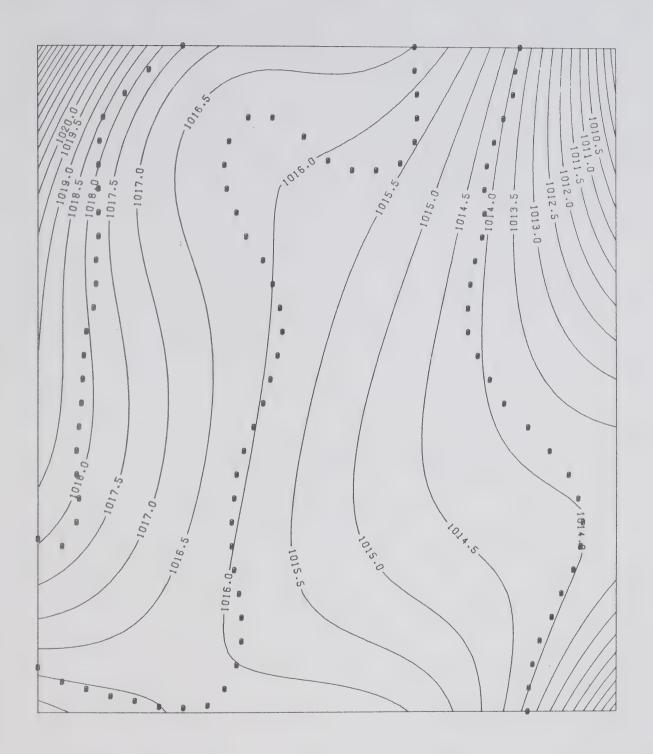
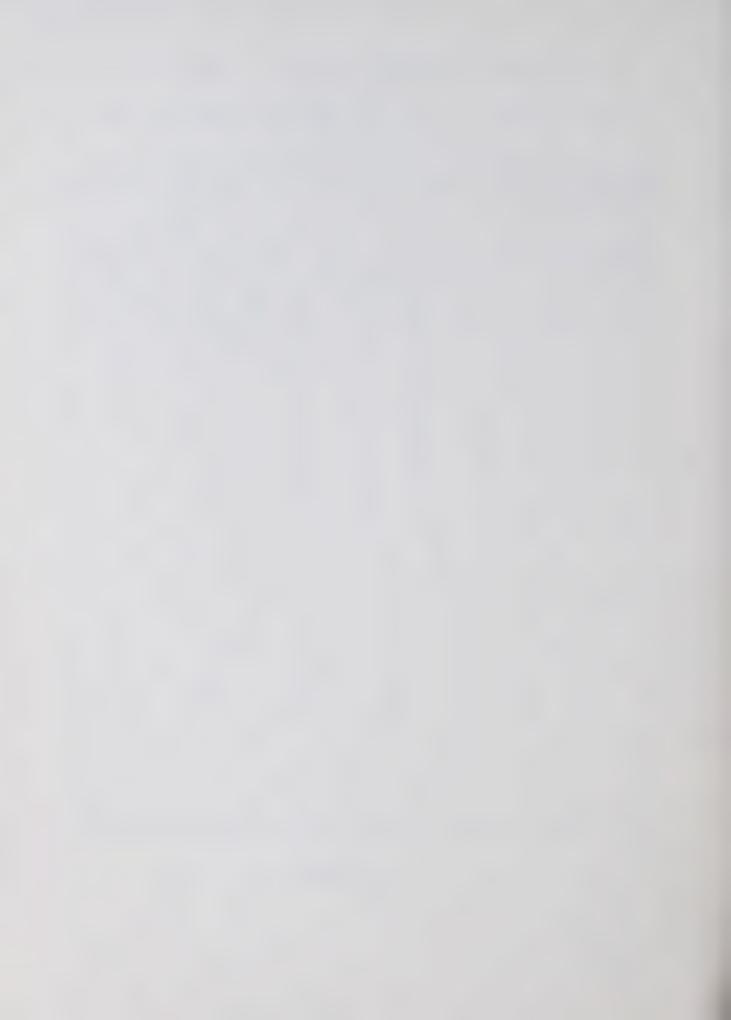


Figure C-11





MANUSCRIPT REPORT SERIES

No. 17

Simulation of tidal motion in complex river systems and inlets by a method of overlapping segments

R. F. HENRY



Marine Sciences Branch

Department of Energy, Mines and Resources, Ottawa



Manuscript Report Series No. 17

RIVER SYSTEMS AND INLETS BY A METHOD OF OVERLAPPING SEGMENTS

R. F. HENRY

0. ABSTRACT

A method is proposed which facilitates digital and hybrid computation of tidal motions for a coastal inlet or river system in which there are many bifurcations, confluences, islands, etc. The inlet is divided into overlapping segments and the tidal motion is computed for each segment separately over a time increment short enough to ensure that errors due to neglect of neighbouring segments are confined to the regions of overlap. The tidal motion for the whole inlet at the end of each time increment is found by discarding erroneous portions of the solutions for the various segments and piecing together the remaining parts.

This approach permits hybrid simulation of large inlet systems even when the amount of analog equipment available is limited. In purely digital computation of tidal motions, the difficulties of programming a single large difference scheme to cover a whole inlet system can be avoided by this proposed process of division into segments. The problem is reduced to linking standard subroutines representing commonly-encountered features such as bifurcations and confluences.

Results are presented of a simple numerical experiment designed to test the validity of the proposed method in a known physical situation and to compare various methods of linking adjacent segments.

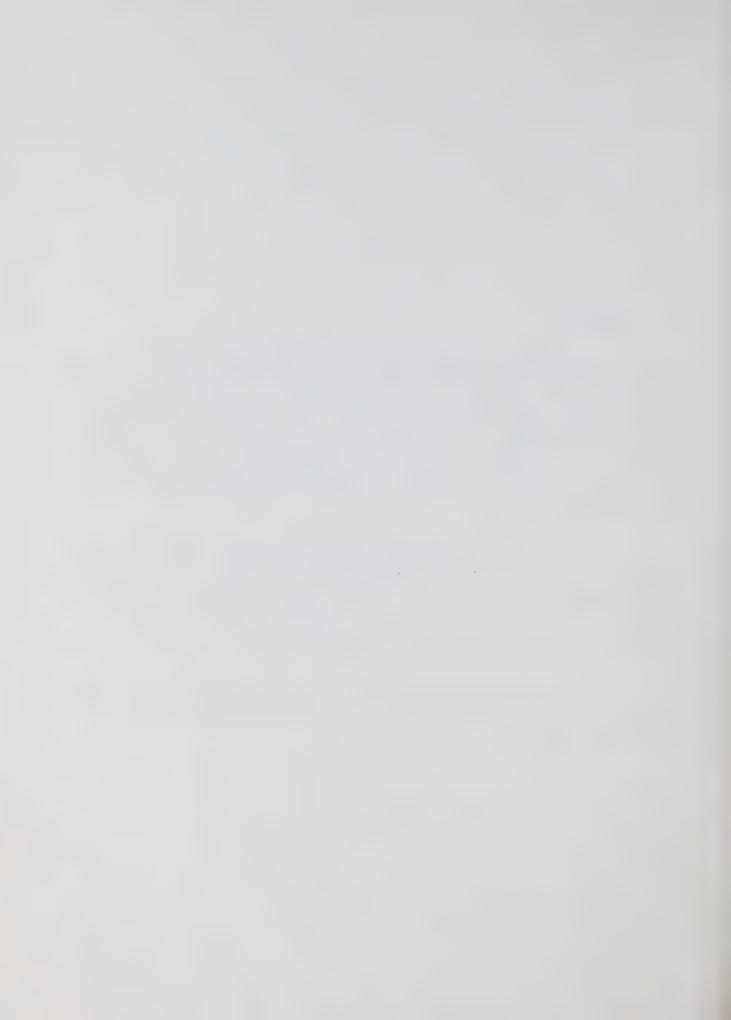


TABLE OF CONTENTS

0.		ABSTRACT	1
1.		INTRODUCTION	1
2.		THE METHOD OF OVERLAPPING SEGMENTS AS APPLIED TO TIDAL MOTION IN RIVERS AND COASTAL INLETS	2
	.1.1	Double or Bilateral Overlap. Combination of numerical solutions at a join with	3
		double overlap.	5
	.2.1	Single or Unilateral Overlap. Combination of numerical solutions at a join with	5
		single overlap.	7
2.	, 3	Prediction of Boundary Conditions at Joins.	8
2.	. 4	Note on Boundary Conditions.	8
3.		A NUMBERICAL EXPERIMENT WITH THE METHOD OF OVERLAPPING SEGMENTS	11
3,	1.1	Application of an Implicit Difference Scheme. Discussion of results.	13
3. 3.	2.1	Application of an Explicit Difference Scheme. Discussion.	19 22
4.		FUTURE DEVELOPMENTS AND APPLICATIONS	23
5.		ACKNOWLEDGEMENTS	29
6.		REFERENCES	30



1. INTRODUCTION

This report deals with digital applications of a method devised originally to facilitate analog and hybrid simulation of systems governed by hyperbolic partial differential equations. A common technique in analog simulation of such systems is to discretize the space variable(s) and so obtain an equivalent system of coupled ordinary differential equations, one for each of the spatial grid points, with time as the independent continuous variable. Applications are limited however by the need for considerable amounts of analog equipment if the domain governed by the equations is large. For a second-order hyperbolic equation, such as that governing tidal motion in inlets or rivers, each grid-point requires two integrators and thus the size of system which can be simulated on a typical general purpose analog computer is quite restricted. A possible solution to this difficulty lies in dividing the domain of interest into segments small enough to be simulated individually with the available equipment and then piecing together the various part solutions so obtained to find the solution over the whole domain. Obviously, it is necessary to implement this type of scheme on a hybrid computer rather than on an analog, since it is impracticable to undertake the required data-handling operations without the assistance of a digital computer.

One such hybrid technique has been suggested by Hsu and Howel for systems governed by parabolic or hyperbolic equations. The spatial domain is divided into a number of smaller segments and the solution for each segment in turn is found using stored solutions from adjacent segments to provide boundary values. Since only one segment at a time can be updated, these boundary values are at first slightly out-of-date and the solution in each segment departs quite rapidly from the true solution. However, if solution proceeds in small time steps, with iteration at each step, the solution in each segment converges to the corresponding part of the correct overall solution.

This paper describes a related but more economical method which, at the cost of some minor extra computation at each time step, eliminates the need for time-consuming iteration. Unlike Hsu and Howe's method, applications are apparently limited to hyperbolic equations since the proposed method requires the condition that physical effects should propagate at finite speeds; this holds for hyperbolic but not for parabolic or elliptic systems. The domain of interest is again divided into small segments but now adjacent segments are arranged to overlap to a certain extent. The solution in each segment is advanced separately over a time interval sufficiently short to prevent errors due to the effective 'freezing' of solutions in adjacent segments penetrating past the region of overlap at each edge.

References are listed on page

After the solutions in all segments have been updated over the same time step, those parts of the solutions which are affected by errors are discarded. Provided the segments overlap sufficiently, the remaining portions of the solutions suffice when pieced together to give the solution over the whole domain at the end of the time step; there is thus no need for iteration.

The practical problem of interest to the writer is the prediction of tidal motion in rivers, estuaries and coastal inlets. Although the proposed "method of overlapping segments" was devised to permit simulation of complex systems on a medium-sized hybrid computer, it became apparent that it could also facilitate digital simulation currently being undertaken and the remainder of this paper is concerned with digital applications.

Similar physical features, for instance, bifurcations, may recur at many places in a long river or inlet, but in the normal method of digital simulation, one large finite difference scheme is set up to cover the whole river. Each bifurcation or other feature is accounted for separately by introducing appropriate special elements into the coefficient matrix of the difference scheme. Economical simulation of a large system requires efficient solution of the difference equations at each time step; with present methods this implies preparation of special algorithms which are specific to a particular difference scheme and physical system. Even minor changes in the simulation, for the same system, may involve lengthy reprogramming, and for any other system, complete reprogramming is normally required. If, as suggested here, the river is first divided into a number of overlapping segments, each of which covers one bifurcation or confluence, etc., the simulation program can be built up quickly by repeated use of a few standard subroutines, one describing a bifurcation, one a confluence, and so on. At every time step, each segment is solved separately by the appropriate subroutine and then the solutions are pieced together to give the updated solution for the whole river. Even major changes in the simulation then often involve alterations in the use of only one or two subroutines. Further, the same subroutines may be used (with appropriate data) in the simulation of any other river or inlet governed by the same type of equations

The simulation of tidal motion used here to illustrate the method is only one of a number of applications in which the method of overlapping segments could facilitate digital solution of complicated hyperbolic systems. Other fields of application and techniques for handling some specific problems are discussed in the concluding section (§4) of this report.

2. THE METHOD OF OVERLAPPING SEGMENTS AS APPLIED TO TIDAL MOTION IN RIVERS AND COASTAL INLETS

inlets it is usually sufficient to use the following one-dimensional form of the shallow water equations 2

$$\frac{\partial h}{\partial t} + u \frac{\partial h}{\partial x} + h \frac{\partial u}{\partial t} = q$$
 (1a)

$$\frac{\partial u}{\partial t} + u \frac{\partial u}{\partial x} + g \frac{\partial h}{\partial x} = g(S_0 - S_f) - \frac{qu}{h}$$
 (1b)

where h = water level, u = velocity, x = distance, t = time, q = lateral inflow, g = acceleration due to gravity, S_0 = channel slope, and S_f = friction slope. Some authors use discharge Q in place of u as the second dependent variable, but whichever form is used, the equations are of hyperbolic type. This is a concise way of stating that the characteristic curves of these equations lie in the real (x,t)-plane; the corresponding physical property is that effects are transmitted at finite speed (ie. wave speed) in such systems. This feature is the basis of the method of overlapping segments.

2.1 Double or Bilateral Overlap

Suppose that the system to be simulated has been divided into a number of overlapping segments and consider the overlap between any two segments, for instance the shaded region around join B between the confluence Segment 1 and the bifurcation Segment 2 in Figure 1. Segment 1 will be taken as extending distance L to the right of B, as far as C, and Segment 2 distance L to the left, as far as A. This case, in which both segments extend past the join, will be referred to as double or bilateral overlap.

The times taken for disturbances to propagate from A to B or from C to B are approximately equal to L/c where c is the wave speed at B. Consequently, if initial conditions are known throughout the river at time t=0, the solution in Segment 1 can be computed over some interval At somewhat less than L/c without errors due to neglect of Segment 2 propagating past B. Similarly, the solution in Segment 2 can be advanced over Δt with errors confined to stretch AB. On discarding the erroneous solutions for stretches BC and AB obtained while solving Segments 1 and 2 respectively, the remaining parts of the separate solutions up to the join B, when considered together, constitute a valid solution for the region covered by the combined segments, including the neighbourhood of the join. Similar operations have to be performed at each time step at all joins between segments, for instance where Segments 1 and 2 overlap adjacent upstream and downstream segments. When the solution has thus been advanced over At for the whole river, the same cycle of computations is then carried out for the next time step, and so on until the desired time range has been covered.

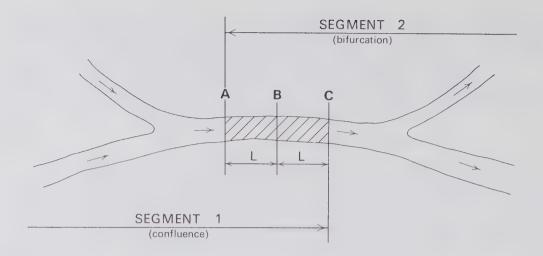


Figure 1 Join with Double or Bilateral Overlap

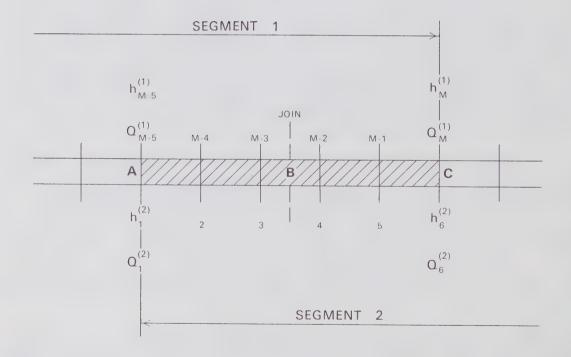


Figure 2 Details of Join with Double Overlap

2.1.1 Combination of numerical solutions at a join with double overlap

For the purpose of discussion, it will be assumed that the dependent variables are discharge Q and water level h and the difference scheme to be used is one in which both O and h are evaluated at every grid-point at each time step; mixed boundary conditions are to be supplied in the form of h1(t) at the first grid-point and Q_M(t) at the Mth (final) grid-point (see § 2.4).

When double or bilateral overlap is employed, the two adjacent segments will usually be arranged to extend an equal number of grid-points past their join B, as for instance in Figure 2, which shows a case with overlap of two and one-half grid sections. Grid-points near the join are considered common to the grid-systems of both Segments 1 and 2. For a given time-step; say (n-1). Δ t to n. Δ t, a set of difference equations with boundary values h_1 (1) (n. Δ t) and Q_M (1) (n. Δ t) has to be solved for the values $h_1^{(1)}(n.\Delta t)$, $Q_1^{(1)}(n.\Delta t)$,..., $h_M^{(1)}(n.\Delta t)$, $Q_M^{(1)}$ (n. Δ t) of h and Q at the M grid-points of Segment 1 and a similar set of equations with boundary values $h_1^{(2)}$ (n. Δ t) and $Q_N^{(2)}(n.\Delta t)$ must be solved for $h_1^{(2)}(n.\Delta t)$, ..., $Q_N^{(2)}(n.\Delta t)$ at the N grid-points of Segment 2. In general, since boundary conditions are given only at the ends of the system, the boundary conditions $Q_M^{(1)}(n.\Delta t)$ and $h_1^{(2)}(n.\Delta t)$ are unknown. Only a small error should occur if $Q_M(1)$ ({n-1}. Δt), which is available from the previous step, is substituted for $Q_{M}^{(1)}$ (n. Δ t) while solving the difference equations for Segment 1 and the same should hold if $h_1^{(2)}(\{n-1\}.\Delta t)$ is used in place of $h_1^{(2)}$ (n. Δt) for Segment 2. The values of h and Q at grid-points close to the ends of the segments must be affected by these approximations, but if At is sufficiently small, appreciable errors should be confined to BC in the case of Segment 1 and to AB in the case of Segment 2. Thus in the example shown in Figure 2, the vector

 $\{\ldots, Q_{M-5}^{(1)}, h_{M-4}^{(1)}, Q_{M-4}^{(1)}, h_{M-3}^{(1)}, Q_{M-3}^{(1)}, h_4^{(2)}, Q_4^{(2)}, h_5^{(2)}, Q_5^{(2)}, h_6^{(2)}, \ldots\}$

should be a satisfactory solution for the region of the join.

2.2 Single or Unilateral Overlap

If the various segments which constitute the system are treated at every time step in a fixed sequence starting from a point at which boundary conditions are prescribed, a system of single or unilateral overlap, which is more economical than double overlap, can be employed. Considering Figure 3, in which Segment 1 extends past the join B as far

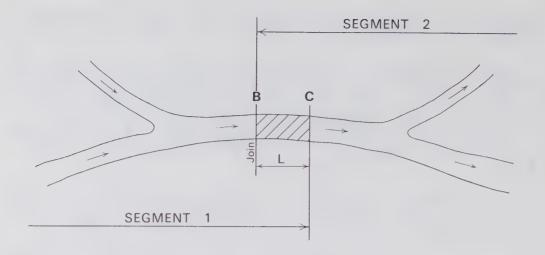


Figure 3 Join with Single or Unilateral Overlap

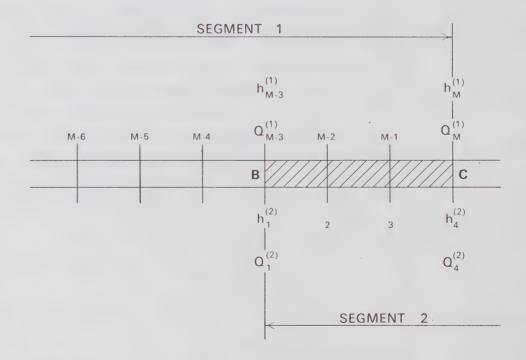


Figure 4 Details of Join with Single Overlap

as C, it can be seen that there is no need for Segment 2 to extend to the left of B provided that Segment 1 is solved before Segment 2. This follows from the fact that if the time-step Δt is less than L/c, error in Segment 1 is confined to the overlap region BC, and the correct updated solution at B is available for use as a left-hand boundary condition in the subsequent solution of Segment 2. If the erroneous solution for BC obtained while solving Segment 1 is discarded, the remaining part plus the solution from Segment 2 constitute a valid solution for the whole region covered by the two segments.

Since solutions must be computed twice in regions of overlap, first when Segment 1 is solved and again for Segment 2, single overlap obviously requires less computing effort than double overlap.

2.2.1 Combination of numerical solutions at a join with single overlap

As an illustration, consider Figure 4, which shows a join with single overlap (extending three grid-sections past join B) at which the intended sequence of solution is Segment 1 followed by Segment 2. For a given time-step, say $(n-1).\Delta t$ to $n.\Delta t$, Segment 1 must be made to extend past join B since the correct right-hand boundary condition $Q_M^{~(1)}(n.\Delta t)$ is unavailable. If the last available value, $Q_M^{~(1)}(\{n-1\}.\Delta t)$, is used in place of $Q_M^{~(1)}(n.\Delta t)$ and if Δt is sufficiently small, error should be confined to the region of overlap BC. Consequently, when Segment 2 is solved, the updated value $h_{M-3}^{~(1)}(n.\Delta t)$ obtained while solving Segment 1 is valid for use as the left-hand boundary condition $h_1^{~(2)}(n.\Delta t)$ of Segment 2, which therefore need not overlap to the left of B. With this method, the vector,

 $\{\ldots, Q_{M-6}^{(1)}, h_{M-5}^{(1)}, Q_{M-5}^{(1)}, h_{M-4}^{(1)}, Q_{M-4}^{(1)}, h_{1}^{(2)}, Q_{1}^{(2)}, h_{2}^{(2)}, Q_{2}^{(2)}, h_{3}^{(2)}, \ldots\}$ should give a satisfactory solution in the region of the join.

In some difference schemes hand Q are evaluated at alternate grid-points on alternate time steps. There is no basic difficulty in employing this type of scheme in conjunction with the single or double overlap variations of the method of segments, but if the amount of overlap has to be changed it must be incremented or decremented in units of two grid sections in order that the grids of adjacent segments should match.

2.3 Prediction of Boundary Conditions at Joins

In the procedures described in §§ 2.1.1, 2.2.1 it was suggested that when an updated boundary condition was unavailable, the most recent value of the same variable should be substituted. For instance, in the illustration of single overlap discussed in §2.2.1, the value $Q_M^{(1)}(\{n-1\}.\Delta t)$ was used as the right-hand boundary condition of Segment 1 in place of the still unknown $Q_M^{(1)}(n.\Delta t)$. An obvious refinement, which requires negligible extra computing effort, is to predict the unknown boundary condition by extrapolation from immediate past values. For instance, the first-order prediction for $Q_M^{(1)}(n.\Delta t)$ is

$$Q_{M}^{(1)}(n.\Delta t) = Q_{M}^{(1)}(\{n-1\}.\Delta t) + \Delta t. [Q_{M}^{(1)}(\{n-1\}.\Delta t) - Q_{M}^{(1)}(\{n-2\}.\Delta t)]$$

Higher-order prediction schemes employing three or more past values could also be used, but these will not be considered here. The scheme described in §2.2.1, where the unknown boundary condition is replaced simply by its last known value, amounts to zeroth-order prediction.

Prediction can be used in the case of double overlap also. Using the terminology of §2.1.1, the first-order prediction for the unknown left-hand boundary value of Segment 2 is

$$h_1^{(2)}(n.\Delta t) = h_1^{(2)}(\{n-1\}.\Delta t) + \Delta t.[h_1^{(2)}(\{n-1\}.\Delta t) - h_1^{(2)}(\{n-2\}.\Delta t)]$$

while the formula for the right-hand boundary value $Q_M^{(1)}$ (n. Δt) of Segment 1 is the same as in the single overlap case above.

The differing effects of using zero and first-order prediction for the unknown boundary conditions are illustrated in §3.

2.4 Note on Boundary Conditions

The illustration used in the foregoing text and the following numerical experiment assumes that h(t) is specified at one boundary while the other dependent variable, Q(t), is specified at the other boundary; this situation, which will be termed the h-Q case, is the one normally encountered in coastal inlets and tidal rivers³, ⁴. However, in studies of straits for instance, it is more likely that h(t) will be known at both ends of the system (from tide gauges) while Q(t) is not known at either end. Possibly in other physical contexts the Q-Q case may occur also.

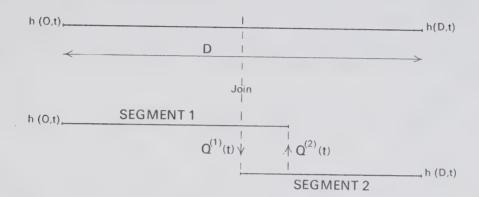


Figure 5 Representation of h-h case as two h-Q cases

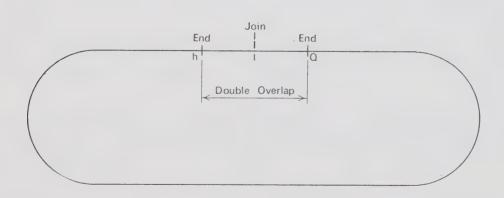


Figure 6 Closed Curve Domain

With ordinary methods, some alteration is required in a program written for one set of boundary conditions before it can be used for either of the other two cases, but the concept of overlapping segments permits a subroutine written for the h-Q case to be used without alteration in h-h and Q-Q problems. Figure 5 shows the reduction of an h-h case to two segments. If appropriate values of Q are exchanged between the segments at each time step, then one segment is an h-Q case and the other Q-h. These are identical from the programming point of view and can be solved by the same subroutine. A Q-Q case permits similar division into Q-h and h-Q cases.

Another illustration of the flexibility of method, though one which is mainly of academic interest, is where the domain of interest is a closed curve such as in Figure 6. The coefficient matrix for a one-dimensional implicit scheme for this domain can readily be seen to have non-zero terms in the upper right and lower left corners and these indicate that a specific inversion algorithm is required for conventional solution of this system. If however the domain is considered as a somewhat longer curve joined at a certain point, beyond which the ends overlap, as shown in Figure 6, then the problem can be treated by the double overlap version of the method of overlapping segments. A standard subroutine for the h-Q case discussed above can be used for this if h and Q values are passed from points overlapped to the respective ends at each time step.

3. A NUMERICAL EXPERIMENT WITH THE METHOD OF OVERLAPPING SEGMENTS

The validity of the proposed method was tested for a simple physical situation in which analytical solutions were available for checking the computed results. The test case chosen was the simulation of one cycle of the standing wave component of the tidal motion in a uniform stretch of river with a bed of rectangular cross-section. In practice, it is unlikely that a uniform stretch of river would be split into segments (except as discussed in § 2.4), but the procedures followed and presumably their effects also are very similar for all types of segment and it was considered unnecessary to complicate the demonstration by introducing bifurcations, confluences, etc.

Assuming negligible friction and zero mean flow, the governing equations for small-amplitude waves in shallow water of depth d in a rectangular channel reduce to

$$\frac{\partial Q}{\partial t} = -gbd \frac{\partial h}{\partial x}$$
 (2a)

$$\frac{\partial h}{\partial t} = -\frac{1}{b} \frac{\partial Q}{\partial x} , \qquad (2b)$$

where b is the channel width. With the mixed boundary conditions

$$h(O,t) = h_1 = H \cos \omega t \tag{3a}$$

$$Q(D,t) = Q_{61} = Hcb \sin \frac{\omega D}{c} \sin \omega t$$
 (3b)

supplied in this test, the analytic solutions to equations (2) are

$$h(x,t) = H \cos \omega t \cos \frac{\omega x}{c}$$
 (4a)

$$Q(x,t) = Hcb \sin \omega t \sin \frac{\omega x}{c}$$
 (4b)

The numerical values chosen correspond to a fairly uniform 60-mile stretch of the St. Lawrence River, which, for the purpose of the test was represented by a grid with one-mile sections. Values used were:

wave-amplitude H=6.5 ft. tidal frequency $\omega=0.00014056$ rad/sec. reach length D=316,800 ft. (i.e. 60 miles) channel width b=50,000 ft. wave speed $c=(gd)^{\frac{1}{2}}=50$ ft.sec. grid section length $\Delta x=5280$ ft.

The accuracy of each solution computed was judged by simultaneously computing rectangular approximations to the following error criteria:

$$E_{h} = \int_{0}^{t} \int_{0}^{D} (h_{computed} - h_{analytic})^{2} dx.dt$$
 (5a)

$$E_{Q} = \int_{0}^{t} \int_{0}^{D} (Q_{computed} - Q_{analytic})^{2} dx.dt$$
 (5b)

Frequent reference will be made in the following sections to the non-dimensional mesh ratio

$$r = \frac{c \cdot \Delta t}{\Delta x} \tag{6}$$

which is an important parameter in finite difference approximations to wave equations. Essentially r represents the number of grid intervals through which effects should propagate during a time interval of length Δt .

Finite difference methods for wave equations and for hyperbolic systems in general can be divided into two classes, explicit and implicit. In explicit schemes, the unknown variables at the end of each time step are expressed explicitly in terms of values known at the end of the immediately preceding time step(s) and so the difference equations to be solved are uncoupled and relatively simple to solve. However, explicit schemes are computationally unstable when the mesh ratio r is greater than unity. Since it may not be possible to predetermine r in non-linear problems, implicit schemes, which are stable for all values of r, are quite often preferred. Other factors, such as their differing effects on wave amplitude and effective speed of propagation also influence the choice of which of the two techniques to use in a given problem.

The main disadvantage of implicit schemes is that they require more programming and computational effort than explicit schemes. The term 'implicit' indicates that at each time step the difference expressions used to find the unknown values at each grid-point include unknown values at neighbouring grid-points and not just known values from previous steps. Consequently, a large set of simultaneous difference equations has to be solved at each time step. The non-zero terms in the coefficient matrices of these schemes are generally grouped close to the main diagonal and very substantial economies in computing time and memory space requirements can be achieved if special algorithms are used for the inversion operation required at each time step instead of general-purpose equation-solving programs.

Features such as bifurcations and confluences in the system being simulated contribute non-zero terms far from the main diagonal of the coefficient matrix which complicate the solution procedure quite out of proportion to their number⁴. Further, since their precise positions in the coefficient matrix depend on the geometry of the particular system being considered, an algorithm written for one river or inlet can very seldom be applied to another. Thus, with the conventional approach, a major programming effort is necessary if an implicit difference solution is required for some new system.

If on the other hand the method of overlapping segments is used, many different systems can be represented as particular combinations of a few standard 'building blocks' (confluence, bifurcation, island, etc.) for each of which a standard subroutine can be used. Writing these subroutines is not a trivial matter, since they themselves have complicated coefficient matrices, but the number of special non-zero off-diagonal terms to be taken into account in any one subroutine is substantially less than in the overall coefficient matrix for the whole system. These subroutines can be checked out individually, and since they may be used in any system governed by the same partial differential equations, it should be worthwhile spending some effort on optimizing their coding.

3.1 Application of an Implicit Difference Scheme

The implicit difference representation of equations (2) chosen for the numerical tests was the well-tried scheme³

$$h_1^n = h_1(n.\Delta t) \tag{7a}$$

$$h_{m+1}^{n} = h_{m}^{n} - \alpha \left[(Q_{m+1}^{n} - Q_{m+1}^{n-1}) + (Q_{m}^{n} - Q_{m}^{n-1}) \right], m = 1, ..., M-1$$
 (7b)

$$Q_{m+1}^{n} = Q_{m}^{n} - \beta \left[(h_{m+1}^{n} - h_{m+1}^{n-1}) + (h_{m}^{n} - h_{m}^{n-1}) \right], m = 1, \dots, M-1$$
 (7c)

$$Q_{M}^{n} = Q_{M}(n.\Delta t)$$
 (7d)

where $\alpha = \frac{\Delta x}{2gbd.\Delta t}$, $\beta = \frac{b.\Delta x}{2.\Delta t}$ and superscripts and subscripts

refer to time and space respectively. $h_1(n.\Delta t)$ and $Q_M(n.\Delta t)$ are of course specified by equations (3) in the present example.

Figures 7 and 8 show the discrepancies E_h and E_Q between computed and analytic solutions of the test problem for the following methods in turn:-

- a) conventional solution of the entire 60-mile stretch of river as one unit, using implicit scheme (7) above.
- b) division of the river near the mid-point into two segments with double overlap at the join and zeroth-order prediction of unknown boundary conditions, as described in §2.1.1.
- c) division into two segments as in b) but with first-order prediction of boundary conditions (§2.3).
- d) division of the river at the mid-point into two segments with single overlap at the join and zeroth-order prediction of the unknown boundary condition for the first segment (§2.2.1).
- e) division into two segments as in d) but with first-order prediction of the boundary condition (§2.3).

Implicit scheme (7) was used throughout for the individual segments. All five cases were run with two different values of the non-dimensional mesh ratio, r=1.0 and 2.5. The former is the limiting value³ of r for explicit schemes (see §3.2 for comparison between implicit and explicit solutions) and r=2.5 lies near the maximum value of r for which the effects of truncation error remain acceptable.

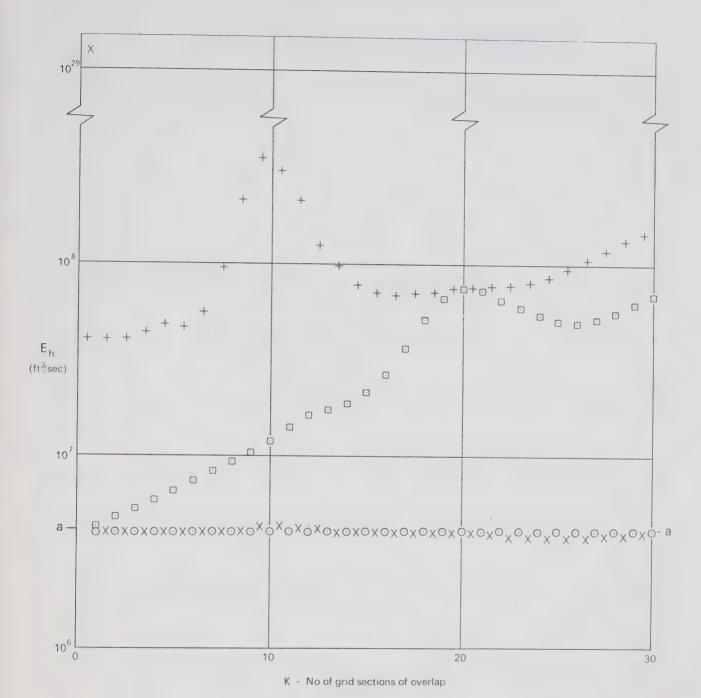
Computations were carried out in single precision FORTRAN on a Univac 1108 36-bit word computer. Round-off error was checked by repeating runs in double precision arithmetic; in all instances this altered E_h and E_Q by less than 1%.

3.1.1 Discussion of results

Results of casesa) to c) for r=1.0 and r=2.5 are presented in Figures 7 and 8 respectively, which show the variation of E_h and E_Q with the number, k, of grid-section lengths of overlap alfotted to each segment at the join. In case a) where the system is solved as a unit, the integral square errors E_h and E_Q are independent of k, since there is no join, and are represented by the horizontal lines a-a on the appropriate figures.

Figures 7 and 8 show clearly that in cases c) and e) the values of E_h and E_Q for all magnitudes of overlap k are very close to the respective values obtained when the system is solved as a unit (case a; line a-a). This means that for the test case studied, both the single overlap and double overlap methods with first order prediction give solutions which are practically identical to those obtained by the conventional method in which the whole system is solved simultaneously. This result, which hopefully will be found to hold for other hyperbolic systems, is most satisfactory since it implies that the method of overlapping segments may be used in conjunction with a given implicit difference scheme without invalidating expertise already acquired in the use of that particular scheme.

Figure 7a Error in h for r = 1.0 versus Extent of Overlap



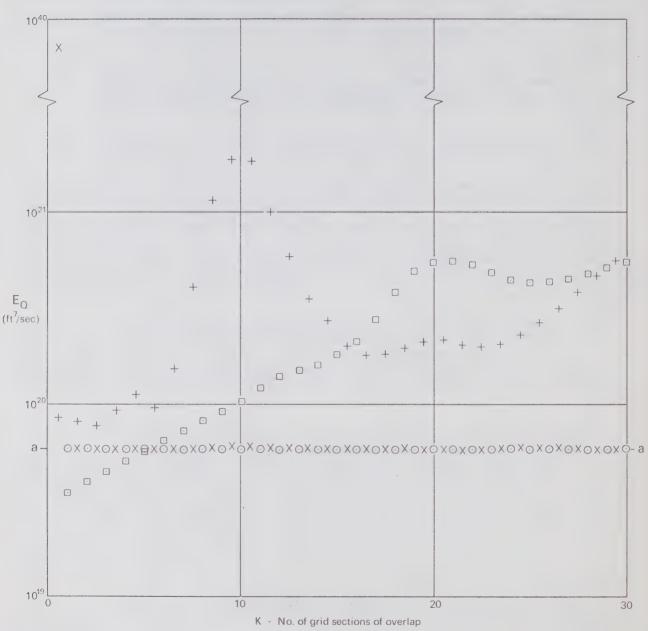
+ Double overlap, zeroth-order prediction - case (b)

X Double overlap, first-order prediction - case (c)

☐ Single overlap zeroth-order prediction - case (d)

O Single overlap, first-order prediction - case (e)

Figure 7b Error in Q for r = 1.0 versus Extent of Overlap



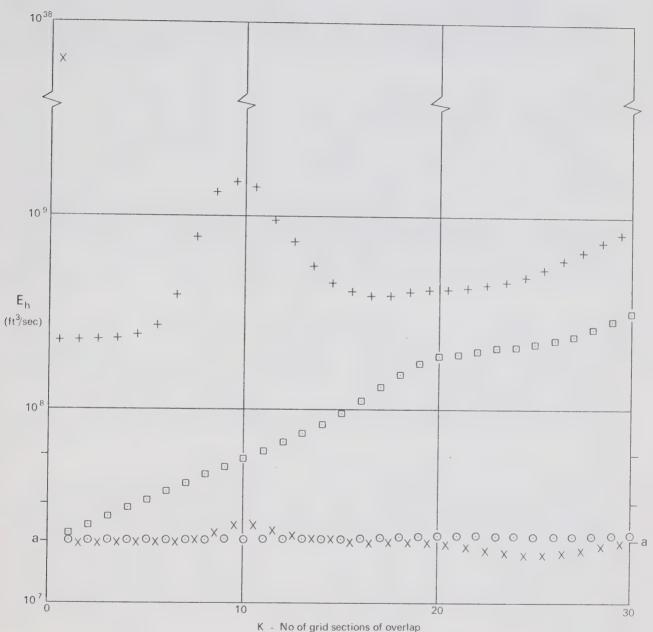
⁺ Double overlap, zeroth-order prediction - case (b)

X Double overlap, first-order prediction - case (c)

[☐] Single overlap zeroth-order prediction - case (d)

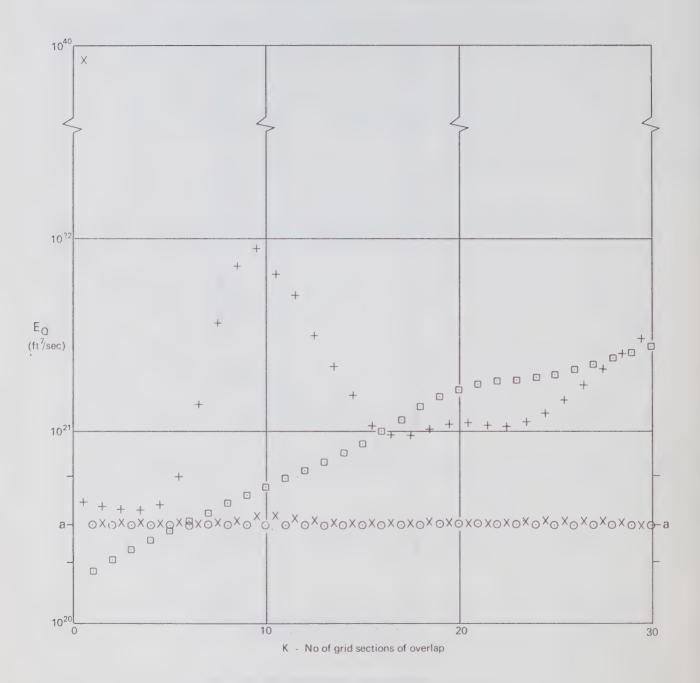
O Single overlap, first-order prediction - case (e)

Figure 8a Error in h for r = 2.5 versus Extent of Overlap



- + Double overlap, zeroth-order prediction case (b)
- X Double overlap, first-order prediction case (c)
- ☐ Single overlap zeroth-order prediction case (d)
- O Single overlap, first-order prediction case (e)

Figure 8b Error in Q for r = 2.5 versus Extent of Overlap



Double overlap, zeroth-order prediction - case (b)

X Double overlap, first-order prediction - case (c)

[☐] Single overlap zeroth-order prediction - case (d)

Single overlap, first-order prediction - case (e)

in conjunction with a given implicit difference scheme without invalidating expertise already acquired in the use of that particular scheme.

It should be pointed out that E_h and E_Q were computed up to much larger values of k than would be contemplated in practice. If the results shown are found to be typical, then it should be adequate to have k=1/2 for double overlap or k=1 for single overlap in all applications, provided that first-order prediction is also used.

Zeroth-order prediction of unknown boundary conditions (cases b and d) on the other hand, gives values of E_h and E_Q which vary considerably with overlap k and which on the whole are greater than E_h and E_Q for case a). For the data used in the test, errors of $E_h=10^8~(\mathrm{ft^3/sec})$ and $E_Q=10^21~(\mathrm{ft^7/sec})$ correspond roughly to average discrepancies between the computed and analytic solutions of about 1% of peak values during the cycle, so that with one exception (k=1/2, case b), the discrepancies found are at worst about 2%. The very large errors in the exceptional case are undoubtedly due to inadequate length of overlap. It is not known why similar large errors do not occur with single overlap (case d), even when r is as large as 2.5.

The improvement obtained by using first-order instead of zero-order prediction indicates that second or higher-order prediction of the unknown boundary conditions should probably bring about even closer conformity between solutions computed using overlapping segments and those obtained by conventional methods. However, agreement is already so close with first-order prediction that higher-order refinements are scarcely worthwhile.

One modification to the first-order prediction technique which might produce a detectable effect would be the introduction of iteration at the very first time step. Since only the most immediate past values, i.e. the initial values, are available on the first step, prediction of unknown boundary values at the ends of segments can only be zeroth-order unless iteration is used. If the first step is performed twice, (or more), values obtained on one attempt can be used as estimates for the unknown boundary conditions during the subsequent one.

3.2 Application of an Explicit Difference Scheme

Provided that certain simple rules concerning arrangement of overlap and exchange of boundary values are followed, solutions obtained when the method of overlapping segments is used in conjunction with an explicit scheme are exactly the same as when the system is treated as a whole

with the same difference scheme. As an example consider the popular 'leap-frog' method 3 , which for equations (2) takes the form

$$Q_{2m}^{2n+1} = Q_{2m}^{2n-1} - \gamma \cdot [h_{2m+1}^{2n} - h_{2m-1}^{2n}], m=1, \dots, \frac{M-2}{2}$$
 (8a)

$$Q_{M}^{2n+1} = Q_{M} (\{2n+1\}.\Delta t)$$
 (8b)

$$h_1^{2n+2} = h_1 (\{2n+2\}.\Delta t)$$
 (8c)

$$h_{2m+1}^{2n+2} = h_{2m+1}^{2n} - \delta \cdot [Q_{2m+2}^{2n+1} - Q_{2m}^{2n+1}], m=1, \dots, \frac{M-1}{2}$$
 (8d)

where $\gamma = \frac{\text{gbd.}\Delta t}{\Delta x}$, $\delta = \frac{\Delta t}{\text{b.}\Delta x}$ and superscripts and subscripts

refer to time and space respectively. Values of h and Q are worked out in this case at alternate points in the space-time grid as shown in part in Figure 9. Double arrows converging on a point in this figure indicate which earlier quantities the value at that point is related to through equations (8).

Suppose that the solution is known up to some arbitrary point in time, say $2n.\Delta t$ and that it is now required to find Q for even-numbered grid points at $(2n+1).\Delta t$ and h for odd-numbered grid-points at $(2n+2).\Delta t$. Considering first the system as a whole, it can be seen that in one complete cycle of computation i.e. two time steps, the value at any given point depends on previous known values spaced at most two grid-points from the point in question e.g. the farthest values on which h^{2n+2}_{2m+1} depends are h^{2n}_{2m-1} and h^{2n}_{2m+3} .

Consider now the situation if, instead, the system is divided into two segments at some grid-point, say 2m+l as indicated in Figure 9, and the individual segments are solved by means of scheme (8). Provided that an overlap of two grid-section lengths is allowed and that the values Q_{2m+2}^{2n-1} , h_{2m+3}^{2n} found for Segment 2 during the previous cycle are attributed to the appropriate grid-points in the region of overlap of Segment 1, then h_{2m+1}^{2n+2} is identical to the value computed when the system is treated as a whole. The same result is obviously true for Q_{2m}^{2n+1} , which does not depend on known values to the right of the join and for all other values computed at $(2n+1).\Delta t$ and $(2n+2).\Delta t$ in both segments. Therefore, in the case of the leap-frog scheme (8), an overlap of two grid-sections plus appropriate transfer of known values between segments ensures identity between the conventional solution and that found by the method of overlapping segments with single overlap. Analogous results hold for double

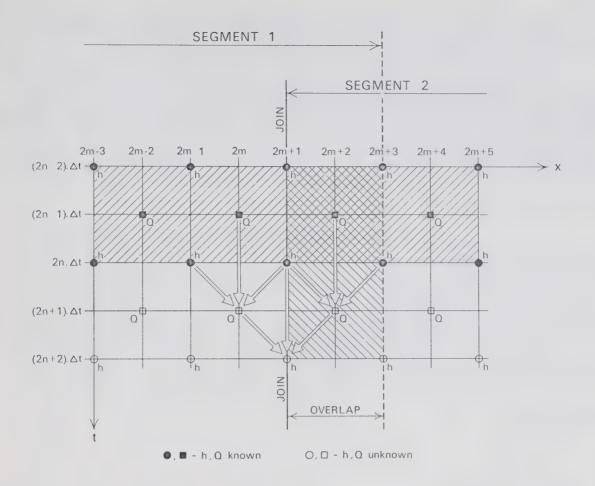


Figure 9 Details near Join for Leapfrog Explicit Scheme

overlap or when other explicit difference schemes are used. Contrary to the situation with implicit schemes (§2.3), the question of prediction of unknown boundary values does not arise.

Values of 1.5 .10 7 and 9.6 .10 19 were found for E_h and E_Q in the test problem when the explicit scheme (8) was applied with r=1.0, the results being the same of course whether the system was solved whole or in two or more segments. For comparison, E_h and E_Q for the system treated as a whole by the implicit scheme (7) were 4.1 .10 6 and 5.9 .10 19 (line a-a in Figure 4).

3.2.1 Discussion

It has been shown that introduction of the method of overlapping segments does not affect solutions when an explicit difference scheme is used. At first sight, programming would appear to be complicated rather than simplified, but for a system with a complicated domain, the advantages of being able to make repeated use of subroutines to solve similar parts of the system would probably outweigh the disadvantages of having to exchange data between segments. The use of the method of overlapping segments in conjunction with explicit schemes is probably best justified in some of the more sophisticated applications mentioned in §4, which are difficult to solve otherwise.

4. FUTURE DEVELOPMENTS AND APPLICATIONS

Work now in progress on simulation of tidal motion in the Fisher-Fitzhugh Inlet, British Columbia, a complicated branching inlet with two bifurcations and six confluences, indicates that the method of overlapping segments yields results which agree well with those of alternate numerical methods. It is hoped to check all the results against field measurements in the near future. Assuming that these and other more extensive numerical tests confirm the validity of the method, a number of interesting and useful applications can be foreseen, some of which are outlined below.

a) Extension to two or three space dimensions

The physical argument on which the method is based applies equally well to hyperbolic systems with more than one space dimension and since the complexity of programming with the conventional approach increases substantially with the number of dimensions involved, it can be expected that the use of overlapping segments will simplify both the conceptual and programming aspects of such problems. This can be foreseen particularly in cases where the governing equations involve different numbers of dimensions in different parts of the system. For example, a river which can be adequately represented for most of its length with one space dimension, perhaps as in equations (2), may widen at some points into lakes or an estuary where two space dimensions may be essential for adequate representation. When this type of system is treated as a whole, particularly when an implicit scheme is employed, programming becomes very involved and division into overlapping one- and two-dimensional segments should make such problems much more manageable.

b) Systems with different time-steps

The method provides a simple means of economizing on computer time where different time-steps are appropriate in different parts of a system. Consider for instance, an inlet which is relatively shallow in its upper reaches. If the section-lengths in the spatial grid are dictated independently by factors such as variation in inlet width, one way to take advantage of the lower wave speeds in the upper reaches is to take larger time-steps in these parts. This is not a simple matter to arrange when one overall difference scheme is used but is easy to program with the method of overlapping segments. The procedure is particularly straightforward if one segment can be given a time-step which is some integer N times that required for another. The latter segment is then solved N times for each step made with the former. Arrangement of overlap and interpolation for intermediate values at the joins is not unduly complicated.

c) Moving high-resolution grids

Closely connected with the proposal in b) above is the possible use of variable spatial grids in a class of meteorological problems. Currently there is need for numerical methods which permit use of a fine grid which moves with a front or hurricane while a more economical coarse grid is used whenever conditions are moderate. The method of overlapping segments seems to offer one straightforward way of coping with this problem.

The domain in question would first be divided into a suitable number of overlapping segments. In the example shown in Figure 10, 11 of the 12 segments (shown without overlaps) would be solved using a coarse grid, but the segment in which the storm was located, in this case Segment 6, would be handled with a finer grid. At some point, as the storm moved towards a neighbouring segment, say 7, it would become necessary to use a fine grid in that segment also, and at times it might be necessary to have more than one segment so treated. Of course, 6 could revert to coarse grid when the storm was well into 7.

The interpolation problem at the boundary between the fine and coarse grids is much the same whether the fine grid moves or not. In this example, each segment would be solved by calling one or two standard subroutines; one assuming a coarse grid, the other using a fine grid and having built-in procedures for interpolating at the segment boundaries. It is convenient to make the coarse grid interval some integer multiple N of the fine grid interval. If an explicit difference scheme is used, N time steps of size $^\Delta t/N$ are taken in the fine grid segments for each step Δt taken in the coarse grid segments. If an implicit scheme is used, the time-steps in both the fine and coarse grid segments could remain the same, provided that the non-dimensional mesh ratio r is nowhere too large.

d) Mixed analytical-numerical models

Once a system is divided into segments, it should be possible to use different techniques for different segments. The most interesting situation would be when some segments were amenable to analytic and others to numerical solution. An example is tidal motion in the inlet shown in lengthwise section in Figure 11. This fjord-type inlet has a sill near the mouth, a deep, practically uniform middle reach and shallows near the head. If the inlet is treated in three segments as shown and the solution in the uniform middle Segment 2 can be represented by some analytic expression while the variable-depth Segments 1 and 3 are treated numerically, the simulation should obviously require less computing time than it would if the whole system were treated numerically. The economies in computer time and storage requirements resulting from this mixed analytical-

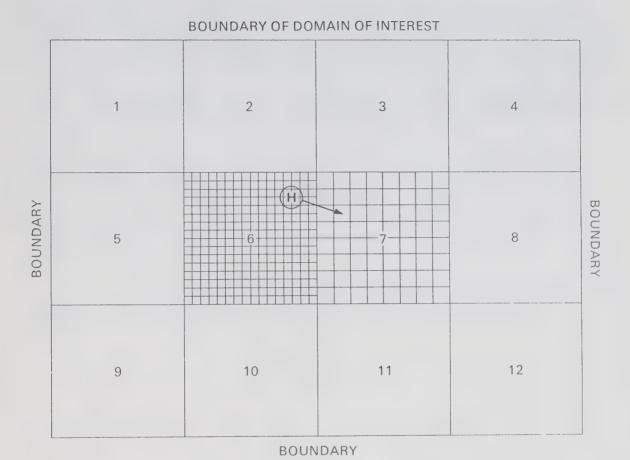


Figure 10 Arrangement of Segments for Moving Grid Example

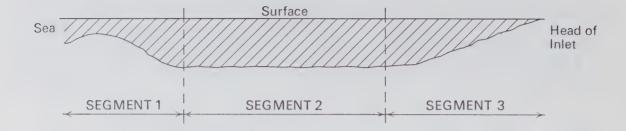


Figure 11 Lengthwise Section of an Inlet

numerical approach could be quite substantial in two and three-dimensional systems. Details of the process of combining solutions from the different segments at the end of each time step remain to be explored.

e) Extension to parabolic and elliptic systems

Although at first sight the dependence of the method on finite speeds of propagation appears to limit applications to hyperbolic systems only, there are grounds for expecting it to work satisfactorily in parabolic systems. While in theory, physical events in diffusive systems produce effects at large distances within an infinitesimal time, in fact the distance over which practically significant effects are apparent is finite. By deciding at what level quantities can be considered insignificant in a given system, it should be possible to determine an upper bound L for the distance over which appreciable effects can be transmitted in a given time interval Δt . This permits introduction of the concept of an equivalent propagation speed L/ Δt , and application of the method of overlapping segments.

Elliptic equations would require temporary augmentation to parabolic or hyperbolic form before the method could be applied. For instance, the Laplace elliptic equation

$$0 = \frac{\partial^2 u}{\partial x^2} + \frac{\partial^2 u}{\partial y^2}$$

could be modified either to the parabolic form

$$\frac{\partial \mathbf{u}}{\partial t} = \frac{\partial^2 \mathbf{u}}{\partial \mathbf{x}^2} + \frac{\partial^2 \mathbf{u}}{\partial \mathbf{y}^2}$$

or to a damped hyperbolic form

$$\frac{\partial^2 \mathbf{u}}{\partial t^2} + \mathbf{c} \frac{\partial \mathbf{u}}{\partial t} = \frac{\partial^2 \mathbf{u}}{\partial \mathbf{x}^2} + \frac{\partial^2 \mathbf{u}}{\partial \mathbf{y}^2}, \quad c > 0$$

The steady-state solution to either of these equations should be the required solution to the Laplace equation, provided identical boundary conditions are supplied. Whether the additional computing effort required by the introduction of the extra independent variable can be justified or not will depend on the complexity of the domain governed by the original elliptic equation and on the prior availability of subroutines to handle the parabolic or hyperbolic forms.

f) Use of several processors

The method of overlapping segments could prove to be a convenient technique for harnessing several computers for real-time simulation of an exceptionally large problem or similarly for making efficient use of multi-processor computers. The domain would be divided into segments fitting the capability of the individual processors, which could then work synchronously in parallel. It should be possible to exchange necessary segment boundary data between processors by using common memory storage.

5. ACKNOWLEDGEMENTS

The writer is indebted to Dr. S. Ince, Hydraulics Laboratory, National Research Council, Ottawa, for drawing his attention to the tidal problems which prompted this work. He also wishes to thank Miss T. Millington for editing this report and Mr. G. Gough for his assistance with the illustrations.

6. REFERENCES

- 1) Dronkers, J.J. 1964. <u>Tidal Computations in Rivers and Coastal Waters</u>. Amsterdam, North-Holland Publishing Company, 518 pages.
- 2) Hsu, S.K.T. and Howe, R.M. "Preliminary Investigation of a Hybrid Method for Solving Partial Differential Equations", 1968 Fall Joint Computer Conference, A.F.I.P.S. Conference Proceedings, Vol. 33, Pt. I., pp 601-609, Thompson Book Co., Washington, D.C.
- 3) Kamphuis, J.W. 1970. Mathematical Tidal Study of St. Lawrence River, <u>Journal of the Hydraulics Division</u>. Vol. 96. Paper 7141.
- 4) Ligget, J.A. and Woolhiser, D.A. 1967. Difference Solutions of the Shallow-Water Equation, Journal of the Engineering Mechanics Division. Vol. 93.









BINDING SECT.

OCT 3 1 1972

